

SUPPLEMENTO
AL VOLUME VI, SERIE X, DEL
NUOVO CIMENTO
A CURA DELLA SOCIETÀ ITALIANA DI FISICA

1957

2° Semestre

N. 3

RENDICONTI

DEL

IV CORSO CHE NELLA VILLA MONASTERO A VARENNA

DAL 15 LUGLIO AL 4 AGOSTO 1956

FU TENUTO A CURA

DELLA SCUOLA INTERNAZIONALE DI FISICA

DELLA SOCIETÀ ITALIANA DI FISICA

INDICE

INTRODUZIONE.

G. POLVANI - Discorso inaugurale	pag. 808
L. GIULOTTO - Prolusione	» 812

Lezioni tenute al corso.

M. H. L. PRYCE - Paramagnetism in Crystals	» 817
J. H. VAN VLECK - Magnetic Properties of Metals	» 857
C. J. GORTER - Paramagnetic Relaxation	» 887

C. KITTEL - Ferromagnetism	pag. 1895
C. J. GORTER - Antiferromagnetism	» 923
L. NÉEL - Les métamagnétiques ou substances antiferromagnétiques	» 942
E. M. PURCELL - Nuclear Magnetism and Nuclear Relaxation	» 961
J. H. VAN VLECK - Line-Breadths and the Theory of Magnetism	» 993
A. ABRAGAM - Influences des électrons sur la résonance des spins nucléaires dans les substances diamagnétiques: le déplacement « chimique » et les interactions indirectes	» 1015
R. KUBO - Stochastic Theory of Magnetic Resonance	» 1063
J. H. VAN VLECK - The Concept of Temperature in Magnetism	» 1081
N. KURTI - Magnetism at Very Low Temperatures and Nuclear Orientation	» 1101
C. KITTEL - Cyclotron Resonance in Crystals	» 1140
A. KASTLER - Les méthodes optique de la résonance hertzienne	» 1148
C. J. GORTER - Magnetic Properties of Superconductors	» 1168

Comunicazioni.

J. SMIT - Hall Effect in Ferromagnetics	» 1177
W. MARSHALL - Critical Scattering of Neutrons from Ferromagnets	» 1183
W. MARSHALL - The Van Vleck Model of Ferromagnetism	» 1186
H. PFEIFER - Influence of the Apparatus on Nuclear Magnetic Resonance	» 1188
J. VAN KRAENDONK - Statistical Theory of Ferro- and Antiferromagnetism	» 1190
J. VAN KRAENDONK - Nuclear Relaxation in Magnetic Materials	» 1192
S. MEIBOOM - The Study of Chemical Exchange Reaction by Nuclear Magnetic Resonance	» 1194
A. ABRAGAM et J. COMBRISSE - Resonance Paramagnétique des impurétés dans un semi-conducteur	» 1197
L. GIULOTTO, G. LANZI and L. TOSCA - Nuclear Magnetic Relaxation in Mixtures of Liquids	» 1213
A. FERRO and G. MONTALENTI - Magnetic After-Effect and Internal Friction at High Temperatures in Iron and some Iron Alloys	» 1214

H. GRÄNICHER and K. A. MÜLLER - Röntgenographic and Paramagnetic Experiments with (Gd-La)AlO ₃ Mixed Crystals	pag. 1216
H. GRÄNICHER - The Electric Analogue to Antiferromagnetism: Antiferroelectricity	» 1220
C. P. ENZ - Magnetic Susceptibility of Electrons in Periodic Fields	» 1224
M. BLOOM - Proton Spin Relaxation in Gaseous and Liquid Hydrogen	» 1230
E. M. PURCELL - The Production of Very Uniform Magnetic Fields	» 1234
J. H. VAN VLECK - The Antiferromagnetic State in the Chrome Alums	» 1235
J. H. VAN VLECK - The Magnetic Susceptibility of Oxygen in a Clathrate Compound	» 1236
P. RHODES - The Dependence of Nuclear Magnetic Resonance Absorption in Metals on Specimen Shape and Size	1237

La Direzione del Corso ringrazia vivamente tutti coloro che hanno collaborato alla raccolta delle lezioni e in particolare i dottori

P. CAMAGNI, G. LANZI, L. TOSCA, G. DALLA PERGOLA, B. BERTOTTI, R. FIESCHI, R. PAPPALARDO, L. VERDINI.

INTRODUZIONE

Discorso inaugurale

DI

G. POLVANI

Presidente della Società Italiana di Fisica.

Quando quattro anni fa la Società Italiana di Fisica iniziò qui a Villa Monastero questi Corsi della nostra Scuola Internazionale di Fisica, la difficoltà maggiore che mi si presentava davanti agli occhi della mente protesi nel futuro con la speranza che detti corsi, come poi è avvenuto, avessero fortuna, non fu tanto quella di trovar modo di rinnovare ogni anno gli argomenti da trattare — la Fisica è cosa così immensa —, nè di trovare i mezzi finanziari per alimentare i corsi — anche la nostra povertà è così immensa — quanto il potere assicurare ogni anno — risum teneatis amici — al povero Presidente della Società, chiunque egli fosse, un nuovo spunto per il suo discorsetto inaugurale del Corso.

Ed io ieri sera ero fortemente imbronciato con me stesso e, Dio me! perdoni, con Varenna stessa, proprio per questo dovere che a me immeritamente per la quarta volta consecutiva incombe.

Ma stamattina presto, verso le quattro e mezzo e le cinque, alzatomi per preparare il discorso, e affacciandomi alla finestra, la vista meravigliosa che dinanzi agli occhi mi si è pòrta — il lago calmo, immobile, lucido come una sfera, il cielo terso e ancor quasi cupo, i « monti sorgenti dall'acqua », l'opposta riva punteggiata di bianche case, il nero promontorio di Bellagio — mi ha riconciliato col mio dovere.

E mi sono detto che veramente valeva la pena che otto secoli fa in seguito alle lotte tra Como e Milano, i Comaschi scacciassero i Comacini dall'Isola, e che alcune monache cistercensi di là fuggiasche, venissero qui a fondare un monastero di cui questi muri sono l'antico oratorio, e che poi accadessero tutte quelle vicende che formano la storia del Monastero e della Villa e di Varenna, affinchè noi, tardi ospiti, si potesse godere oggi, nel loro ricordo, di

ritrovarsi qui, dinanzi a tanto meraviglioso scenario così denso di storia: ritrovarsi qui venuti da ogni parte del mondo a parlare dei nostri studi e profittare della calma tranquillità del luogo più bello del Lago.

E ringraziare, oltre alla Provvidenza che tanto ci ha largito, chi aiutandoci materialmente e moralmente ci concede simile ozio: amici fedeli i cui nomi sono segnati e sul libro dei nostri debiti e nel nostro cuore: il Ministro della Pubblica Istruzione, oggi sua Eccellenza il prof. PAOLO ROSSI; il prefetto della Provincia di Como, il conte dott. GIULIO BIANCHI di Lavagna; il Presidente del Consiglio Nazionale delle Ricerche prof. GUSTAVO COLONNETTI; il Presidente del Consiglio Nazionale delle Ricerche Nucleari, prof. FRANCESCO GIORDANI; il Presidente del Comitato Nazionale per la Fisica, prof. ELIGIO PERUCCA; il Rettore Magnifico dell'Università di Milano, prof. GIUSEPPE MENOTTI DE FRANCESCO; il Direttore generale per l'istruzione superiore, dott. MARIO DE DOMIZIO; il Presidente della RAI, prof. ANTONIO CARRELLI; il Presidente dell'Ente Villa Monastero, avv. GIBERTO BOSISIO, cui va il nostro compiacimento per la confermata carica di Presidente dell'Amministrazione Provinciale di Como; il Sindaco di Varenna, sig. ALEM TANTARDINI, che tanto ha fatto per il suo Comune e che tanto ci vuole bene; il Presidente dell'Ente Provinciale per il Turismo della Provincia di Como, dott. GIUSEPPE RUSSO; il Presidente e il Consigliere delegato della Moto Guzzi di Mandello sul Lario, dott. ENRICO PARODI Cavaliere del Lavoro e rag. BONELLI; il Presidente della Società Fiocchi, comm. GIULIO FIOCCHI; il Presidente della Società Badoni di Lecco, ing. GIUSEPPE BADONI; il Presidente delle Acciaierie del Caleotto, comm. ERNESTO BONAITI; il Presidente della Società Carcano di Mandello, prof. RICCARDO ZELIOLI; il Presidente della Metalgraf di Pescarenico, cav. EGISTO BIFFI; il Presidente della Soc. Serpentino Italiana, ing. on. PIERO AMIGONI; il Consigliere delegato della Società Orobia di Milano, on. ing. prof. NOVERINO FALETTI; il Consigliere delegato della Società Condor di Rho, dottor ing. MARIO MORTARA; l'ing. EUGENIO SOMAINI di Lomazzo, così benemerito dei nostri studi.

A tutti quanti ho nominato vada il ringraziamento più vivo e sentito.

* * *

E non meno calorosa vada la nostra espressione di gratitudine agli scienziati che hanno accolto il nostro invito di salire sulla cattedra di questa Scuola per trattare gli argomenti che formano l'oggetto principale del Corso di quest'anno: le proprietà magnetiche della materia. Permettete che vi presenti questi nostri docenti.

Il prof. PURCELL, premio Nobel, di Cambridge del Massachusetts, il prof. GORTER di Leida, il prof. KITTEL di Berkeley di California, il prof. NÉEL di Grenoble, il prof. PRYCE di Bristol, il prof. VAN VLECK di Cambridge del Massachusetts, il prof. KURTI di Oxford; e ancora i prof. ABRAGAM di Saclay,

KASTLER di Parigi, KUBO di Tokyo, e il prof. LUIGI GIULOTTO di Pavia, al quale va un particolare ringraziamento di tutta la Scuola per il lavoro lungo e non facile dell'organizzazione scientifica di questo quarto Corso.

Al quale dovevano al massimo partecipare, secondo il bando della Scuola, solo trentacinque allievi. Ma le domande ricevute sono state tante che ne abbiamo accolti ben quarantacinque; e, per contentare i molti postulanti, abbiamo introdotto, per quest'anno e in via sperimentale, anche la categoria degli uditori, ben forte di tredici persone.

Non ostante ciò a noi rimane il rammarico di non aver potuto contentare gli altri rimasti esclusi: non potevamo far di più proprio per ragioni finanziarie e tecniche.

Desidero nominarli e presentarli scambievolmente tutti questi studiosi, tornati studenti; e, molti di loro, studenti d'eccezione, se si considera che nel loro paese hanno già alta dignità accademica.

Allievi: P. CAMAGNI (Pavia), Segretario del corso, A. BATTAGLIA (Pisa), C. BERNARDINI (Roma), B. BERTOTTI (Milano), B. BOLOGNA (Roma), P. BROVETTO (Torino), G. DELLA PERGOLA (Roma), G. DIAMBRINI PALAZZI (Roma), A. FERRO MILONE (Torino), R. FIESCHI (Milano), G. GIACOMETTI (Padova), A. GOZZINI (Pisa), G. LANZI (Pavia), M. MAESTRO (Pisa), M. PALMA (Palermo), B. PALMA VITTORELLI (Palermo), R. PAPPALARDO (Pavia), D. PESCECETTI (Torino), E. POLACCO (Pisa), F. PORRECA (Napoli), L. TOSCA (Pavia), L. VERDINI (Roma), M. BLOOM (Canadà), B. BOLGER (Olanda), J. F. C. COCHRAN (Canadà), S. S. DHARMATTI (India), C. ENZ (Svizzera), E. H. FREI (Israele), T. FULTON (U.S.A.), H. GRÄNICH (Svizzera), F. GURSEY (Turchia), A. HRYNKIEWICZ A. (Polonia), B. JACROT (Francia), T. KAHAN (Francia), S. O LUNDQUIST (Svezia), W. MARSHALL (Inghilterra), S. MEIBOOM (Israele), P. RHODES (Inghilterra), D. ROUX (Svizzera), J. SMIT (Olanda), T. TAMURA (Giappone), J. VAN KRANENDONK (Olanda), H. P. J. WIJN (Olanda), J. M. WINTER (Francia), H. J. ZEIGER (U.S.A.).

Uditori: G. CARERI (Roma), F. FUMI (Milano), M. SANTANGELO (Palermo), J. BUTTERWORTH (Inghilterra), W. J. HUISKAMP (Olanda), C. MACLEAN (Olanda), J. C. SEVERIENS (Olanda), T. VANNGARD (Svezia), G. DIETZMANN (Germania Orientale), H. LIPPMANN (Germania Orientale), H. PFEIFER (Germania Orientale), H. K. WEBER (Germania Orientale), J. KACZÉR (Cecoslovacchia).

A tutti maestri, allievi, uditori il ben venuto della Società Italiana di Fisica, quello del Consiglio della Società e mio personale.

* * *

Un'altra novità di questo anno, oltre l'introduzione degli uditori, è la seguente anch'essa in via sperimentale.

Nei due giorni centrali del Corso, cioè il 27 e il 28 Luglio, il Corso, come tale, sospenderà la sua attività per trasformarsi in un Convegno speciale, nel quale saranno discussi lavori, sempre nel campo delle proprietà magnetiche della materia, presentati dai partecipanti al Corso. Al Convegno interverrà anche il premio Nobel, prof. PAULI di Zurigo.

* * *

Altri particolari vi dirà il prof. GIULOTTO, ad ascoltare il quale non voglio porre ulteriore indugio, scusandomi se già troppo a lungo ho parlato.

Chiuderò con l'augurio che possa questa attività della nostra Scuola Internazionale di Fisica, servire la Scienza col più alto scopo che il sapere e la saggezza ricercano: quello dell'umana convivenza nella stima e nel rispetto reciproci.

Prolusione

DI

L. GIULOTTO

Direttore del Corso

Benchè sia solo al suo quarto anno di vita, la Scuola Internazionale di Fisica di Varenna ha ormai una tradizione, che vuole, fra l'altro, che all'inaugurazione la persona alla quale è stata affidata l'organizzazione del Corso ne illustri gli scopi e svolga alcune considerazioni introduttive sugli argomenti che verranno trattati. So di non meritare questo onore, come sentivo di non possedere tutte le doti necessarie quando circa due anni fa, dopo qualche esitazione ho accettato l'incarico che il Consiglio della Società Italiana di Fisica e soprattutto la benevolenza del prof. POLVANI hanno voluto affidarmi.

Nel Corso di quest'anno verranno trattate questioni molto interessanti che costituiscono una delle parti più vive e più dinamiche della Fisica attuale. E mi auguro che questo corso e il corso che si terrà l'anno venturo, che sarà organizzato dal prof. FUMI, contribuiscano ad affermare in Italia le ricerche in campi della Fisica ancor poco coltivati nel nostro paese.

Era pienamente giustificato che in questa Scuola si trattassero in corsi precedenti argomenti riguardanti i raggi cosmici, le particelle elementari e, in generale, la Fisica più strettamente nucleare. In Italia infatti ricerche in questi campi vengono condotte ormai da parecchio tempo con notevole profitto, dimostrato anche recentemente dal contributo italiano ad alcune importanti scoperte.

Ma è altrettanto giustificato e forse più necessario che i piccoli e coraggiosi gruppi di ricercatori italiani che si dedicano da qualche tempo a ricerche in altri campi, trovino ora, qui a Varenna, un riconoscimento, un conforto, una guida.

Questa aspirazione era già stata sentita durante un piccolo convegno che ebbe luogo proprio qui a Varenna due anni fa (*), ed è stata subito ricono-

(*) Vedine i Rendiconti nel N. 2 del *Supplemento* al Vol. I, Serie X del *Nuovo Cimento*, 1955.

sciuta e incoraggiata dal prof. POLVANI e dal Consiglio della Società Italiana di Fisica, che hanno concesso che alla Scuola di Varenna per due anni consecutivi (1956 e 1957) potessero essere svolti alcuni fra i più attuali argomenti di Fisica dello stato solido, dello stato liquido e delle basse temperature.

Dopo varie consultazioni con i gruppi italiani interessati, mi è sembrato che una buona parte degli argomenti da essi proposti potesse venir trattata in un Corso abbastanza omogeneo dedicato alle proprietà magnetiche della materia.

* * *

Il Magnetismo è un capitolo della Fisica che ha avuto negli ultimi decenni nuovi sviluppi che sono più o meno strettamente legati al generale progresso della Fisica e che negli ultimi anni in particolare si è esteso notevolmente con la scoperta e lo studio di fenomeni nuovi. La materia appare ancora oggi, dal punto di vista magnetico, come l'insieme di tanti magnetini elementari, già postulati nelle vecchie teorie sul magnetismo. Ma le nostre conoscenze attuali sui magneti elementari sono ben più profonde. Essi si identificano con gli elettroni, con gli atomi, con i nuclei; così i limiti del capitolo « Magnetismo » appaiono oggi assai più difficili da stabilire che in passato, giungendo fino alle basi stesse della Fisica.

È noto che le prime osservazioni sul Magnetismo risalgono alla più remota antichità e riguardano le singolari proprietà della magnetite capace di attrarre piccoli pezzi di ferro. Così la fenomenologia molto appariscente delle sostanze ferro-magnetiche è la prima ad essere acquisita.

In seguito, col progredire della tecnica sperimentale, si scopre che tutte le sostanze presentano proprietà magnetiche, benchè generalmente in grado molto più piccolo del ferro e delle sostanze ferromagnetiche. Si inizia così, nella seconda metà del secolo diciannovesimo, lo studio del diamagnetismo e del paramagnetismo. I grandi progressi raggiunti in questo secolo nello studio e nell'interpretazione dei fenomeni magnetici sono strettamente legati ai progressi della spettroscopia che portano ad una conoscenza via via più approfondita della struttura degli atomi e delle loro proprietà magnetiche. Spesso accade però in Fisica che i fenomeni più facili da osservare non siano fra quelli di più facile interpretazione.

Le esperienze fondamentali sul ferromagnetismo, tecnicamente abbastanza facili e relativamente antiche, devono così attendere per una loro spiegazione del tutto soddisfacente che altri effetti assai più delicati vengano osservati e si giunga, dopo successive interpretazioni approssimate di tali effetti, alla definitiva formulazione della Meccanica quantistica.

Già all'inizio di questo secolo si era giunti, per merito di LANGEVIN, a una interpretazione di principio abbastanza soddisfacente del diamagnetismo e del paramagnetismo. Di poco posteriore è la teoria di WEISS sul ferromagne-

tismo. Tale teoria però, soddisfacente dal punto di vista fenomenologico, postulava l'esistenza di un « campo molecolare » che sarebbe stato capace di orientare i magneti elementari nell'interno del materiale ferromagnetico, e sarebbe dovuto essere di gran lunga più intenso di quello valutabile in base alle sole azioni magnetiche reciproche.

Solo una ventina di anni dopo il campo di WEISS trova per merito di HEISENBERG una soddisfacente interpretazione quantistica come « forza di scambio ». Successivamente nuove possibilità di interazioni di questo tipo vengono scoperte. NÉEL e la sua scuola sono in grado di accertare che, in alcuni cristalli e in un'opportuno campo di temperatura, i momenti magnetici più prossimi sono orientati antiparallelamente. Si inizia così lo studio dell'antiferromagnetismo e del ferrimagnetismo.

Intanto progrediscono le conoscenze sulle proprietà magnetiche dei nuclei, dapprima soprattutto attraverso l'esame delle strutture iperfini delle righe spettrali, la cui interpretazione esige la esistenza di momenti magnetici nucleari associati a spin nucleari, come è stato ammesso per la prima volta da PAULI già nel 1924; poi grazie alle raffinate esperienze sulla risonanza magnetica nucleare condotte a partire dal 1939 da RABI e collaboratori su fasci di raggi atomici. Per la prima volta queste esperienze avevano permesso di osservare un effetto previsto teoricamente: per l'azione combinata di un campo magnetico costante e di un campo magnetico oscillante ad esso normale e di frequenza opportuna i nuclei scambiano energia col campo oscillante.

Un analogo fenomeno era da aspettarsi anche nella materia condensata. I primi tentativi in questa direzione risalgono al 1936 e al 1942 e sono dovuti a GORTER e collaboratori. I primi successi sono stati raggiunti da PURCELL e collaboratori e da BLOCH e collaboratori poco più di dieci anni fa.

Sono quasi contemporanee alla scoperta della risonanza magnetica nucleare nella materia considerata, le prime osservazioni sulla risonanza paramagnetica elettronica da parte di ZAWOISKY e di altri, che pure hanno aperto nuovi campi di indagine sulle proprietà magnetiche della materia.

* * *

Ha inizio così l'era moderna del Magnetismo, caratterizzata da una sempre maggiore diffusione degli studi, con l'impiego di nuove tecniche, delle proprietà magnetiche della materia. La novità consiste essenzialmente nello studiare il comportamento delle sostanze non più sotto l'azione di un solo campo magnetico costante, ma impiegando contemporaneamente un campo costante e un campo oscillante, la cui frequenza, nelle più comuni condizioni sperimentali, si trova nella gamma delle radiofrequenze per le risonanze nucleari e nella gamma delle microonde per la risonanza elettronica. Nello studio del paramagnetismo elettronico le vecchie bilance magnetiche vengono in gran parte

abbandonate di fronte alle nuove vaste possibilità offerte dalla tecnica delle microonde, mentre, d'altra parte, il fenomeno della risonanza magnetica nucleare costituisce praticamente l'unica possibilità di indagare nel campo del paramagnetismo nucleare.

I nuovi campi di ricerca sembrano dapprima abbastanza accessibili anche ad alcuni laboratori modestamente attrezzati nei quali si cerca di allestire le nuove tecniche con mezzi di fortuna.

Raggiunti però i primi risultati e una loro prima soddisfacente interpretazione teorica si è ormai giunti a uno stadio di notevole perfezionamento nelle tecniche sperimentali e di raffinamento delle teorie. Ci troviamo di fronte a un tipico esempio di progresso rapido e sistematico ad un tempo in un moderno campo di indagine.

Specialmente il fenomeno della risonanza magnetica nucleare ci appare ora, grazie ai più recenti progressi della tecnica, complicato in maniera oltremodo interessante da vari tipi di interazione: interazioni fra gli spin nucleari, interazioni fra momenti di quadrupolo nucleari e campi elettrici cristallini non uniformi e, infine, «chemical shift» e interazioni indirette fra gli spin nucleari.

Nel campo della risonanza elettronica si hanno pure notevoli sviluppi e interessanti novità: oltre a ricerche sempre più accurate e sistematiche sulle interazioni iperfini e col campo elettrico cristallino nei cristalli paramagnetici, l'applicazione della risonanza elettronica allo studio del ferromagnetismo e dell'antiferromagnetismo, i metodi ottici per la rivelazione della risonanza magnetica e ancora un nuovo tipo di risonanza interessante specialmente i semiconduttori, la risonanza ciclotronica. I fenomeni di risonanza magnetica hanno condotto a considerare nuove e delicate questioni sulla larghezza delle righe e strane estensioni del concetto di temperatura.

Infine altro argomento di attualità che può ben inquadrarsi nel magnetismo è rappresentato dallo studio e dalle applicazioni dei vari metodi proposti per l'allineamento nucleare.

È evidente quindi che affinché un corso relativamente breve sul magnetismo possa svolgersi efficacemente occorrerà partire da posizioni abbastanza avanzate sviluppando soprattutto la parte più moderna di questo vasto capitolo della Fisica.

Ciò è del resto nelle tradizioni e nello spirito della Scuola di Varenna che è soprattutto scuola di avanguardia. Ed è veramente una fortunata circostanza, sicura garanzia di successo per il Corso, questa, che ha permesso di riunire fra i docenti buona parte dei responsabili dei più moderni indirizzi di ricerca nel campo del magnetismo. A chiunque si occupi di tali questioni sono ben noti infatti i contributi fondamentali di ABRAGAM, GORTER, KASTLER, KITTEL, KUBO, KURTI, NÉEL, PRYCE, PURCELL, VAN VLECK.

C'era da aspettarsi perciò un notevole interesse per il corso. Assai nume-

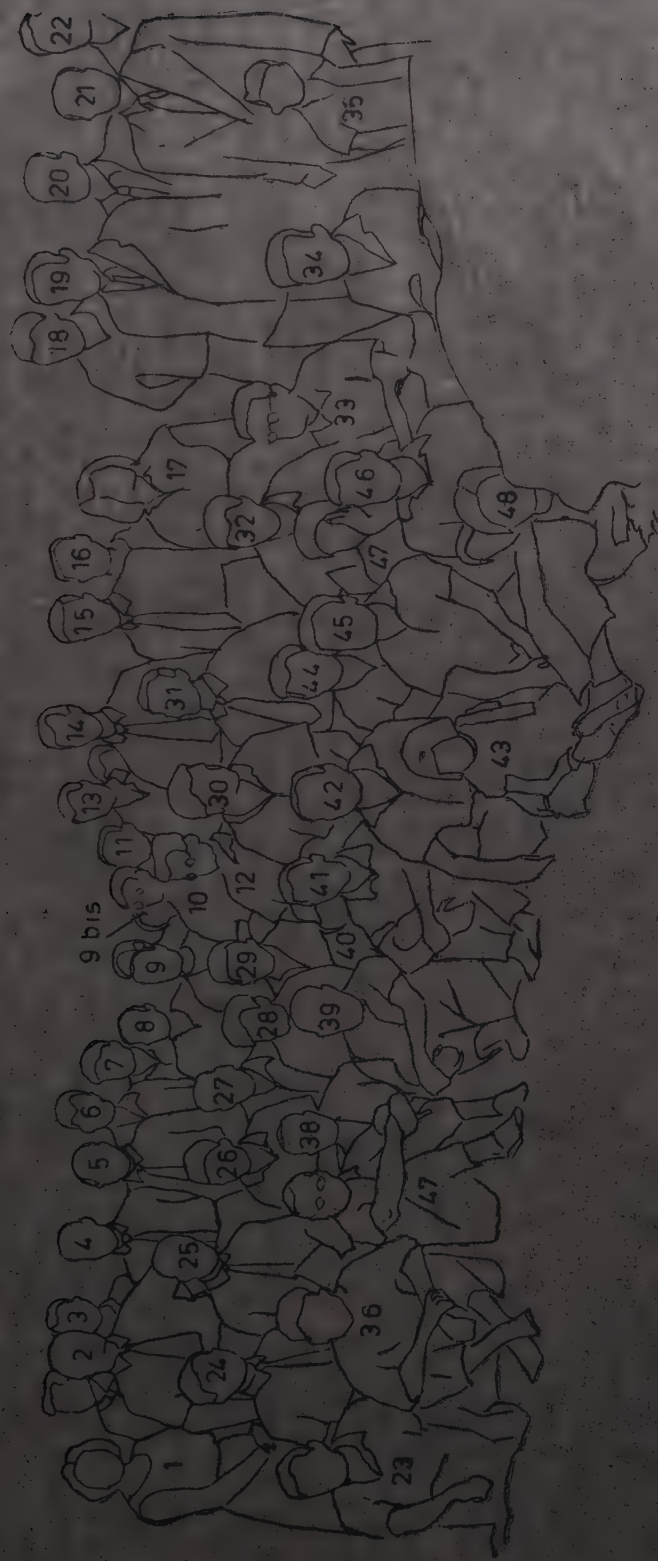
rose sono state infatti le domande di aspiranti allievi, giunte da ogni parte del mondo, ma purtroppo non tutte è stato possibile accogliere.

* * *

Inoltre, poichè fra gli « allievi » e fra gli « uditori » si trovano alcuni ricercatori già affermati, si è creduto opportuno approfittare di tale circostanza per introdurre una novità e dare a tutti i partecipanti la possibilità di portare il proprio contributo all'efficacia del Corso, e quindi in ultima analisi all'avanzamento degli studi sul Magnetismo: la novità consiste nell'inserire durante il periodo del Corso stesso, un piccolo Convegno nel quale docenti, uditori ed allievi potranno presentare i risultati delle loro ricerche o delle loro considerazioni sopra la fenomenologia relativa al Magnetismo. Questa novità è risultata molto gradita, tanto che non pochi sono già gli iscritti a parlare al Convegno, il quale avrà luogo nei giorni 27 e 28 Luglio prossimi.

* * *

Chiudendo infine queste mie brevi parole di prolusione al Corso, mi è gradito ringraziare il prof. POLVANI, animatore della Scuola di Varenna, per l'aiuto dato e i docenti per avere così gentilmente accettato il nostro invito a prestare la loro preziosa opera.



1. Mrs. Gränicher
2. H. Gränicher
3. O. Mac Lean
4. H. Pfeifer
5. A. Ferro Milone
6. E. M. Purcell
7. J. Smit
8. T. Kahan
9. M. Bloom
- 9 bis. A. Gozzini
10. P. Rhodes
11. E. H. Frei
12. B. Bertotti
13. P. Brovotto
14. J. Butterworth
15. A. Hrynkievich
16. P. Camagni
17. G. Giulotto
18. M. Maestro
19. L. Giulotto
20. B. Bolger
21. S. S. Dharmatili
22. M. H. L. Pryce
23. D. Roux
24. T. Tamura
25. H. P. Wijn
26. L. Tosca
27. M. Santangelo
28. C. Enz
29. F. Porreca
30. L. Verdini
31. W. Marshall
32. R. Pappalardo
33. C. Bernardini
34. R. Kubo
35. F. Gozzini
36. J. M. Winter
37. C. Kittel
38. J. H. Van Vleck
39. N. Kurti
40. B. Palma Vittorelli
41. G. Lanzi
42. G. Careri
43. L. Giulotto
44. D. Pescetti
45. B. Bologna
46. S. Meiboom
47. G. Della Pergola
48. G. Della Pergola

SCUOLA INTERNAZIONALE DI FISICA

4° CORSO ESTIVO - VARENNA SUL LAGO DI COMO - VILLA MONASTERO - 15 Luglio - 4 Agosto 1956



LEZIONI TENUTE AL CORSO

Paramagnetism in Crystals.

M. H. L. PRYCE

H. H. Wills Physical Laboratory, University of Bristol

1. - Types of magnetism.

The purpose of these lectures is to deal with paramagnetism in crystals, but it is useful at the start to review briefly the various types of magnetic behaviour one meets in nature.

Diamagnetism is the most frequently observed type, and most simple substances are diamagnetic. Their susceptibility is negative. I.e. a magnetic field induces a magnetic moment in the opposite direction. The absolute value of the susceptibility is very small, and is nearly independent of temperature.

Paramagnetism. In paramagnetic substances a magnetic field induces a moment in the same direction, i.e. the susceptibility is positive. The magnitude of the susceptibility is larger than in diamagnetic substances, and generally increases with decreasing temperature.

Ferromagnetism, antiferromagnetism and ferrimagnetism are more complicated forms of magnetic behaviour, characterized, among other things, by departures from the proportionality between field and magnetic moment. They will be dealt with in other sets of lectures in the summer school, and it will be sufficient for the present purpose to remark that all real paramagnetic substances probably show this behaviour at sufficiently low temperatures; and conversely, these more complicated types become paramagnetic at elevated temperatures.

2. - Fundamentals of paramagnetism.

Many paramagnetic substances obey Curie's law

$$(1) \quad \chi = C/T$$

at least approximately. C is called the Curie constant.

Most paramagnetic crystals, though not all, are ionic. Their paramagnetism can be traced to certain paramagnetic ions, and to a useful extent one can isolate the idea of *ionic susceptibility*. Paramagnetic ions invariably contain transition elements, e.g. Fe^{2+} , Fe^{3+} , Cu^{2+} , $\text{Fe}(\text{CN})_6^{3-}$, Gd^{3+} , UO_2^{2+} , etc.

The susceptibility of a crystal is the sum of the ionic susceptibilities of its components. Since there are diamagnetic and paramagnetic ions in a paramagnetic crystal, the total is made up of a paramagnetic part (temperature dependent) and a diamagnetic part (temperature independent). A more complete expression for the susceptibility would then be

$$(2) \quad \chi = \frac{C}{T} + a,$$

a being a small negative constant. Sometimes a is positive, but still small. We then speak of a temperature-independent contribution to the paramagnetism.

In quoting experimental values of ionic susceptibilities it is usual to correct the measurements for the diamagnetism of the various ions making up the crystal.

Curie's law (2) is a good approximation only for magnetically dilute substances, e.g. those for which the effective field acting on the ion is only the external one. In magnetically dense substances, neighbouring ions influence each other through their magnetic fields and by electron exchange. For magnetically concentrated substances, the Curie-Weiss law often holds:

$$(3) \quad \chi = \frac{C}{T - \Delta} (+a),$$

where Δ is the Weiss constant and is positive for ferromagnetic substances and negative for antiferromagnetic substances. Eq. (3) may hold for magnetically dilute substances too (see (94)).

We shall often in the following, as an approximation, consider atoms and ions as isolated entities. This is not fully correct, for the magnetic properties of a paramagnetic ion in a crystal are strongly influenced by the electric field of the surrounding ions. For instance, in crystals grown from water solution of salts of the first transition group, the magnetic ion is surrounded by six molecules of H_2O , or four molecules of H_2O and two oxygens associated with some acidic ion, such as SO_4^{2-} . In both cases we have six negative charges arranged about the magnetic ion on the vertices of an octahedron. (The H_2O even though neutral, is dipolar and points its negative side towards the metal ion.) For instance, the arrangement for $\text{CuSO}_4 \cdot 5\text{H}_2\text{O}$ is as shown in Fig. 1. A more correct statement is that we shall be considering *ionic complexes* of

this kind, and we shall frequently ignore their mutual interaction, and so regard the complex as an isolated entity.

If the ions or ionic complexes possess no permanent magnetic moment, the effect of an external magnetic field is to induce a moment proportional to the field

$$(4) \quad \mu = \alpha H.$$

The coefficient α is the *ionic polarizability*.

The total moment induced is

$$(5) \quad M = \sum_i N_i \alpha_i H,$$

so that the susceptibility is

$$(6) \quad \chi = M/H = \sum_i N_i \alpha_i,$$

where N_i is the number of ions of species i , whose polarizability is α_i . If the quantity of material involved is one mole, then χ is the molar susceptibility; if it is one gramme, it is the mass-susceptibility; or if one cm^3 , the volume-susceptibility. In the following we shall always talk about molar susceptibilities. For instance, for CaCl_2 , if N_0 is Avogadro's number, we have

$$(7) \quad \chi_{\text{mol.}}(\text{CaCl}_2) = N_0 \alpha(\text{Ca}^{2+}) + 2N_0 \alpha(\text{Cl}^-).$$

If the ions are anisotropic, χ may be very different in different directions. In such a case the induced moment is not, in general, parallel to the applied field, and the polarizability α is then a tensor. An example of an anisotropic ion is NO_3^- . Symmetrical ions, such as Mg^{2+} , Cl^- , SO_4^{2-} , even when in unsymmetrical surroundings, show isotropic susceptibility.

Now although most ions and molecules possess no permanent magnetic moment, there are exceptions. These are the paramagnetic ions. Even without a magnetic field they have a permanent magnetic moment.

The crystal as a whole shows no magnetization when $H = 0$ because the ionic moments are directed at random and cancel out. When a field is applied there is a preponderance of moments with components parallel to the field, because of the difference of energies W of differently oriented moments and of Boltzmann's factor $\exp[-W/kT]$. Net magnetization results.

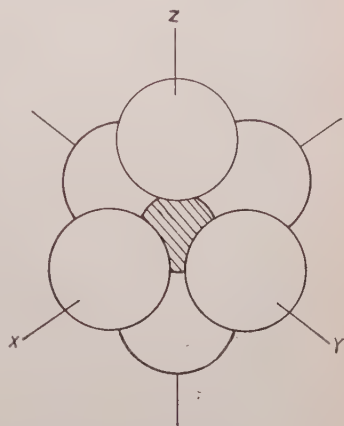


Fig. 1. — Arrangement of neighbour molecules around Cu^{2+} in $\text{CuSO}_4 \cdot 5\text{H}_2\text{O}$. The neighbours in the x - and y -directions are water molecules; in the z -direction, oxygen atoms belonging to SO_4^{2-} ions.

3. - Classical (Langevin) theory of paramagnetism.

Before discussing the quantum theory of paramagnetism it is instructive to run over the classical theory worked out by LANGEVIN. Assume that the ions have moment μ , which in the absence of an external field can point with equal probability in any direction (specified by polar angles θ , φ , say).

When a field H is applied, the ions in a crystal in thermal equilibrium will have a probability distribution given by Boltzmann's law. The probability of having a moment in the direction (θ, φ) will be proportional to:

$$\exp[-W/kT] d(\cos \theta) d\varphi; \quad W = -\mu H \cos \theta.$$

For most paramagnetic materials $W \ll kT$ at room temperature. The distribution of magnetic moments therefore only deviates slightly from a random one. By symmetry, $\bar{\mu}$ is parallel to H and therefore we have:

$$\begin{aligned} (9) \quad \bar{\mu} = \mu \overline{\cos \theta} &= \frac{\int \mu \cos \theta \exp[\mu H \cos \theta / kT] d(\cos \theta) d\varphi}{\int \exp[\mu H \cos \theta / kT] d(\cos \theta) d\varphi} = \\ &= \mu [\coth(\mu H / kT) - (kT / \mu H)]. \end{aligned}$$

Eq. (9) is Langevin's formula. For $\mu H \ll kT$, we can write:

$$\exp[\mu H / kT] \simeq 1 + (\mu H / kT)$$

and we easily find:

$$(10) \quad \bar{\mu} = \mu^2 H / 3kT.$$

The molar susceptibility is:

$$(11) \quad \chi = N_0 \mu^2 / 3kT,$$

in agreement with Curie's law. The Curie constant is

$$(12) \quad C = N_0 \mu^2 / 3k.$$

4. - Quantum theory of paramagnetism.

According to the quantum theory, μ cannot point in all directions. The quantized angular momentum is $J\hbar$, where J is a half integer or integer. For zero magnetic field, there are $2J+1$ states of equal energy. The dege-

neracy is removed when a magnetic field is applied, and one obtains the energy values:

$$(13) \quad W = -\mu H m / J, \quad m = J, J-1, \dots, -J.$$

The magnitude of the component of the magnetic field parallel to H is given by $\mu m / J$. The component of the moment perpendicular to H is not measurable simultaneously with the energy. The average magnetic moment is:

$$(14) \quad \bar{\mu} = \frac{\sum_{m=-J}^J (\mu m / J) \exp [\mu H m / k T J]}{\sum \exp [\mu H m / k T J]}.$$

The sum over m can be performed and yields a somewhat complicated function, the Brillouin function,

$$(15) \quad \bar{\mu} = \mu B_J \left(\frac{\mu H}{k T} \right),$$

where

$$(16) \quad B_J(x) = \left(\frac{2J+1}{2J} \right) \coth \left[\left(\frac{2J+1}{2J} \right) x \right] - \frac{1}{2J} \coth \left(\frac{x}{2J} \right).$$

We are once again interested in the region of small H , where the exponentials can be expanded. For small H , one finds to lowest order in H :

$$(17) \quad \bar{\mu} \simeq (\mu^2 H / k T J^2) \overline{m^2} = (\mu^2 H / 3 k T) \left(\frac{J+1}{J} \right).$$

Eq. (17) reduces to the classical expression, eq. (10), as $J \rightarrow \infty$. The formula for the susceptibility is

$$(18) \quad \chi = (\mu^2 N_0 / 3 k T) \left(\frac{J+1}{J} \right).$$

The natural unit for measuring electronic magnetic moments is the Bohr magneton β :

$$(19) \quad \beta = e \hbar / 2 m c.$$

The magnetic moment is written as

$$(20) \quad \mu = g \beta J,$$

where g is the spectroscopic splitting factor, first introduced by LANDÉ in

atomic spectroscopy. If only orbital angular momentum gives rise to the magnetic moment, $g = 1$. If only spin angular momentum gives rise to the magnetic moment, $g = 2$. (Actually, quantum electrodynamic corrections give $g = 2.0023$, but we shall neglect such subtleties).

For closed shells, $\mathbf{J} = 0$ and therefore $\boldsymbol{\mu} = 0$. One can only have induced moments in such cases. The general case is given by:

$$(21) \quad \boldsymbol{\mu} = g\beta\mathbf{J} + \alpha\mathbf{H},$$

i.e., one allows for both permanent and induced moments.

The real situation is not at all as simple as described in the ideal case above. The internal interactions in a crystal will remove the degeneracy even for zero external field. Further, any ion possesses an infinite number of energy levels, all of which formally enter into the Boltzmann distribution. Of course, one is interested only in the lowest energy levels, for these are the ones which have a non-negligible probability corresponding to them in the Boltzmann distribution.

We may illustrate the types of situations which can arise, by a few examples:

(1) Mn^{2+} , $J = \frac{5}{2}$. There are 6 levels, arranged in 3 degenerate pairs with a spacing of about 0.1 cm^{-1} between the pairs. (A word about units. We shall use cm^{-1} , as in spectroscopy. The energy corresponding to an interval of 1 cm^{-1} corresponds to a temperature interval of 1.4°K). At room temperature, the difference in the exponents in the Boltzmann expression is of the order $10^{-3} \div 10^{-4}$ so that all six levels are essentially equally populated. One has to go down to very low temperatures to detect deviations from the ideal paramagnetic theory developed above. The present case illustrates another point. The crystalline fields do not remove the degeneracy completely. This is an example of Kramers' theorem: « If the number of electrons involved is odd (J is a half integer), internal interactions must lead to a situation in which each level is at least twofold degenerate ». This final Kramers degeneracy requires a magnetic field to remove it.

Ions similar in behaviour to Mn^{2+} are Fe^{3+} ($J = \frac{5}{2}$; 3 pairs) and Gd^{3+} ($J = \frac{7}{2}$; 4 pairs). The pairs have about the same spacing as those in Mn^{2+} . The next nearest energy levels for all these ions lie about 10^4 cm^{-1} higher.

(2) Cu^{2+} . There is one degenerate pair: and the next level lies about 4000 cm^{-1} higher and therefore can be neglected at room temperatures.

(3) Co^{2+} . There are 6 pairs of levels in the region from $0 \div 1000 \text{ cm}^{-1}$. The magnetic properties can therefore arise from the thermal occupation of up to 6 pairs of levels. Thus one has a good deal of variation from one cobaltous compound to another, and the details of the magnetic behaviour are very sensitive to the form of the crystalline fields.

(4) Ni^{2+} . There are 3 single levels, all spaced $0 \div 1 \text{ cm}^{-1}$ apart. (Since in this case we have an even number of electrons, there is no Kramers degeneracy). At room temperature, all levels are essentially equally populated, and the ion acts as if it were in a $J = 1$ degenerate state. However, at $T \sim 1^\circ \text{K}$, the populations of the different levels become noticeably unequal. The next levels lie about 10^4 cm^{-1} above the lowest ones, and are not populated.

(5) Fe^{2+} . There are an even number of electrons. 5 levels lie within $0 \div 100 \text{ cm}^{-1}$ and 10 levels from $500 \div 1000 \text{ cm}^{-1}$.

(6) Cr^{3+} . This ion is similar to the Mn ion. There are two pairs, with about a 0.3 cm^{-1} separation and the next level lies at around 10^4 cm^{-1} above the lower group.

(7) Ce^{3+} . There are 3 groups about 50 cm^{-1} apart and the next level lies over 10^4 cm^{-1} above the lower group.

In addition to the deviation from the ideal case due to the removal of degeneracy by the crystalline field, there are some further difficulties which arise to modify the simple picture of the ideal case:

(a) If the degeneracy is removed by the crystalline field, the simple splitting of energy levels through the linear Zeeman effect, as stated in eq. (13), is no longer correct.

(b) The polarizability of levels which are close together is high, of order $\pm N_0 \beta^2 / \Delta$, where Δ is the energy of splitting.

(c) The anisotropy of the crystal may present further complications.

(d) As mentioned previously, ions can interact with each other either by way of electromagnetic or through exchange effects. This can profoundly influence the properties of magnetically dense crystals.

(e) Though the largest part of the paramagnetic effect arises from the electrons, the nuclei also contribute.

5. - Quantum foundations.

The dominant contribution to the magnetism of ions comes from the electrons. Although nuclei do have a magnetic moment, their contribution is much smaller. We shall therefore start by considering the electronic magnetism only. As our starting point we shall treat the ion as a system of electrons moving in a fixed field of force.

The Hamiltonian of the system is then

$$(22) \quad \mathcal{H} = \sum_i \left[\frac{1}{2m} \left(\mathbf{p}_i + \frac{e\mathbf{A}_i}{c} \right)^2 - e\varphi_i + 2\beta \mathbf{s}_i \cdot \mathbf{H} - \frac{e\hbar}{2m^2c^2} \mathbf{s}_i \cdot \mathbf{E} \wedge \mathbf{p}_i \right] + \sum_{i < k} \frac{e^2}{r_{ik}} +$$

+ smaller terms not involving spin, arising from relativity corrections

+ small terms expressing magnetic interactions between the electrons.

The first term is the kinetic energy; the second is the potential energy of the field of the nucleus and of the surrounding ions; the third expresses the interaction between the spin and the external magnetic field; the fourth is the spin-orbit interaction term; and the fifth is the potential energy of the repulsion between the electrons.

In this expression m stands for electronic mass, e the elementary charge, c the velocity of light, β the Bohr magneton previously defined, \mathbf{p}_i and \mathbf{s}_i the momentum and spin of the i -th electron, φ_i and \mathbf{A}_i the scalar and vector potential at the i -th electron, \mathbf{E}_i and \mathbf{H} (the latter assumed uniform) the electric and magnetic fields, and r_{ik} the distance between the i -th and k -th electrons.

This form of the Hamiltonian is an approximation, derived from Dirac's electron theory for the limiting case of velocities small compared with c , by eliminating the «small» spinor components.

In a central field, the spin-orbit interaction for an electron can be written

$$(23) \quad \frac{e\hbar^2}{2m^2c^2} \left(\frac{E}{r} \right) \mathbf{s} \cdot \mathbf{l}.$$

The expectation value,

$$(24) \quad \frac{e\hbar^2}{2m^2c^2} \left\langle \frac{E}{r} \right\rangle,$$

represents the spin orbit coupling constant, which we call ζ . For many purposes the spin orbit interaction can then be written

$$\sum \zeta_i \mathbf{s}_i \cdot \mathbf{l}_i,$$

where $\hbar \mathbf{l}$ stands for the orbital angular momentum $\mathbf{r} \wedge \mathbf{p}$.

It is convenient to choose a gauge which gives a symmetrical form for the vector potential \mathbf{A} , namely

$$(25) \quad \mathbf{A} = \frac{1}{2} \mathbf{H} \wedge \mathbf{r},$$

the origin being taken at the nucleus, supposed to be at rest. Although the final results of the theory are independent of the gauge, this fact is not obvious at all intermediate stages.

With this choice, the kinetic energy of an electron is

$$\begin{aligned} \frac{1}{2m} \left(\mathbf{p} + \frac{e\mathbf{A}}{c} \right)^2 &= \frac{\mathbf{p}^2}{2m} + \frac{e}{2mc} \mathbf{H} \cdot \mathbf{r} \wedge \mathbf{p} + \frac{e^2}{8mc^2} (\mathbf{H} \wedge \mathbf{r})^2 \\ &= \frac{\mathbf{p}^2}{2m} + \beta \mathbf{l} \cdot \mathbf{H} + \frac{e^2}{8mc^2} (\mathbf{H} \wedge \mathbf{r})^2. \end{aligned}$$

So

$$\begin{aligned} (26) \quad \mathcal{H} &= \left[\sum_i \left(\frac{\mathbf{p}_i^2}{2m} - \frac{Ze^2}{r_i} \right) + \sum_{i < k} \frac{e^2}{r_{ik}} \right] + [V] + [\text{spin-orbit term}] + \\ &+ [\beta \mathbf{H} \cdot (\mathbf{L} + 2\mathbf{S})] + \left[\frac{e^2}{8mc^2} \sum_i (\mathbf{H} \wedge \mathbf{r}_i)^2 \right] + [\text{small terms}], \end{aligned}$$

where $\mathbf{L} = \sum_i \mathbf{l}_i$, $\mathbf{S} = \sum_i \mathbf{s}_i$.

It is convenient to write the several terms in \mathcal{H} in the form $\mathcal{H}_1, \mathcal{H}_2, \mathcal{H}_3, \mathcal{H}_4, \mathcal{H}_5, \mathcal{H}_6$.

\mathcal{H}_1 represents that part of the Hamiltonian of the free ion which is spin-independent. It is usually by far the dominant term. $\mathcal{H}_2 = V$ is that part of the potential energy, which arises from the electrostatic field of the neighbours, frequently called the crystal field. \mathcal{H}_4 and \mathcal{H}_5 represent different aspects of the effect of the applied magnetic field.

$$(27) \quad \mathcal{H}_4 = \beta \mathbf{H} \cdot (\mathbf{L} + 2\mathbf{S}),$$

the « Zeeman term », is mainly responsible for the paramagnetism, while

$$(28) \quad \mathcal{H}_5 = \frac{e^2}{8mc^2} \sum_i (\mathbf{H} \wedge \mathbf{r}_i)^2,$$

is mainly responsible for the diamagnetism.

The operator representing the magnetic moment is obtained by differentiating the Hamiltonian with respect to the magnetic field, i.e.

$$(29) \quad \boldsymbol{\mu} = -\frac{\partial \mathcal{H}}{\partial \mathbf{H}} = -\beta (\mathbf{L} + 2\mathbf{S}) - \frac{e^2}{4mc^2} \sum_i [\mathbf{r}_i^2 \mathbf{H} - (\mathbf{r}_i \cdot \mathbf{H}) \mathbf{r}_i].$$

In this equation, the first term represents a moment present when there is no external field, while the second has the form of an induced moment,

proportional to \mathbf{H} . It arises because the orbital magnetic moment of an electron is $-e\mathbf{r} \wedge \mathbf{v}/2c$, which differs from $-\beta\mathbf{l} = -e\mathbf{r} \wedge \mathbf{p}/2mc$, by just this amount (since $m\mathbf{v} = \mathbf{p} + e\mathbf{A}/c$).

One often takes \mathbf{H} to be in the z -direction, and the « diamagnetic » term in the moment has then the component

$$(30) \quad -\frac{e^2}{4mc^2}(x^2 + y^2)H_z,$$

in the z -direction. It also has components proportional to xz and yz in the perpendicular directions, which give zero average values in isotropic surroundings, but which may not vanish in anisotropic crystals. It will be noticed that this contribution to the moment is opposite in sense to the applied field, i.e. essentially diamagnetic.

The first part $-\beta(\mathbf{L} + 2\mathbf{S})$ is the intrinsic moment, which gives rise to the paramagnetism, as already outlined.

6. – The crystal field.

The problem of studying the energy levels, and their relevance to the magnetic properties, of an ionic complex in a crystal can be approached in stages. One considers first the dominant term in the Hamiltonian. Then one considers the next most important as a perturbation on that. And so on. It is therefore useful to classify the various effects according to the order of magnitude of their contribution to the Hamiltonian. This varies from substance to substance, and we shall for the present confine our attention to the salts of the transition elements of the first long period, Ti to Cu, in which the magnetism arises from an uncompleted $3d$ shell.

For these, the order of magnitude of the energies are

1 (free-ion energies: spin-independent part)	10^5 cm^{-1}
2 (crystal field)	10^4 cm^{-1}
3 (spin-orbit interaction)	10^3 cm^{-1}
4 (Zeeman term)	1 cm^{-1}
5 (diamagnetic term)	10^{-4} cm^{-1}

We are interested only in the energy levels of non-negligible occupancy. Hence the properties of levels more than, say, 10^3 cm^{-1} above the ground level can be ignored as direct contributors to the magnetic properties at room

temperature or lower. The starting point is thus the lowest group of levels of the free-ion Hamiltonian, which is well known from atomic spectroscopy. It is characterized by definite values of L and S , and described by the usual Russell-Saunders coupling. S , although it does not occur in \mathcal{H}_1 , has a well defined value because, via the Pauli principle, it is related to the symmetry properties of the wave-function. L is a good quantum number because it commutes with \mathcal{H}_1 .

In general one can classify the \mathcal{H}_1 energy level more specifically in terms of a « configuration », based on the notion of a self-consistent field, in which each electron is regarded as having its own orbital, and the wave function of the ion is a Slater determinant of individual functions (or simple linear combination of Slater determinants). For the magnetic $3d$ -ions the configuration is $1s^2 2s^2 2p^6 3s^2 3p^6 3d^n$, where $n = 1, \dots, 9$. This is often a sufficient approximation, but occasionally, as for instance to treat certain aspects of hyperfine structure, we have to go back to a more refined starting point in which other configurations (of the same L and S) are mixed in.

For closed-shell ions L and S are both zero, and the ions are consequently diamagnetic. For the paramagnetic ions this is not so, and one has the following table for $3d^n$.

TABLE I.

n	1	2	3	4	5	6	7	8	9
L	2	3	3	2	0	2	3	3	2
S	$\frac{1}{2}$	1	$\frac{3}{2}$	2	$\frac{5}{2}$	2	$\frac{3}{2}$	1	$\frac{1}{2}$

The « free-ion » Hamiltonian \mathcal{H}_1 gives a group of levels which is $(2L+1) \cdot (2S+1)$ -fold degenerate. This degeneracy is partly removed by the effect of the crystalline potential V . This has to be studied next. Its effects will be calculated by first order perturbation methods.

In many of the salts with which we shall be concerned the positive paramagnetic ion is surrounded by an octahedron of negatively charged ions or of polar molecules with a predominance of negative charge oriented towards it. Often the octahedron is not regular. But the field of a regular octahedron furnishes a good starting point for a discussion of the effects.

The electric potential due to this octahedral distribution of charge can be expanded in spherical harmonics. By symmetry the lowest term (apart from a trivial constant) which can occur is of fourth order, for there are no harmonics of order 1, 2 or 3 possessing octahedral symmetry. Odd orders will in any case not occur if the octahedral complex has a centre of symmetry. And if they do, they will not contribute any effects in first order, because only potentials of even parity have non-zero matrix elements coupling states from the same configuration. Higher harmonics than the fourth need not be

considered, for their matrix elements all vanish for d -electrons. We can thus write

$$V = A + G(x^4 + y^4 + z^4 - 3y^2z^2 - 3z^2x^2 - 3x^2y^2) + \dots$$

The first term is the same for all the energy levels, shifting them by a constant amount, and is therefore trivial. The fourth-order term has the symmetry of the octahedron, and satisfies Laplace's equation, as required if the charge distribution of the neighbours does not overlap into the region occupied by the d -electrons.

We can learn a great deal about the effect of V from symmetry considerations.

As an example of the method we shall apply it to the particular case of $\text{Cu}^{2+}6\text{H}_2\text{O}$. Cu^{2+} has the configuration $3d^9$, which may be regarded as one « hole » in the completed shell $3d^{10}$. The effect of V on this is the same as it would be on a single particle of positive charge, moving in a $3d$ orbital.

The ground state of \mathcal{H}_1 for Cu^{2+} (free ion without spin interaction) is 2D . In the real free ion this splits, by spin-orbit interaction, into ${}^2D_{\frac{3}{2}}$ and ${}^2D_{\frac{5}{2}}$, the former being the lower. In the crystalline complex, this classification is invalid, since $\mathcal{H}_2(=V)$ is stronger than \mathcal{H}_3 (spin-orbit) and completely breaks down the free-ion spin-orbit coupling.

There are five linearly independent wave-functions for a d -orbital, and they may be written as the product of a radial factor and a solid harmonic. Appropriate second-order solid harmonics are

$$yz, \quad zx, \quad xy; \quad y^2 - z^2, \quad z^2 - x^2, \quad x^2 - y^2.$$

In the latter group only two (out of three) are linearly independent. We may choose the combinations $2z^2 - x^2 - y^2$ and $x^2 - y^2$ as our basic linear independent ones. This particular set is convenient, as then all five are mutually orthogonal. If we wish to have them in normalized form, we write

$$\begin{aligned} &\sqrt{15} \, yz, \quad \sqrt{15} \, zx, \quad \sqrt{15} \, xy; \\ &\frac{1}{2}\sqrt{5}(2z^2 - x^2 - y^2), \quad \frac{1}{2}\sqrt{15}(x^2 - y^2). \end{aligned}$$

It is clear, by considering the symmetry, that the expectation value of V in each wave function of the first group (often called $d\epsilon$) is the same, also that the matrix elements of V coupling any two different wave-functions vanish. Similarly the expectation value of V in any of the states corresponding to $y^2 - z^2$, $z^2 - x^2$, $x^2 - y^2$, and thus of their linear combinations, are equal. So we conclude that the group $d\epsilon$ all have the same energy; and that the other group, of two independent wave functions, (called $d\gamma$) both have another

energy. I.e. the five-fold degeneracy of a free d -state is split into $3+2$ by the action of a field of octahedral symmetry.

We have ignored electron spin here, for the potential V is spin-independent.

We can decide which of the groups of levels corresponds to the lower energy by the following simple argument. The charge distribution in the wavefunctions xy and $x^2 - y^2$, as seen on the xy -plane, is as shown in Fig. 2a, 2b.

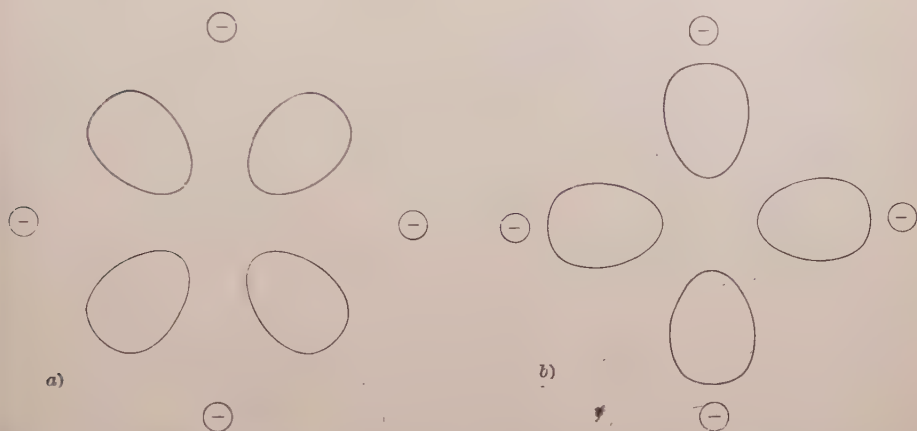


Fig. 2. - 3d charge distribution in Cu^{2+} (a) in xy , (b) in $x^2 - y^2$. The ovals represent contours of charge density equal to half the maximum value. The small circles indicate the position of the negative charges on the neighbours.

The hole, being a positive charge, has a lower energy when the charge distribution points towards the negative charges on the axes as in 2b; and a higher energy when it avoids them, as in 2a. Thus $x^2 - y^2$ has a lower energy than xy . Or, the orbital doublet $d\gamma$ has a lower energy than the triplet $d\epsilon$.

The two-fold degeneracy that is left is further removed if the octahedron of charges or dipoles is distorted. JAHN and TELLER have shown that in a symmetrical molecule with degenerate electronic states, the symmetrical disposition is unstable and the molecule distorts. The same is true of an ionic complex. In $\text{Cu}^{2+}6\text{H}_2\text{O}$ the octahedron is always distorted by elongating along one axis (the z -axis) and contracting along the other two. This removes the degeneracy between $x^2 - y^2$ and $2z^2 - x^2 - y^2$. The former has strong lobes of charge distribution near to the four close dipoles on the x and y axes, while the latter has its charge distribution mainly concentrated towards the more distant dipoles on the z -axis. Thus $x^2 - y^2$ corresponds to a lower energy than $2z^2 - x^2 - y^2$.

By similar arguments we conclude that the $d\epsilon$ degeneracy is partly removed, xy being lower than the degenerate pair yz, zx .

This still leaves the two-fold spin degeneracy. By Kramers' theorem, no external electric field, nor any internal spin-orbit interaction, can remove this. Only an external magnetic field can do so.

But before we consider the magnetic field we must consider the effect of \mathcal{H}_3 , the spin-orbit interaction. This can be represented by

$$\mathcal{H}_3 = \lambda \mathbf{L} \cdot \mathbf{S}.$$

The constant λ is positive if the $3d$ shell is less than half-filled and negative if more than half-filled. For Cu^{2+} , therefore, it is negative. In first order it does not change the energy of either $d\gamma$ level, nor of the xy component of $d\epsilon$. This is so because the diagonal matrix elements of \mathbf{L} all vanish (see later). On the other hand there are non-vanishing matrix elements of \mathbf{L} , and hence of $\mathbf{L} \cdot \mathbf{S}$, connecting the states yz and zx . This results in splitting them into two spin doublets. The final outcome is that, in the absence of an applied magnetic field, the lowest free-ion level of Cu^{2+} is split into five Kramers doublets.

Finally, when a magnetic field is applied, each Kramers doublet is split,

and the last remaining degeneracy is removed. Any further effects lead to quantitative refinements without changing the qualitative picture.

The effects of the several terms in the Hamiltonian on the energy levels are summarized in Fig. 3.

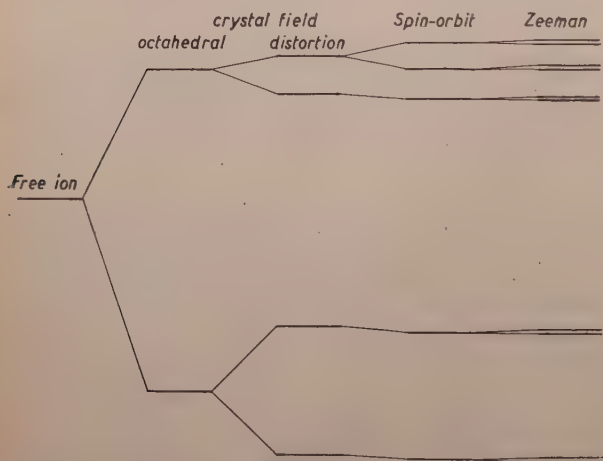


Fig. 3. — Removal of degeneracy in the 2D state of Cu^{2+} by the various perturbations.

7. — The magnetic moment.

Let us consider the spin-orbit interaction in more detail. As discussed above, this interaction is

$\lambda \mathbf{L} \cdot \mathbf{S}$, where λ is a negative constant. It does not change the position of the energy levels to first order, unless they are orbitally degenerate. (One can easily see this by observing that $\langle n | \mathbf{L} | n \rangle = 0$. As an example take

$$L_z = i \left(y \frac{\partial}{\partial z} - z \frac{\partial}{\partial y} \right).$$

L_z is thus a purely imaginary operator. The orbital wave functions can always be chosen to be real because the Hamiltonian (free ion) $+V$ of which they are eigenfunctions is a real operator in the wave function representation. Thus $\langle n|L_z|n\rangle$ is a purely imaginary number. Similar arguments can be made for the diagonal matrix elements of L_x and L_y . Thus, from a calculational standpoint, $\langle n|\lambda\mathbf{L}\cdot\mathbf{S}|n\rangle$ is purely imaginary. From a physical standpoint, however, since it represents a real observable, it must be real. It is therefore identically zero.)

Even though the energy is not changed in first order in orbitally non-degenerate states by the spin-orbit interaction, the wave-function is altered in this order. We concentrate our attention on the two (degenerate) lowest eigenstates corresponding to the energy E_0 and $s_z = \pm\frac{1}{2}$ (represented by the kets $|0, \frac{1}{2}\rangle$ and $|0, -\frac{1}{2}\rangle$). Under the influence of the spin-orbit perturbation, they become respectively:

$$(31) \quad |a\rangle = |0, \frac{1}{2}\rangle - \sum_n' \frac{|n\rangle \langle n|\lambda\mathbf{L}\cdot\mathbf{S}|0, \frac{1}{2}\rangle}{(E_n - E_0)} + O(\lambda^2),$$

and $|b\rangle =$ same as $|a\rangle$, but with $\frac{1}{2}$ replaced by $-\frac{1}{2}$.

The summation is over all energy levels n other than the ground state 0.

The correction term in the wave-function is of the order of $\lambda/(E_n - E_0)$ which is small, but not negligible. For the first transition group which we will be considering, λ ranges from 100 to 1000, while the energy differences are of the order of $10\,000\text{ cm}^{-1}$.

The next perturbation \mathcal{H}_1 , the interaction linear in the magnetic field

$$\beta\mathbf{H}\cdot(\mathbf{L} + 2\mathbf{S}),$$

completely removes the degeneracy. We have to find the correct linear combinations of $|a\rangle$ and $|b\rangle$ which are to be used as zero order wave functions to calculate the perturbation energy.

Assume first that \mathbf{H} is in the z direction, which is chosen to be the axis about which the ion possesses a tetragonal symmetry. It turns out that $|a\rangle$ and $|b\rangle$ are the correct eigenstates for this particular choice of \mathbf{H} , and so only the diagonal part of the Hamiltonian matrix is different from zero. We thus obtain the energy to first order by taking the diagonal matrix elements. Consider, for example, the expression

$$(32) \quad \langle a|\beta\mathbf{H}(\mathbf{L}_z + 2S_z)|a\rangle = \beta H \langle a|L_z|a\rangle + 2\beta H \langle a|S_z|a\rangle,$$

and calculate the right hand side term by term. The first term, written in more detail, is

$$(33) \quad \beta H \left[\langle 0, \frac{1}{2}|L_z|0, \frac{1}{2}\rangle - \sum_n' \left\{ \frac{\langle 0, \frac{1}{2}|L_z|n\rangle \langle n|\lambda\mathbf{L}\cdot\mathbf{S}|0, \frac{1}{2}\rangle}{(E_n - E_0)} + \text{c. c.} \right\} \right].$$

The first term on the right hand side vanishes by the arguments given above. This corresponds to the fact that, in the absence of spin-orbit coupling, the expectation value of the orbital magnetic moment is zero. This phenomenon is known as the *quenching* of the orbital moment.

In addition, we have

$$L_z|0\rangle = i\left(y\frac{\partial}{\partial x} - x\frac{\partial}{\partial y}\right)\frac{1}{2}\sqrt{15}(x^2 - y^2) = 2i\sqrt{15}xy = 2i|2\rangle,$$

so that only one term, corresponding to $n = 2$, enters in the summation in (33) and in its complex conjugate. (The states are numbered as on Fig. 3). We thus obtain

$$(34) \quad \langle 2|L_z|0\rangle = 2i.$$

We have further that

$$(35) \quad \langle 2|L_x|0\rangle = \langle 2|L_y|0\rangle = 0 \quad \text{and} \quad s_z|0, \tfrac{1}{2}\rangle = \tfrac{1}{2}|0, \tfrac{1}{2}\rangle$$

so that

$$(36) \quad \beta H \langle a|L_z|a\rangle = -\frac{4\lambda\beta H}{(E_2 - E_0)}.$$

Since λ is negative, this is positive.

Thus, by virtue of the spin-orbit interaction, the orbital part of the magnetic moment is no longer completely quenched, although there is no effect on the energy to first order.

The second term of eq. (32) gives an expression similar to eq. (33), but with L_z replaced by S_z . Since

$$\langle 0, \tfrac{1}{2}|S_z|n, \tfrac{1}{2}\rangle = \tfrac{1}{2}\delta_{n0},$$

and since the summation over n excludes the state $|0\rangle$, one obtains

$$(37) \quad 2\beta H \langle a|S_z|a\rangle = 2\beta H \langle 0, \tfrac{1}{2}|S_z|0, \tfrac{1}{2}\rangle = \beta H.$$

The energy shift ΔE_a is therefore

$$(38) \quad \Delta E_a = \beta H \left(1 - \frac{4\lambda}{(E_2 - E_0)}\right).$$

In an analogous way, one obtains

$$(39) \quad \Delta E_b = -\beta H \left(1 - \frac{4\lambda}{(E_2 - E_0)}\right).$$

The energy split will be written $g_{\parallel}\beta H$. We thus have

$$g_{\parallel} = 2 \left(1 - \frac{4\lambda}{(E_2 - E_0)} \right).$$

The quantity g_{\parallel} is the spectroscopic splitting factor, or g -value. The experimental value for a typical Cu^{2+} compound is $g_{\parallel} = 2.4$.

When the field is perpendicular to the axis of tetragonal symmetry, say along the x -axis, the energy perturbations are the eigenvalues of the matrix

$$\begin{pmatrix} \langle a | \beta H \cdot (L_x + 2S_x) | a \rangle & \langle a | \beta H \cdot (L_x + 2S_x) | b \rangle \\ \langle b | \beta H \cdot (L_x + 2S_x) | a \rangle & \langle b | \beta H \cdot (L_x + 2S_x) | b \rangle \end{pmatrix}.$$

This time the diagonal matrix elements are zero, as one can see by the following argument. A rotation of π about the z -axis will leave the orbital wave-functions unchanged, and will cause a factor $\pm i$ to appear in front of the spin wave-functions, according as to whether we are dealing with $|a\rangle$ or $|b\rangle$. From a calculational point of view the matrix elements will therefore remain unchanged (since $-i \cdot i = 1$). From a physical point of view, however, it should change sign. Therefore it must vanish. $\#$

We next compute the off-diagonal elements. We have

$$(42) \quad \langle a | L_x | b \rangle = - \left\{ \sum_n' \frac{\langle 0, \frac{1}{2} | L_x | n \rangle \langle n | \lambda \mathbf{L} \cdot \mathbf{S} | 0, -\frac{1}{2} \rangle}{(E_n - E_0)} + \text{c. c.} \right\},$$

since $\langle 0, \frac{1}{2} | L_x | 0, -\frac{1}{2} \rangle = 0$.

One can easily show that

$$(43) \quad L_x | 0 \rangle = -i | 3 \rangle, \quad \text{and so} \quad \langle a | L_x | b \rangle = - \frac{\lambda}{(E_3 - E_0)}.$$

Further $\langle a | S_x | b \rangle = \frac{1}{2}$. Since the other matrix element $\langle b | \beta H (L_x + 2S_x) | a \rangle$ must be equal to the real quantity $\langle a | \beta H (L_x + 2S_x) | b \rangle$, expression (41) becomes

$$(44) \quad \begin{pmatrix} 0 & \beta H \left(1 - \frac{\lambda}{(E_3 - E_0)} \right) \\ \beta H \left(1 - \frac{\lambda}{(E_3 - E_0)} \right) & 0 \end{pmatrix}.$$

The eigenvalues of the matrix (44) are

$$(45) \quad \pm \beta H \left(1 - \frac{\lambda}{(E_3 - E_0)} \right).$$

The energy separation corresponds to a g -value

$$(46) \quad g_{\perp} = 2 \left(1 - \frac{\lambda}{(E_3 - E_0)} \right).$$

As a numerical example, for a typical Cu^{2+} compound, $g_{\perp} = 2.08$.

For a field in the y -direction one obtains instead the matrix

$$(47) \quad \begin{pmatrix} 0 & -i\beta H \left(1 - \frac{\lambda}{(E_4 - E_0)} \right) \\ i\beta H \left(1 - \frac{\lambda}{(E_1 - E_0)} \right) & 0 \end{pmatrix},$$

which has the same eigenvalues as the matrix (44), since $E_4 = E_3$. Usually there is not full tetragonal symmetry and g is not quite the same in the x and y directions.

The above considerations illustrate how the anisotropy of the crystal gives rise to an anisotropy in the magnetic behaviour.

If we have a field in an arbitrary direction, in order to find the energy, we have to diagonalize the matrix

$$(48) \quad \begin{pmatrix} \langle a | \beta \mathbf{H} \cdot (\mathbf{L} + 2\mathbf{S}) | a \rangle & \langle a | \beta \mathbf{H} \cdot (\mathbf{L} + 2\mathbf{S}) | b \rangle \\ \langle b | \beta \mathbf{H} \cdot (\mathbf{L} + 2\mathbf{S}) | a \rangle & \langle b | \beta \mathbf{H} \cdot (\mathbf{L} + 2\mathbf{S}) | b \rangle \end{pmatrix}.$$

Because of the linearity of the matrix in the components of \mathbf{H} , we can just add the results obtained above, and express (48) in the form

$$(49) \quad \begin{pmatrix} g_{\parallel} H_z & g_{\perp} (H_x - iH_y) \\ g_{\perp} (H_x + iH_y) & -g_{\parallel} H_z \end{pmatrix}.$$

We now introduce a fictitious spin S' , whose components are

$$(50) \quad S'_x = \frac{1}{2} \begin{pmatrix} 0 & 1 \\ 1 & 0 \end{pmatrix}, \quad S'_y = \frac{1}{2} \begin{pmatrix} 0 & -i \\ i & 0 \end{pmatrix}, \quad S'_z = \frac{1}{2} \begin{pmatrix} 1 & 0 \\ 0 & -1 \end{pmatrix};$$

and the concept of the spin Hamiltonian

$$(51) \quad \mathcal{H} = \beta \{ g_{\parallel} H_z S'_z + g_{\perp} (H_x S'_x + H_y S'_y) \}.$$

The problem of the energy perturbation in a magnetic field in an arbitrary direction reduces to the one of finding the eigenvalues of the spin Hamil-

tonian (51). If the magnetic field makes an angle, say, θ with the z direction, the eigenvalues of \mathcal{H} are

$$(52) \quad \pm \frac{1}{2} \beta H [g_{\parallel}^2 \cos^2 \theta + g_{\perp}^2 \sin^2 \theta]^{\frac{1}{2}}, \quad \text{so that} \quad g_{\theta} = [g_{\parallel}^2 \cos^2 \theta + g_{\perp}^2 \sin^2 \theta]^{\frac{1}{2}}.$$

8. - Connection with paramagnetic resonance.

The results we have just obtained are of immediate applicability to paramagnetic resonance. This phenomenon arises when a paramagnetic substance in a magnetic field is subjected to a radiofrequency field (in general in the microwave frequency range). When the quantum $h\nu$ of the microwave frequency is equal to the energy separation $g\beta H$, resonant absorption of radiation takes place. This may be regarded as due to the transitions induced between the Zeeman levels by the oscillating magnetic field. There will be a net absorption of radiation, since in thermal equilibrium there is an excess of ions in the lower energy level, so that more transitions take place from lower to upper levels than conversely.

The transition probability, and therefore the absorption, is proportional to the square of the matrix element of the perturbing Hamiltonian. This in turn is proportional to the square of the matrix element of μ_{\perp} , and to the square of the oscillating magnetic field. If, for example, the steady magnetic field is in the z -direction, and the oscillating field is perpendicular to this, then resonant absorption takes place when $h\nu = g_{\parallel} \beta H$, and its strength is proportional to g_{\perp}^2 .

In normal practice ν is kept fixed and H is varied. Resonance takes place when $H = h\nu/g_{\parallel}\beta$.

It will be seen that if g_{\perp} is small or zero, resonance absorption will be weak.

Since the absorption depends on the difference of the populations of the lower and upper levels, which are in the ratio $\exp[g_{\parallel}\beta H/kT] = 1 + g_{\parallel}\beta H/kT$, it will be seen that the factor $g_{\parallel}\beta H/kT$ also enters into the absorption intensity.

9. - The spin Hamiltonian.

The calculations we have done so far show that the leading contribution to the magnetic moment arises from the spin magnetic moment only. For this reason the magnetic properties of the iron-group of elements are often said to approximate to «spin-only» behaviour.

We have then calculated, to the first order in both λ and H , the next term, which gives the contribution of orbital magnetic moment linked to the spin

by means of the spin-orbit interaction. This term is essentially of second order in the perturbing Hamiltonian, but is only one of such terms.

One can easily do the full second order calculation, i.e. calculate the terms of order λ^2 and H^2 , as well as λH . The result can be written in the form of a *spin Hamiltonian*, applicable for any value of S (not merely $S=\frac{1}{2}$, such as in the case of Cu^{2+}) and is easily shown to be

$$(53) \quad \mathcal{H} = E_0 + 2\beta(\delta_{ij} - \lambda A_{ij})S_i H_j - \lambda^2 A_{ij} S_i S_j - \\ - \beta^2 A_{ij} H_i H_j + \frac{e^2}{8mc^2} [H^2 \sum \langle r^2 \rangle - H_i H_j \sum \langle r_i r_j \rangle].$$

The tensor A_{ij} is real, symmetric and positive definite. It is defined by

$$(54) \quad A_{ij} = \sum_n' \frac{\langle 0 | L_i | n \rangle \langle n | L_j | 0 \rangle}{(E_n - E_0)}.$$

Our calculations for Cu^{2+} gave

$$A_{xx} = A_{yy} = \frac{1}{(E_3 - E_0)}, \quad A_{zz} = \frac{4}{(E_2 - E_0)},$$

and all other components zero.

S is the fictitious spin introduced before (the previous notation was S'). The fourth term in (53) is the field-induced paramagnetic term, and the fifth is the diamagnetic term, which includes the diamagnetism of the core as well as that of the outer shell electrons.

The magnetic moment is

$$(55) \quad \mu_i = -\frac{\partial \mathcal{H}}{\partial H_i} = 2\beta(S_i - \lambda A_{ij} S_j) + 2\beta^2 A_{ij} H_j + \\ + (\text{diamagnetic induced moment}).$$

The first term on the right in (55) is the permanent moment, which is present even in zero field. The second term is the induced paramagnetic moment. The term $-2\beta\lambda A_{ij} S_j$ in the permanent moment is the spin-linked orbital moment.

The induced paramagnetic moment is in most paramagnetics larger than the diamagnetic moment, so that we usually have a positive constant as a correction to the Curie law.

In zero external field the magnetic moment reduces to the permanent moment

$$(56) \quad \mu_i = \beta g_{ij} S_j,$$

where

$$(57) \quad g_{ij} = 2(\delta_{ij} - \gamma A_{ij}),$$

is the g -tensor.

If we choose our co-ordinate axes to be the principal axes of the tensor A_{ij} , then g_{ij} will have the principal values g_{xx} , g_{yy} , g_{zz} ; while g_{xy} , etc., are zero.

If the $3d$ -shell is less than half-filled, then the principal g -values are less than 2, since λ is then positive. If it is more than half-filled, λ is negative, and the g -values are greater than 2.

We have not yet mentioned the third term in (53),

$$(58) \quad -\lambda^2 A_{ij} S_i S_j.$$

This term is responsible for splitting the spin multiplet even in the absence of an external field. For if $H=0$, the Hamiltonian reduces to

$$(59) \quad E_0 - \lambda^2 A_{ij} S_i S_j.$$

To study the effect of this without unnecessary complications, let us assume that the ion is in surroundings possessing an axis of symmetry (which may be a three-fold, four-fold or six-fold axis in practical cases). Then we can write $A_{zz} = A_{\parallel}$; $A_{xx} = A_{yy} = A_{\perp}$; and the other tensor components vanish. By using the identity

$$(60) \quad S_x^2 + S_y^2 = S(S+1) - S_z^2,$$

$-\lambda^2 A_{ij} S_i S_j$ simplifies to

$$(61) \quad \lambda^2 (A_{\perp} - A_{\parallel}) S_x^2 - S(S+1) \lambda^2 A_{\perp},$$

which it is usual to write as

$$(62) \quad -\frac{1}{3} S(S+1) \lambda^2 (A_{\parallel} + 2A_{\perp}) + D(S_z^2 - \frac{1}{3} S(S+1)),$$

where

$$(63) \quad D = \lambda^2 (A_{\perp} - A_{\parallel}).$$

The first term in (62) represents a constant shift down of all the levels of the lowest spin-multiplet, while the second corresponds to a splitting of these levels. Since S_z has eigenvalues m_s , with $m_s = S, S-1, \dots, -S$, the eigenvalues of (62) are $Dm_s^2 + \text{const.}$

When we discussed the example of Cu^{2+} , we did not encounter this splitting. This is because when the spin is $\frac{1}{2}$, $m_s = \pm \frac{1}{2}$ and Dm_s^2 is the same for both components. A zero-field splitting occurs only if $S \geq 1$.

A contribution to the Hamiltonian having the same dependence on S_z^2 can arise also from the spin-spin interaction between the electrons, because the spatial arrangement of the electron distribution is anisotropic, so that the magnetic interaction energy between their spin moments depends on the orientation of the resultant spin. In such cases the contribution is incorporated into the coefficient D of the spin-Hamiltonian. Higher approximations will add refinements to the spin-Hamiltonian, but they will be smaller than those already discussed, and will add nothing qualitatively new.

To discuss the effect of splitting on the paramagnetic resonance spectrum we can drop the spin-independent terms from the spin-Hamiltonian, since they shift all levels equally, and so do not enter into the energy differences. We then have

$$(64) \quad \mathcal{H}' = DS_z^2 + g_{\parallel}\beta H_z S_z + g_{\perp}\beta(H_x S_x + H_y S_y).$$

This is the usual, though somewhat incomplete, form of \mathcal{H} used in simple calculations.

If \mathbf{H} is parallel to the axis (z -axis) then the eigenvalues are easily found. For then \mathcal{H} is a function of S_z , and the eigenvalues are

$$(65) \quad E = Dm_s^2 + g_{\parallel}\beta H m_s.$$

Since the selection rules for magnetic resonance are

$$\Delta m_s = \pm 1,$$

we can consider the transitions as going between $m_s = n - \frac{1}{2}$ and $m_s = n + \frac{1}{2}$, when n ranges by integral steps from $S - \frac{1}{2}$ to $-(S - \frac{1}{2})$. So

$$(66) \quad \Delta E = g_{\parallel}\beta H + 2nD.$$

In a resonance experiment, one usually keeps the frequency ν fixed, and varies the magnetic field. The resonance condition $E = h\nu$ thus reduces to

$$(67) \quad H_{\text{res}} = \frac{h\nu}{g_{\parallel}\beta} - n \frac{2D}{g_{\parallel}\beta}.$$

One will therefore observe $2S$ equally spaced lines, whose spacing is

$$(68) \quad \Delta H = \frac{2|D|}{g_{\parallel}\beta}.$$

As already mentioned, the intensity of the resonant absorption is proportional to the square of the matrix element of the perpendicular magnetic

moment. In this simple case this can be shown to be proportional to $(S + \frac{1}{2})^2 - n^2$. This is an important diagnostic in the interpretation of a paramagnetic resonance spectrum, and serves to distinguish the effect of a spin-multiplicity ($2S$ lines) from a nuclear hyperfine structure ($2I+1$ lines), as in the latter case the intensities are all equal.

A typical, though somewhat idealized, example of how this appears is shown in Fig. 4, which corresponds to paramagnetic absorption from Cr^{3+} ($S = \frac{3}{2}$). In this case the intensities are in the ratio 3:4:3.



Fig. 4. — Typical paramagnetic resonance spectrum for $S = \frac{3}{2}$.

10. — Survey of ions of the 3-rd group.

So far we have selected a few simple salient points for detailed discussion. We shall now present a very brief (and incomplete) survey of the situations encountered in the ions of the first transition group. We have already seen (Table I) that the orbital angular momentum L of the free ions can be either 2, 3 or 0. In spectroscopic jargon, the free ions are in either D , F or S states. It will be convenient to treat these three types separately, subdividing into further classifications as we proceed.

11. — D state ions.

In $3d^4$ (Cr^{2+} , Mn^{3+}) and $3d^9$ (Cu^{2+}) the electron charge distribution is similar. The four electrons in $3d^4$ have parallel spins. In $3d^9$ the additional five electrons have their spins parallel to each other and antiparallel to the first four; the charge distribution of five d -electrons all with parallel spins is spherically symmetrical (see S -state ions later) and contribute zero orbital angular momentum. The charge distributions in corresponding orbital sub-states of $3d^4$ and $3d^9$ are therefore the same, and these ions split in the same way in the crystal field.

In the dominant octahedral field the five-fold orbital degeneracy is split into 2+3, as shown on Fig. 5a. Their energy difference is about 10^4 cm^{-1} .

In the ions $3d^1$ (Ti^{3+}) and $3d^6$ (Fe^{2+} , Co^{3+}) the charge distributions are similar to one another, and complementary to $3d^4$, $3d^9$ just discussed. The latter pair can be regarded as one hole in the spherically symmetrical distributions $3d^5$ and $3d^{10}$, while the former pair are to be looked on as one electron added to $3d^0$, $3d^5$. They thus behave alike, but with opposite signs of the charge, since a hole acts like an electron with a positive charge. In the crystal

field the energy levels are therefore inverted, the orbital triplet d_e being lower (Fig. 5b).

In $3d^4$ therefore the behaviour is similar to that discussed for Cu^{3+} , with the modification that $S = 2$ instead of $\frac{1}{2}$, so that there is a zero-field splitting as given by equation (59), and that λ is positive and a good deal smaller in absolute magnitude than for Cu^{2+} (Cr^{2+} : $\lambda = 57$; Cu^{2+} , $\lambda = -828 \text{ cm}^{-1}$).

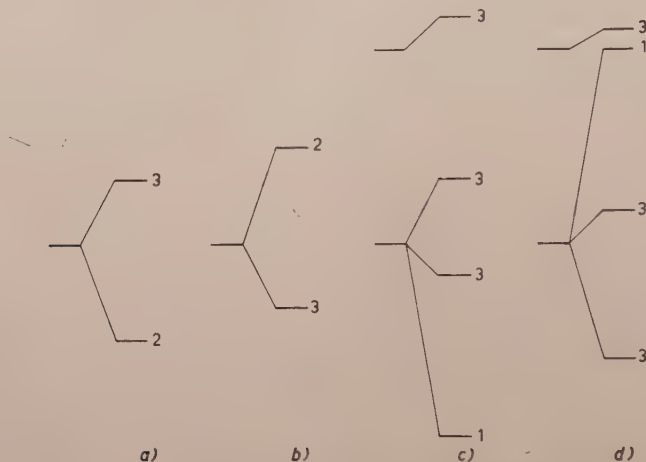


Fig. 5. — Splitting by an octahedral field (a) $3d^4$ and $3d^9$, (b) $3d^1$ and $3d^8$, (c) $3d^3$ and $3d^6$, (d) $3d^2$ and $3d^7$.

In $3d^1$ and $3d^6$, on the other hand, the orbital triplet is lowest. This is further split by distortions from the octahedral symmetry, but these energy separations are much smaller ($\sim 10^3 \text{ cm}^{-1}$). While in $3d^4$ and $3d^9$ the orbital angular momentum is almost totally quenched (λA_{ij} small), in these ions it is largely unquenched. This is so because there are non-zero matrix elements of L coupling the different components of the orbital triplet, and so λA_{ij} is appreciable, because of the small energy denominators. This results in a good deal of variation from salt to salt, both as regards g -values, and, in $3d^6$, as regards zero-field splittings. When the crystal field splitting of the lowest triplet, due to deviations from the regular octahedral shape, are comparable with λ , as happens here, the approximations leading to (53) become poor, and it is better to use other methods to calculate the energy levels.

12. — F -state ions.

In a field of octahedral symmetry, the seven-fold orbital degeneracy of an F -state splits into $1+3+3$. How this comes about can readily be seen by considering the solid harmonics (of order 3) which describe the angular

dependence of an electron in an f -state. Since F -state wave-functions, of any system, transform in the same way under rotations, we can classify their behaviour under the elementary rotations which transform the octahedron into itself. The solid harmonics of order 3 (corresponding to $l = 3$ for an f -electron) can be written

$$(69) \quad \begin{cases} (A_2) & xyz; \\ (T_2) & x(y^2 - z^2), y(z^2 - x^2), z(x^2 - y^2); \\ (T_1) & x(2x^2 - 3y^2 - 3z^2), y(2y^2 - 3z^2 - 3x^2), z(2z^2 - 3x^2 - 3y^2). \end{cases}$$

As written here, they are mutually orthogonal, but not normalized (the normalizing factors are respectively $\sqrt{105}$, $\frac{1}{2}\sqrt{105}$, $\frac{1}{2}\sqrt{7}$ for the three groups). They fall naturally into three groups, which have been labelled A_2 , T_2 and T_1 above, in keeping with the notation introduced by MULLIKEN for the representations of the octahedral group. (In this notation, d_x and d_y , introduced previously, correspond to T_2 and E).

In $3d^3$ (V^{2+} , Cr^{3+}) and $3d^8$ (Ni^{2+}) the orbital singlet A_2 is the lowest level (Fig. 5c). The T_2 states are about 10^4 cm^{-1} higher, and the T_1 states that much again. The situation is a little more complex than this, however, for the free ions of this type have a P -state of the same spin (spectroscopic multiplicity) about $1.5 \cdot 10^4 \text{ cm}^{-1}$ above the F -state, and this perturbs the T_1 -state. This also is shown on Fig. 5c. The lowest level is thus a simple spin multiplet (quartet, $S = \frac{3}{2}$ for $3d^3$; triplet, $S = 1$, for $3d^8$).

The g -value is, using (57) and (53),

$$(70) \quad g = 2 - \frac{8\lambda}{E(T_2) - E(A_2)}.$$

If the octahedron is distorted, T_2 and T_1 are split, and g becomes different in different directions, since $E(T_2)$ must now be taken to refer to the appropriate component of the triplet T_2 . But since this is a small correction to a small term, g is in fact very nearly isotropic for these ions,

If the distortion has an axis of symmetry, T_2 splits into $1+2$; denoting their energies by Δ and Δ' respectively, measured from A_2 as energy zero, (53) shows that

$$(71) \quad A_{\parallel} = \frac{4}{\Delta}, \quad A_{\perp} = \frac{4}{\Delta'},$$

from which, by (63)

$$(72) \quad D = \frac{4\lambda^2(\Delta - \Delta')}{\Delta\Delta'}.$$

Taking, as an order of magnitude, $\lambda = 100 \text{ cm}^{-1}$, $\Delta \approx \Delta' = 10^4 \text{ cm}^{-1}$, $\Delta' - \Delta = 200 \text{ cm}^{-1}$, for Cr^{3+} , one finds $g = 1.92$, $D = -0.08 \text{ cm}^{-1}$. With $\lambda = -300 \text{ cm}^{-1}$ for Ni^{2+} , and the same values of Δ and Δ' , one finds $g = 2.24$, $D = -0.7 \text{ cm}^{-1}$. Typical experimental values are $g = 1.976$, $D = -0.07 \text{ cm}^{-1}$ for Cr^{3+} , and $g = 2.25$, $D = -2 \text{ cm}^{-1}$ for Ni^{2+} . The sign of D depends on the sign of the splitting of the orbital triplet T_2 , and may be different in different compounds, depending on the detailed crystalline symmetry.

It should be remarked that this discussion of D is incomplete. Not only has it ignored the contribution of spin-spin interaction (which is actually very small in these two types of ion), but it has ignored the matrix elements of spin-orbit interaction coupling the ground state with states of different S . In $3d^3$ there are 2D and 2G states, and in $3d^8$, 1D and 1G states, which should be considered in the perturbation calculation. Their contributions do not alter the order of magnitude of the effect, however.

In $3d^2$, (V^{3+}) and $3d^8$ (Co^{2+}) the splitting of the F -state is inverted (Fig. 5d), and the T_1 triplet is the lowest. Although this is further split by the distortion from octahedral symmetry, it means that the orbital moment is far from being totally quenched, and quite large g -values can result. The levels group themselves in a rather complicated fashion, and there is considerable variation from one compound to another. This is particularly marked in cobaltous compounds, whose molar susceptibilities vary within quite wide limits. In Co^{2+} , $S = \frac{3}{2}$, the T_1 orbital triplet, together with the four-fold spin multiplicity, gives rise to 6 Kramers doublets, which lie within 2000 cm^{-1} of one another, several of which are populated at room temperature. In V^{3+} the multiplicity is $3 \cdot 3 = 9$. In vanadic alum the lowest level is single, and there is a doublet 5 cm^{-1} higher, the other six levels being considerably higher.

In paramagnetic resonance experiments with Co^{2+} one has to work at such low temperatures that only the lowest Kramers doublet is populated, and it is convenient to treat this as a system with fictitious spin $S' = \frac{1}{2}$. The g -values then refer to the splitting of this doublet in an external field. Typical values are $g_{\parallel} = 6$, $g_{\perp} = 3$, but there are great variations.

13. - S -state ions.

These are the ions with a half-filled d -shell, $3d^5$, exemplified by Mn^{2+} and Fe^{3+} . In the lowest state $L = 0$ and all five spins are parallel, giving a resultant $S = \frac{5}{2}$. There is no orbital moment associated with this state, and the magnetism arises only from the spin. Since $L = 0$, spin-orbit interaction can have no first order effect.

The charge distribution is spherically symmetrical and in first order the crystal field has no splitting effect on the six-fold spin degeneracy. In crystals

the spin multiplet in fact is always split by a small amount. It is found experimentally that (where an axis of symmetry exists) the spin Hamiltonian can be written

$$(73) \quad \mathcal{H} = \frac{a}{b} \left(S_x^4 + S_y^4 + S_z^4 - \frac{707}{16} \right) + D \left(S_z^2 - \frac{35}{12} \right).$$

In order to account for this splitting one has to calculate to higher orders of perturbation theory than is necessary for the other ions, since the mechanisms we have so far discussed fail to produce any splitting. The first term in (73) has been explained by VAN VLECK and PENNEY as the result of a fifth order perturbation calculation, involving the octahedral field, G , to first order and the spin-orbit interaction, ζ , to fourth order. As regards order of magnitude

$$(74) \quad a \approx \frac{G\zeta^4}{(\Delta E)^4},$$

where ΔE is the energy difference between the 6S and higher terms of the free ion (such as 4P). Taking $G = 10^4 \text{ cm}^{-1}$, $\zeta = 300 \text{ cm}^{-1}$, $\Delta E = 2.5 \cdot 10^4 \text{ cm}^{-1}$ this gives $a \approx 10^{-4} \text{ cm}^{-1}$. It is found to be 10 times larger for Fe^{3+} than for Mn^{2+} . This is understandable, since $\zeta/\Delta E$, which enters as the fourth power, is larger; and since G is larger for a trivalent than for a divalent ion.

The DS_z^2 term, which has the lower symmetry of the distortion from regular octahedral shape, arises from the axial crystalline field. Two mechanisms appear to operate. One (proposed by JUDD and by STEVENS) involves spin-orbit interaction to second order, the octahedral field to first order, and the axial field to first order. This gives a contribution

$$(75a) \quad D \approx \frac{G\zeta^2\Delta}{(\Delta E)^3},$$

where Δ is the axial splitting of a single d -electron. The other mechanism (proposed by ABRAGAM and PRYCE) arises from the small distortion from spherical shape of the charge distribution — the magnetic spin-spin interaction between the electrons then depends on the orientation of S relative to the axis of distortion. Formally, one can describe this by saying that the axial field mixes in some $3d^4 4s$ configuration to the $3d^5$ configuration, thereby giving the spin-density a somewhat ellipsoidal form. The order of magnitude expected is

$$(75b) \quad D \approx \frac{\beta^2 \langle r^{-3} \rangle \Delta}{\Delta E'},$$

where $\Delta E'$ is the energy difference between $3d^4 4s {}^6D$ and $3d^5 {}^6S$, and Δ has

roughly the same magnitude as in (75a) (strictly it is the matrix element $\langle 3d|V|4s \rangle$ while in the other calculation it is $\langle 3d|V|3d \rangle$, but the orders of magnitude are comparable).

Putting $A = 10^3 \text{ cm}^{-1}$, $\Delta E \approx \Delta E' \approx 2.5 \cdot 10^4 \text{ cm}^{-1}$, $\langle r^{-3} \rangle \approx 5$ atomic units, both contributions come to rather less than 10^{-1} cm^{-1} , and of opposite sign. Comparing with the experimental values, it appears that the contribution from (75a) outweighs by a factor 2 that from (75b). Typical experimental values for $|D|$ in Mn^{2+} are 0.03 cm^{-1} . Depending on the nature of the distortion, both signs of D are observed. On the other hand a has a value round 10^{-3} cm^{-1} for all hydrated Mn^{2+} compounds. While for Mn^{2+} the D term in (74) dominates, in Fe^{3+} both are of equal importance.

14. - Susceptibility.

We have seen that the crystalline field affects the energy levels of an ion, in the absence of any other perturbation, in a way which can be broadly described as follows. If the ion has an even number of electrons, the resulting levels will be either all single, which in general will happen in the case of low-symmetry crystals; or, if the crystal is endowed with a high degree of symmetry, there will be usually one singlet and a number of doublets. If the ion has an odd number of electrons, the crystalline field will lead to a number of Kramers doublets.

In considering how the susceptibility looks under these conditions, let us assume that we are dealing with a magnetically dilute crystal. Under an external magnetic field a single level ε_n without an intrinsic magnetic moment will become polarized. The polarizability α_n of the n -th level will in general be a tensor. But with a reasonable degree of symmetry, along the interesting directions the moment is in the same direction as the field, and the polarizability is then a number. The contribution to the gross molar susceptibility is then

$$(76) \quad N\alpha_n \exp[-\varepsilon_n/kT]/Z,$$

with

$$(77) \quad Z = \sum \exp[-\varepsilon_n/kT],$$

($\exp[-\varepsilon_n/kT]/Z$ being the population of the n -th level in the Boltzmann distribution, and N the number of atoms in a mole.

We will not need to consider those levels which are very little populated; for our purposes any level higher than $8kT$ (at room temperature, $\approx 1500 \text{ cm}^{-1}$) can be ignored.

Let us now consider a doublet, whose components split in a magnetic field,

according to equal and opposite magnetic moments. Since the population in the two levels follows a Boltzmann distribution, we have a Brillouin-type susceptibility, following Curie's law. The contribution of the n -th double level to the total susceptibility is then

$$(78) \quad 2N \left(\frac{\mu_n^2}{kT} + \alpha_n \right) / Z,$$

where μ_n is the magnetic moment of the level.

If the levels group together within an energy range small compared with kT , as frequently happens, the calculation can be simplified. On the other hand there are crystals, such as those of Co salts, where one has a number of different levels in the range from 0 to 2000 cm^{-1} , and where computations have to be carried out in detail; the predicted curves of χ against temperature are then complicated, as experiments also show.

It is not at once clear from our formulae whether, when the inter-level spacing is very small compared with kT , the result is the same as the one we derived on the basis of the Brillouin theory. Here we have a part following Curie's law, and a part independent of temperature; when the levels are close together the polarizabilities α_n may become very large. However, we will see that since some of them are positive, some negative, compensation occurs such that the constant part disappears, leaving mainly only the $1/T$ term (when we expand the exponential).

Let us consider the situation in detail. The moment in a doublet whose states are $|n_a\rangle$ and $|n_b\rangle$ is (c.f. (55))

$$(79) \quad \pm \mu_n = \beta \left\langle \begin{matrix} n_a \\ n_b \end{matrix} \middle| L_z + 2S_z \right| \begin{matrix} n_a \\ n_b \end{matrix} \right\rangle,$$

while the polarizability is given by

$$(80) \quad \alpha_n = 2\beta^2 \sum_m \frac{|\langle n | L_z + 2S_z | m \rangle|^2}{E_m - E_n},$$

(plus a negative diamagnetic term for the ionic core, which is usually small).

In (80) it is often useful to separate the sum into two parts: (i) the « low frequency » terms which come from the lowest group of levels, the occupied levels; and (ii) the « high frequency » terms, corresponding to the higher unoccupied, levels.

When two levels are close together $\epsilon_m - \epsilon_n$ becomes very small and α_n gets large; the lower level has a large positive polarizability, the upper one a large negative one. We first consider the « low frequency » terms, corresponding

to those levels which are effectively populated. We can replace $\exp[\varepsilon_n/kT]$ by $(1 - \varepsilon_n/kT)$, assuming that the spread of these levels is small compared with kT . Their contribution to the susceptibility is then

$$(81) \quad \frac{N}{Z} \sum_{n(lf)} \left(\frac{\mu_n^2}{kT} + 2\beta^2 \sum'_m \frac{|\langle m | L_z + 2S_z | n \rangle|^2}{(\varepsilon_m - \varepsilon_n)} \right) \left(1 - \frac{\varepsilon_n}{kT} \right),$$

\sum implying summation over the lowest levels only, each level of a doublet being counted now in contrast to (78)), and \sum' implies $m \neq n$. Now

$$\sum_{n(lf)} \sum'_m \frac{|\langle m | \dots | n \rangle|^2}{(\varepsilon_m - \varepsilon_n)} = 0.$$

since the expression to be summed over is antisymmetric in m and n . For the same reason one obtains

$$\sum_{n(lf)} \sum'_m \frac{|\langle m | \dots | n \rangle|^2 \varepsilon_n}{(\varepsilon_m - \varepsilon_n)} = - \sum_{n(lf)} \sum'_m |\langle m | \dots | n \rangle|^2.$$

If now we insert in (81) the definition of μ_n , (79), and neglect ε_n/kT in comparison with 1, we easily see that the net result is

$$(82) \quad \chi = a + \frac{N\beta^2}{ZkT} \sum_{m(lf)} \sum_{n(lf)} |\langle m | L_z + 2S_z | n \rangle|^2.$$

the summation including $m = n$. Here the Z may be replaced by the number of low-lying states in the group ($2S+1$ for a spin-multiplet). The constant term arises from the high frequency terms, namely

$$(83) \quad a = \frac{2N\beta^3}{(2S+1)} \sum_{n(hf)} \sum_{m(hf)} \frac{|\langle m | L_z + 2S_z | n \rangle|^2}{(\varepsilon_m - \varepsilon_n)},$$

where $\exp[-\varepsilon_n/kT]$ for the occupied levels has been replaced by 1.

(82) is essentially the expression we have in the Brillouin theory. Thus the fact that different levels are split in zero field, and behave differently under an applied magnetic field, does not, in this approximation, change the results obtained by simply assuming complete degeneracy of the levels.

We can do better if the group of levels is described by a spin Hamiltonian. Assuming, for the sake of simplicity, the z -axis to be an axis of symmetry, and taking the magnetic field in this direction, the spin Hamiltonian reads

$$(84) \quad \mathcal{H} = g_{\parallel} \beta H S_{\parallel} + D [S^2 - \frac{1}{3} S(S+1)] - \frac{1}{2} \alpha_{\parallel} H^2.$$

Using the method of diagonal sums we now expand the partition function

$$Z = \sum \exp[-\varepsilon_n/kT]$$

in a power-series in $(kT)^{-1}$, which converges rapidly because only energies small compared with kT are involved. We really need the free energy

$$(85) \quad F = -NkT \ln Z,$$

whose first terms read

$$(86) \quad F = N \left\{ kT \ln (2S+1) + \bar{\varepsilon} - \frac{1}{2kT} \langle (\varepsilon - \bar{\varepsilon})^2 \rangle + \frac{1}{6k^2T^2} \langle (\varepsilon - \bar{\varepsilon})^3 \rangle - \dots \right\},$$

where the symbols $\bar{\varepsilon}$ and $\langle \dots \rangle$ both stand for averages over the $2S+1$ levels. The third and following terms give the deviations from Curie's law. If the magnetic field is in the z direction the result, evaluated from (84), comes to

$$(87) \quad F = N \left\{ kT \ln (2S+1) - \frac{1}{2} \alpha_{\parallel} H^2 - \frac{1}{2kT} \left[\frac{1}{3} S(S+1)(g_{\parallel} \beta H)^2 + p D^2 \right] + \right. \\ \left. + \frac{1}{2k^2T^2} [p D (g_{\parallel} \beta H)^2 + \text{term in } D^3] + \dots \right\},$$

where

$$(88) \quad p = \frac{1}{45} S(S+1)(2S-1)(2S+3).$$

The magnetic moment is

$$M = -(\partial F / \partial H)_T.$$

With another differentiation we get the magnetic susceptibility

$$\chi_{\parallel} = -(\partial^2 F / \partial H^2)_T,$$

whose first terms read

$$(89) \quad \chi_{\parallel} = N \left\{ \alpha_{\parallel} + \frac{S(S+1)}{3kT} g_{\parallel}^2 \beta^2 - \frac{pD}{k^2T^2} g_{\parallel}^2 \beta^2 + \dots \right\}.$$

For a magnetic field in any direction in the (xy) plane, perpendicular to the axis of symmetry, the result is, by similar arguments

$$(90) \quad \chi_{\perp} = N \left\{ \alpha_{\perp} + \frac{S(S+1)}{3kT} g_{\perp}^2 \beta^2 + \frac{pD}{2k^2T^2} g_{\perp}^2 \beta^2 + \dots \right\}.$$

In any other direction of the applied field, the magnetization would not necessarily be in the same direction as \mathbf{H} , but by resolving into components parallel and perpendicular to the axis, it is possible to use these results to obtain the resultant magnetization for any applied field \mathbf{H} .

In cases of lower symmetry we would have to work with a susceptibility tensor χ_{ij} , and

$$(91) \quad M_i = \chi_{ij} H_j.$$

One frequently performs experiments with powders. The experimental susceptibility is then the average

$$(92) \quad \chi = \frac{1}{3}(\chi_{\parallel} + 2\chi_{\perp}).$$

If there were no anisotropy in the g 's the correction terms in $(kT)^{-2}$ in χ_{\parallel} and χ_{\perp} (see (89) and (90)) would exactly cancel out, so that in this case in experiments on powders Curie's law should hold to a very high approximation.

We can represent the initial departure from Curie's law with a formula of the Curie-Weiss type

$$(93) \quad \chi = \frac{C}{(T - \Delta)} + a.$$

The constant Δ turns out to be, for a powder

$$(94) \quad \Delta = \frac{(2S - 1)(2S + 3)}{15} \frac{(g_{\perp}^2 - g_{\parallel}^2)}{(2g_{\perp}^2 + g_{\parallel}^2)} \frac{D}{k}.$$

As normally the g -factors are only slightly anisotropic, Δ is generally small; in other words the finite structure of the spin multiplet gives rise to rather small deviations from Curie's law unless we go down to fairly low temperatures. One finds that Curie's law holds surprisingly well down to temperatures much lower than could be expected on the ground of convergence of series, provided that one averages over all directions. If we are dealing with single crystals the individual susceptibilities may start deviating sooner. Recent measurements of JACKSON in Bristol on $\text{FeSiF}_6 \cdot 6(\text{H}_2\text{O})$ at helium and hydrogen temperatures, where only one spin multiplet with $S = 2$ is populated, and the energy levels lie at about 0° , 25° , and 100° , give a plot of the susceptibility against temperatures as in Fig. 6. At 3°K χ_{\parallel} is smaller than χ_{\perp} by a factor 10^{-3} , yet Curie's law holds for the powder down to about 10°K .

It is unrealistic completely to neglect the interactions among the ions. Let us consider first the effect of the exchange energy, which is of the form

$$(95) \quad -JS_1 \cdot S_2,$$

where S_1 and S_2 are the spins in the spin Hamiltonians for two ions. The deviation in Curie's law caused by (95) can again be computed by the method of diagonal sums, and, when expressed by means of a Curie-Weiss temperature (c.f. (93)), it turns out to yield

$$(96) \quad \Delta = \frac{S(S+1)zJ}{3k},$$

where z is the co-ordination number. In a typical hydrated nickel salt, where $S = 1$, $J \approx 1 \text{ cm}^{-1}$ and $z \approx 6$, $\Delta \approx 6^\circ$, which is not completely negligible. This is very rough, because in a paramagnetic salt, generally speaking, each ion has several types of neighbours, so that we have several different J -values.

The other important interaction is the dipole-dipole interaction. If the symmetry of the crystal reasonably approaches cubic symmetry the contribution to Δ of this interaction turns out to be very small. In an order-of-magnitude calculation one would expect Δ to be

$$\Delta = \frac{\xi\beta^2}{kR^3},$$

where R is the distance of the nearest ions from a given one and ξ is a numerical factor which ordinarily is not greater than $1/10$ and is a measure of the inequality of distances between nearest neighbours.

In comparing these theoretical conclusions with the experiments, one must be careful, because the g -values are really temperature dependent. The deviation of the g -factors from the spin-only value due to the spin-orbit interaction contains in the denominator the splitting of the levels caused by the crystalline field. As a consequence of thermal expansion the ionic distances change, hence the crystalline field splittings and the g -factors change.

One must also always remember that there is a temperature-independent term in χ (e.g. in $\text{CuSO}_4 \cdot 5\text{H}_2\text{O}$ it amounts to 4% of χ at 300°K).

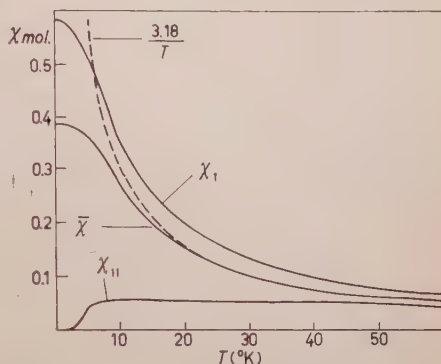


Fig. 6. — Molar susceptibility of $\text{FeSiF}_6 \cdot 6\text{H}_2\text{O}$; preliminary results from L. C. JACKSON (unpublished).

15. — Ions of the rare earths.

We shall now discuss very briefly the situation in the $4f$ series of elements, the rare earths. They differ in several interesting ways from the $3d$ elements, and indeed from any other transition groups. Their unique feature is the

extremely sheltered position of the $4f$ electrons inside the ion. The $4f$ -wave-function is very compact, so that the second and higher harmonics in the crystalline fields arising from the neighbouring molecules give rise to a very small splitting of the degeneracy, 10^2 cm^{-1} , contrasted with 10^4 cm^{-1} in $3d$. (These splittings are proportional to $\langle r^2 \rangle / R^2$, $\langle r^4 \rangle / R^4$, $\langle r^6 \rangle / R^6$ for the harmonics of order 2, 4, 6 which enter, where R is the nearest-neighbour distance, r the $4f$ -radius). The spin-orbit interaction, on the other hand, is some ten times bigger in the rare earths than in the $3d$ ions. Thus the term \mathcal{H}_3 in equation (26) is more important than \mathcal{H}_2 . In dealing with the magnetic properties of the rare earths, then, one treats the crystalline potential \mathcal{H}_2 as a perturbation on the full free-ion Hamiltonian $\mathcal{H}_1 + \mathcal{H}_3$. Since J is a constant of the motion for the free ion, it is a good quantum number to start from in the perturbation calculation.

The crystal field splittings are smaller than kT at room temperature, so that the susceptibility approximates well to that of a free ion at these temperatures. Deviations set in at lower temperatures, however. The paramagnetic resonance behaviour, which has to be studied at very low temperatures, is more difficult to calculate than in the $3d$ -group, in contrast to the apparent simplicity of the variation of susceptibility at the higher temperatures. Partly this is because the values of J met with are high, as contrasted with the value $L = 0, 2$ and 3 in the iron group; partly because it is more difficult to calculate the crystal field splittings when spin and orbit are strongly coupled to form the resultant, J ; and partly because the symmetry around the rare earth ions is not so simple as in the iron group.

The rare earth ions are bigger than the $3d$ -ions, and in their hydrated salts they generally co-ordinate nine water molecules instead of six. These are often arranged in three equilateral triangles with a common three-fold axis of symmetry, one triangle in the equatorial plane and the other two in parallel planes above and below, twisted through 60° relative to the equatorial triangle. The crystal field is therefore quite different from that of an octahedron. Instead of starting from an octahedral field and then considering distortions as small perturbations, in the rare earths one starts from a trigonal field (three-fold symmetry about the axis).

In a field of this type a level with a resultant angular momentum J can be described by the Hamiltonian

$$(97) \quad \mathcal{H} = g_J \beta \mathbf{H} \cdot \mathbf{J} + A_2 J_z^2 + A_4 J_z^4 + A_6^0 J_z^6 + A_6^6 (J_+^6 + J_-^6),$$

where $J_\pm = J_x \pm iJ_y$, and g_J is the Landé splitting factor of the free ion in the level J . Only even powers of J_z etc., can occur, because of parity invariance; and powers higher than the sixth are absent for f -electrons.

Consider as an example Ce^{3+} , with one $4f$ electron. The free-ion state is

$^2F_{3/2}$. In the crystalline field this splits into three Kramers doublets (Fig. 7); experimentally it is found that the two doublets $\pm \frac{1}{2}$ and $\pm \frac{5}{2}$ are close together (about 3 cm^{-1} apart) and the $\pm \frac{3}{2}$ doublet is some 100 cm^{-1} higher.

If a small field is applied parallel to the axis, the $\pm \frac{1}{2}$ doublet separates by an amount $g_{\parallel} \beta H$; and the $\pm \frac{5}{2}$ doublet by $5g_{\parallel} \beta H$. In terms of a fictitious spin $S' = \frac{1}{2}$ for each doublet, this would be interpreted as $g_{\parallel} = g_J = \frac{6}{7} = 0.86$ and $g_{\parallel} = 5g_J = 30/7 = 4.28$. If a small perpendicular field is applied, the $\pm \frac{1}{2}$ doublet separates by $3g_{\perp} \beta H$, and the $\pm \frac{5}{2}$ doublet is not split at all in first order. I.e. $g_{\perp} = 2.57$ and 0 respectively. Experimentally it is found that $g_{\parallel} = 0.96$, $g_{\perp} = 2.19$ for the $\pm \frac{1}{2}$ doublet in cerium ethyl sulphate. The deviations from the calculated values can be explained by a more refined theory, which takes account of the perturbation by the nearby $^2F_{7/2}$ level.

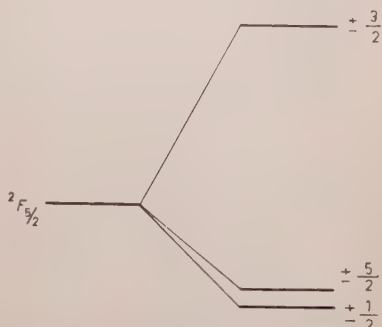


Fig. 7. - Levels in Ce^{3+} , split by crystal field.

Gd^{3+} and Eu^{2+} , which have the half-filled shell structure $4f^7 {}^8S_{7/2}$ analogous to $3d^5 {}^6S_{5/2}$, behave very similarly to Fe^{3+} and Mn^{2+} in having very small splittings and very isotropic g -values.

Further details on the susceptibilities of the rare earths can be found in VAN VLECK *Theory of Electric and Magnetic Susceptibilities*, and on the paramagnetic resonance in the papers of ELLIOT and STEVENS (e.g. *Proc. Roy. Soc.*, A 219, 387 (1953)).

16. - Hyperfine structure. Theory.

So far we have treated the nucleus of the ion as a structureless immobile charged point. Actually it may possess spin, magnetic moment and an electric quadrupole moment. Although these do not interact in any interesting way with the closed-shell electrons, they do with the magnetic electrons. This gives rise to further splittings, because of the further $(2I+1)$ -fold multiplicity associated with the nuclear spin I .

We may look at it as follows. The electrons by virtue of their spin moment and orbital motion set up a magnetic field at the nucleus.

For instance in Cu^{2+} , where the probability distribution for the positive hole is shaped like a four-leafed clover, when the spin is oriented in the positive z -direction (magnetic moment in the negative z -direction since the gyro-magnetic ratio of electrons (and holes) is negative), the magnetic field is also in the positive direction (Fig. 8a shows the lines of force). When the spin is

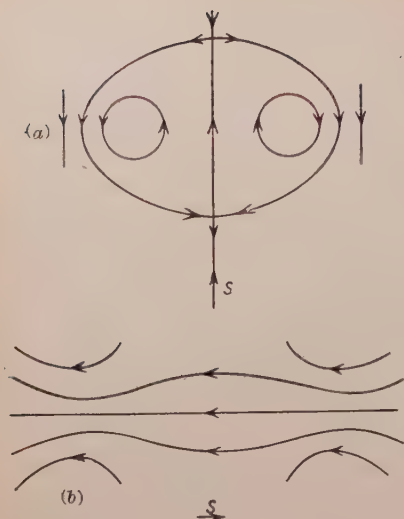


Fig. 8. - Lines of magnetic force inside the Cu^{2+} ion. (a) spin parallel to symmetry axis, (b) spin perpendicular to symmetry axis.

self-consistent field model. As discussed below, indirect mechanisms are responsible for quite a strong contribution from the contact term.

The interaction of this magnetic field with the magnetic moment of the nucleus (parallel to its spin \mathbf{I}) can be written as an addition to the spin-Hamiltonian of the form

$$(98) \quad AS_x I_x + B(S_x I_x + S_y I_y)$$

(again assuming an axis of symmetry).

Since the contribution (A_s , B_s) of the $3d$ -electron spin moment is of the dipole-dipole type there exists an identical relation

$$(99) \quad A_s + 2B_s = 0$$

(in general if the interaction between two dipoles μ , μ' is written $a_{ii}\mu_i\mu_i$, then quite generally $a_{ii} = 0$).

The orbital contributions A_L and B_L are proportional to $(g_{\parallel} - 2)$ and $(g_{\perp} - 2)$.

If one only includes these two, then one finds it impossible to fit the experimental values of A and B . The nature of the discrepancy is most vividly seen in Mn^{2+} , where because $L = 0$ and the electron distribution is spherically symmetrical, both the orbital and spin contributions to the hyperfine structure

perpendicular to the z -axis, the magnetic field is opposite to the spin direction (see Fig. 8b).

Also by virtue of the orbital motion a field of magnitude $-2\beta\langle r^{-3} \rangle \mathbf{L}$ is set up at the nucleus. (This is quenched to the same extent as \mathbf{L} is quenched, since it is proportional to \mathbf{L}). In Cu^{2+} we saw that spin-orbit interaction caused an appreciable unquenching of \mathbf{L} , in the same sense as \mathbf{S} .

Since the probability density for d -electrons (indeed for any but s -electrons) vanishes at the nucleus, the so-called contact term, which gives rise to a magnetic field proportional to spin-density, would appear to vanish for the magnetic electrons. But this conclusion rests on rather too simple-minded a trust in the simple configuration approach suggested by the

vanish. Experimentally, however, there is a prominent hyperfine structure, which can be represented by a term of the form

$$(100) \quad AS \cdot I.$$

Such an interaction, usually called isotropic, can only arise from s -electrons through the contact term. There must therefore be unpaired s -electrons in the ionic structure.

An explanation of how this may arise has been proposed by ABRAGAM. The ionic state in Mn^{2+} is not a pure $1s^2 2s^2 2p^6 3s^2 3p^6 3d^5$ configuration, but contains in its wave-function admixtures from other configurations of the same L and S . In particular it contains some $1s^2 2s^2 2p^6 3s 4s 3p^6 3d^5$, in which the $3s 4s$ are coupled to give 3S_1 , which in turn is coupled to the $3d^5$ $^6S_{\frac{5}{2}}$ to give a resultant $^6S_{\frac{5}{2}}$ as shown in the vector diagram in Fig. 9 (the closed shells give no contribution to either L or S). As a result of this admixture there is an unpaired s -electron density at the nucleus which is linear in the amplitude of the admixture, and which can give a strong magnetic field at the nucleus even when the actual amount of the added configuration (which is given by the square of the amplitude) is quite small.

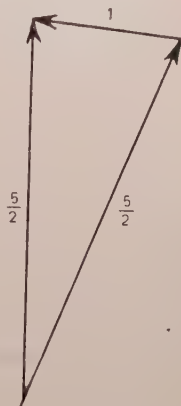


Fig. 9. — Vector diagram to illustrate the hyperfine structure in Mn^{2+} .

Although this explanation appears very plausible, there is still a mystery about this coupling. A computation along these lines, using Hartree wave-functions, has yielded a result from this mechanism which is smaller by a factor 10 than the observed effect (ABRAGAM, HOROWITZ and PRYCE). Experimentally, there is no doubt about the existence of an isotropic term in the hyperfine structure Hamiltonian. In all the $3d$ -ions there is an isotropic term comparable with and often greater than the other terms. No satisfactory alternative to the Abragam mechanism has been proposed. In the trivalent rare-earth ions, however, there is no evidence for an isotropic term in the hyperfine structure, within the experimental error, but it is found in the hyperfine structure of $Eu^{2+}(4f^7 {}^8S_{\frac{7}{2}})$.

On this model for Cu^{2+} , one calculates

$$(101) \quad \begin{cases} A = \frac{2\beta\mu_n}{I} \langle r^{-3} \rangle \left[g_{\parallel} - 2 + \frac{3}{7} (g_{\perp} - 2) - \frac{4}{7} \right] - \mathcal{A}, \\ B = \frac{2\beta\mu_n}{I} \langle r^{-3} \rangle \left[g_{\perp} - 2 - \frac{3}{14} (g_{\perp} - 2) + \frac{2}{7} \right] - \mathcal{A}, \end{cases}$$

where μ_n is the nuclear moment and \mathcal{A} the isotropic coupling, constant. (The middle terms in the bracket, with coefficients $3/7$, $-3/14$ arise from the electron spin moment as corrections because we are dealing with the fictitious spin in (98) and this differs from the real spin; cf. equation (31)).

In the rare earths, where J is a good quantum number, the hyperfine structure of the free ion can be represented by a Hamiltonian $\mathcal{A}\mathbf{J}\cdot\mathbf{I}$, and for a Kramers doublet $|a\rangle$, $|b\rangle$, one has the relations

$$(102) \quad \begin{cases} g_{\parallel} = 2g_J \langle a | J_z | a \rangle, & A = 2\mathcal{A} \langle a | J_z | a \rangle, \\ g_{\perp} = 2g_J \langle a | J_x | b \rangle, & B = 2\mathcal{A} \langle a | J_x | b \rangle, \end{cases}$$

whence

$$(103) \quad \frac{B}{A} = \frac{g_{\perp}}{g_{\parallel}}.$$

In those ions where J really is a good quantum number this relation is found experimentally to hold pretty well, and can be used as an indication of how pure J is in the crystalline state.

The departure of the electronic charge density from spherical symmetry gives rise to a second-order harmonic term in the electric potential near the nucleus (i.e. a gradient of the electric field strength), which interacts with the nuclear quadrupole moment. This is represented by a term of the form

$$(104) \quad P[I_z^2 - \frac{1}{3}I(I+1)]$$

in the spin Hamiltonian.

17. - Hyperfine structure. Observation.

The additional terms (98) and (104) in the Hamiltonian give rise to small splittings of the observed resonance lines, which may be anything from a few gauss to some hundred gauss. As this is the usual order of magnitude of the line width in most paramagnetic crystals, special steps have to be taken to reduce the line width. This arises mainly from two causes, (i) magnetic dipole-dipole interaction between the ions in the crystal, (ii) spin-lattice interactions. The first can be reduced by working with magnetically dilute crystals, in which the magnetic ion is mainly replaced by a diamagnetic ion which forms an isomorphous crystal (e.g. Zn^{2+} for the divalent $3d$ -ions, Al^{3+} for the trivalent ones, La^{3+} for the rare earths). By diluting in this way the line width can be reduced to about 6 gauss, this arising from the magnetic field due to the protons in the water molecules of hydration. By replacing the water by heavy

water, the line width can be further reduced to about 2 gauss, as the deuterons have a smaller magnetic moment than the protons. The spin-lattice broadening can be reduced almost indefinitely by working at sufficiently low temperatures. In practice it is sufficient to work with liquid air ($\sim 90^\circ\text{K}$) for ions whose lowest orbital level is non-degenerate, and for which the spin-lattice coupling is consequently weak; and with liquid hydrogen ($\sim 14^\circ\text{K}$) where there is orbital degeneracy (e.g. Co^{2+}), and in extreme cases such as Ti^{3+} liquid helium ($\sim 4^\circ\text{K}$) may be necessary to attain the necessary resolution.

In simple cases, such as when the magnetic field is parallel to the symmetry axes, the hyperfine structure results in splitting each resonance line into $2I+1$ equally spaced components of equal intensity. The spacing (in magnetic field units) is given by

$$(105) \qquad \Delta H = A/g\beta.$$

18. - Connection with optical spectra.

In calculating the magnetic properties we have had to use the values of the energy differences caused by the crystalline electric fields. These can be estimated from the lattice spacings, the charges and dipole moments on the other ions and molecules in the crystal, etc., but because of the polarizability of the various parts of the crystal many corrections have to be made, and such calculations tend to be unreliable unless done with very great care and thoroughness.

The energy spacings required can, however, be obtained by direct observation of the optical absorption spectrum of the paramagnetic crystal. For instance in $\text{Cu}^{2+} \cdot 6\text{H}_2\text{O}$ $E_{2,3,4} - E_0 \approx 12\,300\text{ cm}^{-1}$, as shown by an absorption band at that frequency. Since the energies involved are nearly all such that the absorption falls either in the visible region, or on the red or violet edges of it, the colours of these crystals are intimately connected with the magnetic properties we have been studying.

When one uses the observed energy spacings, and the value of λ is derived from the spectroscopy of the free ions, one calculates g -values which are close to those observed, but with significant and systematic discrepancies. This can be explained in terms of partial covalent bonding. The model which we have used, in which the ionic complex is treated as a central ion surrounded by water molecules (or other ligands), is too simple. The electrons, or holes, on the ion are really to some extent shared with the ligands. This results in a weakening of those properties, such as the spin-orbit interaction and the nuclear hyperfine structure, which arise predominantly from the proximity of the magnetic electrons to the central nucleus. These considerations can

be put on a quantitative basis, and serve to give a measure of the degree of departure from purely ionic structure.

The sharing of the magnetic electrons with the ligands has been particularly clearly demonstrated in the $4d$ -compound K_2IrCl_6 . In this compound, diluted with diamagnetic K_2PtCl_6 , the hyperfine structure shows that the electrons not only interact with the iridium nucleus, but also with the chlorine nuclei. And it is possible to deduce that the probability of a $4d$ -electron being found located on any one Cl is 3%, and only 82% on the Ir.

Such observations, in which magnetic, optical and chemical data are correlated, promise to yield a greater insight into the structure of crystals and chemical compounds generally.

Magnetic Properties of Metals.

J. H. VAN VLECK

Harvard University - Cambridge, Mass.

I. - The Spin Paramagnetism of Conduction Electrons.

1. - Introduction.

As Professor KITTEL will discuss ferromagnetism, and Professor PRYCE paramagnetism, there is left for me only diamagnetism and feeble paramagnetism. Most materials, however, are diamagnetic or only feebly paramagnetic. The theory which I shall develop in the next two or three lectures at least has applicability to a wider class of materials than do the more spectacular and more commonly discussed theories for highly magnetic substances.

We will begin by treating the part of magnetism which arises from the spin rather than orbital moment. We do so because the spin portion is the simpler to handle, as well as usually the more important contribution. Most of you are doubtless familiar with the fact that the paramagnetic susceptibilities of magnetically dilute salts of the iron group conform to the spin-only formula

$$(1) \quad \chi = \frac{4N\beta^2 S(S+1)}{3kT}.$$

Here and elsewhere β is the Bohr magneton number $he/4\pi mc$, S is the spin quantum number, and N is the number of paramagnetic ions per cm^3 . Eq. (1) is essentially the quantum-mechanical version of the Langevin formula $\chi = N\mu^2/3kT$, as the square of the spin angular momentum is $S(S+1)\hbar^2/4\pi^2$, and the gyromagnetic ratio for spin is e/mc .

We are, however, in these lectures concerned not with insulators but with conducting non-ferromagnetic metals. One is tempted, at first sight, to apply

Eq. (1) to conductors, taking $S = \frac{1}{2}$ and identifying N with the number of conduction electrons per cm^3 . Such a procedure indeed works pretty well if we are, say, describing the paramagnetism associated with color centers in impure insulators, but fails completely in bona fide conductors. The resulting paramagnetism is far too large to agree with experiment, and has, moreover the wrong temperature dependence. The observed susceptibilities of the alkali metals, for instance, depend only slightly on temperature instead of being proportional to temperature.

2. - Simple theory.

The dilemma was solved by PAULI ⁽¹⁾ in an epoch-making paper which marked the first practical use of Fermi-Dirac statistics in metals and so is an appropriate starting point to develop magnetic theory. We shall develop the theory at first only for the vicinity of $T = 0$, as then the calculation is particularly simple. (See remarks following Eq. (35) for the more general case). Since room temperatures are small compared to the Fermi threshold temperatures, the correction terms ascribable to the fact that the temperature is not zero are of little importance. (The first correction term is calculated in the literature ⁽²⁾, and turns out to be proportional to the square of the temperature).

At the absolute zero the distribution is, of course, that of minimum energy. Before application of an external field this situation is achieved when the $\frac{1}{2}n$ orbital states of lowest energy are filled each with two electrons of oppositely directed spin. Here n is the total number of electrons, so that $n = NV$. When a magnetic field is applied, the configuration of minimum energy is no longer that in which the electrons are paired in these $\frac{1}{2}n$ orbital states. Instead we may suppose that the $\frac{1}{2}n - k$ states of least original energy have their full quota of two magnetically paired electrons, but that the next succeeding $2k$ cells each have a single electron with $m_s = -\frac{1}{2}$. As $k \ll n$, we may to a sufficient approximation regard these $2k$ cells as equally spaced in unperturbed energy, with the same spacing ΔE as that in the vicinity of the highest originally occupied cells, which we shall call the critical spacing. The change from the original complete pairing to the new distribution involves an increase of amount $k^2 \Delta E$ in the « unperturbed » part of the energy, as taking an electron from cell $\frac{1}{2}n - x$ to $\frac{1}{2}n + x$ changes this energy by an amount $2x \Delta E$, and to a sufficient approximation $\sum x = \frac{1}{2}k^2$. However, this change in the distribution diminishes by an amount $2\beta kH$ the part of the energy due

(1) W. PAULI, jr.: *Zeits. f. Phys.*, **41**, 81 (1927).

(2) F. BLOCH: *Zeits. f. Phys.*, **53**, 216 (1929).

to the magnetic field, since « turning over » an electron from $m_s = \frac{1}{2}$ to $m_s = -\frac{1}{2}$ gives an alteration $2\beta H$. The value of k appropriate to the absolute zero is that which minimizes the total energy $k^2 \Delta E - 2\beta kH + \text{const.}$, and is hence $k = \beta H / \Delta E$. As $2k$ electrons now have spins aligned along the field, the susceptibility per unit-volume is

$$(2) \quad \chi_s = \frac{2\beta^2}{V\Delta E}.$$

The value of the critical spacing ΔE will depend on whether we consider the conduction electrons as absolutely free, or consider the binding effect of the atoms through which they migrate. We shall treat first the case that the electrons are completely free. The critical energy, or energy of the highest state occupied at $T = 0$ is well known to be

$$(3) \quad E_{\max} = \frac{h^2}{8mV^{\frac{2}{3}}} \left(\frac{3n}{\pi} \right)^{\frac{2}{3}} = \frac{h^2}{8m} \left(\frac{3N}{\pi} \right)^{\frac{2}{3}}.$$

The spacing of energy levels near the actual upper limit is

$$\Delta E = 2 \left(\frac{dE}{dn} \right).$$

The expression (2) for the susceptibility hence becomes

$$(4) \quad \chi_s = \beta^2 \left[\frac{12m}{h^2} N^{\frac{1}{3}} \left(\frac{\pi}{3} \right)^{\frac{2}{3}} \right].$$

Actually, the electrons are never completely free, as supposed in the Sommerfeld model, but, as usual, this fact is circumvented by using in (4) an effective mass which is not the same as the true mass, and which is deduced empirically. This amounts to employing in (2) a realistic value of the energy spacing ΔE .

3. - Exchange and correlation corrections.

There is in addition an important correction because of the exchange forces between the conduction electrons. The ordinary Coulomb forces, either between these electrons or between electrons and positive ions, do not depend on spin alignment, and so do not affect the susceptibility. The exchange terms, however, influence the results materially. Because of the anti-symmetrization associated with the exclusion principle, it is unlikely that two electrons with

parallel spin be close together. Instead, each electron has around it the so-called « Fermi-hole » ⁽³⁾ in the statistical electron charge cloud distribution.

From pure considerations of symmetry and dimensions, one can show that the reduction in energy per unit volume due to the Fermi hole effect has the form

$$(5) \quad E_{\text{ex}} = ae^2(N_+^{\frac{1}{3}} + N_-^{\frac{1}{3}}),$$

where a is a purely numerical constant and N_+ , N_- are the number of electrons of $+$ or $-$ spin direction respectively per unit volume. The absence of cross terms is an expression of the fact that the exchange correlation effects, in the simple free electron picture which does not include polarization corrections, exist only between electrons of similar spin. There are, of course, identical coefficients for N_+ and N_- since there is symmetry between north and south directions except as influenced by the external field. The expression for E_{ex} must be quadratic in e because it is a first-order effect in the Coulomb energy. The expression (5) now follows from purely dimensional considerations, as E_{ex} must have the dimensions of energy/unit-volume, i.e. of e^2/l^4 and as the dimensions of N_+ , N_- , being numbers/unit volume, are $1/l^3$. (There is no ambiguous dimensionless combination of constants which can enter from the disposable constants h , N , m involved in connection with antisymmetrization.)

Detailed calculation ⁽³⁾, which we omit, shows that the value of the constant a is

$$a = -0.229 \left(\frac{4\pi}{3} \right)^{\frac{1}{3}}.$$

The ordinary Fermi energy, on which we based the uncorrected formula (4) for the susceptibility, has the form $b(N_+^{\frac{2}{3}} + N_-^{\frac{2}{3}})$ with

$$b = \frac{3}{10} \frac{h^2}{8m} \left(\frac{3}{\pi} \right)^{\frac{2}{3}} 2^{\frac{1}{3}},$$

as is seen from (3) since the total energy is $\int_0^F E(N) dN$. Our problem is now to minimize the total energy in a magnetic field, viz.,

$$(6) \quad E = -\beta H(N_+ - N_-) + b(N_+^{\frac{2}{3}} + N_-^{\frac{2}{3}}) + a(N_+^{\frac{1}{3}} + N_-^{\frac{1}{3}})e^2,$$

subject to the requirements $N_+ + N_- = N$. We omit writing down terms in the energy which depend solely on N , since they are of no interest for our

⁽³⁾ F. SEITZ: *The Modern Theory of Solids*, p. 359 ff.

purposes. We now set $N_+ = \frac{1}{2}N = \frac{1}{2}N_- = \Delta N$ in (6), drop cubic terms in ΔN (which correspond to incipient saturation effects in the field, which we neglect), and minimize (6) with respect to the ΔN . With an elementary calculation, we thus find that the exchange-corrected susceptibility is

$$(7) \quad \chi_s = \frac{2\beta \Delta N}{H} = \frac{9\beta^2 N}{10 E_F + 4 E_{ex}},$$

where $E_F = b(N/2)^{\frac{2}{3}}$ and $E_{ex} = ae^2(N/2)^{\frac{1}{3}}$

are respectively the mean Fermi and Fermi-hole energies per conduction electron in the absence of the field. We express our results in terms of E_{ex} and E_F rather than a , b since the former are the parameters usually recorded in books on solid-state physics. If we neglect E_{ex} , (7) is of course the same as (4). Even this result is not sufficiently realistic, because it is not corrected for the effect of what is called in solid-state physics the correlation energy, i.e. the correction to the energy, because electrons of opposite spin tend to repel each other. The equilibrium distribution hence is one in which electrons even of anti-parallel spin have some relative correlation in position. (This polarization effect is a dynamical one, not to be confused with the purely kinematical one involved in the antisymmetrization leading to the Fermi hole; there is some dynamical correlation even between parallel spins, but it is unimportant in view of the large superimposed kinematical mechanism.) We will not try to go into the details of the calculation of the correlation energy as it is one of the trickiest subjects in solid state physics. It has the effect of making the exchange corrections less important than (7) would imply. It is clear that the correlation effects should work in this direction, since it makes relative spin alignment less important energetically, there being, so to speak, holes both for parallel and antiparallel cases. The correlation corrections have been most thoroughly examined by PINES (4).

4. - Comparison with experiment by means of measurements of magnetic resonance.

One's first reaction is that a direct comparison with experiment is out of the question, for in the usual experiments one measures the total susceptibility, which is the sum of the spin contributions which we have considered and the orbital diamagnetism both of the conduction electrons and of the positive ions.

(4) D. PINES: *Phys. Rev.*, **95**, 1090 (1954).

However, SCHUMACHER and SLICHTER ⁽⁵⁾ have shown that by means of magnetic resonance it is possible to isolate the spin susceptibility. The point is essentially that the diamagnetic effects make no observable contribution to the magnetic resonance.

Schumacher and Slichter's procedure is perhaps best explained in terms of the so-called Kramers-Kronig relations ⁽⁶⁾ between the real and imaginary parts of the susceptibility. It is particularly appropriate to mention these relations at this conference here at Varenna, since KRAMERS first proposed them at the Volta conference in Como in 1927. Let us consider the complex susceptibility $\chi(\omega) = \chi'(\omega) - i\chi''(\omega)$.

Then it is well known that the absorption coefficient at angular frequency ω ($= 2\pi\nu$) is $\alpha = (4\pi\omega/c)\chi''$ while the ordinary, i.e. static susceptibility is $\chi'(0)$. KRONIG and KRAMERS ⁽⁶⁾ show that

$$(8) \quad \chi'(\omega_0) = \frac{2}{\pi} \int_0^{\infty} \frac{\omega \chi''(\omega)}{\omega^2 - \omega_0^2} d\omega + \chi'(\infty).$$

This relation is very general, as it is based on certain assumptions concerning the location of singularities in the complex plane which are tantamount merely to supposing that disturbances do not antecede in time the fields that produce them. In practice one varies the magnetic field rather than impressed frequency. However, the absorption is important only in the vicinity of resonance, and is, very approximately, a function only of $\omega - \omega_R$, where ω_R is the resonance angular frequency $\omega_R = g(e/2mc)H$. Hence (8) can be rewritten for the case $|\omega - \omega_R| \ll \omega_R$, as

$$(9) \quad \chi_s = \chi'(0) = \frac{2}{\pi\omega_R} \left(\frac{ge}{2mc} \right) \int_0^{\infty} \chi'' dH,$$

if we assume the susceptibility at infinite frequency is zero. The susceptibility can hence be evaluated if the absorption is known. However, the difficult feature in any absorption measurement is the calibration of the absolute amount of the absorption. SLICHTER and his collaborators ingeniously overcame this difficulty by measuring nuclear resonance absorption with the same apparatus. This they did, preserving the same value of ω_R , by using fields of a few thousand gauss in the nuclear case as compared with a few gauss in the

⁽⁵⁾ R. T. SCHUMACHER and C. P. SLICHTER: *Phys. Rev.*, **101**, 58 (1957); R. T. SCHUMACHER, T. R. CARVER and C. P. SLICHTER: *Phys. Rev.*, **95**, 1089 (1954).

⁽⁶⁾ H. A. KRAMERS: *Atti Congr. Fis.*, Como, p. 545 (1927); R. DE L. KRONIG: *Journ. Opt. Soc. Amer.*, **12**, 547 (1926).

electronic one. As adapted to the nuclear case, Eq. (9) becomes

$$(10) \quad N g_I^2 \frac{I(I+1) \beta_N^2}{3kT} = \frac{2}{\pi \omega_R} \left(\frac{g_I e}{2 M_R c} \right) \int_0^\infty \chi'' dH,$$

where g_I and β_N are respectively the nuclear g factor and magneton. $\beta_N = \hbar e / 4\pi M_R c$, I is the nuclear spin, and $\omega_R = H(e/2 M_R c)g_I$ is the nuclear resonance frequency.

It is thus possible to determine the spin susceptibility by measuring the area under the resonance absorption curve calibrated against the known area for the nuclear case. The reader perhaps wonders why the absorption measurements do not furnish the total rather than spin susceptibility. The answer is that in principle there should be resonance connected with the eigenvalues of the orbital energy (cf. our later discussion following Eq. (40)). These are Kittel's cyclotron resonance frequencies, and coincide with the spin resonance frequency if $g = 2$ and we assume the effective mass is the same as the actual mass for conduction electrons (which actually is not true). However, the orbital resonance is so exceedingly broad as to be virtually unobservable, because of broadening caused by orbit-lattice coupling and other effects. The spin lines are much narrower, because relaxation connected with lattice effects here enters only in connection with higher order terms involving spin-orbit coupling. Incidentally, in the orbital case the susceptibility at infinite frequency is not zero (though it is for the spin resonance absorption). In other words, the additive constant $\chi(\infty)$ in (8), instead of being zero, is negative in the orbital case. Otherwise one could not have a negative susceptibility at zero frequency, for the integral in (9) is essentially positive.

The experimental measurement of the spin susceptibility by the resonance method has so far been confined to lithium and sodium. Table I shows the spin susceptibility, as measured by SCHUMACHER and SLICHTER, in comparison with values calculated exclusive and inclusive of the various corrections which we have discussed. In each case, the value of m used in the various formulas is the effective mass, which is 1.46 times the true mass of the electron in the case of Lithium, and 0.985 in the case of Sodium (⁷).

The first column gives the value calculated without any correction for exchange. The second column gives the value calculated by our formula (7), which includes the effect of the Fermi hole, but not the correction for the correlation between anti-parallel spins. Finally, the third column gives the value calculated by PINES, which includes a rather refined correction for correlation. It is seen that the theoretical values inclusive of all corrections agree

(⁷) H. BROOKS: unpublished calculations.

with experiment almost within the errors of measurement. On the other hand, the less refined calculations give unsatisfactory results. Inclusion of the Fermi hole, but not correlation, for instance, overcorrects the susceptibility as compared with the free electron value. It should be emphasized that in this connection any calculation based on the free electron model and not allowing for the forces between electrons which give rise to exchange and correlation is quite inadequate. In the computation of cohesive binding energies it is quite a good approximation to forget about the forces between electrons entirely—in other words, the corrections due to the Fermi hole and correlation practically cancel the direct Coulomb term. No such simple procedure works in calculating the susceptibility. We should, however, note that the calculations of cohesive binding energies indicate that the correlation energy is about $\frac{1}{3}$ of the Fermi hole energy; if, by analogy, we insert a factor $\frac{2}{3}$ in the E_{ex} term of the denominator of (7), the calculated susceptibility becomes $2.5 \cdot 10^{-6}$ for Li and $1.1 \cdot 10^{-6}$ for Na, in moderate agreement with experiment. Measurements of the Slichter type on the spin susceptibility furnish one of the best ways of verifying whether a calculation for the effect of correlation is correctly made. The earlier primitive calculation of the correlation energy by SAMPSON and SEITZ⁽⁸⁾, for instance, yields $\chi_s = 2.92 \cdot 10^{-6}$ for Li, in disagreement with experiment.

TABLE I. — *Theoretical and experimental spin susceptibilities.*

	Calc., Eq. (4)	Calc., Eq. (7)	Calc., PINES	Experiment
Li	$1.17 \cdot 10^{-6}$	$5.3 \cdot 10^{-6}$	$1.87 \cdot 10^{-6}$	$(2.08 \pm 0.1) \cdot 10^{-6}$
Na	$0.64 \cdot 10^{-6}$	$1.7 \cdot 10^{-6}$	$0.85 \cdot 10^{-6}$	$(0.95 \pm 0.1) \cdot 10^{-6}$

We should mention that, besides the Schumacher-Slichter procedure, there is another method, semi-theoretical, semi-experimental, for determining the spin-paramagnetism χ_s . This is the fact that the so called Knight shift is proportional to $|\psi(0)|^2 \chi_s$, where $\psi(0)$ is the value of the wave function at the nucleus for the conduction electrons with energies at the Fermi threshold. It is possible to compute $|\psi(0)|^2$ from theory with fair accuracy, and if we rely on the theoretical value of this proportionality factor, it is possible to determine χ_s from measurements of the Knight shift. The values of $\chi_s \cdot 10^6$ obtained in this fashion are⁽⁸⁾ respectively 1.85 ± 0.20 and $0.83 \pm .03$ for Li and Na. The agreement both with experiment and with PINES calculation, is reassuring.

(8) J. B. SAMPSON and F. SEITZ: *Phys. Rev.*, **56**, 633 (1940).

II. - The Diamagnetism of Free Electrons in Boltzmann Statistics.

5. - Introduction.

Let us now turn to the theory of the orbital susceptibility or diamagnetism of perfectly free electrons, exemplified in practice, to a certain degree, by the conduction electrons in metals. There were numerous papers early in the century, including some by distinguished physicists, that purported to get a non-vanishing diamagnetism, but such results are, of course, wrong, for Miss Van Leeuwen's theorem⁽⁹⁾ tells us that in pure classical theory, there can be no magnetism at all. The reason that non-vanishing results were obtained was that the boundary electrons were not properly taken into account. They creep around the boundary in an opposite sense from the interior electrons which do not touch the boundary, and the effect of the two just cancels. The situation is shown schematically in Fig. 1. The boundary electrons 1 cancel the diamagnetic contribution of the interior electrons 2, 3, 4. The calculation of the magnetism of the conduction electrons is, in fact a rather tricky subject, especially in quantum mechanics. It is precisely this property which makes the subject of interest to the applied mathematician, and by now there is a sizable literature on the subject. From the standpoint, however, of the physicist, the subject is perhaps less vital, as the amount of information which can be obtained regarding the metallic state from measurement of diamagnetism is somewhat limited, though by no means insignificant.

The calculation of diamagnetism can be effected in one of two ways: either by adding up contributions of the moments associated with the individual energy states, or by computing the dependence of the partition function on the field

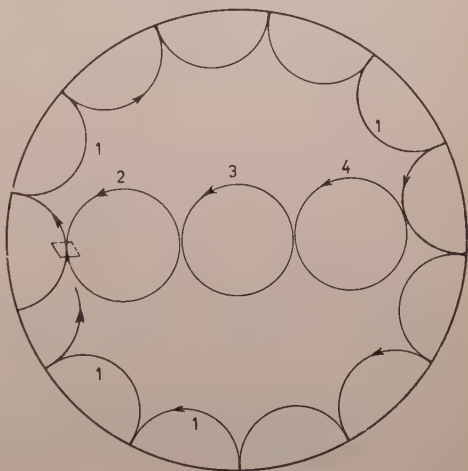


Fig. 1.

⁽⁹⁾ J. H. VAN LEEUWEN: *Dissertation*, Leiden (1919); *Journ. de Phys.*, 2, 361 (1921); also N. BOHR: *Dissertation*, Copenhagen (1911); summary by J. H. VAN VLECK in *The Theory of Electric and Magnetic Susceptibilities*, Sections 24-26.

strength ⁽¹⁰⁾. The latter procedure is the simpler, and more foolproof, though less explicit, as it is not necessary to trace through the contribution of the individual states as influenced by the boundary.

6. — Mathematical preliminaries.

At this stage it is necessary to say a few words about the mathematical framework by which magnetic moments are computed. As you all know, the Hamiltonian function for an electron subject to a vector potential \mathbf{A} and a scalar potential φ is:

$$(11) \quad \mathcal{H} = \frac{1}{2m} (\mathbf{p} + \frac{e}{c} \mathbf{A})^2 - e\varphi.$$

The canonical momentum \mathbf{p} is connected with the velocity \mathbf{v} in the fashion $m\mathbf{v} = \mathbf{p} + (e/c)\mathbf{A}$. Let us suppose the applied magnetic field is directed along the z -axis. Then in an anisotropic medium we can identify the magnetic moment with its z -component:

$$M_z = -N(e/2mc)(x\dot{y} - y\dot{x}).$$

The average magnetic moment, i.e. the expectation value of the magnetic moment in a given state n of energy E_n , classical or quantal, is

$$(12) \quad \langle M_n \rangle = - \frac{\partial E_n}{\partial H}.$$

This well-known relation is verified by substituting

$$(13) \quad A_x = -\frac{1}{2}Hy, \quad A_y = \frac{1}{2}Hx, \quad A_z = 0,$$

⁽¹⁰⁾ The correct expression for the diamagnetism of free electrons in quantum mechanics in weak fields was first obtained by LANDAU: *Zeits. f. Phys.*, **64**, 629 (1930); other subsequent treatments of this problem include E. TELLER: *Zeits. f. Phys.*, **67**, 311 (1931); J. H. VAN VLECK: *The Theory of Electric and Magnetic Susceptibilities*, Section 81; C. G. DARWIN: *Proc. Camb. Phil. Soc.*, **27**, 86 (1930); E. H. SONDEHEIMER and A. H. WILSON: *Proc. Roy. Soc.*, A **210**, 173 (1951); E. W. ELCOCK: *Proc. Roy. Soc.*, A **222**, 239 (1954); R. B. DINGLE: *Proc. Roy. Soc.*, **211**, 500, 517 (1952); F. S. HAM: *Phys. Rev.*, **92**, 1113 (1953); M. C. STEELE: *Phys. Rev.*, **88**, 451 (1952); M. F. M. OSBORNE: *Phys. Rev.*, **88**, 438 (1952); M. BLACKMAN: *Proc. Roy. Soc.*, A **166**, 1 (1938).

Our method of developing the theory in the present lectures, though obtained independently, shows considerable resemblance to that of R. PEIERLS: *Zeits. f. Phys.*, **80**, 763 (1933). Both Peierl's treatment and the present one develop the partition function as an ascending series in \hbar , and avoid the necessity of summing the various quantum states explicitly.

in (11), differentiating with respect to H , and remembering that the energy is the expectation value of the Hamiltonian function. In some cases it is more convenient to take

$$(14) \quad A_x = -Hy, \quad A_y = 0, \quad A_z = 0,$$

which corresponds to a different choice of gauge. The relation (12) still retains its validity if (14) is used rather than (13), as we expect physically, since gauge invariance is necessary in any self-consistent theory. One can verify the invariance mathematically by noting that the extra terms which substitution of (14) for (13) contributes to (12) are proportional to

$$x\dot{y} + y\dot{x} = d(xy)/dt$$

and so vanish for periodic or bounded orbits. The relation (12) is incidentally readily shown to still be valid even when one includes spin, which we omit for the present.

With Boltzmann statistics, the partition function is

$$Z = \sum_n \exp[-E_n/kT],$$

where the summation is over all states, and becomes an integration if the distribution is continuous. If there are N atoms per cm^3 , the mean moment per unit volume is

$$(15) \quad M = \frac{N \sum_n \langle M_n \rangle \exp[-E_n/kT]}{\sum_n \exp[-E_n/kT]}.$$

In terms of the partition function, the magnetic moment is

$$(16) \quad M = NkT \frac{\partial \log Z}{\partial H},$$

as one can verify readily by differentiation and use of (12). This result applies in both classical and quantum mechanics, provided Boltzmann statistics are used.

7. - Classical theory.

As applied to the Hamiltonian function (11) with a vector potential (13) for electrons in a box of volume l^3 , the partition function is

$$(17) \quad Z = \int_{-\infty}^{\infty} \int_{-\infty}^{\infty} \int_{-\infty}^{\infty} \int_0^l \int_0^l \int_0^l \exp \left[\frac{(p_x - \frac{1}{2}ec^{-1}Hy)^2 + (p_y + \frac{1}{2}ec^{-1}Hx)^2 + p_z^2 - 2eq\varphi m}{2mkT} \right] \cdot dp_x dp_y dp_z dx dy dz.$$

By changing the variable from p_x to $p_x = p_x - \frac{1}{2}ec^{-1}Hy$, with an analogous change for p_y , one sees immediately that (17) is independent of H . This constitutes the theorem of Miss van Leeuwen, also contained in the doctor's dissertation of NIELS BOHR, who obtained it independently. Our proof is general for a one electron system; the extension to coupled many particle systems is readily made.

8. - Quantum theory for weak fields.

The explicit calculation in quantum mechanics is excessively difficult unless we take $\varphi = 0$, i.e. consider only the case of free electrons, as we do henceforth.

In quantum mechanics the partition function is a diagonal sum or trace, and instead of (17) one has

$$(18) \quad Z = \frac{2}{h^3} \int_{-\infty}^{\infty} \int_{-\infty}^{\infty} \int_{-\infty}^{\infty} \int_0^l \int_0^l \int_0^l \exp \left[-\frac{2\pi i(\mathbf{p} \cdot \mathbf{r})}{h} \right] \cdot \exp[(a+b)] \exp \left[\frac{2\pi i \mathbf{p} \cdot \mathbf{r}}{h} \right] dp_x dp_y dp_z dx dy dz,$$

where

$$(19) \quad \begin{cases} -kTa = \frac{p_x^2 + p_y^2 + p_z^2}{2m} + \frac{He}{2mc} (xp_y - yp_x), \\ -kTb = \frac{H^2 e^2}{8mc^2} (x^2 + y^2). \end{cases}$$

In (19) p_x must be interpreted as the operator $(\hbar/2\pi i) \partial/\partial x$, etc., or alternatively x as $(-\hbar/2\pi i) \partial/\partial p_x$, since one has one's choice of using the coordinate or momentum system of representation. We will find it more con-

venient to use the momentum system, so that (19) becomes

$$(20) \quad \begin{cases} -kTa = \frac{p_x^2 + p_y^2 + p_z^2}{2m} + \frac{Heh}{4\pi imc} \left(p_y \frac{\partial}{\partial p_x} - p_x \frac{\partial}{\partial p_y} \right), \\ -kTb = \frac{H^2 e^2}{8mc^2} \left(\frac{h}{2\pi i} \right)^2 \left(\frac{\partial^2}{\partial p_x^2} + \frac{\partial^2}{\partial p_y^2} \right). \end{cases}$$

In eq. (18) we have used wave functions corresponding to free electrons, but this involves no loss of generality, for the invariance of the diagonal sum insures us of obtaining the proper final answer regardless of the system of representation which is used. The normalization factor $2/h^3$ in (18) is used to insure the proper enumeration of the number of systems (a factor not, however really necessary until we later convert to Fermi-Dirac statistics); it can be obtained either by noting that there is one state for each area of amount h in the phase space $dp_x dx$, or, if preferred, by quantizing the electron in a box of infinite potential barriers. The factor 2 is to allow for the two possible spin orientations, which effectively doubles the orbital statistical weight. The translational states in a box are discrete rather than continuous, but as the box becomes infinitely large, the discrete manifolds becomes virtually a continuum. The integrand of (18) is, except for a factor, the density matrix of quantum mechanics in the free electron system of representation.

Why is it that one obtains a non-vanishing susceptibility in quantum mechanics? It is because p_x does not commute with x , etc., in matrix multiplication, or, more specifically, because $\exp[a+b]$ is not the same thing as $\exp[a] \exp[b]$ when a, b are non-commutative operators. The angular canonical angular momentum $xp_y - yp_x$ agreeably commutes with both $p_x^2 + p_y^2 + p_z^2$ and $x^2 + y^2$. So we incorporate the linear term in H in the definition of a , since its ordering poses no trouble. On the other hand $x^2 + y^2$ does not commute with $p_x^2 + p_y^2$. If we were to let the operators in (20) work on only the exponential $\exp[2\pi i(\mathbf{p} \cdot \mathbf{r})/h]$ in (18), we would obtain, except for an unimportant normalization factor, precisely the same integral for Z as in (17), and hence a partition function independent of H and zero magnetic moment. Actually, of course, this is not right. What do we mean by the exponential function of an operator? It is something defined by means of series, and leads us into rather intricate algebra if terms of arbitrary order are considered. However, if b is a small operator of which higher powers may be disregarded, then

$$(21) \quad \exp[a+b] = \exp[a] + \int_0^1 \exp[(1-\lambda)a] b \exp[\lambda a] d\lambda,$$

if we neglect terms beginning with b^2 . The result (21) is readily established by

remembering that the fundamental definition of the exponential function is

$$\exp[a+b] = \lim_{N \rightarrow \infty} \left(1 + \frac{a+b}{N}\right)^N.$$

In applying (21), certain terms, e.g. those linear in H can be omitted, as any part of the integrand which is an odd function of H integrates to zero, and so can be omitted. Hence the only terms which enter are those in which both differential operators work entirely on the wave function factor $\exp[2\pi i(\mathbf{p} \cdot \mathbf{r})/h]$ (the classical terms) or else both on the part of the exponential that is involved to the right of the operator in (21). Thus to terms in H^2 , (18) is the same as

$$(22) \quad Z = A \int_{-\infty}^{\infty} \exp[-p_x^2/2mkT] dp_x - \frac{2AH^2e^2}{8mc^2kT} \int_{-\infty}^{\infty} \int_0^1 \exp[-p_x^2(1-\lambda)/2mkT] \cdot \left(-\frac{h}{2\pi i}\right)^2 \frac{\partial^2}{\partial p_x^2} \exp[-\lambda p_x^2/2mkT] dp_x d\lambda,$$

where

$$A = \frac{2}{h^3} \int_{-\infty}^{\infty} \int_{-\infty}^{\infty} \int_0^l \int_0^l \int_0^l \exp[-(\lambda p_y^2 + p_z^2)/2mkT] dp_y dp_z dx dy dz = (2/h^3)(2\pi m V k T).$$

In writing (22), we have omitted the H^2 portion of the contributions from the working of the operators $\partial/\partial p_x$ and $\partial/\partial p_y$ on the wave functions $\exp[2\pi i(\mathbf{p} \cdot \mathbf{r})/h]$, for it must vanish in toto because of Miss van Leeuwen's theorem, as is also easily verified by explicit calculation. Also, instead of writing down the term $\partial^2/\partial p_y^2$ in (22) we have multiplied by 2 that in $\partial^2/\partial p_x^2$, as the two terms make equal contributions because of their symmetry.

The integrals in (22) are elementary, and their evaluation gives

$$(23) \quad Z = (2\pi mkT)^{\frac{3}{2}} \left(1 - \frac{1}{6} \frac{H^2 \beta^2}{k^2 T^2}\right) (2V/h^3).$$

As $\log \alpha(1+\beta) \sim \log \alpha + \beta$ if β is small, the susceptibility corresponding to (23) is by (16)

$$(24) \quad \chi = -\frac{N\beta^2}{3kT}.$$

The negative sign means that there is diamagnetism.

III. - The Diamagnetism of Free Electrons in Fermi-Dirac Statistics for Weak Fields.

To apply results to an actual metal we must, of course, use the Fermi-Dirac rather than Boltzmann statistics. With the F.-D. statistics, the magnetic moment per unit volume is given by

$$(25) \quad M = - \frac{\partial F}{\partial H},$$

where F is the free energy function

$$(26) \quad F = N\zeta - 2kT \sum_i \log (1 + \exp [(\xi - E_i)/kT]).$$

The threshold parameter ξ is determined by the requirement that F be a minimum. This yields a relation

$$(27) \quad N = 2 \sum_i \frac{1}{\exp [(E_i - \xi)/kT] + 1} = 2 \sum f_i,$$

which is equivalent to the requirement that the total number of atoms per cm^3 be N , for f_i as defined by (27) is simply the familiar occupancy factor or Fermi function of the F.-D. statistics. The factor 2 arises from the spin, as we are not enumerating spin states in the summation. Similarly, formula (25) is equivalent to

$$(28) \quad M = - 2 \sum_i \frac{\partial E_i}{\partial H} f_i,$$

as we should expect. However, (28) is only useful if we have diagonalized the energy. If instead we use a different system of representation, e.g. the free electron system of representation, in which the extra Zeeman terms are operators, then trouble arises from ordering, and it is necessary to go back to (25). When recast as a trace in the free electron system of representation, (26) is equivalent to

$$(29) \quad F = N\zeta - \frac{2kT}{h^3} \iiint \exp [-2\pi i(\mathbf{p} \cdot \mathbf{r})/h] \log (1 + \exp [(\zeta/kT) + a + b]) \cdot \\ \cdot \exp [2\pi i(\mathbf{p} \cdot \mathbf{r})/h] dp_x dp_y dp_z,$$

with a, b defined as in (20). We omit the integration over $dx dy dz$ as the volume factor deriving from this is unity if we are dealing with free energy/unit

volume. What do we mean by the logarithm of an operator O ? Probably the most fundamental definition is in terms of a parametric integration:

$$(30) \quad \log(1 + O) = \int_0^1 \frac{O}{1 + uO} du.$$

If c_2 is small compared to c_1 and c_1, c_2 are non-commutative operators, then

$$\frac{1}{c_1 + c_2} = \frac{1}{c_1} - \frac{1}{c_1} c_2 \frac{1}{c_1}$$

as one readily verifies. Thus

$$(31) \quad \log(1 + c_1 + c_2) = \log(1 + c_1) + \int_0^1 \frac{1}{1 + uc_1} c_2 \frac{1}{1 + uc_1} du.$$

This result can also be established by developing the logarithm as a series in $(c_1 + c_2)$, but we believe the derivation of (31) by means of (30) is better, as we do not require that $|c_1 + c_2| \ll 1$ as is essential for rigor in the series method. In virtue of (21) and (31) we see that (29) becomes

$$(32) \quad F = \text{terms independent of } H - \frac{2kT}{h^3} \int_0^1 \int_0^1 \int_{-\infty}^{\infty} \int_{-\infty}^{\infty} \int_{-\infty}^{\infty} \frac{\exp[\xi']}{1 + u \exp[a_0 + \xi']} \cdot \exp[(1 - \lambda)a_0] b \exp[+\lambda a_0] \frac{1}{1 + u \exp[a_0 + \xi']} d u d \lambda d p_x d p_y d p_z$$

where a_0 denotes the operator a with $H = 0$, and $\xi' = \xi/kT$.

Here we have omitted, or rather incorporated in the part of F which is independent of H , the terms due to the working of the operators directly on the wave function, as such operators will not give any H dependence because of Miss van Leeuwen's theorem. Usually this theorem is used for Boltzmann statistics, but it applies equally well to Fermi-Dirac ones, as all that is involved in the proof is the shift in the variable of integration. Written out explicitly, (32) is (cf. eq. (22))

$$F = \text{const.} - \frac{2mH^2\beta^2}{h^3} \int_0^1 \int_0^1 \int_{-\infty}^{\infty} \int_{-\infty}^{\infty} \int_{-\infty}^{\infty} \frac{\exp[\xi' + a_0] \exp[\lambda p_x^2/2mkT]}{1 + u \exp[\xi' + a_0]} \cdot \frac{\partial^2}{\partial p_x^2} \frac{\exp[-\lambda p_x^2/2mkT]}{1 + u \exp[\xi' + a_0]} d \lambda d u d p_x d p_y d p_z.$$

The computation from here on is elementary. Carrying out the differentiation, one has

$$\begin{aligned}
 F &= \text{const.} - \frac{2H^2\beta^2}{h^3kT} \int_0^1 \int_0^1 \int_{-\infty}^{\infty} \frac{\exp[\xi' + a_0]}{(1 + u \exp[\xi' + a_0])^2} \left[-\lambda + \frac{\lambda^2 p_x^2}{mkT} + \left(1 - \frac{p_x^2(1 + 2\lambda)}{mkT} \right) \right. \\
 &\quad \left. + \left(\frac{\exp[\xi' + a_0]u}{1 + u \exp[\xi' + a_0]} \right) + \frac{2p_x^2 u^2 \exp[2(\xi' + a_0)]}{mkT(1 + u \exp[\xi' + a_0])^2} \right] d\lambda du dp_x dp_y dp_z = \\
 &= \text{const.} - \frac{2H^2\beta^2}{h^3kT} \int_0^1 \int_0^1 \int_{-\infty}^{\infty} \frac{\exp[\xi' + a_0]}{(1 + u \exp[\xi' + a_0])^2} \left[1 - \lambda + \frac{p_x^2}{mkT} (\lambda^2 + 1 - 2\lambda) - \right. \\
 &\quad \left. - \frac{1 + (p_x^2/mkT)(3 - 2\lambda)}{1 + u \exp[\xi' + a_0]} + \frac{2p_x^2}{mkT(1 + u \exp[\xi' + a_0])^2} \right] d\lambda du dp_x dp_y dp_z.
 \end{aligned}$$

Performing the integration over u and λ one obtains

$$\begin{aligned}
 F &= \text{const.} + \frac{2H^2\beta^2}{h^3kT} \iiint \left[\frac{\frac{1}{2} + \frac{1}{3} p_x^2/mkT}{1 + \exp[\xi' + a_0]} - \left(\frac{1}{2} + p_x^2/mkT \right) \cdot \right. \\
 &\quad \left. \cdot \frac{1}{(1 + \exp[\xi' + a_0])^2} + \frac{2p_x^2}{3mkT(1 + \exp[\xi' + a_0])^3} \right] dp_x dp_y dp_z = \\
 &= \text{const.} + \frac{2H^2\beta^2}{h^3kT} \iiint \left[\frac{1}{2(1 + \exp[\xi' + a_0])} - \frac{1}{2(1 + \exp[\xi' + a_0])^2} + \right. \\
 &\quad \left. + \frac{1}{3} \frac{p_x^2 \exp[\xi' + a_0]}{mkT(1 + \exp[\xi' + a_0])^2} - \frac{2 \exp[\xi' + a_0] p_x^2}{3(1 + \exp[\xi' + a_0])^3 mkT} \right] dp_x dp_y dp_z.
 \end{aligned}$$

Partial integration converts the result to

$$(33) \quad F = \text{const.} + \frac{H^2\beta^2}{3h^3kT} \iiint \frac{\exp[\xi' + a_0]}{(1 + \exp[\xi' + a_0])^2} dp_x dp_y dp_z.$$

This expression can be simplified slightly by shifting in the usual way to polar co-ordinates in momentum space, performing the isotropic angular integration, and taking the remaining variable of integration as the energy. The expression for the magnetic moment then becomes

$$(34) \quad M = -\frac{\partial F}{\partial H} = -\frac{2H\beta^2 m^{\frac{3}{2}} 2^{\frac{1}{2}} 4\pi}{3h^3kT} \int_0^{\infty} \frac{\exp[(\xi - E)kT] E^{\frac{1}{2}}}{(1 + \exp[(\xi - E)/kT])^2} dE.$$

The same value of the threshold parameter ξ may be used as for $H = 0$; and tables of M in the general temperature region are found in the literature. For most purposes it is sufficient to compute only the leading term under the

assumption that the temperature is small compared with the threshold temperature. This term can be computed by observing that most of the contribution to the integral (34) comes from the threshold region $E \sim \xi$ and without appreciable error we can replace the slowly varying factor $E^{\frac{1}{2}}$ by $\xi^{\frac{1}{2}}$. Furthermore for $T = 0$ the value of ξ is $N^{\frac{1}{3}}\hbar^2(3/\pi)^{\frac{2}{3}}/8m$ (cf. Eq. (3)), as one sees from the fact that the occupied region in momentum space is a sphere of volume $N/2$. Since $\xi/kT \gg 1$ near $T = 0$, the integral (34) is approximately $kT\xi^{\frac{1}{2}}$. Hence for $T \sim 0$ the expression for the susceptibility becomes

$$(35) \quad \chi_{\text{dia}} = \frac{M}{H} = -\frac{4m\beta^2}{\hbar^2} N^{\frac{1}{3}}(\pi/3)^{\frac{2}{3}}.$$

If we compare (24) with (1) (with $S = \frac{1}{2}$), and (35) with (4), we note the remarkable result that for the free electron model, the diamagnetism is, except for sign, just one-third as great as the spin paramagnetism, both in the Boltzmann statistics and in the ordinary low temperature case of the Fermi-Dirac statistics. In the following paragraph we shall show that this result applies even without the restriction that the temperature be low in the F.-D. statistics. Since the Boltzmann statistics can be regarded as essentially a special high temperature case of the F.-D., we see that for the completely free electron model the spin paramagnetism is three times as great as the orbital diamagnetism over the entire temperature range, and the two types of susceptibilities have consequently the same kind of temperature dependence. We should, however, mention that the simple relation of proportionality holds only in weak fields, where the moment is linear in H , and so loses its validity, when, for instance, there is a de Haas-van Alphen effect (to be discussed later).

In Sect. 1 we computed the spin susceptibility in the F.-D. statistics only for low temperatures. To compute this for the free electron model at arbitrary temperatures we need only note that the term added to the Hamiltonian function by the spin is $2\beta H s_z$, with $s_z = \pm \frac{1}{2}$. Since the factor 2 in (26) is due to the two possibilities for spin, we see that the extra terms added to the free energy because of the Zeeman energy of electron spin are

$$(36) \quad F = -\frac{kT}{\hbar^3} \iiint \{ \log(1 + \exp[\xi' + a_0 - \beta H/kT]) + \\ + \log(1 + \exp[\xi' + a_0 + \beta H/kT]) - 2 \log(1 + \exp[\xi' + a_0]) \} dp_x dp_y dp_z,$$

provided we disregard higher order terms in the field strength, so that the spin and orbital contributions to the susceptibility may be considered additive. If we expand the integrand to terms in H^2 (the first non-vanishing order), we find that (36), is, except for sign, just three times the part of (33) which is proportional to H^2 . Since the susceptibility is obtained from the free energy

by a simple differentiation, the generality of the proportionality factor 3 is established.

9. - Comparison with experiment.

One way to make comparison with experiment is to compare the sum of the spin and orbital susceptibilities with the observed over-all susceptibility. However in the case of the alkali metals, the spin paramagnetism usually dominates the orbital diamagnetism—we have seen that according to the simplest theory the former is three times as big as the latter.

Hence, no very sensitive test of the orbital portion of the theory is provided by a comparison of this type. Instead, probably the most significant comparison is obtained by using those materials, viz. Li and Na, for which the spin susceptibility has been measured quite accurately by the resonance method, and subtracting the spin susceptibility from the total susceptibility.

However, even then, not too much accuracy can be attached to the experimental results, for the feeble susceptibilities of the alkalis are hard to measure with precision. In fact, there has in some cases (notably Cs) been even uncertainty as to the sign of the total susceptibility. Before comparison with experiment can be made, it is also necessary to subtract the contribution which positive ions make to the diamagnetic susceptibility.

This contribution can be estimated from the well-known formula of Pauli:

$$\chi_{\text{ion}} = -\frac{Ne^2}{6Mc^2} \sum_i \langle r_i^2 \rangle_{\text{av.}},$$

where the sum is over the mean square radii of all the electrons bound to the positive ions, i.e. the non-conduction or non-valence electrons. The mean square radii can be estimated pretty well from our knowledge of ionic radii or from the estimated contribution of individual ions to the total diamagnetism of saturated compounds (Pascal's additivity relations). To have a realistic theory, it is necessary to utilize an effective rather than real electronic mass. In introducing this, particular care should be taken of the fact that the electronic mass is implicitly contained in the Bohr magneton $\beta = \hbar e / 4\pi mc$. In formula (4) involving the spin paramagnetism, an effective mass should not be used in connection with β , as the spin magnetic moment (except for the Schwinger electrodynamic corrections) is always exactly β . On the other hand, in the orbital problems β entered merely in connection with a certain combination of constants, so that β should be replaced by $\hbar e / 4\pi m_{\text{eff}} c$.

Thus instead of having

$$(37) \quad \chi_{\text{dia}} = -\frac{1}{3} \chi_{\text{free spin}}$$

as (4) and (35) would suggest, we have instead

$$(38) \quad \chi_{\text{dia}} = -\frac{1}{3} \frac{m^2}{m_{\text{eff}}^2} \chi_{\text{free spin}}$$

The subscript free spin means that the spin susceptibility is computed without exchange or correlation correlations. Since (4) is proportional to (m_{eff}/m) if an effective mass is used, χ_{dia} is proportional to (m/m_{eff}) .

With a low effective mass, the diamagnetism can therefore be greater than the spin paramagnetism, and this is doubtless connected with the fact that there are diamagnetic conductors. (Li and Na, however, are paramagnetic.) In using (37) and (38) one must employ on the right side the theoretical values computed without regard to the Fermi hole or correlation (not the experimental values) as otherwise these relations cease to be valid. The values of the computed diamagnetism of the conduction electrons, computed with and without use of an effective mass, are given in Table II, in comparison with experiment.

TABLE II. — *Susceptibilities for Li and Na (in units of 10^{-6}).*

	χ_{total}	χ_{spin}	χ_{ion}	$\chi_{\text{dia}} (\text{exp})$	$\chi_{\text{dia}} (th, m)$	$\chi_{\text{dia}} (th, m_{\text{eff}})$
Li	1.89 ± 0.05	2.08 ± 0.1	-0.05	-0.14 ± 0.15	-0.28	-0.19
Na	0.70 ± 0.03	0.95 ± 0.1	-0.18	-0.07 ± 0.13	-0.22	-0.22

The experimental values of the total susceptibilities given in the first column are by PUGH and GOLDMAN⁽¹¹⁾ for Li and by BOWERS for Na⁽¹²⁾; these are the most recent determinations, and presumably the most accurate. The experimental spin susceptibilities in the second column are by SCHUMACHER and SLICHTER,—the same as quoted in Table I. The ionic susceptibilities in the third column are old values given by the writer some 25 years ago⁽¹³⁾, but are presumably sufficiently accurate for present purposes. As explained previously, the experimental value of the diamagnetic susceptibilities of the conduction electrons is the first column minus the sum of the second and third columns. The last two columns are computed from Eqs. (37) and (38), or, what is equivalent, from (35) without and with the artifice of an effective mass, (in this correction it must be noted that (4) itself is to be taken proportional to m or m_{eff}). The values of the effective mass $1.46 m$ and $0.95 m$ for Li and Na, are derived by BROOKS. It is seen that if the effective mass is used, the agreement with experiment is well within the experimental error.

⁽¹¹⁾ W. PUGH and J. E. GOLDMAN: *Phys. Rev.*, **99**, 1641 (1955).

⁽¹²⁾ R. BOWERS: *Phys. Rev.*, **100**, 1141 (1955).

⁽¹³⁾ J. H. VAN VLECK: *The Theory of Electric and Magnetic Susceptibilities*, p. 359.

More refined values of χ_{dia} , -- 0.20 and -- 0.24 calculated by PINES⁽¹⁴⁾ for Li and Na are not appreciably different from those in the last column.

In the case of the other alkalis, there are not sufficient experimental data to warrant a detailed comparison of theory and experiment⁽¹⁵⁾.

The noble metals Cu, Ag, Au, show a negative over-all susceptibility,—probably not to be attributed to anything as simple as an abnormally small effective mass, since the conduction band widths for these metals are not abnormally large. Zn and Cd have a strong anisotropy in their diamagnetism, an unexplained dependence on temperature, and also at low temperature exhibit the complexities of the deHaas-van Alphen effect to be discussed later.

IV. — Saturation Corrections. The de Haas-van Alphen Effect.

So far we have considered only the terms in the magnetic moment which are linear in the field strength. For certain purposes, notably study of the de Haas-van Alphen effect, it is necessary to consider the higher order terms in H . It is then necessary to compute⁽¹⁶⁾ the partition function or free energy accurately rather to terms in H^2 .

10. — Boltzmann statistics.

The accurate computation of the partition function in Boltzmann statistics is most easily accomplished by choosing the gauge so that the vector potential has the form (14) rather than (13). The Hamiltonian function is then:

$$\mathcal{H} = \frac{1}{2m} \left[\left(p_x - \frac{e}{c} Hy \right)^2 + p_y^2 + p_z^2 \right],$$

(14) D. PINES: p. 38 of the *Report of the Solway Congress for 1954*, « *Les Electrons dans les Métaux* ».

(15) For a very recent, refined theory of the diamagnetism of electrons in metals, which includes corrections for binding, etc., see T. KJELDAAS jr., and W. KOHN: *Phys. Rev.*, **105**, 806 (1957) and references there to earlier work. The susceptibilities which they calculate for Li and Na are respectively -- 0.07 and -- 0.26. For a generalization of the standard theory, see also P. G. HARPER: *Proc. Phys. Soc.*, A **68**, 879 (1955).

(16) The theory for the de Haas-van Alphen effect was first developed qualitatively by R. PEIERLS: *Zeits. f. Phys.*, **81**, 186 (1933) and first put in quantitative form by LANDAU (see appendix to SHOENBERG's paper in *Proc. Roy. Soc.*, A **170**, 341 (1939)). For detailed exposition of the theory, see R. PEIERLS: *The Magnetic Properties of Metals*, p. 144 or H. A. WILSON: *The Theory of Metals*, p. 160.

and the x -component of momentum is then a constant of the motion if we assume periodic or von Karman type boundary conditions in the x direction. Since p_x can be treated as a constant, it is legitimate to change variables from y to $y' = y - (c/eH)p_x$, and p_y is canonically conjugate equally well to y or y' . The partition function then factors into

$$(39) \quad Z = (2/h^2) \int_{-\infty}^{\infty} \exp[-p_z^2/2mkT] dp_z \int_0^{l_3} dz \int_0^{l_1} dx \int_0^{l_2 He/c} dp_x \cdot \\ \cdot (1/h) \int_{-\infty}^{\infty} \int_{-\infty}^{\infty} \exp[-2\pi i p_y y'/h] \exp[-\mathcal{H}'/kT] \exp[2\pi i p_y y'/h] dp_y dy',$$

with

$$\mathcal{H}' = (1/2m)(p_y^2 + e^2 H^2 c^{-2} y'^2).$$

We assume that the solid is a rectangular parallelepiped of volume V and edges l_1, l_2, l_3 . The free electron wave functions have been omitted from the x, p_x and z, p_z integrals, as they cancel out since the relevant Boltzmann exponent involves only momentum. The integral over y, p_y could in principle be computed in the free electron system of representation, but actually the operator technique such as we used in Sect. 8 is not feasible.

Instead we note that the double integral over y' and p_y when multiplied by the weight factor $1/h$, is just the partition function

$$(40) \quad \sum_{n=0}^{\infty} \exp[-(n + \frac{1}{2})h\nu/kT] = \exp[-h\nu/2kT]/(1 - \exp[-h\nu/kT])$$

of a harmonic oscillator of frequency $\nu = He/2\pi mc$. This frequency corresponds to the spacing of orbital eigenvalues associated with the y motion and is the same as the Kittel cyclotron frequency. The integration limits for p_x require some comment. Not to be influenced by the walls (whose explicit effect we omit), the equilibrium position of the harmonic oscillator must be inside the cubical box of magnetic material. Hence we must have

$$0 < (c/He)p_x < l_2,$$

giving us the limits listed in (39). Actually one may claim that more than the equilibrium position, also the liberation limits of the oscillator problem must fall inside the box. This complication we have overlooked as we have taken the limit of integration for y to be $-\infty$ and ∞ in (39), which is not really correct even when this inequality is satisfied. Rigorously the limits should be $-(c/eH)p_x$ and $l_2 - (c/eH)p_x$. The resulting correction gives in

very weak fields a dependance on the size of the vessel which has been considered by DINGLE, STEELE, OSBORNE and HAM⁽¹⁰⁾.

If we take into account the preceding observations, and evaluate the integrals in (39), this expression becomes:

$$(41) \quad Z = (2/\hbar^2)(2\pi m k T)^{\frac{3}{2}} V (eH/c) [2 \sinh (ehH/4\pi m c k T)]^{-1}.$$

The magnetic moment is readily computed by means of (16), and is

$$(42) \quad M = -N\beta L(\beta H/kT),$$

where $L(x)$ is the well-known Langevin-function $L(x) = (1/x) - \coth x$ and β is the Bohr magneton $he/4\pi mc$.

It should be noted that, as we should expect, (41) becomes independent of H , and (42) reduces to zero in the classical limit $\hbar = 0$. Also in weak fields, (42) should agree with (24), as indeed it does.

Our purpose in computing the higher powers in the field strengths is presumably to examine saturation effects. Eq. (42) predicts that in high fields, the moment should approach monotonically a limiting value $-N\beta$ in the characteristic fashion of a Langevin function. Actually, no such behaviour is found. Instead, for certain materials, notably bismuth, the susceptibility depends on the field strength in an irregular, highly oscillatory fashion. For an appreciable length of time, this behaviour, known as the de Haas-van Alphen effect, was a mystery. This, for instance, was the case when the author wrote his book on *Electric and Magnetic Susceptibilities* in 1932. Soon thereafter, however, PEIERLS and LANDAU⁽¹⁶⁾ showed that the existence of the de Haas-van Alphen effect was a necessary consequence of the quantum theory of the diamagnetism of free electrons. The point is, that when one uses the Fermi-Dirac statistics, the dependence of field strength is quite different than when one employs Boltzmann statistics.

11. - Fermi-Dirac statistics.

If we write the partition function as

$$(43) \quad Z = \int_0^{\infty} z(E) \exp [-E/kT] dE,$$

then obviously $z(E)$ is the number of energy levels in the interval $E, E+dE$. In the F.-D. statistics, the free energy F from which the magnetic moment

can be computed by means of (25) is

$$(44) \quad \left\{ \begin{aligned} F &= \zeta N - kT \int_0^{\infty} z(E) \log \{1 + \exp[(\zeta - E)/kT]\} dE \\ &= \zeta N - \int_0^{\infty} \frac{W(E)}{\exp[(E - \zeta)/kT] + 1} dE, \end{aligned} \right.$$

where

$$W(E) = \int_0^E z(E) dE,$$

is the number of states with energy inferior to E . If we regard Z as a function of $\lambda = 1/kT$, then (43) is closely related to a Laplace integral, as it has the form

$$\int f(\lambda) \exp[-\lambda E] dE.$$

If by explicit computation, as in (41), the dependence of the classical partition function Z on λ is known, then it can be shown that the problem of finding $z(E)$ and hence getting an explicit expression for (44) is substantially equivalent to finding the Laplace transform of Z . The passage from the Boltzmann to F.-D. statistics can thus be regarded as a purely mathematical exercise in Laplace transforms and contour integration. In this fashion, Wilson⁽¹⁶⁾ derived the expression for the magnetic moment in F.-D. statistics. We can, however, proceed in a somewhat more physical, though fundamentally equivalent fashion. The number of states with energies inferior to E is

$$(45) \quad \left\{ \begin{aligned} W(E) &= (2/\hbar^2) \sum_{n=0}^{n'} \int_{-\sqrt{2m[E-(n+\frac{1}{2})\hbar\nu]}}^{\sqrt{2m[E-(n+\frac{1}{2})\hbar\nu]}} dp_x (He/c) l_1 l_2 l_3 \\ &= (4/\hbar^2) (He/c) V \sum_{n=0}^{n'} \sqrt{2m[E-(n+\frac{1}{2})\hbar\nu]}, \end{aligned} \right.$$

where n' is the maximum value of n for which the radicand is positive. To derive (45) we need only note that, if we suppress the exponential $\exp[-p_z^2/2mkT]$, the first line of (39) is the number of states associated with the x and z components of motion for a given eigenvalue of the y motion. The eigenvalues of the energy connected with the y motion are $(n + \frac{1}{2})\hbar\nu$, and so the maximum allowable value of $p_z^2/2m$ for a given n is $(n + \frac{1}{2})\hbar\nu$.

If we substitute (45) in (44), the calculation of the free energy is reduced to evaluation of an integral and a sum. By means of a rather lengthy procedure, involving contour integration, it is possible to evaluate the integral and throw the expression for the free energy into the form

$$(46) \quad F = \text{term independent of } H + (2m\beta^2/h^2)N^{\frac{1}{2}}(\pi/3)^{\frac{1}{2}}H^2 + \\ + \frac{8(2)^{\frac{1}{2}}\pi m^{\frac{1}{2}}(\beta H)^{\frac{3}{2}}kT}{h^3} \sum_{l=1}^{\infty} (-1)^l \frac{\cos [(\pi l \zeta / \beta H) - (\pi/4)]}{l^{\frac{1}{2}} \sinh (\pi^2 l k T / \beta H)}.$$

Even this rather formidable expression is obtained only with certain simplifying assumptions, notably that, as is usually true, the temperature be low compared to the Fermi threshold temperature. Also certain terms of rather complicated form which are of little interest at field strengths ordinarily obtainable have been omitted.

For obvious reasons, we will not spend time on the derivation of the quite complicated expression (46), as it is lengthy and a purely mathematical process which is not particularly instructive as regards the physics of the situation. The magnetic moment is obtained as $-\partial F/\partial H$.

The term proportional to H^2 in (46) is the same as that previously derived in connection with Eq. (35).

The wiggles connected with the de Haas-van Alphen effect are obtained from the last line of (46). The remarkable thing is the way this expression involves both a trigonometric and hyperbolic function of the reciprocal of the field strength. An oscillation in this term will have occurred when $\zeta/\beta H$, regarded as a function of H , increases by 2. This modulus of periodicity can be understood in a purely elementary fashion without going through elaborate calculations. At low temperatures the maximum eigenvalue of the harmonic oscillator part of the problem (the y component) is determined by the maximum integral value of n compatible with $(n + \frac{1}{2})\hbar\nu \leq \zeta$, since ζ is the threshold energy. An extra value of n will come into play if $\Delta(\zeta/\hbar\nu)=1$; i.e. if $\Delta(\zeta/\beta H)=2$, since $\nu = He/2\pi mc$, $\beta = \hbar e/4\pi mc$.

It is the successive de-occupancy of more and more values of n as H becomes larger and larger that gives the oscillations of the de Haas-van Alphen effect.

The predictions of the theory agree remarkably well with experiment, though the accord is perhaps more qualitative than quantitative.

In the first place, the phenomenon is observable only at low temperatures, as one would expect from the occurrence of the hyperbolic sine in the denominator of (46). Secondly, and particularly noteworthy, when plotted against $1/H$, the oscillations of the susceptibility come at regular intervals.

Some of Shoenberg's experimental results ⁽¹⁷⁾ for gallium are shown in

(17) D. SHOENBERG: *Phil. Trans. Roy. Soc.*, **245**, 1 (1952).

Fig. 2. The ordinate is the anisotropy $\chi_c - \chi_a$ or $\chi_b - \chi_a$ in the susceptibility rather than the susceptibility itself. At the lowest temperature only the envelope of the wiggles is graphed.

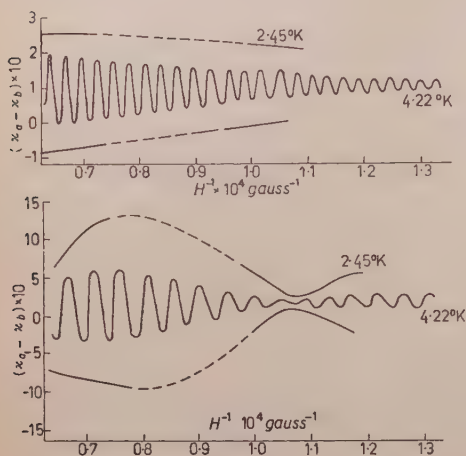


Fig. 2.

From the period of the oscillations, it should be possible to deduce the Fermi threshold energy. In fact, efforts have already been made in this direction ⁽¹⁸⁾. In principle, the study of the de Haas-van Alphen effect should be an excellent method of studying the Fermi surfaces. Actually, this procedure is anything but simple. In the first place, the experiments must be made at very low temperatures for the effects to be perceptible. Secondly, the diamagnetic susceptibility must be large.

Originally the observations, though now including other substances, were confined to bismuth, which is abnormally diamagnetic corresponding to an effective mass only about 1/300 of the normal electronic mass.

Also, besides the experiments being difficult, a realistic theory is far more complicated than one which we have presented. Obviously, substances with an effective mass 1/300 of the real mass cannot be but qualitatively approximated by the free electron model even if a fictitious mass is used. Furthermore, bismuth is highly anisotropic magnetically. In strong fields, the spin and orbital effects are not at all additive, and cross terms should be considered. Also, the free electron approximation should be corrected for quasi-binding. There is an appreciable literature ^(16,18,19) on this point, but we shall not attempt to discuss it.

⁽¹⁸⁾ L. ONSAGER: *Phil. Mag.*, **45**, 100 (1952); A. B. PIPPARD: *Solvay Congress Report*, 1954, « *Les Electrons dans les Métaux* », p. 132.

⁽¹⁹⁾ V. HEINE: *Proc. Phys. Soc. London*, A **69**, 505 (1956); I. M. LIFSHITZ and A. M. KOSEWITCH: *Dokl. Akad. Nauk SSSR*, **96**, 963 (1954).

V. - Relation of Pauli. Feeble Paramagnetism to Antiferromagnetism.

12. - Other causes of feeble paramagnetism.

Besides the Pauli spin paramagnetism, there are other mechanisms for obtaining a weak paramagnetism which is independent of temperature

One cause is the existence of matrix elements $\mu(n, n')$ of magnetic moment involving an energy separation $h\nu(n; n')$ from the ground state n which is large compared to kT (« high frequency terms »). If the matrix elements of magnetic moment are solely of this character, the susceptibility is readily shown to be:

$$(47) \quad \chi = 2N \sum_n \frac{|\mu(n; n')|^2}{h\nu(n'; n)}.$$

This type of situation may arise for one of two reasons (I) and (II).

(I) A paramagnetic atom which when free obeys Curie's law, may have in the solid state its magnetism quenched, i.e. its matrix elements of magnetic moment transformed into those of the high frequency type. This situation does not commonly arise, since even though the orbital angular momentum is quenched, the spin usually is not (except at exceedingly low temperatures); in fact, when there are an odd number of electrons/atom Kramer's theorem tells us that this is impossible as long as a one-atom model is applicable. (Singlet atomic states with $L \neq 0$ should, to be sure, give the type of situation (47), but the ground states of atoms which are singlets practically always are S states, for which the matrix elements in (47) vanish if we use the free atom values in the solid state).

(II) High frequency matrix elements may, however, be created in atoms which are in S states when free, by the deviations from central symmetry when they are bound in the solid state. The fact that most saturated chemical compounds are diamagnetic rather than paramagnetic indicates that this situation is not too likely to arise, for the deviations from central symmetry caused by chemical binding are no doubt usually greater than those caused by the force of cohesion in the solid state.

13. - Antiferromagnetism.

The subject of antiferromagnetism is being covered by Prof. GORTER, and so is outside the scope of the present lectures. It should however be pointed

out that antiferromagnetism with a high Curie or better called, Néel temperature T_n , is the commonest cause of feeble paramagnetism. An antiferromagnetic medium is essentially one in which the exchange integrals J_{ij} are negative in the Heisenberg exchange energy

$$(48) \quad -2 \sum_j J_{ij} \mathbf{S}_i \cdot \mathbf{S}_j.$$

Since J_{ij} is usually a short-range affair, the important pairs i, j are only those which are nearest neighbours. If we denote by J the value of J_{ij} for neighbouring atoms, then it can be shown that for values of $T \ll T_n$ the susceptibility is

$$(49) \quad \chi = \frac{N\beta^2 S(S+1)}{3kT_n} \quad \text{with } T_n \sim J$$

independent of temperature.

A characteristic of antiferromagnetism is a maximum in the susceptibility at the Néel point, but if the temperature is very low compared to this critical temperature, the susceptibility is effectively constant, as in (49), and there is no a-priori way of distinguishing between an antiferromagnetic and other feebly paramagnetic materials. Nor would it be proper to say that there is a sharp dividing line between the antiferromagnetic model of feeble paramagnetism and the Pauli theory for free electrons.

It is well known that in the theory of chemical binding there are two types of approximation: the Heitler-London-Slater-Pauling model in which the electrons are localized on the individual atoms, and the Hund-Mulliken itinerant electron model. The latter neglects completely the fact that ionization potentials are usually higher than electron affinities, so that the energy is increased when an electron is transferred from one atom to another giving a polar rather than electrically neutral configuration. On the other hand the H-L-S-P model does not allow for any wandering tendencies of electrons.

It is often remarked that in the theory of ferromagnetism, the Heisenberg model stands in the same relation to the Slater collective electron model as does the H-L-S-P to the H-M theory of valence. We wish to point out that precisely the same parallelism also exists in the antiferromagnetic *vis-à-vis* the Pauli free electron model of feeble paramagnetism. This point does not seem to be generally recognized in the literature, and is our reason for going into it in some detail here.

In the free electron theory of Pauli, it is assumed that an electron can pass freely from one place to another without reference to where the other electrons are. Actually, as we have already mentioned, the polar configuration involves higher energies, and correlation corrections of course reduce this excess.

The other extreme is where there is exactly one valence electron on each atom. We, for simplicity, assume an alkali-like situation so as not to have the complications of orbital degeneracy.

A configuration in which there is always exactly one electron per atom would have no conductivity. The conducting properties come in through perturbations by excited polar states. In other words in zero approximation we have a completely Heitler-London type of situation, but actually there is some admixture of polar states which give the conducting properties. The effect of this admixture is to give a coupling of type (48) even though true exchange is negligible.

Let the wave functions of adjacent atoms be $\psi_A(1)$, $\psi_B(2)$, and let us assume that the traditional exchange integral

$$\int \psi_A(1) \psi_B(2) V \psi_B(1) \psi_A(2) dV_1 dV_2$$

is unimportant. If the wave functions are orthogonal, it would vanish, for instance, in the one-electron self-consistent field model, where V is only the sum of one-electron functions.

On the other hand, let us assume that the one electron transfer integral

$$50) \quad U = \int \psi_A(1) V \psi_B(1) dV_1,$$

is appreciable. (We are tacitly assuming that the wave functions ψ_A , ψ_B are orthogonal: actually they are not. The non-orthogonality difficulties may, however, be avoided by introducing some sort of Schmidt or Wannier orthogonalization procedure, or, more simply, if the perturbations are small, by replacing V by $V - E_0$ in (50) where E_0 is the energy of the unperturbed ground state.)

Let us consider just the two-atoms system A , B . The ground or non-ionic states are:

$$\frac{1}{\sqrt{2}} [\psi_A(1) \psi_B(2) \pm \psi_B(1) \psi_A(2)],$$

with the upper and lower signs corresponding respectively to the singlet and triplet. Only the former will be perturbed by the excited states $\psi_A(1)\psi_A(2)$ and $\psi_B(1)\psi_B(2)$ and it is depressed by an amount

$$\frac{4U^2}{\hbar\nu}$$

if the energy interval $h\nu$ between the polar and ground state is large. This difference between the singlet and triplet is equivalent to giving the exchange integral J_{AB} the value $-2U^2/h\nu$.

So far we have considered only interaction between a pair of atoms, but allowance for all excited states is equivalent to introduction of the complete Hamiltonian (48) with each J between neighboring atoms giving the value $-2U^2/h\nu$. We thus have an antiferromagnetic situation just in virtue of the correction of the non-polar Heitler-London model for ionic or wandering effects.

This model is of course a good approximation only in the case $U \ll h\nu$ whereas the free electron model neglects $h\nu$ in comparison with U . If we imagine $h\nu$ hypothetically to increase from 0 to a value large in comparison with U we pass gradually from the Pauli to the antiferromagnetic model. Actually, we are probably in the intermediate case in most instances, just the region hard to treat quantitatively. The correlation corrections which we have discussed in Section 3 can be regarded as essentially an attempt to treat the intermediate situation as quantitatively as possible.

Perhaps the best way of deciding whether the conduction or antiferromagnetic model is closest to the truth is to study the temperature variation of the susceptibility. If it increases with increasing temperature (as does that of an antiferromagnetic below the Néel point) the antiferromagnetic model is indicated, while if it decreases, the behaviour is that of the free electron model in which kT is not negligible compared with the threshold energy. (The latter behavior can also be explained by assuming that we have an antiferromagnetic with a low Néel point, but a very low Néel temperature is then required).

From the foregoing discussion, it may seem that almost any conductor should be feebly paramagnetic, and one is tempted to inquire how does ferromagnetism ever arise?

The answer, we believe, is that the preceding discussion has overlooked the orbital degeneracy. If this is present, some of the excited states can have as big a spin as the parallel configuration in the ground state, and so can depress the latter. The excited ionic states of maximum spin will, because of the exclusion principle, be less numerous than those of minimum spin, but may be more effective as perturbers because they are deeper (because of the Hund rule) and so lead to smaller frequency denominators in the perturbation formulae. On this view, and this is our reasoned opinion, ferromagnetism is to be attributed to a large positive intra-atomic exchange integral concomitant with orbital degeneracy.

Ferromagnetism is, however, a digression from our purported study of feeble magnetism, and so this is the good place for us to stop.

Paramagnetic Relaxation.

C. J. GORTER

Kamerling Onnes Laboratorium der Rijksuniversiteit - Leiden

I.

Paramagnetic relaxation is concerned with the study of the establishment of thermal equilibrium in the spin system of a paramagnetic salt. The relaxation can be studied by means of an alternating field $h \cos \omega t$ superposed on a constant field H_0 . We shall consider the important case that these two fields are parallel to each other. Then we can write:

$$H = H_0 + h \cos \omega t, \quad M = \chi_0 H_0 + \chi' h \cos \omega t + \chi'' h \sin \omega t,$$

in which χ characterizes the component of the magnetization M that is in phase with the alternating field, while χ'' characterizes the out of phase component of M . χ' can be measured by observing the change in the resonance frequency of a tuned circuit on insertion of the sample, while χ'' can be measured by observing the resulting absorption by calorimetric methods. By using bridge methods, one can measure both χ' and χ'' . A twin T bridge is convenient for radiofrequencies, while a Hartshorn bridge can be used at audiodrequencies. The frequency range and approximate accuracy of the various methods are given in the following Table.

Method	LC circuit	twin T bridge	calorim.	H. bridge
Frequency range . .	$10^5 \div 2 \cdot 10^7$	$10^5 \div 2 \cdot 10^7$	$10^5 \div 10^8$	$1 \div 1200$
Accuracy	$10^{-3} \div 3 \cdot 10^{-3}$	$10^{-3} \div 3 \cdot 10^{-3}$	10^{-8}	10^{-7}
Quantity measured .	χ'	χ', χ''	χ''	χ', χ''

The calorimetric method is useful at and below liquid hydrogen temperatures where the electrical conductivity and the specific heat are small.

1. - Theory of Casimir and du Pré.

In the limit of very low frequencies we have $\chi = \chi_0$, the static susceptibility. At very high frequencies, on the other hand, the spins cannot exchange energy with the lattice and we then have $\chi = \chi_{ad}$, where $\chi_{ad} < \chi_0$. If there were no interaction between the spins and no electrical splitting due to the crystalline field, we would have $\chi_{ad} = 0$. The specific heat at constant magnetization can be shown to be given by $C_M = b/T^2$, where the constant b arises from the interaction between the spins and from the electrical splitting. If Curie's law holds, i.e. if $M = CH/T$, we have $C_H = (b + CH_o^2)/T^2$, while C_M is then independent of H_o . By thermodynamic reasoning Debye showed that in general

$$\chi_{ad}/\chi_0 = C_M/C_H.$$

Finally, we define a dimensionless quantity F by

$$C_M/C_H = 1 - F.$$

If Curie's law holds, we have

$$F = CH_o^2/(b + CH_o^2).$$

CASIMIR and DU PRÉ assumed that, even in the absence of thermal equilibrium, the distribution over the energy levels of the isolated spin system is given by a Boltzmann distribution appropriate to a temperature T_s , the spin temperature, which may, however, be different from the temperature T of the surroundings. For low frequencies, we have $T_s = T$ and $\chi = \chi_0$. As the frequency increases, T_s becomes different from T and transfer of energy between the lattice and the spin system becomes possible. CASIMIR and DU PRÉ assumed that the heat flow is proportional to the temperature difference

$$dQ/dT = \alpha(T - T_s).$$

A simple calculation then gives

$$\frac{\chi'}{\chi_0} = \frac{F}{1 + \tau^2\omega^2} + 1 - F, \quad \frac{\chi''}{\chi_0} = \frac{F\tau\omega}{1 + \tau^2\omega^2},$$

where the spin-lattice relaxation time τ is given by

$$\tau = \frac{C_H}{\alpha} = \frac{b + CH_o^2}{\alpha T^2}.$$

Nearly all the experimental data, except those at liquid helium temperatures, can be fitted very well with these Debye formulae for χ' and χ'' . By measuring χ' one can determine $1 - F$, while by measuring the height of the maximum in χ'' one determines $F/2$. Thus the quantity obtained from such measurements is the constant b , i.e. the specific heat C_M . This can be compared with the theoretical value of b , and with the experimentally determined C_M from adiabatic demagnetization or paramagnetic resonance data. One can also measure τ as a function of H_0 and T . The dependence on H_0 can be described by the Brons-Van Vleck formula

$$\tau = \tau_0 \frac{b + CH_0^2}{b + pCH_0^2},$$

where the dimensionless parameter p lies between 0 and 1. The dependence of τ on the temperature is more complicated. τ decreases in general with increasing temperature, $1/\tau$ varying from a few Hz to 10^8 Hz.

Many measurements have been done from room temperature down to liquid air temperature, and at liquid helium temperature. The results depend crucially on the type of magnetic ions in the salt, as shown in the figures.

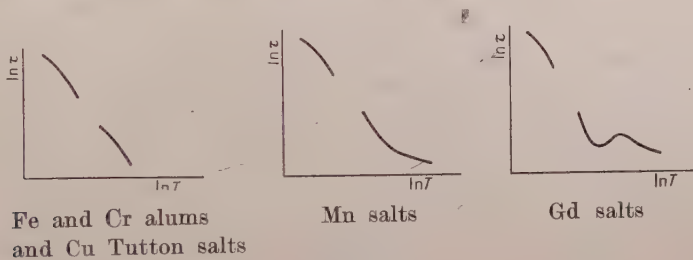


Fig. 1.

In contradiction to alums and Cu Tutton salts, the curves giving $\ln \tau$ as a function of $\ln T$ level off at high temperatures for the Mn salts, so that the τ for Mn salts can be measured easily even at room temperature. The Gd salts have a still more complicated behaviour, the curve even showing a minimum.

Theoretical calculations about the relaxation time τ have been carried out among others by WALLER, KRONIG, VAN VLECK, FIERZ and BROER. There are two different mechanisms for the establishment of thermal equilibrium, viz. the spin-lattice relaxation discussed above, and the spin-spin relaxation due to rearrangements taking place entirely within the spin system.

At high temperatures the spin-lattice relaxation is due to the inelastic scattering of phonons, the so called quasi-Raman effect. For $T \gg \theta_D$, where

θ_D is the Debye temperature of the lattice, one finds $\tau \propto T^{-2}$, while for $T \ll \theta_D$ one gets $\tau \propto T^{-7}$. In general this is roughly in agreement with experiments.

At liquid helium temperatures the spin-lattice relaxation time should be due to direct phonon processes consisting of emission or absorption of a single phonon. This leads to $\tau \propto T^{-1}$ and $\tau \propto H_\sigma^{-2}$.

Experimentally one does not find the T^{-1} law, but rather T^{-3} or T^{-5} , while the dependence on H_σ is also quite different, τ increasing rather than decreasing with increasing H_σ . We will come back to these points later on.

2. - Spin-spin absorption.

For $H_\sigma = 0$ we have $F = 0$ and hence $\chi'' = 0$. Experimentally one finds, however, that an extra absorption appears at high frequencies, for $H_\sigma = 0$, which tends to zero for high fields. This spin absorption can be represented by a term $(1 - F)\tau'\omega$, so that we now get

$$\chi''/\chi_0 = \frac{F\tau\omega}{1 + \tau^2\omega^2} + (1 - F)\tau'\omega.$$

The relaxation time τ' is of the order of 10^{-9} s so that $\tau'\omega \ll 1$ for the frequencies used and it is not surprising that the absorption is linear in ω . τ' is the spin-spin relaxation time, considered already by WALLER and later recalculated by BROER, which describes the time required for the isolated spin system to adjust its magnetization to an applied field. The calculated value of τ' is

$$\tau' = (2\pi)^{\frac{1}{2}}\hbar/4\beta H_i,$$

where β is the Bohr magneton, and H_i is the root mean square of the local field at the position of a spin:

$$H_i = (H_{\text{local}})^{\frac{1}{2}}.$$

This τ' is of the correct order of magnitude, but there are a number of complications concerned with the influence of the electrical splitting. The theoretical value given here holds only in the absence of an electrical splitting. The theory of τ' with electrical splitting will be discussed later on.

Finally we mention that in salts with a larger exchange interaction between the ions, such as the Cu salts or in hydrated MnSO_4 and MnCl_2 , τ' is much larger than in salts without exchange interaction and absorption is accordingly larger. Apparently the effective value of H_i is smaller in these salts. This

effect is connected with the phenomenon of exchange narrowing of paramagnetic resonance lines. The width of these lines is also determined by H_i , and a narrowing therefore means also a smaller effective value of H_i .

II.

At liquid helium temperatures the experimental data do not follow the Debye formula for χ' and χ'' derived formerly.

We must remark that there is sometimes an effect due to the coupling of the crystal with the bath. One finds experimentally that there is then a difference between a powder and a large crystal, which is due to this effect. The resulting dispersion curves are flattened out and the absorption curves may become asymmetrical.

When this effect has been corrected for, the resulting curves are, however, still too broad, i.e. the dispersion curves fall off over a frequency range that is larger than according to a Debye formula. One must introduce a whole group of relaxation times, which we shall characterize by an average value τ_{av} .

According to the theory already discussed, in which the spin-lattice relaxation was ascribed to direct phonon processes, τ should be proportional to H_o^{-2} . In undiluted iron alum one finds, however, that τ_{av} increases with increasing H_o .

According to VAN DER MAREL and VAN DEN BROEK, dilution of the iron alum gives an increase in τ_{av} , while for high dilution, τ_{av} starts actually to decrease at high fields H_o . One also finds that the temperature dependance of τ_{av} depends on the dilution.

For pure iron alum $\tau_{av} \propto T^{-n}$, where $n \approx 5$, while for a dilution of 1:60 one finds $n \approx 1.2$.

As pointed out in 1941 by VAN VLECK, there are a number of complications arising in the theory of the relaxation time due to direct phonon processes. In the first place we mention the problem of how the energy, taken up by the lattice oscillators that are on speaking terms with the spins, i.e. which have an angular frequency ω such that $\hbar\omega$ is equal to the energy required for a spin flip, is transported to the bath. The oscillators that are on speaking terms with the spins are coupled with the other lattice oscillators by the anharmonicity of the elastic forces, the irregularities of the grain boundaries, etc. At liquid helium temperatures the anharmonicity is rather ineffective, and the coupling is presumably to the crystal irregularities. In the second place,

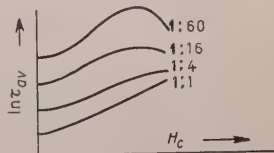


Fig. 2. — τ_{av} for different dilutions of iron alum as a function of H_c .

we mention the problem of the coupling of the spins to the lattice vibrations. As VAN VLECK has shown, the oscillators that are on speaking terms with the spins are interrupted so frequently by the spin relaxation that the levels of these oscillators are broadened enormously. We then get a complicated system consisting of the spins coupled strongly to the oscillators that are on speaking terms which in turn are coupled weakly to the other lattice oscillators. We can describe this situation roughly by saying that, because of the broadening of the oscillator levels, the spin can exchange energy with a whole range of oscillators extending from $\omega = 0$ to a maximum frequency of ω_{msp} , the maximum frequency with which the spins are on speaking terms. The coupling of these oscillators with $\omega < \omega_{\text{msp}}$ with the rest of the oscillators, and hence with the bath, is for low ω due to the irregularities in the crystal, while for high ω and not too low T it is due to the anharmonicity.

Upon dilution ω_{msp} will decrease because the broadening discussed above will decrease since the oscillators are now less frequently interrupted. The probability for a spin to flip then decreases since there are fewer oscillators on speaking terms in spite of the fact that there are now more oscillators of a given frequency per spin than before dilution. We can thus understand the increase of τ_{av} upon dilution. With increasing H_o , the quantity ω_{msp} increases because the spin flip energy $\hbar\omega$ increases with increasing H_o .

The increase in ω_{msp} will start at smaller H_o in diluted salts than in concentrated salts since there ω_{msp} is much larger in the concentrated salts. This accounts for the bending down of the curves showing τ_{av} as a function of H_o at high dilution. We thus see that with the help of this picture of a whole band of oscillators on speaking terms with the spins, we get a qualitative understanding of the behaviour of τ_{av} at helium temperatures.

TEMPERLEY, on the other hand, has suggested that neighbouring spins may make simultaneous flips, so that they can exchange energy with oscillators of double the original frequency, of which there are four times as many according to the Debye theory, etc.

This suggestion has been criticized by VAN VLECK, but we must now admit that the decrease of τ_{av} with H_o at high dilution could be understood on the basis of Temperley's theory.

3. — Spin-spin relaxation.

The question may be raised whether the τ and τ' introduced here are similar to the t_1 and t_2 introduced for the relaxation of nuclear resonance.

τ and t_1 are analogous, but τ' and t_2 are different, because in the present case we always have $M \parallel H_o$, whereas in the case of t_2 one studies the component of $M \perp H_o$. Therefore τ' and t_2 are not so simply related.

At liquid air temperatures ω is not high enough to eliminate the lattice relaxation completely, and one has therefore done measurements at liquid hydrogen temperatures, where $\tau \sim 10^{-3}$ s while $\tau' \sim 10^{-9}$ s.

The experiments of SMITS and VERSTELLE show that the quantity

$$\frac{\chi^4}{\chi_0(1-F)},$$

is not at all independent of H_0 , as it should be on the basis of the relevant formula formerly proposed.

We can roughly divide the substances into three categories, characterized by the following three pictures:

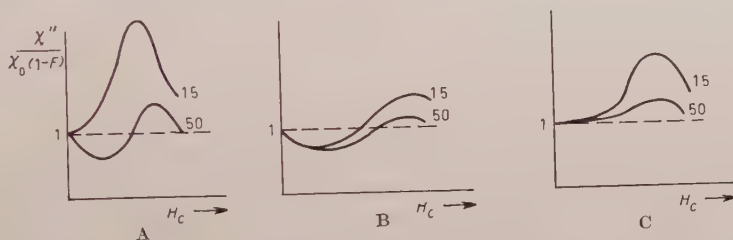


Fig. 3. — A - Cr alums; B - Fe alums; Mn Tutton salts; C - Cu Tutton salts

The two curves in each figure correspond to ω equal to 15 and 50 MHz. Group A shows large electrical splittings Δ_{el} of the ions in the crystalline field, so that $\beta H_i \ll \Delta_{el}$, where H_i is the effective internal field. Group B shows strong magnetic interactions between the ions, as in the Fe alums and the Mn Tutton salts. Thus in B we have $\beta H_i \approx \Delta_{el}$. Finally, group C is characterized by very small electrical splittings so that $\beta H_i \gg \Delta_{el} \approx 0$. A substance of group B may be made to go over to group A by dilution since this diminishes the value of H_i .

Let us now consider the corresponding dispersion χ'/χ_0 . In Cr alum at 1.5 and 20 MHz we get the curve shown in the figure 4, while for still larger frequencies the curves are the same as for 20 MHz. This effect of the appearance of a «hole» in the χ' curve at higher frequencies does not depend on the temperature, and can therefore have nothing to do with the lattice oscillations. In concentrated Fe alum the effect does not appear and this fact lends support to the division into the groups A, B and C.

We see that this new relaxation effect occurs in a relatively small range of external field H_0 . For substances of group A it occurs in small H_0 , for substances of groups B and C it is less pronounced and occurs in larger fields. The electrical field splitting thus plays an important role in this phenomenon,

and we must therefore investigate theoretically the spin-spin relaxation in the presence of an electrical splitting.

According to an old theory of KRONIG and BOUWKAMP, the dependence of τ' on H_o should be given by

$$\tau'_{H_o} = \tau'_0 \exp [H_o^2/H_i^2],$$

where H_i is the internal field. The argument runs as follows. The local field H_{local} is a fluctuating function of the time. Because of energy conservation a spin can flip only if $H_{\text{local}} + H_o = 0$, if we consider only single spin processes. But the probability to find $H_{\text{local}} = -H_o$ decreases with increasing H_o , and τ' will increase in a Gaussian fashion with increasing H_o . If a large Δ is present τ' may slowly decrease rather than rapidly increase as predicted by KRONIG and BOUWKAMP.

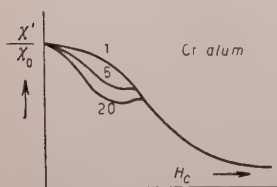


Fig. 4.

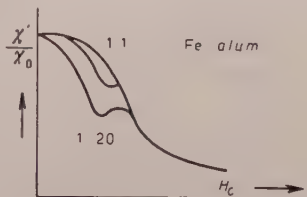


Fig. 5.

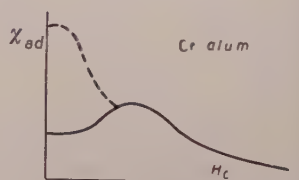


Fig. 6.

In salts in which an electrical splitting occurs, only part of the susceptibility is due to re-establishment of a Boltzmann distribution, while the rest is due to polarization, as has been argued by Prof. PRYCE. BROER has plotted the fraction due to this second part as a function of the external field, as shown in the figure for Cr-alum by the drawn curve. χ_{ad}/χ_0 should be equal to this fraction in fields H_o higher than H_i . In lower fields also the re-establishment of the distribution in the Kramers pairs of levels should contribute to χ_{ad} , and this contribution is shown by the dotted line. The agreement of the present experimental curves with the curve given here is strikingly proving that the treatment of KRONIG and BOUWKAMP has to be preferred over that of BROER.

Ferromagnetism.

C. KITTEL

Department of Physics, University of California - Berkeley, Cal.

The lectures will deal with the following problems,

- (1) Saturation magnetization and exchange,
- (2) Domain Theory.
- (3) High frequency properties of ferromagnetics and ferrites.

My object here is to give a qualitative physical understanding of the principal results; more quantitative calculations and references to the original papers may be found in standard books and reviews of ferromagnetism. The occurrence of ferromagnetism shows that the effective internal field H_{eff} tending to align the elementary magnetic moments must be at least of the order 10^7 Oe. This follows from the requirement that

$$(1) \quad kT_c \approx \mu_B H_{\text{eff}},$$

where μ_B is the Bohr magneton. Now the field at one lattice site due to a Bohr magneton at a neighboring site is of order

$$\mu_B/a^3 \approx 10^4 \text{ Oe},$$

so something else is needed to account for ferromagnetism. We know the exchange interaction is responsible. The usual isotopic exchange interaction between two electrons is given by

$$\mathcal{H}_{\text{ex}} = -2JS_1 \cdot S_2,$$

where J is the exchange integral. In the classical limit, the electrons behave as if there were a strong cosine coupling between their spins, although basically

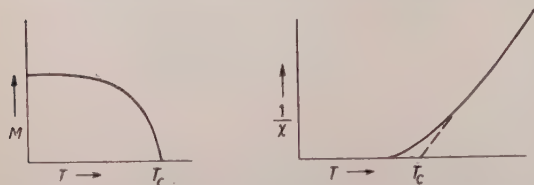


Fig. 1. — Temperature dependence of the magnetization and susceptibility in a ferromagnet.

we know the exchange interaction is an electrostatic effect arising from the exclusion principle. For a small angle θ between a pair of spins the exchange energy is $JS^2\theta^2$, as we see on expanding \mathcal{H}_{ex} classically. The temperature dependence of the magnetization and susceptibility

in a ferromagnetic substance is shown in Fig. 1.

Except in the immediate vicinity of T_c , we have for $T > T_c$,

$$\chi = \frac{C}{T - T_c}.$$

In a normal paramagnetic material we have Curie's law

$$(2) \quad \chi = \frac{M}{H} = \frac{C}{T}.$$

P. WEISS accounted for the ferromagnetic behavior by assuming the existence, in a ferromagnetic substance, of a « molecular field » proportional to the magnetization. He assumed that the H_{eff} of Eqn. (1) was the sum of this molecular field and the applied field, namely $H_{\text{eff}} = H + \lambda M$, where λ is called the « molecular field constant » or « Weiss constant ». Using this on (2)

$$\chi = \frac{M}{H_{\text{eff}}} = \frac{C}{T},$$

we get, with no trouble at all,

$$\chi = \frac{C}{T - \lambda C}.$$

Evidently the Curie temperature T_c is λC . In using (2) we are considering the limiting case where $\mu_B H_{\text{eff}} \ll kT$. For more generality we might replace (2) with the Langevin equation or, better, the quantum mechanical expression involving the Brillouin function. For example, using the Langevin equation we would put

$$M = M_0 L \left(\frac{\mu}{kT} [H + \lambda M] \right).$$

For different values of the parameter T , plots of H vs. M can be made, and from these, the saturation curve $M = f(T)$ can be constructed. When the Langevin equation is used the slope at the origin is finite. The correct slope (zero) is obtained when the Brillouin expression is used. The experimental results can generally be represented by

$$M = M_0(1 - AT^{\frac{3}{2}})$$

at low temperatures, $T < T_c/5$; while at higher temperatures

$$M = M_0(1 - BT^2)$$

usually gives a better fit. The $T^{\frac{3}{2}}$ behavior here is called the Bloch law. We shall discuss this further below.

An exercise exhibiting the usefulness of the molecular field method we consider the model of ZENER and VONSOVSKY in which the interaction between ions is assumed to occur indirectly via the electrons in the conduction band. One ion polarizes the band and then the band polarizes the other ions. This is represented in Fig. 2.

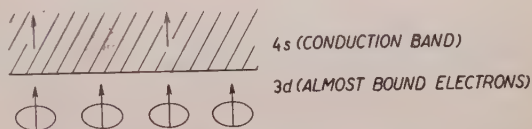


Fig. 2. — Zener-Vonsovsky model of the indirect exchange interaction.

We assume no significant interaction between the electrons in the same band, so that the effective fields are

$$H_1 = H + \lambda M_2;$$

$$H_2 = H + \lambda M_1.$$

Here M_1 is the magnetization of the ion cores (i.e. almost bound electrons) and M_2 is that of the conduction electrons. This treatment will result in the desired ferromagnetic property. We assume a Curie law behavior for M_1 :

$$M_1/H_1 = C/T$$

and a Pauli susceptibility for the conduction electrons

$$\frac{M_2}{H_2} = F \equiv \frac{N\mu_s^2}{E_F},$$

where E_F is the Fermi energy. From these relations we have

$$TM_1 = CH_1 = C(H + \lambda M_2);$$

$$M_2 = FH_2 = F(H + \lambda M_1).$$

Then if

$$\begin{vmatrix} T & -C\lambda \\ -F\beta & 1 \end{vmatrix} = 0,$$

these equations will have non-trivial solutions for M_1, M_2 when $H=0$, i.e., the crystal could exhibit a spontaneous moment. This is a condition on T , namely

$$T = FC\lambda^2 \equiv T_c,$$

which involves λ^2 , in keeping with the second order nature of the interaction mechanism.

1. - Short treatment of spin waves.

We want to indicate qualitatively on a semi-classical model how the Bloch $T^{\frac{1}{2}}$ law for the magnetization of a ferromagnetic at low temperatures comes out of the spin wave picture. We are not giving a proof here; rather, we are



Fig. 3. - Spin wave on a line of atoms.

trying to suggest the reason why $\omega \sim k^2$ is the dispersion relation for a spin wave in a ferromagnet. Let us consider a line of N spins with spacing a , as in Fig. 3.

Here ε is the amplitude of the spin wave. We first want to find the energy of the wave in terms of ε and the wave vector $k = 2\pi/\lambda$. We consider the case of long wavelength where $\lambda \gg a$, and the angle θ between adjacent spins is small. Then the exchange energy associated with the wave can be written

$$E \approx NJS^2\theta^2.$$

Referring to Fig. 4 we see

$$\theta \approx \frac{2\pi a}{\lambda} \frac{\varepsilon}{S} = \frac{ka\varepsilon}{S},$$

so that

$$E(\varepsilon, k) \approx NJ\varepsilon^2 k^2 a^2.$$

The change in the Z -component of the spin is

$$S - (S^2 - \varepsilon^2)^{\frac{1}{2}} \approx \varepsilon^2/2S.$$

We consider first the spin as a strictly classical vector. Our object is not so much rigor as to gain some feeling for the problem. For the whole wave we will have a change then of $N\varepsilon^2/2S$ in the Z-component which we can set equal to the number of reversed spins. Using this in (3) gives

$$E(n, k) \approx 2JSk^2a^2n = n\hbar\omega,$$

where we are using the fact that n is quantized and that a wave is analogous to a harmonic oscillator.

We now consider the properties of a system of spin waves in thermal equilibrium at a temperature $T < T_c/5$. Waves with $\hbar\omega > kT$ will not be appreciably excited. Waves with $\hbar\omega < kT$ will be excited to at least $n = 1$, and *some* waves (of low ω) will have $n > 1$. However, the number of states with energy less than *some* E goes as k^3 , where k is the wave vector associated by Eq. (3) with that value of the energy. One can fairly say that most of the states which are excited at all (at low temperatures) have $n \approx 1$ and $E \approx kT$. Then we have, very roughly, that

$$(4) \quad \Delta M \approx \frac{k^3}{k_{\max}^3} M \approx \frac{(kT)^{\frac{3}{2}}}{J^{\frac{1}{2}}} M$$

for the magnetization reversal, as the energy of a spin wave of the maximum k permitted by the crystal structure must be of the order of the exchange energy J . Eq. (4) expresses the Bloch $T^{\frac{3}{2}}$ law for the temperature dependence of the saturation magnetization in the low temperature region.

The internal energy U of the spin wave system is proportional to $T^{\frac{5}{2}}$, as the number of modes excited is proportional to $T^{\frac{3}{2}}$ by the argument above and the average energy of an excited mode is of the order of kT . The product gives $U \propto T^{\frac{5}{2}}$. The associated spin wave heat capacity is obviously

$$C \approx Nk(kT/J)^{\frac{5}{2}}.$$

In ferrites one would expect the heat capacity at sufficiently low temperatures to go as $T^{\frac{3}{2}}$, and this has been verified for magnetite by Kouvel.

We note in passing that there is some point in writing the energy of a spin wave as $(n + \frac{1}{2})\hbar\omega$ rather than as $n\hbar\omega$. For a reversal of half a spin we have $N\varepsilon^2/2S = \frac{1}{2}$ or $\varepsilon^2 = S/N$. There are a total of N possible spin waves on the line; if ε_0 denotes the total deflection of all the zero-point modes we

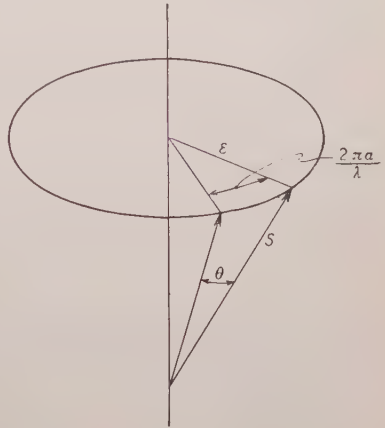


Fig. 4. — Angle relations in a spin wave.

have

$$\varepsilon_0^2 = N\varepsilon^2 = S,$$

just as required to account for the difference between the maximum value S of S_z and the magnitude $\sqrt{S(S+1)}$ of the spin. We observe that $S(S+1) - S^2 = S = \varepsilon_0^2$.

On collective electron theory in the simplest form we have

$$C \propto T$$

and

$$\frac{\Delta M}{M} = AT^2.$$

In the analysis of experimental results, the temperature dependence of the lowest exponent usually shows up most prominently, so that for metals we might expect

$$C \propto T, \quad \frac{\Delta M}{M} \propto T^{\frac{3}{2}},$$

in agreement with observation. The actual behavior of ferromagnetic metals probably corresponds to a combination of spin wave theory and collective electron theory.

2. - Some remarks on crystal anisotropy.

When we magnetize a single crystal of a ferromagnetic material, we discover that the magnetization curve depends on the orientation of the field with respect to the crystal. Thus we have «easy» directions in the crystal. For hexagonal cobalt the easy direction is parallel to the hexagonal axis; any direction perpendicular to this is a hard direction. This is illustrated in the Fig. 5 which shows M vs. H along the easy (\parallel) and the hard (\perp) directions.

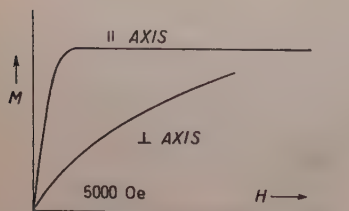


Fig. 5. - Magnetization curves of a single crystal of cobalt in the easy and hard directions of magnetization.

In iron, which has a cubic structure, the saturation magnetization is reached with a field of 1 Oe or less in a $[100]$ type direction while about 500 Oe are required to reach saturation in a $[111]$ direction. This property

naturally carries with it an anisotropy in the energy of a crystal with respect to its direction of magnetization. The excess energy of a crystal magnetized

in an arbitrary direction over what it would have magnetized in an easy direction is known as its anisotropy energy.

The crystal anisotropy cannot be derived from the usual isotropic exchange interactions which depend only on the relative orientation of the spin vectors and have nothing to do with directions in the crystal. Since the classical dipole-dipole interaction contains only the second power of cosines, the resulting anisotropy energy can contain only squares of cosines also, and can therefore exist only in crystals with a symmetry lower than cubic. In hexagonal cobalt the dipole-dipole interaction presumably contributes a small part to the observed anisotropy at room temperature. In cubic crystals there is a quantum mechanical dipolar contribution to the anisotropy resulting from the zero-point amplitude of the spin waves. The spins not being strictly parallel, it is possible to have a dipolar anisotropy.

The major part of anisotropy is accounted for by including the spin orbit interaction which is neglected in using the usual exchange integral expression.

One of several mechanisms by which the spin-orbit interaction gives anisotropy will be described. The distribution of $3d$ electron charge must have the symmetry of the crystal, in the absence of spin-orbit interaction. For simplicity, however, we draw the charge distribution as spherical in Fig. 6. Spin-orbit

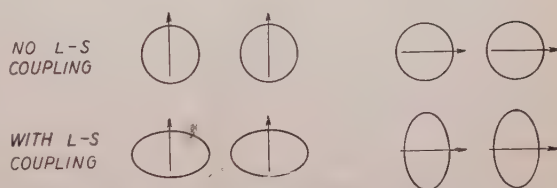


Fig. 6. — A mechanism for ferromagnetic anisotropy.

coupling mixes into the ground state wave function components which change when the spin direction is changed. Thus the overlap of wave functions and the exchange interaction will contain a component which depends on the direction of magnetization relative to the crystal axes.

The magnitude of the anisotropy energy will be of the order

$$E_{\text{anis.}} \sim C(\lambda/\Delta)^2 \sim (g-2)^2 J \sim 10^{-14} \cdot 10^{-2} \sim 10^{-16} \text{ erg} \approx 10^4 \text{ Oe},$$

C is an interaction energy which may be of the order of magnitude of the exchange energy, J ; Δ is an energy difference between states mixed by the spin-orbit energy λ . (Note: $1^\circ\text{K} \approx 1 \text{ cm}^{-1} \approx 10^{-4} \text{ eV} \approx 10^4 \text{ Oe} \approx 10^{-16} \text{ erg}$.)

In cobalt anisotropy has not been observed in the plane perpendicular to the hexagonal axis. Thus the anisotropy energy can be expressed in the form:

$$f_K = K'_1 \sin^2 \vartheta + K'_2 \sin^4 \vartheta + \dots,$$

here ϑ is the angle between the magnetization and the hexagonal axis. The

values of the constants are:

$$K'_1 = 4.1 \cdot 10^6 \text{ erg/cm}^3; \quad K'_2 = 1.0 \cdot 10^6 \text{ erg/cm}^3.$$

In the case of iron let the direction cosines relative to the crystal axes be $\alpha_1, \alpha_2, \alpha_3$. Then we have, in accordance with cubic symmetry:

$$f_K = K_1(\alpha_1^2\alpha_2^2 + \alpha_2^2\alpha_3^2 + \alpha_3^2\alpha_1^2) + K_2\alpha_1^2\alpha_2^2\alpha_3^2.$$

The quadratic term with cubic symmetry, $\alpha_1^2 + \alpha_2^2 + \alpha_3^2$, is identically unity and therefore does not enter into the formula. The fourth power term can be manipulated to the form $\alpha_1^4 + \alpha_2^4 + \alpha_3^4$ by noticing that $(\alpha_1^2 + \alpha_2^2 + \alpha_3^2)^2 = 1$. For iron at room temperature it is found that

$$K_1 = 4.2 \cdot 10^5 \text{ erg/cm}^3; \quad K_2 = 1.5 \cdot 10^5 \text{ erg/cm}^3.$$

The maximum energy is required to magnetize the crystal in the $[111]$ direction.

3. - Magnetostriction.

Magnetostriction occurs because the anisotropy energy depends on the state of strain of the crystal. The crystal deforms in order to minimize the energy. The energy in question consists of three parts which we can indicate schematically as follows:

$$f = K(\alpha) + \frac{1}{2}c\varepsilon^2 + B(\alpha)\varepsilon.$$

The first term is the usual anisotropy energy density and depends on α , the direction of magnetization; the second is the elastic energy density which depends linearly on the elastic moduli and quadratically on the strain tensor components, indicated here collectively by c and ε respectively; last, we have terms indicating a first order correction (linear in the ε_{ij}) to the anisotropy energy as a result of the strain, also a function of α . We can find the magnetostriction, i.e. $\delta l/l$ in any given direction β by minimizing this expression with respect to ε_{ij} .

4. - Ferromagnetic domains.

It is found experimentally that an applied field of 10^{-3} Oe will sometimes suffice to reverse the magnetization of a ferromagnetic specimen. The exchange interaction gives rise to an effective molecular field on the order of 10^7 Oe,

as we have seen. How is it possible for so small an applied field to have such a profound effect on the gross magnetic moment? Also, how is it possible for the gross magnetic moment to be zero in a zero applied field in view of this exceedingly large molecular field?

WEISS gave the answer to these questions when he suggested that the magnetic moment of a specimen is broken up into small parts, called domains, each magnetized to saturation in its individual direction. A change in the net magnetic moment of a specimen can proceed by the following two mechanisms: 1) movement of the boundary wherein those domains which are favorably oriented with respect to an applied field increase in size at the expense of their neighbors; 2) rotation of the direction of magnetization of the domains. Normally the first mechanism predominates at weak fields.

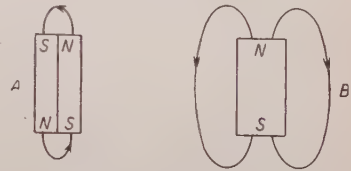


Fig. 7. - Origin of domains.

The next question is, why do domains exist? The answer to this is that the specimen lowers its energy by dividing itself up into domains oriented in such a way that the magnetic energy in the demagnetizing field is reduced. For example, in sample (A), Fig. 7, consisting of two domains, the magnetic energy

$$\frac{1}{8\pi} \int H^2 dv,$$

is lower than in (B) where the field has a substantial value over a large volume. Other domain structures, without free poles, can occur as shown in Fig. 8.

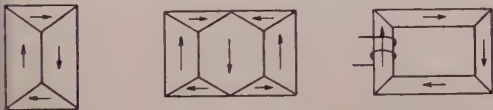


Fig. 8. - Domain structures with closed flux patterns.

The magnetic energy can generally be lowered by forming more domains, but we observe that energy is required to form a boundary. The process of subdivision can continue therefore only as long as the *total* energy continues to decrease. Sufficiently small particles contain only

a single domain. Later we shall estimate the critical size for which this must be the case. Now we will consider the boundaries themselves.

5. - The Bloch wall.

If the transition in magnetization direction were abrupt the energy of the boundary would amount to the full exchange energy due to the spins on each

side. BLOCH pointed out that there is a cheaper way, namely by making a gradual transition over several atomic layers, as shown in Fig. 9. The shorter arrows represent spins which are directed, to varying degrees, into the paper.



Fig. 9. — The Bloch wall.

Suppose N spins are involved equally in the angular change of π . The angle between a pair of neighboring spins is π/N , and their contribution to the exchange energy is $J(\pi/N)^2$. If there are $1/a^2$ atoms per unit area of wall, then the total exchange energy, per unit area, is

$$\sigma_{\text{exch.}} = \frac{1}{a^2} J \pi^2 / N .$$

The energy can be lowered by making the wall thicker. The wall is prevented from becoming indefinitely thick because the spins inside the wall have a higher energy because of anisotropy. Roughly,

$$\sigma_{\text{anis.}} \approx K N a$$

per unit area of wall. Here K is the anisotropy constant and $N a$ is the wall thickness.

The optimum wall thickness is that for which the total energy,

$$\sigma = \sigma_{\text{exch.}} + \sigma_{\text{anis.}} \approx \frac{J \pi^2}{a^2 N} + K N a ,$$

is a minimum. We find easily that

$$N \approx \left(\frac{J \pi^2}{K a^3} \right)^{\frac{1}{2}} ,$$

so that

$$\sigma \approx 2 \left(\frac{J \pi^2 K}{a} \right)^{\frac{1}{2}} ,$$

and

$$\sigma_{\text{exch.}} \approx \sigma_{\text{anis.}} .$$

We can easily make an estimate of the orders of magnitude of the relevant quantities. For example if

$$J \sim k T_c \sim 10^{-13} \text{ erg} ; \quad K \sim 10^5 \text{ erg cm}^3 ; \quad a \sim 10^{-8} \text{ cm} ;$$

then

$$N \sim 1000 ,$$

and

$$\sigma \sim 1 \text{ erg/cm}^2.$$

When the anisotropy constant is small, then σ is small; N is large; and the Bloch wall is thick.

Now we want to calculate the order of magnitude of the dimensions of a ferromagnetic domain. With the arrangement shown in Fig. 10, the wall energy per unit thickness and length is

$$E_w \approx \sigma L N,$$

if there are N walls, each of length L .

Also

$$E_{\text{anis.}} \approx D^2 N K = K/N,$$

because

$$D = 1/N.$$

After minimizing $E_w + E_{\text{anis.}}$ with respect to N , we have

$$N \approx (K/\sigma L)^{\frac{1}{2}}.$$

If we take $L = 1 \text{ cm}$, $K = 10^5 \text{ erg cm}^{-3}$, $\sigma = 1 \text{ erg cm}^{-2}$, we find

$$N \approx 300 \text{ per cm}.$$

We now estimate the critical size for single domain particles. We consider a sphere of radius R , magnetized to saturation. For this case one can show directly that the field energy is given by

$$E_0 = \frac{1}{2} \left(\frac{4\pi}{3} \right) M_s^2 \left(\frac{4\pi}{3} R^3 \right).$$

If the sphere consisted of two domains, oppositely magnetized, then a reasonable guess for the field energy would be $E_0/2$. If we add the wall energy, we get

$$E_1 \approx \frac{1}{4} \frac{4\pi}{3} M_s^2 \frac{4\pi}{3} R^3 + \sigma \pi R^2.$$

If E_0 and E_1 are to be the same, then R must satisfy, *very roughly*,

$$M_s^2 R_c \approx \frac{1}{2} M_s^2 R_c + \sigma$$

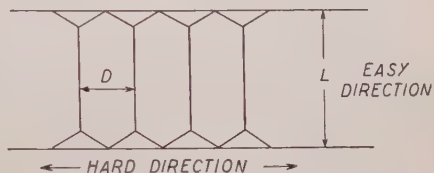


Fig. 10. - Model for calculation of domain dimensions.

or

$$R_e \approx \sigma / M_s^2 \approx 10^{-6} \text{ cm}.$$

This estimate is in order of magnitude agreement with the experimental results.

6. - Equivalent anisotropy fields.

The effect of both crystal and shape anisotropy upon the spins can be described by a fictitious magnetic field provided that the angle ϑ between the easy direction and the magnetization is small.

(i) *Crystal anisotropy*. - In a uniaxial crystal such as cobalt, the anisotropy energy is given by

$$E = K \sin^2 \vartheta + \dots$$

For small ϑ we have, to first order

$$E = K \vartheta^2.$$

This expression will also apply to cubic crystals if ϑ is measured from a [100] direction. We may think of the anisotropy energy density as an added effective field in the direction of the easy axis:

$$E = -H_a M_s \cos \vartheta = -H_a M_s (1 - \frac{1}{2} \vartheta^2 + \dots),$$

so

$$H_a = \frac{2K}{M_s}.$$

This field tends to align M_s along the easy axis. For a spherical oriented single domain particle (i.e., having no shape anisotropy) H_a should be equal to the coercivity. In iron at room temperature the order of magnitude of H_a is

$$H_a \approx \frac{10^6}{2 \cdot 10^3} = 500 \text{ Oe}.$$

(ii) *Shape anisotropy*. - The angular dependent part of the magnetostatic energy density of a magnetized ellipsoid of revolution is

$$E = \frac{1}{2} (N_1 - N_2) M_s^2 \sin^2 \vartheta = \frac{1}{2} \Delta N M_s^2 \sin^2 \vartheta,$$

where θ is the angle between \mathbf{M} and the axis, and N_1, N_2 are demagnetization factors. Therefore there is a uniaxial anisotropy with anisotropy constant:

$$K_{\text{eff}} = \frac{1}{2} M_s^2 4N,$$

and an effective anisotropy field

$$H_{\text{eff}} = 4NM_s.$$

This has its maximum value for an infinite circular cylinder, namely

$$H_{\text{eff}}^{\text{max}} = 2\pi M_s.$$

7. - The moving Bloch wall.

We want to show that the Bloch wall has an effective mass in the sense that its energy per unit area may be expressed in the form

$$\sigma = \sigma_0 + \sigma_1 v^2.$$

Let φ_i be the angle between the spin i in the wall and a fixed direction in the wall. Since there are many spins in the wall we will consider φ a continuous function of z , the normal direction. When the wall moves with a velocity v the spins will rotate at a rate

$$\omega \equiv \frac{d\varphi}{dt} = -v \frac{d\varphi}{dz}.$$

We can calculate the energy involved by attributing this rotation to an effective internal field H_i normal to the wall such that

$$\omega = \frac{ge}{2mc} H_i = \gamma H_i,$$

or

$$-v \frac{d\varphi}{dz} = \gamma H_i.$$

We get then, for the energy due to the motion

$$\sigma - \sigma_0 = \frac{1}{8\pi} \int H_i^2 dz = \frac{v^2}{8\pi\gamma^2} \int \left(\frac{d\varphi}{dz} \right)^2 dz.$$

We may take dq/dc as essentially constant through the wall and equal to π/δ . Then

$$\sigma - \sigma_0 \approx \frac{v^2}{8\pi\gamma^2} \left(\frac{\pi}{\delta} \right)^2 \cdot \delta = \frac{1}{2} \cdot \frac{\pi}{4\delta\gamma^2} \cdot v^2.$$

i.e., the wall has an effective mass per unit area of $\pi/4\delta\gamma^2$, in order of magnitude. The complete derivation is due to W. DÖRING. Experimental verification may be found in the wall resonance experiments of RADO and co-workers, and also in work at Eindhoven. It is also possible to show that the wall must have a viscous drag which in an appropriate limit makes $r \propto H/\lambda$, where λ is the Landau-Lifshitz relaxation frequency.

8. – Ferromagnetic resonance.

In this Section we deduce the condition for ferromagnetic resonance. We start with the equation of motion of the total magnetization \mathbf{M} ,

$$\frac{d\mathbf{M}}{dt} = \gamma \mathbf{M} \times \mathbf{H},$$

The magnitude of \mathbf{M} is constant, because

$$\frac{dM^2}{dt} = 2\mathbf{M} \cdot \frac{d\mathbf{M}}{dt} = 2\mathbf{M} \cdot \gamma \mathbf{M} \times \mathbf{H} \equiv 0.$$

In contrast with the case of nuclear magnetic resonance, it is not easily possible to change the magnitude of the magnetization because of the strong exchange interaction.

GRIFFITHS found in 1946 that the magnetic field at which resonance occurs does not satisfy the usual condition for paramagnetic resonance. We may ask whether the exchange field prevents the resonance from occurring at the normal Zeeman frequency. However, for homogeneous magnetization the exchange field does not enter. We give two arguments for this result. The exchange field is proportional to the magnetization

$$\mathbf{H}_{\text{exch.}} = \lambda \mathbf{M}.$$

Using this we have

$$\mathbf{M} \times \mathbf{H}_{\text{exch.}} = \lambda \mathbf{M} \times \mathbf{M} = 0.$$

A similar argument applies to the Lorentz field, $4\pi\mathbf{M}/3$. A better argument,

however, is the following: The commutator of the *total* spin, $\sum_i \mathbf{S}_i$, with the exchange energy, $\sum_{i>j} \mathbf{S}_i \cdot \mathbf{S}_j$, vanishes

$$\left[\sum_i \mathbf{S}_i, \sum_{i>j} \mathbf{S}_i \cdot \mathbf{S}_j \right] = 0.$$

The exchange energy can therefore have no effect on the time dependence of the magnetization.

We now derive the resonance condition for a thin plate when the applied field, H , lies in the plane of the plate, in z direction. The r.f. magnetic field will be in the same plane and in the x direction. The demagnetization factors are then

$$N_x = N_z = 0; \quad N_y = 4\pi.$$

The equation of motion becomes

$$i\omega M_x = \gamma(M_y H_z - M_z H_x);$$

$$i\omega M_y = \gamma(M_z H_x - M_x H_z);$$

$$i\omega M_z = \gamma(M_x H_y - M_y H_x^{\text{eff}});$$

on assuming a general periodic motion for \mathbf{M} . If the amplitude of the r.f. field is small compared to H_0 ($= H_z$) then M_x , H_y , and M_y will also be small so the variation in M_z is small to the second order and we will consider it zero (i.e. $M_z = \text{const}$). Now

$$H_y = -4\pi M_y,$$

and arises when in the course of the precession the magnetization acquires a component in the y direction. The first equation is then

$$i\omega M_y = \gamma(M_y H_z + M_z 4\pi M_y) = \gamma M_y B_z.$$

In the second equation $M_z H_x$ drops out in the absence of a driving field, leaving

$$i\omega M_y = \gamma(-M_x H_z) = -\gamma H_0 M_x.$$

Thus we find the natural frequency

$$\omega = \pm \gamma \sqrt{BH_0} = \gamma H_{\text{eff}}.$$

9. - The general ellipsoid.

We have developed the resonance condition for the special case of a thin plate specimen parallel to the magnetic field. For the case of a general ellipsoid with demagnetizing factors N_x , N_y and N_z , we find for the resonance frequency,

$$\omega_0 = \gamma \sqrt{[H_0 + (N_x - N_z)M_s][H_0 + (N_y - N_z)M_s]},$$

taking the external field in the direction of the z -axis, Fig. 11. In the derivation of this expression anisotropy effects are neglected, and it is assumed that the r.f. field is uniform in the sample. The specimen should therefore be small in comparison to the skin depth and the wave length of the rf field in that material. In the case of ferromagnetic metals this expression would apply only to very small samples. In experiments on metals the flat geometry is used most often. If the plate is not very thin, then in the expression for the resonance frequency, the N_z of the whole plate is appropriate, *i.e.*

$$H'_0 = H_0 - N_z M,$$

while N_x and N_y refer to the geometry determined by the skin depth and would be ≈ 0 if the normal to the plate is in the z direction.

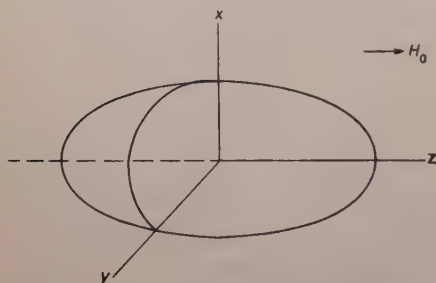


Fig. 11. - General ellipsoid in a ferromagnetic resonance experiment.

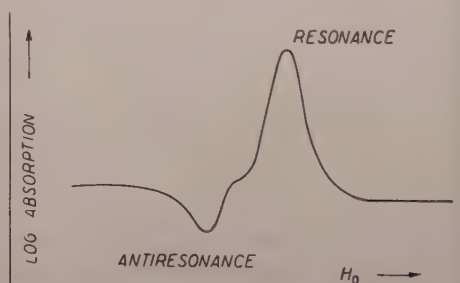


Fig. 12. - Antiresonant and resonant points in ferromagnetic resonance.

Another particular point on the absorption curve is the anti-resonance condition. This describes a minimum in the absorption as shown in Fig. 12, and takes place at a field which is smaller than the resonance field. In order to find how this comes about, we have to solve the equations of motion

$$\frac{d\mathbf{M}}{dt} = \gamma \mathbf{M} \times \mathbf{H}.$$

for a general ellipsoid, as before, but this time taking account of an applied rf field in the x direction. If this is $h \exp[i\omega t]$, we find for the x -component of the magnetization

$$M_x = \frac{\chi_{0x} h \exp[i\omega t]}{1 - (\omega/\omega_0)^2},$$

where

$$\chi_{0x} = \frac{M_s}{H_0 + (N_x - N_z)M_s}.$$

Antiresonance occurs when the permeability

$$\mu_x = 1 + 4\pi\chi_x = 0,$$

and the resultant x component of the flux vanishes inside the specimen. Thus if

$$\chi_x = \frac{\chi_{0x}}{1 - (\omega/\omega_0)^2} = -\frac{1}{4\pi},$$

then

$$\omega_{\text{antires.}} = \omega_0 \sqrt{1 + 4\pi\chi_{0x}} = \gamma H_{\text{eff}}^{\text{res}} \sqrt{1 + 4\pi\chi_0} = \gamma H_{\text{eff; antires.}},$$

where

$$H_{\text{eff; antires.}} = \sqrt{[H_0 + (4\pi + N_x - N_z)M_s][H_0 + (N_y - N_z)M_s]}.$$

In the following table we have collected the resonance field values for some different cases:

shape	$H_{\text{eff; resonance}}$	$H_{\text{eff; antiresonance}}$
sphere	H_0	$\sqrt{BH_0}$
flat sheet, \perp field	$H_0 - 4\pi M_s$	$\sqrt{H_0(H_0 - 4\pi M_s)}$
flat sheet, \parallel field	$\sqrt{BH_0}$	B

10. - The relaxation problem in ferromagnetic resonance.

It is not known exactly what the relaxation mechanism is, but we will consider some of the forms that have been tried in the equation of motion:

$$\frac{d\mathbf{M}}{dt} = \gamma \mathbf{M} \times \mathbf{H} + \text{relaxation term},$$

where the relaxation term tends to return \mathbf{M} to the direction of \mathbf{H} .

(i) One form is

$$-\lambda'(M-\chi_0H)_{x,y},$$

for the x and y components. The agreement with experiment is very poor at low H unless λ' is taken proportional to H ; this seems an artificial assumption.

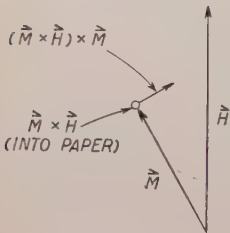


Fig. 13. - Landau and Lifshitz relaxation term.

(ii) The second form is due to Landau and Lifshitz:

$$-\lambda\left[\frac{\vec{H}\cdot\vec{M}}{M^2}-\vec{H}\right]\equiv\lambda\frac{(\vec{M}\times\vec{H})\times\vec{M}}{M^2}.$$

As shown in Fig. 13, this is a vector perpendicular to \vec{M} . It amounts to a rotation of \vec{M} back toward the direction of \vec{H} and does not effect the magnitude of \vec{M} .

(iii) A third possibility is the formulation of Bloch where the relaxation terms are

$$\frac{-M_x}{T_2}; \quad \frac{-M_y}{T_2}; \quad \frac{-(M_z-M_0)}{T_1},$$

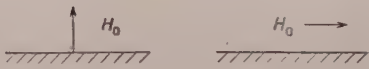


Fig. 14. - Field configurations used by Uehling and Young.

for the x , y and z components respectively; T_2 is the transverse relaxation time; T_1 governs magnetization changes along the field direction, and is called the spin-lattice relaxation time.

UEHLING and YOUNG performed experiments using two different configurations as shown in Fig. 14. A consistent fit was obtained with the Bloch equations with essentially the same T_1 and T_2 in both cases. The Landau-Lifshitz expression, on the other hand, required somewhat different values of λ for the two configurations.

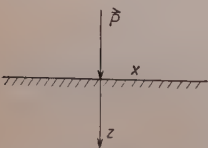


Fig.15.- Coordinate system for discussion of the surface impedance.

We conclude by making some remarks about the interpretation of the observed quantities. Consider an electromagnetic wave incident on a plane surface as in Fig. 15. We can define the characteristic surface impedance Z in terms of the Poynting vector as follows:

$$\vec{P}=\frac{c}{4\pi}\vec{E}\times\vec{H}=\frac{c}{4\pi}H_t^2\frac{\vec{E}_t}{H_t}=\frac{c}{4\pi}H_t^2Z.$$

The usual eddy current equation is

$$\frac{\partial^2 H_x}{\partial z^2} = 4\pi\sigma\omega\mu i H_x.$$

A solution is

$$H_x = H_t \exp[-kz],$$

if

$$k^2 = 4\pi\sigma\omega\mu i.$$

In addition, E_y and H_x are related by one of Maxwell's equations

$$(\text{curl } \mathbf{H})_y = \frac{\partial H_x}{\partial z} = -k \exp[-kz] H_t = \frac{4\pi\sigma}{c} E_y.$$

Applying this relation to the surface gives

$$\frac{E_t}{H_t} = Z = \frac{c}{4\pi\sigma} k \propto (1 + i) \sqrt{\mu}.$$

In some applications, the susceptibility is small, and we can write

$$\sqrt{\mu} = \sqrt{1 + 4p(\chi' - i\chi'')} \approx 1 + 2p(\chi' - i\chi''),$$

and

$$Z \propto 1 + i + 2p[(\chi' + \chi'') + i(\chi' - \chi'')].$$

The real part of Z is responsible for absorption; the imaginary part gives rise to dispersion. The shape of the absorption line is as $\chi' + \chi''$, as shown in Fig. 16.

The approximation that χ is small is applicable to nuclear resonance in metals, but for ferromagnetic resonance calculations the full development of $\mu^{\frac{1}{2}}$ must be used.

The measured g -values are generally higher than the free spin value ($g = 2.0023$):

$$\text{Fe } 2.1; \quad \text{Co } 2.2; \quad \text{Ni } 2.2; \quad \text{Heusler alloy } 2.0(1).$$

As shown by Wiener and Hoskins, the g -factor varies with frequency for Fe-Ni

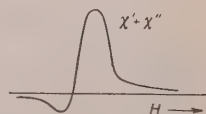


Fig. 16. - Shape of absorption line under eddy current conditions.

alloys in the composition range 35-50% Ni; they found $g \approx 2.2$ to 2.3 at 3 cm, $g \approx 2.13$ at 1.2 cm, and $g \approx 2.09$ at 0.6 cm. We will have more to say later on about these values.

11. - Crystal anisotropy effects in ferromagnetic resonance.

Consider a uniaxial crystal having an easy direction of magnetization and a hard direction as indicated in Fig. 17. If an external magnetic field H is applied in the easy direction the effective field acting on the spins is $H + H_a$, while for H in the hard direction the effective field is $H - H'_a$; H_a is the usual anisotropy field, and H'_a is the effective field tending to oppose magnetization in the hard direction.

For $H \gg H_a$ and oriented at an arbitrary

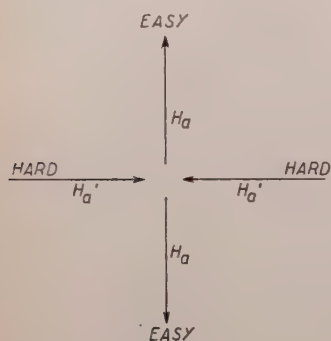


Fig. 17. - Anisotropy field effects in ferromagnetic resonance.

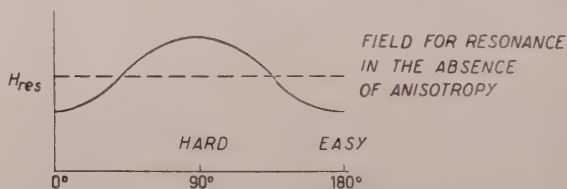


Fig. 18. - Dependence of resonance field on angle from crystal axis in a uniaxial crystal with positive anisotropy.

angle θ with respect to the easy axis, it is easy to show that, for a microwave field at fixed frequency, the value of H at which resonance occurs as a function of θ is of the form shown in Fig. 18. For H not much greater than H_a , the solution is more complicated. KIP and ARNOLD found an extra resonance line for such a case in a SiFe crystal, and such extra lines have since been observed by others.

12. - g -values.

The spectroscopic splitting factor g is defined from the equation for the frequency at which ferromagnetic resonance occurs after all corrections due to sample shape, etc. have been made:

$$\hbar\omega = g\mu_B H_{\text{eff}}.$$

Microwave resonance experiments usually give values of g ranging between 2.1 and 2.3. In Einstein-de Haas and Barnett magnetomechanical experiments one finds factors g' with values often in the range 1.86 to 1.92. As we shall see the two types of experiments actually measure different, but related,

quantities. The theory of the effect of spin-orbit interaction suggests that g and g' should be related by the equation

$$(1) \quad g - 2 \cong 2 - g'.$$

The Einstein-de Haas experiment measures the rotation of a freely suspended sample when an applied magnetic field in the vertical direction is reversed. We have

$$\Delta M = \text{change in magnetization} = \Delta(M_{\text{spin}} + M_{\text{orb}} + M_{\text{latt}}),$$

$$\Delta J = \text{change in ang. momentum per unit vol.} = \Delta(J_{\text{spin}} + J_{\text{orb}} + J_{\text{latt}}),$$

M_l is negligible since it is of order $m/M \sim 10^{-4}$ with respect to the other contributions; here m is the electronic mass, and M is the ionic mass. Since $\Delta J = 0$ when the field is reversed

$$\Delta J_l = -\Delta(J_s + J_0),$$

and the experiment measures the ratio

$$\left| \frac{\Delta M}{\Delta J_l} \right| = \left| \frac{\Delta(M_s + M_0)}{\Delta(J_s + J_0)} \right|.$$

Recalling the wave functions discussed by PRYCE for the case when spin-orbit interaction couples two levels separated by an energy Δ , we consider a quantity

$$\varepsilon \approx -\frac{\lambda}{\Delta},$$

where λ is the spin orbit coupling constant. If we define ε by $M_0/M_s = \varepsilon$, then we have $J_0/J_s = 2\varepsilon$. Then

$$\frac{\Delta M}{\Delta J_l} = \frac{M_s}{J_s} \frac{(1 + \varepsilon)}{(1 + 2\varepsilon)} \cong \frac{2e}{2mc} (1 - \varepsilon) = \frac{g'e}{2mc}.$$

Therefore

$$g' \cong 2(1 - \varepsilon).$$

In microwave resonance wave functions involved are such that the spin change absorbs all the angular momentum in the radiation field to first order so that $\Delta J_0 + \Delta J_l = 0$ and

$$\frac{d}{dt} \mathbf{J}_s = (\mathbf{M}_s + \mathbf{M}_0 + \mathbf{M}_l) \times \mathbf{H}.$$

On neglecting M_l this becomes

$$\frac{d}{dt} \mathbf{J}_s \cong (\mathbf{M}_s + \mathbf{M}_0) \times \mathbf{H}.$$

So

$$\gamma = \frac{ge}{2mc} = \frac{M_s + M_0}{J_s} = \frac{2e}{2mc} (1 + \epsilon).$$

Then

$$g = 2(1 + \epsilon),$$

and

$$g - 2 \cong 2 - g'.$$

Experimentally one finds for Fe, Ni and FeNi alloys that $g - 2$ is somewhat larger than $2 - g'$. Measurements of g in FeNi alloys at three frequencies by HOSKINS and WIENER show that g depends on frequency in the manner shown

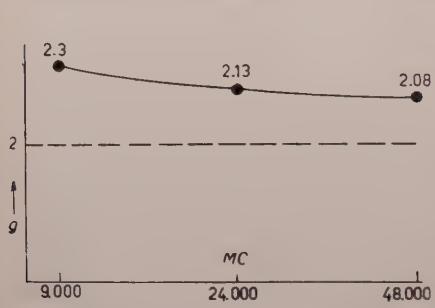


Fig. 19. - Schematic variation of g with frequency in FeNi alloys.

in Fig. 19. The value 2.08 is almost low enough to satisfy (1). To agree with these experiments and also to satisfy (1), one requires an effective internal field H_i of the order of 200 Oe on the $3d$ electrons so that

$$\hbar\omega = g\mu_B(H + H_i).$$

Such a field could arise from the Zener-Vonsovsky mechanism for ferromagnetism in which the $3d$ electron spins are coupled indirectly by exchange interaction with the $4s$ electron spins. The resulting reaction of the $4s$ magnetization on the $3d$ electrons gives rise to H_i . If S is a $3d$ electron spin and s is a $4s$ electron spin, then

$$\mathcal{H}_{\text{ex}} = -AS \cdot s,$$

and the magnetization of the $4s$ electrons is

$$M_{4s} \approx N\mu_B \left(\frac{A}{E_F} \right),$$

where E_F is the Fermi energy and N the number of $4s$ electrons per unit

volume. Then

$$H_i \approx \frac{A}{E_F} \frac{A}{g\mu_B}.$$

To get $H_i \approx 100$ Oe, we must have $A \approx 1/100$ eV. This magnitude of A is of course much too small to explain the ferromagnetic transition temperature, which would require that A be of the order of $\frac{1}{2}$ eV.

The value of A needed to explain H_i is of interest for another reason, namely that \mathcal{H}_{ex} can provide a relaxation mechanism for the $3d$ electrons in the same way that the $\mathbf{I} \cdot \mathbf{S}$ interaction relaxes nuclear spins. The fact that $\mathbf{S} \cdot \mathbf{s}$ commutes with $\mathbf{S} + \mathbf{s}$ does not affect the validity of this argument if the $4s$ electrons have an additional interaction with the lattice which would enable them to relax much more quickly than the $3d$ electrons. The Elliott spin-orbit mechanism probably provides this. For $A \approx 1/100$ eV, MITCHELL computes a spin-lattice relaxation time of $\approx 10^{-8}$ s for the $3d$ electrons, which is of the order of magnitude of the observed time.

13. - Spin waves in antiferromagnetics and ferrites.

For an antiferromagnetic array as in Fig. 20*a*, we picture the spins on the two sublattices precessing about crystalline anisotropy fields H_a oriented in opposite directions for the two sublattices. Neighboring spins precess in opposite directions as in Fig. 20*b*, getting in and out of phase with each other as in Fig. 20*c* and 20*d*. The effective field acting on the spins is different for 20*c* and 20*d*, being approximately $2H_{\text{ex}} + H_a$

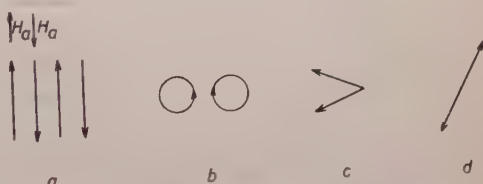


Fig. 20. - Antiferromagnetic resonance.

for the former case and H_a for the latter. The resultant effective field will be the geometric mean of these two fields, following procedures we used in the ferromagnetic resonance case:

$$H_{\text{eff}} = \sqrt{H_a(2H_{\text{ex}} + H_a)}.$$

For $H_{\text{ex}} \approx 10^6$ Oe and $H_a \approx 10^4$ Oe, we get $H_{\text{eff}} \approx 10^5$ Oe corresponding to an interaction energy of 0.1 cm^{-1} for the lowest ($k = 0$) spin waves. One must therefore heat such an antiferromagnet up to $\sim 10^\circ$ K before exciting spin waves. This threshold energy for the excitation of spin waves leads to an exponential dependence on temperature for the spin contribution to the specific heat in the low temperature region.

For higher energy spin waves we do not change the term $2H_{\text{ex}} + H_a$ for

the Fig. 20c case, but we change the term H_a of the Fig. 20d case to

$$H_a + \frac{Ja^2k^2}{g\mu_B}.$$

For

$$\frac{Ja^2k^2}{g\mu_B} \gg H_a,$$

the energy of the spin waves is then linear in the wave vector k , leading to a T^3 contribution to the heat capacity, the same as for phonons. For a ferrite there are two or more branches in the $E(k)$ vs. k curve.

14. - s - d interaction.

We will discuss one aspect of the work of OWEN *et al.*, concerning the s - d exchange interaction in Cu-Mn alloys. Mn^{++} has five electrons in the $3d$ shell and a total spin of $\frac{5}{2}$. For low Mn concentrations, one might expect the Mn^{++} to substitute for Cu^+ , the $4s$ electrons of the Mn becoming conduction electrons along with those of the copper.

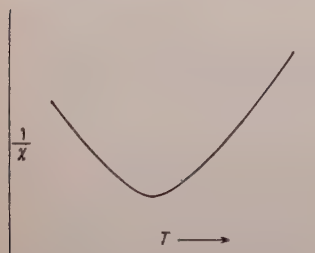


Fig. 21. - Susceptibility of dilute solid solution of Mn in Cu.

The exchange interaction between $3d$ core electrons and a $4s$ electron in Mn^+ is known from spectroscopic data to be of the order 9400 cm^{-1} or somewhat over 1 eV . Allowing for screening by the conduction electrons, one might expect an exchange interaction between a $4s$ conduction and a Mn ion core of $\approx \frac{1}{3} \text{ V}$. The Cu-Mn system therefore seemed suitable for the observation of ferromagnetism produced by the indirect exchange

mechanism of ZENER, PAULING and VONSOVSKY. Fig. 21 shows the experimentally observed plot of $1/\chi$ vs. T . This plot indicates the onset of antiferromagnetism so that another interaction must be present.

The electronic Knight shift of the Mn^{++} $3d$ electron resonance is expected to be proportional to A^2 , while the Cu nuclear resonance Knight shift should be proportional to Aa . Here A is the coupling constant in the $AS \cdot s$ interaction between $3d$ and $4s$ electrons, and a is the hyperfine coupling constant between Cu nuclei and the $4s$ conduction electrons.

For 0.03% Mn, the Néel temperature is safely below 1°K . At 1°K the Mn^{++} ion cores may be polarized by brute force with a field of $10\,000 \text{ G}$. Under such conditions one calculates that the Cu nuclear Knight shift would be 6 times that of pure copper if the s - d interaction were 1 eV . Experiment-

ally one finds the Knight shift to be less than 1/10-th that in pure copper. Taking account of the demagnetizing field, one deduces that the polarization of the 4s electrons is less than perhaps 1/50-th of that expected. The explanation of this discrepancy is not yet known. It does not seem to be adequate to stop the perturbation calculation with the first order term.

15. - Ferrites.

The simplest ferrites are of the form MFe_2O_3 , where M is a divalent cation such as Mn, Co, Ni, Cu, Mg, Zn, Fe^{++} , Cd, or some mixture of these. Ferrites have acquired great practical interest because of their high resistivities which are in the range 10^{-2} to $10^8 \Omega \text{ cm}$.

The fact that Fe^{++} and Fe^{+++} have magnetic moments of $4\mu_B$ and $5\mu_B$ respectively would lead to a saturation moment of $14\mu_B$ per molecule in $\text{Fe}^{++}\text{O Fe}_2^{+++}\text{O}_3$ if all the magnetic moments were lined up in the same direction. The observed saturation magnetization of magnetite is $4.07\mu_B$ per molecule. A simple model to explain this characteristic behavior of the saturation magnetization in ferrites has been proposed by Néel. He suggests that the two Fe^{+++} spins are lined up antiparallel to each other; the observed magnetic moment arises in effect only from the Fe^{++} spins.

From the spinel structure of this substance, one recognizes two types of environments for the magnetic ions:

A - sites surrounded by 4 oxygens on a tetrahedron, Fe^{+++} ;

B - sites surrounded by 6 oxygens on an octahedron, Fe^{++} , Fe^{+++} .

There will then be three types of interaction: A-A, B-B and A-B. All of these are assumed by Néel to be antiferromagnetic interactions. In order for A and B to be antiparallel, the A-B interaction must be the strongest. All the A's are forced to be parallel, and all the B's are forced to be parallel when the A-B interaction is strongly antiferromagnetic. Thus from $9\mu_B$ per molecule on B and $5\mu_B$ per molecule on A, we arrive at the saturation magnetization by subtraction. A comparison of the susceptibility of ferrites with antiferromagnetic and ferromagnetic substances is shown in Fig. 22. The solid line shows the behavior of ferrites.

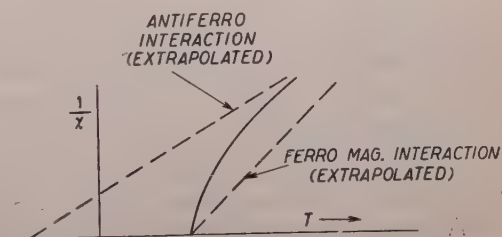


Fig. 22. - Susceptibility of a ferrite above the Curie temperature.

The structure described above, with trivalent ions on each type of site, is

called the inverse spinel structure. The normal spinel is typified by the $\text{ZnO Fe}_2\text{O}_3$ ferrite which has Zn^{++} on the A sites and Fe^{+++} on the B sites. Neutron diffraction studies show antiferromagnetism at low temperatures which indicates an anti-parallel alignment of Fe^{+++} . The details of the observed antiferromagnetism, such as the sublattice structure and the low Néel temperature, are not explained by the simple Néel theory.

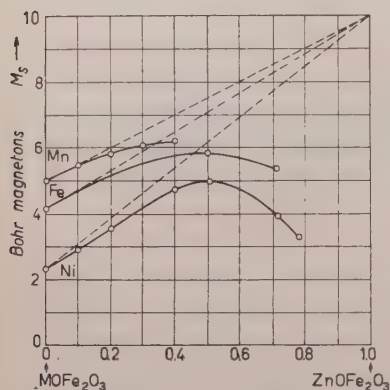


Fig. 23. — Saturation magnetization of mixed Mn-Zn, Fe-Zn, and Ni-Zn ferrites, as a function of the zinc content. [After J. J. WENT and E. W. GORTER].

The line width, ΔH , observed in microwave resonance in ferrites is found sometimes to increase at lower temperatures. The mechanism proposed by Galt to explain this line broadening is that an exchange of charge may be taking place between Fe^{++} and Fe^{+++} , i.e.



This type of exchange is analogous to electron diffusion. The maximum effect on the line width will occur when the exchange frequency approaches the relaxation frequency. Thus if the exchange is much faster than the relaxation frequency at high temperatures, the effect of lowering the temperature is to lower the exchange rate and thus make it more effective in broadening the line. At a sufficiently low temperature, one expects a maximum in ΔH according to this mechanism.

J. K. GALT, using a hollow ferrite rectangle cut along the easy axis found that

$$\frac{v}{H} = \frac{\text{velocity of Bloch wall}}{\text{external field}} = \text{constant}.$$

The relaxation time he evaluated from the observed velocity agreed with the relaxation time evaluated from the line width in microwave resonance.

Fig. 23 shows the effective magnetic moment « per molecule » of the mixed ferrite $\text{Zn}_x\text{M}_{1-x}\text{O Fe}_2\text{O}_3$ as a function of x . It is consistent with the Néel picture; the addition of Zn is assumed to squeeze the Fe^{++} ions out of the tetrahedral sites.

16. — Spin resonance in ferrites.

The g -values are unaffected by the exchange interactions in the common ferrites. One can compound in an appropriate way the g -values of the individual ions and obtain the observed g -values.

17. - Some spin wave aspects of ferrites.

As mentioned earlier, the lower branch of the $E(k)$ vs. k curve should be parabolic in an ideal ferromagnet. For a spherical specimen this is satisfied, but for other geometries it may be shown that the energy of $k \approx 0$ spin waves will be shifted because of the effect of the demagnetizing field, as indicated in Fig. 24. The $E(k)$ vs. k curves for the different geometries should join the k^2 curve in some manner as indicated by the dotted lines. The $k = 0$ state will therefore be degenerate with states of higher k for some geometries. This degeneracy will enable the $k = 0$ state to be mixed by crystal magnetic imperfections with higher spin wave states rather easily and provides a mechanism for the broadening of the microwave absorption line. Workers at the Bell Laboratories are reported to have observed geometrical effects on the microwave absorption line width.

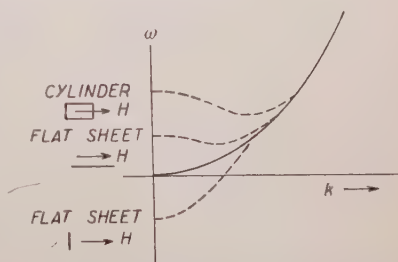


Fig. 24. - Spin wave spectrum for various specimen geometries.

18. - Microwave gyrator.

A ferrite magnetized as indicated in Fig. 25 rotates the plane of polarization of microwaves incident upon it. Going in the opposite direction, the plane of polarization is rotated again in the same sense. The gyrator is very useful in isolating the source in microwave equipment from reflected waves. If microwaves from a rectangular wave guide are passed through a gyrator arranged to rotate the plane of polarization by 45° , the reflected wave, upon passing back through the gyrator, will be rotated through another 45° and will not be accepted by the original rectangular wave guide.

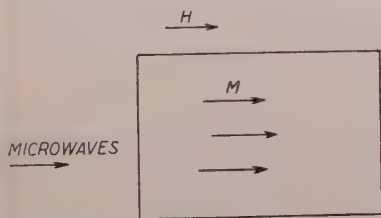


Fig. 25. - Gyrator arrangement.

The angle through which a plane polarized wave is rotated is given by

$$\vartheta \cong \frac{1}{2c} \sqrt{\epsilon} \frac{ge}{2mc} 4\pi \tilde{M} l,$$

where \tilde{M} is the average magnetization of the ferrite, l is its length and ϵ is the dielectric constant.

This result may be derived most easily by substituting

$$\frac{d\mathbf{M}}{dt} = \gamma \mathbf{M} \times \mathbf{H},$$

directly into the Maxwell equation

$$\nabla \times \mathbf{E} = -\frac{1}{c} \left(\frac{d\mathbf{H}}{dt} + 4\pi \frac{d\mathbf{M}}{dt} \right).$$

Antiferromagnetism.

C. J. GORTER

Kamerlingh Onnes Laboratorium der Rijksuniversiteit - Leiden

1. - Introduction: molecular field model.

Experimental facts connected with antiferromagnetism are known for a considerable time, mainly from work done by the schools of HONDA, WEISS, and KAMERLINGH ONNES. These early investigations were done on crystal powders like Cr_2O_3 , NiCl_2 , CoCl_2 , FeCl_2 , CuSO_4 . In these materials the susceptibility follows the Curie-Weiss law with positive or negative θ quite well at higher temperatures, but shows an anomalous behaviour at lower temperatures (see Fig. 1). Below the transition point (Néel temperature), the magnetization M is not a linear function of the magnetic field H . This is illustrated in Fig. 2 for FeCl_2 . Some hysteresis effects are also sometimes apparent. More recently, SCHUBNIKOV observed an anomaly in the specific heat, having the shape of a λ point, at the Néel temperature (Fig. 3).

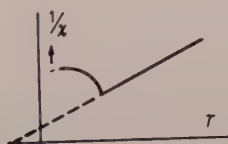


Fig. 1.

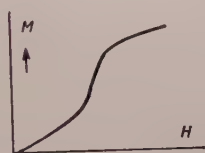


Fig. 2.

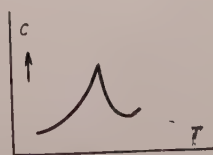


Fig. 3.

BIZETTE found that dilution by non-paramagnetic salts lowers the Néel temperature. KURTI and SIMON found similar abnormal behaviour below 0.1°K in materials which follow Curie's law quite well above this temperature (e.g. iron- and chromium alums).

The anomalous behaviour described above, and other similar effects, were called cryogenic anomalies. They remained unexplained till the thought of

antiferromagnetism was put forward independently by NÉEL, LANDAU and KRAMERS.

NÉEL in 1932 was the first to suggest that in paramagnetic samples an arrangement of alternating spins might occur. This is shown schematically in Fig. 4 and 5. Such an arrangement was supposed to be caused by an exchange-interaction similar, but of opposite sign, to the ferromagnetic interaction. NÉEL developed a theory based on the Weiss concept of the molecular field. He considered the crystal lattice to consist of two sublattices, having opposite directions of ionic magnetic moments.



Fig. 4.



Fig. 5.

A ion in one sublattice will be exposed to an effective field H_{eff} , consisting of the external field H and a molecular field proportional to the opposite of the magnetization of the other sublattice. NÉEL wrote accordingly

$$(1) \quad \begin{cases} H'_{\text{eff}} = H - A M'' \\ H''_{\text{eff}} = H - A M' \end{cases}$$

where the quantities with one prime refer to one sublattice, and the quantities with double prime refer to the other sublattice. The magnetization per ion of the sublattices is then given by

$$(2) \quad \begin{cases} M' = \mu \tanh \mu H'_{\text{eff}} / kT \\ M'' = \mu \tanh \mu H''_{\text{eff}} / kT \end{cases}$$

and the total magnetization per ion by

$$(3) \quad M = (M' + M'')/2.$$

Similar ideas were put forward by LANDAU (1933). Landau's starting point was the observation that the anhydrous chlorides, which show cryogenic anomalies, have a layer structure. He assumed that a ferromagnetic interaction exists between the ions in each layer, tending to put the spins parallel, while an interaction of opposite sign exists between ions in adjacent layers (Fig. 4).

In a later paper NÉEL also adopted the idea of a ferromagnetic interaction

within each sublattice. The equations for the effective field become then

$$(4) \quad \begin{cases} H'_{\text{eff}} = H - AM'' + DM' = H - (A + D)M'' + 2DM \\ H''_{\text{eff}} = H - AM' + DM'' = H - (A + D)M' + 2DM. \end{cases}$$

The interaction energy is given by

$$(5) \quad U = \frac{1}{2}N[AM'M'' - \frac{1}{2}D(M'^2 + M''^2)] = \frac{1}{2}N[(A + D)M'M'' - 2DM^2].$$

The second form of the above equations is most suggestive below the Néel temperature where the material is antiferromagnetic, while the first form is the more natural one above the Néel temperature, where the Curie-Weiss law

$$C/[T - \mu^2(A - D)/k]$$

applies.

KRAMERS (1934) based his treatment on the Heisenberg theory of ferromagnetism. He asked himself what would happen if the sign of the exchange interaction is the opposite to the one giving ferromagnetism. A mathematical treatment carried out in co-operation with HULTHÉN for the case $T = 0^\circ\text{K}$ results in the conclusion that even in this case a completely regular alternating arrangement of the spins would not occur. Nevertheless there is a pronounced tendency of the spins to be surrounded by spins of opposite sign. This theory was further developed by ANDERSON, who arrived at the conclusion that the chance of finding opposite neighbouring spins is high, of the order of 0.90, but still not one at $T = 0^\circ\text{K}$. Kramers' theory is the most exact, but its mathematical difficulties are great, especially for $T \neq 0$ where the so-called spin wave theory should apply.

At an early stage in the development of his theory NÉEL already considered the possibility that the two sublattices are not completely identical. In such materials $M \neq 0$ at $T = 0$; $H = 0$. This behaviour was called ferromagnetism by NÉEL.

What is the direct experimental evidence for the existence of an antiferromagnetic state? At the Néel temperature, below which the alternating arrangement of the spin starts, there occurs a loss of symmetry of the crystal.

This can be observed by a rapid but gradual change in lattice constant and in elastic properties.

The sublattices as such cannot be distinguished by X-rays as the X-ray scattering is independent of spin.

However in some cases a small loss in symmetry of the crystal structure can be observed below the Néel temperature. Neutron diffraction experiments do give direct evidence as to the existence of the sublattices. As neutrons

have a spin $\frac{1}{2}$, their scattering is spin dependent. SHULL, ERICKSON and others have made important contributions using this technique.

A totally different proof as to the physical reality of the sublattices has been obtained by POULIS in Leiden.

POULIS studied the proton magnetic resonance spectrum of single crystals of $\text{CuCl}_2 \cdot 2\text{H}_2\text{O}$.

Because of dipole-dipole interaction with the neighbouring cupric ions, the protons show a number of resonance frequencies. Fig. 6 shows schematically the proton frequencies as function of crystal orientation as the crystal is turned about one of its principal axes. This figure shows a periodicity of 180° in the angle φ as it is to be expected for dipole-dipole interaction, when the average spin moment of the cupric ions adjusts itself in the direction of the magnetic field. The above pattern is observed above the Néel temperature. On passing the Néel temperature the pattern changes abruptly to the one indicated in Fig. 7, showing at not too high fields a periodicity of 360° . This is understandable if the ionic moments are no longer free, but turn with the crystal lattice, as is the case in the antiferromagnetic state. The symmetry of this figure is proof of the existence of the two sublattices.

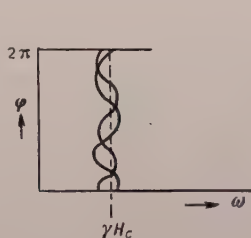


Fig. 6.

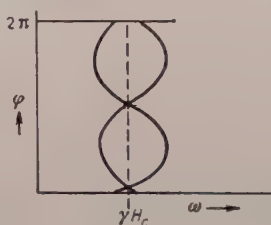


Fig. 7.

2. - Three types of solutions in a orthorhombic crystal.

We will now discuss the solutions of the Néel equations for a crystal of orthorhombic symmetry. For simplicity twofold degenerate levels and an isotropic magnetic moment will be assumed. The following form of the equations will be adopted:

$$(6) \quad \begin{cases} H'_x = H - A_x M''_x + D_x M'_x \\ H''_x = H - A_x M'_x + D_x M''_x \end{cases}$$

and similar equations for the y - and z -components;

$$(7) \quad M'_x = \frac{\mu H_x}{(H_x'^2 + H_y'^2 + H_z'^2)^{\frac{1}{2}}} \tanh \frac{\mu(H_x'^2 + H_y'^2 + H_z'^2)^{\frac{1}{2}}}{kT},$$

and similar equations for $M''_x, M'_y, M''_y, M'_z, M''_z$. We have accordingly 12 equations with 12 unknowns.

It should be remarked that the way in which the anisotropy energy has been introduced in the above equations is different from the form used generally in the theory of ferromagnetism. In the latter case the anisotropy is taken to be determined by the angle between magnetization direction and crystal axes, the relevant energy terms being e.g. of the form:

$$K_x \frac{M_x^2}{M_x^2 + M_y^2 + M_z^2} + \text{cyclic permutations}.$$

In the formulation used here the anisotropy energy is given by terms of the following general form:

$$(N/2)D_x \frac{M_x'^2 + M_x''^2}{2} + \text{cyclic permutations}.$$

The physical interpretation of this equation is that the anisotropy energy is the result of the interaction between crystalline field and magnetic moments. The main difference with the first equation is the absence of the normalizing denominator. NÉEL in his theory uses the first form, and sometimes takes the anisotropy constants K to be experimentally adjustable parameters which are functions of T . YOSIDA also uses the first form, but assumes the K 's to be proportional to $|M|^2$. This is essentially equivalent to the present formulation. In the present treatment the A 's and B 's will be taken to be independent of temperature.

We will first discuss the solution of (6) and (7) for the case $T=0$. Then the tgh is equal to 1. Even with this restriction we have 6 linear equations and 6 equations of the 4-th degree in M . Some of the unknowns can be eliminated and 8 equations of the second degree obtained. These equations have $2^8 = 256$ solutions. With the co-operation of the late Prof. HAANTJES these solutions have been discussed. It turns out that some of the solutions have been introduced by squaring of equations, some are identical, others have no physical meaning. After eliminating all non relevant solutions four remain, of which one can be shown always to be thermodynamically unstable.

We will discuss the remaining three solutions for the simplest case that H is in the direction of antiferromagnetic alignment. We choose the axes so that

$$H_x = H, \quad H_y = H_z = 0$$

$$(A_x + D_x) > (A_y + D_y) > (A_z + D_z).$$

The three solutions are then

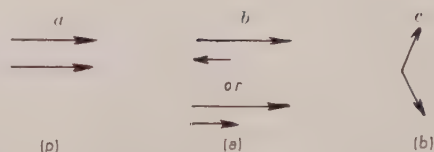


Fig. 8 *a-b-c*.

- 1) The *p*-solution (paramagnetic solution), characterized by

$$M'_x = M''_x; \quad M'_y = M''_y = M'_z = M''_z = 0. \quad (\text{Fig. 8a}).$$

- 2) The *a*-solution (antiferromagnetic), characterized by

$$M'_x \neq M''_x, \quad M'_y = M''_y = M'_z = M''_z = 0 \quad (\text{Fig. 8b}).$$

- 3) The *b*-solution (antiferromagnetic), characterized by

$$M'_x = M''_x, \quad M'_y = -M''_y, \quad M'_z = M''_z = 0 \quad (\text{Fig. 8c}).$$

It should be remarked that if D is very large in the y -direction, while A is very large in the x direction, two more solutions are possible. These solutions have not yet been analyzed in detail and, as they will only appear in very special cases, they will be disregarded here.

3. - Discussion of the above solutions.

In principle the solutions can be obtained by computing the free enthalpy and then minimizing the latter. This has been done by NÉEL for the case $T=0$. For an arbitrary temperature the minimizing process becomes impracticable. With the co-operation of Mrs. VAN PESKI the equations have been solved for arbitrary temperature by using a graphical method, based on the classical construction given by WEISS for the ferromagnetic case. In the latter case the two equations

$$H_{\text{eff}} = H + \lambda M,$$

$$M = \mu \tanh \frac{\mu H_{\text{eff}}}{kT},$$

have to be solved for M . The Weiss construction consists simply of plotting M as function of H_{eff} (Fig. 9). The first equation gives a straight line HP and the second the S -shaped curve (Langevin-function, \tanh , or Brillouin function).

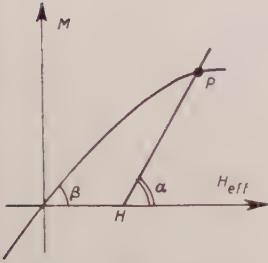


Fig. 9.

The solution is the point of intersection P . It will be observed that if $\alpha > \beta$ the material is paramagnetic: at $H = 0$ there is no intersection except the origin at which $M = 0$.

If $\alpha < \beta$ the material is ferromagnetic, as it can be easily shown that of three intersection points, the one at the origin is unstable and the two other points represent states of spontaneous polarization. The condition $\alpha < \beta$ gives the well-known condition for the existence of ferromagnetism $1/\lambda < \mu^2/kT$.

Applying now the Weiss construction to the case of antiferromagnetism, we have for the p -solution: $M'_x = M''_x$, while the y - and z -components are zero. Eqs. (6) and (7) reduce accordingly to the two eqs.

$$H'_x = H''_x = H - (A - D)M'_x$$

$$M'_x = M''_x = \mu \tanh \frac{\mu H'_x}{kT},$$

and the Weiss construction applies directly. Point P in Fig. 10 represents accordingly the p -solution.

In order to obtain the a -solution a straight line RS is drawn, making an angle $\arctg 1/(A + D)$ with the H'_x -axis. The position of this line is such that $AR = AS$. Point A then gives the a -solution. That this is true can easily be seen by subtracting and adding eqs. (6).

Dropping the suffix x we obtain

$$\frac{H' + H''}{2} = H - (A - D) \frac{M' + M''}{2},$$

$$H' - H'' = (A + D)(M' - M'').$$

The first of these equations describes the line HP , and the second the line QRS . The point R corresponds to the values H'' ; M'' ; point S to H' ; M' and A to $(H' + H'')/2$; $(M' + M'')/2 = M_r$.

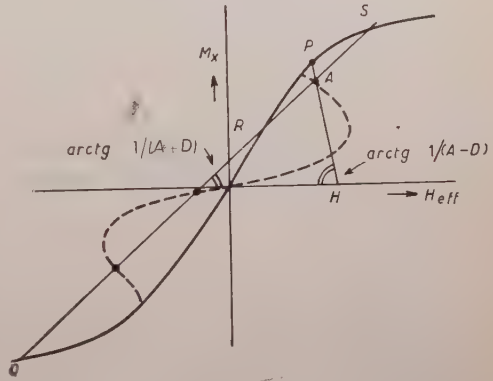


Fig. 10.

As the line QRS is shifted parallel to itself the center points of the sections QR , RS and QS describe a locus, indicated, by the dotted line in the figure.

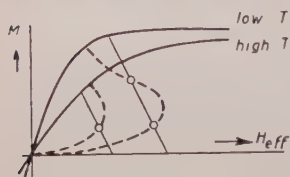


Fig. 11.

We shall now discuss the behaviour of the p - a - and b -solutions as a function of the temperature T and the external field H . In the construction used in Fig. 10. for the p - and a -solutions, the Brillouin curve depends on the temperature, and the locus of midpoints used in this construction therefore also changes with temperature, as shown by the dashed curves in Fig. 11.

The antiferromagnetic solution can occur only if $1/(A+D) < \mu^2/kT$, i.e. for $T < T_N = (A+D)\mu^2/k$. For $T > T_N$, the locus of midpoints, and hence the antiferromagnetic solution, has disappeared.

For small H , the a -solution has $M'' \approx -M'$, while for increasing H the quantity M' increases and $|M''|$ decreases. This gives rise to a susceptibility which increases with increasing H , and which (for small H) is smaller the lower T is. We get three possibilities according to whether the line through the point H cuts the locus of midpoints in 1, 2 or 3 points.

1) If there is one intersection, we get an a -solution which simply ends in the p -solution at a certain value of H , where the a - and p -solutions have become identical. The transition is of the second order: there is no jump in M and the free enthalpy G and its first derivative

$$M = -\frac{\partial G}{\partial H},$$

are continuous. The drawn curves in Fig. 12 correspond to the thermodynamically stable solutions, since they correspond to the lowest value of G . The curve $G(H)$ can be obtained by integrating the curve $M(H)$.

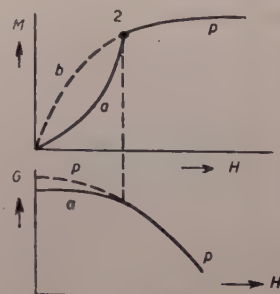


Fig. 12.

2) If there are two intersections we get a G -curve somewhat similar to that pertaining to the gas-liquid transition. We now get a first-order transition such that the two hatched surfaces in Fig. 13 are of equal area. There now occurs a jump in M .

The drawn curves are again the thermodynamically stable states, as they correspond to the lowest G value.

3) If there are three intersections we get a first order transition within the a -solution and a second-order transition into the p -solution (Fig. 14).

The first-order transitions occurring in the cases 2) and 3) disappear above a certain temperature,

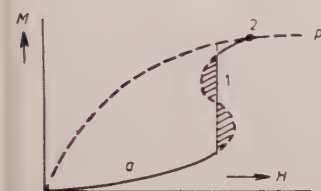


Fig. 14.

which in case 2) is a second-order a - p transition point, while in case 3)

a critical point occurs which is quite similar to the critical temperature. At these points the triangle appearing in the G -curve of a liquid-gas transition has contracted to a point, similar to what occurs at the gas-liquid critical temperature.

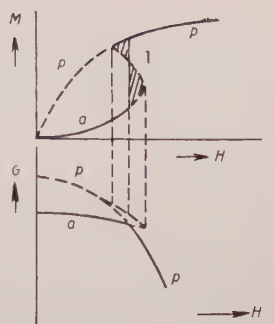


Fig. 13.

4. - Phase diagrams.

We shall now construct the corresponding phase diagrams. We shall first leave the b -solution out of consideration. The phase diagram for the a - p transition is drawn in Fig. 15.

H_x may also be negative, and the diagram is symmetrical around the T axis. Below $T = \mu^2(A_x + D_x)/k$, the a -solution is realized up till a certain value of H_x where the a -solution goes over in the p -solution.

The second order line reaches the H_x axis at the point $\mu_x(A_x - D_x)$. This part of the curve is often not realized, however, in view of the neighbouring first order transition line.

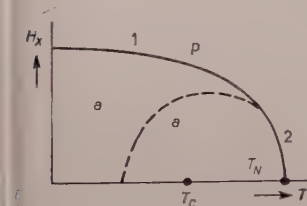


Fig. 16.

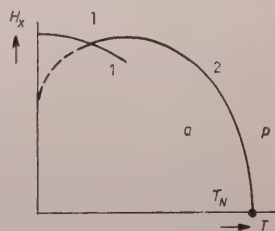


Fig. 15.

A different diagram is obtained if $D_x > A_x$, as in the theory of Landau for instance. Then $(A_x - D_x)$ becomes negative, and we may get the following diagram (Fig. 16).

Near the origin there is now an unstable ferromagnetic region, the ferromagnetic line on the T axis ending at a point $T_c = \mu^2(D_x - A_x)/k$.

p-solution. - For $H_x = 0$ the magnetizations now are along the $\pm y$ axis: $M'_y = -M''_y$. With increasing H_x , M' and M'' approach the x axis and finally

the p -solution is reached again. The susceptibility becomes independent of H and T for this solution,

$$M_x = \frac{H_x}{(A_x + A_y - D_x + D_y)}.$$

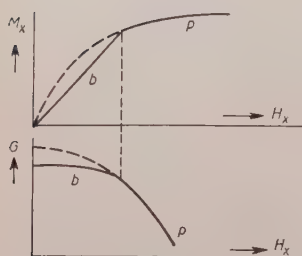


Fig. 17.

The transition from b - to p -solution (Fig. 17) is of the second order. The drawn curves again correspond to the thermodynamically stable solutions.

In the molecular field approximation one often encounters equations of the form:

$$M = H_{\text{eff}}/\lambda = \mu \operatorname{tgh} (\mu H_{\text{eff}}/kT).$$

Putting

$$t = \frac{kT}{\lambda\mu^2} \quad \text{and} \quad p = \frac{M}{\mu},$$

we get

$$p = \operatorname{tgh} (p/t)$$

with the solution

$$p = \eta(t),$$



Fig. 18.

where the function η can be obtained graphically (cf. Fig. 9 and Fig. 18).

a-solution. — For $H = 0$ the sublattice magnetizations M' and M'' are given by $\mu\eta(t)$ with

$$t = \frac{kT}{\mu^2(A_x + D_x)}.$$

b-solution. — Here we have:

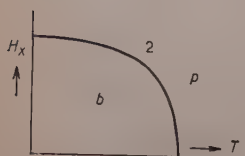


Fig. 19.

with

$$\sqrt{(M'_x)^2 + (M'_y)^2} = \mu\eta(t)$$

$$t = \frac{kT}{\mu^2(A_y + D_y)}.$$

We finally give the phase diagram for the b -solution (Fig. 19). This gives

a single second order line:

$$H_x = \mu(A_x + A_y - D_x + D_y) \cdot \eta(kT/\mu^2(A_y + D_y)) .$$

[cutting the T axis at

$$T = \mu^2(A_y + D_y)/k$$

and the H_x axis at

$$H_x = \mu(A_x + A_y + D_y - D_x)/k] .$$

We have previously discussed two types of phase diagrams for an external field in the preferred direction of magnetic alignment: 1) considering only magnetizations in that direction, (a, p); 2) considering an alignment of the sublattices in two other directions, as well as the paramagnetic state (b, p) (Fig. 20).

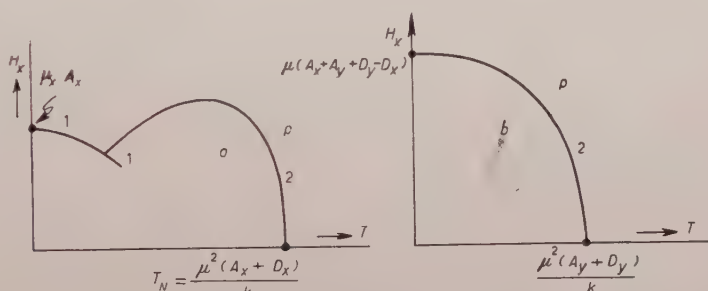


Fig. 20.

In the case for which $(A_y + D_y) > D_x$: there exists the possibility for a transition from the a - to the b -solution, which we shall now consider. In Fig. 21 are shown the magnetization and free enthalpy corresponding to the three different solutions.

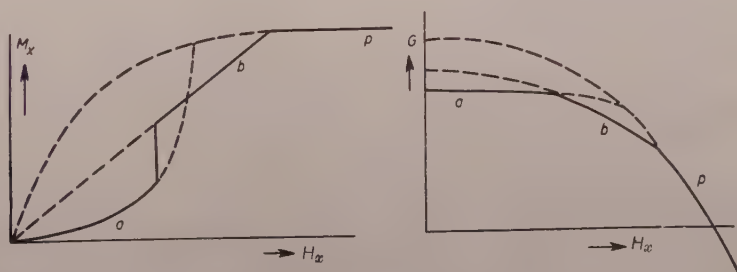


Fig. 21.

At first as the external field increases from zero the a -solution corresponds to the state of lowest free enthalpy, G , and is therefore the stable state.

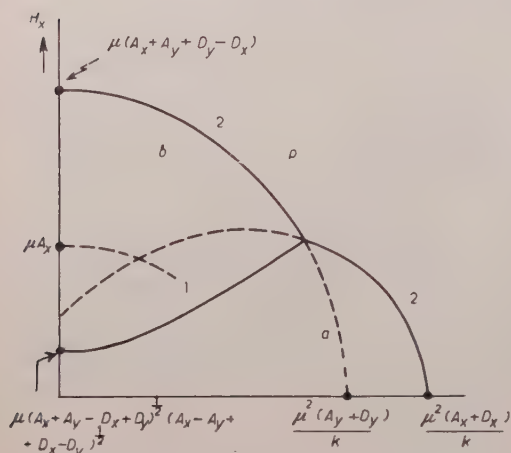


Fig. 22.

parallel to the external field, but as H_x increases a threshold field, which for small anisotropies is given by

$$\mu[2A\Delta(A+D)]^{\frac{1}{2}},$$

is reached at which the sublattice magnetizations become equal in magnitude but do not lie parallel to H_x . Upon further increase of H_x the magnetization

vectors fold in towards H_x .

5. - Other directions of the field.

Now consider the case for which again the preferred direction of magnetization of the sublattices is parallel to x , but now the external field is applied in the y -direction. Then one has only to deal with a solution of the b -type so that the susceptibility in the y -direction varies with the temperature as shown in Fig. 23.

The behaviour for fields applied in the y - and z -directions is similar, so that

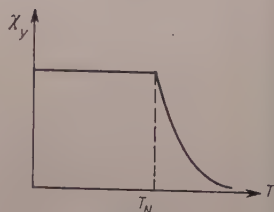


Fig. 23.

in the powder at $T=0$ where $\chi_x = 0$, one has:

$$\chi = \frac{1}{3}(\chi_y + \chi_z),$$

and

$$\frac{\chi(T=0)}{\chi(T=T_N)} = \frac{\chi_y + \chi_z}{\chi_x(T=T_N) + \chi_y + \chi_z} = \frac{2}{3},$$

for small anisotropies.

For applied fields lying in the H_x, H_z plane one also gets a threshold field at which the magnetization jumps discontinuously (Fig. 24). The asymptotes of the threshold hyperbola give information about $A_z + D_z$.

Throughout the foregoing discussion it has been assumed that the A 's and the D 's are temperature independent. This may not be strictly true, and in some cases the experimental data can be explained by using temperature dependent A and D .

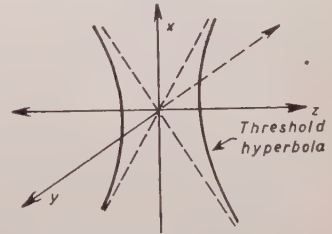


Fig. 24.

6. - Other models.

The antiferromagnetic transitions arise from the exchange energy between an atom and its neighbours and are therefore similar to the order-disorder transitions which occur in alloys. In the alloy case one has to deal with a configurational energy which depends upon the kind of neighbouring atoms surrounding a given atom in the lattice. Arguments similar to those used by BETHE and PEIERLS for the alloys can be applied to the antiferromagnetic transition, and improves the theory in the following respects.

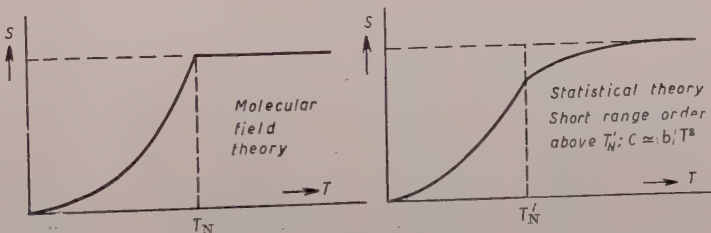


Fig. 25.

1) Above the Néel temperature short range order of the spins still persists, so that the entropy does not become strictly constant above T_N as is predicted by the simple molecular field model which takes into account only long range order (Fig. 25).

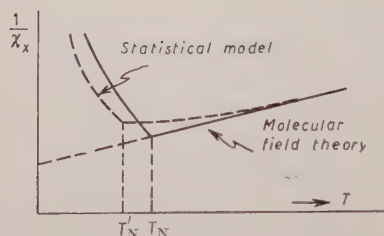


Fig. 26.

2 nearest neighbours. The difference between T_N and T'_N already appears in the susceptibility above T_N (Fig. 26).

2) Given an interaction between neighbouring spins, the Néel temperature, T_N , turns out to be slightly lower than that given by the molecular field model, so that $T'_N < T_N$, where $(T_N - T'_N)$ depends upon the number of nearest neighbours. For a large number of nearest neighbours $(T_N - T'_N)$ is small, but it becomes quite large for only

7. - Spin wave model.

At $T=0$ there is no complete saturation of the spins, i.e. only about 90% of the spins on each sublattice point in the same direction. The spin wave model predicts that for

$$T < \frac{\mu^2}{k} (2A \Delta A)^{\frac{1}{2}},$$

C_v , $(M'_0 - M')$, χ_x all go exponentially to zero, and above this temperature $C_v \sim T^3$, $(M'_0 - M') \sim T^2$, $\chi_x \sim T^2$. M'_0 is the spontaneous magnetization of the sublattice at $T=0$. Also according to spin wave theory, χ_v near $T=0$ should decrease somewhat with increasing temperature.

8. - Hysteresis.

Some antiferromagnetic materials show a very weak ferromagnetic hysteresis, of the order of 0.01 of a percent of the saturation magnetization. This has been explained by NÉEL from the assumption that antiferromagnetic domains exist. Between the domains would exist a gradual transition (wall), shown schematically in Fig. 27. It will be noticed that the number of atoms in the domain wall, which is of the order of ten atoms thick, is such that no regular antiferromagnetic arrangement is possible. NÉEL argues that such a domain wall would have a magnetic moment, which would be the cause of the weak ferromagnetism observed.



Fig. 27.

It should be remarked that the above hysteresis has not been observed in all antiferromagnetic materials, and $\text{CuCl}_2 \cdot 2\text{H}_2\text{O}$ a.o. does not show it.

9. - Experimental data.

We will discuss here only measurements on single crystals, as these give the greatest amount of information and so provide the best test of the theory. The material most investigated is $\text{CuCl}_2 \cdot 2\text{H}_2\text{O}$. Some measurements are also available on single crystals of $\text{CuBr}_2 \cdot 2\text{H}_2\text{O}$, $\text{MnCl}_2 \cdot 4\text{H}_2\text{O}$, $\text{MnBr}_2 \cdot 4\text{H}_2\text{O}$, MnF_2 and a few other halides and oxydes. Measurements on powders have shown antiferromagnetism to exist in a great number of materials.

We will now compare the main features of the molecular field theory with the experimental results.

The existence of a threshold field, corresponding to the a - b transition (Fig. 28) is confirmed experimentally. In $\text{CuCl}_2 \cdot 2\text{H}_2\text{O}$ the threshold field is 6500 Oe at $T=0$, rising to 8500 Oe at the Néel temperature. As at $T=0$

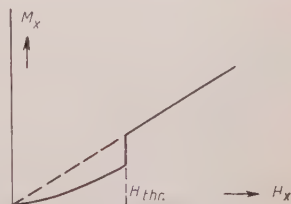


Fig. 28.

$$H_{\text{thr.}} = \mu [2A \Delta(A + D)]^{\frac{1}{2}},$$

the anisotropy $\Delta(A + D)/(A + D)$ can be calculated and is found to be small (about $\frac{1}{2}$ percent), and it is also found to vary little with temperature.

The spin wave theory predicts that in the antiferromagnetic region, except at very low temperatures, χ_x should vary as T^2 , $M'_0 - M'$ as T^2 and C_v as T^3 . This behaviour is found experimentally to a reasonable approximation.

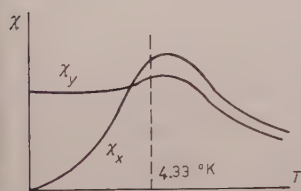


Fig. 29.

The behaviour of χ near the Néel temperature, shows marked deviations from the molecular field theory. Experimental results for $\text{CuCl}_2 \cdot 2\text{H}_2\text{O}$ are shown in Fig. 29. Instead of the sharp maximum at the Néel temperature, χ_x shows a broader maximum somewhat above the Néel temperature, and only a small change of slope at the transition. The behaviour of χ_y is nearly as expected from theory, the weak maximum possibly being due to imper-

fect alignment of the crystal, so that there would actually be some contribution from χ_x .

At temperatures appreciably above the Néel temperature the data for the susceptibility fit a Curie-Weiss law $\chi = C/(T - \theta)$ with θ approximately -4°K which indicates $D \ll A$. The difference in magnitude of χ_x and χ_y far above T_N is due to the anisotropy of the magnetic moment.

Below the Néel temperature (T_N) the molecular field theory gives the relation

$$\chi_y = \frac{1}{2A} \quad \text{while} \quad T_N = \mu^2(A + D)/k.$$

As D is considerably smaller than A , T_N can be calculated approximately from the experimental value of χ . The results of this calculation is $T_N \approx 7.5^\circ\text{K}$, which is not in good agreement with the observed value of $T_N = 4.33^\circ\text{K}$.

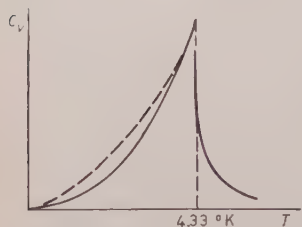


Fig. 30.

The behaviour of the specific heat (C_v) as a function of temperature is sketched in Fig. 30 for $\text{CuCl}_2 \cdot 2\text{H}_2\text{O}$. The solid line represents the experimental results and the dashed line the prediction from molecular field theory. The most evident discrepancy is the « tail » of the experimental curve above the Néel temperature. This tail contains about 35% of the entropy.

The entropy S as function of temperature is given in Fig. 31 and 32. The first of these figures gives theoretical curves for the molecular field model and the second the corresponding experimental curves.

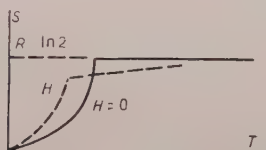


Fig. 31.

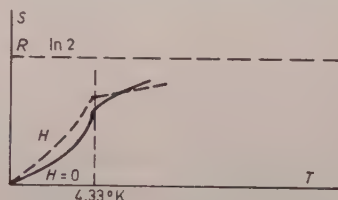


Fig. 32.

From the above discussion it appears that the molecular field model describes the experimental facts reasonably well, appreciable discrepancies occurring only in the temperature range just above the Néel temperature. The experimental curves suggest that some amount of order persists in this temperature range. This is in agreement, at least qualitatively, with the prediction of the Bethe-Peierls theory.

10. – Antiferromagnetic resonance.

In the ferromagnetic state the exchange energy causes no shift of the resonance frequency. This results from the fact, that the effective exchange field H_{exch} is parallel to the magnetization M , so that $\vec{M} \wedge \vec{H}_{\text{exch}} = 0$. In quantum formulation the exchange energy and Zeeman energy commute. The above, however, is not true for the antiferromagnetic state. Here we have two sublattices with different magnetizations. In the molecular field model the total magnetic moment of each sublattice will precess in a magnetic field which is

the sum of the effective field due to the other equally precessing sublattice and the external field. This leads to two resonance frequencies for each value of the external field, and this is what is actually observed.

In a formal treatment we can write down the three Bloch equations for each of the sublattices, obtaining six equations. These equations will give six solutions for the resonance frequencies, of which only two are real and thus have physical meaning. On the basis of the molecular field theory described in these lectures, these solutions have been obtained for the case $T=0$ by UBBINK. The case $T > 0$ has been treated by YOSIDA, who however made a number of simplifying assumptions. Details of the solutions have been worked out by GERRITSEN.

The dependence of the resonance frequencies on the external magnetic field H_x is given in Fig. 33 for the case $T=0$. Even at $H_x = 0$ there are two different resonance frequencies. This is because in the orthorhombic crystal considered here the y - and z -directions are not equivalent. As the external field is increased, one of the frequencies increases, while the other decreases to reach zero at the threshold field. Above the a - b threshold field there exist two branches up to the b - p critical field. At the latter point one of the branches becomes identical with the paramagnetic resonance frequency (the continuation of the dashed line), while the other branch ends on the H_x -axis.

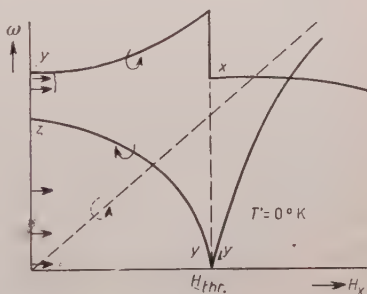


Fig. 33.

In $\text{CuCl}_2 \cdot 2\text{H}_2\text{O}$ this would be in a very large field of about 200 000 Oe. The horizontal arrows indicate the frequencies used in the experimental verification (31 000 ÷ 33 000 MHz; 9 400 MHz; 4 000 MHz; 10 MHz).

11. — Polarization of antiferromagnetic resonance.

The magnetic polarization of antiferromagnetic resonance has been analyzed theoretically and experimentally by GERRITSEN. The two normal modes of oscillation of the magnetizations of the sublattices have been obtained on the basis of the molecular field model. Adding the oscillations of the two sublattices, taking the phase difference into account, gives the magnetic polarization of the radiation. Some results of the calculation of the magnetic polarization have been indicated by letters near certain parts of the resonance curves in Fig. 33 and by the sense of arrows in the case of circular polarisation. In the rising branches the sense of rotation is the same as that in paramagnetic resonance, in the descending branches it has the opposite sense.

At the threshold field, where the transition from the a - to the b -solution occurs, there is a wide range of possible orientations of the magnetization, of resonance frequencies and of polarizations. This is called orientation resonance.

The Fig. 34 and 35 give the much simpler diagrams in case the external magnetic field is orientated in the y - and z -direction respectively.

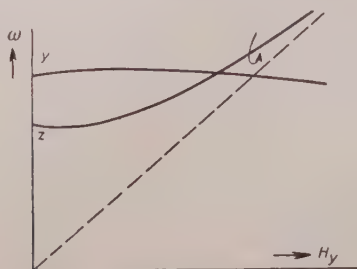


Fig. 34.

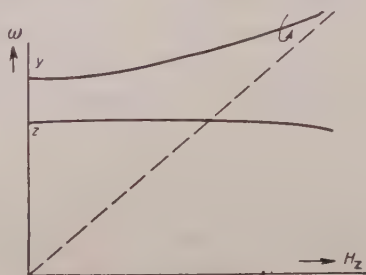


Fig. 35.

All essential results of this analysis have been confirmed by experimental results far below the Néel temperature of $\text{CuCl}_2 \cdot 2\text{H}_2\text{O}$.

12. - Antiferromagnetic resonance at higher temperatures.

When the temperature increases the resonance frequencies at zero field decrease in proportion with the magnetization of the sublattices. Simultaneously the threshold field increases slowly. Just above the threshold field both resonance frequencies differ from zero. At the threshold field itself orientation resonance occurs also at very low frequencies. These are the main

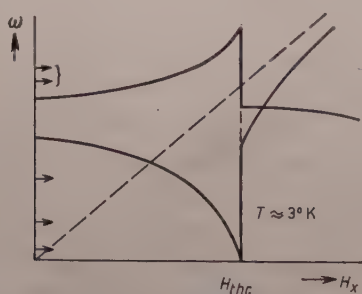


Fig. 36.

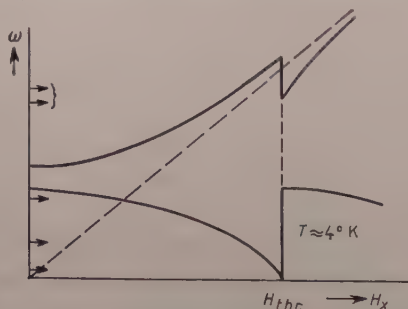


Fig. 37.

differences with the zero temperature case. The Fig. 36 and 37 give a sketch of the resonance diagram in $\text{CuCl}_2 \cdot 2\text{H}_2\text{O}$ at two temperatures.

A few small anomalies in the frequencies and the dependence of the line widths on temperature have not yet been interpreted.

The negative results of the attempts to observe antiferromagnetic resonance in crystals with much higher Néel temperatures indicate that also the anisotropies of the exchange interactions are much larger than in $\text{CuCl}_2 \cdot 2\text{H}_2\text{O}$. This must have increased the required frequencies and fields to such an extent that at the lower temperatures they lie outside the available range. As a matter of fact vague resonances have been observed just below the Néel temperatures.

13. – Proton magnetic resonances.

The proton magnetic resonance measurements of POULIS and HARDEMAN reveal the vector sum of the external field and the local field at the position of the protons. From this a wealth of information on the antiferromagnetic behaviour may be derived. In the introduction (Fig. 7) it was stressed that it produces a straightforward proof of the reality of the two sublattices. Also the structure of the sublattices and the positions of the protons may be derived. Further accurate information is obtained on the value of the Néel temperature and on the a - p and b - p transition lines near it, on the a - b threshold hyperbolae in the a - c plane and on the dependence of the spontaneous magnetization of the sublattices on the temperature.

Quite recently the proton spin relaxation time t_1 has been studied for different temperatures and directions of the field. This time depends on the fluctuations of the magnetizations of the sublattices. It has been analyzed theoretically by BLOOM and Van KRANENDONK and by POULIS and HARDEMAN.

A number of data have also been obtained on proton resonances in other antiferromagnetic crystals.

Les métamagnétiques ou substances antiferromagnétiques à champ seuil.

L. NÉEL

Institut Fourier, Université - Grenoble

1. — Introduction et rappel de résultats antérieurs.

Malgré son peu de rigueur, la théorie du champ moléculaire reste encore aujourd'hui le meilleur guide dans l'interprétation des propriétés magnétiques des substances antiferromagnétiques et ferrimagnétiques: nous voulons l'appliquer ici à une catégorie particulière de substances antiferromagnétiques, douées de propriétés spécifiques, et que nous nous proposons d'englober sous le nom de *substances métamagnétiques*, attribué déjà à certaines d'entre elles par J. BECQUEREL ⁽¹⁾.

La théorie de l'antiferromagnétisme que nous avons proposée depuis assez longtemps ⁽²⁾ consiste à diviser le réseau des ions magnétiques en deux sous-réseaux équivalents *A* et *B* dont nous désignons les aimantations par M_a et M_b . Nous exprimons les différentes interactions d'échange ou de superéchange entre les ions par deux champs moléculaires H_a et H_b , agissant respectivement sur les sous-réseaux *A* et *B* et donnés par les relations:

$$(1) \quad H_a = n' M_a - n M_b; \quad H_b = n' M_b - n M_a.$$

n et *n'* sont deux coefficients de champ moléculaire; le coefficient *n* est essentiellement positif.

A haute température $M_a = M_b$ et la substance obéit à une loi de Curie-

⁽¹⁾ J. BECQUEREL: *Journ. de Phys.*, **10**, 10 (1939); *Réunion Internationale de Magnétisme* (Strasbourg, 1939), tome I, p. 97.

⁽²⁾ L. NÉEL: *Ann. de Phys.*, **17**, 5 (1932); *Journ. de Phys.*, **3**, 160 (1932); *Ann. de Phys.*, **5**, 232 (1936); *Compl. Rend. Ac. Sci.*, **203**, 304 (1936).

Weiss classique; l'aimantation J s'écrit:

$$(2) \quad J = \frac{CH}{T - \theta_p},$$

où C possède la valeur classique de la constante de Curie et où:

$$(3) \quad \theta_p = \frac{1}{2}C(n' - n).$$

Au dessous d'une certaine température T_n , un ordre s'établit dans l'orientation des moments magnétiques et les deux sous-réseaux prennent des aimantations spontanées égales mais orientées en sens inverses l'une de l'autre: nous désignons par $\frac{1}{2}M$ la grandeur de l'aimantation spontanée de chaque sous-réseau. C'est une fonction de la température. Tout se passe comme si chaque sous-réseau était ferromagnétique pour son propre compte et prenait sous l'action d'un champ moléculaire positif $H_m = (n' + n)M/2$ une aimantation spontanée $M/2$. Il en résulte que T_n est donné par:

$$(4) \quad T_n = \frac{1}{2}C(n' + n).$$

A la température $T = T_n$, la susceptibilité s est donnée par:

$$(5) \quad s = \frac{1}{n}.$$

2. - Les différentes catégories de substances antiferromagnétiques.

La valeur de n étant donnée, celle de n' n'est pas quelconque: on conçoit en effet que si n' était négatif et grand en valeur absolue devant n , il devrait exister une autre décomposition du réseau principal en deux sous-réseaux correspondant à une énergie libre plus faible que celle de la décomposition primitivement adoptée. Nous ne dirons rien de plus sur cette question très complexe de stabilité des sous-réseaux qui est liée à l'architecture du réseau cristallin et aux interactions entre un atome donné et ses voisins plus ou moins éloignés.

Les coefficients n et n' peuvent se déterminer au moyen des formules (3) et (4), connaissant les valeurs de la température de Curie paramagnétique θ_p et de la température de transition T_n . Lorsqu'on effectue ces déterminations sur les quelques dizaines de substances antiferromagnétiques actuellement connues et étudiées, on s'aperçoit qu'il convient de les partager en trois groupes principaux. Un premier groupe comprenant des substances telles que FeO ,

MnO, etc., correspond à des valeurs de n' négatives comprises entre $-0.51 n$ et $-0.57 n$; les dispositions relatives des ions dérivent de celles d'un réseau cubique à faces centrées. Un deuxième groupe comprenant des substances comme FeF_2 , CoF_2 , etc., correspond à des valeurs de n' négatives comprises entre $-0.16 n$ et $-0.28 n$. Les dispositions relatives des ions dérivent de celles du cube centré: tous les proches voisins d'un atome d'un sous-réseau donné appartiennent à l'autre sous-réseau. Enfin, un troisième groupe comprenant des substances telles que NiCl_2 , CoCl_2 , etc., correspond à des valeurs de n' positives, souvent très grandes vis-à-vis de n . C'est ce troisième groupe de substances que nous nous proposons plus spécialement d'étudier dans ce mémoire.

3. — Les couplages magnéto-cristallins.

Pour compléter la description des propriétés d'une substance antiferromagnétique, il est nécessaire maintenant de tenir compte des couplages magnéto-cristallins. Ces couplages font apparaître dans l'expression de l'énergie totale un terme E_c qui dépend de l'orientation de la direction d'antiferromagnétisme par rapport aux axes du cristal. Supposons par exemple qu'il s'agisse d'une substance uniaxe, placée dans un champ magnétique nul; les aimantations M_a et M_b des deux sous-réseaux sont rigoureusement antiparallèles et ce terme s'écrit en première approximation sous la forme:

$$(6) \quad E_c = -K' \cos^2 \theta,$$

où θ représente l'angle avec l'axe de la direction d'antiferromagnétisme, c'est-à-dire de la direction parallèle à M_a et à M_b . Si par exemple, la constante K' est positive, la direction d'antiferromagnétisme coïncide avec l'axe. Nous sommes très peu renseignés sur les valeurs de K' ; nous sommes cependant en droit d'admettre qu'elles sont du même ordre de grandeur que les constantes d'anisotropie des substances ferromagnétiques, c'est-à-dire de l'ordre de 10^4 à 10^6 erg/g.

En l'absence de perturbations extérieures, les directions d'antiferromagnétisme occupent donc des directions privilégiées correspondant aux minima de E_c . On peut évidemment rapprocher ces directions privilégiées des directions privilégiées de l'aimantation spontanée, dans un corps ferromagnétique, mais il existe cependant une différence fort importante. En effet, l'application d'un champ H correspond, dans une substance ferromagnétique, à un couple sur l'aimantation spontanée qui est de l'ordre de MH ; au contraire, dans une substance antiferromagnétique, le couple qui agit sur la direction d'antiferromagnétisme est beaucoup plus petit, puisque de l'ordre de H^2/n .

Il en résulte que les directions d'antiferromagnétisme sont probablement beaucoup plus difficiles à modifier que les directions d'aimantation spontanée.

4. — Susceptibilités parallèle et perpendiculaire.

Du fait même de l'existence des directions privilégiées d'antiferromagnétisme, il convient de distinguer deux cas lorsqu'on applique un champ magnétique à un système antiferromagnétique: le cas où le champ appliqué est perpendiculaire à la direction privilégiée et le cas où le champ lui est parallèle.

Lorsque le champ est perpendiculaire à la direction privilégiée, le système prend une aimantation J parallèle à H donnée par:

$$(7) \quad J = H/n ;$$

la susceptibilité J/H est indépendante de H et égale à $1/n$. On la désigne sous le nom de susceptibilité perpendiculaire et on la désigne par s_n .

Lorsque le champ H est parallèle à la direction privilégiée d'antiferromagnétisme, la susceptibilité parallèle $s_p = J/H$ est toujours indépendante du champ, mais sa valeur est donnée par une expression plus compliquée:

$$(8) \quad \frac{1}{s_p} = n - \frac{1}{2} (n + n') \frac{M}{T} \frac{dT}{dM},$$

où $\frac{1}{2}M$ représente l'aimantation spontanée de chacun des sous-réseaux, brièvement étudiée plus haut. A la température de transition T_n , le facteur $(M/T) dT/dM$ tend vers zéro, de sorte que s_p tend vers $1/n$, c'est-à-dire vers la valeur de s_n . Au contraire lorsque la température tend vers le zéro absolu, $(M/T) dT/dM$ tend vers l'infini, de sorte que s_p tend vers zéro.

Ainsi, lorsque n' est de l'ordre de grandeur de n , la susceptibilité s_p varie d'une manière relativement progressive de 0 à $1/n$, lorsque T varie du zéro absolu jusqu'à la température de transition T_n . Au contraire lorsque n' est très grand devant n , la susceptibilité s_p reste égale à zéro jusqu'à une température voisine de T_n , puis varie très rapidement pour atteindre la même valeur $1/n$ pour $T = T_n$.

Lorsque le champ magnétique est parallèle à la direction privilégiée d'antiferromagnétisme, l'aimantation du système provient d'une augmentation de l'aimantation M_a du sous-réseau dont l'aimantation est dirigée dans le même sens que H et d'une diminution de M_b , mais les orientations de M_a et de M_b restent invariables ainsi que la direction d'antiferromagnétisme. Au contraire, lorsque le champ est perpendiculaire à la direction d'antiferromagnétisme, M_a et M_b ne restent plus antiparallèles et tendent à s'aligner dans la direction

du champ. On peut dans ce cas convenir d'appeler direction d'antiferromagnétisme la *bissectrice extérieure* de \mathbf{M}_a et de \mathbf{M}_b : la direction d'antiferromagnétisme reste alors invariable, quel que soit \mathbf{H} .

5. - Le phénomène de découplage; le champ seuil.

Une étude plus détaillée des phénomènes, dans le cas où le champ magnétique est parallèle à la direction d'antiferromagnétisme, montre qu'il existe une valeur critique du champ, appelée *champ seuil*, pour laquelle la direction d'antiferromagnétisme se découple brusquement de la direction privilégiée et lui devient perpendiculaire, avec variation discontinue de la susceptibilité qui de s_p passe brusquement à la valeur $1/n$, égale à s_n . Ce champ seuil est donné par:

$$(9) \quad H_s^2 = 2K'n.$$

Nous avons signalé ce phénomène dès 1936 ⁽³⁾ et il a été retrouvé en 1952, par C. J. GORTER et ses collaborateurs au cours d'une série de magnifiques travaux consacrés à l'étude des propriétés magnétiques de $\text{CuCl}_2 \cdot 2\text{H}_2\text{O}$ ⁽⁴⁾.

Il convient ici de remarquer que dans le cas où K' est nul, c'est-à-dire en l'absence de couplage entre le réseau cristallin et la direction d'antiferromagnétisme, la direction d'antiferromagnétisme s'oriente toujours dans un sens perpendiculaire au champ appliqué et la susceptibilité conserve toujours une valeur égale à $1/n$.

Dans la plupart des substances antiferromagnétiques, la valeur H_s du champ seuil est probablement très élevée, de sorte que la susceptibilité reste indépendante du champ jusqu'aux valeurs les plus élevées qu'il soit possible d'atteindre, mais il ne doit pas en être de même lorsque n est petit: notamment lorsque le rapport n'/n est grand.

6. - Les constantes K_0 et K_1 d'anisotropie d'un antiferromagnétique.

Nous nous proposons maintenant de discuter l'influence de l'énergie magnétocristalline sur l'existence d'un champ seuil. Pour ne pas compliquer outre mesure la discussion, nous nous limiterons à un cas type simple: celui d'une *substance uniaxe* dans laquelle le rapport n'/n est grand. Dans ce cas, les modifications de l'état du système provoquées par l'action d'un champ extérieur

⁽³⁾ L. NÉEL: *Ann. de Phys.*, **5**, 232 (1936).

⁽⁴⁾ C. J. GORTER et H. HAANTJES: *Physica*, **17**, 285 (1952); J. UBBINK, J. A. POULIS et C. J. GORTER: *Physica*, **17**, 213 (1951); **18**, 361 (1952).

se réduisent à de simples changements d'orientation des aimantations spontanées \mathbf{M}_a et \mathbf{M}_b des deux sous-réseaux, ces aimantations conservant une grandeur égale à $\frac{1}{2}M$ qui ne dépend que de la température T . L'énergie totale du système est la somme de l'énergie d'échange de Weiss-Heisenberg, de l'énergie du système dans le champ extérieur \mathbf{H} et de l'énergie magnétocristalline. La partie E_w de l'énergie d'échange qui ne dépend que de l'angle de \mathbf{M}_a avec \mathbf{M}_b s'écrit :

$$(10) \quad E_w = n\mathbf{M}_a\mathbf{M}_b,$$

tandis que l'énergie dans le champ extérieur est donnée par :

$$(11) \quad E_h = -\mathbf{H}(\mathbf{M}_a + \mathbf{M}_b).$$

En ce qui concerne maintenant l'énergie magnétocristalline E_c , l'état du système est défini par les angles θ et θ' de \mathbf{M}_a et de \mathbf{M}_b avec l'axe ainsi que par l'angle φ que font entre eux les plans méridiens contenant \mathbf{M}_a et \mathbf{M}_b . Compte-tenu du fait que dans l'expression générale de E_c il existe des termes qui ne dépendent que de l'angle de \mathbf{M}_a avec \mathbf{M}_b et que ces termes, possédant ainsi un caractère isotrope, peuvent être intégrés dans les termes d'échange en modifiant convenablement la valeur du coefficient n , on démontre que l'expression générale de l'énergie magnétocristalline E_c d'une substance antiferromagnétique uniaxe, limitée aux termes du second degré par rapport aux cosinus directeurs de \mathbf{M}_a et de \mathbf{M}_b , ne dépend que de deux constantes K_0 et K_1 et s'écrit ⁽⁵⁾ :

$$(12) \quad E = -\frac{1}{2}K_0(\cos^2 \theta + \cos^2 \theta') - K_1 \cos \theta \cos \theta'.$$

7. - Etats d'équilibre du système.

Dans un champ magnétique extérieur nul, l'état d'équilibre du système s'obtient en déterminant le minimum de $E_w + E_c$; par raison de symétrie, il correspond toujours à $\varphi = 0$. Trois états sont possibles : 2 états antiferromagnétiques et un état ferromagnétique. Dans les deux états antiferromagnétiques, (Ap) et (An), les directions d'antiferromagnétisme sont respectivement parallèle et normale à l'axe. Dans l'état ferromagnétique (Fp), la direction privilégiée de l'aimantation spontanée est parallèle à l'axe du cristal.

Pour exprimer d'une manière simple les résultats, nous utiliserons deux variables réduites auxiliaires r et r' , dont les dimensions sont celles d'un nombre,

(5) L. NÉEL : *Compt. Rend. Ac. Sci.*, **242**, 1549 (1956).

définies, par les relations suivantes:

$$(13) \quad r = \frac{2(K_0 + K_1)}{nM^2}, \quad r' = \frac{2(K_0 - K_1)}{nM^2}.$$

On trouve alors ⁽⁵⁾ que lorsque r' est négatif, le système prend l'état (An) lorsque r est inférieur à 1 et l'état (Fp) lorsque r est supérieur à 1. Lorsque r' est positif, le système prend l'état (Ap) lorsque $r - r'$ est inférieur à 1 et l'état (Fp) lorsque $r - r'$ est supérieur à 1.

En portant sur un graphique (Fig. 1) des points représentatifs, de coordonnées rectangulaires r et r' , on peut ainsi diviser le plan (r, r') en deux régions par la ligne brisée PQS: à droite la région ferromagnétique, à gauche la région antiferromagnétique.

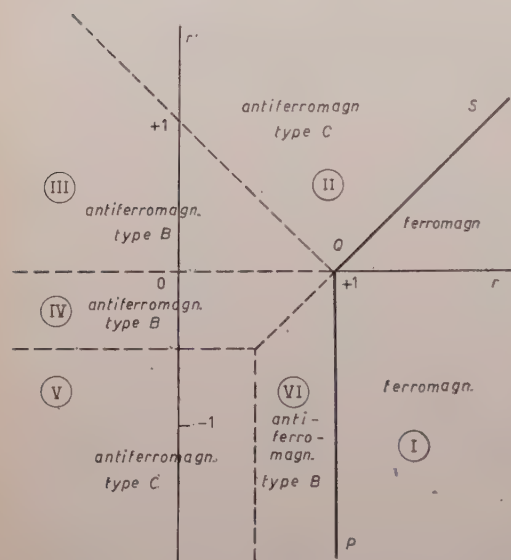


Fig. 1. — Diagramme d'état dans le plan (r, r') (antiferromagnétisme ou ferromagnétisme). Quand r' est positif, l'axe cristallin et la direction d'antiferromagnétisme sont parallèles; ils sont perpendiculaires quand r' est négatif.

8. — Action d'un champ magnétique extérieur.

Il importe maintenant de compléter l'étude de la région antiferromagnétique par la détermination de l'aimantation obtenue en soumettant le système à un champ extérieur H . Il suffit pour cela d'ajouter à l'énergie du système le terme E_h donné plus haut par la relation (11) et d'écrire la condition d'énergie minimale. Les calculs sont toujours très élémentaires aussi nous nous contenterons d'en énoncer seulement les résultats, qui sous une forme partielle avaient déjà fait l'objet d'une publication antérieure ⁽⁶⁾. Pour abréger l'écriture, nous exprimerons en outre les champs magnétiques H par l'intermédiaire d'une variable

⁽⁶⁾ L. NÉEL: *X^e Conseil de Physique Solvay* (Bruxelles, Septembre 1954). (*Les électrons dans les métaux*, R. STOOPS, éditeur, Bruxelles, 1955, p. 251).

réduite:

$$(14) \quad h = \frac{2H}{nM}.$$

On constate d'abord qu'en appliquant le *champ magnétique* H dans une *direction perpendiculaire* à la *direction d'antiferromagnétisme* l'aimantation reste proportionnelle à H jusqu'à ce que la saturation M soit atteinte. La susceptibilité s_n conserve donc une valeur constante jusqu'à ce que le champ réduit h atteigne une valeur h_1 et on obtient une courbe d'aimantation du type A (Fig. 2). L'inverse $1/s_n$ de la susceptibilité perpendiculaire prend la valeur $n(1 + r')$ lorsque r' est positif et la valeur $n(1 - r)$ lorsque r' est négatif (dans le premier cas la direction d'antiferromagnétisme est parallèle à l'axe, dans le second cas, elle lui est perpendiculaire).

Ainsi, dans les deux cas, nous obtenons une valeur

de la susceptibilité s_n nettement différente de la valeur conventionnelle égale à $1/n$. Cette observation a son intérêt car, comme nous le précisons plus loin, la variable r' est susceptible de varier d'une manière extrêmement importante avec la température, beaucoup plus que n . On pourrait peut-être expliquer ainsi à partir de cette remarque les variations anormales de s_n qui ont parfois été observées.

Les lois de l'aimantation du système dans un *champ parallèle* à la *direction d'antiferromagnétisme* sont beaucoup plus compliquées que dans le cas précédent, comme conséquence de l'existence nécessaire d'un champ seuil. En effet, dans la phase initiale de l'aimantation la direction d'antiferromagnétisme, définie comme la bissectrice extérieure de \mathbf{M}_a et \mathbf{M}_b , est parallèle à la direction du champ, tandis que dans la phase finale, au moment où \mathbf{M}_a et \mathbf{M}_b sont devenus parallèles, elle est perpendiculaire à la direction du champ: il y a donc eu discontinuité pour un certain champ seuil h_s . Deux types B et C de loi d'aimantation se rencontrent: un type B dans lequel l'aimantation reste nulle jusqu'à ce que le champ atteigne une valeur seuil h_2 (Fig. 2) pour laquelle l'aimantation varie d'une manière discontinue et atteint une valeur inférieure à l'aimantation à saturation M . Ensuite, l'aimantation reste proportionnelle au champ, avec un rapport constant $J/H = s_p$, puis atteint la saturation pour $h = h_3$. Dans le type C , la discontinuité qui se produit pour le champ seuil h_4 est telle que la saturation M est atteinte d'emblée.

Dans cette description, nous supposons que la susceptibilité est nulle dans la phase initiale, au-dessous du champ seuil. Nous rappelons, comme cela a

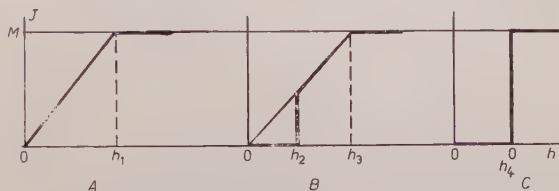


Fig. 2.

été précisé plus haut (cf. Sect. 4), que cette hypothèse est correcte jusqu'à une température très proche de la température de transition T_n , puisque nous nous sommes placés par hypothèse dans le cas où n' est grand vis-à-vis de n .

Nous avons déterminé, en fonction de r et de r' , les types de lois d'aimantation rencontrés ainsi que les valeurs des champs critiques h_2 , h_3 , h_4 .

Le plan (r, r') est divisé, comme le montre la Fig. 1, en 6 régions par les 6 droites $r' = 0$; $r = 1$; $r' = -\frac{1}{2}$; $r = \frac{1}{2}$; $r - r' = 1$; $r + r' = 1$. Le Tableau I rassemble le résultat des calculs.

Lorsqu'au lieu d'étudier un monocristal on étudie une poudre agglomérée, composée de cristallites orientés au hasard, la susceptibilité moyenne s_m s'obtient en première approximation par la relation:

$$(15) \quad s_m = 2s_n + s_p.$$

Cette formule n'est pas rigoureuse pour deux raisons: elle néglige les interactions magnétiques entre les cristallites et elle néglige aussi la rotation de la direction d'antiferromagnétisme qui se produit lorsque le champ est appliqué obliquement par rapport à la direction d'antiferromagnétisme (cette rotation est de l'ordre de h^2 , tandis que la rotation de \mathbf{M}_a ou de \mathbf{M}_b est de l'ordre de h). A cause de sa simplicité, nous utiliserons néanmoins la formule (15): elle montre que la présence d'un champ seuil se manifeste, dans le cas d'une poudre, par une variation beaucoup plus rapide de l'aimantation en fonction de h .

9. — Hystérésis paramagnétique.

Les résultats qui ont été résumés dans le Tableau I ont été obtenus en supposant que le système prend toujours la configuration qui correspond à l'énergie la plus basse. En réalité, de faux équilibres sont possibles; l'analyse des phénomènes, relatifs au type *B* d'aimantation par exemple, montre ⁽⁶⁾ qu'à champ magnétique croissant le découplage de la direction d'antiferromagnétisme ne doit se produire que pour un champ h'_2 supérieur à h_2 ; à champ décroissant, le retour à sa position initiale de la direction d'antiferromagnétisme ne se produit que pour un champ h''_2 inférieur à h_2 . On obtient ainsi de véritables phénomènes d'hystérésis.

Du point de vue expérimental, nous ne connaissons rien de précis à ce sujet. Nous n'insisterons donc pas davantage d'autant plus qu'il est fort possible qu'il existe un mécanisme qui permette au système de prendre automatiquement la configuration d'énergie minimale. On sait qu'un tel mécanisme, à savoir le *déplacement des parois de Bloch*, permet, dans un corps ferromagné-

TABEAU I. — Valeurs, suivant les différentes régions du plan (r, r'), des susceptibilités s_n et s_p et des champs critiques.

Région du plan (r, r')	Position de la direction d'anti-ferromagnétisme	Valeurs de s_n (type A)	Aimantation parallèle à l'axe		
			Type de la loi d'aimantation	Valeurs de s_p	Valeurs des champs critiques
(II)	parallèle à l'axe du cristal	$s_n = \frac{1}{n(1+r')}$ $h_1 = 2(1+r')$	\mathcal{O}	—	$h_4 = 1 + r' - r$
(III)	parallèle à l'axe du cristal	$s_n = \frac{1}{n(1+r')}$ $h_1 = 2(1+r')$	\mathcal{O}	$s_p = \frac{1}{n(1-r)}$	$h_2 = 2(1-r)^{\frac{1}{3}}r^{\frac{1}{3}}$ $h_3 = 2(1-r)$
(IV)	normale à l'axe du cristal	$s_n = \frac{1}{n(1-r)}$ $h_1 = 2(1-r)$	\mathcal{B}	$s_p = \frac{1}{n(1+r')}$	$h_2 = 2(-r')^{\frac{1}{3}}(1+r')^{\frac{1}{3}}$ $h_3 = 2(1+r')$
(V)	normale à l'axe du cristal	$s_n = \frac{1}{n(1-r)}$ $h_1 = 2(1-r)$	\mathcal{O}	—	$h_4 = 1$
(VI)	normale à l'axe du cristal	$s_n = \frac{1}{n(1-r)}$ $h_1 = 2(1-r)$	\mathcal{B}	$s_p = \frac{1}{nr}$	$h_2 = 2r^{\frac{1}{3}}(1-r)^{\frac{1}{3}}$ $h_3 = 2r$
(I)	Le système est ferromagnétique; la direction privilégiée de l'aimantation spontanée est perpendiculaire à l'axe.				

tique, le choix, entre deux phases aimantées en sens inverse, de la phase d'énergie minimale pour un champ appliqué sensiblement nul, tandis que le passage réversible d'une phase à l'autre exigerait des champs magnétiques très élevés. On peut de même, dans une substance antiferromagnétique, supposer qu'il existe *toujours*, mais en proportions variables, deux phases dont l'une correspond à une direction d'antiferromagnétisme parallèle à l'axe, l'autre à une direction perpendiculaire et imaginer que les changements de proportion entre les phases s'effectuent par le déplacement de la paroi qui les sépare.

10. — Application aux chlorures anhydres.

Les considérations développées plus haut s'appliquent immédiatement aux chlorures anhydres, NiCl_2 , CoCl_2 , FeCl_2 , comme nous avons eu l'occasion de le montrer récemment ⁽⁶⁾.

Les chlorures NiCl_2 , CoCl_2 appartiennent très probablement au type *B*, comme le montre le fait que la susceptibilité dans des champs de l'ordre de 1000 Oe est nettement plus faible, de l'ordre des deux tiers, que la susceptibilité dans 10000 Oe: c'est à quoi il faut s'attendre, dans le cas d'une poudre, lorsqu'il existe un champ seuil de valeur intermédiaire. Les données expérimentales ne permettent pas de déterminer les 4 constantes n' , n , r et r' car il existe seulement deux bonnes données, la température de transition T_n et la susceptibilité dans les champs forts pratiquement égale à s_n , et une donnée très mal connue: la valeur du champ seuil. Si on suppose, tout gratuitement d'ailleurs, $r = r'$, on obtient, en rapportant les aimantations à 1 gramme, les valeurs indiquées dans le Tableau II. Les points représentatifs seraient ainsi situés dans la région (III) du plan (r, r') , sur la première bissectrice.

TABLEAU II.

Substance	NiCl_2	CoCl_2	FeCl_2
n'	11 000	3 000	3 400
n	1 300	340	130
r	0.001 6	0.054	0.5

Pour FeCl_2 , l'amplitude de la discontinuité correspondant au champ seuil devient extrêmement importante, de l'ordre de grandeur de l'aimantation à saturation: on a affaire au type *C* (Fig. 2) et le point représentatif passe dans la région (II) du plan (r, r') .

Pour les trois chlorures, le rapport n'/n est élevé: 10 au moins. La susceptibilité initiale varie comme l'inverse de $n(1+r)$; quand r est petit, l'expérience

montre que la susceptibilité est pratiquement indépendante de la température, d'où on déduit que n est aussi pratiquement indépendant de la température. C'est un résultat tout à fait logique, puisque n représente des interactions d'échange. Au contraire, la susceptibilité initiale de FeCl_2 varie beaucoup avec T : il faut certainement voir là l'influence de la variation thermique de r qui, étant égal à 0.5 n'est plus négligeable devant l'unité.

11. — Application à MnAu_2 .

A. MEYER et P. TAGLANG ont récemment montré ⁽⁷⁾ que la susceptibilité magnétique du composé métallique MnAu_2 restait indépendante de la température de 100 °K à 300 °K et du champ magnétique jusqu'à 10 000 Oe environ. Au voisinage de cette valeur du champ, l'aimantation J_s varie d'une manière beaucoup plus rapide puis tend ensuite vers la saturation selon une loi d'approche de la forme:

$$(16) \quad J = J_s \left(1 - \frac{b}{H^2} \right).$$

Comme nous l'avons déjà exposé ⁽⁵⁾ c'est exactement le comportement qu'il faut attendre de la part d'une substance antiferromagnétique, caractérisée par une loi d'aimantation du type C et un champ seuil voisin de 10 000 Oe. On peut supposer que le point représentatif soit situé dans la région (II) du plan (r, r') .

De la valeur de la susceptibilité initiale $s_m = 3.76 \cdot 10^{-4}$, mesurée sur un polycristal, on tire:

$$(17) \quad n(1 + r') = 1770$$

de 100 °K à 300 °K. De la détermination du champ seuil H_s et de la valeur de l'aimantation à saturation M , on déduit que dans le même intervalle de température H_s/M reste voisin de 270, d'où:

$$(18) \quad n(1 + r' - r) = 540,$$

mais cela ne suffit pas encore pour déterminer n , r' et r .

On peut remarquer cependant que dans le cas du fer et du nickel, les mieux étudiés des ferromagnétiques, le rapport K/M^2 de la constante d'aniso-

(7) A. MEYER et P. TAGLANG: *Compt. Rend. Ac. Sci.*, **239**, 961, 1611 (1954); *Journ. de Phys. Rad.*, **17**, (1956), sous presse.

tropie au carré de l'aimantation spontanée tend vers zéro au point de Curie. Par analogie, il est logique d'admettre que dans les substances antiferromagnétiques r et r' tendent aussi tous les deux vers zéro au point de transition T_n . Il en résulte alors que la susceptibilité pour $T = T_n$ est simplement égale à $1/n$. Les mesures de A. MEYER et P. TAGLANG montrent que la susceptibilité de MnAu_2 passe, au voisinage de $T_n = 370^\circ\text{K}$, par un maximum aigu égal à $1.1 \cdot 10^{-3}$ qui correspond à $n = 900$ environ.

En admettant alors que n ne varie pas avec T , on déduit alors des deux formules (17) et (18) que dans le domaine de température compris entre 100°K et 300°K , r et r' sont respectivement voisins de 1.4 et de 1.0.

D'autre part, on déduit $n' - n$ de la valeur du point de Curie paramagnétique ($\theta_p = 451^\circ\text{K}$) et de la constante de Curie spécifique ($C = 7.12 \cdot 10^{-3}$) en utilisant la formule (3), ce qui donne $n' = 128\,000$ environ. Le rapport $n'/n = 142$ est ici particulièrement grand. Cette grandeur du rapport n'/n , jointe au fait que r et r' passent de la valeur 0 aux valeurs 1.4 et 1.0 quand la température s'abaisse de 370°K à 300°K , permet de comprendre pourquoi le maximum de la susceptibilité initiale à $T = T_n$ est aussi aigu. Un autre fait confirme l'exactitude de notre interprétation: lorsque le champ appliqué est suffisamment élevé [$h > 2(1+r')$], les deux aimantations spontanées M_a et M_b coïncident dans chacun de tous les cristallites et tout se passe comme si nous avions affaire à une substance ferromagnétique uniaxe et d'énergie d'anisotropie égale à $-(K_0 + K_1) \cos^2 \theta$. La loi d'approche à la saturation est alors du type (16), avec:

$$(19) \quad b = \frac{4K^2}{nM^2} = \frac{n^2 r^2 M^2}{15}.$$

D'après les mesures de MEYER et TAGLANG, b/M^2 reste, de 100 à 300°K , voisin de $0.64 \cdot 10^5$ d'où l'on déduit $nr = 980$, alors qu'on déduit $nr = 1260$ des données antérieurement admises: c'est un résultat très satisfaisant eu égard au caractère extrêmement schématique de la théorie.

12. - La variation thermique de r et de r' : transition entre ferromagnétisme et antiferromagnétisme.

Nous avons déjà précisé plus haut les raisons expérimentales qui amènent à penser que r et r' tendent vers zéro à la température T_n de disparition de l'aimantation spontanée. Ces arguments sont d'ailleurs confirmés par les résultats d'une théorie due à AKULOV⁽⁸⁾ selon laquelle la constante d'aniso-

⁽⁸⁾ N. AKULOV: *Zeits. f. Phys.*, **100**, 197 (1936).

tropie d'un corps cubique ferromagnétique varierait au voisinage du point de Curie comme la dixième puissance de l'aimantation spontanée d'où il résulte que r et r' varieraient comme M^8 et seraient nuls pour $T = T_n$. Nous considérerons désormais ce point comme acquis.

Loin du point de transition, les constantes d'anisotropie sont quelquefois proportionnelles au carré de l'aimantation spontanée: r et r' sont alors constants, comme cela se passe pour MnAu_2 au-dessous de 300°K . Mais il existe beaucoup d'autres cas où la constante d'anisotropie varie d'une manière très importante et beaucoup plus compliquée par exemple dans des substances hexagonales comme Co ou MnBi . Dans le cobalt, K diminue de $4.7 \cdot 10^7$ erg/mole à zéro, lorsque la température passe de -200°C à $+200^\circ\text{C}$, dans un domaine où la diminution de M^2 est seulement de l'ordre de 5%. De même, entre 84°K et 300°K , la constante K du composé MnBi augmente de 0 à $3.5 \cdot 10^8$ erg/mole tandis que M^2 diminue légèrement ⁽⁹⁾.

Finalement, nous arrivons à la conclusion ⁽¹⁰⁾ que le point représentatif R de l'état du système antiferromagnétique se déplace dans le plan (r, r') en fonction de la température pour aboutir à l'origine, à $T = T_n$. Il peut arriver notamment que R , situé initialement à basse température dans la partie de la région (I) où r' est positif (Fig. 1), se déplace, franchisse à une certaine température T_a la frontière QS entre les régions (I) et (II), franchisse ensuite à une température T_b la frontière entre les régions (II) et (III) pour aboutir à l'origine 0, quand $T = T_n$. Nous serions donc ainsi en présence d'une substance qui est ferromagnétique à basse température et qui devient ensuite antiferromagnétique à $T = T_a$. L'antiferromagnétisme appartiendrait au type C pour $T < T_b$ et au type B pour $T_b < T < T_n$.

Il résulte des des considérations développées plus haut que, dans la région (II) ($T_a < T < T_b$), le champ seuil H_s et l'aimantation spontanée M sont liées par la relation:

$$(20) \quad \frac{H_s}{M} = \frac{1}{2} n(1 + r' - r).$$

On remarque d'abord que le champ seuil H_s tend vers zéro quand T tend vers T_a puisque l'équation de la frontière QS entre les régions (I) et (II) est précisément $1 + r' - r = 0$. Il en résulte qu'en portant H_s/M en fonction de T on obtient une courbe qui d'une part tend vers 0 lorsque T tend vers T_a et qui d'autre part, extrapolée vers $T = T_n$, tend vers $\frac{1}{2}n$. Il faut bien noter que cette extrapolation doit se faire à travers la région (II) ($T_b < T < T_n$), à l'intérieur de laquelle il existe bien encore un champ seuil, mais donné par une formule différente: $H_s/M = n(1 - r)^{\frac{1}{2}}r'^{\frac{1}{2}}$.

⁽⁹⁾ C. GUILLAUD: *Thèse* (Strasbourg, 1943).

⁽¹⁰⁾ L. NÉEL: *Compt. Rend. Ac. Sci.*, **242**, 1549, 1824 (1956).

13. - Autre type de transition entre ferromagnétisme et antiferromagnétisme.

Dans le type de transition étudié plus haut, r' est positif. On peut concevoir aussi un autre type de transition correspondant au cas où r' est négatif. Le point représentatif R' , situé initialement à basse température dans la partie inférieure de la région (I) du plan (r, r') , se déplace, franchit à une certaine température T_a la frontière PQ entre les régions (I) et (VI), traverse ensuite les régions (VI), (IV) et éventuellement la région (V) pour aboutir finalement à l'origine 0.

Ce deuxième type de transition entre ferromagnétisme et antiferromagnétisme est bien différent du premier. En effet, dans la région (VI), la loi d'aimantation est du type B et le champ seuil, qui est donné par la relation $H_s/M = n(1 - r)^{\frac{1}{2}}r^{\frac{1}{2}}$, tend également vers zéro quand $T = T_a$ puisque l'équation de la frontière PQ est $r = 1$. Mais il y a une différence essentielle: dans ce deuxième type, la discontinuité d'aimantation qui est associée au champ seuil tend vers zéro quand T tend vers T_a tandis que dans le type précédent l'amplitude de la discontinuité d'aimantation restait égale à M . Il doit donc être relativement facile de distinguer les deux cas du point de vue expérimental.

14. - Autres mécanismes de transition.

L'étude du rôle des couplages magnétocristallins sur la stabilité des différentes configurations possibles vient de nous montrer que la variation thermique des constantes d'anisotropie pouvait donner naissance, pour une substance donnée, à une transition d'un état ferromagnétique à un état antiferromagnétique. Ce mécanisme de transition n'est naturellement pas le seul possible. J. S. SMART⁽¹¹⁾ a déjà discuté les différentes manières suivant lesquelles l'ordre pouvait s'établir dans une substance magnétique, pour différents réseaux cristallins, en fonction de la valeur des interactions d'échange ou de superéchange entre un atome et ses voisins plus ou moins proches. Si ces interactions varient, c'est-à-dire en somme si n et n' sont des fonctions de T , il peut se produire des transitions de l'état ferro- à l'état antiferromagnétique.

La théorie de Smart, appliquée par cet auteur au cas de $MnBi$ et de $MnAs$, n'invoque que la variation thermique des interactions *isotropes* d'échange ou de superéchange: elle ignore complètement le rôle des constantes d'anisotropie et l'existence du champ seuil. Elle ne conduit donc à aucune relation entre la valeur du champ seuil et la température de transition. Il n'est pas certain

⁽¹¹⁾ J. S. SMART: Naval Res. Rep., no. 2113 (Juillet 1951), U.S. Naval Ordnance Lab.; *Phys. Rev.*, **90**, 55 (1953).

d'autre part que la variation thermique de n et de n' soit suffisante pour faire apparaître de tels phénomènes: au surplus on a le moyen de savoir si les coefficients de champ moléculaire dépendent de la température. Nous avons en effet montré autrefois ⁽¹²⁾ que dans une substance présentant un paramagnétisme du type Langevin-Weiss (c'est le cas des substances antiferromagnétiques au-dessus de leur température T_n de transition) la constante de Curie n'était égale à sa valeur théorique, relative à un paramagnétisme pur sans champ moléculaire, que dans les cas où les coefficients de champ moléculaire étaient indépendants de la température. Dans les autres cas, il y a un terme correctif.

15. — Application à l'interprétation des propriétés magnétiques du dysprosium.

Les propriétés magnétiques du dysprosium métallique ont fait l'objet, ces dernières années, d'études détaillées de F. TROMBE ⁽¹³⁾ et de F. J. ELLIOTT, S. LEGVOLD et F. H. SPEDDING ⁽¹⁴⁾ elles sont très complexes et fort curieuses. Dans un domaine A correspondant aux températures inférieures à 90 °K, le dysprosium se comporte comme un ferromagnétique classique. Dans un domaine B (90 °K < T < 160 °K), les isothermes d'aimantation présentent l'allure schématique suivante: l'aimantation commence par varier à peu près proportionnellement au champ jusqu'à un certain champ seuil H_s , pour lequel s'amorce une variation beaucoup plus rapide de l'aimantation qui se termine finalement par une approche à la saturation en $1/H^2$. Ces isothermes présentent une analogie très frappante avec celles de $MnAu_2$, mais tandis que le champ seuil de $MnAu_2$ varie assez peu avec la température celui de Dy varie au contraire beaucoup: de 2500 à 10000 Oe, quand T passe de 103 °K à 153 °K.

Plus loin, dans une région C située au-dessus de 160 °K, le dysprosium devient paramagnétique avec une susceptibilité spécifique qui commence par croître avec la température, passe à 178 °K par un maximum aigu voisin de $4 \cdot 10^{-3}$, puis décroît quand la température augmente davantage, en obéissant à une loi de Curie-Weiss définie par une constante de Curie spécifique $C = 0.087$ et un point de Curie paramagnétique $\theta_p = 157$ °K.

Il s'agit certainement dans cette région C d'un antiferromagnétisme de point de transition $T_n = 178$ °K. On obtient le coefficient n par la relation $n = 1/s$, où s est la susceptibilité pour $T = T_n$, soit $4 \cdot 10^{-3}$, ce qui donne $n = 250$. On a d'autre part $n' - n = 2\theta_p/C$, d'où $n' - n = 3600$ et finalement $n' = 4100$. Le rapport n'/n est ainsi assez grand, voisin de 16, de sorte que le dysprosium

⁽¹²⁾ L. NÉEL: *Ann. de Phys.*, II^e Série, **8**, 237 (1937).

⁽¹³⁾ F. TROMBE: *Journ. Rech. CNRS*, no. 23 (Juin 1953), p. 61.

⁽¹⁴⁾ F. J. ELLIOTT, S. LEGVOLD et F. H. SPEDDING: *Phys. Rev.*, **94**, 1143 (1954).

appartient à la même famille antiferromagnétique que FeCl_2 et MnAu_2 et que l'existence d'un champ seuil paraît ainsi parfaitement normale.

Quant à la transition vers un ferromagnétisme qui se produit quand la température s'abaisse en dessous de 100°K , nous proposons de l'attribuer à la variation thermique des constantes d'anisotropie K_0 et K_1 . Le fait que la discontinuité d'aimantation reste extrêmement importante au voisinage du point de transition T_a montre que la transition appartient au premier type.

Pour appuyer cette interprétation, nous avons déterminé H_s et M d'après les données expérimentales et représenté H_s/M en fonction de la température (Fig. 3). Nous obtenons ainsi une courbe qui coupe l'axe des abscisses à

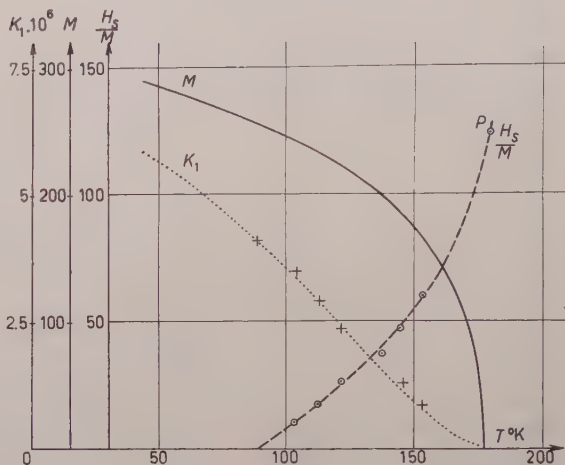


Fig. 3.

90°K au voisinage immédiat du point T_a estimé plus haut être voisin de 100°K . D'autre part, cette même courbe extrapolée vers $T = T_n$ donne une valeur très voisine de $125 = n/2$, conformément aux prévisions théoriques relatives au premier type de transition. Ces faits apportent une preuve décisive en faveur de l'interprétation que nous proposons.

Au contraire une interprétation basée sur la variation thermique des champs moléculaires se heurte, d'une part à l'objection qu'elle n'explique pas la relation étroite révélée par l'expérience entre le champ seuil et la température T_a de transition et d'autre part au fait que la constante de Curie spécifique, dans l'état paramagnétique, possède une valeur pratiquement égale à la valeur théorique correspondant à Dy^{+++} , ce qui montre que la variation thermique des coefficients de champ moléculaire est très faible, comme nous l'avons rappelé plus haut.

16. - Valeur de la constante d'anisotropie K_1 .

De la valeur du champ seuil H_s , connaissant d'autre part n et M , il est possible d'en déduire $r - r'$, puis K_1 . Ces valeurs ont été reportées sur la Fig. 3 en fonction de T . On trouve ainsi qu'à 90°K , la constante K_1 est voisine de $4 \cdot 10^6$ erg/g, soit environ $6.5 \cdot 10^8$ erg/mole. Cette valeur est à rap-

procher de la valeur de la constante d'anisotropie du composé MnBi, égale à $3.5 \cdot 10^8$ erg/mole. Ainsi les constantes d'anisotropie qu'il est nécessaire d'introduire dans notre système d'interprétation sont du même ordre de grandeur que celles de corps ferromagnétiques connus.

La susceptibilité initiale moyenne s_m décroît de $4 \cdot 10^{-3}$ à $2.8 \cdot 10^{-3}$ quand la température s'abaisse de 178°K à 168°K . Cette décroissance est attribuable à la diminution de s_p et de s_n . La susceptibilité parallèle s_p est donnée par l'équation (8); à 10° au-dessous T_n , de on trouve que $(M/T)dT/dM$ est approximativement égal à -0.13 , d'où finalement $s_p = 1.9 \cdot 10^{-3}$ soit sensiblement la moitié de la valeur correspondant à $T = T_n$. La croissance de r' à mesure que l'on s'écarte de T_n produit une diminution de $s_n = 1/n(1+r')$. L'expérience ne donne que $r - r'$ qui est égal à 0.30 à 10° au-dessous de T_n . Si on pose $r' = kr$, il faut donner à k la valeur raisonnable de 0.43 pour obtenir finalement une valeur de s_m égale à la valeur expérimentale (en négligeant l'effet de la croissance de r' sur s_p).

En admettant maintenant que k conserve la valeur 0.43 quand la température varie, on en déduit que $r+r'$ prend la valeur 1 pour $T = T_b = 160^\circ\text{K}$, ce qui donne la température T_b à laquelle se produit le passage du point représentatif de la région (II) à la région (III): les valeurs du champ seuil que nous avons utilisées correspondent à des températures inférieures, c'est-à-dire à la région (II) comme nous l'avions admis implicitement.

17. - Application à l'erbium.

Les propriétés magnétiques de l'erbium, bien que connues avec moins de précision ⁽¹⁵⁾, sont analogues à celles du dysprosium: on y distingue les mêmes trois régions *A*, *B* et *C*.

Dans la région *C*, à $T_n = 76^\circ\text{K}$ environ, apparaît un maximum de susceptibilité égal à $2.4 \cdot 10^{-3}$: il correspond à $n = 420$. Au-dessus de T_n , on a affaire à un paramagnétisme de Curie-Weiss caractérisé par un point de Curie paramagnétique $\theta_p = +40^\circ\text{K}$ et une constante de Curie spécifique voisine de $C = 0.069$, valeur théorique. On obtient ainsi $n' - n = 2\theta_p/C = 1160$, soit $n' = 1580$. Le rapport $n'/n = 3.8$ est bien plus petit que dans le cas du dysprosium.

Dans la région *B* apparaît un champ seuil qui s'annule vers 30°K . Le rapport H_s/M croît à peu près linéairement en fonction de la température et s'extrapole pour $T = T_n$ vers la valeur 190 , fort proche, compte-tenu de grosses incertitudes expérimentales, de la valeur théorique $\frac{1}{2}n = 210$. A 30°K , la

⁽¹⁵⁾ F. J. ELLIOTT, S. LEGVOLD et F. H. SPEDDING: *Phys. Rev.*, **100**, 1595 (1955).

constante d'anisotropie K_1 , calculée avec la même méthode que celle du dysprosium, est voisine de $6 \cdot 10^6$ erg/g ou 10^9 erg/mole.

18. — Conclusions.

En résumé, l'expérience permet de distinguer parmi les substances antiferromagnétiques une catégorie bien individualisée correspondant à des valeurs positives de n' , c'est-à-dire à des interactions positives à l'intérieur de chaque sous-réseau et à des valeurs de n petites devant n' . Ces conditions favorisent l'observation du champ seuil (FeCl_2 , MnAu_2 , ...) et éventuellement le passage de l'état antiferromagnétique à l'état ferromagnétique sous l'influence de la variation thermique des constantes d'anisotropie K_0 et K_1 .

Les mêmes conditions favorisent également la présence d'un moment magnétique permanent superficiel, lié aux parois de Bloch séparant les domaines élémentaires antiferromagnétiques, comme nous l'avons montré antérieurement ⁽⁶⁾.

Il semble donc justifié de ranger ces substances dans une catégorie spéciale: celle des substances *métamagnétiques*, reprenant ainsi une vieille dénomination forgée par BECQUEREL ⁽¹⁾ pour certaines d'entre elles (CoCl_2 , NiCl_2 , ...), avant que la signification de leurs assez étranges propriétés magnétiques ait été élucidée.

Il faut toutefois s'attendre à ce que, dans le domaine des très basses températures, la théorie exposée ci-dessus ne suffise pas à rendre compte de toutes les propriétés magnétiques de la substance, notamment quand les porteurs de magnétisme possèdent un moment orbital. Il faut alors tenir compte de la décomposition des niveaux magnétiques dans le champ électrique cristallin. Si l'écartement de ces niveaux est de l'ordre de nM^2 ou de $n'M^2$, les phénomènes deviennent extrêmement compliqués et ne peuvent plus s'interpréter d'une manière intuitive.

Nuclear Magnetism and Nuclear Relaxation.

E. M. PURCELL

Harvard University, Cambridge, Mass.

1. - Introduction.

The theory of electronic paramagnetism is inseparably bound up with the theory of atomic structure. To regard a paramagnetic atom as having under all circumstances a fixed magnetic moment and spin is an approximation at best, and often a bad one. Especially the orbital contribution to the magnetization is affected by the environment of the atom or ion. In this respect *nuclear* paramagnetism is different, and simpler. The nuclear ground state is separated from the excited nuclear states by an energy gap so vast in comparison with any external perturbations we have to deal with, that we may treat the nuclear properties as given constants. That is, the subject of nuclear magnetism falls into two distinct parts: the question of the origin of the nuclear spins and moments, which is an important problem in nuclear theory but one that we shall ignore, and the study of the magnetic behavior of matter in bulk which arises from the nuclear magnetic moments, which is our topic in these lectures.

We are concerned with the following properties of the nucleus:

a) The intrinsic angular momentum I . We recall that nuclei of even mass number A have $I=0$, or 2, or 4, etc., while for odd- A nuclei, $I=\frac{1}{2}, \frac{3}{2}, \dots$. Of course $I\hbar$ is merely the maximum component of angular momentum in a given direction; the quantity which is truly a constant of the motion is the square of the nuclear angular momentum, with eigenvalue $I(I+1)\hbar^2$.

b) The magnetic moment $\mu = g\mu_0 I = \hbar\gamma I$, where μ_0 , the so-called « nuclear magneton » is defined as $e\hbar/2Mc$, M being the mass of a bare proton. We call γ the gyromagnetic ratio. We shall often use $\boldsymbol{\mu}$ as the vector magnetic moment, or magnetic moment operator.

c) The electric quadrupole moment Q , a measure of the departure from sphericity of the nuclear charge distribution. For reasons of parity, quadrupole moments are not observable unless $I \geq 1$, and they will not concern us through most of these lectures.

2. - The static paramagnetism of a collection of nuclei.

The possibility of nuclear polarization, analogous to electronic polarization, was first suggested by GORTER ⁽¹⁾ and later, independently, by KURTI and SIMON ⁽²⁾, in connection with the subject of magnetic cooling. We use as a model a collection of N similar nuclei with given spin I and given magnetic moment μ . The nuclei are held fixed in a crystal which is in an external applied field \mathbf{H} . If the crystal is electronically diamagnetic, so that there are no uncompensated electron moments to produce internal fields, and if the nuclei do not interact with one another, the nuclear Hamiltonian is

$$(1) \quad \mathcal{H} = \sum_j \mathcal{H}_j,$$

where \mathcal{H}_j , the Hamiltonian for the j -th nucleus is

$$(2) \quad \mathcal{H}_j = -\boldsymbol{\mu}_j \cdot \mathbf{H}.$$

A nucleus of spin I may have $2I+1$ spin orientations. The external field removes the spin degeneracy and the energy levels of each nucleus are labelled by m , ranging from $-I$ to I , with energies given by

$$(3) \quad E_m = -m\mu H/I.$$

A description of the system is furnished by the set of numbers n_m , where n_m is the number of nuclei in the m -th state. If thermal equilibrium prevails, these occupation numbers will be governed by the Boltzmann factor, $\exp[-W_m/kT]$. But if (1) and (2) represented the exact Hamiltonian there would be no mechanism for setting up this equilibrium, and so the n_m would not change from the values they had before the field was applied. Therefore, if thermal equilibrium is to be attained, there must be some interactions (if only very weak ones) besides the interactions with the external field.

Suppose that thermal equilibrium is somehow brought about. Then the

⁽¹⁾ C. J. GORTER: *Phys. Zeits.*, **35**, 928 (1934).

⁽²⁾ N. KURTI and F. SIMON: *Proc. Roy. Soc.*, A **149**, 175 (1935).

magnetic moment of the system will be along \mathbf{H} and its magnitude will be

$$(4) \quad M = (N\mu/I) \frac{\sum_m m \exp [m\mu H/IkT]}{\sum_m \exp [m\mu H/IkT]},$$

which reduces in the limit $H\mu \ll kT$, to

$$M = \frac{N\mu^2}{3kT} \left(\frac{I+1}{I} \right) H.$$

Introducing the static paramagnetic susceptibility χ_0 , we may write this as $M = \chi_0 H$, with

$$(5) \quad \chi_0 = \frac{N\mu^2}{3kT} \left(\frac{I+1}{I} \right).$$

If μ is a typical nuclear magnetic moment, $H\mu/kT \sim 10^{-10}$, so that under all but the most extreme conditions Eq. (5) should be an excellent approximation. Nuclear paramagnetism conforms extremely closely to Curie's law at ordinary temperatures and magnetic field strengths.

In 1937 LASAREV and SCHUBNIKOV⁽³⁾ detected the static nuclear susceptibility of solid hydrogen. In the vicinity of 2 °K, they were able to separate the diamagnetic electronic contribution from the nuclear contribution through the temperature dependence of the latter, and their results were sufficiently accurate to prove that the magnetic moment of the proton is not just μ_0 .

More recently EVANS⁽⁴⁾ has measured at room temperature the static nuclear susceptibility of hexamethylbenzene, $C_6(CH_3)_6$. The sample was mounted at the end of a rod with a quartz bar fixed at right angles to help balance out diamagnetic effects, the whole being suspended by a quartz fibre in an inhomogeneous magnetic field. The nuclear magnetization was destroyed by a radio-frequency field which was then switched off. As the nuclear polarization returned, at a rate governed by the nuclear relaxation time, the torque experienced by the specimen and the resulting torsional deflection changed with time. The diamagnetism of the specimen, though much larger than the nuclear paramagnetism, does not depend on the time in this way.

An interesting departure from Curie's law is shown by liquid ^3He , which, below 2 °K, deviates from Curie's law in the antiferromagnetic direction. Here the Pauli exclusion principle is beginning to operate on the ^3He spins, owing to some overlap of the nuclear wave functions. The experiment which

(3) B. G. LASAREV and L. W. SCHUBNIKOV: *Phys. Zeits. d. Sov. U.*, **11**, 445 (1937).

(4) D. F. EVANS: *Phil. Mag.*, **1**, 370 (1956).

revealed this effect ⁽⁵⁾ was actually a measurement not of χ_0 but of the magnetic resonance absorption which, as we shall presently see, is proportional to χ_0 but far easier to detect.

3. — The dynamic behavior of nuclear spins.

We begin our investigation of the dynamic behaviour of a nuclear spin system by asking two questions:

- 1) Given a time dependent applied field $H_0(t)$, what is the behavior of the total magnetic moment of our system, $M(t)$?
- 2) How do the individual nuclear moments interact with one another and with the other dynamical variables of the system; in particular, how does the spin system reach thermal equilibrium?

We shall take up these questions separately.

As a first approximation, consider the case of spins which interact only with the applied field $H(t)$ and not with each other. The Hamiltonian is given by Eqs. (1) and (2). The x -component of the magnetic moment of the j -th nucleus obeys

$$(6) \quad \frac{d\mu_{jx}}{dt} = \frac{i}{\hbar} [\mathcal{H} \mu_{jx}].$$

Replacing μ_{jx} by $\gamma\hbar I_{jx}$ and making use of the commutation rules connecting I_{jx} , I_{jy} and I_{jz} , we are led to one component of the vector equation

$$(7) \quad \frac{d\bar{\mu}_j}{dt} = -\gamma_j H(t) \times \bar{\mu}_j.$$

We introduce here $\bar{\mu}$ as the *expectation value* of the vector magnetic moment of the j -th nucleus. Now the total magnetic moment of our system, at any time, is

$$M = \sum_j \bar{\mu}_j,$$

so that, on the assumption that $H(t)$ is uniform throughout the system,

$$(8) \quad \frac{dM}{dt} = -H(t) \sum_j \gamma_j \bar{\mu}_j.$$

⁽⁵⁾ W. M. FAIRBANK, W. B. ARD and G. K. WALTERS: *Phys. Rev.*, **95**, 566 (1954).

If we further assume that all the γ_j 's are the same and equal to γ , we get simply

$$(9) \quad \frac{d\mathbf{M}}{dt} = -\gamma \mathbf{H} \times \mathbf{M}.$$

Eq. (9) is the basic equation of nuclear magnetic resonance. We derived it under the following assumptions:

- a) All the γ_j 's are equal. This is not an important restriction; if we deal with a substance containing different nuclear species, we merely write an equation like Eq. (9) for each species separately. At least, we may do this whenever our next assumption *b*) holds.
- b) There are no interactions other than those with the applied field. This is a very severe restriction. Nevertheless we shall be able to treat interactions, in certain cases, through the device of an «internal field».
- c) Only magnetic coupling is involved. Eq. (9) does not hold, for instance, if the nuclei have electric quadrupole moments and are situated in strongly inhomogeneous electric fields.

Note that we have *not* had to assume that the various $\bar{\mu}_j$'s are the same or have the same history.

Eq. (9) predicts that our system should behave, with respect to its macroscopic magnetic moment \mathbf{M} , like a magnetic top. Indeed, its behavior is even simpler than that of an ordinary top, which would obey an equation like (9) only in the limit of infinite spin velocity. How does this simplicity arise? It comes essentially from the exclusion of the possibility of excited nuclear states, so that I and μ are truly constants of the motion. In the language of top theory, the precession frequency must be very small compared to the rotation frequency, if we are to have this situation. Now the precession frequencies, for nuclear magnetic moments in ordinary fields, lie in the range of 10^7 s^{-1} , whereas nuclear *rotation* frequencies are typically in the range of γ -rays, around 10^{-18} s^{-1} . The assumption is therefore a safe one.

As our first example, let $\mathbf{H}(t)$ be a field constant in time: $\mathbf{H} = \mathbf{H}_0$. Then \mathbf{M} precesses around the direction of \mathbf{H}_0 with an angular velocity

$$(10) \quad \omega_0 = \gamma H_0.$$

Consider, as a second example, the field described by $H_x = H_y = 0$, $H_z = H_0 \cos \omega t$. The motion of \mathbf{M} is here a precession around the z -axis with varying angular velocity. If φ is the angle between the xz plane and the plane which contains \mathbf{M} and the z -axis, we have from Eq. (9) $\varphi = (\gamma H_0 / \omega) \sin \omega t + \delta$,

so that M , varies as $\cos [(\gamma H_0/\omega) \sin \omega t + \delta]$, etc. As this example emphasizes, our system is *not*, in general, linear in its response to applied fields.

A problem of greater interest for us is described by: $H_x = H_1 \sin \omega t$, $H_y = H_0 \cos \omega t$, $H_z = H_0$. A constant field along the z -axis is accompanied by a rotating transverse field. To analyze this situation we introduce rectangular co-ordinates x' , y' , z' , which rotate with respect to fixed co-ordinates x , y , z , with angular velocity ω_r . If $d\mathbf{M}/dt$ is the rate of change of \mathbf{M} with t in the fixed co-ordinates, and $\partial\mathbf{M}/\partial t$ is the rate of change of \mathbf{M} referred to $x'y'z'$,

$$(11) \quad \frac{d\mathbf{M}}{dt} = \frac{\partial\mathbf{M}}{\partial t} + \boldsymbol{\omega}_r \times \mathbf{M}.$$

From (9), then $\partial\mathbf{M}/\partial t = \gamma\mathbf{M} \times \mathbf{H} + \mathbf{M} \times \boldsymbol{\omega}_r$, or

$$(12) \quad \frac{\partial\mathbf{M}}{\partial t} = \gamma\mathbf{M} \times \mathbf{H}_{\text{eff}}, \quad \text{where} \quad \mathbf{H}_{\text{eff}} = \mathbf{H} + \boldsymbol{\omega}_r/\gamma.$$

Eq. (12) shows that the motion of \mathbf{M} , as seen from the rotating co-ordinates, is the same as it would be in fixed co-ordinates if the applied field were $\mathbf{H} + \boldsymbol{\omega}_r/\gamma$. A completely quantum mechanical derivation of this theorem can be given⁽⁶⁾; one has only to assume that the Hamiltonian is $\mathcal{H} = -\gamma\hbar\mathbf{I} \cdot \mathbf{H}$, where \mathbf{I} is the total angular momentum.

Returning to our immediate problem, we direct $\boldsymbol{\omega}_r$ along z and choose $\boldsymbol{\omega}_r = \omega$. Then the components of \mathbf{H}_{eff} , referred to the rotating co-ordinates, are constant in time and are

$$(13) \quad H_{x'} = 0, \quad H_{y'} = H_1, \quad H_{z'} = H_0 + \frac{\omega}{\gamma}.$$

(By choice of phase, we have made $H_{x'} = 0$). Given some initial magnetization \mathbf{M}_0 , the subsequent motion of \mathbf{M} , in the rotating system, is simply a precession around the direction of \mathbf{H}_{eff} . It is now easy to describe $M_{x'}(t)$, $M_{y'}(t)$, and $M_{z'}(t)$, and from these we can recover $M_x(t)$, etc., by transforming back to the fixed co-ordinates. More complicated situations can sometimes be sorted out by applying two successive transformations of this sort. Examples are given in the article of RABI, RAMSEY and SCHWINGER⁽⁶⁾.

We are mainly interested in the *resonance* condition

$$(14) \quad \omega = -\gamma H_0.$$

The sign in Eq. (14) is connected with the sense of rotation of the transverse field. It should be remembered, too, that γ may be positive or negative,

(6) I. I. RABI, N. F. RAMSEY and J. SCHWINGER: *Rev. Mod. Phys.*, **26**, 167 (1954).

depending on the nuclear species. If one looks in the direction of H_0 , in fixed co-ordinates, nuclei with *positive* gyromagnetic ratio will be observed to precess *counter-clockwise*. In the rotating co-ordinate system, \mathbf{M} simply rotates about the y' axis.

Now the condition (14) is, from another point of view, precisely the Planck condition for transitions between adjacent eigenstates of I_z , the Zeeman levels of this system in the constant field H_0 . For a single nucleus of moment μ and spin I we would have $2I+1$ levels separated according to Eq. (3), by

$$\Delta E = \mu H_0 / I,$$

so that

$$\Delta E / \hbar = \frac{\mu H_0}{I \hbar} = \gamma H_0.$$

Quantum mechanically speaking, the rotating field H_1 is a perturbation which causes transitions between the stationary states of the spin system in the constant field H_0 . It may be instructive to review the connection between the behavior of the expectation value of \mathbf{M} , which obeys the classical equation of motion Eq. (9), and the quantum mechanical transition probability. Consider a single spin with $I = \frac{1}{2}$; there are two eigenstates in the field H_0 , $m_z = \pm \frac{1}{2}$. Let $\bar{\mu}$ be the expectation value of the magnetic moment. Supposing the system to be in the state $m = +\frac{1}{2}$ at $t = 0$, when H_1 is suddenly switched on, what is the probability of finding the system in the other state at time t thereafter? Let $U(t)$ denote this probability. Now initially $\bar{\mu}_z = \mu$, $\bar{\mu}_x = \bar{\mu}_y = 0$. At any later time, $\bar{\mu}_z = -\mu U + \mu(1 - U)$, so that

$$(15) \quad U(t) = \frac{1}{2}[1 - \bar{\mu}_z(t)/\mu].$$

But we know that the vector $\bar{\mu}$, which lies initially along z , rotates about y' with angular speed γH_1 , if (14) is satisfied. Hence $\bar{\mu}_z = \mu \cos \gamma H_1 t$ from which we get, using (15),

$$(16) \quad U(t) = \sin^2 (\gamma H_1 t / 2).$$

The off-resonance case can be solved nearly as easily. In that case one finds

$$(17) \quad U(t) = \cos^2 \delta \sin^2 (\gamma H_1 t / 2 \cos \delta),$$

where

$$(18) \quad \delta = \text{tg}^{-1} (\gamma H_0 - \omega) / H_1.$$

We are accustomed to describing most radiation and absorption processes in terms of a constant time-independent transition probability W . W would

be just dU/dt , if the latter quantity were constant. But here it is not, so we cannot speak of a transition probability in the usual sense. This is a consequence of our assumption that the system has sharply defined energy levels and is perturbed by a field that is a precisely known function of the time. We shall see that if either restriction is removed, we obtain Uxt , at least for some range of t .

Even in the absence of other disturbances, the state of a dipole is not changeless. All excited states have a finite life-time because of the possibility of spontaneous emission, which causes a broadening of the resonance line. In the case of electric dipole emission states in the optical range, the lifetime is of the order of 10^{-8} s. The lifetime is given by the approximate formula $T \approx \hbar \lambda^3 / \mu^2$. For a nuclear magnetic state, the lifetime is much larger than 10^{-8} s for three reasons; λ , the wavelength, is about 10^7 times an optical wavelength; μ is a magnetic moment, not an electric one, and is thus smaller by a factor 137; μ is also a *nuclear* magneton, not a Bohr magneton, and is thus smaller by about 10^3 . Hence in this case $T \sim 10^{25}$ s, or 10^8 times the lifetime of the universe! This value of T was derived from the formula for radiation into free space. T is much shorter if the system is coupled to a resonant circuit of dimensions small compared to λ , but it is still ridiculously long. We have to look elsewhere for the source of line-broadening in nuclear resonance.

Below, we shall obtain a transition probability U which is proportional to t by two means: firstly, by assuming a slight broadening of the energy levels of the magnetic dipoles in the field H_0 and secondly, by subjecting the system to quasi-random disturbing fields.

Suppose that the perturbing field H_1 is uniform throughout the sample but the steady field H_0 is *not* uniform throughout the sample so that there is a distribution of resonant frequencies. The fraction of nuclei with resonant frequencies between ω_0 and $\omega_0 + d\omega_0$ is $g(\omega_0) d\omega_0$, the distribution being normalized so that $\int_{-\infty}^{\infty} g(\omega_0) d\omega_0 = 1$. The transverse field H_1 , at frequency ω , is switched on at $t = 0$, when all N spins, in the system, say, are in the level $m = \frac{1}{2}$. The expected number in the upper state, $m = -\frac{1}{2}$, at time t is then

$$(19) \quad N\bar{U}(t) = N \int_{-\infty}^{\infty} g(\omega_0) U(t, \omega_0) d\omega_0,$$

where $U(t, \omega_0)$ is given by Eq. (17). Explicitly,

$$(20) \quad \bar{U}(t) = \int_{-\infty}^{\infty} g(\omega_0) \left[1 - \left(\frac{\omega_0 - \omega}{\gamma H_1} \right)^2 \right]^{-1} \sin^2 \left\{ \frac{\gamma H_1 t}{2} \left[1 + \left(\frac{\omega_0 - \omega}{\gamma H_1} \right)^2 \right]^{\frac{1}{2}} \right\} d\omega_0.$$

The main contribution to this integral comes from the neighborhood of ω . Let us assume provisionally that $g(\omega_0)$ varies so little over this region that it can be replaced by $g(\omega)$. The integral remaining can be evaluated, with the following result:

$$(21) \quad \bar{U}(t) = \frac{\pi}{2} \gamma H_1 g(\omega_0) \int_0^{\gamma H_1 t} J_0(z) dz.$$

According to Eq. (21), $\bar{U}(t)$ will be proportional to t for $\gamma H_1 \ll 1$, so that we may speak of a constant transition probability per unit time, so long as t is not too great:

$$W = \frac{d\bar{U}}{dt} \approx \frac{\pi}{2} \gamma^2 H_1^2 g(\omega), \quad \gamma H_1 t \ll 1.$$

For very short times, however, the assumption that $g(\omega_0)$ can be replaced by $g(\omega)$ in (20) is untenable, and (21) does not hold. Examination of this limit shows that for time t less than $\Delta\omega_0^{-1}$, where $\Delta\omega_0$ is a measure of the width of the distribution $g(\omega_0)$, $\bar{U}(t)$ is proportional to t^2 rather than t .

In the foregoing example it was the «smearing out» of the resonance frequencies which was responsible for the linear growth, over a restricted period of time, of $\bar{U}(t)$. Something like this happens⁸ if we introduce, not a distribution of ω_0 , but a spectral distribution of the perturbing field H_1 , that is, a distribution of ω . This is what we have if the field H_1 is in some degree a *random* function of the time.

To keep the mathematics simple, we imagine a particular type of random variation of phase and amplitude of the rotating field H_1 . The field shall rotate with constant frequency and amplitude for a time τ_0 , at the end of which both phase and amplitude change suddenly and arbitrarily to new values. The field rotates then with the same frequency, but with the new phase and amplitude for a second period of the same length τ_0 , as before. The process continues, each new phase and amplitude having no predictable relation to the previous ones, but the frequency and period remaining constant throughout.

Suppose that ω coincides with the resonance frequency $\omega_0 = \gamma H_0$ which is in this example the same for all nuclei. Then in the rotating co-ordinate system the z -component of \mathbf{H}_{eff} vanishes. \mathbf{H}_{eff} is a vector lying in the $x'y'$ plane; it remains fixed in both magnitude and direction for a period τ_0 , and then changes its amplitude and direction suddenly, all directions in the $x'y'$ plane being equally likely. Let us start with the vector \mathbf{M} in the z -direction at $t = 0$ and let us impose the important restriction $\gamma H_1 t \ll 1$. The precession of \mathbf{M} about \mathbf{H}_{eff} during each of a succession of intervals τ_0 causes the tip of the vector \mathbf{M} , to execute a two-dimensional random walk in the neighborhood of the pole. We are interested in the mean square displacement of \mathbf{M} from

the z -axis, at time t , the mean being understood to be taken over an ensemble of spins for each of which the random variation of \mathbf{H}_1 is different. Since exactly t/τ_0 steps occur in time t , and the square of a step length is $\gamma^2\tau_0^2(H_x^2 + H_y^2)$, we have at once

$$(23) \quad \bar{\theta}^2 = \gamma^2 \bar{H}_1^2 \tau_0 t.$$

Here \bar{H}_1^2 is the mean square amplitude of the transverse rotating field.

Now $U(t)$, the expectation that a spin will be found in the state $m = -\frac{1}{2}$, is related to the projection of \mathbf{M} on the z -axis. That is,

$$U(t) = \frac{1}{2}(1 - \cos \theta).$$

If θ is small, $\bar{U}(t)$ can be written down at once using our result in Eq. (23):

$$(24) \quad \bar{U}(t) = \frac{1}{4} \bar{\theta}^2 = \frac{1}{4} \gamma^2 \bar{H}_1^2 \tau_0 t,$$

or in terms of a transition probability per unit time,

$$(25) \quad W = \frac{d\bar{U}}{dt} = \frac{1}{4} \gamma^2 \bar{H}_1^2 \tau_0.$$

Again there is a restriction on the validity of our result. The time t must be long enough to include several intervals τ_0 . It is easy to see that during the *first* step, $\bar{U}(t)$ must grow quadratically with t , as the vector \mathbf{M} precesses at constant speed away from the pole. This is closely related to the restriction $t > \Delta\omega^{-1}$ in our previous example. In both examples, the linearity ceases when t is too great, but the reasons are not the same. The former example, with the given distribution of ω_0 , lacks the essential randomness we have introduced in our second example.

This calculation has provided us with a simple model of a spin system perturbed by a randomly fluctuation field which is characterized merely by its mean square amplitude and a certain time-constant τ_0 . We shall use this model to discuss, in a very elementary way, *thermal relaxation* in a spin system.

4. - The approach to thermal equilibrium.

It obviously makes no difference in the above argument if we start with \mathbf{M} along $-z$ rather than z . That is, the probability of a transition from $m = \frac{1}{2}$ to $m = -\frac{1}{2}$ in a given time, is the same as the probability of transition from $m = -\frac{1}{2}$ to $n = \frac{1}{2}$. This is the well-known equality of probabilities for

stimulated emission and absorption, in a given perturbing field. Yet it is only through the agency of some statistical perturbations that our spin system can acquire the Boltzmann distribution appropriate to the temperature of its surroundings. How does this come about?

Think of a macroscopic quantity of substance, an assembly of N spins with $I = \frac{1}{2}$ and gyromagnetic ratio γ , in a magnetic field H_0 . Each spin has two energy levels and the macroscopic state is described by the occupation numbers n_+ and n_- . At the time the field is applied, $n_+ = n_- = N/2$. As a result of perturbations caused by internal fields H_i (different at different nuclear sites) we have $n_+ W_\uparrow$ per second transitions up and $n_- W_\downarrow$ per second transitions down. W_\downarrow stands for the probability, per second, that a spin in the upper or «anti-parallel» state will make a transition to the lower state, and W_\uparrow for the converse. We have just argued that $W_\uparrow = W_\downarrow$, but that is not quite correct. The reason is that we have neglected part of our system. We want our spin system to reach thermal equilibrium at the temperature T , which requires that we must have a heat bath with which the spins interact and which determines this final temperature. By the conservation of energy, any transition of a spin must be accompanied by a transition in the heat bath. It is the coupling with the bath which causes the difference in W_\uparrow and W_\downarrow . Let us see what this difference must be.

When the assembly of spins reaches a stationary state, we shall have

$$(26) \quad W_\uparrow n_+ = W_\downarrow n_-$$

so that

$$(27) \quad (W_\uparrow/W_\downarrow)_{\text{equil.}} = (n_-/n_+)_{\text{equil.}} = \exp[-2\mu H_0/kT].$$

Now, the probability that a given spin will make a transition is independent of the states of the other spins (except in «super-radiant states») (*). This probability is determined completely by the fact that the heat bath with which the spins interact is in equilibrium at the temperature T . As long as the interaction energy is small compared to the total energy of the bath, the bath remains in equilibrium at the same temperature and the ratio W_\uparrow/W_\downarrow is independent of the occupation numbers n_+ and n_- .

How the difference in W_\uparrow and W_\downarrow arises we need not always trace in detail, but perhaps we may indicate how it comes about in one special case. Let us consider a heat bath composed of a very large number of harmonic oscillators which happen to be conveniently chosen to have the same frequency

(*) These are the case discussed by R. H. DICKE [*Phys. Rev.*, **93**, 99 (1954)] where a definite phase relationship exists among the spins, so that the spins «radiate coherently». This case will not occur in our work.

as our spin resonance. At the start, the oscillators are in thermal equilibrium at the temperature T_0 . Quantum mechanically we can describe the behavior of the oscillators as follows. Each oscillator has an infinite number of energy levels uniformly spaced by $\varepsilon = \hbar\omega_0$. At any time the macroscopic state of the bath is described by occupation numbers ν_0, ν_1, \dots where ν_j is the occupation number of the j -th oscillator energy level. If the bath is in equilibrium, we know that the occupation numbers will be proportional to successively diminishing Boltzmann factors

$$(28) \quad \nu_j \sim \exp[-j\varepsilon/kT_0].$$

If a nuclear spin makes a transition up, $(+\frac{1}{2} \rightarrow -\frac{1}{2})$, at the same time an oscillator goes from its j -th to $(j-1)$ -th state: when a spin makes a transition down, $(-\frac{1}{2} \rightarrow +\frac{1}{2})$ an oscillator goes from j to $j+1$. The probabilities of the transitions we can write down by examining the matrix element P of the interaction between spins and oscillators. The probabilities of the two processes would look something like this

$$(29) \quad W_{\uparrow} \sim \sum_{j=1}^{\infty} |\langle +, j | P | -, j-1 \rangle|^2 \exp[-j\varepsilon/kT_0]$$

and

$$(30) \quad W_{\downarrow} \sim \sum_{j=0}^{\infty} |\langle -, j | P | +, j+1 \rangle|^2 \exp[-j\varepsilon/kT_0] = \\ = \exp[\varepsilon/kT_0] \sum_{j=1}^{\infty} |\langle -, j-1 | P | +, j \rangle|^2 \exp[-j\varepsilon/kT_0].$$

Comparison of (29) and (30) verifies, for this model at least, that

$$(31) \quad W_{\uparrow}/W_{\downarrow} = \exp[-\varepsilon/kT_0]$$

at all times, provided that the heat bath remains in thermal equilibrium at the initial temperature T_0 . This may be insured by coupling the ensemble of oscillators in turn to an infinite heat reservoir, or more directly by considering the collection of oscillators to be so large that its energy of interaction with the nuclear spins is negligible compared to the total energy of the oscillators themselves.

A general treatment of the coupling of bath and nuclear system such as that of BLOCH and WANGSNESS⁽⁷⁾, or Bloch's even more general theory⁽⁸⁾, leads to such a result.

(7) R. K. WANGSNESS and F. BLOCH: *Phys. Rev.*, **89**, 728 (1953).

(8) F. BLOCH: *Phys. Rev.*, **102**, 104 (1956).

In our case of N spins with $I = \frac{1}{2}$, $n_+ + n_- = N$. Let

$$(32) \quad W_{\downarrow} = W \exp[\mu H_0/kT], \quad W_{\uparrow} = W \exp[-\mu H_0/kT].$$

The rates of change of the occupation numbers are

$$(33) \quad \frac{dn_+}{dt} = -\frac{dn_-}{dt} = n_- W_{\downarrow} - n_+ W_{\uparrow}.$$

We assume $\mu H_0/kT \ll 1$, and expand the exponentials in (32), obtaining

$$(34) \quad \frac{d}{dt}(n_+ - n_-) = -2W \left[n_+ - n_- - (n_+ + n_-) \frac{\mu H_0}{kT} \right].$$

Multiplying both sides of this equation by μ and using the relations

$$\frac{N\mu^2}{kT} H_0 = \chi_0 H_0 = M_0, \quad \mu(n_+ - n_-) = M_z,$$

we get the fundamental differential equation of paramagnetic relaxation in the form

$$(35) \quad \frac{dM_z}{dt} = -2W(M_z - M_0).$$

The exponential relaxation described by this equation is characterized by the time constant $T_1 = (2W)^{-1}$. We call T_1 the spin lattice relaxation time, or frequently, after Bloch, the longitudinal relaxation time. For our particular perturbation characterized by $\overline{H_i^2}$ and τ_0 , we may set $W = \frac{1}{2}\gamma^2 \overline{H_i^2} \tau_0$, obtaining an explicit formula for the relaxation time

$$(36) \quad T_1 = 2/(\gamma^2 \overline{H_i^2} \tau_0).$$

It is perhaps not completely obvious that we are entitled to derive W from a theory which failed to account for a difference between W_{\uparrow} and W_{\downarrow} . The justification is that this difference, being of magnitude $(\mu H_0/kT)W$, is here quite small compared to W itself.

The magnetization always relaxes toward its equilibrium value $M_0 = \chi_0 H_0$. The exponential decrease of the difference $M_z - M_0$ holds only under the assumption $\mu H_0 \ll kT$. As we have seen, this is not an important restriction for nuclear magnetism. Experimentally one finds indeed an exponential behavior. Experimental values of relaxation times T_1 of various substances lie between 10^{-4} and 10^4 s. The factor 10^8 indicates the enormous variations.

in the transition probabilities in substances which are often superficially not very different. Fig. 1 shows a simple case of relaxation. It is the growth of the nuclear polarization of protons in NH_4Br as a function of the time. The relaxation time T_1 is about half a minute in this case.

The extension of our analysis to $I > \frac{1}{2}$ is not quite trivial. One finds that with a pure magnetic perturbation, the behaviour of M_z will still be a simple exponential. The relaxation time does not depend on the spin. For constant

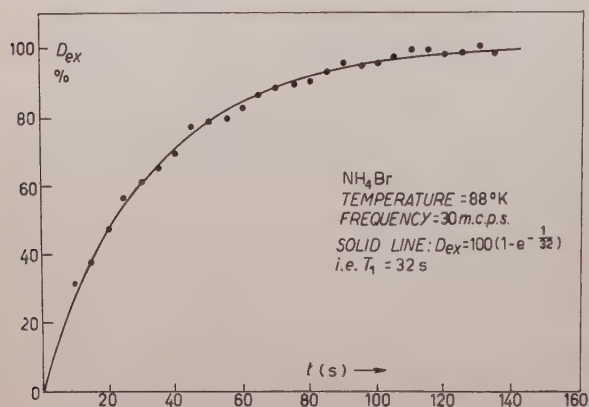


Fig. 1. — Exponential recovery of nuclear polarization in an ammonium bromide crystal. The points were obtained experimentally by measuring the intensity of the nuclear resonance absorption, using a measuring field too weak to disturb the polarization. (Unpublished work of A. SACHS and E. TURNER).

intensity of the internal field, T_1 is in fact determined by γ^2 for given $\overline{H_i^2}$ and τ_0 . A certain restriction must be introduced for the initial state; large departures of the n_m from the equilibrium values are not permitted. This assumption was not needed in the case of spin $\frac{1}{2}$. However, so long as the departures are small, they may be otherwise arbitrary. We do not require a Boltzmann distribution. We may have the system in an initial distribution over the spin states which cannot be described by a spin temperature; such a distribution

will change gradually into an equilibrium distribution adjusted to the bath temperature, exhibiting a simple exponential behavior of the magnetization in the process. However, if the original distribution is a Boltzmann distribution described by a spin-temperature, T_s different from the bath temperature T_0 then it remains a true Boltzmann distribution throughout the relaxation process. The spin system remains, so to speak, in internal equilibrium given by temperature T_s while T_s slowly approaches T_0 . This follows from the relations between the transition probabilities of the different levels.

Our analysis lacks generality in one important respect. We have assumed the spins to be coupled independently to the bath, and not to each other. In many substances, the interactions among the spins play an important or even dominant role in coupling the spins to the bath. A common example is the magnetic dipole-dipole interaction between nuclear spins on different atoms in the same molecule, the modulation of which, by the thermally excited rotation of the molecule, serves to couple the spin system to the rotational

degrees of freedom of the molecule. The latter serves as the bath. In this situation the concept of a random local field leads to a useful approximate description, but it fails to account for certain interesting and sometimes conspicuous properties of the system.

For our immediate purpose the simple «local field» model of the relaxation process will do well enough. Some of the effective sources of magnetic perturbations, in addition to the nuclear dipole-dipole interaction already mentioned, are: the magnetic field in a molecule which arises from the rotation of the whole molecular charge distribution; the magnetic field arising from the nuclear moments, or molecular rotation moments, of neighboring molecules; magnetic fields from unpaired electron spins, as in substances containing paramagnetic ions, or even metallic conductors. To give one homely example, the nuclear spin-lattice relaxation in ordinary tap water is due in large part to the dissolved oxygen.⁽⁹⁾ Here one source of the field H_i at a hydrogen nucleus is the pair of electron spins on some nearby O_2 molecule, a molecule which enjoys the rare distinction of a magnetic ground state, $^3\Sigma$.

What determines the characteristic time τ_0 in which such a field fluctuates, will vary from case to case. We need only remark now that the fluctuation is often extremely rapid, that is, τ_0 can be very short. In liquids, for instance, most interactions that we shall consider are characterized by fluctuation times less than 10^{-10} s. This has an important bearing on the question we now turn to.

5. - Relaxation of the transverse components of the magnetization.

The equilibrium value of the transverse components of magnetization, if there is no applied field except H_0 , is of course zero. If a transverse component of \mathbf{M} is somehow created, we may expect it to relax to zero. Indeed, processes very much like those just described can bring about such a relaxation. If we look at the system from the rotating co-ordinates, it is evident that an effective field, H_{eff} , which has randomly fluctuation components along all three axes x' , y' and z' , will cause the spin vectors (by which of course we mean the expectation values of the μ_i 's) to execute random walks over the sphere from any starting point, so that in the end the average of $\bar{\mu}_x$ and $\bar{\mu}_y$ over the ensemble will approach zero.

It is not obvious that the transverse components will relax at the same rate as the longitudinal component of \mathbf{M} . In general they will not, because the variation in time of $(H_{\text{eff}})_z$ in the rotating system will often be very different from that of $(H_{\text{eff}})_x$, and $(H_{\text{eff}})_y$. We may anticipate the appearance of a trans-

(9) G. CHIAROTTI, G. CRISTIANI and L. GIULOTTO: *Nuovo Cimento*, **1**, 863 (1955).

verse relaxation time, T_2 , distinct from the longitudinal relaxation time, T_1 . However, in one case of common occurrence the transverse and longitudinal components relax alike. If the local or internal field, \mathbf{H}_i , is on the average isotropic, and if it fluctuates with such rapidity that the characteristic time τ_0 is much less than ω_0^{-1} , then a transformation to co-ordinates rotating at angular velocity ω_0 will have practically no effect on the character of \mathbf{H}_i . It will be isotropic in its strength and in its behaviour in the $x'y'z'$ system as well. It follows, from arguments identical to those we have used to predict the behavior of M_z , that M_x and M_y will obey

$$(37) \quad \frac{dM_x}{dt} = -\frac{M_x}{T}, \quad \frac{dM_y}{dt} = -\frac{M_y}{T},$$

while

$$\frac{dM_z}{dt} = -\frac{1}{T}(M_z - M_0).$$

All components relax with the same time constant: the only difference is that the transverse components relax to zero, their equilibrium value. This is the usual situation in liquids, where, as we have already remarked, the prevailing interactions fluctuate in times as short as 10^{-10} or even 10^{-11} s. The equality of the transverse and longitudinal relaxation times in such systems is experimentally well established.

At the other extreme is the situation often found in crystals. Here the spins are subject to local fields which, although they vary randomly from one spin to another, have components that are nearly constant in time. Such static or nearly static components of \mathbf{H}_i will obviously look entirely different in rotating co-ordinates, for the transformation will endow them with a rotation at a frequency close to ω itself. The x' and y' components of \mathbf{H}_{eff} then lose their effectiveness to relax M_z . The z -component of \mathbf{H}_i on the other hand is unmodified by the transformation and appears as a static contribution, in the z' direction, to \mathbf{H}_{eff} . For a given spin, this merely shifts ω_0 , in effect. For the ensemble of spins, it is equivalent to a distribution of H_0 or ω_0 values. It results in a decay of M_x and M_y simply because the precession of the various $\bar{\mu}_x$ and $\bar{\mu}_y$'s that contribute to M_x and M_y gets out of step. The decay of M_x and M_y will be much faster than that of M_z in such cases. That is, T_2 will be much shorter than T_1 . But the transverse decay need not in fact be exponential, so that the specification of a relaxation time is not an adequate description of the process. The behavior of the transverse components of \mathbf{M} is sometimes called spin-spin relaxation.

An important distinction between longitudinal and transverse relaxation is the necessity, in longitudinal relaxation, for a net transfer of energy between

the nuclear spins and the « bath », owing to the presence of the strong field H_0 which defines the longitudinal direction. No net transfer of energy is involved in changing M_x and M_y , and such changes may therefore be effected by interactions wholly internal to the spin system.

Transverse relaxation is closely related to resonance line shape. The shorter the transverse relaxation time T_2 , the broader the line. More precisely, the line shape is the Fourier transform of the decay of the transverse magnetization. We postpone further examination of both problems to Sect. 9. Our present discussion is intended only as an introduction to the various kinds of relaxation we find in nuclear resonance experiments. To complete it, we remark that many substances do display a simple exponential relaxation of the transverse magnetization, with a time constant T_2 distinctly different from the longitudinal relaxation time of the system.

6. - The behavior of the system in a field that varies in time.

Let a field $H_a(t)$ be applied to the system, along with the constant field H_0 . The total external field is then $H(t) = H_0 + H_a(t)$. The internal fields to which we have ascribed relaxation effects remain, but we want to avoid dealing with them explicitly. That is, we seek equations connecting $M(t)$ with $H(t)$, suitably modified to take account of the relaxation process. The first attempt by BLOCH ⁽¹⁰⁾ to provide such a phenomenological description was notably successful. The Bloch equations are

$$(38) \quad \begin{cases} \dot{M}_x = -M_x/T_2 + \gamma(M_y H_0 - M_z H_y) \\ \dot{M}_y = -M_y/T_2 + \gamma(M_z H_x - M_x H_0) \\ \dot{M}_z = -(M_z - \chi_0 H_0)/T_1 + \gamma(M_x H_y - M_y H_x) \end{cases}$$

The z -direction has been taken along H_0 , it is assumed that $H_0 \gg H_a$, and H_a is assumed to be transverse. These are the conditions in most nuclear resonance experiments.

The Bloch equations amount to an amalgamation of the dynamical equation, Eq. (9), here applied only to the external field, with the equation for pure relaxation (37). One may say that motion of the magnetization vector M in the applied field, and the relaxation of the magnetization proceed independently. The justification for this is the success of the Bloch equations in describing a wide variety of phenomena. Nuclear magnetic resonance ab-

⁽¹⁰⁾ F. BLOCH: *Phys. Rev.*, **70**, 460 (1946).

sorption and dispersion, nuclear induction, saturation and transient effects—all these are accurately described by Eq. (38). The application of the Bloch equations to most of these phenomena has been thoroughly discussed in the literature and we will not review it here.

Still, the Bloch equations have their limitations. In many systems the transverse magnetization does not decay exponentially. Also, the relaxation processes are sometimes modified by the applied field \mathbf{H}_a , if \mathbf{H}_a is relatively strong. It may be instructive to examine a case in which a more general equation can be written. If all internal fields fluctuate very rapidly, so that $\tau \ll \omega^{-1}$ with the result that $T_1 = T_2 = T$, it will be the *total* instantaneous applied field $\mathbf{H} = \mathbf{H}_0 + \mathbf{H}_a$ which defines the vector \mathbf{M}_0 toward which \mathbf{M} is relaxing. It is only the total field which, at one instant, establishes a unique direction; the rapidly fluctuating microscopic fields do not, in themselves, provide a « memory » for earlier conditions. For such a system we have, in place of the approximate Bloch equations, the single vector equation

$$(39) \quad \dot{\mathbf{M}} = -T_1^{-1}(\mathbf{M} - \chi_0 \mathbf{H}) + \gamma \mathbf{M} \times \mathbf{H},$$

\mathbf{H} includes both \mathbf{H}_a and \mathbf{H}_0 and there is no restriction on the magnitude of either part. In particular, we may apply Eq. (39) when \mathbf{H}_0 is small or even zero. The latter case is the simplest case of *paramagnetic relaxation*, discovered long ago in electronic paramagnetism by GORTER.

We investigate the response of the system to an alternating field in the presence of a constant field at right angles:

$$(40) \quad H_x = H_1 \cos \omega t, \quad H_y = 0, \quad H_z = H_0.$$

The substitution of (40) into Eq. (39) presents us with the problem of forced oscillations of a damped, *non-linear* oscillator. We look for solutions of the form

$$(41) \quad \left\{ \begin{array}{l} M_x = \sum_n a_n \cos n\omega t + b_n \sin n\omega t \\ M_y = \sum_n c_n \cos n\omega t + d_n \sin n\omega t \\ M_z = \sum_n e_n \cos n\omega t + f_n \sin n\omega t. \end{array} \right.$$

Let

$$\gamma H_0 T_1 = \omega_0 T_1 = q_0, \quad \gamma H_1 T_1 = 2q_1, \quad \omega T_1 = q.$$

Substituting (41) into our differential equation, and assuming that amplitudes of the higher harmonics are small so that terms arising from the mixing of

harmonics can be neglected, we are able to obtain an approximate solution for the amplitudes of the fundamental terms:

$$(42) \quad \left\{ \begin{array}{l} a_0 = c_0 = e_1 = f_1 = 0 \\ a_1 = \chi_0 H_1 D^{-1} [(1 + q_0^2)^2 + q^2(1 - q_0^2) + 2q_1^2(1 + q_0^2)] \\ b_1 = \chi_0 H_1 D^{-1} q(1 + q_0^2 + q^2 + 2q_1^2) \\ c_1 = 2\chi_0 H_1 D^{-1} q_0 q^2 \\ d_1 = -\chi_0 H_1 D^{-1} q q_0 (1 + q_0^2 - q^2 + 2q_1^2) \\ e_0 = \chi_0 H_0 - q_1 c_1 \\ D = (1 + q^2 - q_0^2)^2 + 4q_0^2 + 2q_1^2(1 + q^2 + q_0^2) \end{array} \right.$$

We note that D is a «resonance denominator», but we want to discuss first the non-resonant case, $H_0 = 0$. With $q_0 = 0$, we have a drastic simplification. The system becomes completely linear and the *exact* solution is

$$(43) \quad M_x = \chi_0 H_1 \frac{\cos \omega t + q \sin \omega t}{1 + q^2}, \quad M_y = M_z = 0.$$

The oscillating field in the x direction produces a magnetization in the x -direction which oscillates out of phase with the field, the phase lag being $\text{tg}^{-1} q$. This behavior, like that of any linear system, is conveniently described by a complex susceptibility $\chi = \chi' - i\chi''$, defined as follows: let H_x be the real part of $H_1 \exp[i\omega t]$ and M_x the real part of $\chi H_1 \exp[i\omega t]$. For the case at hand,

$$(44) \quad \chi' = \chi_0 / (1 + q^2), \quad \chi'' = q\chi_0 / (1 + q^2).$$

The behavior is just like that of the complex dielectric susceptibility in the phenomenon of dielectric dispersion and relaxation studied by DEBYE.

Returning to the case of resonance, suppose that $q_0 \gg 1$ (implying a relatively sharp resonance) and consider the behavior for frequencies ω close to ω_0 , that is, for q near q_0 . Suppose also that $H_1 \ll H_0$. Let $\delta = q - q_0$. It is convenient to introduce two complex susceptibilities:

$$(45) \quad \left\{ \begin{array}{l} \chi_{\parallel} = \chi'_{\parallel} - i\chi''_{\parallel} = (a_1 - ib_2)/H_1, \\ \chi_{\perp} = \chi'_{\perp} - i\chi''_{\perp} = (-d_1 - ic_1)/H_1. \end{array} \right.$$

From Eq. (42), neglecting small quantities, we now find, for the «parallel

susceptibility »:

$$(46) \quad \begin{cases} \chi'_{\parallel} = -\frac{1}{2}\chi_0 q_0 \delta (1 + \delta^2 + q_1^2)^{-1} \\ \chi''_{\parallel} = \frac{1}{2}\chi_0 q_0 (1 + \delta^2 + q_1^2)^{-1} \end{cases}$$

and to this approximation, $\chi'_{\perp} = \chi'_{\parallel}$ and $\chi''_{\perp} = \chi''_{\parallel}$.

Two points should be noted. First, the maximum value of χ'' is $\frac{1}{2}q_0\chi_0$; thanks to the factor q_0 , which is often as large as 10^7 , resonance methods enjoy an enormous practical advantage over static methods of measurement of nuclear magnetic susceptibility.

The second point concerns the linearity of the system. In a restricted sense the system is linear, as, at least in the present approximation, a sinusoidal field H_1 leads to a sinusoidal response at the same frequency. Only this justified our calling quantities like a_1/H_1 susceptibilities. Strictly speaking, however, the system is not linear, for the amplitude of the oscillating field appears in the denominator in Eq. (46). With increasing amplitude, a saturation effect enters. A close analogy is provided by the resistance of a wire to alternating current, when the resistance depends on the temperature of the wire. At constant power the wire displays a constant resistance, so long as the frequency is high compared to the thermal relaxation rate of the wire. But if the a.c. amplitude changes, so does the resistance. Whether such a system ought to be called linear is a question of taste; but one must at any rate be cautious about applying to such a system general theorems predicated on linearity.

Saturation effects are of great practical and theoretical interest in nuclear resonance, being direct manifestations of relaxation processes. But let us exclude them for the following discussion by the restriction $q_1 \ll 1$. It is easy to show that in the limit of vanishing q_1 the higher harmonics, $n > 1$, in the solution (41) of Eq. (39) all vanish, the system becomes truly linear, and the susceptibilities are given exactly by

$$(47) \quad \begin{cases} \chi'_{\parallel} = \chi_0 [(1 + q_0^2)^2 + q^2(1 - q_0^2)][(1 + q^2 - q_1^2)^2 + 4q_0^2]^{-1} \\ \chi''_{\parallel} = \chi_0 q(1 + q_0^2 + q^2)[(1 + q^2 - q_0^2)^2 + 4q_0^2]^{-1} \\ \chi'_{\perp} = -\chi_0 q q_0 (1 + q_0^2 - q^2)[(1 + q^2 - q_0^2)^2 + 4q_0^2]^{-1} \\ \chi''_{\perp} = 2\chi_0 q_0 q^2 [(1 + q^2 - q_0^2)^2 + 4q_0^2]^{-1} \end{cases}$$

There is no restriction on the magnitudes of q_0 and q in Eq. (47). These Eqs. are capable, for example, of describing the transition from the non-resonant case, Eq. (44), to which (47) reduces with $q_0 = 0$, to the resonant situation. Fig. 2 shows a family of curves, plotted from Eq. (47) for various values of q_0 .

Usually, in nuclear resonance, the situation is very different from any case

shown in Fig. 2, in that q_0 is a very large number. Then the difference between Eq. (47) and Eq. (46) is minor. Still it is of some interest to assess the difference. According to (47) the peak of the resonance is not precisely at $\omega = \omega_0$, nor do the dispersion terms χ'_\parallel and χ'_\perp go through zero precisely there. Instead there are small shifts, but these are, in order of magnitude, $1/q_0$ times the line width itself, and hence negligible for all practical purposes. Note that we have here been able to discuss exactly the behavior of the system in a linearly oscillating field, something the rotating co-ordinate treatment does not facilitate.

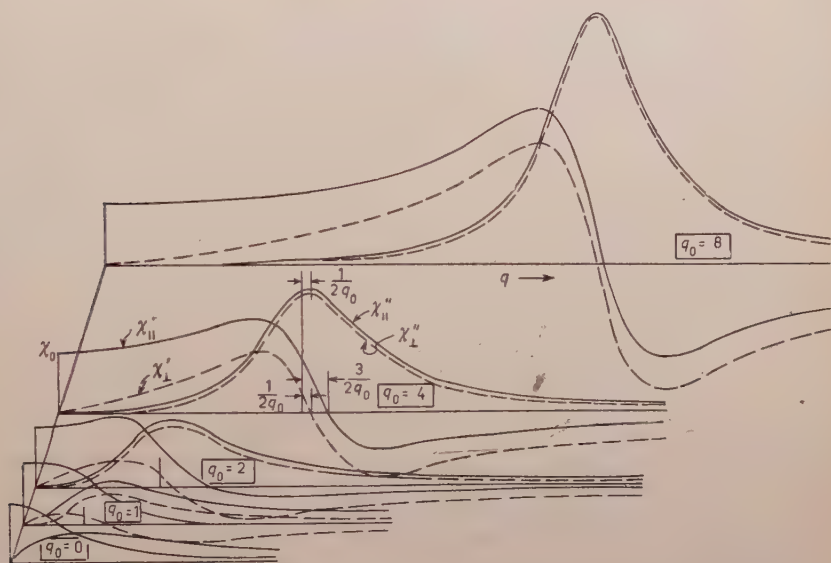


Fig. 2. - The four transverse susceptibilities given by Eq. (47), plotted for various values of the parameter q_0 , which is a measure of the relative sharpness of the resonance.

It is well known that the real and imaginary parts of the generalized susceptibility of any linear system are connected by the Kronig-Kramers integral relations:

$$(48) \quad \begin{cases} \chi''(\omega) = -\frac{2}{\pi} \int_0^\infty \frac{\omega_1 \chi'(\omega_1) d\omega_1}{\omega_1^2 - \omega^2}, \\ \chi'(\omega) = \frac{2}{\pi} \int_0^\infty \frac{\omega_1 \chi''(\omega_1) d\omega_1}{\omega_1^2 - \omega^2} + \chi'(\infty). \end{cases}$$

It is not hard to show by a contour integration that both χ_\parallel and χ_\perp , as given by Eq. (47), exemplify the relations (48).

The relation we have already noticed in Eq. (46) between the maximum value attained by χ'' and the sharpness of the resonance, that is, $\chi''_{\max} = \frac{1}{2}g_0\chi_0$, is a very general feature of resonance absorption in a linear system. Suppose we have a system with a single absorption line of width $\Delta\omega$ at ω_0 , the width being defined so that width \times height = area, or

$$\int_0^{\infty} \chi'' d\omega = \chi''_{\max} \Delta\omega.$$

If we now set $\omega = 0$ in the second of the Kronig-Kramers equations (48) and assume that the integrand is appreciable only in the neighborhood of ω_0 , we get at once

$$(49) \quad \chi'_0 - \chi'_\infty = \frac{2}{\pi} \chi''_{\max} \frac{\Delta\omega}{\omega_0}.$$

In our case, of course, $\chi'_\infty = 0$.

7. - Pulses and transients.

In many nuclear resonance experiments it is not the steady state of the system but its *transient* response which is important. Examples are the fast passage experiments described by BLOCH⁽¹⁰⁾ and used in recent investigations of relaxation, the pulse method of TORREY⁽¹¹⁾, and, perhaps most widely known, the «spin-echo» methods of HAHN⁽¹²⁾. There is an extensive literature on such topics which we shall not review here. But some general comments may be useful to the reader who wishes to concern himself with pulse or transient methods.

Pulse techniques have been applied mostly, though by no means exclusively to systems in which $T_1 = T_2$. Our remarks will be mainly directed at that case, with spin-echo methods in mind. Typically, one applies to the polarized system one or more radiofrequency pulses of short duration and relatively high intensity; one observes the transverse components of the polarization \mathbf{M} some time thereafter, by amplifying the voltage induced in the now quiescent coil by the precessing vector \mathbf{M} . The behavior of the system under such treatment is by no means linear. Nevertheless, it is easier than one might think to analyze and explain what goes on. The question can be separated into two parts, each fairly simple. We may ask how the system behaves while the radio-frequency pulse is applied, and how it behaves in the absence of

⁽¹¹⁾ H. C. TORREY: *Phys. Rev.*, **76**, 1059 (1949).

⁽¹²⁾ E. L. HAHN: *Phys. Rev.*, **80**, 580 (1950).

any such field. In the presence of a strong radio-frequency pulse, $H_z = 2H_1 \cos \omega t$, of short duration, relaxation processes may often be neglected. In the particular case of spin-echo experiments, the pulse duration is of the order of magnitude ($\gamma H_1 T$). If this is very short compared to the relaxation time T , that is if $\gamma H_1 T \ll 1$, we may ignore relaxation and describe the system by the dynamical equation

$$(50) \quad \dot{\mathbf{M}} = -\gamma \mathbf{H} \times \mathbf{M},$$

in which \mathbf{H} represents only the applied field, $\mathbf{H}_0 + \mathbf{H}_1$. (If these fields are not sufficiently homogeneous over the system their distribution of values will need to be taken into account in applying Eq. (50)). In the remainder of the time, between or after r-f pulses, the only applied field is \mathbf{H}_0 and only relaxation accompanied by simple precession about \mathbf{H}_0 occurs.

We are already acquainted with the use of rotating co-ordinates in problems governed by Eq. (50). There are some advantages in using the same trick to describe relaxation effects. In fact, Eq. (39), in which relaxation appears explicitly, can be transformed without difficulty into rotating co-ordinates. As before, let $\mathbf{H}_{\text{eff}} = \mathbf{H}' + \boldsymbol{\omega}_r/\gamma$ and define \mathbf{M}_0 by $\mathbf{M}_0 = -\chi_0 \boldsymbol{\omega}_r/\gamma$. Then Eq. (39) transforms as follows:

$$(51) \quad T\dot{\mathbf{M}}' = \mathbf{M}_0 + \chi_0 \mathbf{H}_{\text{eff}} - \mathbf{M}' + \gamma T \mathbf{M}' \times \mathbf{H}_{\text{eff}}.$$

The primes denote vectors described in the rotating co-ordinates.

Thus the behavior of \mathbf{M}' , in relation to \mathbf{H}_{eff} is like that of \mathbf{M} in relation to \mathbf{H} as described in Eq. (39), except that \mathbf{M}' relaxes to $\chi_0 \mathbf{H}_{\text{eff}} + \mathbf{M}_0$ rather than to $\chi_0 \mathbf{H}_{\text{eff}}$ alone. Of course, this was to be expected, for the fictitious field $\boldsymbol{\omega}_r/\gamma$ which enters into the composition of \mathbf{H}_{eff} cannot change the relaxation. In particular, if we are able to choose a co-ordinate system in which $\mathbf{H}_{\text{eff}} = 0$, the vector \mathbf{M}' simply relaxes toward \mathbf{M}_0 , the tip of the \mathbf{M}' vector moving along a straight line as it does so.

The more general case with $T_2 \neq T_1$ cannot be analyzed so easily. The Bloch equations (38) can be used if the radiofrequency field \mathbf{H}_1 is not too strong, and if the system has a simple transverse relaxation. The meaning of the latter condition will be discussed when we consider resonance line shape. Relaxation in the presence of a strong oscillating field has been studied in an important paper by REDFIELD⁽¹³⁾, who has shown, among other things, that there are circumstances in which the transverse polarization does not decay rapidly even though T_2 , as ordinarily defined, is very short. This result has an interesting application in magnetic resonance experiments on crystals with

(13) A. REDFIELD: *Phys. Rev.*, **98**, 1787 (1955).

very long spin-lattice relaxation times. Ordinarily the maximum sensitivity for detection is reached at a very low value of the strength H_1 of the oscillating field. Further increase of H_1 only brings saturation with no further improvement in sensitivity. By properly using a much stronger oscillating field, and observing the dispersive rather than the absorptive component of the nuclear susceptibility, it is possible to avoid saturation and attain substantially higher sensitivity. The technique was used by Holzman and coworkers⁽¹⁴⁾ to study the ^{29}Si resonance in silica samples with extremely long relaxation times.

8. - Line widths and line shapes.

In this section we shall forget about relaxation processes and discuss the interactions between nuclear spins in crystals. The most important interactions are usually the dipole-dipole interactions. Let us write the Hamiltonian for a system of nuclear spins placed in a field H_0 along the z -axis. Including dipole-dipole interactions between all nuclei, it is:

$$(52) \quad \mathcal{H} = -\gamma\hbar H_0 \sum_j I_{jz} + \gamma^2\hbar^2 \sum_{k>j} \sum_j r_{jk}^{-3} [\mathbf{I}_j \cdot \mathbf{I}_k - 3r_{jk}^{-2} (\mathbf{I}_j \cdot \mathbf{r}_{jk})(\mathbf{I}_k \cdot \mathbf{r}_{jk})].$$

First of all let us consider the case where pairs of nuclei are close together and these pairs relatively widely spaced, so that to a first approximation we can neglect the interaction between different pairs. Then for a typical pair the Hamiltonian is

$$(53) \quad \mathcal{H}_{12} = -\gamma\hbar H_0 (I_{1z} + I_{2z}) + \gamma^2\hbar^2 r_{12}^{-3} [\mathbf{I}_1 \cdot \mathbf{I}_2 - 3r_{12}^{-2} (\mathbf{I}_1 \cdot \mathbf{r}_{12})(\mathbf{I}_2 \cdot \mathbf{r}_{12})].$$

Now for typical internuclear distances and a field H_0 of several thousand gauss, the dipole-dipole term amounts to no more than one percent of the Zeeman energy, so we can treat it as a small perturbation. Then if the nuclei have the same spin and g -values, the eigenstates of the Zeeman term alone can be specified by the value of the total spin $I = I_1 + I_2$ and the total z -component $I_z = I_{1z} + I_{2z}$. These are, for the case of spin $\frac{1}{2}$ nuclei

$$(54) \quad \left\{ \begin{array}{llll} I = 0; & I_z = 0, & E = 0, & \psi = 2^{-\frac{1}{2}}(\alpha_1\beta_2 - \alpha_2\beta_1) \\ I = 1; & I_z = -1, & E = \gamma\hbar H_0, & \psi = \beta_1\beta_2 \\ I = 1; & I_z = 0, & E = 0, & \psi = 2^{-\frac{1}{2}}(\alpha_1\beta_2 + \alpha_2\beta_1) \\ I = 1; & I_z = 1, & E = -\gamma\hbar H_0, & \psi = \alpha_1\alpha_2. \end{array} \right.$$

⁽¹⁴⁾ G. R. HOLZMAN, P. C. LAUTERBUR, J. H. ANDERSON and W. KOTH: *Journ. Chem. Phys.*, **25**, 172 (1956).

The first of these states, the singlet, is magnetically inert so we can forget about it. For the others it is a matter of elementary matrix algebra to calculate the shifts of the levels as a first order perturbation; these shifts are shown in Fig. 3, in units of Δ where $\Delta = \frac{1}{4}\gamma^2\hbar^2r^{-3}(3\cos^2\theta - 1)$ and θ is the angle between \mathbf{r} , the vector joining the two nuclei, and the magnetic field. In this diagram we have assumed $\Delta > 0$, i.e. $\cos\theta > 3^{-\frac{1}{2}}$. It is clear that instead of the single line of frequency $\omega_0 = \gamma H_0$ which we would get if there were no interactions, we see two distinct resonance lines at $\omega_0 + 3\Delta$ and $\omega_0 - 3\Delta$. The separation of these lines is

$$(55) \quad \Delta\omega = 6\Delta = \frac{3}{2}\gamma^2\hbar^2r^{-3}(3\cos^2\theta - 1).$$

This characteristic feature of the spin $\frac{1}{2}$ dipole pair interaction, a doublet line with splitting dependent on the orientation of the pair axis in the field, was first demonstrated experimentally by PAKE⁽¹⁵⁾, in the crystal $\text{CaSO}_4 \cdot 2\text{H}_2\text{O}$. In this crystal, in most orientations, two distinct values of θ occur, so that one sees two doublets, or four lines. The lines are not narrow compared to their spacing, the broadening being a result of interactions of each dipole with neighbors other than its immediate partner, interactions included in our completed Hamiltonian (52) but neglected in the subsequent calculation. This broadening by neighbors can be evaluated by the methods described by VAN VLECK, of which we shall have more to say in a moment.

It is possible to treat groups larger than two in the above manner, but the problem rapidly grows cumbersome. The case of three spins has been studied⁽¹⁶⁾, that of four has been solved in particular cases⁽¹⁷⁾. In more complicated cases one has to resort to Van Vleck's theory of dipolar broadening⁽¹⁸⁾ which, although it does not yield the multiplet structure of the resonance, does provide us with rigorously calculable quantities that can be compared with experiment, the moments of the overall line shape. Actually the complicated multiplets would not be resolved experimentally; a many-spin group yields a rather featureless line, as a rule. Some suitable measure

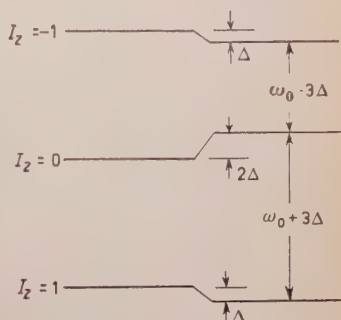


Fig. 3. — Perturbation of the Zeeman levels of a two-spin system by dipole-dipole interaction.

⁽¹⁵⁾ G. E. PAKE: *Journ. Chem. Phys.*, **16**, 327 (1948).

⁽¹⁶⁾ E. R. ANDREW and R. BERSOHN: *Journ. Chem. Phys.*, **18**, 159 (1950) and **20**, 924 (1950).

⁽¹⁷⁾ R. BERSOHN and H. S. GUTOWSKY: *Journ. Chem. Phys.*, **22**, 651 (1954).

⁽¹⁸⁾ J. H. VAN VLECK: *Phys. Rev.*, **74**, 1168 (1948) and these lectures: *Nuovo Cimento*.

of the width, such as the second moment, is the most significant feature experimentally as well as theoretically.

A good example of this application of these methods is the work of ANDREW and HYNDMAN on the structure of the urea molecule⁽¹⁹⁾. By observing the dependence on crystal orientation of the width of the hydrogen resonance in this substance, and comparing the result with the predictions of Van Vleck's theory, they were able to rule out decisively one hypothetical structure for the molecule and establish another.

We have been talking about single crystals. In a powdered or polycrystalline sample, all values of θ occur, and the resonance line shape is an average of the shapes for various orientations. In this average most features of the line structure are lost. The two- and three-spin groups still show characteristic shapes, the former a two-humped curve, the latter a three-humped curve. For more complicated cases one has to fall back again on Van Vleck's formula, now averaged over all orientations.

9. - The effect of molecular motion on line width and relaxation.

We have looked at two different aspects of nuclear magnetic resonance, from two very different points of view. In Sect. 5 we discussed the relaxation of the longitudinal polarization to its equilibrium value, imagining the cause of this relaxation to reside in rapidly and randomly fluctuating internal fields. Indeed we paid special attention to the case in which the fluctuation occurs rapidly compared to the nuclear precession, and in which, as we saw in Sect. 5, the transverse and the longitudinal relaxation behave alike. We then observed, in Sect. 6, that the width of the resonance absorption line, in this extreme case, is essentially T^{-1} on a frequency scale. More precisely, the resonance absorption, $\chi''(\omega)$ has the simple « Lorentz » shape in the neighborhood of resonance: $\chi'' \sim [1 + (\omega - \omega_0)^2/\Delta\omega^2]^{-1}$, with $\Delta\omega$, the half width of the absorption at half maximum, being given by $\Delta\omega = T^{-1}$.

At the other extreme lies the problem we examined in Sect. 8, the shape of the resonance line in the presence of nuclear dipole-dipole interactions which are not explicitly time-dependent. Instead of a simple resonance line we find here lines of various shapes, including lines split into multiplets. Even when the multiplets coalesce into a single line the shape is far from the Lorentz form. It is evident from this fact that the Bloch equations do not hold in this situation.

It is evident also that the interactions that appear in the Hamiltonian of

(19) E. R. ANDREW and D. HYNDMAN: *Proc. Phys. Soc. Lond.*, A **66**, 1187 (1953).

Eq. (52) cannot bring about an exchange of energy between the spin system and a temperature bath so long as the \mathbf{r}_{jk} , the only co-ordinates which could connect the system with a bath, are constant in time. That is to say, our Hamiltonian with time-independent Zeeman and dipole-dipole terms cannot account for spin-lattice relaxation. To be precise we ought to distinguish here between *longitudinal relaxation*, by which we ordinarily mean the relaxation of M_z , and *spin-lattice* relaxation. It is really the latter which requires exchange of energy between spin-system and bath, or lattice. Actually, because the dipole-dipole part of (52) does not commute with $M_z = \gamma\hbar \sum_j I_{jz}$, M_z may change even while the total energy of the spin system remains constant. Usually this reservation is not very important because the dipole-dipole interaction is weak compared to the interaction with the external field. But it is a warning that the «independent-spin» model upon which our earlier description of relaxation was based is only an approximation to the truth.

We want to discuss now the behavior of the nuclear spin system between the two extremes which we may call respectively the «rapid fluctuation» limit and the «frozen-lattice» limit. A rigorous treatment is extremely difficult but a very simple model will help us to understand the main features of nuclear relaxation as they are revealed by experimental measurements of T_1 , T_2 and the width or shape of the resonance line. We are going to develop a little further the «local field» description introduced in Sect. 3 and used again in Sect. 5.

Suppose the j -th nucleus in our spin system is subject to, in addition to the applied field H_0 , small fields from a number of nearby sources in the lattice:

$$(56) \quad \mathbf{H}_j = \mathbf{h}_{j1} + \mathbf{h}_{j2} + \dots + \mathbf{h}_{j\alpha} \dots$$

The sources are assumed statistically independent, and numerous enough to permit us to apply the Central Limit Theorem to the sum in Eq. (56). \mathbf{H}_j has then a Gaussian distribution and furthermore \mathbf{H}_j and \mathbf{H}_k are, at any instant, statistically independent. Now the components of $\mathbf{h}_{j\alpha}$ are stationary random functions of the time and we shall characterize their behavior by a *correlation function* defined in the usual way by:

$$(57) \quad g_z(\tau) = \langle h_z(t)h_z(t-\tau) \rangle / \langle (h_z(t))^2 \rangle.$$

All the fields $\mathbf{h}_{j\alpha}$, though statistically independent, are supposed to have the same correlation function. The brackets $\langle \rangle$ denote a time average over the stationary random function. The various local fields \mathbf{H}_j are thus statistically similar in their behavior, and are of course stationary random functions of the time because they are composed of the $\mathbf{h}_{j\alpha}$ which are themselves stationary

random functions. Regarding the H_j as an ensemble of random functions, we may therefore replace a time average by an ensemble average whenever we choose to do so.

About the function $g(\tau)$ we may remark at once that necessarily $g(\tau) = g(-\tau)$ and $g(0) = 1$. Let us suppose that the local field has no component that persists for all time, either as a constant component or as a periodic component of constant amplitude. Any such perturbation would have to be treated separately. We assume, in other words, that for two instants sufficiently remote in time the values of the local field are completely uncorrelated, an assumption expressed by the statement $g(\infty) = 0$. In a given case the persistence of correlation may be specified roughly by a *correlation time* τ_c with the property that $g(\tau) \ll 1$ for all $\tau \gg \tau_c$. Taking the rather special random variation postulated in Sect. 3 as an example, we find for that field

$$g(\tau) = 1 - \tau/\tau_0, \quad 0 \leq \tau \leq \tau_0; \quad g(\tau) = 0, \quad \tau > \tau_0.$$

In that case obviously one might with reason call τ_0 the correlation time.

Suppose we have at $t = 0$ a transverse polarization, $M_j = M_0$, along the x' axis, an axis rotating with speed $\omega_r = \gamma H_0$. At the site of the j -th spin the z -component of the local field, $H_{jz} = h_{j1z} + h_{j2z} + \dots$ will cause a precession of $\bar{\mu}$ with respect to x' such that the vector $\bar{\mu}$, the expectation value of the moment of the j -th spin, will have advanced in time t by the angle

$$(58) \quad \varphi_j(t) = \gamma \int_0^t H_{jz} dt = \gamma \sum_{\alpha} \int_0^t h_{j\alpha z} dt.$$

We seek the distribution of the φ_j 's, at time t , over the spin ensemble. That is, we seek the function $\Phi(\varphi, t)$ such that $\Phi d\varphi$ is the expected fraction of spins whose angular displacement from the x' axis at time t will be between φ and $\varphi + d\varphi$. (We are for the present ignoring the possibility of rotation out of the equatorial plane, which we may do if H_j varies *slowly* enough so that H_{jx} and H_{jy} transform into rapidly oscillating components $H_{jx'}$ and $H_{jy'}$ in the rotating co-ordinate system.)

If now we can apply the Central Limit Theorem to the sum in Eq. (59), it follows that Φ is a normal distribution and we have only to calculate its variance. Since the $h_{j\alpha}$'s are independent with average value zero, we have

$$(59) \quad \langle (\varphi_j(t))^2 \rangle = \sum_{\alpha} \left\langle \left[\int_0^{\infty} \gamma h_{j\alpha z} dt \right]^2 \right\rangle,$$

which the statistical similarity of the h_α 's allows us to write as

$$(60) \quad \langle (\varphi_j(t))^2 \rangle = \gamma^2 \left\{ \left\langle \left[\int_0^t h_{\alpha z} dt \right]^2 \right\rangle / \langle h_{\alpha z}^2 \rangle \right\} \sum_{\alpha} \langle h_{\alpha z}^2 \rangle.$$

The quantity in curly brackets can be expressed in terms of the correlation function $g(\tau)$, as follows (*). Write

$$\left[\int_0^t h dt \right]^2 = \int_0^t dt' \int_0^t h(t') h(t'') dt'',$$

and substitute the new variable $\tau = t' - t''$, thus obtaining

$$(61) \quad \left[\int_0^t h dt \right]^2 = \int_0^t dt' \int_{t'-t}^{t'} h(t') h(t' - \tau) d\tau.$$

Reversing the order of integration, with due attention to the limits of the integration over t' , we get

$$(62) \quad \left[\int_0^t h dt \right]^2 = \int_0^t d\tau \int_{\tau}^t h(t') h(t' - \tau) dt' + \int_{-t}^0 d\tau \int_0^{t+\tau} h(t') h(t' - \tau) dt'.$$

The average we are now required to take may as well be a time average as an ensemble average, and if we take the average before integrating, in (62), we have, remembering the definition of $g(\tau)$:

$$(63) \quad \left\langle \left[\int_0^t h dt \right]^2 \right\rangle / \langle h^2(t) \rangle = \int_0^t (t - \tau) g(\tau) d\tau + \int_{-t}^0 (t + \tau) g(\tau) d\tau = 2 \int_0^t (t - \tau) g(\tau) d\tau.$$

Writing $\langle H^2 \rangle$ for $\sum_{\alpha} \langle h_{\alpha z}^2 \rangle$, the mean square local field at a site, we have finally

$$(64) \quad \langle (\varphi(t))^2 \rangle = 2\gamma^2 \langle H_z^2 \rangle \int_0^t (t - \tau) g(\tau) d\tau,$$

(*) The argument is an adaptation of that of ABRAGAM and POUND: *Phys. Rev.*, **92**, 943 (1953).

for the variance of the normal distribution $\Phi(q, t)$. Call this simply $\langle q^2 \rangle$. Then

$$(65) \quad \Phi(\varphi, t) = [2\pi\langle\varphi^2\rangle]^{-\frac{1}{2}} \exp[-\tfrac{1}{2}\varphi^2/\langle\varphi^2\rangle].$$

To find the transverse polarization which remains at time t we have

$$M_{x'}(t) = M_0 \int_{-\infty}^{\infty} \Phi(\varphi, t) \cos \varphi \, d\varphi = M_0 \exp[-\tfrac{1}{2}\langle\varphi^2\rangle],$$

so that, explicitly,

$$(66) \quad M_{x'}(t) = M_0 \exp\left[-\gamma^2\langle H_z^2\rangle \int_0^t (t-\tau)g(\tau) \, d\tau\right].$$

Eq. (66) describes the relaxation of the transverse polarization in our model. We could obtain the absorption line shape by taking the Fourier transform of $M_{x'}(T)$; a short proof of this connection is given by ANDERSON⁽²⁰⁾. But let us discuss the relaxation itself.

Whatever the form of $g(\tau)$, for $\tau \ll \tau_c$, $g(\tau) \approx 1$, so that if $t \ll \tau_c$, $M_{x'}$ will behave as follows

$$(67) \quad M_{x'} \approx M_0 \exp[-\tfrac{1}{2}\gamma^2\langle H_z^2\rangle t^2].$$

On the other hand, for $t \gg \tau_c$

$$(68) \quad M_{x'} \approx M_0 \exp[-\text{constant} \cdot t].$$

The simple exponential decay is found only when $t \gg \tau_c$; only in that range does our system conform to the Bloch equations.

We now adopt a special form for $g(\tau)$, namely

$$(69) \quad g(\tau) = \exp[-|\tau|/\tau_0].$$

This is the correlation function for a simple stochastic model, a field which changes abruptly to a new value at *random* instants, the changes occurring at the average rate $1/\tau_0$. The constant in Eq. (68) is now easily evaluated, and we find $M_{x'}(t) = M_0 \exp[-t/T_2]$ with

$$(70) \quad T_2 = [\gamma^2\langle H_z^2\rangle\tau_0]^{-1}.$$

Now the above arguments are valid only if $\tau_0 \gg \omega^{-1}$, so that the local

(20) P. W. ANDERSON: *Journ. Phys. Soc. of Japan*, **9**, 316 (1954).

field components H_x and H_y may be ignored. We shall only indicate here what happens as τ_0 approaches ω^{-1} . First, the component H_y , begins to play a role in the relaxation of M_z , and in the end, for $\tau_0 \ll \omega^{-1}$, the transverse relaxation rate is simply doubled by this effect, if we assume \mathbf{H} to be statistically isotropic. Second, the component H_x and H_y begin to be effective in producing *longitudinal* relaxation, the situation that finally prevails when $\tau_0 \ll \omega^{-1}$ being that already discussed in Sect. 3 for the less general model there assumed. In the limit $\tau_0 \ll \omega^{-1}$ we find, as we found before, $T_1 = T_2$. Omitting the further details of the analysis, we give only its result, which describes both transverse and longitudinal relaxation in our model over the whole range for which both behave in a simple exponential fashion:

$$(71) \quad \begin{cases} \frac{1}{T_2} = \frac{1}{3} \gamma^2 \langle H^2 \rangle \left[\tau_0 + \frac{\tau_0}{1 + \omega^2 \tau_0^2} \right] \\ \frac{1}{T_1} = \frac{1}{3} \gamma^2 \langle H^2 \rangle \left[\frac{2\tau_0}{1 + \omega^2 \tau_0^2} \right] \end{cases}$$

These equations hold for $\tau_0^2 \gamma^2 \langle H^2 \rangle \ll 1$. $\langle H^2 \rangle$ is the mean square intensity of the local field which is assumed to be statistically isotropic. That is, $\langle H^2 \rangle = 3\langle H_x^2 \rangle$, etc.

If $\tau_0^2 \gamma^2 \langle H^2 \rangle > 1$, the decay of M_x is almost entirely of the form described by Eq. (67) so that T_2 has no unique meaning.[†] However, the formula for T_1 should remain valid even as we approach this frozen-lattice limit. Fig. 4 summarizes the predicted behavior.

We now have to relate this to the world of real substances, where the sources of the local fields may be, for instance, the neighboring nuclear dipoles, and the cause of their random fluctuation may be the thermal agitation of the atoms or molecules which are the carriers of the nuclear dipoles. In this world we find an enormous range of correlation times. In tightly bound crystals, setting aside the weak modulation of the local fields caused by lattice vibrations, there occurs only rarely a drastic change in local configuration. Then τ_0 may be so great that we have the frozen-lattice limit so far as T_1 is concerned. In liquids τ_0 is typically in the neighborhood of 10^{-11} s, which takes us far out into the « rapid-

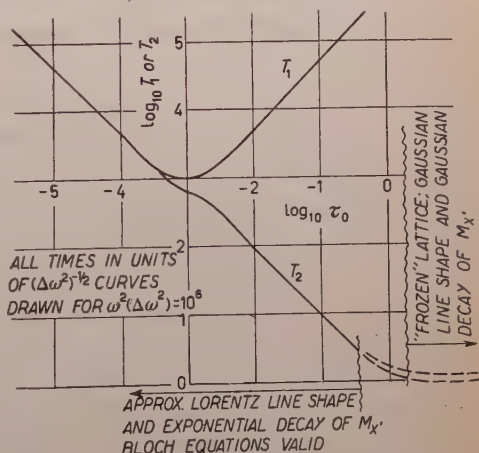


Fig. 4. — The behavior of T_1 and T_2 as functions of the correlation time τ_0 , as given by the simple «local field» theory outlined in the text.

fluctuation » domain. As we pass from liquid to solid, or better, say, from liquid to glass, by changing the viscosity of the substance, all intermediate states are traversed. Indeed the whole range of behavior described by Fig. 4 has been experimentally observed.

A striking feature of the T_1 curve is the minimum in the neighborhood of $\tau_0 = \omega^{-1}$. This is a manifestation of the fact that interactions which fluctuate at a rate comparable to the Zeeman frequency are most effective in inducing transitions between the Zeeman levels; the existence of this minimum has been experimentally demonstrated in many cases.

As for line width and shape our particular model displays, in the frozen-lattice limit, a Gaussian line. The line remains unaffected by fluctuations in the interaction until the correlation time becomes as small as $[\gamma^2 \langle H^2 \rangle]^{-\frac{1}{2}}$. With further shortening of τ_0 the line narrows progressively. Moreover, as soon as $\tau_0 \ll [\gamma^2 \langle H^2 \rangle]^{-\frac{1}{2}}$ the shape of the line is substantially Lorentzian. It is never precisely Lorentzian, for a Lorentzian line has an infinite second moment, whereas it is possible to show that the second moment of the line for our model—and even for more general models—must remain constant independent of τ_0 . It does so thanks to a departure from Lorentzian shape far out in the wings of the narrowed line, a departure which is closely connected with the fact that for a very short time, initially, the M_2 decay goes not as $\exp[-\text{constant} \cdot t]$ but as $\exp[-\text{constant} \cdot t^2]$.

The model we have used is an instructive one which helps us to see the physical connection between nuclear relaxation and molecular motions, but it has some fundamental defects which need to be emphasized. Even in the simple case of dipole coupling between pairs of like nuclei, a system with the Hamiltonian of Eq. (53), the field of one nucleus at the other cannot be treated as an independent local field. Instead we have to consider, quantum-mechanically, transitions of the coupled system induced by modulation of the interaction. This can be done⁽²¹⁾ and, broadly speaking, much the same behavior is predicted as we have already described, with some quantitative details altered. But systems are known, only a little more complicated, for which a «local-field» description would be quite inadequate.

On the other hand it is no easy task to provide a rigorous theory of line shape and relaxation in the intermediate domain where \hbar/τ_0 is neither large nor small compared to the interaction energy. This problem is discussed in the lecture of Prof. KUBO and, in a somewhat different context, in those of Prof. VAN VLECK. It is hoped that the remarks above may serve as an introduction to the more recent and more ambitious attempts to deal with this problem.

⁽²¹⁾ N. BLOEMBERGEN, E. M. PURCELL and R. V. POUND: *Phys. Rev.*, **73**, 679 (1948).

Line-Breadths and the Theory of Magnetism.

J. H. VAN VLECK

Harvard University - Cambridge Mass.

I.

At first sight, the subject of line breadths seems rather remote from magnetism, but actually from the subject of line structures a great deal can be learned about the correlation and relaxation effects which are so important for the present-day theory of magnetism, both electronic and nuclear.

1. - The Lorentz phase interruption model.

The traditional starting point for any discussion of line breadths is the simple collision theory of Lorentz ⁽¹⁾. We can omit radiation damping, for it is unimportant in the microwave region. The Lorentz model is basically a harmonic oscillator subject to collisions of exceedingly short duration. At each such impact there is a sudden change in phase. It is further assumed that there is no persistence or « hang-over » in phase, so that after collision one value of the phase is as likely as another. (Actually, as shown by VAN VLECK and WEISSKOPF ⁽²⁾, the various phases should be weighted somewhat unevenly conforming to the Boltzmann factor for the instantaneous value of the energy in the applied field. The resulting corrections, however, introduce only terms in $1/(\omega + \omega_0)$ rather than $1/(\omega - \omega_0)$, and are of no importance near resonance. We shall omit them).

The mathematical analysis for the Lorentz model runs as follows. The differential equation for a harmonic oscillator subject to a periodic field

⁽¹⁾ H. A. LORENTZ: *The Theory of Electrons*, note 57.

⁽²⁾ J. H. VAN VLECK and V. F. WEISSKOPF: *Rev. Mod. Phys.*, **17**, 227 (1945).

$E \cos \omega t$ is

$$m\ddot{x} + ax = -eE \cos \omega t.$$

The general solution is

$$(1) \quad x = \operatorname{Re} \left[\frac{eE \exp[i\omega t]}{m(\omega^2 - \omega_0^2)} + A \exp[i\omega_0 t] + B \exp[-i\omega_0 t] \right],$$

where $\omega_0 = (a/m)^{1/2}$, and A and B are constants of integration. Let us assume that the last collision took place at $t = t_0$. We can further suppose that after collision $x = \dot{x} = 0$. For an individual oscillator this statement would not be true, but if the new phases after collision are randomly distributed, then for an ensemble of atoms, positive and negative values of either x or \dot{x} are equally probable after collision, so that on averaging over the ensemble, one has $x = \dot{x} = 0$. We thus have for the average effect of the oscillator whose last collision was at $t = t_0$

$$x(t, t_0) = \operatorname{Re} \left[\frac{eE}{m(\omega^2 - \omega_0^2)} \cdot (\exp[i\omega t] - \exp[i\omega t_0]) \cos \omega_0(t - t_0) - i\omega\omega_0^{-1} \exp[i\omega t_0] \sin \omega_0(t - t_0) \right].$$

So far we have considered only the collisions which take place at t_0 . We have further to average over all times of collision. If τ is the mean life between collisions, the probability that the last collision took place at $t = t_0$ is $(1/\tau) \exp[-(t - t_0)/\tau]$ and so on the average

$$x(t) = \frac{1}{\tau} \int_{-\infty}^{t_0} x(t, t_0) \exp[-(t - t_0)/\tau] dt_0.$$

We shall omit terms which on integration give denominators $\omega + \omega_0$ rather than $\omega - \omega_0$, and so are unimportant near resonance. Integration then gives

$$(2) \quad x(t) = \operatorname{Re} \left[\frac{eE \exp[i\omega t](i(\omega - \omega_0))}{m(\omega^2 - \omega_0^2)[(1/\tau) + i(\omega - \omega_0)]} \right].$$

The rate of absorption of energy is

$$(3) \quad \left\langle -eE \cos \omega t \cdot \frac{dx}{dt} \right\rangle_{\text{av}} = \frac{e^2 E^2}{4m} \frac{1/\tau}{(1/\tau)^2 + (\omega - \omega_0)^2}.$$

Eq. (3) embodies the familiar Lorentz structure for the line shape.

The Lorentz model and resulting line-shape are standard for treating the shape of collision-broadened lines in gases. It represents, for instance, the shape of magnetic resonance lines in oxygen gas. Most magnetic resonance experiments, however, are concerned with solids, and here the Lorentz model loses its validity. We have, however, nevertheless included the basic Lorentz treatment because, quite apart from its applicability to gases, it is needed as a starting point for some of our later discussions.

The reason that the Lorentz model does not apply to solids is not hard to see. The basic feature of a solid is that its atoms maintain spacings which are constant in time. On the other hand the impacts envisaged by the Lorentz theory can be realized only in gases, or perhaps liquids, where there are sudden approaches and recessions of atoms to and from each other.

2. - The Gaussian model.

A more appropriate approach to the description of line structure in solids is furnished by the so-called statistical theory, which assumes that the effect of other atoms on a given atom can be approximated by a static field rather than represented by a sudden impact. The line shape is due to the fact that different atoms are exposed to different fields or, equivalently, that the field is only quasi-static, and varies slowly with time. The observable quantity is essentially the time exposure over a long time interval. The approximations of the statistical theory are tantamount to treating the collision as of infinitely long duration. Even in gases the proper limiting theory to use well-out in the wings of the lines is the statistical one, for it can be shown⁽³⁾ that the Lorentz impact and the statistical theories apply respectively to the limiting cases $T \ll |\omega - \omega_0|^{-1}$ and $T \gg |\omega - \omega_0|^{-1}$, where T is the duration of a collision, and $\omega - \omega_0$ is the displacement from the center of the line.

The shape of the line in the statistical theory is determined by the distribution of the instantaneous fields over a variety of atoms. If a given atom interacts with a large number of neighbors, so that the total field is compounded from a large number of small fields, the distribution of resultant fields should presumably be approximately Gaussian, for the Gaussian situation is a quite general consequence of the statistics of the aggregates of a large number of objects. It should however, be cautioned that the statistical theory does not necessarily imply Gaussian line shape, and vice versa. In gases, for instance, the shape of the line in the wings is determined primarily by considering

(3) For a broad review of the general subject of collision broadening, and copious references, see. R. G. BREENE, Jr.: *Rev. Mod. Phys.*, **29**, 94 (1957).

the field of a single atom at collision rather than by multiple simultaneous weak fields from many atoms; the determining factors are then the variations of the field with regard to interatomic distance, and the distribution of the latter in time. The multiple compounding which gives birth to a Gaussian distribution is hence not necessarily realized. On the other hand, the best situation for the generation of a Gaussian shape is realized in the case of solids composed of regularly spaced atoms in which the only interactions between the moments of different atoms are dipolar ones which vary slowly with distance, so that a given atom feels the influence of many atoms.

3. - The method of moments ⁽⁴⁾.

The Gaussian expression for the line shape normalized to unity is

$$(4) \quad f(\omega) = \left[\frac{1}{2\pi \langle \Delta\omega^2 \rangle_{AV}} \right]^{\frac{1}{2}} \exp \left[-(\omega - \omega_0)^2 / 2 \langle \Delta\omega^2 \rangle_{AV} \right].$$

There is only a single parameter, viz. the mean square deviation $\langle \Delta\omega^2 \rangle_{AV}$ from the mean or central angular frequency ω_0 .

It is fairly easy to calculate this parameter by the method of moments, as it is essentially the second moment. The eigenvalue problem connected with the interaction of 10^{23} dipoles is, of course, of far too high an order to calculate exactly. But, thanks to the invariance of the diagonal sum, it is possible to obtain explicit expressions for the moments of lowest order.

The quantum-mechanical formula for the mean square moment of a magnetic resonance line arising from the application of an oscillating magnetic field along the x direction is

$$(5) \quad \langle \Delta\omega^2 \rangle_{AV} = \frac{\sum_{n,n'} \omega_{n,n'}^2 | (S_x)_{nn'} |^2}{\sum_{n,n'} | (S_x)_{nn'} |^2} - \omega_0^2,$$

where $(S_x)_{nn'}$ is the matrix element of the spin moment connecting states n and n' . Both the numerator and denominator can be expressed as diagonal sums or traces, and (5) can also be written as

$$(6) \quad \langle \Delta\omega^2 \rangle_{AV} = - \frac{4\pi^2}{h^2} \frac{\text{Tr} [\mathcal{H} S_x - S_x \mathcal{H}]^2}{\text{Tr} S_x^2} - \omega_0^2,$$

⁽⁴⁾ The presentation in the present section is a condensed version of that originally given by J. H. VAN VLECK: *Phys. Rev.*, **74**, 1168 (1948), to which the reader is referred for further details. The general method of quantum-mechanical moments was first proposed by I. WALLER: *Zeits. f. Phys.*, **79**, 370 (1932).

where \mathcal{H} is the Hamiltonian function. Because of the invariance of the trace or diagonal sum, (6) can be evaluated in any system of representation, and is most conveniently calculated in a system of representation in which the spin of each atom is individually space quantized.

Let us assume that there is, as is customary in magnetic resonance experiments, a constant magnetic field applied perpendicular to the measuring field. The direction of the constant field we shall take as the z axis. If we assume that the only interactions between the spins of the different atoms are dipolar and exchange coupling, the Hamiltonian functions is

$$(7) \quad \mathcal{H} = Hg\beta \sum_j S_{z_j} + \sum_{k>j} \tilde{A}_{jk} \mathbf{S}_j \cdot \mathbf{S}_k + \sum_{k>j} \tilde{B}_{jk} [(\mathbf{S}_j \cdot \mathbf{S}_k) - 3r_{jk}^{-2} (\mathbf{r}_{jk} \cdot \mathbf{S}_j)(\mathbf{r}_{jk} \cdot \mathbf{S}_k)].$$

Here the first, second, and third members are respectively the Zeeman, exchange, and dipolar energies. The constants \tilde{A}_{jk} and \tilde{B}_{jk} have respectively the significance

$$(8) \quad \tilde{A}_{jk} = -2J_{jk}, \quad \tilde{B}_{jk} = g^2\beta^2/r_{jk}^3,$$

in terms of the exchange integral J_{jk} and the interatomic spacing r_{jk} . The symbol S_{z_j} denotes the z component of the spin angular momentum vector of atom j , which may be either electronic or nuclear, since as yet we do not need to specify whether the calculation is applying to nuclear or electronic resonance. Exchange coupling is, of course, absent in the nuclear case, but RAMSEY and PURCELL () have shown that even here higher order perturbation effects can give rise to coupling that is exchange-like in form in that it is proportional to the scalar product $\mathbf{S}_j \cdot \mathbf{S}_k$. The letters β and g are to be interpreted as nuclear or electronic Bohr magnetons and g -factors according to the case we are considering. It is assumed that all atoms have the same spin, and, since the crystalline Stark energy is omitted, in writing (7), the effect of crystalline fields on the line breadth is neglected.

In order to exhibit clearly the effect of the quantization of the z component of spin, we write scalar products such as $\mathbf{r}_{jk} \cdot \mathbf{S}_j$ in the explicit form $r_{jk}(\alpha_{jk}S_{x_j} + \beta_{jk}S_{y_j} + \gamma_{jk}S_{z_j})$ where $\alpha_{jk}, \beta_{jk}, \gamma_{jk}$ are the direction cosines of r_{jk} relative to the x, y, z axes. When this is done, Eq. (7) becomes

$$(9) \quad \mathcal{H} = Hg\beta \sum_j S_{z_j} + \sum_{k>j} \tilde{A}_{jk} \mathbf{S}_j \cdot \mathbf{S}_k + \\ + \sum_{k>j} \tilde{B}_{jk} [\mathbf{S}_j \cdot \mathbf{S}_k - 3\gamma_{jk}^2 S_{z_j} S_{z_k} - \frac{3}{4}(\alpha_{jk}^2 + \beta_{jk}^2)(S_{j+} S_{k-} + S_{j-} S_{k+})] + \\ + \left\{ \sum_{k>j} \tilde{B}_{jk} \left[-\frac{3}{4}(\alpha_{jk}^2 - \beta_{jk}^2)(S_{j+} S_{k+} + S_{j-} S_{k-}) + 3i\alpha_{jk}\beta_{jk}(S_{j+} S_{k+} - S_{j-} S_{k-}) - \right. \right. \\ \left. \left. - \frac{3}{2}\gamma_{jk}(\alpha_{jk} - i\beta_{jk})(S_{j+} S_{z_k} + S_{z_j} S_{k+}) - \frac{3}{2}\gamma_{jk}(\alpha_{jk} + i\beta_{jk})(S_{j-} S_{z_k} + S_{z_j} S_{k-}) \right] \right\}.$$

(⁵) N. F. RAMSEY and E. M. PURCELL: *Phys. Rev.*, **85**, 143 (1952); N. F. RAMSEY: *Phys. Rev.*, **91**, 303 (1953).

Here we have used the abbreviations S_{j+} , S_{j-} for the combinations $S_{x_j} + iS_{y_j}$, $S_{x_j} - iS_{y_j}$. If the Zeeman energy is large compared to the dipolar and exchange interactions, the part of the Hamiltonian function (9) which is inclosed in the parentheses $\{ \}$ should be omitted in computing the mean square breadth $\langle \Delta\omega^2 \rangle_{av}$, for it is readily shown that the effect of these bracketed terms is to generate weak transitions, or satellites whose frequencies are near 0, $2g\beta H/h$, $3g\beta H/h$ and are of no interest to us, as we are interested in the structure of the main line centering about $g\beta H$. This process of omitting the irrelevant or bracketed part of (9) is known as truncation.

The calculation of the traces (6) with the truncated Hamiltonian function (9) is readily made with the aid of the commutation relations

$$S_{x_j} S_{y_k} - S_{y_j} S_{x_k} = \delta_{jk} S_{z_j} \cdot i$$

etc. One finds

$$(10) \quad \langle \Delta\omega^2 \rangle_{av} = \frac{1}{3} (S(S+1)) \frac{4\pi^2}{h^2} \cdot q \sum_k \tilde{B}_{jk}^2 \left(\frac{3}{2} \gamma_{jk}^2 - \frac{1}{2} \right)^2.$$

The lattice sums involved in (10) converge rapidly, for in virtue of the expression (8) for \tilde{B}_{jk} they converge as the inverse sixth power of the radius. For a simple cubic lattice, the explicit form of (10) turns out to be

$$(11) \quad \langle \Delta\omega^2 \rangle_{av} = 36.8 g^4 \beta^4 (2\pi/h)^2 d^{-6} \left[\frac{1}{3} S(S+1) \right] (\lambda_1^4 + \lambda_2^4 + \lambda_3^4 - 0.187),$$

where λ_1 , λ_2 , λ_3 are the direction cosines of the applied field H relative to the principal cubic axes, and where d is the spin lattice constant, i.e. the distance between neighboring magnetic atoms located on a simple cubic grating. (Our constant d need not be the same as the conventional lattice constant, since there may be intervening atoms devoid of spin which are irrelevant for our problem).

With the powder, rather than a single crystal, (10) reduces quite generally to the expression

$$(12) \quad \langle \Delta\omega^2 \rangle_{av} = \frac{3}{5} \left(\frac{2\pi}{h} \right)^2 S(S+1) \sum_k \tilde{B}_{jk}^2,$$

regardless of whether or not the lattice is cubic.

In principle, fourth, sixth, and all higher order moments should be capable of calculation by means of the method of diagonal sums. If all the moments are known, the shape of the line is completely rigorous and does not even involve the approximations of statistical theory. Actually, even the fourth moment is fairly difficult to compute. Its calculation, however, furnishes a test of how good an approximation the Gaussian assumption is. According

to the Gaussian formula (4) for the line shape one has $\langle \Delta\omega^4 \rangle_{Av} = 3[\langle \Delta\omega^2 \rangle_{Av}]^2$ so that

$$(13) \quad \sqrt[4]{\langle \Delta\omega^4 \rangle_{Av}} = 1.32 \sqrt{\langle \Delta\omega^2 \rangle_{Av}}.$$

Because of the complicated dependence on the direction cosines, it is difficult to compute the mean fourth moment for an arbitrary direction of the applied field relative to the principal cubic axes. However, explicit computation of $\langle \Delta\omega^4 \rangle_{Av}$ by the rigorous method of moments gives a factor 1.25 rather than 1.32 in (13) if $S = \frac{1}{2}$ and if the field is directed along the 100 axis. If it is directed along the 111 axis, or if $S > \frac{1}{2}$ the calculated departures from (13) are even less. In these calculations of $\langle \Delta\omega^4 \rangle_{Av}$ it is assumed that there is no exchange coupling, i.e. $\tilde{A}_{jk} = 0$ in (7). We can therefore conclude that as long as exchange effects, crystalline fields, and quadrupole moments are absent, the line shape should be nearly Gaussian.

4. - Nuclear resonance - Confirmation of the results of the method of moments in CaF_2 .

The predictions based on the method of moments are best tested in nuclear rather than electronic resonance, for then there is not the complication of exchange interaction. The material should be diamagnetic, as the presence of electronic paramagnetism overpowers or at least profoundly alters any purely nuclear effects. Furthermore, the substance should be one devoid of nuclear quadrupole moments, as we have omitted them from our Hamiltonian function (7), and they profoundly alter the line structure.

Calcium fluoride is a crystal *par excellence* for testing the theory of pure dipolar broadening. The only spin is that of the fluorine nucleus, and the fluorine nuclei are arranged in a simple cubic lattice. Furthermore, the spin of the F nucleus is $\frac{1}{2}$, so that there can be no complications arising from quadrupole moments. The nuclear resonance absorption by a single crystal of CaF_2 has been measured by PURCELL, BLOEMBERGEN and POUND⁽⁶⁾.

The directional effects are most simply tested in a preliminary way by study of the variation of the peak absorption at the center of the line when the orientation of the magnetic field relative to the principal axes of the crystal is changed. The peak is easier to measure than the breadth, and exhibits the salient features of the directional trends. With the Gaussian assumption (4),

(6) E. M. PURCELL, N. BLOEMBERGEN and R. V. POUND: *Phys. Rev.*, **70**, 988 (1946).

the peak absorption should be inversely proportional to the r.m.s. line breadth, and so should have an angular factor which is the square root of the reciprocal of that given in (11). The angular dependence calculated on this basis when

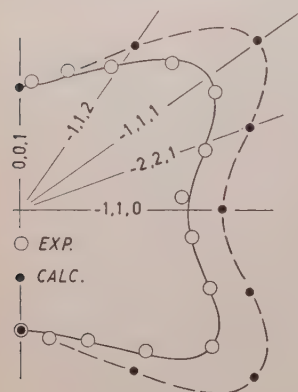


Fig. 1.

the magnetic field is rotated through various positions in the 110 plane is shown by the dashed line in Fig. 1, taken from the paper by PURCELL, BLOEMBERGEN and POUND. The measured peak absorption is shown by the solid line. The constant of proportionality is determined so as to give agreement in the 001 direction.

On the whole, the accord between theory and experiment in Fig. 1 is satisfying. Exact agreement cannot be expected, since the Gaussian assumption on which the theoretical curve is predicated is not rigorous. Since, experimentally, only the relative rather than absolute values of the peak absorption are known, measurements of the type shown in Fig. 1 do not provide a test of the calculated absolute magnitude of the line breadth.

In order to examine the absolute value of the width, and in order to study its directional dependence in a refined fashion not contingent on the Gaussian hypothesis, the r.m.s. width has subsequently been directly determined experimentally for three angles by PAKE and PURCELL⁽⁷⁾. The comparison of theory and experiment is given in Table I.

TABLE I. — Calculated and observed r.m.s. frequency deviations in CaF_2 .

Direction	$\sqrt{\langle(\Delta\omega)^2\rangle_{\text{Av}}}$ (calc.)	$\sqrt{\langle(\Delta\omega)^2\rangle_{\text{Av}}}$ (obs.)
100	3.60 gauss	(3.68 ± 0.20) gauss
110	2.24 »	(2.25 ± 0.20) »
111	1.53 »	(1.77 ± 0.20) »

In making this comparison we follow the customary practice of expressing the frequency in terms of the magnetic field which will produce a Zeeman shift equal to the frequency interval in question.

PAKE and PURCELL have pushed the comparison of theory and experiment a step further by measuring the root mean fourth frequency deviation for the 100 direction. The observed value of the ratio $\sqrt[4]{\langle(\Delta\omega)^4\rangle_{\text{Av}}}/\sqrt{\langle(\Delta\omega)^2\rangle_{\text{Av}}}$ is 1.24. The rectangular, triangular and Gaussian approximations to the line shape would yield ratios 1.158, 1.245 and 1.316.

(7) G. E. PAKE and E. M. PURCELL: *Phys. Rev.*, **74**, 1184 (1948); **75**, 534 (1948).

The agreement is gratifying especially when it is remembered that no undetermined constants are involved. The discrepancy in the 111 measurement may in part be due to crystal imperfections which make the line along the purported 111 direction less peaked than the theoretical value, inasmuch as partial or incipient mixture of other directions makes the line broader.

II.

5. - Electronic paramagnetic resonance. Exchange narrowing.

Let us now try to apply our theory to resonance caused by electron rather than nuclear spin. In the electronic case, line shapes cannot be so successfully calculated by the method of moments and the Gaussian hypotheses. If there are no complications caused by crystalline fields, and if we are dealing with a salt which conforms to the spin only formula, the expression for the mean square moment of the line, caused by dipolar broadening, should still be given by (11) or (12) if now we, of course, interpret S , $g\beta$ as electronic rather than nuclear spins and magnetic moments. It is difficult to determine experimentally the total area under the absorption curve, and it is much easier to measure the « half-breadth » (i.e., separation of the two angular frequencies at which the absorption has half the maximum value.) If the line is Gaussian in shape, the relation between the half-width and root mean-square deviation (square root of the second moment) is

$$(14) \quad \Delta\omega_{\frac{1}{2}} = 2.35 \{ \langle \Delta\omega^2 \rangle_{Av} \}^{\frac{1}{2}}.$$

The line widths calculated by means of (14) and (12) agree with experiment however, only if the magnetic dilution is high. Without water of hydration, or other diluting materials, the observed line widths are usually much smaller than those computed. In ferromagnetic materials, one would expect on the basis of (14) an enormous broadening, because of the very close spacing of the ions, but such a behavior is not observed.

The most extensive, and probably the most accurate studies of the effect of dilution on line breadth are found in recent measurements of MACLEAN and KOR⁽⁸⁾ on a large number of manganous salts, of which a selected but typical group are shown in our Table II. Here the line breadths are expressed

(8) C. MACLEAN and G. J. W. KOR: *Appl. Sci. Res.*, B, 4, 425 (1956).

in gauss rather than frequency units ($\Delta H = h \Delta \omega / 2\pi g \beta$) since in the experiments the field rather than frequency is swept. There is also an extensive body of data by various workers on cupric salts, leading to the same general conclusions, but the manganous salts are a better proving ground for the theory since the Mn^{++} ion is in an S state, has an isotropic g factor, and shows very little Stark splitting.

TABLE II.

Substance	$(\Delta H_{\frac{1}{2}})_{\text{exp}}$	$(\Delta H_{\frac{1}{2}})_{\text{calc}}$	$\langle \Delta H^4 \rangle_{\text{Av}}^{1/4} / \langle \Delta H^2 \rangle_{\text{Av}}^{1/2}$
$MnCl_2 \cdot 4H_2O$	1410 gauss	1530 gauss	1.23
$MnCl_2$	750 »	2950 »	1.40
$MnSO_4 \cdot 4H_2O$	1150 »	1560 »	1.28
$MnSO_4 \cdot 1H_2O$	320 »	2870 »	1.46
$MnSO_4$	665 »	3520 »	1.35
$MnCO_3$ (cryst.)	460 »	4460 »	1.43
$Mn_3(PO_4)_2 \cdot 3H_2O$. .	465 »	1246 »	1.38
$Mn_2P_2O_7 \cdot 3H_2O$	1070 »	1250 »	1.32
$Mn(NO_3)_2 \cdot 6H_2O$. . .	1210 »	1033 »	1.31
MnF_2	470 »	7020 »	1.39
MnS	780 »	7520 »	1.40

Reference to Table II shows that whereas the theory usually works quite well for materials of high magnetic dilution, the calculated half-breadths for the undiluted salts are much higher than those observed. ($MnSO_4 \cdot 1H_2O$, apparently is an exceptional case, whose explanation is not clear, and it is surprising that the breadth should be so much larger with four than one water of hydration. MACLEAN and KOR's results are confirmed in Japanese work but are in disagreement with some earlier American measurements ()).

It is now generally agreed that the abnormally small breadths found in electronic paramagnetic salts are to be ascribed to the phenomenon of « exchange narrowing », a mechanism first proposed by GORTER and VAN VLECK⁽⁹⁾. Qualitatively or physically, this process can be described by saying that the spin waves arising from exchange spoil the coherence, and, hence, the effectiveness of the dipolar interactions. Mathematically, the behavior can be characterized by the fact that inclusion of the exchange interaction enhances the fourth moment compared with the value that would be calculated from the second moment with the Gaussian hypothesis.

The reason that the exchange interaction enhances the fourth but not the

⁽⁹⁾ For references, see MACLEAN and KOR: l. c. ⁽⁸⁾.

⁽¹⁰⁾ C. J. GORTER and J. H. VAN VLECK: *Phys. Rev.*, **72**, 1128 (1947); J. H. VAN VLECK: l. c. ⁽⁴⁾.

second moment is the following. The exchange (\tilde{A}) term in the Hamiltonian function (9) commutes with \mathbf{S} , and, therefore, does not contribute to the second moment given by (6). However, $\mathcal{H}_{\text{dipolar}}$ and \mathbf{S} do not commute, and $\mathcal{H}_{\text{exchange}}$ does not commute with $\mathcal{H}_{\text{dipolar}}$. In consequence, $\mathcal{H}_{\text{exchange}}$ does contribute to the fourth moment, which can be shown to be given by the expression

$$(15) \quad \langle \Delta \omega^4 \rangle_{\text{Av}} = \langle \omega - \omega_0 \rangle_{\text{Av}}^4 = \langle \omega^4 \rangle_{\text{Av}} - 6\omega_0^2 \langle \omega^2 \rangle_{\text{Av}} + \omega_0^4,$$

where

$$\left(\frac{h}{2\pi} \right)^4 \langle \omega \rangle_{\text{Av}} = \frac{\text{Tr} [\mathcal{H}U - U\mathcal{H}]^2}{\text{Tr} S_x^2},$$

with

$$\omega_0 = g\beta H, \quad V = \mathcal{H}S_x - S_x\mathcal{H}.$$

The result for the fourth moment turns out to be ⁽⁶⁾

$$(16) \quad \langle \Delta \omega^4 \rangle_{\text{Av}} = a \{ \langle \Delta \omega^2 \rangle_{\text{Av}} \}^2 + b \langle \Delta \omega^2 \rangle_{\text{Av}} (2\pi/h)^2 J^2,$$

where a and b are dimensionless numerical constants. The explicit value of b for a powder with a simple cubic lattice is $b = 8.48(\pi/2)[S(S+1)/3]$. The a term is that caused by dipolar broadening alone. With a strictly Gaussian shape, the value of a would be exactly $3 = (1.32)^4$. Actual explicit calculations show that a is probably slightly smaller than 3, probably explaining why the observed values of the ratios in the last column of Table II are sometimes less than 1.32 in some of the dilute salts. However, our main concern is the fact that inclusion of the exchange terms increases the ratio. In consequence, the fact that it exceeds 1.32 in the compact salts in Table II is explained. The exchange contributions to the fourth moment should be im-

portant only in the undiluted salts, since the exchange integral decreases rapidly with the distance between the paramagnetic ions.

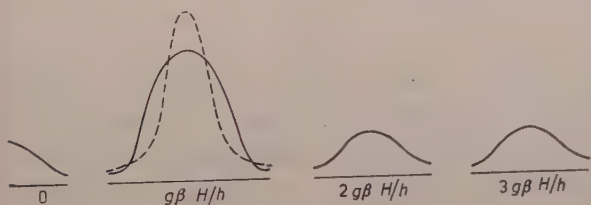


Fig. 2.

line is shrunk near the center, and tapers off more gradually in the wings. The total area under the absorption (more accurately the total line strength) is preserved but the half-width is diminished. The behavior is shown schematically in Fig. 2, where the dashed curve represents the shape after the

When the fourth moment is increased, and the second moment is unaltered, the

exchange effects are included. (The lines at 0, $2g\beta H/h$, $3g\beta H/h$ are very weak satellites caused by the part of (9) in braces. They are not relevant for the present discussion, and it was to avoid their spurious effect that truncation was introduced in computing the moment of the main line.

6. - Bloembergen-Purcell-Pound migratory narrowing.

Another example of where enhancement of the fourth moment narrows the line is found in the theory and experiments of BLOEMBERGEN, POUND and PURCELL⁽¹¹⁾ on magnetic resonance lines in liquids. The half-breadths which they find are much narrower than one would compute from the dipolar interaction under the Gaussian assumption. These authors interpret their results in terms of the motional averaging out of the dipolar fields. Instead of their very elegant correlation theory, one can also give an explanation by the method of moments. The translational kinetic energy connected with the migration of the ions relative to each other enhances the fourth but not the second moment of the resonance lines, because this energy, while commuting with any component of spin, does not commute with the dipolar Hamiltonian inasmuch as the latter involves r_{ij} and θ_{ij} .

7. - Narrowing and broadening by frequency interruption or modulation.

We now turn to a different mechanism of broadening than the phase interruption model of Lorentz or the statistical Gaussian theory. This is what may be termed the frequency-change mechanism. In many cases of magnetic resonance, the frequency of the resonant system may alter at random times, and the line structure is then modified. This type of process, which is another idealized limiting case quite different from the one considered by Lorentz, has been rather overlooked until fairly recently, but often has important physical applications.

The simplest model and illustrative example is that of an oscillator with two characteristic frequencies ω_1 and ω_2 . It has one frequency part of the time, and the other the remainder. The time of switching from one frequency to the other, which we term a collision, is random. This type of model has been examined independently by ARCHER⁽¹²⁾, by ANDERSON⁽¹³⁾, and by

⁽¹¹⁾ N. BLOEMBERGEN, E. M. PURCELL and R. V. POUND: *Phys. Rev.*, **73**, 679 (1948); N. BLOEMBERGEN: *Thesis* (Leiden, 1948).

⁽¹²⁾ D. H. ARCHER: *Thesis* (Harvard, 1953).

⁽¹³⁾ P. W. ANDERSON: *Journ. Phys. Soc. Japan*, **9**, 316 (1954).

GUTOWSKY, McCALL and SLICHTER⁽¹⁴⁾. Our approach is similar to that of GUTOWSKY, McCALL and SLICHTER, which is the simplest, but ours is based on the harmonic oscillator rather than Bloch equations.

The results with this frequency modulation model depend on whether there is no persistence in position or velocity after the collision that changes the frequency, or whether instead there is some degree of «hangover».

Let us first consider the case that there is no persistence. Then after each collision the oscillator has no memory of what happened before, and the fact that the frequency changed at collision is irrelevant as far as the mean rate of absorption in each phase is concerned. The absorption is consequently half the sum of two Lorentz expressions (3) of appropriate frequency and is hence

$$(17) \quad \frac{e^2 E^2}{8m} \left[\frac{(1/\tau)}{(\omega - \omega_1)^2 + (1/\tau)^2} + \frac{(1/\tau)}{(\omega - \omega_2)^2 + (1/\tau)^2} \right],$$

where τ is the mean time between frequency changes.

Let us now turn to the more complicated case that there is complete persistence in position and velocity at each collision. In this case, the solutions of the equations of motion for phases 1 and 2 are respectively (cf. Eq. (1))

$$(18) \quad \begin{cases} x_1(t) = \frac{eE}{m(\omega^2 - \omega_1^2)} \{ \exp[i\omega t] + A_1 \exp[i\omega_1 t] + B_1 \exp[-i\omega_1 t] \}, \\ x_2(t) = \frac{eE}{m(\omega^2 - \omega_2^2)} \{ \exp[i\omega t] + A_2 \exp[i\omega_2 t] + B_2 \exp[-i\omega_2 t] \}, \end{cases}$$

with the A 's and B 's to be determined by the boundary conditions that x and \dot{x} are continuous at collision. Let us introduce the averages over a large number of oscillators with random different histories. The equations can be satisfied by assuming that

$$\langle x_1(t) \rangle_{Av} = X_1 \exp[i\omega t], \quad \langle x_2(t) \rangle_{Av} = X_2 \exp[i\omega t],$$

with X_1, X_2 independent of t .

Let us now consider the subaverages for those oscillators whose last collisions or frequency change was at time t_0 . The boundary conditions yield

$$(19) \quad \langle x_1(t_0) \rangle_{sub Av} = X_2 \exp[i\omega t_0], \quad \langle x_2(t_0) \rangle_{sub Av} = X_1 \exp[i\omega t_0],$$

$$(20) \quad \langle \dot{x}_1(t_0) \rangle_{sub Av} = i\omega X_2 \exp[i\omega t_0], \quad \langle \dot{x}_2(t_0) \rangle_{sub Av} = i\omega X_1 \exp[i\omega t_0].$$

(14) H. S. GUTOWSKY, D. W. McCALL and C. P. SLICHTER: *Journ. Chem. Phys.*, **21**, 279 (1953).

Furthermore, $\langle x_1(t) \rangle_{\text{sub. Av}}$, $\langle x_2(t) \rangle_{\text{sub. Av}}$ are given by the expressions (18) if we use average values of the constants A , B . These averages are determined so as to satisfy (19) and (20). Hence

$$\begin{aligned}\langle x_1(t) \rangle_{\text{sub. Av}} &= \frac{eE}{m(\omega^2 - \omega_1^2)} \{ \exp[i\omega t] - \exp[i(\omega - \omega_1)t_0] \exp[i\omega_1 t] \} + \\ &\quad + X_2 \exp[i(\omega - \omega_1)t_0] \exp[i\omega_1 t], \\ \langle x_2(t) \rangle_{\text{sub. Av}} &= \frac{eE}{m(\omega^2 - \omega_2^2)} \{ \exp[i\omega t] - \exp[i(\omega - \omega_2)t_0] \exp[i\omega_2 t] \} + \\ &\quad + X_1 \exp[i(\omega - \omega_2)t_0] \exp[i\omega_2 t].\end{aligned}$$

Here, for simplicity, we assume that $|\omega - \omega_1|$, $|\omega - \omega_2|$ are small compared to ω . Otherwise, it would be necessary to introduce terms in $\exp[-i\omega_1 t]$ and $\exp[-i\omega_2 t]$ in order to satisfy (19), (20) more accurately. Such extra terms are unimportant near resonance.

The subaverages are converted to full averages by integrating over all values of t_0 . The probability that t_0 fall in the interval t_0 , $t_0 + dt_0$ is $(1/\tau) \exp[-(t - t_0)/\tau] dt_0$, and so, on performing the integration, as in obtaining (2) from (1), one finds

$$\begin{cases} X_1 \exp[i\omega t] = \left[\frac{\exp[i\omega t]}{i(\omega - \omega_1) + (1/\tau)} \right] \left[\frac{iE}{2m\omega} + \frac{X_2}{\tau} \right], \\ X_2 \exp[i\omega t] = \left[\frac{\exp[i\omega t]}{i(\omega - \omega_2) + (1/\tau)} \right] \left[\frac{iE}{2m\omega} + \frac{X_1}{\tau} \right]. \end{cases}$$

These equations can immediately be solved for $X_1 + X_2$. The absorption is $\frac{1}{2} eE \cdot \text{Re}[-i\omega(\frac{1}{2}X_1 + \frac{1}{2}X_2)]$, as the system spends equal time in phases 1 and 2. (The other factor $\frac{1}{2}$ appears as the mean value of $\cos^2 \omega t$). Hence, the absorption is

$$\begin{aligned}(21) \quad & -\text{Re} \left[\frac{ie^2 E^2 [(\omega - \omega_c) - (2i/\tau)]}{4m[(\omega - \omega_c)^2 - (\Delta\omega)^2 - (2i/\tau)(\omega - \omega_c)]} \right] = \\ & = \frac{e^2 E^2 (\Delta\omega)^2 (1/\tau)}{2m \{ (\omega - \omega_c)^4 + (\Delta\omega)^4 + (\omega - \omega_c)^2 [(4/\tau^2) - 2(\Delta\omega)^2] \}},\end{aligned}$$

where

$$\omega_c = \frac{1}{2}(\omega_1 + \omega_2), \quad \Delta\omega = \frac{1}{2}(\omega_1 - \omega_2).$$

The important thing is that according to Eq. (21), if τ is sufficiently small, the line is narrowed to a single line centering around the mean frequency ω_c , and the line gets more peaked and sharper as τ becomes smaller and smaller. An illustrative plot from ARCHER's thesis is shown in Fig. 3.

Note especially that according to (21), the absorption at the central frequency ω_c is proportional to $1/\tau$, whereas if instead one uses the formula (17) based on no persistence, the absorption here is proportional to τ if $\omega = \omega_c$ and $1/\tau \gg \Delta\omega$. In other words, with no persistence, decreasing τ merely has the effect of blurring the two resonance frequencies, and if $1/\tau$ is sufficiently large, the maximum may come at $\omega = \omega_c$, but the line is not sharpened. On the other hand, with complete persistence of «hang-over», the lines are sharpened.

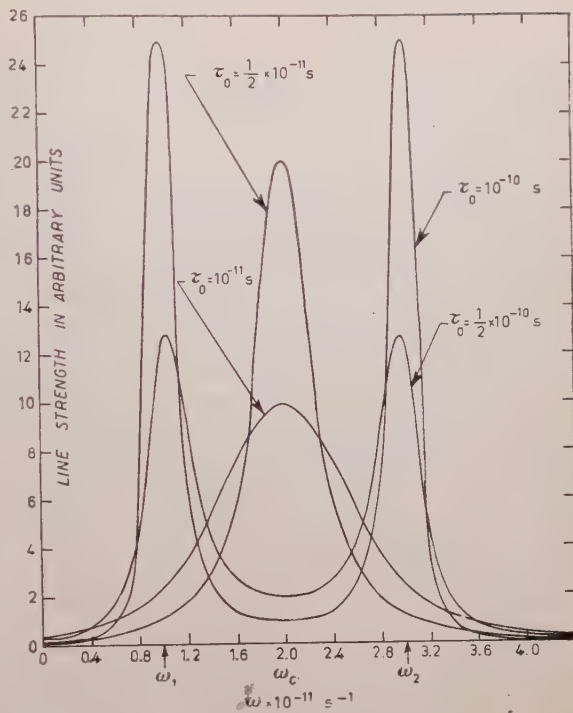


Fig. 3.

8. - Pressure narrowing.

What is the physical application of this model? One application is to the pressure narrowing of nuclear resonance lines. PURCELL, POUND, and BLOEMBERGEN⁽¹⁵⁾ find that in the nuclear resonance absorption of the protons in hydrogen gas the absorption line actually sharpens as the pressure increases. To be sure, the line is so narrow that they do not directly measure its width, and so instead determine by saturation measurements the relaxation time T_1 associated with the transfer of energy between the proton spin system and the rest of the universe. However, under the conditions of their experiments, there is every reason to believe that T_1 is the same as the characteristic time T_2 associated with the line width. The two different frequencies in the model which we have considered correspond schematically to two different orientations of the resultant spin of the protons in H_2 with respect to the rest of the molecule. In strong magnetic fields, powerful enough to Paschen-Back the hyperfine structure, the vectors \mathbf{I} (resultant nuclear spin) and \mathbf{J} (resultant angular

⁽¹⁵⁾ E. M. PURCELL, R. V. POUND and N. BLOEMBERGEN: *Phys. Rev.*, **70**, 986 (1946).

momentum of the molecule exclusive of nuclear spin) will be separately space quantized with respect to the field. The frequency of precession of \mathbf{I} will be slightly influenced by the setting of \mathbf{J} . There will, in general be more than two quantized orientations of \mathbf{J} , and so our model with only two frequencies is oversimplified, but the principle is the same. The higher the pressure, the more frequently will there be collisions which change the orientation of \mathbf{J} , and the smaller the value of τ . The underlying physical basis is that the more often the frequency changes, the better the approximation it is to say that we have resonance at the mean frequency.

Another example to which the model might apply is an electron which is continually switching its attachment from one kind of ion to another in a solution. The resonance frequencies will be slightly different for the two kinds of ion. The more frequent the switch between ions, the more perfectly and sharply the resonance centers around the mean of the two frequencies.

III.

9. - Relation between the various theories.

So far we have considered three theories of line breadth:

- (1) The Lorentz phase interruption model,
- (2) the statistical theory of line broadening based on the method of moments,
- (3) the frequency modulation model with two frequencies and persistence of position and velocity.

Before proceeding further, it is well to recapitulate and discuss the conditions under which the various theories are applicable. First, we will elaborate a little on the origin of line broadening in quantum theory⁽³⁾.

Subject to certain restrictions, into whose details we shall not enter and which are not very relevant for the present discussion, the expressions for the line shape in quantum mechanics can be obtained by assuming that because of interatomic interactions or collisions, the energy of a stationary state, instead of being independent of time as in ordinary time-independent perturbation theory, is a function of the time. The expression for the line structure

associated with a transition $1 \rightarrow 2$ then takes the form

$$(22) \quad I(\omega) = \text{const.} \left| \frac{1}{\pi} \int_{-\infty}^{\infty} \exp[-i\omega_0 t] \exp \left[(2\pi i/h) \int_{-\infty}^t [\mathcal{H}_2(t') - \mathcal{H}_1(t')] dt' \right] dt \right|^2.$$

When there are no collisions, the energies \mathcal{H}_2 and \mathcal{H}_1 of the upper and lower state are constants and the integral is a δ function located at frequency ω_0 .

Because of collisions, the functions \mathcal{H}_1 , \mathcal{H}_2 cease to be constant, and the phase factor in the wave function $\psi(x) \exp[(2\pi i/h) \int \mathcal{H} dt]$ looks at collision somewhat as shown in Fig. 4. In terms of this picture, the quantum-mechanical significance of the various models which we have discussed is as follows:

(1) The Lorentz model assumes that the change in phase is infinitely abrupt at collision. This will be the case in the close oscillations are very, very narrow in Fig. 4. It is further necessary that the change in phase $\int_{\text{collision}} \mathcal{H} dt$ be different for the upper and lower state, as otherwise the exponent in (22) is not changed by collision. The Lorentz model applies primarily to electronic resonance in gases.



Fig. 4.

(2) The statistical model supposes that the changes in frequency take place very slowly. The integration in (22) is then equivalent to generating a distribution of values for the frequency $\omega_{12} = (\mathcal{H}_2 - \mathcal{H}_1)/h$ and the curve of $I(\omega)$ is the same as that of this distribution function. The latter may be expected to be approximately Gaussian if the number of interacting spins is large. This will be roughly the case for dipolar interaction, but because the number of nearest neighbors is finite, there will be small corrections to Gaussian shape. Dipolar broadening in a crystal such as CaF_2 is the ideal case for such a procedure, since the atoms are regularly spaced; and there are no sudden collisions.

(3) Suppose that the nuclear spin and the rest of the molecule are pretty well decoupled so that the wave function factors into a product of nuclear spin and molecular wave functions. If we are dealing with a nuclear transition, the molecular state will be the same for the upper and lower level; the change in the phase will be the same for states 1, 2 in (22), and there is, hence, no resulting contribution to the line-broadening. Furthermore, collisions will in general not reorient the nuclear spins since these are decoupled, and since the

intermolecular forces do not depend on nuclear spin alignment. The collision may, however, alter the alignment of the rest of the molecule. In consequence, the energy of interaction between these two components is changed, differently for the upper and lower nuclear state, so that essentially a change of frequency is generated at collision, but no change in phase. The frequency modulation model may hence be expected to describe proton resonance in hydrogen in a strong molecular field. On the other hand, one should not use this model for the electron spin resonance in O_2 , since the spin is here so strongly coupled to the rest of the molecular (coupling energy $\sim 4 \text{ cm}^{-1}$) that an ordinary magnetic field is not able to decouple the spin, and, as a result, the electron spin participates in the change of phase at collision. The Lorentz model is hence used to describe paramagnetic resonance in oxygen.

Let us revert now to crystals with regularly spaced atoms. The various mutual orientations of the magnetic dipoles give rise to internal fields. These will change slowly with time because of the dipolar interactions themselves (assuming no other interactions present), but these changes will be slow. It is, hence, a good approximation in a crystal like CaF_2 to regard the inner field as constant in time, and to average over a distribution of fields. The presence of exchange interaction in a material such as the manganous salts may be regarded as giving rise to rapid changes in the inner fields, and correspondingly in the resonance frequencies. We can, therefore, picture the frequency as shifting back and forth between a continuum of values, or in other words sweeping irregularly through a continuum of values whose distribution is approximately Gaussian. However, the frequency spectrum will not be Gaussian if the fluctuations are rapid, just as in Fig. 3 one does not have two sharp monochromatic lines except in the limit $\tau = \infty$. The more rapid the fluctuations, the more nearly the spectrum will condense around the central frequency, corresponding to the fact that in Fig. 3, the frequency centers increasingly around ω_c as $\tau \rightarrow 0$. We, thus, can see qualitatively why the modulations caused by exchange interactions and their attendant spin waves narrow the resonance lines in paramagnetic crystals.

A mathematical implementation of these ideas has been achieved in a quite remarkable theory of ANDERSON and WEISS⁽¹⁶⁾, which gives a quantitative model for exchange narrowing, or for the Bloembergen-Purcell-Pound migratory narrowing. A more refined mathematical formulation of the Anderson-Weiss theory has been published by KUBO and TOMITA⁽¹⁷⁾.

⁽¹⁶⁾ P. W. ANDERSON and P. WEISS: *Rev. Mod. Phys.*, **25**, 269 (1952); P. W. ANDERSON: *l. c.* ⁽¹³⁾.

⁽¹⁷⁾ R. KUBO and K. TOMITA: *Journ. Phys. Soc. Japan*, **9**, 888 (1954).

10. - The theory of Anderson and Weiss.

ANDERSON and WEISS consider the dipole-dipole interaction as producing a Gaussian distribution of internal fields. In addition, this field is modulated in a random fashion. Their theory can be regarded as a generalization of our previous frequency modulation model to the case of infinitely many rather than two frequencies. The simplest assumption is a Gaussian distribution with a Gaussian modulation. The mathematical problem is essentially the same as that of Gaussian noise in f.m. In this case, the line shape can be shown to be given by

$$(23) \quad I(\omega) = \frac{I_0}{\pi} \operatorname{Re} \int_0^{\infty} \exp \left[-i(\omega - \omega_0)t - \omega_p^2 \int_0^t (t - t') \exp \left[-\frac{1}{4}\pi\omega_e^2 t'^2 \right] dt' \right] dt,$$

with $\omega_0 = 2\pi g\beta H/h$ and I_0 the total intensity of the line. Here ω_p , ω_e are characteristic frequencies associated respectively with the amount of frequency deviation and with the rate of sweep of the f.m. In the wings of the lines, one has $|\omega - \omega_0| \gg \omega_e$. Then only small t is important the integral in the exponent is approximately $\frac{1}{2}t^2$, and

$$(24) \quad I(\omega) = \frac{I_0}{(2\pi)^{\frac{1}{2}}\omega_p} \exp \left[-(\omega - \omega_0)^2 / 2\omega_p^2 \right].$$

The other extreme realized near the center of the line is $|\omega - \omega_0| \ll \omega_e$. Then large values of t make most of the contribution to the integral in the exponent, which becomes t/ω_e and

$$(25) \quad I(\omega) = \frac{I_0}{\pi} \frac{\omega_p^2/\omega_e}{(\omega - \omega_0)^2 + (\omega_p^2/\omega_e)^2}.$$

The corresponding half-width is

$$(26) \quad \Delta\omega_{\frac{1}{2}} = 2\omega_p^2/\omega_e$$

instead of (14). Thus, modulation by exchange or other causes gives a Lorentz line shape near the center of the line, but a Gaussian structure in the wings, so that the various moments are given by convergent expressions.

The modulation frequency ω_e does not affect the second moment of the line, which is

$$(27) \quad \langle \Delta\omega^2 \rangle_{\text{AV}} = \omega_p^2.$$

This property is a remarkable reflection of the fact that in quantum mechanics,

the second moment is unaffected by terms, such as exchange, which commute with the spin vector.

The fourth moment is found to be

$$(28) \quad \langle \Delta \omega^4 \rangle_{Av} = 3\omega_p^4 + \frac{1}{2} \pi \omega_p^2 \omega_e^2.$$

The possibility of choosing ω_p , ω , so as to give the proper second and fourth moment immediately suggests itself. Then, all the parameters in the Anderson-Weiss theory are determined, and an explicit model for exchange narrowing is thereby obtained. Comparison with (16) yields for a simple cubic lattice

$$(29) \quad \omega_e^2 = 8.48 (2\pi J/h)^2 [S(S+1)/3].$$

11. - The « 10/3 effect ».

In applying (23) in this fashion to cases in which $\omega_e \gg \omega_p$, i.e., in which the exchange narrowing is pronounced, one should use for the second moment, that which one calculates from (6) without truncation, i.e., no longer omitting the part of (9) that is in braces $\{ \}$. When (9) is thus not truncated, the mean square $\langle \Delta \omega^2 \rangle_{Av}$ is increased by a factor 10/3, and the value of $\langle \Delta \omega^2 \rangle_{Av}$ to be used in (27) is 10/3 times the right side of (12)

Although we have seen that (9) should be truncated when there is no appreciable exchange narrowing, the impropriety of truncating when such narrowing is important is established by empirical and theoretical evidence. In the first place, ANDERSON and WEISS find that the values of the exchange integral obtained by means of (26) and (29) from empirical line widths do not agree at all well with those obtained from the Curie temperatures unless the 10/3 correction is introduced. Theoretically, there are sound grounds for abandoning truncation when J is large; namely, in the perturbing effect of dipolar interaction the energy differences arising from the Larmor term are blurred out when the exchange energy is high. (There is not a similar blurring of the spin resonance, since the spin moment commutes with the exchange energy, whereas the dipolar potential does not). In other words, because a perturbing member involves a change in Zeeman energy, it is not necessarily a high-frequency or satellite-producing perturbation, as there can be changes in exchange energy which just compensate those in Zeeman energy, so that part of the perturbation becomes of the low-frequency or line-broadening type. Additional evidence for the 10/3 effect is found in the fact that it can be shown that the line breadth constant $T_2 = (\omega_p^2/\omega_e)^{-1}$ yielded by the Anderson-Weiss theory for large ω reduces, as it should, to the saturation relaxation time T_1 of Bloembergen's theory only if the 10/3 factor is included. Some Japanese

experiments show that the $10/3$ factor tends to disappear if one goes to very high microwave frequencies ⁽¹⁸⁾. This behavior is to be expected, for the higher the value of H relative to J , the more the part of (9) enclosed in braces tends to produce satellites rather than broaden the line, and the better approximation it is to truncate.

12. - The « 4/9 effect ».

In the preceding section, we saw that in certain cases, viz. large exchange or migratory narrowing, the truncation introduced in our first presentation of the theory was excessive. There is, also, a case where it is insufficient. This is the case of nuclear resonance (where there is no exchange narrowing) whenever two species of nuclei, I , I' , with different moments are present. Then a transition of the form $\Delta M_{I'} = -\Delta M_I$, becomes a satellite-producing, rather than line-broadening, perturbation, for the changes in Zeeman energy of atoms I and I' do not compensate. As a result, we should truncate still further and delete from (9) terms of the form $S_{j+} \cdot S_{k-}$ and $S_{j-} \cdot S_{k+}$ when they connect atoms of different moments. The contribution of dipolar interactions between atoms of unlike moments to the mean square line breadth is thereby decreased by a factor $4/9$. The reality of this effect is most strikingly confirmed in the experiments of BLOEMBERGEN and ROWLAND ⁽¹⁹⁾ on the nuclear magnetic resonance of ^{203}Tl and ^{205}Tl .

13. - Exchange broadening.

So far we have given the impression that the exchange energy does not contribute to the mean square line breadth. This is no longer the case when there are two nuclear species with unlike g -factors, or when there are crystalline electric fields. Under such circumstances, the exchange energy makes a contribution to the relevant second moment, since it does not commute with $g_j S_j + g_k S_k$ if $g_j \neq g_k$, or with the modified spin moment obtained from the total moment by a projection operator to include only intensity for one particular transition in the crystalline field energy. Then the second moment contains a term proportional to J^2 and exchange widens rather than narrows

⁽¹⁸⁾ Cf. H. KUMAGAI: *Proceedings of the International Conference of Theoretical Physics*, Kyoto and Tokio, p. 791 K. TOMITA: *Proceedings of the International Conference of Theoretical Physics*, Kyoto and Tokyo, p. 797.

⁽¹⁹⁾ N. BLOEMBERGEN and T. L. ROWLAND: *Phys. Rev.*, **97**, 1679 (1955).

the line ^(20,21). One can even try ⁽²¹⁾ to estimate the exchange integral J from the amount of exchange broadening, but, like estimates obtained in the case of exchange narrowing, it is difficult to obtain precision in the determination of J in this fashion, because the moments of the lines are often hard to measure with accuracy, and because the theory involves certain approximations.

* * *

From the various topics we have treated, we see that there are, indeed, many ramifications to the subject of the breadth of magnetic resonance lines, even in the solid state where the atoms are regularly spaced, and that it is a topic which is a powerful tool for studying the relaxation and exchange mechanisms connected with the magnetization processes.

⁽²⁰⁾ Cf. M. H. L. PRYCE: *Nature*, **162**, 538 (1948); J. WHEATLEY, D. HALLIDAY and J. H. VAN VLECK: *Phys. Rev.*, **74**, 1211 (1948); M. YOKOTA and S. KOIDE: *Journ. Phys. Soc. Japan*, **9**, 953 (1954).

⁽²¹⁾ Cf., for instance, E. ISHIGURO, K. KAMBE and T. USUI: *Physica*, **17**, 310 (1951); K. KAMBE and J. F. OLLUM: *Journ. Phys. Soc. Japan*, **11**, 50 (1956); N. BLOEMBERGEN and T. L. ROWLAND: *l. c.* ⁽¹⁹⁾.

Influence des électrons sur la résonance des spins nucléaires dans les substances diamagnétiques: le déplacement « chimique » et les interactions indirectes.

A. ABRAGAM

Centre d'Études Nucléaires de Saclay

1. — Introduction.

Nous abordons l'étude de l'influence des électrons sur la résonance nucléaire, dans des substances strictement diamagnétiques où il n'existe pour les électrons, ni paramagnétisme orbital, ni paramagnétisme de spin. L'absence de paramagnétisme électronique, dans une molécule, se traduit par le fait que les valeurs moyennes de toutes les composantes de son moment électronique total, aussi bien orbital, soit $\langle \psi_0 | L_a | \psi_0 \rangle$, que de spin, soit $\langle \psi_0 | S_a | \psi_0 \rangle$, sont nulles. ψ_0 est la fonction d'onde électronique totale (des coordonnées d'espace et de spin) de la molécule dans son état fondamental.

Malgré une symétrie apparente, il existe entre le comportement du spin et du moment orbital une différence essentielle dont les conséquences sont importantes pour ce qui suit. Les forces entre les atomes qui composent la molécule sont essentiellement des forces électriques et les forces qui dépendent des spins sont négligeables. Il en résulte que le spin total est un bon nombre quantique. Si les valeurs moyennes de toutes les composante de S sont nulles, on a nécessairement $S = 0$.

Une conclusion analogue n'est pas vraie pour le moment orbital car le moment orbital L n'est pas un bon nombre quantique et l'on peut dans l'état fondamental avoir $\langle L_a \rangle = 0$, $L \neq 0$.

Considérons, par exemple, la fonction d'onde $p_x = (\psi_1 + \psi_{-1})/\sqrt{2}$ d'un électron p , combinaison linéaire des 2 états $L_z = 1$ et $L_z = -1$. On vérifie aisément sur cette fonction que $\langle L_x \rangle = \langle L_y \rangle = \langle L_z \rangle = 0$, et pourtant $L = 1$ puisqu'il s'agit d'un électron p . VAN VLECK, à qui est due cette remarque, dit qu'en pareil cas le moment orbital est bloqué (quenched). Il est inté-

ressant de remarquer que l'absence de dégénérescence orbitale est une condition suffisante pour le blocage du moment orbital. Le raisonnement est le suivant: soit ψ un état propre, supposé non dégénéré, d'un système atomique ou moléculaire quelconque. Si l'on néglige les forces magnétiques, toujours faibles, l'Hamiltonien du système, somme de son énergie cinétique et de l'énergie électrostatique des charges qui le composent, est un opérateur réel. On peut alors supposer que ψ est réel. En effet si ψ était complexe, de la forme $\psi_1 + i\psi_2$, l'Hamiltonien étant réel, ψ_1 et ψ_2 seraient séparément des états propres du système, avec la même valeur propre et ψ serait dégénéré contrairement à l'hypothèse. L'opérateur

$$L_z = \frac{1}{i} \sum \left(x_k \frac{\delta}{\delta y_k} - y_k \frac{\delta}{\delta x_k} \right),$$

est imaginaire pur et sa valeur moyenne prise sur une fonction réelle est aussi imaginaire pure. En même temps, puisque L_z est un opérateur hermitique cette valeur moyenne est un nombre réel. Elle est donc nulle. q.e.d.

Dans le cas d'un atome isolé, l'existence d'états pour lesquels la valeur moyenne d'une composante de \mathbf{L} n'est pas nulle est intimement liée à la dégénérescence de rotation qui reflète la symétrie sphérique de l'Hamiltonien de l'atome, symétrie qui n'existe pas dans une molécule ou un crystal.

Nous supposons dans ce qui suit que l'état fondamental électronique ψ_0 du système que nous considérons n'a ni dégénérescence orbitale, ni dégénérescence de spin, ce qui, nous venons de le voir, entraîne la valeur $S = 0$ pour le spin total du système, ainsi que la nullité des valeurs moyennes des trois composantes de son moment orbital.

Nous verrons bientôt que la nature de l'interaction magnétique des électrons avec les spins nucléaires est telle que la valeur moyenne de cette interaction, calculée à l'aide de la fonction d'onde ψ_0 est nulle et l'on peut en première approximation négliger l'influence des couches électroniques sur la résonance nucléaire. C'est ce que nous avons fait jusqu'ici. La précision accrue des moyens d'observation de la résonance nucléaire oblige toutefois à tenir compte d'effets plus fins dont il existe essentiellement deux types.

1.1. Les déplacements de la fréquence de résonance. — Lorsqu'on place l'échantillon dans un champ magnétique la fréquence de résonance d'un spin nucléaire n'est pas tout à fait la même que pour le noyau « nu ». Il y a à cela deux raisons:

a) En présence d'un champ magnétique, aux mouvements des électrons périphériques se trouve superposé un mouvement de précession d'ensemble où précession de Larmor. Ce mouvement supplémentaire correspond à l'existence d'un courant électrique qui produit à l'emplacement du noyau un

champ H_d qui vient se superposer au champ appliqué H_0 . Comme le courant est proportionnel à H_0 il en est de même du champ H_d qu'il produit.

b) Le champ H_0 appliqué a pour effet de déformer les couches électroniques en les polarisant. Ces couches ainsi polarisées produisent à l'emplacement du noyau un champ magnétique H_p qui n'est plus nul comme en l'absence de H_0 . Là encore H_p est proportionnel à H_0 .

Le champ global vu par le noyau est $H = H_0 + H_d + H_p = H_0(1 + \sigma)$, où σ est indépendant de la grandeur de H_0 . Il en résulte un déplacement relatif σ de la fréquence de Larmor $\omega = \omega_0(1 + \sigma)$ du spin nucléaire. Ce déplacement σ dépend de la distribution des électrons autour du noyau. Il est naturel qu'il ait des valeurs différentes dans les composés chimiques différents, d'où le nom de déplacement chimique qui lui est donné.

1'2. *Les couplages indirects entre les spins.* — En plus des interactions dipolaires entre les spins nucléaires que nous connaissons bien, il existe entre ces spins des interactions supplémentaires dites interactions indirectes dont l'origine est la suivante:

Un moment nucléaire μ_1 produit à l'emplacement des divers électrons, un champ magnétique qui a pour effet de déformer en les polarisant les couches électroniques. Les couches électroniques ainsi déformées peuvent produire un champ magnétique H' non nul à l'emplacement d'un autre moment nucléaire μ_2 . Comme H' dépend de μ_1 , son interaction avec μ_2 équivaut à un couplage entre μ_1 et μ_2 .

Nous allons dans les paragraphes qui suivent préciser toutes ces idées par le calcul. La théorie du déplacement chimiques est due essentiellement à N. RAMSEY. Celle des interactions indirectes à PURCELL, RAMSEY, BLOEMBERGEN, KITTEL et RUDERMAN, GUTOWSKY, MCCALL et SLICHTER, etc.

2. — Le déplacement chimique.

2'1. *Généralités.* — Pour calculer ce déplacement nous devons écrire explicitement l'expression de l'Hamiltonien de couplage entre les électrons d'une part, les spins nucléaires et le champ appliqué H_0 d'autre part. Cet Hamiltonien comprend des termes d'orbite et des termes de spin. Les termes d'orbite s'obtiennent comme il est bien connu, à partir de l'Hamiltonien non relativiste de l'équation de Schrödinger des électrons en remplaçant dans le terme d'énergie cinétique le vecteur impulsion \mathbf{p} par $\mathbf{p} - (\varepsilon \mathbf{A}/C)$ où $\varepsilon = -e$ est la valeur algébrique de la charge de l'électron et \mathbf{A} est le potentiel vecteur d'où dérive le champ magnétique total, somme du champ magnétique appliqué H_0 et du champ magnétique produit par les spins nucléaires.

Les termes de spin ne sont pas donnés directement par la théorie non relativiste. On peut soit les dériver de l'équation de Dirac, soit les obtenir d'une façon phénoménologique en attachant à l'électron un moment magnétique $\mu_e = -2\beta s$ (β est le magnéton de Bohr) dont la distribution dans l'espace est la même que celle de la charge de l'électron. Bien que, comme nous allons le voir, les termes de spin n'interviennent pas dans le calcul du déplacement chimique, ils jouent un rôle prépondérant dans le calcul ultérieur des interactions indirectes et nous allons les écrire explicitement dès maintenant pour éviter des redites.

L'Hamiltonien d'une molécule peut en vertu de ce qui précède, s'écrire:

$$(1) \quad \mathcal{H} = V + \frac{1}{2m} \sum_k \left(\mathbf{p}_k + \frac{e}{c} \mathbf{A}_k \right)^2 + 2\beta \sum_k \mathbf{s}_k \text{ rot } \mathbf{A}_k.$$

Dans (1), \mathbf{p}_k est l'impulsion de l'électron k , \mathbf{s}_k son spin, V l'énergie potentielle du système que nous n'avons pas à expliciter, $\mathbf{A}_k = \mathbf{A}$, (\mathbf{r}_k) est le potentiel vecteur à l'emplacement \mathbf{r}_k de l'électron k .

Le potentiel vecteur \mathbf{A}_k se compose de deux parties, le potentiel vecteur \mathbf{A}_k^0 dont dérive le champ appliqué \mathbf{H}_0 et qui est donné par la formule:

$$(2) \quad \mathbf{A}_k^0 = \frac{1}{2} \mathbf{H}_0 \wedge \mathbf{r}_k,$$

et le potentiel $\mathbf{A}_k' = \sum_N \mathbf{A}_k^N$ produit par les différents moment nucléaires μ_N .

Nous n'avons pas précisé dans la définition de \mathbf{A}_k^0 , quelle origine nous choisissons pour les vecteurs \mathbf{r}_k et les résultats physiques doivent être indépendants de ce choix. Lorsqu'on a affaire à un atome isolé il est naturel de choisir comme origine le noyau de cet atome qui coïncide pratiquement avec le centre de gravité de l'atome. Dans une molécule lorsqu'on calcule le déplacement chimique pour un noyau déterminé N_0 , il pourra être commode de choisir ce noyau comme origine. Nous y reviendrons un peu plus loin.

Si l'on néglige la pénétration de l'électron à l'intérieur du noyau (ce qu'on n'est pas toujours en droit de faire dans certaines expériences de haute précision) on peut représenter \mathbf{A}_k^N par la formule donnant le potentiel vecteur d'un dipole élémentaire,

$$(3) \quad \mathbf{A}_k^N = \text{rot} \left(\frac{\mu_N}{r_{Nk}} \right) = \frac{\mu_N \wedge \mathbf{r}_{Nk}}{r_{Nk}^3},$$

où $\mu_N = \gamma \hbar \mathbf{I}_N$ est l'opérateur moment magnétique du noyau et $\mathbf{r}_{Nk} = \mathbf{r}_k - \mathbf{r}_N$ est le rayon vecteur de l'électron k par rapport au noyau N . L'Hamiltonien (1) ne contient pas toutes les interactions magnétiques qui existent dans la molécule. En sont absents:

a) les couplages magnétiques entre les électrons qui ne jouent aucun rôle dans le problème,

b) le couplage Zeeman des moments nucléaires avec le champ appliqué H_0 et les couplages dipolaires des moments magnétiques entre eux, interactions que nous connaissons bien.

(1) peut se récrire:

$$(4) \quad \mathcal{H} - V = \frac{1}{2m} \sum_k \left(\mathbf{p}_k + \frac{e}{c} \mathbf{A}_k^0 + \frac{e}{c} \sum_N \mathbf{A}_k^N \right)^2 + 2\beta \sum_k \mathbf{s}_k \cdot \text{rot } \mathbf{A}_k^0 + 2\beta \sum_{Nk} \mathbf{s}_k \cdot \text{rot } \mathbf{A}_k^N.$$

(4) peut, compte tenu de (2) et de (3), se récrire:

$$(5) \quad \mathcal{H} - V = T + Z_L + D + O_1 + O_2 + O_3 + Z_S + S_1 + S_2,$$

où

$$T = \frac{1}{2m} \sum_k \mathbf{p}_k^2, \quad D = \frac{e^2}{2mc^2} \sum_k (\mathbf{A}_k^0)^2 = \frac{e^2}{8mc^2} \sum_k (\mathbf{r}_k \wedge \mathbf{H}_0)^2,$$

$$Z_L = \frac{e}{2mc} \sum_k (\mathbf{p}_k \cdot \mathbf{A}_k^0 + \mathbf{A}_k^0 \cdot \mathbf{p}_k) = \frac{e\mathbf{H}_0}{2mc} \cdot \left(\sum_k \mathbf{r}_k \wedge \mathbf{p}_k \right) = \beta \mathbf{H}_0 \cdot \mathbf{L},$$

$$O_1 = \frac{e}{2mc} \sum_{k,N} (\mathbf{p}_k \cdot \mathbf{A}_k^N + \mathbf{A}_k^N \cdot \mathbf{p}_k) = 2\beta \sum_{N,k} \frac{\gamma_N (\mathbf{r}_{kN} \wedge \mathbf{p}_k) \cdot \mathbf{I}_N}{r_{kN}^3} = 2\beta \sum_{N,k} \frac{e_{kN} \cdot \boldsymbol{\mu}_N}{r_{kN}^3},$$

$$O_2 = \frac{e^2}{2mc^2} \sum_{k,N} \mathbf{A}_k^0 \cdot \mathbf{A}_k^N = \frac{e^2}{2mc^2} \sum_{k,N} (\mathbf{H}_0 \wedge \mathbf{r}_k) (\mathbf{r}_{kN} \wedge \boldsymbol{\mu}_N) / r_{kN}^3,$$

$$O_3 = \frac{e^2}{2mc^2} \sum_{k,N,N'} \mathbf{A}_k^N \cdot \mathbf{A}_k^{N'} = \frac{e^2}{2mc^2} \sum_{k,N,N'} \frac{(\boldsymbol{\mu}_N \wedge \mathbf{r}_{kN}) \cdot (\boldsymbol{\mu}_{N'} \wedge \mathbf{r}_{kN'})}{r_{kN}^3 r_{kN'}^3},$$

$$Z_S = 2\beta \mathbf{H}_0 \cdot \mathbf{S},$$

$$S_1 = 2\beta \sum_{k,N} \frac{1}{r_{kN}^3} \left\{ \frac{3(\mathbf{s}_k \cdot \mathbf{r}_k)(\boldsymbol{\mu}_N \cdot \mathbf{r}_{kN})}{r_{kN}^2} - (\mathbf{s}_k \cdot \boldsymbol{\mu}_N) \right\},$$

$$S_2 = \frac{16\pi}{3} \beta \sum_{N,k} (\mathbf{s}_k \cdot \boldsymbol{\mu}_N) \delta(\mathbf{r}_{kN}).$$

Passons en revue les différents termes de (5). Les six premiers, de T à O_3 , sont des termes orbitaux provenant du développement du carré dans le second membre de (4), T est l'énergie cinétique, Z_L est l'énergie orbitale Zeeman de la molécule représentant le couplage de son moment magnétique orbital $-\beta \mathbf{L}$ avec le champ appliqué H_0 , D est le terme diamagnétique classique. Si l'on choisit comme axe Oz la direction de H_0 , il peut se récrire $D = (e^2/8mc^2) H_0^2 \cdot \sum (x_k^2 + y_k^2)$. Pour un atome n'ayant que des couches fermées, $\langle x_k^2 + y_k^2 \rangle = \frac{2}{3} \langle r_k^2 \rangle$ et peut être remplacé par l'expression équivalente $D = (e^2/6mc^2) H_0^2 \cdot \sum r_k^2$. O_1 est le couplage magnétique des orbites électroniques avec les moments

magnétiques nucléaires. O_2 est un terme bilinéaire en H_0 et I_N . C'est l'interaction dont on a parlé dans l'introduction, qui représente le couplage avec les moments nucléaires du champ magnétique produit par le courant électronique résultant de la précession de Larmor des électrons dans le champ appliqué H_0 .

Enfin O_3 est une expression bilinéaire en I_N et $I_{N'}$, qui n'est pas leur interaction dipolaire habituelle.

Parmi les termes de spin, le premier Z_s est l'énergie Zeeman représentant le couplage du moment magnétique électronique de spin, $-\beta 2S$, avec le champ appliqué H_0 . Les deux derniers termes S_1 et S_2 représentent le couplage des spins électroniques avec les spins nucléaires. Ils s'obtiennent à partir du dernier terme de (4), par un calcul qui demande quelques précautions par suite de la singularité de **rot** A_k^N à l'origine. L'interprétation du 1^{er} terme S_1 est simple: c'est une interaction dipolaire entre les spins électroniques et les spins nucléaires. L'interprétation du 2^{ème} terme est moins immédiate: c'est l'interaction, de contact ou interaction de Fermi qui n'apporte une contribution que si la fonction d'onde électronique a une valeur non nulle à l'emplacement du noyau mais qui dans ce cas est en général prépondérante.

Nous allons grouper les termes de (5) de la façon suivante:

$$(6) \quad \mathcal{H} - V = (T + D) + (Z_L + Z_s) + (O_1 + S_1 + S_2) + (O_2 + O_3).$$

La première parenthèse contient l'énergie cinétique des électrons et leur énergie diamagnétique. Ces termes ne joueront aucun rôle dans ce qui suit et n'appellent aucun commentaire. La 2^{ème} parenthèse est l'énergie Zeeman de la molécule. Il résulte des hypothèses que $(Z_L + Z_s) = 0$. La 3^{ème} parenthèse contient les termes responsables de ce qu'on appelle la structure hyperfine des atomes et des molécules, et la valeur moyenne de chacun de ces termes est nulle. En ce qui concerne O_1 ceci résulte immédiatement du fait que l'on peut reprendre textuellement pour chaque opérateur l_{kN} , moment orbital de l'électron k par rapport au noyau N , le raisonnement fait dans l'introduction sur l'opérateur L . Pour S_1 et S_2 ceci résulte expressément de notre hypothèse que ψ_0 est un état de spin $S = 0$ et du fait que la valeur moyenne de toute composante d'un spin électronique quelconque est nulle dans un tel état. Enfin en ce qui concerne les quantités O_2 et O_3 , les hypothèses faites n'entraînent pas leur nullité.

Avant de passer au calcul du déplacement chimique il faut préciser comment nous définissons l'état fondamental de la molécule. Sa fonction d'onde électronique définit le mouvement des électrons par rapport au système de référence rigide formé par les noyaux composant la molécule, mais il faut de plus tenir compte de la possibilité d'un mouvement de rotation d'ensemble de la molécule au cours duquel l'orientation du champ appliqué H_0 , par rap-

port à la molécule change. Cette rotation dans les liquides peut en général être décrite d'une façon classique. Nous représentons l'état fondamental de la molécule par le symbole $(0, \lambda)$ où (0) décrit l'état électronique et (λ) spécifie l'orientation de la molécule. La sommation sur λ correspond à la moyenne sur les diverses orientations.

2.2. *Calcul du déplacement chimique.* — Si nous revenons à (5) et (6), nous voyons que le seul terme bilinéaire par rapport à \mathbf{H}_0 et \mathbf{I}_N est O_2 . Nous intéressant à un noyau spécifique N_0 , nous le choisissons comme origine des vecteurs. Nous nous limiterons au cas des liquides car dans les solides la largeur de raie, bien supérieure au déplacement de fréquence, rend le calcul de ce dernier illusoire.

Il vient alors:

$$(7) \quad A_1 = \langle O_2 \rangle = \sum_{\lambda} \langle 0\lambda | O_2 | 0\lambda \rangle = \frac{e^2}{2mc^2} \sum_{\lambda} \left(0\lambda \left| \sum_k \frac{(\mathbf{H}_0 \wedge \mathbf{r}_k)(\mathbf{r}_k \wedge \boldsymbol{\mu}_N)}{r_k^3} \right| 0\lambda \right) = \\ = \frac{e^2}{2mc^2} \sum_{\lambda k} \left(0\lambda \left| \frac{(\mathbf{H}_0, \mathbf{r}_k)(\boldsymbol{\mu}_N \cdot \mathbf{r}_k)}{r_k^3} - \frac{(\boldsymbol{\mu}_N \cdot \mathbf{H}_0)}{r_k} \right| 0\lambda \right).$$

On peut remarquer que (7) doit être considéré comme une petite perturbation de l'interaction directe $-\boldsymbol{\mu}_N \cdot \mathbf{H}_0$ du moment nucléaire avec le champ appliqué, et que l'on peut donc dans (7) remplacer $\boldsymbol{\mu}_N$ par sa composante le long de \mathbf{H}_0 . Il vient alors:

$$(8) \quad \langle O_2 \rangle = -\frac{e^2}{2mc^2} (\boldsymbol{\mu}_N \cdot \mathbf{H}_0) \sum_{\lambda k} \left(0\lambda \left| \frac{1 - \cos^2 \theta_k}{r_k} \right| 0\lambda \right),$$

où θ_k est l'angle du vecteur \mathbf{r}_k avec \mathbf{H}_0 ou encore, si l'on fait la moyenne sur toutes les orientations de la molécule

$$(9) \quad \left\{ \begin{array}{l} \langle O_2 \rangle = \frac{e^2}{3mc^2} (\boldsymbol{\mu}_N \cdot \mathbf{H}_0) \sum_k \left(0 \left| \frac{1}{r_k} \right| 0 \right), \\ \sigma_1 = \frac{e^2}{3mc^2} \sum_k \left(0 \left| \frac{1}{r_k} \right| 0 \right), \end{array} \right.$$

où σ_1 est la contribution de $\langle O_2 \rangle$ au déplacement fréquence.

Pour avoir une idée de l'ordre de grandeur de σ_1 on peut remarquer que e^2/mc^2 est le rayon classique de l'électron, r_0 , relié au rayon a_0 de la première orbite de Bohr par:

$$r_0 = \alpha^2 a_0,$$

où $\alpha = 1/137$ est la constante de structure fine. Si l'on admet que les valeurs moyennes $(0|1/r_k|0)$ sont de l'ordre de $1/a_0$ on voit que σ_1 sera d'ordre de grandeur α^2 , c'est-à-dire entre 10^{-4} et 10^{-5} .

Il est possible d'obtenir un autre terme d'énergie Δ_2 , bilinéaire par rapport à μ_N et H_0 , et apportant par conséquent une contribution à σ , en combinant par la théorie des perturbations du second ordre un terme A de (5) linéaire en μ_N avec un terme B linéaire en H_0 . Pour que le résultat ne soit pas identiquement nul il faut que les 2 termes A et B aient tous les deux des éléments de matrice non nuls avec des états électroniques excités (n) de la molécule, d'après la formule:

$$(10) \quad \Delta_2 = \sum'_n \frac{(0|A|n)(n|B|0)}{E_0 - E_n} + \text{c.c.}$$

Nous sous-entendons pour abrégier les indices λ relatifs à l'orientation. Comme terme A on pourrait prendre O_1 , S_1 ou S_2 comme terme B , Z_L ou Z_S ce qui a priori donnerait 6 combinaisons différentes pour (10). On peut toutefois se convaincre que seule la combinaison des termes orbitaux (O_1 , Z_L) donne un résultat différent de zéro.

Le fait que toute combinaison contenant Z_S ne donne pas de contribution à (10) résulte du fait que $|0\rangle$ est un état propre $S = 0$ du spin électronique total et que par conséquent $Z_S |0\rangle = 0$. Le terme B est donc nécessairement Z_L . Pour montrer que ni S_1 ni S_2 ne peuvent être des termes A on doit remarquer que (10) peut se récrire:

$$(11) \quad \Delta_2 = (0|ACB|0) + \text{c.c.},$$

où C est défini comme l'opérateur $\sum_n |n\rangle\langle n|/(E_0 - E_n)$.

Si les forces dépendant des spins sont négligeables, C est un opérateur qui ne dépend que des variables d'orbite. S_1 et S_2 étant des opérateurs linéaires par rapport aux spins des divers électrons, il est alors évident que $(0|S_1 CZ_L|0)$ et $(0|S_2 CZ_L|0)$ sont nuls. On a donc:

$$(12) \quad \Delta_2 = \sum'_n \frac{(0|Z_L|n)(n|O_1|0)}{E_0 - E_n} + \text{c.c.},$$

ou en réintroduisant l'indice λ et choisissant comme axe des z la direction de H_0 :

$$(12') \quad \Delta_2 = 2\beta^2 \sum'_{n,k,\lambda} \frac{(0\lambda|L_z \cdot H_0|n) \left(n \left| \frac{\mu_N \cdot \mathbf{I}_k}{r_k^3} \right| 0\lambda \right)}{E_0 - E_n} + \text{c.c.}$$

L'évaluation numérique de (12) est beaucoup plus compliquée que celle de (7) puisqu'elle requiert la connaissance des états excités de la molécule.

Une approximation que l'on fait souvent pour essayer d'obtenir l'ordre de grandeur de (12) consiste à remplacer les dénominateurs d'énergie par une valeur moyenne $1/\Delta E = \langle 1/(E_n - E_0) \rangle$. Il vient alors :

$$(13) \quad \Delta_2 = -\frac{2\beta^2}{\Delta E} \sum_{k,\lambda} \left\{ \left(0\lambda \left| (L \cdot H_0) \left(\frac{\mu_N \cdot l_k}{r_k^3} \right) \right| 0\lambda \right) + \text{c.c.} \right\},$$

ce qui par le même raisonnement que pour Δ_1 donne :

$$(14) \quad \sigma_2 = -\frac{4\beta^2}{3\Delta E} \sum_k \left(0 \left| \frac{\mathbf{L} \cdot \mathbf{l}_k}{r_k^3} \right| 0 \right).$$

Pour obtenir une estimation très grossière de l'ordre de grandeur de σ_2 on peut supposer que $(0|\mathbf{L} \cdot \mathbf{l}_k)/r_k^3|0)$ est de l'ordre de $1/\alpha_0^3$ et ΔE , distance entre états électroniques, de l'ordre de $\frac{1}{2}(c^2/a_0)$, énergie d'ionisation de l'atome d'hydrogène.

On retrouve alors pour σ_2 le même ordre de grandeur que pour σ_1 , c'est-à-dire α^2 , carré de la constante de structure fine.

Les 2 termes σ_1 et σ_2 sont donc a priori du même ordre. On remarquera que σ_1 est le seul qui existe pour un atome ou ion qui ne possède que des couches fermées, σ_2 étant alors nul. C'est donc essentiellement σ_2 qui est responsable du déplacement chimique lorsque le même atome fait partie de molécules différentes.

On remarquera aussi que dans (12), (12'), (13) et (14) les moments orbitaux qui y figurent sont pris par rapport au noyau N_0 considéré. Il en est nécessairement ainsi pour le facteur \mathbf{l}_k/r_k^3 . Pour le facteur \mathbf{L} , ceci résulte du choix arbitraire de N_0 , comme origine des coordonnées.

2.3. *Cas de molécules diatomiques.* — RAMSEY a montré que σ_z , qui est très difficile à calculer, peut être relié à la constante de couplage H' qui figure dans l'interaction

$$(15) \quad W = -H' \mu_N \cdot \mathbf{J}$$

entre le moment de rotation \mathbf{J} d'une molécule linéaire dans l'état $^1\Sigma$ et un spin nucléaire μ_N de cette molécule.

Nous ferons pour simplifier le raisonnement sur la molécule d'hydrogène. L'extension à une autre molécule linéaire est immédiate.

Le champ magnétique $H'\mathbf{J}$ produit à l'emplacement d'un proton P_1 par la rotation de la molécule, a 2 composantes. La première est le champ magnétique produit par le mouvement du 2^{ème} proton P_2 . Ce champ $H'_1\mathbf{J}$ est donné

par la formule:

$$(16) \quad \begin{cases} H_1' \mathbf{J} = - \left(\frac{\mathbf{v}}{c} \wedge \frac{e\mathbf{b}}{b^3} \right) = - \left(\frac{\boldsymbol{\omega}}{c} \wedge \mathbf{b} \right) \wedge \frac{e\mathbf{b}}{b^3}, \\ \quad \quad \quad = - \left(\frac{\hbar \mathbf{J}}{Ic} \wedge \mathbf{b} \right) \wedge \frac{e\mathbf{b}}{b^3} = \frac{e\hbar}{Ibc} \mathbf{J}. \end{cases}$$

Dans (16), \mathbf{b} est le rayon vecteur $\mathbf{P}_1\mathbf{P}_2$, $\boldsymbol{\omega}$ est le vecteur rotation de la molécule égal à $\hbar \mathbf{J}/I$, où I est le moment d'inertie de la molécule. \mathbf{v} est la vitesse relative de P_2 par rapport à P_1 . On a tenu compte dans (16) du fait que \mathbf{J} est évidemment normal à \mathbf{b} .

La 2^{ème} contribution à H' provient de la rotation des électrons. C'est un effet du second ordre. Si \mathbf{L} est le moment cinétique des électrons par rapport à un référentiel rigide lié à la molécule, il existe entre \mathbf{L} et le moment cinétique total \mathbf{J} , un couplage

$$O' = - \frac{\hbar^2}{2I} \mathbf{L} \cdot \mathbf{J}.$$

Ceci résulte du fait que l'énergie cinétique de rotation de la molécule est:

$$(17) \quad T_R = \frac{\hbar^2}{2I} (\mathbf{K})^2 = \frac{\hbar^2}{2I} (\mathbf{J} - \mathbf{L})^2,$$

où \mathbf{K} est la contribution au moment cinétique total, provenant de la rotation des noyaux. En développant (17) on trouve immédiatement le terme de couplage O' .

C'est là un terme qui s'annule au premier ordre puisque la molécule est dans un état $^1\Sigma$, mais a des éléments de matrice avec les états électroniques excités de la molécule.

On peut répéter exactement les calculs, qui à partir de Z_L et de O_2 nous avaient donné avec Δ_2 un terme bilinéaire en H_0 et μ_N , pour obtenir à partir de O' et de O_2 un terme bilinéaire en \mathbf{J} et μ_N . Il faut toutefois tenir compte du fait que H_0 pouvait occuper toutes les orientations par rapport à l'axe de la molécule alors que \mathbf{J} est nécessairement normal à cet axe.

On aura donc pour cette seconde contribution au champ magnétique de rotation:

$$(18) \quad H_2' \mathbf{J} = \frac{3}{2} \frac{\hbar^2}{\beta I} \sigma^2 \mathbf{J}.$$

Le facteur $\hbar^2/\beta I$ dans (18) est le rapport des coefficients, \hbar^2/I dans O' , et β dans Z_L .

Le facteur $\frac{3}{2}$ provient du fait que dans la moyenne sur les orientations de la molécule \mathbf{J} est nécessairement normal à l'axe de la molécule mais non H_0 .

En effet la somme $\sum_{\lambda} (0\lambda||)(||0\lambda)$ qui donne A_2 dans (12') peut s'écrire:

$$(19) \quad \overline{\sin^2 \theta} (0\sigma||)(||0\sigma) + \overline{\cos^2 \theta} (0\pi||)(||0\pi),$$

où σ est un état de la molécule où son axe est perpendiculaire à H_0 , π un état où l'axe est parallèle à H_0 , et θ est l'angle de cet axe avec H_0 .

On vérifie aisément que $(0\pi||)(||0\pi)$ est nul car L_z dans ce cas commute avec l'Hamiltonien électronique et n'a que des éléments de matrice diagonaux,

$$\sum_{\lambda} (0\lambda||0\lambda)$$

peut donc s'écrire:

$$\overline{\sin^2 \theta} (0\sigma||0\sigma) = \frac{2}{3} (0\sigma||0\sigma).$$

Dans le calcul de H'_2 les mêmes considérations s'appliquent, sauf que J étant toujours perpendiculaire à l'axe de la molécule $\overline{\sin^2 \theta} = 1$ q.e.d.

D'où:

$$\begin{aligned} \sigma &= \sigma_1 + \sigma_2 \\ &= \sigma_1 + \frac{2\beta I}{3\hbar^2} H'_2 \\ &= \sigma_1 + \frac{2\beta I}{3\hbar^2} (H' - H_1) \\ (20) \quad \sigma &= \frac{e^2}{3mc^2} \sum_k \left(0 \left| \frac{1}{r_k} \right| 0 \right) + \frac{2\beta I}{3\hbar^2} \frac{H' - e\hbar}{Ibc}. \end{aligned}$$

Lorsque H' est connu expérimentalement, comme c'est le cas pour la molécule d'hydrogène, σ peut être évalué avec précision. Pour la molécule d'hydrogène RAMSEY donne: $\sigma = 2.6 \cdot 10^{-5}$.

2.4. *L'invariance de jauge; application aux molécules contenant des atomes lourds.* — Il est bien connu en théorie de l'électromagnétisme que l'on peut toujours ajouter à un potentiel vecteur A un gradient ∇A , où A est une fonction scalaire indépendante du temps soumise à la seule condition $\nabla^2 A = 0$ à condition de multiplier la fonction d'onde par un facteur de phase $\exp[(e\hbar/c)A]$. On vérifie aisément que cette double modification laisse l'équation de Schrödinger inchangée (la généralisation au cas où A dépend du temps ne nous intéresse pas ici). C'est ce que l'on appelle l'invariance de jauge. En particulier un déplacement de l'origine des vecteurs \mathbf{r}_k dans la molécule par un vecteur \mathbf{R} revient à ajouter à tous les $A^0(k)$, le vecteur $\frac{1}{2}(\mathbf{R} \wedge \mathbf{H})$ et à multiplier simultanément la fonction d'onde par $\exp[-(ie/2\hbar c)(\mathbf{R} \wedge \mathbf{H}) \cdot \sum \mathbf{r}_k]$. L'intérêt de cette remarque est le suivant. Si nous retournons à l'expression (9) de σ_1 , nous constatons que cette expression varie comme $1/r_k$, donc très lentement avec la distance de l'électron k au noyau considéré N_0 . Nous arrivons

ainsi à la conclusion, physiquement choquante, que même des électrons appartenant à des atomes assez éloignés apportent une contribution assez importante au déplacement chimique de la fréquence du noyau N_0 . L'explication de ce paradoxe réside dans le fait que le terme du second ordre σ_2 apporte lui aussi une contribution importante de la part d'atomes éloignés et que ces contributions se compensent approximativement. Il serait donc intéressant de pouvoir modifier l'expression de σ_1 et σ_2 de façon que leur somme ne s'exprime plus comme différence des valeurs absolues des 2 quantités grandes et presque égales.

Supposons que la molécule se compose de p atomes N_1, N_2, \dots, N_p et que les orbitales électroniques de la molécule supposées mutuellement orthogonales puissent se classer en un certain nombre d'orbitales localisées sur les différents atomes et formant des couches fermées, plus un certain nombre d'orbitales qui ne sont pas localisées sur un atome particulier, que nous appellerons orbitales de valence. $\Phi_{N_1}, \Phi_{N_2}, \dots, \Phi_{N_p}$ représentent respectivement les couches fermées des noyaux N_1, N_2, \dots, N_p , Φ_v représente les électrons de valence.

Nous ferons l'hypothèse simplificatrice (peut-être excessive mais commode) que l'empiètement (overlap) de 2 orbitales appartenant à 2 groupes différents est négligeable. D'après un résultat général de mécanique quantique ceci permet de traiter les électrons appartenant à 2 groupes différents comme discernables (mais non les électrons à l'intérieur d'un même groupe).

On peut alors à l'intérieur de chaque groupe faire un changement de jauge différent, de façon à ramener l'origine des vecteurs \mathbf{r}_k dans (2), au noyau N_i pour les électrons de l'atome N_i . On s'aperçoit alors que la contribution au terme paramagnétique Δ_2 apportée par les couches fermées disparaît.

En ce qui concerne les électrons de valence l'origine des vecteurs \mathbf{r}_k reste arbitraire. On pourra par exemple prendre comme origine le noyau N_0 particulier dont on calcule le déplacement chimique. L'expression de Δ_1 et Δ_2 devient alors:

$$(21) \quad \Delta_1 = \frac{e^2}{2mc^2} \sum_{N_i, \lambda} \sum_{k=1}^{q_{N_i}} \left(\Phi_{N_i} \lambda \left| \frac{(\mathbf{H}_0 \wedge \mathbf{r}_{kN_i})(\mathbf{r}_{kN_0} \wedge \boldsymbol{\mu}_{N_0})}{r_{kN_0}^3} \right| \Phi_{N_i}, \lambda \right) + \\ + \frac{e^2}{2mc^2} \sum_{k=1}^{q_v} \left(\Phi_v, \lambda \left| \frac{(\mathbf{H}_0 \wedge \mathbf{r}_k)(\mathbf{r}_{kN_0} \wedge \boldsymbol{\mu}_{N_0})}{r_{kN_0}^3} \right| \Phi_v, \lambda \right).$$

Dans cette formule q_{N_1}, \dots, q_v représentent les nombres des électrons dans les groupes d'orbitales, $\Phi_{N_1}, \dots, \Phi_v$.

On remarquera que dans le premier terme de Δ_1 pour $N_i \neq N_0$, r_{kN_i} distance de l'électron k au noyau N_i est beaucoup plus petite que sa distance r_{kN_0} au noyau d'un atome distant N_0 . La quantité dont on calcule la valeur moyenne, décroît donc comme $1/r_{kN_0}^2$ et non comme $1/r_{kN_0}$ avant le changement de jauge et cette contribution à Δ_1 pourra être négligée en première approximation.

Passons à Δ_2 .

Ce terme provient maintenant uniquement des électrons de valence et peut s'écrire :

$$(22) \quad A_2 = -\frac{2\beta^2}{\Delta E} \sum_{\lambda} \sum_{k=1}^{q_v} \left\{ \left(\Phi_v, \lambda \left| \frac{(\mathbf{L} \cdot \mathbf{H}_0)(\boldsymbol{\mu}_{N_0} \cdot \mathbf{l}_{kN_0})}{r_{kN_0}^3} \right| \Phi_v, \lambda \right) + \text{c.c.} \right\}.$$

\mathbf{L} est ici le moment orbital par rapport à l'origine arbitraire choisie pour les électrons de valence.

Si l'on veut calculer le déplacement chimique relatif d'un noyau N_0 dans 2 environnements chimiques différents, la contribution essentielle à ce déplacement relatif sera le terme paramagnétique A_2 des électrons de valence. En effet les termes A_1 provenant des couches fermées des autres atomes sont petits, les termes A_1 provenant de l'atome considéré sont les mêmes dans les deux cas, et les termes A_1 provenant des électrons de valence, petits, si ces électrons sont peu nombreux.

L'influence du terme A_2 est particulièrement grande lorsque la molécule possède des états excités voisins de l'état fondamental. Si la distance de ces états excités voisins de l'état fondamental est suffisamment petite pour que leurs populations ne soient pas négligeables à la température de l'expérience on obtient des déplacements chimiques dépendants de la température.

C'est le cas par exemple, de certains composés diamagnétiques du cobalt (PROCTOR et YU: *Phys. Rev.*, **81**, 20 (1951)).

Il faut naturellement admettre que les transitions entre les différents états qui correspondent à des déplacements chimiques différents, sont suffisamment rapides pour que seule une valeur moyenne du déplacement soit observée.

L'étude systématique du déplacement chimique dans le but d'établir une corrélation, ne fut-ce qu'empirique, avec la distribution des électrons dans les molécules a été poursuivie activement par GUTOWSKY et ses collaborateurs. On trouvera une tentative d'interprétation quantitative des résultats pour la molécule F_2 dans l'article de SLICHTER et SAIKA (*Journ. Chem. Phys.*, **22**, 26 (1954)).

Le déplacement chimique se manifeste d'une façon spectaculaire par une structure fine de la raie de résonance lorsque plusieurs atomes du même élément occupent dans la molécule des positions qui ne sont pas équivalentes. L'exemple le plus fameux est celui de l'alcool éthylique CH_3-CH_2-OH dont les 3 pics sur la Fig. 1 correspondent à la résonance des protons à 3 groupes, méthyl, méthylène et hydroxyl.

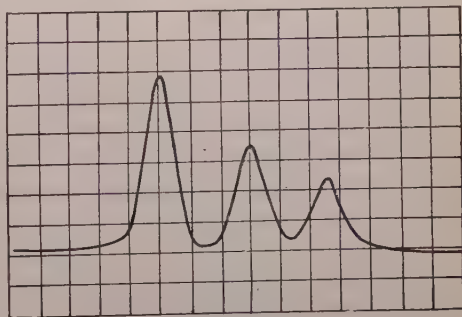


Fig. 1.

3. — Interactions indirectes entre spins nucléaires.

La découverte de ces interactions remonte à 1951 environ et la responsabilité pour cette découverte est partagée entre de nombreux auteurs. Parmi ceux qui ont contribué à débrouiller le phénomène nous citerons HAHN, GUTOWSKY, SLICHTER, RAMSEY, PURCELL, etc. Le fait que ces interactions n'aient été mises en évidence que plus de 5 ans après la découverte de la résonance nucléaire s'explique par la petitesse des effets observés et la nécessité d'une résolution que les premiers appareils ne possédaient pas. Les interactions indirectes ont été surtout étudiées dans les liquides car dans les solides elles sont, en général (mais non toujours comme nous le verrons), masquées par les interactions dipolaires directes beaucoup plus grandes, alors que dans les liquides l'effet des interactions dipolaires est éliminé au premier ordre par le mouvement brownien des noyaux.

Dans une première partie de cet exposé nous verrons comment l'existence de ces interactions se rattache à la structure atomique et moléculaire de la matière, puis dans une seconde partie nous verrons comment ces interactions permettent de comprendre la structure fine des raies de résonance nucléaire observées dans les liquides ainsi que le rôle qu'elles peuvent jouer dans certains solides.

L'interaction entre 2 spins I_N et $I_{N'}$, est de la forme $I_N \mathcal{J}_{NN'} I_{N'}$, où $\mathcal{J}_{NN'}$ est un certain tenseur. Une simplification importante de la forme de cette interaction interviendra dans les liquides. Les axes principaux du tenseur \mathcal{J} sont liés à la molécule et si celle-ci subit rapidement des réorientations spatiales, comme c'est le cas dans les liquides, il est facile de voir que le tenseur \mathcal{J} sera remplacé par un tenseur moyen $\bar{\mathcal{J}}$ avec $(\bar{\mathcal{J}})_{ik} = J \delta_{ik}$, J étant la trace de \mathcal{J} , et que l'interaction indirecte deviendra un simple produit scalaire $J \cdot I_{N_0} I_{N'}$.

C'est précisément parce que la trace de l'interaction habituelle dipole considérée comme un tenseur est nulle que cette interaction disparaît au premier ordre dans les liquides rendant possible l'observation de l'interaction indirecte $J(I_{N_0} I_{N'})$ qu'elle masquerait autrement dans la plupart des cas.

3.1. Théorie atomistique des interactions nucléaires. — Les bases de cette théorie se trouvent contenues dans la décomposition (5') de l'Hamiltonien électronique d'une molécule. Nous cherchons une interaction bilinéaire par rapport aux moments nucléaires. Une seule interaction de ce type existe dans (5'), c'est O_3 . Si nous calculons $\langle O_3 \rangle = (\Psi_0 | O_3 | \Psi_0)$, valeur moyenne de O_3 , prise sur la fonction d'onde électronique Ψ_0 de l'état fondamental de la molécule, nous trouverons bien une interaction du type $I_N \cdot \mathcal{J} \cdot I_{N'}$, où \mathcal{J} est un tenseur qui dépend de la structure électronique de la molécule.

Bien qu'effet du premier ordre, la contribution de $\langle O_3 \rangle$ est toujours très

petite. Ceci tient essentiellement au fait que O_3 est une somme d'opérateurs à un électron et que lorsque dans le produit $((\boldsymbol{\mu}_N \wedge \mathbf{r}_{Nk})/r_{Nk}^3) \cdot ((\boldsymbol{\mu}_{N'} \wedge \mathbf{r}_{N'k})/r_{N'k}^3)$ le 1^{er} facteur est relativement grand, l'électron k se trouvant près du noyau N , l'autre facteur est petit car l'électron k se trouve alors relativement loin de N' .

De plus la contribution à $\langle O_3 \rangle$ des orbites des couches profondes de l'un ou l'autre atome, pour lesquelles un facteur tel que $\langle 1/r_{Nk}^3 \rangle$ est grand, est réduite considérablement par un facteur angulaire. En effet, si $|a_N\rangle$ est une orbite de l'atome N , dont les dimensions sont beaucoup plus petites que la distance internucléaire NN' , on aura approximativement sur cette orbite $\mathbf{r}_{N'} \cong \mathbf{R}_{NN'} = \text{const.}$ et la contribution correspondante à $\langle O_3 \rangle$ sera approximativement:

$$\left(a_N \left| \frac{\boldsymbol{\mu}_N \wedge \mathbf{r}_N}{r_N^3} \right| a_N \right) \cdot \frac{\boldsymbol{\mu}_N \wedge \mathbf{R}_{NN'}}{R_{NN'}^3},$$

qui est nul car l'orbite atomique $|a_N\rangle$ possède une parité définie par rapport au noyau N .

L'ordre de grandeur de $\langle O_3 \rangle$ est difficile à estimer. On peut toutefois penser qu'une partie non négligeable de cette expression provient d'électrons à peu près à égale distance des deux noyaux N et N' .

On a donc

$$\langle O_3 \rangle \sim \frac{e^2}{2mc^2} \frac{\boldsymbol{\mu}_N \cdot \boldsymbol{\mu}_{N'}}{(R_{NN'})^4} \sim \frac{\boldsymbol{\mu}_N \boldsymbol{\mu}_{N'}}{R_{NN'}^3} \cdot \frac{8r_0}{R_{NN'}},$$

où r_0 est le rayon classique de l'électron.

Le rapport de cette interaction à l'interaction directe serait donc de l'ordre de:

$$\frac{8}{137^2} \frac{a_0}{R_{NM'}},$$

où a_0 est la première orbite de Bohr.

Pour une distance internucléaire NN' de 2 Å ce rapport serait de l'ordre de 10^{-4} .

Puisque dans certains cas (exceptionnels il est vrai) l'interaction indirecte en arrive à excéder l'interaction directe, il faut chercher d'autres mécanismes.

Comme dans le cas du déplacement chimique, nous pouvons obtenir un terme bilinéaire en $\boldsymbol{\mu}_N$ et $\boldsymbol{\mu}_{N'}$ en combinant par une perturbation du 2^{ème} ordre deux termes de (5'), linéaires en $\boldsymbol{\mu}_N$.

Ces termes sont O_1 , S_1 et S_2 .

(Le terme O_2 , bilinéaire en $\boldsymbol{\mu}_N$ et H_0 et qui a fourni une contribution du 1^{er} ordre à σ , fournirait au second ordre un terme trilinéaire en $\boldsymbol{\mu}_N$, $\boldsymbol{\mu}_{N'}$ et H_0 d'un ordre de grandeur bien inférieur).

Il y a donc a priori 6 façons de combiner O_1 , S_1 et S_2 , mais il est facile de voir par un raisonnement analogue à celui fait à propos du déplacement chimique, que le terme orbital ne se combine pas au terme de spin et que les seules combinaisons sont donc (O_1, O_1) , (S_1, S_1) , (S_1, S_2) , (S_2, S_2) .

Il est peut être bon de remarquer à ce point que si les termes quadratiques par rapport aux spins électroniques n'apportent pas de contribution au déplacement chimique, c'est que là l'un des deux facteurs de chacun de ces termes est nécessairement $Z_s = 2\beta\mathbf{H}_0 \cdot \mathbf{S}$ et que comme on l'a vu, tous les éléments non diagonaux $\langle O | Z_s | n \rangle$ sont nuls.

Avant de passer au calcul de tous ces termes, remarquons, encore, que, comme du reste dans le cas des déplacements chimiques la difficulté des calculs est telle que sauf des cas exceptionnels on ne pourra espérer obtenir mieux qu'un ordre de grandeur ce qui justifiera un certain nombre d'approximations a priori discutables. En particulier nous continuerons à faire un large usage de l'approximation de clôture qui consiste à remplacer dans (10) les dénominateurs d'énergie par une valeur moyenne ΔE .

3.1.1. L'approximation de Heitler-London.

Application au cas de la molécule d'hydrogène et à l'acétate de cuivre. — Suivant HEITLER et LONDON nous décrivons une liaison chimique entre deux atomes N et N' par une fonction d'onde à deux électrons du type

$$(23) \quad \Psi(1, 2) = \frac{1}{\sqrt{2(1 + A^2)}} \{ \Phi_N(1)\Phi_{N'}(2) + \Phi_{N'}(1)\Phi_N(2) \} \chi(1, 2),$$

où Φ_N et $\Phi_{N'}$ sont des orbitales (où combinaison linéaires d'orbitales) appartenant respectivement aux atomes N et N' et où $\chi(1, 2)$ est une fonction des deux spins 1 et 2 correspondant à l'état $S = 0$ (remarquons incidemment que (23) n'est pas un déterminant de Slater unique mais une somme de deux tels déterminants).

$A = \int \Phi_N^*(1) \Phi_{N'}(1) d\tau_1$ est une mesure du recouvrement des deux orbitales.

L'énergie d'interaction entre deux spins μ_N et $\mu_{N'}$ se calcule d'après (10) et avec l'approximation de clôture est donnée par

$$(24) \quad - \frac{1}{\Delta E} (\Psi(1, 2) \{ \mathcal{H}_N(1) + \mathcal{H}_{N'}(1) + \mathcal{H}_N(2) + \mathcal{H}_{N'}(2) \}^2 \Psi(1, 2)),$$

où \mathcal{H}_N et $\mathcal{H}_{N'}$ représentent dans $O_1 + S_1 + S_2$ la somme des termes contenant μ_N ou $\mu_{N'}$, respectivement. Il ne faut naturellement prendre dans (24) que les termes bilinéaires en \mathcal{H}_N et $\mathcal{H}_{N'}$.

Si nous développons alors (24), compte tenu de (23), nous trouverons 5 es-

de termes de la forme:

$$(25) \quad \left\{ \begin{array}{l} (\Phi_N | \mathcal{H}_N | \Phi_N)(\Phi_{N'} | \mathcal{H}_{N'} | \Phi_{N'}) \\ (\Phi_N | \mathcal{H}_N | \Phi_{N'})(\Phi_{N'} | \mathcal{H}_{N'} | \Phi_N) \\ (\Phi_N | \mathcal{H}_{N'} | \Phi_N)(\Phi_{N'} | \mathcal{H}_N | \Phi_{N'}) \\ (\Phi_N | \mathcal{H}_N \mathcal{H}_{N'} | \Phi_N) \\ (\Phi_N | \mathcal{H}_N \mathcal{H}_{N'} | \Phi_{N'}) \end{array} \right.$$

Les termes de première espèce sont beaucoup plus grands que tous les autres car Φ_N et \mathcal{H}_N sont beaucoup plus grands au voisinage du noyau N que du noyau N' . Ce sont les seuls que nous conserverons.

Si les fonctions d'onde orbitales sont réelles on a $(\Phi_N | O_1 | \Phi_N) = 0$, en vertu des remarques faites dans l'introduction, et seuls les termes de spin demeurent. On peut alors écrire $(\Phi_N | \mathcal{H}_N | \Phi_N) = \mathbf{I}_N \cdot \mathbf{a}_N \cdot \mathbf{s}$, où \mathbf{a}_N est un certain tenseur symétrique.

\mathbf{a}_N décrirait la structure hyperfine de l'atome N si l'on pouvait admettre que la forme de l'orbite Φ_N n'est pas modifiée par le voisinage de l'atome N' .

On trouve des exemples de structure hyperfine anisotrope dont la description se fait par un tenseur, dans certains sels paramagnétiques du groupe du fer (voir ABRAGAM et PRYCE: *Proc. Roy. Soc.* (1951)).

L'interaction entre les deux spins N et N' s'écrit alors $\mathbf{I}_N \cdot \mathcal{J}_{NN'} \cdot \mathbf{I}_{N'}$, où $\mathcal{J}_{NN'}$ est un tenseur symétrique défini par:

$$(26) \quad \mathbf{I}_N \cdot \mathcal{J}_{NN'} \cdot \mathbf{I}_{N'} = - \frac{2\hbar^2 \nu_N \nu_{N'}}{(1 + A^2) \Delta E} (\chi(1, 2) \{ (\mathbf{I}_N \cdot \mathbf{a}_N \cdot \mathbf{s}_1) \cdot (\mathbf{I}_{N'} \cdot \mathbf{a}_{N'} \cdot \mathbf{s}_2) \} \chi(1, 2)) ,$$

où $\{A, B\}$ représente le produit symétrique $\frac{1}{2}(AB + BA)$. Si l'on remarque que, $\chi(1, 2)$ étant la fonction de spin singulet, on a $(\chi | s_{1x} s_{2x} | \chi) = -\frac{1}{4}$, $(\chi | s_{1x} s_{2y} | \chi) = 0$, il vient

$$(27) \quad \mathcal{J}_{NN'} = - \frac{\hbar^2 \nu_N \nu_{N'}}{2(1 + A^2) \Delta E} \{ \mathbf{a}_N \cdot \mathbf{a}_{N'} \} ,$$

où $\{ \mathbf{a}_N \cdot \mathbf{a}_{N'} \}$ est le produit contracté et symétrisé des deux tenseurs \mathbf{a}_N et $\mathbf{a}_{N'}$.

On voit aisément que si \mathbf{a}_N et $\mathbf{a}_{N'}$ sont des tenseurs symétriques il en est de même de \mathcal{J} .

(27) montre que l'ordre de grandeur de \mathcal{J} est:

$$(28) \quad \frac{\mathcal{J}}{\hbar} \sim \frac{\nu_N \cdot \nu_{N'}}{\nu_0} ,$$

où ν_N et $\nu_{N'}$ sont les largeurs respectives des structures hyperfines des atomes

N et N' et ν_0 la fréquence qui sépare l'état fondamental de la molécule d'un état excité. Il y aura donc lieu de s'attendre à des couplages J importants lorsque:

a) les atomes N et N' sont des atomes lourds ayant des structures hyperfines importantes;

b) lorsque pour une raison accidentelle un état électronique excité (paramagnétique) de la molécule, se trouve anormalement près de l'état fondamental.

Application à la molécule d'hydrogène deutérié. — La constante J de l'interaction indirecte a été mesurée dans la molécule HD et trouvée égale en Hz à 43 Hz (nous verrons dans 2) pourquoi l'expérience ne peut pas se faire sur la molécule H_2).

Pour comparer ce résultat à la théorie, le plus simple est de partir de la formule (27) où l'on considérera la distance moyenne ΔE des états excités comme une inconnue et de voir si l'on trouve pour cette quantité une valeur raisonnable.

Si pour Φ_N et $\Phi_{N'}$ on prend des orbitales 1s des deux atomes d'hydrogène et du deutérium, a_N , $a_{N'}$ et $\mathcal{J}_{NN'}$ deviennent des scalaires (il en serait du reste ainsi de \mathcal{J} quelle que soit la fonction d'onde $\Psi(1, 2)$ choisie, l'expérience ayant été faite dans un gaz) et il vient

$$(29) \quad \frac{J}{\hbar} = \frac{\nu_D}{\nu_H} \cdot \frac{(\Delta\nu_H)^2}{2(1 + A^2)(\Delta E/\hbar)},$$

où $\Delta\nu_H$ est l'intervalle de fréquence hyperfine de l'hydrogène. Avec $J/\hbar = 43$ Hz, $\Delta\nu_H = 1400$ MHz, $\nu_D/\nu_H = 0.156$ on trouve $\Delta E \sim 10$ eV.

Au lieu d'utiliser une fonction électronique de Heitler-London et de négliger dans (25) tous les termes sauf le premier, approximation d'autant meilleure que les distances internucléaires sont plus grandes par rapport au rayon des orbitales atomiques Φ_N et $\Phi_{N'}$, on peut dans le cas de HD utiliser directement la formule (24) avec la meilleure fonction $\psi(1, 2)$ dont on dispose. C'est ce qu'a fait RAMSEY en utilisant la fonction de James et Coolidge pour cette molécule. Il n'a toutefois retenu dans \mathcal{H}_N et $\mathcal{H}_{N'}$ que le terme S_2 dont il estime à juste titre l'influence prépondérante. Il trouve $\Delta E \simeq 19$ eV.

Ni l'une ni l'autre valeur ne sont déraisonnables. L'énergie de l'état excité triplet calculée par JAMES et COOLIDGE est d'environ 9 eV au-dessous de l'état fondamental singulet.

Bien que la fonction de James et Coolidge soit incontestablement meilleure que la fonction de Heitler et London pour la description de l'état fondamental, les incertitudes liées à l'approximation de clôture sont telles qu'il paraît illusoire de spéculer davantage sur la comparaison de ces deux valeurs de ΔE .

Application à l'acétate de cuivre solide. — Bien qu'il n'existe pas de résultats expérimentaux sur l'existence d'une interaction indirecte entre les spins des noyaux de cuivre dans cette substance la théorie permet de prévoir pour cette interaction des propriétés très spéciales qui justifient une étude rapide. Des expériences de résonance électronique faites sur cette substance à Oxford par B. BLEANEY et ses collaborateurs ont permis de montrer que dans le crystal d'acétate les ions cuivre Cu^{++} , dont chacun a un spin électronique $\frac{1}{2}$, se trouvent groupés par paires relativement isolées les unes des autres et qu'entre les spins électroniques s_1 et s_2 des ions d'une même paire existe une interaction d'échange du type $A s_1 \cdot s_2$. Le signe de A est positif et sa grandeur de l'ordre de $1/20$ d'électron-volt. La paire d'ions possède donc un état fondamental diamagnétique $S = 0$ et un état excité paramagnétique $S = 1$ qui est celui où BLEANEY a observé la résonance électronique. L'analogie avec la molécule diatomique HD est évidente et le calcul de l'interaction indirecte entre les deux spins nucléaires des ions cuivre de la paire se fait immédiatement par la formule (27) où l'on prend $\Delta E = A$.

La comparaison avec le cas de HD appelle les commentaires suivants:

a) ΔE au lieu d'être de l'ordre de 10 eV est seulement de $1/20 \text{ eV}$, c'est-à-dire 200 fois plus petit dans l'acétate de cuivre que dans HD et par conséquent, \mathcal{J} serait toutes choses égales 200 fois plus grand.

b) Du fait que l'influence de l'état électronique excité qui est anormalement bas, l'emporte de beaucoup sur celle des autres états excités, l'approximation de clôture est bien justifiée dans ce cas.

c) Si l'on fait dans (27), $|a_N/k| \sim |a_{N'}/k| \sim 0.01 \text{ cm}^{-1}$ qui sont les valeurs expérimentales obtenues par BLEANEY à partir de ses expériences sur l'état $S = 1$, et $\Delta E = 400 \text{ cm}^{-1}$, on trouve $\mathcal{J}/k \sim 7500 \text{ Hz}$ qui est près de 20 fois supérieur à l'interaction dipole dipole directe des deux noyaux de cuivre de la paire. L'interaction indirecte ne risque donc pas d'être masquée par l'interaction directe et peut être observée dans l'état solide.

d) Les structures hyperfines de deux ions de la paire sont très anisotropes et l'une des valeurs principales des tenseurs a_N et $a_{N'}$ qui les décrivent, est beaucoup plus grande que les autres (c'est à celle-là que correspond la valeur 0.01 cm^{-1} citée plus haut). L'anisotropie d'est-à-dire le rapport entre la plus grande valeur principale et les deux autres qui sont approximativement égales est de l'ordre de 7. Il en résulte que le tenseur \mathcal{J} , produit contracté des deux tenseurs a_N et $a_{N'}$ (dont les axes principaux se trouvent être parallèles) devrait avoir une anisotropie de l'ordre de 50.

Il serait intéressant de faire une expérience de résonance nucléaire sur l'acétate de cuivre, à la température de l'hélium liquide, où l'état paramagnétique est inoccupé, pour essayer de contrôler ces prédictions de la théorie.

Remarque. — Nous avons admis plus haut que l'absence de dégénérescence orbitale permettrait de négliger le couplage orbital O_1 des électrons avec les spins nucléaires et de décrire par l'expression $(\Phi_N | \mathcal{H}_N | \Phi_N) = \mathbf{I}_N \cdot \mathbf{a}_N \cdot \mathbf{s}$, la structure hyperfine de l'atome N .

On peut montrer, que l'expression ci-dessus est encore valable lorsque (comme c'est le cas notamment dans Cu^{2+}) un couplage spin orbite important a pour effet de rendre la valeur moyenne du moment orbital différente de zéro dans l'état Φ_N .

3'1.2. La méthode des orbitales.

Application aux métaux et aux isolants. — Le résultat relativement simple (27) obtenu pour l'interaction indirecte entre les spins nucléaires de deux atomes liés par un couplage de Heitler-London reposait sur l'utilisation d'orbitales localisées sur l'un ou l'autre des atomes considérés.

La méthode des orbitales moléculaires non localisées permet de s'affranchir de cette restriction.

Cette méthode a des bases théoriques solides puisqu'elle est une extension au cas des molécules, de la méthode de champ self consistant qui donne de très bons résultats dans les atomes. Au lieu d'un champ self consistant central comme dans les atomes on cherche un champ self consistant ayant la symétrie de la molécule. En fait le problème est difficile et l'on emploie une approximation où sans s'occuper de la self-consistance on représente chaque orbite moléculaire par une combinaison linéaire d'orbitales appartenant aux différents atomes composant la molécule. Nous pouvons en principe appliquer cette approximation ou MOLCAO (molecular orbitals, linear combinations of atomic orbitals) à notre problème.

Nous supposons que la molécule a $2r$ électrons et p orbitales moléculaires Ψ_1, \dots, Ψ_p orthogonales, chaque orbite logeant deux électrons.

Avec ces orbitales, compte tenu du spin on forme $2p$ états avec lesquels on construit un déterminant de SLATER Ψ_0 . Il reste à calculer l'interaction in directe par

$$(30) \quad \sum_N' \sum_{N', N''} \sum_{k, k'=1}^{2p} \frac{(\Psi_0 | \mathcal{H}_N(k) | n)(n | \mathcal{H}_{N'}(k') | \Psi_0)}{E_0 - E_n},$$

ou si l'on utilise l'approximation de clôture, par

$$(31) \quad - \frac{1}{\Delta E} \sum_{N, N'} \sum_{k, k'} (\Psi_0 | \mathcal{H}_N(k) \mathcal{H}_{N'}(k') | \Psi_0).$$

Dans le développement de (3), compte tenu des règles de calcul des déterminants de Slater, on trouvera des éléments de matrice à une particule du type $(\Psi_p | \mathcal{H}_N \mathcal{H}_{N'} | \Psi_p)$ et des éléments de matrice à deux particules du type nor-

mal, soit :

$$(\Psi_p(1)\Psi_q(2)|\mathcal{H}_N(1)\mathcal{H}_{N'}(2)|\Psi_p(1)\Psi_q(2)) .$$

ou du type échange

$$(\Psi_p(1)\Psi_q(2)|\mathcal{H}_N(1)\mathcal{H}_{N'}(2)|\Psi_q(1)\Psi_p(2)) .$$

Chaque orbite étant supposée une combinaison linéaire du type

$$\Psi_p = \sum_{q,N} C_{qN}^p \varphi_{qN} ,$$

où les φ_{qN} sont des orbitales atomiques appartenant aux différents atomes composant la molécule, il est en principe possible d'évaluer (31) si les φ_{qN} et les coefficients C_{qN}^p sont connus.

On trouvera une discussion détaillée de cette méthode dans l'article de McCONNELL (*Journ. Chem. Phys.* (1955)).

Une extension intéressante de la méthode des orbitales non localisées se présente avec le cas des métaux où, comme il est bien connu, les électrons de conduction ont des fonctions d'onde qui s'étendent au métal tout entier.

Le calcul a été fait sur un modèle simplifié du métal par RUDERMAN et KITTEL et indépendamment par BLOEMBERGEN et nous allons en esquisser les grandes lignes sur l'exemple d'un métal monovalent.

Cette fois-ci la « molécule » est le métal tout entier. Nous ne considérons que les électrons de conduction en supposant que l'excitation des électrons des couches internes demande trop d'énergie pour apporter une contribution appréciable à (30).

Les orbitales électroniques individuelles sont dans ce modèle fonctions bien connues de Bloch de la forme $\exp[i\mathbf{k} \cdot \mathbf{r}] \cdot u_{\mathbf{k}}(\mathbf{r})$, où les fonctions $u_{\mathbf{k}}(\mathbf{r})$ ont la périodicité du réseau et sont normalisées dans un volume unité. Au voisinage d'un noyau la fonction $u_{\mathbf{k}}(\mathbf{r})$ se comporte comme la fonction Ψ de l'atome libre et l'on a $|u_{\mathbf{k}}|^2 = (\xi/N) |\Psi|^2$, où N est le nombre d'atomes par unité de volume ($2N$ est le nombre des électrons) et $\xi = \xi(\mathbf{k})$ un coefficient de l'ordre de l'unité. La fonction d'onde électronique globale est un déterminant de Slater bâti à partir de fonctions de Bloch dont l'énergie $E_{\mathbf{k}}$ varie depuis zéro jusqu'à une valeur maximum $E_{k_0} = E_F$ dite énergie de Fermi.

Cette représentation de l'état fondamental du métal est valable tant que le gaz électronique auquel on assimile les électrons de conduction peut être considéré comme complètement dégénéré, ce qui est le cas à température ordinaire.

Dans ce modèle nous n'aurons pas recours à l'approximation de clôture

car une représentation simple d'un état excité est fournie par la promotion d'un électron d'un état d'énergie E_k inférieure à E_{k_0} à un état d'énergie $E_k > E_{k_0}$. Nous supposons pour simplifier que E_k s'étend de E_{k_0} à $+\infty$.

On pourrait évidemment considérer la promotion de plus d'un électron mais de tels états ne seraient pas couplés au fondamental par O_1 , S_1 et S_2 qui sont des opérateurs à un électron.

Pour compter nos états et évaluer les énergies d'excitation nous utiliserons l'approximation des électrons libres où l'énergie E_k est indépendante de la direction du vecteur d'onde et donnée par $\hbar^2 k^2 / 2m^*$, où m^* est la masse effective.

Le nombre $Z(\mathbf{k})$ d'états compris dans l'élément de volume d^3k , est, comme il est bien connu, $1/(2\pi)^3$ pour chaque orientation du spin (pour un volume de métal unité).

KITTEL et RUDERMAN se limitent à la considération de l'interaction de contact qui est certainement la plus importante si la fonction d'onde électronique $u_k(r)$ a une proportion importante d'état s au voisinage des noyaux. C'est en particulier le cas des métaux alcalins.

Dans ce cas on montre facilement que l'interaction J est scalaire même à l'état solide.

Compte tenu de l'expression (5') de S_2 , l'interaction entre deux spins I_N et $I_{N'}$ s'écrira:

$$(32) \quad \left(\frac{16\pi\beta\hbar}{3} \right)^2 \gamma_N \gamma_{N'} \sum_{\mathbf{k}, \mathbf{k}'} \frac{(\mathbf{k} | \delta(\mathbf{r}_N)(\mathbf{s} \cdot \mathbf{I}_N) | \mathbf{k}') (\mathbf{k}' | \delta(\mathbf{r}_{N'}) (\mathbf{s} \cdot \mathbf{I}_{N'}) | \mathbf{k})}{E_k - E_{k'}} + \text{c.c.}$$

\mathbf{r}_N est le rayon vecteur joignant le noyau N à l'électron, $|k\rangle$ est la fonction de Bloch $\exp[i\mathbf{k} \cdot \mathbf{r}] u_k(\mathbf{r}) \chi$, où χ est une fonction de spin. Si l'on fait la somme sur les deux orientations possibles du spin dans l'état \mathbf{k} ce qui donne un facteur $+\frac{1}{2}$ l'interaction peut s'écrire

$$(33) \quad J_{NN'} = \frac{1}{2} \left(\frac{16\pi}{3} \beta\hbar \right)^2 \gamma_N \gamma_{N'} \left\{ \sum_{\mathbf{k}, \mathbf{k}'} \frac{(\mathbf{k} | \delta(r_N) | \mathbf{k}') (\mathbf{k} | \delta(r_{N'}) | \mathbf{k})}{E_k - E_{k'}} + \text{c.c.} \right\}$$

Si nous remplaçons la sommation dans (33) par une intégration il vient

$$(34) \quad J_{NN'} = \frac{1}{2} \left(\frac{16\pi}{3} \beta\hbar \right)^2 \frac{1}{(2\pi)^6} \gamma_N \gamma_{N'} \int_0^{k_0} d^3k \int_{k_0}^{\infty} d^3k' \frac{\exp[i(\mathbf{k} - \mathbf{k}') \cdot \mathbf{R}_{NN'}] | (u_k | \delta(\mathbf{r}_N) | u_{k'}) |^2}{(\hbar^2/2m^*)(k^2 - k'^2)} + \text{c.c.}$$

L'intégration sur les angles donne

$$(35) \quad J_{NN'} = \left(\frac{16\pi}{3} \beta \hbar \right)^2 \frac{1}{(2\pi)^4} \frac{2m^*}{\hbar^2} \frac{1}{R_{NN'}^2} \int_{-k_0}^{k_0} k \, dk \left\{ \int_{-\infty}^{k_0} k' \, dk' \frac{\exp[i(k+k')R_{NN'}]}{k^2 - k'^2} \right\} |\Delta_{kk'}|^2,$$

où l'on a posé $|(u_k|\delta(r_N)|u_{k'})|^2 = |\Delta_{kk'}|^2$.

L'intégrale double dans (35) s'évalue facilement par la méthode des résidus si on remarque qu'elle peut se mettre sous la forme

$$(36) \quad \int_{-k_0}^{k_0} dk \left\{ \int_{-\infty}^{-k_0} + \int_{k_0}^{\infty} \right\} f(k, k') \, dk',$$

où $f(k, k')$ est une fonction antisymétrique de k et k' qui présente des pôles pour $k^2 - k'^2 = 0$.

(36) peut se récrire:

$$\int_{-k_0}^{k_0} dk PP \int_{-\infty}^{\infty} f(k, k') \, dk, \quad \text{car} \quad \int_{-k_0}^{k_0} dk \int_{-\infty}^{k_0} dk' f(k, k') = 0.$$

La contribution principale à cette intégrale provenant des valeurs de k et de k' pour lesquelles $k^2 - k'^2$ est petit, on peut remplacer $|\Delta_{kk'}|^2$ qui est une fonction lentement variable de k et de k' par

$$|\Delta_{k_0 k_0}|^2 = \frac{1}{N^2} \xi_0^2 |\Psi(0)|^4.$$

Si l'on pose alors $(16\pi/3)\beta|\Psi(0)|^2\gamma_N\hbar = a_{N'}$, coefficient du couplage de structure hyperfine de l'atome, il vient:

$$(37) \quad J_{NN'} = \frac{a_N a_{N'} \xi_0^2}{N^2} \frac{1}{(2\pi)^4} \frac{2m^*}{\hbar^2} \frac{1}{R_{NN'}^2} \int_{-k_0}^{k_0} k \, dk \cdot PP \int_{-\infty}^{\infty} \frac{k' \, dk' \exp[i(k+k') \cdot R_{NN'}]}{k'^2 - k^2}.$$

L'intégrale double s'évalue aisément et donne:

$$\frac{\pi}{4R_{NN'}^2} [2k_0 R_{NN'} \cos(2k_0 R_{NN'}) \sin(2k_0 R_{NN'})].$$

D'où

$$(38) \quad J_{NN'} = \frac{1}{32\pi^3} \frac{m^*}{\hbar^2} a_N a_{N'} \xi_0^2 \Omega^2 \frac{1}{R_{NN'}^4} [2k_0 R_{NN'} \cos(2k_0 R_{NN'}) - \sin(2k_0 R_{NN'})],$$

où l'on a appelé $\Omega = 1/N$, le volume atomique, ou encore en posant

$$a_N = \frac{2}{2I+1} k \Delta\nu_N,$$

où $\Delta\nu_N$ est l'intervalle de structure hyperfine de l'atome N

$$(39) \quad J_{NN'} = \frac{m^* \Delta\nu_N \Delta\nu_{N'}}{2\pi(2I+1)(2I'+1)} \frac{\xi_0^2 \Omega^2}{R_{NN}^4} [2(k_0 R_{NN}) \cos(2k_0 R_{NN}) - \sin(2k_0 R_{NN})].$$

Pour apprécier l'ordre de grandeur de $J_{NN'}$ donné par (38) ou (39) on peut remarquer pour des noyaux plus proches voisins Ω_0 est de l'ordre de $R_{NN'}^3$ et donc en prenant $\xi_0 = 1$ et posant $E_F = \hbar^2 k_0^2 / 2m^*$

$$(40) \quad J_{NN'} \sim \frac{a_N a_{N'}}{4E_F} \left(\frac{k_0 R_{NN'}}{2\pi} \right)^3;$$

c'est une formule du même type que (38) avec en plus le facteur sans dimension

$$\left(\frac{k_0 R_{NN'}}{2\pi} \right)^3 = \left(\frac{R_{NN'}}{\lambda_0} \right)^3,$$

où λ_0 est la longueur d'onde d'un électron libre ayant l'énergie de Fermi.

Ce facteur est de l'ordre de l'unité dans les métaux usuels, fait qui exprime la possibilité de localiser un paquet d'ondes électroniques au voisinage d'un atome déterminé.

Une autre propriété de l'interaction $J_{NN'}$, apparente sur (38) est son grand rayon d'action et son signe variable. Nous remettons la comparaison des résultats avec l'expérience à un autre paragraphe.

Des résultats expérimentaux obtenus par BLOEMBERGEN, il résulte aussi que l'interaction J n'est pas toujours entièrement scalaire dans les métaux et que la considération du seul couplage électron noyau S_2 est insuffisante. BLOEMBERGEN (*Phys. Rev.* (1955)) a effectué des calculs détaillés et assez pénibles sur la contribution à l'interaction J du terme croisé (S_1, S_2) qui est le plus important après (S_2, S_2) , que nous venons de calculer.

Les conclusions, du reste attendues, auxquelles il arrive sont:

a) L'interaction anisotrope à trace nulle entre deux spins nucléaires \mathbf{I}_N et $\mathbf{I}_{N'}$ qui résulte de la combinaison (S_1, S_2) a la dépendance angulaire d'une interaction dipole-dipole

$$(40') \quad B_{NN'} = B \{ \mathbf{I}_N \cdot \mathbf{I}_{N'} - 3(\mathbf{I}_N \cdot \mathbf{n})(\mathbf{I}_{N'} \cdot \mathbf{n}) \},$$

où \mathbf{n} est le vecteur unité porté par NN' .

La forme de (40) était du reste imposée a priori par des considérations d'invariance par rotation.

b) Le rapport de la constante B à la constante J de l'interaction scalaire est de l'ordre de $\alpha_p a_p / \alpha_s a_s$, où α_p et α_s sont les poids d'état p et d'état s dans la fonction $u_k(r)$ au voisinage de la surface de Fermi et a_p et a_s sont les largeurs des structures hyperfines correspondant respectivement aux états p et s .

c) Comme l'interaction scalaire, l'interaction B ou interaction pseudo-dipolaire, est à longue portée.

Pour terminer l'étude atomistique des interactions indirectes nous résumons le calcul par Bloembergen de ces interactions dans un isolant.

Le modèle choisi pour l'isolant (Fig. 2) est très analogue à celui pris pour le métal, avec la seule différence que dans l'isolant la bande de valence est pleine et la bande de conduction qui en est séparée par une énergie $\hbar^2 k^2 / 2m^*$ est vide.

Pour l'interaction scalaire le calcul est très analogue à celui fait pour le métal avec la différence qu'en prenant l'origine des énergies au sommet de la bande de valence, l'intégration sur k se fait toujours de 0 à k_0 , mais celle sur k' de K à $+\infty$ et que le dénominateur $(k^2 - k'^2)$ est remplacé par $(k'^2 + K^2)$ (on néglige pour simplifier, la largeur de la bande de valence par rapport à sa distance à la bande de conduction).

Un calcul de résidus identique au précédent montre que la formule (38) du métal doit être remplacée par:

$$(41) \quad J_{NN'} = \frac{1}{4\pi^3} \frac{m^*}{\hbar^2} a_N a_{N'} \xi^2 \Omega^2 \frac{1}{R_{NN'}^4} \{ (k_0 R_{NN'}) \cos(k_0 R_{NN'}) - \sin(k_0 R_{NN'}) \} \exp[-K R_{NN'}].$$

Ce qui différencie surtout (41) de (38) est son court rayon d'action conditionné par le facteur exponentiel $\exp[-KR]$. C'est là un résultat physiquement raisonnable puisque dans un isolant les électrons peuvent être considérés comme pratiquement localisés sur un atome déterminé et n'on donc qu'une probabilité très faible de coupler entre eux les spins nucléaires de deux atomes éloignés.

Par contre ce modèle est probablement beaucoup trop grossier pour que les conclusions qu'on peut tirer de (41) quant au signe de $J_{NN'}$ et à la possibilité d'un ferromagnétisme ou antiferromagnétisme nucléaire aux très basses températures ne soient pas illusoirs.

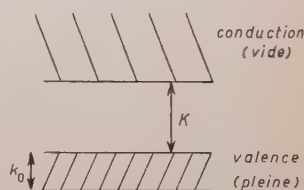


Fig. 2.

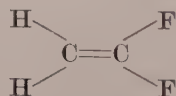
L'interaction pseudo-dipolaire se calcule comme dans le cas du métal et sa relation à l'interaction scalaire a le même caractère que dans le métal.

3'2. Structures en multiplets des raies de résonance dans les liquides. — Nous avons vu dans 3'1. qu'il doit exister entre les spin nucléaires des interactions bilinéaires qui dans les liquides ont la forme d'un produit scalaire $\hbar J \mathbf{I}_1 \cdot \mathbf{I}_2$ (nous écrirons désormais $\hbar J$ au lieu de J , pour que J ait les dimensions d'une fréquence). Nous nous proposons d'expliquer à l'aide de ces interactions les structures des multiplets observés dans certaines raies de résonance nucléaire. Bien que la découverte de ces structures ne remonte qu'à 1951, la quantité d'informations expérimentales accumulées est immense. Nous nous contenterons d'analyser un certain nombre de situations typiques que nous examinerons par ordre de complexité théorique croissante.

Introduisons d'abord quelques définitions. Considérons, dans une molécule, des spins nucléaires qui ont la même fréquence de Larmor dans un champ H_0 donné, ce qui exige non seulement qu'ils appartiennent au même isotope mais encore qu'ils aient le même déplacement chimique. Ce sera le cas s'ils occupent dans la molécule des positions qui peuvent être amenées en coïncidence par une opération du groupe de symétrie de la molécule. Nous dirons que de tels spins sont semblables.

Soit un groupe G de spins semblables entre eux. Nous dirons que les spins de ce groupe sont équivalents si tout spin n'appartenant pas à G a même couplage avec tous les spins de G .

Par exemple, les deux protons sont équivalents dans le difluoro-méthane CH_2F_2 mais non dans le difluoroéthylène



où chaque fluor a des couplages différents avec les deux protons.

On remarquera que cette définition n'implique nullement l'égalité des couplages qui peuvent exister entre les différents spins équivalents. Ainsi dans BrF_5 , qui a la forme d'une pyramide de base carrée, avec un fluor au sommet de la pyramide et les 4 autres aux 4 sommets du carré, les fluors de base qui sont évidemment semblables, sont équivalents avec notre définition bien que les couplages entre 2 fluors adjacents ne soient pas les mêmes qu'entre 2 fluor apposés.

L'intérêt de cette définition réside dans le théorème suivant: les interactions scalaires entre des spins équivalents sont inobservables dans une expérience de résonance nucléaire.

Soient I_1, I_2, \dots, I_p , un groupe de spins équivalents et I'_1, \dots, I'_p , tous les

autres spins de la molécule. En présence d'un champ magnétique constant H_0 dirigé suivant Oz et d'un champ magnétique $H_1 \cos \omega t$ dirigé suivant Ox , l'Hamiltonien du système peut, avec les hypothèses faites, s'écrire:

$$(42) \quad -\gamma \hbar H_0 I_z - \gamma \hbar H_1 \cos \omega t \cdot I_x + \frac{\hbar}{2} \sum_{p,q} J_{pq} \mathbf{I}_p \cdot \mathbf{I}_q + \mathbf{I} \cdot \sum_{p'} h J_p \mathbf{I}_{p'} + \mathcal{H}(\mathbf{I}),$$

où $\mathbf{I} = \mathbf{I}_1 + \dots + \mathbf{I}_p$ et $\mathcal{H}_1(\mathbf{I})$ est la partie de l'Hamiltonien qui ne dépend pas des spins \mathbf{I}_p . On a tenu compte dans (42) de l'hypothèse que les spins \mathbf{I}_p sont équivalents en prenant le même coefficient J'_p pour l'interaction d'un spin $\mathbf{I}_{p'}$, avec tous les spins \mathbf{I}_p .

On remarquera que l'opérateur $\mathcal{H}_a = \frac{1}{2} \sum_{p,q} \hbar J_{pq} \mathbf{I}_p \cdot \mathbf{I}_q$ commute avec tous les autres termes de l'Hamiltonien. Posons $\mathcal{H} = \mathcal{H}_a + \mathcal{H}_b$. L'équations de Schrödinger du système peut s'écrire:

$$i\hbar \frac{\delta \Psi}{\delta t} = \mathcal{H} \Psi = (\mathcal{H}_a + \mathcal{H}_b) \Psi,$$

ou encore en posant

$$(43) \quad \Psi = \exp \left[-\frac{i}{\hbar} \mathcal{H}_a t \Phi \right],$$

$$i\hbar \frac{\delta \Phi}{\delta t} = \mathcal{H}_b \Phi.$$

Pour obtenir (43) on a tenu compte de $[\mathcal{H}_a, \mathcal{H}_b] = 0$.

Le signal observé dans un dispositif de résonance nucléaire est proportionnel à

$$S = \frac{d}{dt} (\Psi(t) | M_x | \Psi(t)),$$

ou encore à

$$S = \frac{d}{dt} \left(\Phi(t) \left| \exp \left[\frac{i}{\hbar} \mathcal{H}_a t \right] M_x \exp \left[-\frac{i}{\hbar} \mathcal{H}_a t \right] \right| \Phi(t) \right),$$

où M_x est la composante suivant l'axe des x du moment magnétique total du système. Comme M_x commute lui aussi avec \mathcal{H}_a on a:

$$(44) \quad S = \frac{d}{dt} (\Phi(t) | M_x | \Phi(t)).$$

Nous voyons sur (44) que le signal observé est entièrement déterminé par la connaissance de $\Phi(t)$. Or d'après (43) \mathcal{H}_a n'intervient pas dans la détermination de $\Phi(t)$.

Le signal est indépendant de \mathcal{H}_a qui est donc inobservable.

La démonstration ci-dessus, due à GUTOWSKY, McNEILL et SLICHTER a l'avantage d'être très générale et de s'appliquer en particulier lorsque le signal a un caractère transitoire comme dans la méthode des échos de spin lorsque les considérations d'états stationnaires sont insuffisantes. Nous allons à présent considérer quelques exemples en supposant d'abord que tous les spins semblables sont équivalents.

A) *Cas de deux groupes G et G' de spins équivalents I_k et I'_k dont le couplage mutuel J/\hbar est très petit par rapport à la différence δ de leurs fréquences de Larmor.*

Cette condition est toujours réalisée lorsque les deux groupes correspondent à des espèces nucléaires différentes.

L'Hamiltonien, simplifié, en vertu du théorème précédent, par l'omission des interactions entre noyaux équivalents, peut s'écrire:

$$(45) \quad \mathcal{H} = -(\gamma\hbar I_z + \gamma'\hbar I'_z)H_0 + \hbar J \mathbf{I} \cdot \mathbf{I}',$$

où

$$\mathbf{I} = \sum \mathbf{I}_k, \quad \mathbf{I}' = \sum \mathbf{I}'_k.$$

Dans la définition de γ et de γ' , l'on a fait entrer les constantes σ des déplacements chimiques.

Notre hypothèse sur la petitesse de J peut se formuler:

$$|H_0(\gamma - \gamma')| \gg J.$$

On peut dans ce cas utiliser une méthode de perturbation et remplacer $J \mathbf{I} \cdot \mathbf{I}'$ par sa partie diagonale $J I_z \cdot I'_z$. Les niveaux d'énergie du système sont alors donnés par:

$$(46) \quad E = -(\gamma\hbar H_0 M + \gamma'\hbar H_0 M') + \hbar J M M',$$

où M et M' sont les valeurs propres de I_z et I'_z . Les raies de résonance des spins I_k et I'_k ont des fréquences données par

$$(47) \quad \begin{cases} \omega = -\gamma H_0 + J M', \\ \omega' = -\gamma' H_0 + J M. \end{cases}$$

On voit que ces raies forment des multiplets, ayant respectivement $2I'_M + 1$ composantes équidistantes pour la résonance des I_k et $2I_M + 1$ composantes pour la résonance de I'_k .

Les nombres I_M et I'_M , valeurs maxima de I_z et I'_z , sont données respectivement par pi et $p'i'$, où i est le spin de chacun des spins équivalents I_k et p leur nombre, et de même pour i' et p' . L'intensité d'une raie des spins I_k correspondant à une valeur M' de I'_z , est proportionnelle au nombre de façons dont on peut former l'état $I'_z = M'$ avec les p' spins, I'_k . C'est le coefficient de $x^{M'}$ dans le développement de

$$(48) \quad p(x) = (x^{i'} + x^{i'-1} + \dots + x^{-i'})^{p'}.$$

On remarquera que si l'on opère à fréquence constante en balayant le champ H_0 , en vertu de (47), les écarts ΔH et $\Delta H'$ entre deux composantes contigües des multiplets I et I' , seront dans le rapport γ'/γ .

Remarquons enfin que l'écart entre les raies d'un même multiplet est en vertu de (47) indépendant du champ appliqué H_0 . Les confirmations expérimentales des résultats précédents sont extrêmement nombreuses.

Considérons à titre d'exemple le cas de BrF_5 où (GUTOWSKY, MCCALL et SLICHTER: *Journ. Chem. Phys.*, **21**, 279 (1953)) les deux groupes G et G' se composent respectivement d'un fluor F au sommet d'une pyramide à base carrée et des quatre fluors F à la base. La structure observée se compose de deux multiplets, un quintuplet et un doublet séparés par 0.876 gauss dans un champ H_0 de 6365 gauss, l'écartement entre les composantes d'un même multiplet étant de 0.019 gauss. L'expérience montre également que l'écart entre les multiplets est proportionnel au champ appliqué alors que l'écart entre deux raies d'un même multiplet en est indépendant.

Nous interprétons le quintuplet comme correspondant à la résonance du fluor F et le doublet à la résonance des fluors F' . L'écart entre les fréquences des multiplets étant beaucoup plus grand que leur largeur, la méthode des perturbations est applicable. La raie de résonance de F doit avoir $2I'_M + 1 = 2p'i' + 1 = (2 \cdot 4 \cdot \frac{1}{2}) + 1 = 5$ composantes, et celle de F' $(2 \cdot 1 \cdot \frac{1}{2}) + 1 = 2$ composantes, d'accord avec l'expérience.

D'après (48), les intensités des composantes du quintuplet doivent être proportionnelles aux nombres 1, 4, 6, 4, 1, celles du doublet doivent être égales entre elles. De plus l'intensité totale du doublet qui correspond à la résonance des quatre fluors F' doit être quatre fois celle du quintuplet, ce qui conduit à attribuer à chacune des composantes du doublet le coefficient 32. Tout ceci est confirmé par l'expérience.

Comme autre exemple nous citerons la structure de la résonance de H et de D dans la molécule HD, observée dans le gaz HD comprimé, par WIMETT à M.I.T. (Fig. 3).

Le triplet correspond à la résonance du proton (spin du deuton égal à 1) et le doublet au deuton (spin du proton $\frac{1}{2}$).

Les deux résonances sont observées dans le même champ H_0 , en utilisant

deux champs de radiofréquence, de fréquence respectives

$$\omega_H = \gamma_H H_0 \quad \text{et} \quad \omega_D = \gamma_D H_0.$$

Le théorème démontré au début du paragraphe indique que l'interaction indirecte est inobservable dans la molécule H_2 .

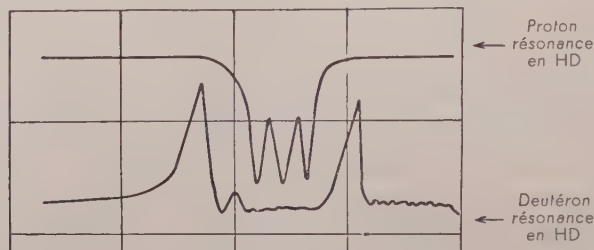


Fig. 3. — Résonance du proton et du deuteron en HD.

Les cas où il y a plus de deux groupes de spin équivalents se traite de la même façon mais les structures se compliquent.

B) *Cas de deux spins $\frac{1}{2}$.* L'Hamiltonien de ce système peut s'écrire:

$$(49) \quad \frac{\mathcal{H}}{\hbar} = \omega_0(s_z + s'_z) + \delta(s_z - s'_z) + J\mathbf{s}_1 \cdot \mathbf{s}_2,$$

où l'on a posé

$$\omega_0 = -\frac{\gamma + \gamma'}{2} H_0, \quad \delta = -(\gamma - \gamma') H_0.$$

On peut toujours supposer $\delta > 0$.

Les états propres et les valeurs de \mathcal{H} s'obtiennent facilement par résolution d'une équation du second degré.

Ce sont

$$\begin{aligned} |a\rangle &= |+, +\rangle \\ |b\rangle &= p|+, -\rangle + q|-, +\rangle \\ |c\rangle &= q|+, -\rangle - p|-, +\rangle \\ |d\rangle &= |--, -\rangle, \end{aligned}$$

où p et q sont donnés par:

$$(49) \quad p^2 = 1 - q^2 = \frac{1}{2} \left\{ 1 + \frac{\delta}{\sqrt{J^2 + \delta^2}} \right\}.$$

On peut sans restreindre la généralité prendre dans (49) $p > 0$. Le signe de q est alors déterminé par:

$$(50) \quad q = p \frac{\sqrt{\delta^2 + J^2} - \delta}{J}.$$

Les niveaux d'énergie sont

$$(51) \quad \left\{ \begin{array}{l} E_a/\hbar = \omega_0 + \frac{J}{4}, \\ E/\hbar = -\frac{J}{4} + \frac{1}{2}\sqrt{J^2 + \delta^2}, \\ E_c/\hbar = -\frac{J}{4} - \frac{1}{2}\sqrt{J^2 + \delta^2}, \\ E_d/\hbar = -\omega_0 + \frac{J}{4}. \end{array} \right.$$

Les fréquences correspondantes sont:

$$(52) \quad \left\{ \begin{array}{l} \omega_{ab} = \omega_0 + \frac{J}{2} - \frac{1}{2}\sqrt{J^2 + \delta^2}, \\ \omega_{ac} = \omega_0 + \frac{J}{2} + \frac{1}{2}\sqrt{J^2 + \delta^2}, \\ \omega_{bd} = \omega_0 - \frac{J}{2} + \frac{1}{2}\sqrt{J^2 + \delta^2}, \\ \omega_{cd} = \omega_0 - \frac{J}{2} - \frac{1}{2}\sqrt{J^2 + \delta^2}. \end{array} \right.$$

On a posé $\omega_0 = -\gamma_0 H_0$.

Enfin leurs intensités relatives sont respectivement:

$$(53) \quad \left\{ \begin{array}{l} P_{ab} \simeq |(a|s_x + s'_x|b)|^2 \simeq (p+q)^2 = 1 + \frac{J}{\sqrt{\delta^2 + J^2}}, \\ P_{ac} \simeq (p-q)^2 = 1 - \frac{J}{\sqrt{\delta^2 + J^2}}, \\ P_{bd} = P_{ab}, \\ P_{cd} = P_{ac}. \end{array} \right.$$

Il est facile de voir que les transitions $a \rightarrow d$ et $b \rightarrow c$ sont interdites.

Les formules (49) à (53) sont des formules exactes qui donnent la forme du spectre quelles que soient les valeurs relatives de J et δ . Il est intéressant de voir quelle est l'allure du spectre dans les deux cas extrêmes $J/\delta \ll 1$ et $J/\delta \gg 1$ (Fig. 4 et 5).

a) $\frac{J}{\delta} \ll 1 \cdot p \rightarrow 1, q \rightarrow 0.$

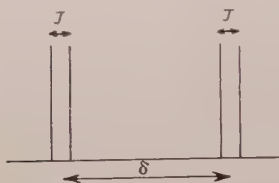


Fig. 4.

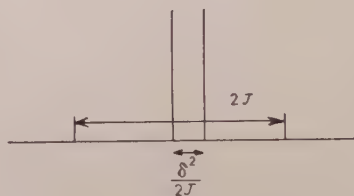


Fig. 5.

$P_{ab}, P_{ac}, P_{bd}, P_{cd} \rightarrow 1$, les intensités des quatre raies deviennent égales. D'autre part

$$\omega_a \rightarrow -\frac{\delta}{2} + \frac{J}{2} + \omega_0,$$

$$\omega_{cd} \rightarrow -\frac{\delta}{2} - \frac{J}{2} + \omega_0,$$

$$\omega_{ac} \rightarrow +\frac{\delta}{2} + \frac{J}{2} + \omega_0,$$

$$\omega_{bd} \rightarrow +\frac{\delta}{2} - \frac{J}{2} + \omega_0.$$

On a, d'accord avec la théorie simplifiée du paragraphe précédent, deux doublets dont les centres sont distants de δ , l'écartement de chacun des doublets devenant égal à J et donc indépendant du champ appliqué H_0 dès que $J \ll \delta$.

(b) $J/\delta \gg 1.$

On a alors:

$$P_{ab} = P_{cd} \rightarrow 2$$

$$P_{ac} = P_{bd} \rightarrow \frac{\delta^2}{2J^2},$$

$$\omega_{ab} \rightarrow \omega_0 - \frac{\delta^2}{4J},$$

$$\omega_{bd} \rightarrow \omega_0 + \frac{\delta^2}{4J},$$

$$\omega_{ac} \rightarrow \omega_0 + J$$

$$\omega_{cd} \rightarrow \omega_0 - J.$$

On voit qu'à la limite quand $\delta \rightarrow 0$, les deux spins devenant équivalents, les deux raies centrales viennent se confondre, et les deux raies latérales disparaissent, l'interaction J pour deux noyaux équivalents devenant ainsi inobservable, en accord avec le théorème général.

A titre d'exemple on peut considérer la résonance des protons dans la dichloroacétaldéhyde (Fig. 6).

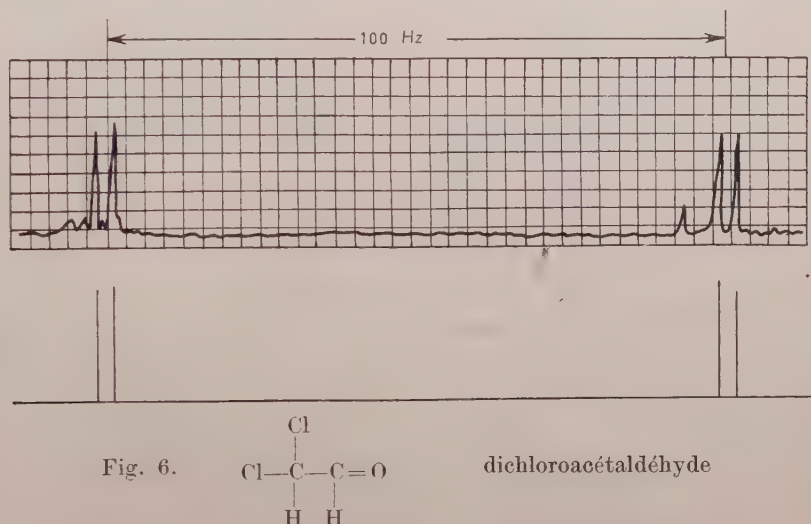
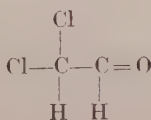


Fig. 6.



dichloroacétaldéhyde

(Le petit pic à gauche du doublet de droite est dû à une impureté).

On voit que l'on est dans le cas où $J/\delta \ll 1$. L'expérience qui a été faite par ANDERSON à 30.5 MHz donne en effet:

$$\frac{\delta}{2\pi} = (990 \pm 5) \text{ Hz},$$

$$\frac{J}{2\pi} = (2.7 \pm 0.2) \text{ Hz}.$$

Comme autre exemple, où J et δ sont cette fois comparables, on peut prendre le cas des protons du 2-bromo-5-chlorothiophène (Fig. 7), où ANDERSON trouve:

$$\frac{\delta}{2\pi} = 4.7 \text{ cps}, \quad \frac{J}{2\pi} = 3.9 \text{ cps}.$$

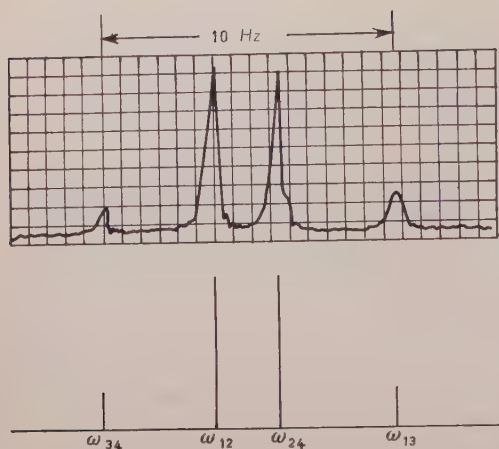
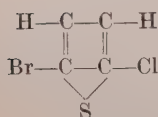


Fig. 7.



2-bromo-5-chlorothiophène

$$F'_z = I_z + I'_z,$$

$$|I|^2 = I_x^2 + I_y^2 + I_z^2 = I(I+1)$$

et

$$|I'|^2 = I_x'^2 + I_y'^2 + I_z'^2 = I'(I'+1).$$

Nous chercherons les états propres $|\zeta\rangle$ de (45) sous la forme:

$$(54) \quad |\zeta\rangle = \sum_M C_M |F_z, I, I', M\rangle,$$

où $M = I_z$ n'est pas un bon nombre quantique pour l'Hamiltonien (45) (on pourrait aussi bien utiliser $M' = I'_z$).

Le problème se résout alors comme suit.

Les groupes G et G' contenant respectivement p spins i et p' spins i' , on commence par classer les états du système suivant les valeurs de F_z , I et I' .

A toute combinaison F_z , I , I' permise par les règles habituelles de couplage des moments angulaires correspondra une équation séculaire séparée dont l'ordre, en vertu de (54), sera, au plus, le plus petit des deux nombres $(2I+1)$, $(2I'+1)$. C'est ainsi que si l'un des spins I est $\frac{1}{2}$ toutes les équations séculaires sont du second degré au plus.

On trouvera dans l'article de BANERJEE, DAS et SAHA (*Proc. Roy. Soc.*, A 226, 490 (1954)) les cas $I = \frac{1}{2}$; $I' = \frac{1}{2}$, 1, $\frac{3}{2}$, 2 traités en détail (avec un déploiement de moyens mathématiques impressionnant mais peut être superflu, le problème étant au fond très simple). On peut ensuite calculer les proba-

C) Cas de deux groupes de spins équivalents, J et δ étant du même ordre de grandeur.

Le problème est de diagonaliser l'Hamiltonien (45) où l'on n'a plus le droit comme dans A) de remplacer $JI \cdot I'$ par sa partie diagonale $JI_z I'_z$. Il a été résolu dans B) pour le cas où chacun des groupes se compose d'un seul spin $\frac{1}{2}$, l'équation séculaire étant alors du second degré.

Ce problème se simplifie considérablement si l'on remarque que l'Hamiltonien (45) admet comme bons nombres quantiques

bilités de transition entre deux états $|\zeta\rangle$ et $|\zeta'\rangle$ par la formule:

$$(55) \quad P_{\zeta\zeta'} \simeq |\langle \zeta | I_x + I'_x | \zeta' \rangle|^2.$$

On a négligé dans (55) la petite différence entre γ et γ' . $I_x + I'_x$ commutant avec I et I' , seules les transitions $\Delta I = 0$, $\Delta I' = 0$, $\Delta F_z = \pm 1$ sont permises.

Nous avons raisonné jusqu'ici comme si la donnée de I , I' , F_z , I_z déterminait entièrement un état du système. En fait il peut exister plusieurs façons de former un état $|I, I', F_z, I_z\rangle$. Par exemple si le groupe G se compose de trois spins $i = \frac{1}{2}$ on peut avec ces spins former deux états $I = \frac{1}{2}$ orthogonaux. Nous pouvons introduire un nombre quantique supplémentaire λ pour tenir compte de cette circonstance et écrire nos états $|I, I', F_z, I_z, \lambda\rangle$.

Les états correspondant à des valeurs différentes de λ présentent des caractères de symétrie différents par rapport à une permutation des spins i entre eux, ou des spins i' entre eux.

L'Hamiltonien (45) étant une fonction symétrique de spins i comme de spins i' , ses éléments de matrice non diagonaux en λ , $\langle \lambda | \mathcal{H} | \lambda' \rangle$ sont nuls et ses éléments diagonaux $\langle \lambda | \mathcal{H} | \lambda \rangle$ ne dépendent pas de λ . Il en résulte que ses niveaux d'énergie $E(I, I', \dots)$ présenteront une dégénérescence essentielle d'ordre \mathcal{N} , où \mathcal{N} est le nombre de façons dont la combinaison (I, I') peut être réalisée.

Comme l'opérateur $I_x + I'_x$ dont dépendent les transitions est lui aussi indépendant de λ , on peut faire le calcul des fréquences et des probabilités de transition en ignorant complètement la dégénérescence λ à condition d'affecter ensuite chaque transition $\zeta(F_z, I, I', \dots) \rightarrow \zeta(F_z \pm 1, I, I', \dots)$ d'un poids égal à l'ordre \mathcal{N} de cette dégénérescence.

Toutes les considérations précédentes se généralisent immédiatement au cas où il y a plus de deux groupes de spins équivalents.

A titre d'exemple considérons, le cas où chacun des deux groupes G et G' contient deux spins $\frac{1}{2}$ et demandons-nous quel est le nombre maximum de raies que l'on puisse observer.

Les niveaux et les transitions se classent en trois groupes indépendants:

$$I = 0, I' = 1; \quad I = 1, I' = 0; \quad I = 1, I' = 1.$$

Le 1^{er} et le 2^{ème} groupe donnent évidemment chacun une raie. Pour évaluer la contribution du 3^{ème} groupe il suffit de voir quel est le nombre d'états propres pour une valeur donnée de F_z . Il y a un état $F_z = 2$, deux états $F_z = 1$, trois états $F_z = 0$.

D'où 2 transitions	$F_z = 2 \rightarrow F_z = 1$
6 »	$F_z = 1 \rightarrow F_z = 0$
6 »	$F_z = 0 \rightarrow F_z = -1$
2 »	$F_z = 1 \rightarrow F_z = -2$

D'où 16 transitions pour le 3^{ème} groupe.

18 est le nombre total de raies que l'on devrait pouvoir observer pour $J \sim \delta$.

Avant de comparer ce résultat avec l'expérience nous étudierons dans le paragraphe suivant une méthode de perturbation.

D) Méthode de perturbation. — Lors J/δ sans être très petit, est nettement inférieur à 1, on a intérêt à pousser jusqu'au second ordre la méthode de perturbation que l'on avait limitée au premier ordre dans *B*). C'est ce qu'a fait W. ANDERSON dont nous allons exposer la méthode.

Supposons que la molécule contienne R groupes G_1, G_2, \dots, G_R de spins équivalents.

Comme on l'a vu dans *C*), nous pouvons nous limiter à la considération des états du système où le spin total des différents groupes $G_A \dots G_R$ a des valeurs déterminées $I_A \dots I_R$.

Les contributions de différentes combinaisons au spectre observé sont en effet additives et peuvent être calculées séparément.

L'Hamiltonien du système peut s'écrire: $\mathcal{H} = \mathcal{H}^{(0)} + \mathcal{H}^{(1)}$ avec: $\mathcal{H}^{(0)} = - \sum_R \omega_R I_z^R$

$$(56) \quad \mathcal{H}^{(1)} = - \frac{1}{2} \sum_{R \neq S} \sum J_{RS} (I_z^R I_z^S + I_+^R I_-^S).$$

$\mathcal{H}^{(1)}$ est traité comme une perturbation de $\mathcal{H}^{(0)}$.

A l'ordre zéro les fonctions d'onde du système sont: $\Psi_i^{(0)} = |m_A, \dots, m_R\rangle$, où m_R est la valeur de I_z^R et les valeurs propres de l'énergie sont

$$(57) \quad E_i^{(0)} = - \sum_R \omega_R m_R.$$

Les corrections du premier ordre aux états d'énergie sont:

$$E_i^{(1)} = \langle \Psi_i^0 | \mathcal{H}^{(1)} | \Psi_i^0 \rangle = - \frac{1}{2} \sum_{R \neq S} J_{RS} m_R m_S.$$

Ce sont les seules considérées en *A*).

Les corrections du second ordre $E_i^{(2)}$ seront:

$$(58) \quad E_i^{(2)} = \sum_{y \neq i} \frac{(\Psi_i^0 | \mathcal{H}^{(1)} | \Psi_y^0)(\Psi_y^0 | \mathcal{H}^{(1)} | \Psi_i^0)}{E_i^{(0)} - E_y^{(0)}} = \\ = \frac{1}{4} \sum_{R \neq S} \frac{J_{RS}^2}{\omega_R - \omega_S} \{ m_R (I_S^2 + I_S - m_S^2) - m_S (I_R^2 + I_R - m_R^2) \}.$$

(58) est une conséquence immédiate des formules qui donnent les éléments de matrice I_{\pm}^R .

Les fréquences de transition entre un niveau $E(m_A, m_B, \dots, m_R)$ et un autre d'énergie $E(m_A - 1, m_B, \dots, m_R)$ sont, compte tenu des corrections $E^{(1)}$ et $E^{(2)}$, données par

$$(59) \quad \omega = \omega_A + \sum_{R \neq A} J_{AR} m_R + \frac{1}{2} \sum_{R \neq A} \frac{J_{AR}^2}{(\omega_A - \omega_R)} \{I_R(I_R + 1) - m_R(m_R + 1) + 2m_A m_R\}.$$

Le nombre de lignes que l'on obtient ainsi est beaucoup plus grand que dans le cas de l'approximation A). On voit en particulier que la fréquence d'une transition $m_A \rightarrow m_A - 1$ dépend non seulement des valeurs m_R des autres groupes comme dans le cas B) mais aussi de leur spin total I_R et de la valeur m_A elle-même.

La correction (58) des niveaux d'énergie s'accompagne d'une correction analogue pour les fonctions d'onde $\Psi_i^{(0)}$ et donc pour les probabilités de transition (59) est donné par:

$$(60) \quad P = (I_A - m_A + 1)(I_A + m_A) \left\{ 1 - \sum_{R \neq A} \frac{2J_{AR} m_R}{\omega_A - \omega_R} \right\}.$$

La démonstration de cette formule qui se fait d'une façon très analogue à celle de (58) se trouve dans l'article d'ANDERSON (*Phys. Rev.* (1956) à paraître) où l'on trouve également le calcul de la correction du 3^{ème} ordre $E^{(3)}$ de l'énergie.

Si nous reprenons l'exemple de deux groupes G_A et G_B contenant chacun deux spins $\frac{1}{2}$ la théorie des perturbations prévoit 14 raies au total.

Les combinaisons $I_A = 1, I_B = 0$ et $I_A = 0, I_B = 1$ donnent chacun une raie.

La combinaison $I_A = 1, I_B = 1$ donne 12 raies.

Il y a en effet 6 transitions $m_A \rightarrow m_A - 1$ qui sont $m_A = 1; m_B = 0, \pm 1$ et $m_A = 0; m_B = 0, \pm 1$ et de même 6 transitions $m_B \rightarrow m_B - 1$ (si l'on se limite à la formule du 2^{ème} ordre (59) les transitions $m_B = 0, I_A = I_B = 1, m_A = 1 \rightarrow m_A = 0$ et $m_A = 0 \rightarrow m_A = -1$ sont confondues mais se séparent si l'on pousse le calcul au 3^{ème} ordre). On remarquera qu'en C) nous avions prévu 18 raies pour le même problème.

L'explication de ce désaccord est la suivante.

Dans la méthode de perturbation on considère les m_R comme approximativement bons nombres quantiques. Il en résulte que les deux états propres $F_z = 1$ seront approximativement $(1, 0)$ et $(0, 1)$ et les trois états propres $F_z = 0$ seront approximativement $(1, -1), (0, 0), (-1, 1)$. Dans C) nous avions admis qu'entre $F_z = 1$ et $F_z = 0$ il y avait $2 \cdot 3 = 6$ transitions possibles.

Mais les transitions $|1, 0\rangle \rightarrow |-1, 1\rangle$ et $|0, 1\rangle \rightarrow |1, -1\rangle$ qui seraient rigoureusement interdites si les m_R étaient de bons nombres quantiques, les sont

encore approximativement si les m_R sont approximativement de bons nombres quantiques, c'est-à-dire si J/δ est petit. Les deux raies correspondantes ainsi que deux raies analogues de la transition $F_z = 0 \rightarrow F_z = -1$ que la théorie des perturbations ne prévoit pas, seront faibles tant que J/δ est petit, c'est-à-dire en fait tant que la théorie des perturbations est valable. La Fig. 8

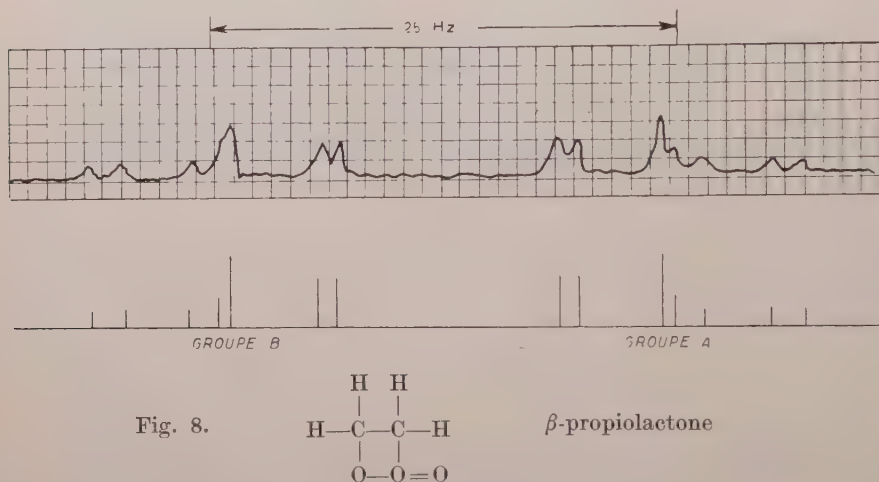


Fig. 8.

représente le spectre expérimental du propiolactone, dont la molécule contient deux groupes de deux protons équivalents, observé par ANDERSON, avec au-dessous le spectre théorique calculé par lui. L'accord avec l'expérience est remarquable. La valeur trouvée $J/\delta = 0.265$ est suffisamment petite pour que les quatre raies supplémentaires prévues par la théorie exacte, échappent à l'observation.

E) Cas général. — Un cas plus compliqué que tous ceux examinés jusqu'ici est celui où la molécule possède des noyaux semblables mais non équivalents.

Il est facile de voir que dans ce cas le spin total I_A d'un groupe G_A de spins semblables n'est plus un bon nombre quantique ce qui complique considérablement la solution du problème. On trouvera dans l'article de McCONNEL, McLEAN et REILLY (*Journ. Chem. Phys.*, **23**, 1156 (1955)) des indications sur la façon dont la théorie des groupes permet, en utilisant les propriétés de symétrie de la molécule, de choisir convenablement les fonctions d'onde de départ de manière à simplifier les calculs au maximum.

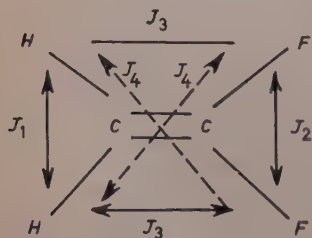


Fig. 9.

Nous nous contenterons ici d'étudier un exemple

particulier, le difluoroéthylène déjà mentionné dont la structure (Fig. 9) est suffisamment simple pour que les simplifications résultant de la symétrie de la molécule puissent être obtenues sans faire appel à l'appareil général, assez peu maniable de la théorie des groupes.

Appelons s et s' les spin de deux protons, i et i' ceux des deux fluors.

L'Hamiltonien du système peut s'écrire:

$$(61) \quad \frac{\mathcal{H}}{\hbar} = +\omega_H(s_z + s'_z) + \omega_F(i_z + i'_z) + \\ + J_1 \mathbf{s} \cdot \mathbf{s}' + J_2 \mathbf{i} \cdot \mathbf{i}' + J_3 (\mathbf{i} \cdot \mathbf{s} + \mathbf{i}' \cdot \mathbf{s}') + J_4 (\mathbf{i} \cdot \mathbf{s}' + \mathbf{i}' \cdot \mathbf{s}).$$

Il est facile de voir sur (61) que le spin total S des protons et le spin total I des fluors ne sont plus de bons nombres quantiques. Par contre une simplification importante résulte du fait que la différence $\omega_H - \omega_F$ est beaucoup plus grande que tous les coefficients J et que les termes en J peuvent être traités comme une perturbation des deux premiers termes de (61). Il est toutefois instructif, en vue d'une comparaison avec le cas traité en C) et D), de ne pas introduire cette simplification dès le début permettant ainsi d'étendre nos considérations au cas d'une molécule contenant deux groupes de deux protons, les proton d'un même groupe étant semblables mais non équivalents.

Il existe toujours un bon nombre quantique pour (61).

$$F_z = s_z + s'_z + i_z + i'_z.$$

La symétrie de la molécule et donc de l'Hamiltonien (61) par rapport à un plan passant par l'axe CC et normal au plan de la molécule permet d'en introduire un second, qui est la parité par rapport à cette transformation. Nous pouvons classer les états du système en états pairs que cette symétrie laisse inchangés et en états impairs qu'elle multiplie par -1 . Si nous nous rappelons qu'une fonction d'onde triplet de deux spins $\frac{1}{2}$ est paire par rapport aux deux spins composants alors qu'une fonction singulet est impaire nous pouvons facilement dresser un tableau des différents états du système. Nous utiliserons une notation telle que $^3S \pm 1$, ou 3S_0 pour indiquer un état triplet des spins s et s' où S_z est ± 1 ou 0 . De même 1S_0 représentera l'état singulet. Le tableau des états du système prend alors la forme suivante:

$$\begin{array}{ll} \frac{F_z}{2+} \left\{ \begin{array}{ll} ^3S_1 & ^3I_1 \\ ^3S_1 & ^3I_0 \end{array} \right. & \begin{array}{l} A_1 \\ B_1 \end{array} \\ 1+ \left\{ \begin{array}{ll} ^3S_0 & ^3I_1 \\ ^3S_1 & ^3I_0 \end{array} \right. & B_1 \\ 1- \left\{ \begin{array}{ll} ^1S_0 & ^3I_1 \\ ^3S_1 & ^1I_0 \end{array} \right. & \begin{array}{l} C_1 \\ C_2 \end{array} \end{array} \quad \begin{array}{l} F_z \left\{ \begin{array}{ll} ^3S_{-1} & ^3I_1 \\ ^3S_1 & ^3I_{-1} \\ ^3S_0 & ^3I_0 \end{array} \right. \begin{array}{l} D_1 \\ D_2 \\ D_3 \end{array} \\ 0+ \left\{ \begin{array}{ll} ^1S_0 & ^1I_0 \end{array} \right. & D_4 \\ 0- \left\{ \begin{array}{ll} ^1S_0 & ^3I_0 \\ ^3S_0 & ^1I_0 \end{array} \right. & \begin{array}{l} E_1 \\ E_2 \end{array} \end{array}$$

L'indice \pm , indique les états pairs. On n'a pas écrit les états qui correspondent à des valeurs négatives de F_z . On voit que l'équation séculaire de l'Hamiltonien (61) se factorise en deux équations du 1^{er} degré, cinq équations du 2^{ème} degré et une équation du 4^{ème} degré. Si l'on remarque de plus que les transitions ne se font qu'entre des états de même parité et que la règle $\Delta F_z = \pm 1$ est toujours valable on trouve facilement que le nombre total de transitions permises est 28. Ceci est à confronter avec le cas traité précédemment où les spins de chaque groupe étaient équivalents, et l'équation séculaire d'ordre le plus élevé était du 3^{ème} degré. Introduisons à présent la simplification $\omega_H - \omega_F \gg J$. Sur le tableau précédent on voit que les seuls états qui ont la même énergie à l'ordre zéro et qui par conséquent sont couplés par les interactions J sont (D_3, D_4) et (E_1, E_2) . L'équation séculaire se factorise en deux équations du second degré et 12 équations du 1^{er} degré. On a un spectre des protons et un spectre analogue des fluors. Le spectre des protons se compose des 6 transitions:

$$A_1 \rightarrow B_1, \quad B_1 \rightarrow D_1, \quad B_2 \rightarrow \zeta, \quad B_2 \rightarrow \eta, \quad C_2 \rightarrow \zeta', \quad C_2 \rightarrow \eta',$$

où ζ et η sont deux combinaisons linéaires de D_3 et D_4 et ζ' et η' deux combinaisons linéaires de E_1 et E_2 , et de 6 transitions analogues pour les F_z négatifs. Les 12 fréquences correspondantes se réduisent à 10 car, comme on le trouve aisément, les deux fréquences $A_1 \rightarrow B_1$ et $B_1 \rightarrow D_1$ sont égales de même que les fréquences correspondantes pour les F_z négatifs.

Le spectre total se compose donc de 20 raies. Les indications précédentes devraient permettre au lecteur d'en calculer complètement les fréquences à partir des constantes de l'Hamiltonien (61) ce qu'il est vivement engagé à faire en exercice,

Le point le plus important est que ce calcul permet de déterminer les interactions J_1 et J_2 qui existent entre des spins semblables. Dans le difluoroéthylène McCONNELL *et al.* ont trouvé $J_1 \sim 5$ Hz, $J_2 \sim 37$ Hz. Il faut insister encore sur ce point: un couplage entre spins *semblables* peut être observable, seul un couplage entre spin *équivalents* est inobservable.

F) *L'influence des durées de vie des niveaux d'énergie de système sur la forme du spectre.* — Dans les paragraphes précédents nous avons essayé de prédire les positions et les intensités des raies sans tenir compte des phénomènes, qui comme la relaxation, l'échange chimique, ou l'action d'un champ de radiofréquence intense limitent les temps de vie des niveaux énergétiques des spins nucléaires.

Une théorie générale de ces effets est compliqué. FÉLIX BLOCH (*Phys. Rev.*, **102**, 104 (1956)) en a tracé le cadre général et a pu dans les cas les plus simples pousser les calculs jusqu'au bout. Nous nous contenterons, dans ce

chapitre, de considérations très simples qui permettent d'expliquer qualitativement l'allure d'un certain nombre de phénomènes.

a) L'absence de certains multiplets. — Dans un certain nombre d'exemples précédemment traités comme le pentafluorure de brome BrF_5 , le dichloroacétaldéhyde, etc., nous avons raisonné comme si les moments magnétiques des noyaux brome et chlore étaient absents, en accord avec la forme du spectre observé. L'explication réside dans le fait que ces noyaux dont le spin est $\geq \frac{1}{2}$, possèdent des moments quadrupolaires fortement couplés aux champs électriques qui existent dans la molécule et qui fluctuent rapidement par suite de sa rotation due au mouvement brownien. Il en résulte pour leurs spins des temps de relaxation T_1 très courts, qui limitent considérablement le temps de vie d'un spin dans un état donné. Nous avons vu que, sous certaines conditions les fréquences de résonance d'un spin I' couplé à un spin I par une interaction $\hbar J \mathbf{I} \cdot \mathbf{I}'$ étaient données par la formule

$$(47) \quad \omega = -\gamma H_0 + J M',$$

où $M' = I'_z$ pouvait prendre $(2I' + 1)$ valeurs. Sous l'effet de la relaxation du noyau I' , ce dernier passe d'un état $I'_z = M'$ à un autre avec une fréquence moyenne de l'ordre de $1/T_1$ entraînant des variations simultanées de la fréquence ω du noyau I . (On peut montrer qu'un multiplet est remplacé par une raie unique si la fréquence moyenne des sauts qui est $1/T_1$ est grande par rapport à la largeur J du multiplet). Par conséquent, en général les noyaux doués d'un moment quadrupolaire n'apportent pas de contributions aux spectres de multiplets. Des exceptions comme celles du bore dans les diboranes ou dans NaBH_4 , où le spin $I > \frac{1}{2}$ du bore est responsable de la structure en multiplets de la raie de résonance des protons, s'expliquent par la symétrie de ces molécules qui conduit à des gradients de champ électrique très faibles à l'emplacement du noyau de bore.

Une autre cause de disparition des multiplets est l'échange chimique.

Lorsque dans une molécule donnée, un noyau I' est remplacé à des intervalles fréquents par un autre noyau semblable, tout se passe pour la résonance du noyau I , dont I' causait la structure en multiplet, comme si c'était le même noyau I' qui sans quitter la molécule effectuait une transition. Formellement ce cas peut donc se ramener au cas précédent.

La situation est encore la même lorsque c'est le noyau résonant I lui-même qui s'échange entre des molécules différentes. Un exemple remarquable de ce phénomène a été observé par J. ARNOLD pour le proton du groupe hydroxyl de l'alcool éthylique $\text{C}_2\text{H}_5\text{OH}$. L'échange de ce proton est catalysé par la présence d'ions H^+ ou H^- en proportions très faibles (inférieures à 10^{-5}) et il faut prendre des précautions spéciales dans la préparation des échantillons

d'alcool pour éviter cet échange. La Fig. 10 montre le spectre complet des protons de l'alcool éthylique, dans le cas de l'alcool impur (en haut) et de l'alcool pur (en bas). Si l'on compare les spectres du groupe hydroxyl sur ces deux figures on est frappé par la différence suivante: la ligne de l'hydroxyl

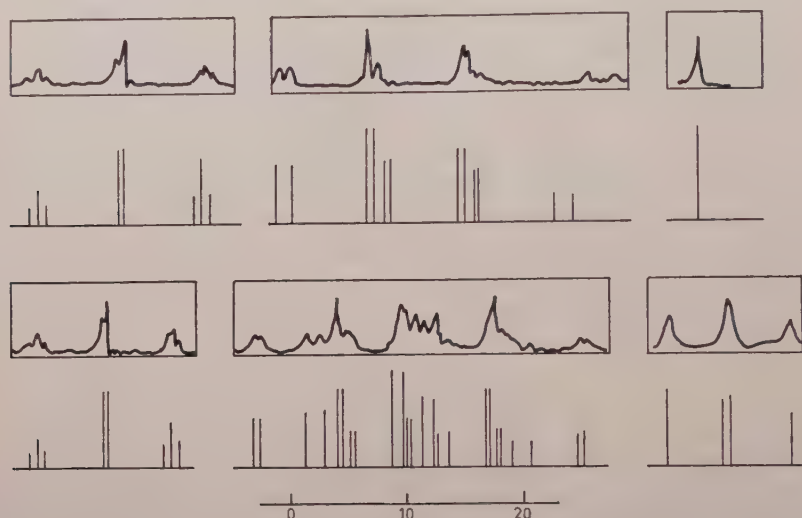


Fig. 10. — Spectre des protons de l'alcool éthylique impur (en haut) et pur (en bas).

est comme il se doit, un triplet dans la figure du bas par suite de son couplage avec le groupe méthylène CH_2 , mais ce triplet est devenu une ligne unique dans la figure du haut par suite de l'échange chimique. En étudiant la forme du spectre de l'hydroxyl en fonction de la concentration en ions H^+ et OH^- , ARNOLD a pu réaliser toutes les formes intermédiaires entre ces deux figures et relier la concentration à la vitesse d'échange.

La Fig. 11 montre la forme théorique du spectre de l'hydroxyl en fonction du temps caractéristique d'échange.

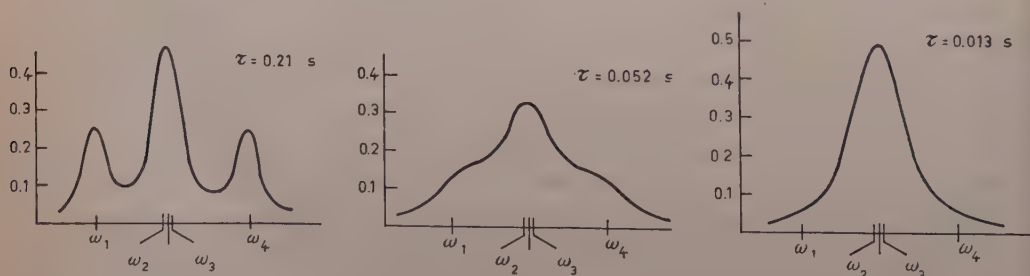


Fig. 11.

La comparaison des spectres du groupe méthylène dans les deux figures est également instructive, la complexité beaucoup plus grande dans le cas de l'alcool pur étant due au couplage avec le groupe hydroxyl, couplage supprimé par l'échange dans l'alcool impur.

On voit que l'échange a pour effet de découpler complètement l'hydroxyl du méthylène.

b) Variation dans la largeur des raies. — Pour calculer l'intensité des raies correspondant à une transition $|\zeta\rangle \rightarrow |\zeta'\rangle$ nous avons utilisé la formule $P_{\zeta\zeta'} \sim |\zeta(I|\zeta')|^2$ qui est bien vérifiée par l'expérience pour l'intensité intégrée donnée par l'aire de la courbe de résonance mais non pour la hauteur des divers pics qui ont donc des largeurs différentes. Ceci est très naturel, car il est clair que la largeur d'une raie faisant partie d'un multiplet qui correspond à une transition d'un spin I donné dépend évidemment de la vie moyenne du spin voisin I' dont les diverses orientations donnent naissance à ce multiplet.

Le calcul de ces largeurs peut en principe se faire par la théorie générale, moyennant des hypothèses sur le mécanisme de la relaxation dans la molécule. C'est dans un cas compliqué comme celui de l'alcool un calcul d'une extrême complexité, qui a été fait par F. BLOCH dans des cas simples et avec des hypothèses simples sur le mécanisme de relaxation. Nous nous contenterons ici d'attirer l'attention sur le cas particulièrement frappant de la raie double au centre du triplet du groupe méthyl de l'alcool (Fig. 11). Les deux composantes de cette raie correspondent toutes les deux à $m_R = 0$ mais à $I_B = 0$ et $I_B = 1$ respectivement où l'indice B est relatif aux protons du groupe méthylène. Alors que les intensités intégrées de ces deux raies, sont égales à la précision expérimentale, leurs hauteurs et donc leurs largeurs sont très inégales, la raie qui correspond à $I_B = 0$ étant la plus haute. Ceci est très naturel car l'état singulet $I_B = 0$ étant dépourvu de magnétisme nucléaire a certainement une vie beaucoup plus longue que l'état triplet.

c) Double irradiation. — La disparition de la structure fine de la résonance d'un spin I couplé à un spin I' , lorsque ce dernier subit des transitions fréquentes suggère naturellement l'expérience de double irradiation qui consiste à appliquer un champ de radio fréquence intense H'_1 à la fréquence ω' du spin I' et à observer simultanément la résonance de I avec un champ faible H_1 à la fréquence ω . FÉLIX BLOCH et indépendamment J. SHOOLERY, sont les premiers à avoir eu cette idée. On constate effectivement que si l'intensité du champ H'_1 est suffisante, la structure fine de la résonance de I disparaît.

On peut être tenté d'assimiler entièrement ce phénomène à celui décrit en a) et de dire que la probabilité de transition sous l'effet du champ fort H'_1

$\gamma^2 H_1'^2 T_2'$ joue le même rôle que l'inverse $1/T_1'$ du temps de relaxation de I' ou que l'inverse $1/\tau$ du temps caractéristique de l'échange chimique de ce noyau.

Ce raisonnement est tout à fait incorrect car il ne tient pas compte du fait que le champ HF , H_1' impose aux spins I' un mouvement *cohérent*, contrairement à ce qui se passe pour les phénomènes dus à la relaxation et l'échange chimique. Expérimentalement, lorsque l'on fait croître le champ H_1' à partir de zéro, jusqu'à des valeurs élevées, le passage de la structure en multiplet à une ligne unique a une allure complètement différente de ce qui est observé lorsque au moyen d'un catalyseur on fait croître la fréquence $1/\tau$ de l'échange chimique.

La théorie du nombre, des positions et des intensités des raies du spectre de I , lorsqu'on irradie I' est fort compliquée et nous ne la donnerons pas ici nous contentant de quelques remarques simples [voir BLOOM et SHOOLERY (*Phys. Rev.*, **97**, 1261 (1955)), dont la théorie approchée ne donne pas correctement les intensités relatives, et FÉLIX BLOCH (*Phys. Rev.*, **102**, 104 (1956)) pour une théorie plus complète].

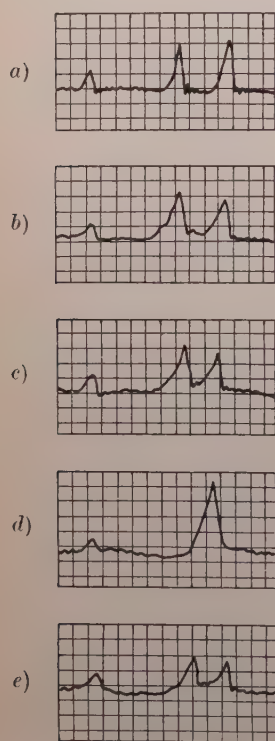


Fig. 12. — a) sans irradiation; b) 110 Hz; c) 105 Hz; d) 100 Hz; e) 95 Hz.

1) L'Hamiltonien du système dans un référentiel tournant à la fréquence ω' du champ H_1' , supposée égale à la fréquence de Larmor ω_1' du spin I' peut s'écrire:

$$(62) \quad \frac{\mathcal{H}}{\hbar} = (\omega_0 - \omega')I_z - \gamma' H_1' I_x' + J \mathbf{I} \cdot \mathbf{I}'.$$

Si $\gamma' H_1' \gg J$ on peut y traiter $J \mathbf{I} \cdot \mathbf{I}'$ comme une perturbation. On voit que $I_z = m$, $I_x' = m'$ sont de bons nombres quantiques pour la partie non perturbée de l'Hamiltonien $(\omega_0 - \omega')I_z - \gamma' H_1' I_x'$ et que par conséquent au premier ordre $J \mathbf{I} \cdot \mathbf{I}'$ n'apporte pas de contribution à l'énergie du système. Les spins I et I' sont découplés et la résonance de I donne une raie simple. Le critère pour qu'il en soit ainsi est $\gamma' H_1' \gg J$ et ce raisonnement est à substituer à celui basé sur les probabilités de transition, utilisé pour a).

2) L'intérêt principal des expériences de double irradiation est de permettre de débrouiller les spectres compliqués en neutralisant par un champ de radiofréquence les couplages avec noyau (ou

un groupe G de noyaux semblables). La Fig. 12 montre comment varie la forme de deux pics dans le dichloroacétaldéhyde observés avec un faible champ h.f., H_1 de fréquence ω lorsqu'on irradie les deux autres pics avec un champ h.f., H'_1 intense, dont on fait varier la fréquence. On a porté sur la figure les valeurs de $(\omega' - \omega)/2\pi$.

3) On peut par cette méthode mesurer la fréquence de Larmor d'un noyau sans utiliser un dispositif de détection pour cette fréquence. C'est ainsi que VIRGINA ROYDEN (*Phys. Rev.*, **96**, 543 (1954)) a mesuré la fréquence de Larmor du carbone-13 dans l'iodure de méthyl CH_3I , enrichi en ^{13}C en déterminant la fréquence ω' du champ H'_1 pour laquelle la résonance des protons, dédoublée par leur couplage avec le spin $I' = \frac{1}{2}$ de ^{13}C , devient simple. Cette méthode pourrait devenir intéressante pour la mesure des moments magnétiques faibles dont les fréquences de Larmor dans un domaine où le rapport signal/bruit est mauvais, en utilisant pour détecter le passage par la résonance, la disparition de la structure fine de la résonance d'un autre noyau dont le spin est couplé à celui dont on cherche le moment magnétique.

1) Les méthodes de double irradiation appellent une remarque générale reliée aux considérations développées dans le premier chapitre. Nous y avons dit que de toutes les méthodes de mesure utilisant le principe de résonance, seule celle des jets de Rabi n'exigeait pas l'inégalité des populations de deux états entre lesquels se faisaient les transitions résonantes. La double irradiation en fournit un second exemple. Le facteur de Boltzmann des deux états de ^{13}C ne joue aucun rôle dans l'expérience de V. ROYDEN.

Il est bon de remarquer à ce propos que la description que l'on donne quelquefois de la méthode de double irradiation en disant qu'on observe la résonance du noyau I tout en saturant celle du noyau I' , est profondément incorrecte. Il ne s'agit pas de saturer la résonance de I' , ce qui exige $\gamma'^2 H_1'^2 T_2' \gg 1/T_1'$ mais de découpler le noyau I' du noyau I en rendant sa fréquence de précession $\gamma H_1'$ dans un champ d'amplitude H_1' beaucoup plus rapide que sa fréquence de précession J , due à son couplage avec le noyau I .

d) Relaxation par interaction indirecte. — Le fait qu'un échange chimique rapide rende inobservable la structure fine due à un couplage scalaire $J\mathbf{I}_1 \cdot \mathbf{I}_2$, ne signifie pas pourtant que ce couplage n'a aucune conséquence observable. Une situation analogue s'était déjà présentée à nous dans le cas de l'interaction dipole-dipole entre les protons d'une molécule d'eau. Si la molécule appartient à un solide rigide, la raie de résonance a une structure fine, que les expériences de Pake ont mise en évidence. Dans l'eau liquide cette structure disparaît par suite de la rotation brownienne des molécules, mais l'interaction dipole-dipole entre les protons de la molécule est, par un effet du second ordre, responsable de leur relaxation. On peut calculer les

temps de relaxation correspondants par la méthode des fonctions aléatoires de BPP. Cette méthode peut s'étendre au cas de l'interaction scalaire où le caractère aléatoire est introduit par l'échange chimique. Un exemple est fourni par la molécule HF où cet effet a été mis en évidence par la première fois (I. SOLOMON et N. BLOEMBERGEN: *Journ. Chem. Phys.*, à paraître). On admet que dans cette substance les protons peuvent s'échanger rapidement entre les molécules, cet échange étant par la présence de quantités d'eau minimales.

Mathématiquement on peut décrire l'interaction scalaire entre les spins des protons et des fluors en présence d'échange par une expression de la forme:

$$\mathcal{H} = \sum_{i,k} J_{ik} S_{i0} \cdot I_k,$$

où les S_i sont les spins des protons et les I_k ceux des fluors. Les coefficients J_{ik} sont des fonctions aléatoires du temps qui obéissent aux conditions suivantes: pour un indice i donné, à chaque instant t tous les coefficients J_{ik} sont nuls sauf un seul $J_{ik_0} = J$, l'indice k_0 étant relatif au fluor particulier avec lequel le proton i forme une molécule à l'instant t .

Par suite de l'échange chimique le proton i saute d'une molécule à l'autre avec un intervalle moyen τ_e entre deux sauts consécutifs et un changement à chaque saut de l'indice k_0 défini précédemment.

On montre facilement en utilisant la méthode des fonctions aléatoires que la variation de la polarisation $\langle S_z \rangle$ des spins S est décrite par l'équation

$$(63) \quad \frac{d\langle S_z \rangle}{dt} = -\frac{J^2}{2} \frac{\tau_e}{1 + (\omega_I - \omega_S)^2 \tau_e^2} \{ (\langle S_z \rangle - S_0)(\langle I_z \rangle - I_0) \}$$

On peut remarquer que bien que dans des molécules légères comme HF la valeur absolue de l'interaction $\hbar J$ soit beaucoup plus faible que celle de l'interaction dipole-dipole $\gamma_I \gamma_S \hbar^2 / r^3$, du fait que le temps de corrélation τ_e lié à l'échange chimique, peut être beaucoup plus long que le temps de corrélation τ_c relatif à la rotation de la molécule, le mécanisme de relaxation par interaction indirecte et échange chimique peut atteindre une importance égale et même supérieure à celui de la relaxation par interaction dipole-dipole.

Ce fait a été démontré expérimentalement par I. SOLOMON (I. SOLOMON et N. BLOEMBERGEN, ref. citée) qui a pu faire varier le temps d'échange τ_e en modifiant le contenu en eau des échantillons d'acide fluorhydrique. Bien qu'il n'ait jamais pu obtenir un échantillon suffisamment sec pour avoir $1/\tau_e < J$ et résoudre la structure fine de la résonance, il a pu par une étude systématique de la relaxation déterminer la constante J qui est de 600 Hz environ. Nous reviendrons sur cette étude et sur une discussion de l'équation (69) à propos de l'effet Overhauser.

3.3. *Les interactions indirectes dans des solides.* — Comme nous l'avons déjà remarqué, l'importance des interactions indirectes dans les solides est très réduite car contrairement à ce qui se passe pour les liquides, elles sont, à moins de circonstances spéciales, complètement masquées par les interactions directes dipole-dipole. Nous nous contenterons ici de décrire d'une façon très schématique le beau travail de BLOEMBERGEN et ROWLAND (*Phys. Rev.*, **97**, 1679 (1955)) sur la résonance magnétique du thallium dans l'oxyde de thallium et dans le métal, qui a permis de mettre en évidence d'une façon indiscutable l'existence d'interactions indirectes importantes dans les solides. Les faits expérimentaux sont les suivants:

Le thallium a deux isotopes ^{203}Tl et ^{205}Tl ayant tous deux un spin $\frac{1}{2}$, et des moments magnétiques différent de 1 pour cent environ. Les proportions isotopiques dans l'élément naturel sont 29.5 pour cent et 70.5 pour cent environ. Le premier fait expérimental extrêmement frappant est que la résonance de ^{203}Tl est beaucoup plus large que celle de ^{205}Tl ce qui a première vue est complètement incompréhensible. On peut penser au fait que des voisins semblables sont plus efficaces que des voisins différents pour l'élargissement, ce qui se traduit par un facteur $9/4$ pour le second moment de la raie mais alors c'est ^{205}Tl qui est l'isotope le plus abondant qui devrait avoir la raie la plus large, contrairement à l'expérience.

Pour expliquer ce fait BLOEMBERGEN a eu l'idée d'invoquer entre les spins nucléaires une interaction indirecte du type scalaire ou d'échange, $\mathbf{J}\mathbf{I} \cdot \mathbf{I}'$ beaucoup plus forte que l'interaction dipole-dipole directe. On sait que de telles interactions, si elles ont lieu entre des voisins semblables rétrécissent la raie alors qu'elles l'élargissent dans le cas de voisins différents. On conçoit alors que le ^{205}Tl qui a 7 voisins semblables pour 3 voisins différents ait une raie plus étroite que ^{203}Tl pour lequel la situation est renversée.

Pour vérifier ce raisonnement, BLOEMBERGEN a observé la résonance des deux isotopes dans des échantillons à contenu isotopique variable. La Fig. 13 montre bien que la raie d'un isotope donné a une largeur minimum lorsque cet isotope est pratiquement seul dans l'échantillon et que les raies des deux isotopes ont même largeur si leurs proportions sont égales.

On peut voir toutefois que l'hypothèse d'une interaction indirecte purement scalaire est insuffisante. En effet dans cette hypothèse, par suite du rétrécissement par échange, la largeur de la raie de l'isotope devrait être beaucoup plus faible que la largeur dipolaire alors que c'est le contraire qui a lieu, la largeur observée étant encore pour l'isotope isolé plusieurs fois la largeur dipolaire. BLOEMBERGEN l'explique en supposant que l'interaction indirecte, en plus du couplage scalaire $\mathbf{J}\mathbf{I}_1 \cdot \mathbf{I}_2$ comporte une partie pseudo-dipolaire $B\{\mathbf{I}_1 \cdot \mathbf{I}_2 - 3(\mathbf{I}_1 \cdot \mathbf{n})(\mathbf{I}_2 \cdot \mathbf{n})\}$ qui contribue à l'élargissement, même entre spins semblables. Le problème est encore compliqué par l'existence d'un déplace-

ment anisotrope de la fréquence de résonance qui est une cause supplémentaire d'élargissement.

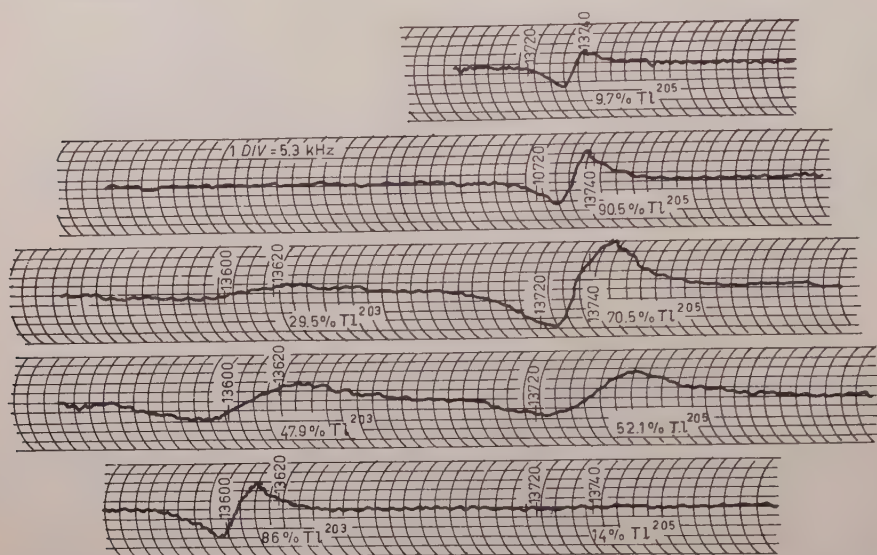


Fig. 13. -- resonances de ^{203}Tl et ^{205}Tl dans un champ H_0 de 5560 Oe sur des échantillons en poudre enrichés de Tl_2O_3 à 77 °K. Les fréquences sont indiquées en kHz.

La situation devient alors très complexe et nous nous contenterons de signaler qu'en invoquant ces deux phénomènes: interaction indirecte anisotrope et déplacement anisotrope de la fréquence de résonance BLOEMBERGEN arrive à donner une explication cohérente de tous les faits observés. Les valeurs de $J \sim 10$ kHz et de $B \sim 2$ à 3 kHz, entre plus proches voisins, utilisées dans cette explication, sont en accord raisonnable avec les valeurs calculées à partir des premiers principes, par les méthodes développées dans la Sect. 3.

Bien entendu, comme on l'a déjà signalé, c'est parce qu'il s'agit d'une interaction entre deux atomes lourds ayant des structures hyperfines très larges, que les interactions indirectes atteignent des valeurs aussi importantes.

Stochastic Theory of Magnetic Resonance.

R. KUBO

Department of Physics, University of Tokyo - Tokyo

1. - Correlation function ^(1,2).

This is a brief review of the theory of line-shape problems in magnetic resonance phenomena from the view point of the stochastic theory. My subject is more of mathematical nature than physical. Also the time is too short to go into any discussion of real physical cases which should be done otherwise. Here we have to confine ourselves to a certain mathematical model of the physical processes.

Let us begin with a general consideration of the nature of complex susceptibility for a finite frequency of external field. This will make one understand how the stochastic theory is related to the resonance problem.

The magnetic susceptibility χ is written as

$$(1) \quad \chi = \chi' - i\chi'',$$

the real and the imaginary parts being functions of ω , the frequency of external magnetic field. Usually we consider the case where a static field H_0 is present besides the alternating field, so that χ is a tensor. But let us consider only the component χ_{xx} because this is enough when the alternating field is linearly polarized.

The first theorem, which is the basis of the whole theory, is that $\chi''_{xx}(\omega)$ is essentially a Fourier-transform of the correlation function of the magne-

(1) R. KUBO and K. TOMITA: *Journ. Phys. Soc. Japan*, **9**, 888 (1954)

(2) A detailed discussion was made by the author in a preliminary report. *Busseironkenkyu*, **89**, 79 (1955). A full paper will appear in *Journ. Phys. Soc. Japan*.

tization $M'_x(t)$ which fluctuates spontaneously. Expressed by a formula, the theorem is that

$$(2) \quad \chi''_{xx}(\omega) = \frac{2}{\hbar\omega} \operatorname{tgh} \frac{\hbar\omega}{2kT} \int_0^\infty \langle \{M'_x(t_0 + t) M'_x(t_0)\} \rangle \cos \omega t \, dt,$$

where M'_x means

$$M'_x = M_x - \bar{M}_x.$$

This is the deviation of the magnetization from the average value. M'_x changes in time with the internal motion of the magnetic system, so it is a function of time.

It should be noticed here that the internal motion here is a natural motion of the system in the absence of the alternating field. The integrand, $\langle \{M'_x(t_0 + t) M'_x(t_0)\} \rangle$, is the correlation function of the motion of $M'_x(t)$ for the time interval t . The average is taken over all distributions of the system, and the bracket means the symmetrization of the product to take care of the situation that M'_x for different time points do not necessarily commute.

Since the motion $M'_x(t)$ is a natural motion in a certain equilibrium state of the system, it is *stationary* in the mathematical terminology used for stochastic processes. That is, the nature of the time variation is independent of the change of the origin of time, so that, for instance, we should have

$$\frac{1}{T} \int_0^T \langle M'_x(t) \rangle \, dt = \frac{1}{T} \int_0^T \langle M'_x(t + t_0) \rangle \, dt,$$

and

$$\langle M'_x(t) M'_x(0) \rangle = \frac{1}{T} \int_0^T \langle M'_x(t + t_0) M'_x(t_0) \rangle \, dt_0.$$

The latter as a function of t is the correlation function (not normalized) of M'_x by definition. By the assumption of ergodicity, the time average for $T \rightarrow \infty$ is replaced by the ensemble average, which was indicated in (2) by $\langle \rangle$, that is

$$(3) \quad \Psi(t) = \lim_{T \rightarrow \infty} \frac{1}{T} \int_0^T M'_x(t + t_0) M'_x(t_0) \, dt_0 \rightarrow \\ \rightarrow \langle \{M'_x(t_0 + t) M'_x(t_0)\} \rangle = \operatorname{Tr} \varrho \{M'_x(t_0 + t) M'_x(t_0)\},$$

ϱ being the density operator for the statistical distribution of the system.

Thus, looking at $M'_x(t)$ as a stochastic variable, the theorem (2) says that the imaginary part $\chi''_{xx}(\omega)$ is essentially the Fourier transform of $\Psi(t)$.

This theorem is exact, as far as the perturbing field (alternating field) has only small amplitude so that we could assume a linear response (that is the magnetization induced by this perturbation is considered to be proportional to the amplitude of the perturbing field). The derivation of the theorem is given in the Appendix I.

For practical applications of the theorem (2), it can be simplified as

$$(4) \quad \chi''_{xx}(\omega) = \frac{1}{kT} \int_0^{\infty} \langle \{M'_x(t_0 + t)M'_x(t_0)\} \rangle \cos \omega t dt = \frac{1}{kT} \int_0^{\infty} \Psi(t) \cos \omega t dt,$$

because ω is usually so small that the condition

$$\hbar\omega \ll kT$$

is satisfied even at low temperatures.

Eq. (4) is nothing but what is used commonly in literatures as the expression of the absorption intensity written in terms of matrix elements of M_x . One can easily convince oneself by making use of the integral expression of the δ -function. But Eq. (2) or (4) shows that the spectral distribution of the absorption can be interpreted as the spectrum of the correlation of $M'_x(t)$.

Actually, Eq. (2) is a particular case of the « fluctuation dissipation theorem » which states generally the existence of such a relation between the impedance function and the correlation function (3).

A well known and old example of this theorem is Niquist's theorem about the thermal noise of a resistive circuit (4).

2. - Relaxation function (1,2).

It might be worthwhile to add here a few remarks. It is well known that the real and the imaginary parts, $\chi'(\omega)$ and $\chi''(\omega)$, are connected to each other by the Kramers-Kronig relation. This comes from the fact that there exists a function $\Phi(t)$, which we call relaxation function, by means of which the complex

(3) See for instance CALLEN and WELTON: *Phys. Rev.*, **83**, 34 (1951).

(4) H. NIQUIST: *Phys. Rev.*, **32**, 110 (1928).

susceptibility is expressed as

$$(5) \quad \chi^*(\omega) = \chi'(\omega) - i\chi''(\omega) = \chi(0) - i\omega \int_0^{\infty} \Phi(t) \exp[-i\omega t] dt = \\ = - \int_0^{\infty} \frac{d\Phi}{dt} \exp[-i\omega t] dt$$

The function $\Phi(t)$ represents the relaxation process of the magnetization when a constant disturbance is removed. Eq. (5) is easily understood since $-d\Phi/dt$ is the response to a pulse. The fundamental assumption for (5) is again the linearity of the response.

It can be proved in general that the relaxation function and correlation function are mutually connected by a certain integral transformation which involves a quantum mechanical time constant \hbar/kT . In the limit of $\hbar/kT \rightarrow 0$ (or high temperature) this degenerates into the classical relation

$$(6) \quad \text{relaxation function} = \text{correlation function}/kT.$$

If one admits (6), one sees at once that Eq. (5) leads to Eq. (4). More generally Eq. (6) or Eq. (4) holds if the frequencies involved in the correlation function are limited to the low-frequency region ($\hbar\omega \ll kT$). This will be the case for most of the practical applications (but not always).

3. - Random modulation of resonance frequency.

The natural motion of $\mu'_x(t)$ is generally expressed as a multiperiodic motion, i.e.

$$(7) \quad M'_x(t) = \sum_{\alpha} M'_{x\alpha} \exp[i\omega_{\alpha} t].$$

When one inserts this into Eq. (4), one gets a series of resonance lines at the frequencies ω_{α} . The absorption A is

$$(8) \quad A = \frac{1}{kT} \sum_{\alpha} \omega_{\alpha}^2 \langle |M'_{x\alpha}|^2 \rangle \delta(\omega - \omega_{\alpha}).$$

The intensity of each line is given by the average of the square of its amplitude, which corresponds to the matrix element connecting two levels with the energy spacing $\hbar\omega_{\alpha}$.

The decomposition (7) is done with respect to the whole system. It is sometimes more convenient to think of other decompositions. For instance, the total magnetic moment is the sum of atomic moments. Each of the atomic moments (spins) is now considered as the unit. Then each spin makes a very complicated motion, which can be conceived as a stochastic process. Let us consider a very simple example. Each spin is now precessing under the influence of the constant external field \mathfrak{H}_0 and an effective field \mathfrak{H}_i , the latter representing the force due to the surroundings. For simplicity, we further consider the component H_i of \mathfrak{H}_i parallel to \mathfrak{H}_0 . Generally H_i varies from a spin to another, and also it may change in the course of time, so H_i is now supposed to be a stochastic variable. The motion of a spin is effectively represented by the equation

$$(9) \quad \dot{\mu} = i(\omega_0 + \omega'(t))\mu,$$

where ω_0 is the precessional frequency due to the static external field and $\omega'(t)$ is the modulation caused by the fluctuation of the local field H_i . Eq. (9) gives

$$(10) \quad \mu(t) = \mu(0) \exp[i\omega_0 t] \exp\left[i \int_0^t \omega'(t') dt'\right].$$

Therefore Eq. (4) is now written as

$$(11) \quad \chi'_{xx}(\omega) = \frac{N}{kT} \int_0^\infty \left\langle |\mu(0)|^2 \exp\left[i \int_0^t \omega'(t') dt'\right] \right\rangle \exp[i(\omega_0 - \omega)t] dt,$$

N being the total number of spins per unit volume.

The main problem here is the effect of the random modulation of frequency. This was already discussed by Professors VAN VLECK and PURCELL, but a short discussion will be worth while.

Let us define a function $g(t)$ by

$$(12) \quad g(t) = \left\langle \exp\left[i \int_0^t \omega'(t') dt'\right] \right\rangle,$$

which is essentially the correlation function and determines the line shape. We are considering here simply only one resonance line broadened by the local field H_i . We have now two important time constants. The first

is defined by

$$(13) \quad \omega_p^2 = \langle \omega'(t)^2 \rangle,$$

($\langle \omega'(t) \rangle$ may be assumed to be zero without loss in generality). The second is ω_c which measures the rate of the time variation of $\omega'(t)$. This is defined by

$$(14) \quad \int_0^\infty \langle \omega'(0)\omega'(t) \rangle dt / \omega_p^2 = 1/\omega_c = \tau_c,$$

$\tau_c = 1/\omega_c$ may be called the correlation time of the local field. In the two following cases, we can make general predictions about the line shape.

a) $\omega_p \gg \omega_c$. The variation of ω' can be regarded essentially as static. The line shape is directly determined by the probability distribution of ω' or H_i . The intensity distribution simply reflects the distribution of ω' . A rough measure of the width is ω_p .

b) $\omega_p \ll \omega_c$. If ω' changes rapidly an averaging effect occurs which produces the narrowing of the resonance line. The line-shape in the limit will be generally Lorentzian with the half-width

$$(15) \quad \Delta\omega = \omega_p^2/\omega_c = \omega_p^2\tau_c.$$

4. - Gaussian process.

To find the line shape from Eq. (12), one has to know the stochastic nature of $\omega'(t)$. An easy example is afforded by a Gaussian process. If the local field H_i is the resultant of a large number of contributions from many neighbors (liquids or crystals), we may generally expect $\omega'(t)$ to be a so-called Gaussian process. That is, we write

$$(16) \quad \omega' = \sum_{i=1}^n \Delta\omega'_i \quad n \gg 1.$$

Each $\Delta\omega'_i$ itself may be considered as a stochastic quantity. By the central-limit theorem, we may expect that the random variable ω' at a certain moment will have a Gaussian distribution (normal distribution), and also we may assume that the stochastic process $\omega'(t)$ will be a Gaussian process. This means that the probability distribution of the values of ω' at different time-points, that is $\omega'(t_1)$, $\omega'(t_2)$, ..., $\omega'(t_r)$, is Gaussian. Namely it is given by the distri-

bution density

$$(17) \quad f(\omega'(t_1), \omega'(t_2), \dots, \omega'(t_r)) = C \exp \left[-\frac{1}{2} \sum_i^r \sum_j^r a_{ij} \omega'(t_i) \omega'(t_j) \right].$$

It is then easy to establish the relation

$$(18) \quad g(t) = \exp \left[-\omega_p^2 \int_0^t (t - \tau) \varphi(\tau) d\tau \right],$$

where $\varphi(\tau)$ is now the correlation function of $\omega'(t)$, i.e.,

$$(19) \quad \varphi(\tau) = \langle \omega'(\tau) \omega'(0) \rangle / \omega_p^2.$$

Eq. (18) is derived in Appendix II. To measure the rate of the variation of $\omega'(t)$, we can take the correlation time τ_c of $\omega'(t)$ defined by

$$(20) \quad \tau_c = 1/\omega_c = \int_0^\infty \varphi(\tau) d\tau,$$

where ω_c may be called the correlation frequency of $\omega'(t)$.

It is now easy to examine the two limiting cases mentioned in the previous section. The intensity of absorption is practically limited in the frequency region $(\omega_0 - \omega_p, \omega_0 + \omega_p)$ around the centre ω_0 . Therefore, in the Fourier inverse of (18) the most important contribution comes from the region of $t \gtrsim 1/\omega_p$. Thus we need only know the behaviour of $g(t)$ for $t \gtrsim 1/\omega_p$. If ω_c is small compared with ω_p ($\omega_c \ll \omega_p$), $\varphi(\tau)$ in the integral in Eq. (18) can be replaced by its initial value $\varphi(0)$ which is equal to 1. Then we have

$$(21) \quad g(t) \sim \exp \left[-\frac{\omega_p^2}{2} t^2 \right].$$

The Fourier-transform of this gives a Gaussian shape with the second moment ω_p^2 . This is the limiting case of a rigid lattice.

If $\omega_c \gg \omega_p$, $\varphi(\tau)$ in Eq. (19) changes rapidly in the range of integration, so that we may approximate (19) by

$$(22) \quad g(t) \sim \exp \left[-\omega_p^2(t) \int_0^\infty \varphi(\tau) d\tau \right] = \exp \left[-\frac{\omega_p^2}{\omega_c} t \right].$$

The Fourier-transform of this will give a Lorentzian distribution of the absorption intensity, i.e.,

$$(23) \quad I(\omega) \propto \frac{1}{\pi} \frac{\omega_p^2 \tau_c}{(\omega - \omega_0)^2 + (\omega_p^2 \tau_c)^2}.$$

The half width is

$$(23) \quad \Delta\omega = \omega_p^2 \tau_c = \omega_p^2 / \omega_c.$$

Since we assumed that

$$\omega_p^2 \tau_c = \omega_p^2 / \omega_c \gg \omega_p,$$

this is an extreme narrowing.

The narrowing thus takes place when the modulation ω' of the resonance frequency changes rapidly in a time of the order of $1/\omega_p$. Evidently the narrowing itself has nothing to do with the unperturbed frequency ω_0 . The local field H_i will change by virtue of some internal motion of the system, either atomic motion or other kind of motion (for instance, a coupled motion of spins due to the exchange interaction). The narrowing is generally called the motional narrowing, which is the averaging effect of the local fields.

Between the two limits of slow and rapid motion, the line shape can be computed if the correlation function is known. Two typical functions are often assumed. One is a simple exponential function of the type

$$(24) \quad \varphi(\tau) = \exp[-\tau/\tau_c]$$

and the other is

$$\varphi(\tau) = \exp\left[-\frac{\pi}{4} \omega_c^2 \tau^2\right].$$

The half width for any stage of narrowing can be calculated with these assumptions. The former is used often for the motional narrowing due to atomic motion ⁽⁶⁾ and the latter often for the exchange narrowing ⁽⁵⁾.

⁽⁵⁾ P. W. ANDERSON and P. R. WEISS: *Rev. Mod. Phys.*, **25**, 316 (1954). The same problem has been discussed in connection with communication problem, for instance, L. A. ZADEH: *Proc. I.R.E.*, **39**, 425 (1951) and Z. KIYASU: *Inst. Elect. Comm. Eng. Japan*, **34**, 605 (1951).

⁽⁶⁾ N. BLOEMBERGEN, E. M. PURCELL and R. V. POUND: *Phys. Rev.*, **73**, 679 (1948).

We did not consider so far the non-adiabatic effects of the local field. If the local field change involves the frequency of natural resonance ω_0 , it will induce transitions and limit the life of energy levels. This will result in a broadening effect. The non-adiabatic broadening thus occurs when ω_c is comparable with ω_0 . The additional breadth will decrease when ω_c becomes larger than ω_0 , but it will remain to be an appreciable part of the breadth even in the limit of $\omega_c \gg \omega_0$, because there the breadth of the secular effect of the local field (that is the part described by ω') is strongly narrowed. In a simple case of dipolar broadening, the non adiabatic broadening gives 7/3 of the secular broadening, so that the breadth in the limit of rapid motion will be 10/3 of the width (23'). This is the 10/3 effect (^{1,5,6}).

As a matter of fact, a rigorous calculation has to be done in a quantum-mechanical way. The naive picture we described above will fail to give a right answer if it is taken too literally. (This was pointed out by VAN VLECK for the calculation of the second moment of dipolar broadening). But the above will be enough to show how a stochastic theory is related to a certain case of magnetic resonance problem.

5. - Markoffian process (⁷).

Now we turn to another mathematical model which has certain physical applications. Suppose each of the resonating units in the system has a set of eigenstates which will be denoted by E_1, E_2, \dots, E_r . The resonance frequency in the state E_j is ω_j , and $P_j(t)$ will be the probability that an unit is found in the state E_j at the time t .

We assume that the probability changes in time following the kinetic equation

$$(26) \quad \frac{dP_j}{dt} = -C_j P_j + \sum_k P_k C_k p_{kj} = -\sum_k D_{kj} p_k,$$

where C_j is the life time of the state E_j , and p_{kj} is the transition probability from E_k to E_j . This is normalized to

$$\sum_j p_{kj} = 1.$$

(⁷) P. W. ANDERSON: *Journ. Phys. Soc. Japan*, **9**, 316 (1954); R. KUBO: *Journ. Phys. Soc. Japan*, **9**, 935 (1954).

Equation (26) is an example of Markoffian process. Our problem is now to investigate the effect of the transition on the observed resonance spectrum.

It can be shown (see Appendix III) that $g(t)$, Eq. (12), is given by

$$(27) \quad g(t) = \sum_j u_j(t),$$

where $u_j(t)$ is found as the solution of the differential equations

$$(28) \quad \left(\frac{d}{dt} - i\omega_j \right) u_j(t) + \sum_k D_{kj} u_k(t) = 0, \quad (j = 1, 2, \dots, r),$$

with the initial conditions

$$(29) \quad u_j(0) = P_j^0,$$

P_j^0 being the equilibrium distribution (satisfying the condition $dP_j^0/dt = 0$).

Eq. (28) describes a set of oscillators ($j=1, 2, \dots, r$) with eigenfrequencies ω_j and with a coupling of damping type.

One can show further that the intensity distribution itself is expressed as a sort of forced-oscillation solution of Eq. (28). Namely, the absorption spectrum $I(\omega)$ is given by

$$(30) \quad I(\omega) = \frac{1}{\pi} \operatorname{Re} \sum_j x_j(\omega),$$

with $x_j(\omega)$ determined as the solution of the algebraic equations

$$(31) \quad i(\omega - \omega_j)x_j + \sum_k D_{kj}x_k = P_j^0 \quad (j = 1, 2, \dots, r).$$

Thus the model adopted here allows for a fairly simple treatment. The transitions between the states induce a damping-type coupling between the unperturbed oscillators.

A simple example of this is the resonance spectrum of a molecule which can take two states, the transition being induced by a certain collision process. We may write then the matrix (D_{kj}) as

$$(32) \quad (D_{kj}) = \begin{pmatrix} \omega'_c & -\omega'_c \\ -\omega''_c & \omega''_c \end{pmatrix}.$$

The equilibrium probabilities P_j^0 are

$$P_1^0 = \omega''_c / \omega_c, \quad P_2^0 = \omega'_c / \omega_c, \quad (\omega_c = \omega'_c + \omega''_c).$$

Eqs. (30) and (31) will give then at once

$$(33) \quad I(\omega) = \frac{\omega_c P_1^0 P_2^0}{\pi} \frac{(\omega_1 - \omega_2)^2}{(\omega - \omega_1)^2 (\omega - \omega_2)^2 + \omega_c^2 (\omega - \bar{\omega})^2},$$

where

$$\bar{\omega} = P_1^0 \omega_1 + P_2^0 \omega_2,$$

is the average of the two frequencies ω_1 and ω_2 . In the limit $\omega_c \rightarrow \infty$, the spectrum will be a sharp line at $\omega = \bar{\omega}$. In the opposite limit $\omega_c \rightarrow 0$, we have two peaks at ω_1 and ω_2 , the intensities of which are proportional to P_1^0 and P_2^0 .

Thus when ω_c increases (say through increase of temperature) two sharp lines will first broaden, will then overlap, the maxima approaching each other, and finally merge into one single line. Such behaviour is often observed in various cases. For instance a molecule *A* will change into another molecule *B* by collision or reaction. If the nuclear resonance of an atom which remains in both states is observed, the difference of chemical shift will give different resonance at ω_1 and ω_2 if the reaction is slow. In the limit of very rapid reaction one will observe a single line.

Another example is the proton resonance line in solid hydrogen. The rotational level of orthohydrogen ($J=1$) will be split into three sublevels if the rotation is hindered in the crystal by some crystalline field. The dipolar interaction of hydrogen atoms will give different resonance frequencies in these sublevels. Thermal agitation will, on the other hand, induce transition between sublevels. Thus one would expect a change in the resonance spectrum with temperature. This is the model adopted by PURCELL and REIF⁽⁸⁾ to explain a growth of the central peak when the temperature is increased. This kind of problem is easily solved using Eq. (30) and (31).

6. - Concluding remarks.

The above is certainly only one simple case of the theory, but it will be enough to show certain features of the problem. It is sometimes essential to treat the problem with direct connection to quantum mechanics. It is, however, to be noticed that simple theories of such kinds as discussed here will be very helpful for a mathematical formulation and also for a physical understanding, in order to develop a quantum mechanical or dynamical theory.

A recent work of BLOCH⁽⁹⁾ is quite interesting from this point of view.

⁽⁸⁾ F. REIF and E. M. PURCELL: *Phys. Rev.*, **91**, 631 (1953).

⁽⁹⁾ F. BLOCH: *Phys. Rev.*, **102**, 104 (1956).

APPENDIX I

Let the Hamiltonian of the magnetic system be denoted by \mathcal{H} and the energy due to the external field by $\mathcal{H}'(t)$. The latter is

$$(A1.1) \quad \mathcal{H}' = -H_1(t)M,$$

where $H_1(t)$ is the magnetic field varying with time (a constant field is included in \mathcal{H}). The equation of motion of the density matrix ϱ of the system is

$$(A1.2) \quad \dot{\varrho}(t) = \frac{1}{i\hbar} [\mathcal{H} + \mathcal{H}'(t), \varrho(t)].$$

Transforming Eq. (A1.2) into the interaction representation, i.e.,

$$\varrho(t) = \exp[-i\mathcal{H}/\hbar] \bar{\varrho}(t) \exp[i\mathcal{H}/\hbar],$$

we have

$$(A1.3) \quad \dot{\bar{\varrho}}(t) = \frac{1}{i\hbar} [\bar{\varrho}(t), M(t)]H_1(t),$$

where $M(t)$, defined by

$$M(t) = \exp[i\mathcal{H}/\hbar]M \exp[-i\mathcal{H}/\hbar],$$

represents the Heisenberg motion of M . Eq. (A1.3) is easily integrated to give

$$\bar{\varrho}(t) = \bar{\varrho}(-\infty) + \frac{1}{i\hbar} \int_{-\infty}^t [\bar{\varrho}(-\infty), M(t')]H_1(t') dt' + 0(H_1^2).$$

Thus, to the first order in H_1 , $\varrho(t)$ is expressed as

$$(A1.4) \quad \varrho(t) = \varrho_0 + \frac{1}{i\hbar} \int_{-\infty}^t [\varrho_0, M(t'-t)]H_1(t') dt',$$

ϱ_0 being the equilibrium density matrix since we assume that the system was in equilibrium at $t = -\infty$. Eq. (A1.4) gives the expectation of M as.

$$\langle M(t') \rangle = \text{Tr} \varrho_0 M + \frac{1}{i\hbar} \int_{-\infty}^t \text{Tr} \{ [\varrho_0 M(t'-t)] \cdot H_1(t') M \} dt'.$$

Defining the deviation of M from the constant value

$$M_0 = \text{Tr } \varrho_0 M,$$

as $M'(t)$, we have

$$(A1.5) \quad \langle M'(t) \rangle = \frac{1}{i\hbar} \int_{-\infty}^t \text{Tr} \{ [\varrho_0 M'(t'-t)] \cdot H_1(t') M' \} dt'.$$

This corresponds to the representation (5) in the text, when the relaxation function (tensor) is defined as

$$(A1.6) \quad \frac{d\varphi_{xy}(\tau)}{d\tau} = \frac{i}{\hbar} \text{Tr } \varrho_0 [M'_x(\tau), M'_y] = \frac{i}{\hbar} \text{Tr} [\varrho_0 M'_x(\tau)] M'_y.$$

If the equilibrium density matrix is taken as

$$\varrho_0 = \exp [-\beta \mathcal{H}] / \text{Tr } \exp [-\beta \mathcal{H}], \quad (\beta = 1/kT),$$

Eq. (A1.6) can be transformed into

$$(A1.7) \quad \varphi_{xy}(\tau) = \int_0^\beta \text{Tr } \varrho_0 \exp [\lambda \mathcal{H}] M'_x(\tau) \exp [-\lambda \mathcal{H}] M'_y d\lambda.$$

For this we may use the identity

$$\begin{aligned} (A, \exp [-\beta \mathcal{H}]) &= \exp [-\beta \mathcal{H}] \int_0^\beta \exp [\lambda \mathcal{H}] [\mathcal{H}, A] \exp [-\lambda \mathcal{H}] d\lambda = \\ &= \frac{\hbar}{i} \exp [-\beta \mathcal{H}] \int_0^\beta \exp [\lambda \mathcal{H}] \dot{A} \exp [-\lambda \mathcal{H}] d\lambda. \end{aligned}$$

With the use of this (A1.6) is rewritten and integrated to give (A1.7). It is evident that (A1.7) goes in the limit $\hbar \rightarrow 0$ to

$$\varphi_{xy} = \frac{1}{kT} \text{Tr } \varrho_0 \{ M'_x(\tau) M'_y \} = \frac{1}{kT} \langle \{ M'_x(\tau) M'_y \} \rangle.$$

The easiest way to reach Eq. (2) from (A1.7) is to write down the expression explicitly in the representation which diagonalizes \mathcal{H} . Another way is to use

the formula

$$(A1.8) \quad \int_{-\infty}^{\infty} \text{Tr } \varrho_0 A B(t) \exp[-i\omega t] dt = \exp[\beta\hbar\omega] \int_{-\infty}^{\infty} \text{Tr } \varrho_0 B(t) A \exp[-i\omega t] dt.$$

which holds provided that the functions $\langle AB(t) \rangle$ and $\langle B(t)A \rangle$ vanish for $t = \pm\infty$ (relaxation) and that they have no singularity for $0 \geq I_m t \geq i\hbar\beta$. We shall not give here a general discussion, but only mention that $\varphi_{xx}(\tau)$ is symmetric in τ so that

$$\begin{aligned} \int_0^{\infty} \varphi_{xx}(t) \cos \omega t &= \frac{1}{2} \int_{-\infty}^{\infty} \varphi_{xx}(t) \exp[-i\omega t] dt = \frac{1}{2} \int_{-\infty}^{\infty} \int_0^{\beta} \text{Tr } \varrho_0 \exp[\lambda \mathcal{H}] M'_x(t) \cdot \\ &\cdot \exp[-\lambda \mathcal{H}] M'_x(0) \exp[-i\omega t] dt d\lambda = \frac{1}{2} \int_{-\infty}^{\infty} \int_0^{\beta} \text{Tr } \varrho_0 M'_x(t - i\hbar\lambda) M'_x(0) \exp[-i\omega t] dt d\lambda. \end{aligned}$$

The last expression is transformed as

$$\begin{aligned} \frac{1}{2} \int_{-\infty}^{\infty} dt \int_0^{\beta} d\lambda \text{Tr } \varrho_0 M'_x(t - i\hbar\lambda) M'_x(0) \exp[-i\omega(t - i\hbar\lambda) + \hbar\omega\lambda] &= \\ = \frac{1}{2} \int_{-\infty}^{\infty} dt \int_0^{\beta} d\lambda \exp[\hbar\omega\lambda] \text{Tr} \{ \varrho_0 M'_x(t) M'_x(0) \} \exp[-i\omega t] &= \\ = \frac{\exp[\beta\hbar\omega] - 1}{\hbar\omega} \cdot \frac{1}{2} \int_{-\infty}^{\infty} dt \text{Tr} \{ \varrho_0 M'_x(t) M'_x(0) \} \exp[-i\omega t], \end{aligned}$$

where we assumed the regularity of the function $\text{Tr } \varrho_0 M'_x(t) M'_x(0)$ as mentioned above. The last expression is transformed with the use of (A1.8) into

$$\begin{aligned} \frac{\exp[\beta\hbar\omega] - 1}{\hbar\omega} \cdot \frac{1}{1 + \exp[\beta\hbar\omega]} \cdot \frac{1}{2} \int_{-\infty}^{\infty} dt \text{Tr } \varrho_0 \frac{1}{2} (M'_x(t) M'_x(0) + M'_x(0) M'_x(t)) \exp[-i\omega t] &= \\ = \frac{1}{2\hbar\omega} \text{tgh} \frac{\beta\hbar\omega}{2} \cdot \int_0^{\infty} dt \text{Tr } \varrho_0 \{ M'_x(t) M'_x(0) \} \cos \omega t, \end{aligned}$$

which is Eq. (2) in the text. The regularity condition used here is actually the same as one would assume when explicit matrix representations are used, to assure the interchange of the double summation and the convergence of that double series.

APPENDIX II

Derivation of Eq. (18).

By definition, we may write

$$(A2.1) \quad g(t) = \lim_{N \rightarrow \infty} \langle \exp [i \sum_{j=1}^N \omega'(t_j) \Delta t] \rangle \quad \left(\Delta t = \frac{t}{N} \right),$$

where t_j marks equally dividing time points. An important formula for a multidimensional Gaussian (normal) distribution is

$$(A2.2) \quad \int_{-\infty}^{\infty} \dots \int_{-\infty}^{\infty} \exp \left[-\frac{1}{2} \sum_i \sum_j a_{ij} x_i x_j - i \sum_j s_j x_j \right] dx_1 \dots dx_N = \\ = \frac{(2\pi)^{N/2}}{|\det(a_{ij})|^{\frac{1}{2}}} \exp \left[-\frac{1}{2} \sum \sum A_{jk} s_j s_k \right],$$

where A_{jk} represent the matrix inverse to (a) , that is,

$$(A_{jk}) = (a_{jk})^{-1}.$$

Eq. (A2.2) tells us at once that $\overline{x_j x_k}$, the average of $x_j x_k$ over the Gaussian distribution, is given by

$$(A2.3) \quad \overline{x_j x_k} = A_{jk}.$$

This is easily seen by differentiating (A2.2) with respect to s_j and s_k and putting $s_j = 0$ afterwards. Applying (A2.2) and (A2.3) to (A2.1), we get

$$(A2.4) \quad g(t) = \lim_{N \rightarrow \infty} \lim \exp \left[-\frac{1}{2} \sum \langle \omega'(t_j) \omega'(t_k) \rangle \Delta t^2 \right] = \\ = \exp \left[-\frac{1}{2} \int_0^t \int_0^t \langle \omega'(t_1) \omega'(t_2) \rangle dt_1 dt_2 \right].$$

Further, we assume the stochastic process $\omega'(t)$ to be stationary so that the above formula may be written as

$$g(t) = \exp \left[-\int_0^t (t - \tau) \langle \omega'(\tau) \omega'(0) \rangle d\tau \right],$$

using the condition

$$\langle \omega'(t_1) \omega'(t_2) \rangle = \langle \omega'(t_1 - t_2) \omega'(0) \rangle.$$

APPENDIX III

Derivation of Eq. (28 - 31).

A Markoffian process is defined by the Chapman-Kolomologov equation.

$$(A3.1) \quad P_{jk}(t) = \sum_m P_{jm}(t - \tau) P_{mk}(h),$$

where $P_{jk}(t)$ is the probability that a system will be found in the state k after the time t when it was in j at $t = 0$. Under the assumption that

$$P_{jj}(t) = 1 - C_j t + o(t),$$

$$P_{jk}(t) = C_j p_{jk} t + o(t),$$

(for small t) (A3.1) is transformed into the differential equation

$$(A3.2) \quad \dot{P}_{jk}(t) = -C_k P_{jk}(t) + \sum_m P_{jm}(t) C_m p_{mk},$$

where p_{mk} is the transition probability for the jump from m to k and satisfies the condition

$$(A3.3) \quad \sum_k p_{mk} = 1.$$

Let us write Eq. (A3.2) as

$$(A3.4) \quad \dot{q}_l = -\varphi_l D,$$

where φ_l is the row vector

$$(A3.5) \quad \varphi_l = (P_{l1}, P_{l2}, \dots, P_{lr}),$$

Eq. (A3.4) is the same as Eq. (26) except that here the suffix l is explicitly written to indicate the initial state at $t = 0$. The equilibrium distribution (the existence of which we naturally assume) is independent of l and is the unique solution of

$$(A3.6) \quad \dot{q}^0 = 0 \quad \text{or} \quad \varphi^0 D = 0,$$

where φ^0 is the row vector

$$\varphi^0 = (P_1^0, P_2^0, \dots, P_r^0),$$

P_j^0 being the probability of j -th state in equilibrium. Corresponding to the existence of φ^0 , the column vector

$$\psi_0 = \begin{pmatrix} 1 \\ 1 \\ \cdot \\ \cdot \\ \cdot \\ 1 \end{pmatrix},$$

satisfies

$$D\psi_0 = 0.$$

Now we introduce the matrix $Q_{jk}(t)$ by the definition

$$(A3.8) \quad Q_{lk}(t) = \left\langle \exp \left[i \int_0^t \omega'(t') dt' \right] \right\rangle_k,$$

that is the expectation of $\exp \left[i \int_0^t \omega'(t') dt' \right]$ under the condition that the system is initially in the l -th state and finds itself in the k -th state after the time t . Corresponding to (A3.1) we see that this satisfies the equation

$$(A3.9) \quad Q_{lk}(t) = \sum_m Q_{lm}(t - \tau) Q_{mk}(\tau).$$

Now we have

$$Q_{jj}(\tau) = (1 - C_j \tau) \exp[i\tau\omega_j] + o(\tau),$$

$$Q_{jk}(\tau) = C_j p_{jk} \tau + o(\tau),$$

so that Eq. (A3.9) is transformed into

$$(A3.10) \quad \dot{Q}_{lk}(t) = (i\omega_k - C_k)Q_{lk}(t) + \sum_m Q_{lm}(t)C_m p_{mk}.$$

which is in a concise form

$$(A3.11) \quad \dot{Q}(t) = iQ\Omega - QD,$$

Q being a matrix and Ω being the matrix with the diagonal elements $\omega_1 \dots \omega_r$. (A3.11) is solved easily to give

$$Q(t) = Q(0) \exp[(i\Omega - D)t].$$

Since we assume the equilibrium distribution for the unperturbed state the initial distribution is q^0 , and the final state should be summed up over all possible states. Thus we find that

$$(A3.12) \quad g(t) = \varphi_0 \exp [(i\Omega - D)t] \varphi^0,$$

is the generating function to give the intensity distribution.

We may define a row vector $u(t)$ by

$$u(t) = \varphi_0 \exp [(i\Omega - D)t],$$

which satisfies the equation

$$(A3.13) \quad \dot{u}(t) = u(t)(i\Omega - D), \quad u(0) = \varphi_0.$$

The intensity distribution of the absorption is given by

$$\begin{aligned} (A3.14) \quad I(\omega) &= \frac{1}{2\pi} \int_{-\infty}^{\infty} g(t) \exp[-i\omega t] dt \\ &= \frac{1}{2\pi} \int_{-\infty}^{\infty} u(t) \cdot \varphi_0 \exp[-i\omega t] dt \\ &= \frac{1}{\pi} \operatorname{Re} \int_0^{\infty} u(t) \exp[-i\omega t] dt \cdot \varphi_0. \end{aligned}$$

The last expression introduces

$$(A3.15) \quad x_j(\omega) = \int_0^{\infty} u_j(t) \exp[-i\omega t] dt,$$

in terms of which $I(\omega)$ is written as

$$I(\omega) = \frac{1}{\pi} \operatorname{Re} \sum_j x_j(\omega).$$

Eq. (A3.13) is Eq. (28), and $x_j(\omega)$ defined by (A3.15) satisfy the vector equation

$$x(\omega)(i\omega - \Omega) + x(\omega)D = q^0,$$

which is Eq. (31) of the text.

The Concept of Temperature in Magnetism.

J. H. VAN VLECK

Harvard University - Cambridge, Mass.

Simultaneous temperatures.

In these lectures I shall discuss three thermal phenomena in magnetism, viz. the Overhauser effect, the Bloembergen exchange energy reservoir, and negative temperatures, all rather different. There is, however, a unifying thread in these diverse topics, for they all relate to the co-existence of systems at different temperatures when the thermal contacts between them are weak. Somewhat surprising effects can result, and the title strange thermal phenomena in magnetism would perhaps be more descriptive, but we use the title that we do because in our opinion the study of these three examples helps us understand conceptually the role of temperature in the Boltzmann distribution factors involved in magnetic problems.

When a single temperature is relevant, the Boltzmann factor has the form $\exp[-\mathcal{H}/kT]$. In our examples, we will be concerned with two or three terms in the Hamiltonian function which are associated with different temperatures, so that the distribution function is,

$$(1) \quad \exp \left[\frac{\mathcal{H}_1}{kT_1} - \frac{\mathcal{H}_2}{kT_2} \right] \quad \text{or} \quad \exp \left[-\frac{\mathcal{H}_1}{kT_1} - \frac{\mathcal{H}_2}{kT_2} - \frac{\mathcal{H}_3}{kT_3} \right].$$

Obviously, distributions of this kind are at best quasi-stationary. The different components must be kept at their respective temperatures through external agencies, and the contacts between the different parts must be small for otherwise the various temperatures will equalize themselves when equilibrium is reached. Situations of this type are well known classically. For instance, we often consider transport of heat between two boxes of stirred gases respectively at temperature T_1 and T_2 , and the collective distribution function

is indeed of the first type in (1) if \mathcal{H}_1 denotes the translational kinetic energy of box 1, and \mathcal{H}_2 that of box 2. We are rather less used to thinking of simultaneous temperatures for systems which are not physically separated, as when \mathcal{H}_1 , \mathcal{H}_2 , \mathcal{H}_3 relate to different terms in the magnetic energy of a given volume element. Analogous classical examples are, however, by no means unknown. In acoustical theory, for example, one often deals with different rotational and translational molecular temperatures. In our applications \mathcal{H}_1 , \mathcal{H}_2 , \mathcal{H}_3 are quantum mechanical matrices rather than ordinary classical functions. The concept of a quantum mechanical density matrix, however, has become a familiar one, and there is no reason why the temperatures for different Boltzmann factors need be the same in order for the concept of a matrix representing distribution to have meaning.

If we have a system with two constituents at different temperatures T_1 , T_2 the coupling between them will tend to equalize these two temperatures as one would expect. Very strange things, however, can happen when we have a system of which three components are at temperatures T_1 , T_2 , T_3 wherein T_1 and T_2 are preserved because of external agencies or large heat capacities, and component 3 has as its only external contact transfer processes in which there are simultaneous changes in the energies of components 1 and 2. It turns out that T_3 need not be intermediate between T_1 and T_2 . This is the case in Overhauser effect; here T_1 , T_2 , T_3 correspond respectively to the temperatures T_g , T_k , T_i which we will explain shortly.

1. - The Overhauser effect.

In the Overhauser effect⁽¹⁾, one deals with a paramagnetic metal with nuclear spin, usually a feebly paramagnetic alkali, in which the paramagnetism arises from the conduction electrons. A strong constant magnetic field H is applied, whose direction we take as the z axis. The electrons are exposed to a microwave field of a frequency which is resonant to the value of H employed and which is powerful enough to give a considerable degree of saturation. The nuclear resonance is observed with a weak r.f. field of appropriate frequency. It is found that saturating the electronic system enhances the nuclear resonance. This is the opposite behavior from what one would naively expect. Saturation tends to equalize the population of the upper and lower Zeeman states, and so produce a higher effective temperature. One might anticipate that the nuclear resonance is correspondingly weakened. Actually, the reverse is found. The explanation of this paradox, as we shall see, is that the electronic and nuclear Zeeman temperatures are not the same, and that when one is raised the other is lowered.

(1) A. OVERHAUSER: *Phys. Rev.*, **91**, 476 (1953); **92**, 411 (1953).

Let T_z be the electron Zeeman temperature. This is the temperature associated with the distribution between Zeeman components of a given level. Notice that this is not necessarily the temperature associated with the electronic distribution among the different translational levels. In our opinion, the concept of a Zeeman temperature different from other temperatures is a fruitful one, although it is not yet very much used in the literature. Let T_k be the temperature of the electronic translational motion, and finally let T_I be the Zeeman temperature for the nuclei.

Let us first use Boltzmann statistics. Then in treating the interaction of a conduction electron with a nuclear spin the relevant distribution function is

$$(2) \quad \exp \left[-\frac{k^2 \hbar^2}{8\pi^2 m^* k T_k} \right] \exp \left[-\frac{g\beta H S_z}{k T_z} \right] \exp \left[\frac{g_I \beta_N H I_z}{k T_I} \right],$$

where β and β_N are respectively electronic and nuclear Bohr magnetons. The gyromagnetic ratio of the electron is negative and is $-ge/2mc = -g\beta/(\hbar/2\pi)$ since the ordinary electronic g -factor is defined in such a way as to be positive. The electron spin Zeeman energy is correspondingly $+g\beta H S_z$. The nuclear g factor is so defined that $+g_I \beta_N/(\hbar/2\pi)$ is the nuclear spin gyromagnetic ratio. The nuclear Zeeman energy is hence $-g_I \beta_N H I_z$, and this fact explains the different sign of the two Zeeman terms in (2). Most nuclei have a positive g_I , but cases are known for which g_I is negative. The interaction Hamiltonian, which is considered too small to figure in the Boltzmann factor is

$$(3) \quad \mathcal{H}_{\text{inter}} = (8\pi/3)\beta\beta_N g g_I (\mathbf{I}_j \cdot \mathbf{S}_k) \delta(r_{jk}),$$

where r_{jk} is the distance from nucleus j to electron k . The expression (3) is of the « Fermi » or « contact » type and is the most important part of the hyperfine interaction. Its structure requires particular comment. It represents an interaction in which $I_z + S_z$ is conserved, and this fact is essential to the existence of the Overhauser effect. A transition in which $\Delta S_z = +1$ also implies $\Delta I_z = -1$, and vice versa.

There are two ways of handling transfer processes. One is to use time-dependent perturbation theory, the other to apply conservation of energy, including enough ingredients in the system so that the total energy is necessarily conserved. We will follow the latter procedure. Let us consider a process of the following type

$$(4) \quad (I_z, S_z, k) \leftrightarrow (I_z - 1, S_z + 1, k').$$

Conservation of energy requires that

$$(5) \quad E'_k = E_k - Hg\beta - Hg_I\beta_N.$$

The number of transitions from left to right in (4) is equal to the transition probability A times the triple product of the occupancy factors N_k , N_{s_z} , N_{I_z} for the states participating in the process, and is hence, $AN_k N_{s_z} N_{I_z}$. The corresponding expression for the inverse process is $A'N_k' N_{s_z-1} N_{I_z-1}$. The principle of detailed balancing tells us that $A = A'$.

A quasi-stationary condition is reached when the number of systems undergoing the transitions \rightarrow and \leftarrow are equal, to wit when

$$(6) \quad \frac{N_{k'}}{N_k} \frac{N_{s_z+1}}{N_{s_z}} \frac{N_{I_z-1}}{N_{I_z}} = 1.$$

Using the Boltzmann factors (2) and the conservation of energy (5), we can write (6) in the form

$$(7) \quad \exp \left[-\frac{H(g\beta + g_I\beta_N)}{kT_k} \right] \exp \left[-\frac{Hg\beta}{kT_z} \right] \exp \left[-\frac{Hg_I\beta_N}{kT_I} \right] = 1,$$

and so

$$(8) \quad \frac{1}{T_I} = \frac{(g\beta + g_I\beta_N)}{g_I\beta_N T_k} - \frac{g\beta}{g_I\beta_N T_z}.$$

The calculation which we have presented has been on the basis of the Boltzmann statistics. Actually one should use the Fermi-Dirac statistics. However, Eq. (7) still retains its validity. One way of seeing that this is true is to note that with F.D. statistics the upward and downward precesses are respectively proportional to $f_1(1-f_2)$ and $f_2(1-f_1)$, where f_1 and f_2 are the occupancy factors for the lower and upper state. Since

$$f = \frac{1}{\exp[(E_i - \zeta)/kT] + 1},$$

the ratio

$$\frac{f_2(1-f_1)}{f_1(1-f_2)},$$

has the same value

$$\exp[-(E_2 - E_1)/kT]$$

as the occupancy ratio in Boltzmann statistics, and the condition for the process $N_{I_z}, N_{s_z}, N_k \leftrightarrow N_{I_z}, N_{s_z}, N_k$ being stationary, i.e. having as many upward or downward transitions, is the same as before. More fundamentally, one can see that the F.D. statistics do not modify the fundamental equations because F.D. statistics can be regarded merely as the application of Boltzmann statistics to the whole solid regarded as one big system but with only

such states as can be described by antisymmetric wave functions. The condition $A = A'$ applies to each individual transition of the ensemble, and so (7) remains valid; Eq. (6) does if we consider individual states of the ensemble, and do not incorporate what is essentially a weight factor for the distribution function for the individual atoms as compared to the complete system.

If the electronic spin is completely saturated (equal population in its upper and lower states) the temperature T_z can be regarded as infinite. There is no corresponding increase in T_k , since the electronic translational system serves as a reservoir because of its good heat contacts and high heat capacity. As a first approximation, we can hence identify T_k with the ordinary room temperature T . Actually because of r.f. heating T_k is higher than T , and is about 70 °C in the experiments of CARVER and SLICHTER. Furthermore, β is enormously greater than β_N and so

$$(9) \quad T_I = T_k (g_I \beta_N / g \beta).$$

The sign of (9) requires particular comment. In most cases such as the stable alkali isotopes, the nuclear g_I 's are positive. There are, however, a few nuclei which have negative gyromagnetic ratios and hence negative values of g_I . In the Overhauser effect, such nuclei should yield negative temperatures, such as we discuss later. Existing measurements, however, are on materials for which g_I is positive.

In the case of ^7Li , $g\beta$ is $1690 g_I \beta_N$, and we are led to the prediction

$$(10) \quad T_I = T_k / 1690.$$

The Overhauser effect thus offers the possibility of an enormous reduction in T_I , and hence an enormous enhancement of the nuclear resonance absorption, which is proportional to

$$[N_I - N_{I-1}] \sim \frac{g_I \beta_N H}{k T_I (2I + 1)}.$$

CARVER and SLICHTER⁽²⁾ do indeed find that saturating the electronic system does indeed greatly increase the nuclear absorption, as Fig. 1 shows. The upper curve is one without the saturating microwave field. Here the nuclear resonance of ^7Li is lost in noise, but it shows up sharply in the middle curve, where this field has been applied. The lower curve is one of proton resonance in glycerin used merely for monitoring purposes.

The enhancement factor observed by CARVER and SLICHTER⁽²⁾ is less than

(²) T. R. CARVER and C. P. SLICHTER: *Phys. Rev.*, **92**, 212 (1953); **102**, 975 (1956) A quite different approach to the concept of temperature in the Overhauser effect has been developed by SLICHTER who shows that in a properly chosen rotating system, the nucleus and electron can be regarded as having the same temperature (*Phys. Rev.*, **99**, 1822 (1955)).

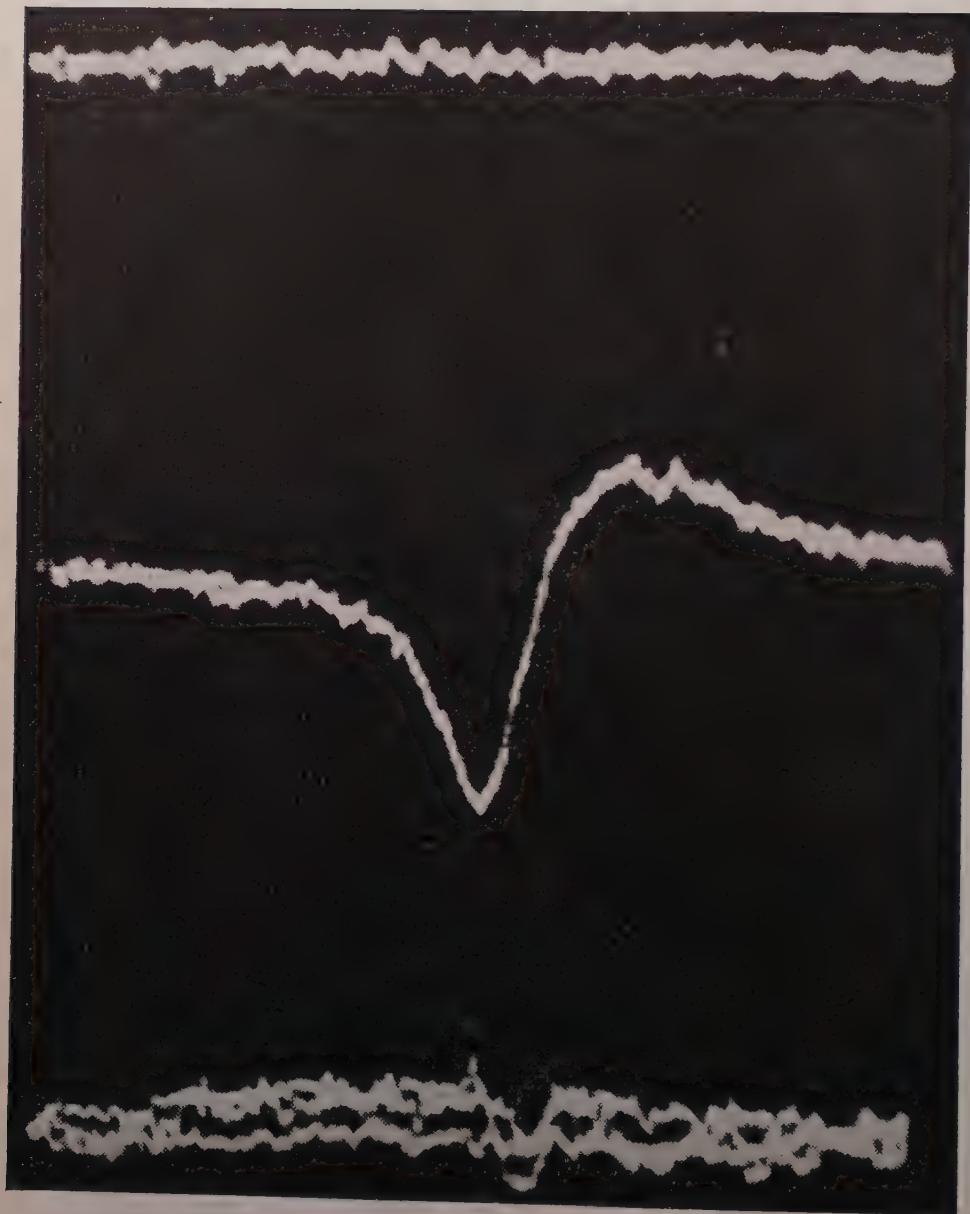


Fig. 1.

one tenth of that 1690 predicted by (10). One reason for the lower value is that the electron spin is not being completely saturated, and so, instead of being infinite, the electron Zeeman temperature is

$$(11) \quad T_z = T_k / (1 - s),$$

where s is the so-called saturation factor. A derivation and explanation of (11) is given in fine print below.

Derivation of Eq. (11). The calculation of the Pauli paramagnetism when the temperature parameters are different in the Zeeman and translational energies is obviously more complex than that which we made in our earlier lecture (series on the magnetism of metals) under the normal assumption $T_k = T_z$, especially since it is essential to use F.D. rather than Boltzmann statistics. The requisite generalization, however, becomes apparent when we remember that the Fermi-Dirac statistics are the distributions for individual, undifferentiated electrons obtained by applying Boltzmann statistics to the entire collection or supersystem regarded as a single unit.

The « super-partition function » is

$$(12) \quad Z = \sum [-(\mathbf{k}^2 \hbar^2 / 8\pi^2 m^* T_k) - (\beta g S_z H / k T_z)],$$

where now the unit is the entire solid rather than individual atom.

We note that Z is a function of the ratio H/T_z and of T_k . Therefore, the magnetic moment

$$(13) \quad M = NkT_z \frac{\partial \log Z}{\partial H},$$

can also be written as

$$(14) \quad M = Nk \frac{\partial \log Z}{\partial (H/T_z)}.$$

Without going into any detail we can see that M is a function of T_k and H/T_z alone:

$$M = \varphi(T_k, H/T_z).$$

The formula for the moment must yield the same result for the moment as a calculation based on the F.D. statistics when we use one atom as a unit. From our calculations of the Pauli spin susceptibility, we know that at ordinary temperatures and field strengths the moment is of the form:

$$(15) \quad M = aH,$$

a being independent of field and temperature. In our case, because of the above functional dependence, one sees that in the region in which M is linear in H

$$(16) \quad M = aH \frac{T_k}{T_z}.$$

When the two temperatures coalesce, (15) is restored. Saturation consists essentially in increasing T_z with respect to T_k ; it is commonly calibrated by the saturation parameter s . The quantity $1 - s$ is the ratio of the moment in the presence of the saturating microwave field to that in its absence, with the tacit understanding that the lattice temperature is unaltered. In terms of our temperature concepts, the saturation parameter is seen to have the significance

$$(17) \quad 1 - s = \frac{T_k}{T_z}.$$

By means of (17) we can eliminate T_z in the formula (8) for equilibrium if we wish to be more conventional and express our results in terms of s rather than T_z .

Actually, there is another effect which gives a far more important correction than that for incomplete saturation. Besides the Overhauser processes, which are essentially triple collisions, there is another type of nuclear collision, wherein the nuclei simply exchange energy with the lattice. The «lattice» here does not mean thermal vibrations, but represents the diffusion of the ions, like in a liquid. Let τ_l be the relaxation time for such a process, and τ_o the relaxation time for the Overhauser electronic-spin nucleus interaction, which we have discussed. Then, in the approximation in which all the exponentials are small, we can write the condition of equilibrium as

$$(18) \quad \frac{1}{\tau_o} + \frac{1}{\tau_l} = \frac{1}{\tau_o} \left[1 - \frac{g_I \beta_N H}{k T_I} - \frac{g \beta H (1 - s)}{k T_k} + \frac{(g \beta + g_I \beta_N) H}{k T_k} \right] + \\ + \frac{1}{\tau_l} \left[1 - \frac{g_I \beta_N H}{k T_I} + \frac{g \beta_N H}{k T_l} \right].$$

Here T_l is the temperature of the lattice, that is, the ordinary room temperature; in good approximation it is equal to T_k . If $\tau_l \ll \tau_o$, the controlling factor is the second member, and the nuclear temperature τ_l is approximately equal to τ_i ; whereas if $\tau_l \gg \tau_o$, the Overhauser mechanism predominates and (8) is a good approximation. In actual practice it is not warranted to neglect either member of (18); in other words, the Overhauser process is to a certain extent short-circuited by more orthodox processes in which the distribution of electronic spins is not involved.

In the experiments carried out for Li, s was about .7; from the measurements of HOLCOMB and NORBERG on relaxation time and line-widths, CARVER and SLICHTER⁽²⁾ deduce in a rather devious and perhaps questionable fashion that $\tau_o/\tau_l = 8$.

The theory which we have presented predicts that with perfect saturation and no short-circuiting the nuclear resonance is enhanced by a factor 1690. By taking into account the non-complete saturation and other corrections, i.e. using (18) rather than (9), the factor is cut down to 140, while the expe-

periments give 110, in fairly good agreement. In the case of Na the saturation is less (.01) and one gets a much less pronounced Overhauser effect.

It cannot be too strongly emphasized that the conventional Overhauser effect is based on the predominance of « Fermi » or « contact-type coupling » (3). With predominantly dipolar coupling, transitions of the type $I_z, S_z \leftrightarrow I_z + 1, S_z + 1$ are more prevalent than those of the category $I_z, S_z \leftrightarrow I_z - 1, S_z + 1$. As a result, the value of T_i ultimately changes sign if the dipolar coupling becomes sufficiently pronounced compared to the Fermi type (3). The normal sign is observed (2) in the proton resonance in anhydrous NH_3 containing Na. This fact shows that the electrons liberated by the sodium ions penetrate the NH_3 system and have appreciable contact with the protons.

2. — The Bloembergen exchange-energy reservoir.

The idea that in the phenomena of spin-lattice relaxation there may be two temperatures, one of the spin system, the other of the lattice is a comparatively old and well-established one dating back to the classic thermodynamical theory of CASIMIR and DU PRÉ (4). More recently, BLOEMBERGEN and WANG (5) have suggested that there may be two temperatures within the spin system,—one T_z relating to the distribution of Zeeman energy $\mathcal{H}_z = \sum g\beta H S_z$, the other T_e to the exchange energy $\mathcal{H}_{ex} = -2 \sum J_{ij} \mathbf{S}_i \cdot \mathbf{S}_j$. Neither need necessarily be the same as that T_l of the lattice vibrations, whose Hamiltonian function we denote by \mathcal{H}_l . If all three temperatures co-exist, the distribution function is of the form

$$(19) \quad \exp \left[-\frac{\mathcal{H}_z}{kT_z} \right] \exp \left[-\frac{\mathcal{H}_{ex}}{kT_e} \right] \exp \left[\frac{\mathcal{H}_l}{kT_l} \right].$$

There can be energy exchange between the Z and ex systems because of dipolar interaction, between the ex and l systems because of the modulation of exchange or dipolar energy by lattice vibrations, and between the Z and l systems because of the modulations of dipolar energy by lattice vibrations. The corresponding relaxation times will, following BLOEMBERGEN and WANG, be denoted by t_{He} , t_{el} , t_{Hl} . The situation is shown symbolically in Fig. 2, taken from their paper. BLOEMBERGEN and WANG give convincing arguments that

(3) Cf. F. BLOCH: *Phys. Rev.*, **93**, 944 (1954) and the interesting experiments of I. SOLOMON on the controlled or generalized Overhauser effect (*Phys. Rev.*, **99**, 559 (1955)).

(4) H. B. G. CASIMIR and F. K. DU PRÉ: *Physica*, **5**, 507 (1938).

(5) N. BLOEMBERGEN and S. WANG: *Phys. Rev.*, **93**, 72 (1954).

when the exchange energy is large, as in ferrites or anhydrous salts, the transfer of energy between the Zeeman components and the lattice via the direct t_{Hl}

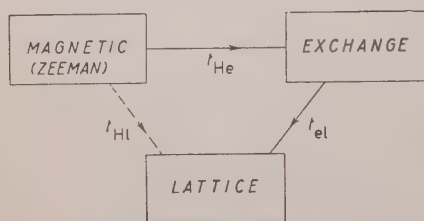


Fig. 2.

process is negligible compared to that via the route t_{He} followed by t_{el} . It is, in fact, clear theoretically that the direct route should be of minor importance, for the lattice vibrational modulation of the dipolar interactions is the smallest of the types of perturbation we have mentioned if the exchange energy is large. (T_{He} can result from dipolar interaction without invoking vibrations.) If α_{He} , α_{el} be respectively

the Zeeman-exchange and exchange-lattice heat conductivities, and if the temperature differences are small enough that the heat transfer is linear therein, then T_e is connected with T_z , T_l by the relation

$$\frac{T_z - T_e}{T_e - T_l} = \frac{\alpha_{el}}{\alpha_{He}},$$

when heat is continuously being supplied to the Zeeman system by a r.f. field. BLOEMBERGEN and WANG give arguments to show that $\alpha_{el} \gg \alpha_{He}$. For one thing, the fact that in a material such as the organic free radical which they study (α - α -diphenyl- β -picryl-hydrazil) the relaxation is independent of temperature is evidence that the bottleneck arises from the α_{He} rather than α_{el} part, for otherwise it would be strongly dependent on temperature. The relaxation time t_{el} is, to be sure, probably longer than t_{He} ,—in fact one of the arguments which BLOEMBERGEN and WANG advance is that a shorter relaxation time than one would estimate for t_{el} is observed in decay experiments. Although t_{el} is larger than t_{He} , the specific heat is much larger for the exchange than for the Zeeman system. The conductivity is essentially the quotient of specific heat by relaxation time. The specific heat of the exchange system is so much greater than that associated with redistribution of the Zeeman components that T_e is much closer to T_l than T_z in the materials with large exchange energy which they study.

The main purpose of the present discussion is not, however to discuss the relative magnitudes of T_z , T_e , T_l but rather to stress that more exact physical significance can be given to the temperatures T_z and T_e than BLOEMBERGEN and WANG realized. They introduced the temperatures in a qualitative order of magnitude fashion, but actually a certain degree of quantitative significance can be given to a Zeeman temperature distinct from the exchange energy. The point is essentially that the Zeeman and exchange

energies commute, and the existence of the exchange (unlike dipolar) coupling does not interfere with the imparting of a definite Zeeman temperature to the spin system by the magnetic field. Suppose first that one applies a slowly changing, otherwise constant magnetic field. The Zeeman energy is $Hg\beta M'$, where M' is the total magnetic quantum number of the entire crystal. If H changes adiabatically, the distribution of values is unchanged and T_z is proportional to H . If the unit were a single atom, this argument would be trivial. Actually for given M' , any value $\leq |M'|$ is possible for the spin quantum number S' of the crystal. There is a vast choice of different eigenvalues for the exchange energy because there is a great variety of quantum numbers associated with the various vector coupling possibilities for the component spin vectors compounded to S' . The point is that all the different Zeeman components have a distribution corresponding to one and the same T_z , unaffected by the value of the temperature parameter T_e which determines the distribution of the exchange eigenvalues.

Now let us consider the case of heating by a r.f. field. In his thesis ⁽⁶⁾, Bloembergen points out that for a free atom not subject to any coupling or crystalline field, the effect of a r.f. field applied perpendicular to a constant field is simply to redistribute the atoms among the Zeeman components in such a way as can be accounted for simply by changing the Zeeman temperature as a parameter. In other words, without any external agency except the r.f. field, the Zeeman components stay in thermal equilibrium, but with a slowly rising temperature. Bloembergen's proof runs essentially as follows. The rate of growth of the number of atoms N_M in a given Zeeman component M is given by

$$(20) \quad \frac{dN_M}{dt} = A_{M-1 \rightarrow M} N_{M-1} - A_{M \rightarrow M+1} N_M,$$

inasmuch as the r.f. field only induces transition probabilities of the form $\Delta M = \pm 1$. Here $A_{M \rightarrow M'}$ is the transition probability because of exposure to the r.f. field. Quantum mechanics shows that

$$(21) \quad A_{M \rightarrow M+1} = A[S(S+1) - M(M+1)],$$

where A is a constant proportional to the square of the r.f. field, but independent of the amount of spin S possessed by the atom. If originally the atoms were in thermal equilibrium, we have initially

$$(22) \quad N_M^0 = [N/(2S+1)] \exp[-Mg\beta H/kT_z],$$

⁽⁶⁾ N. BLOEMBERGEN: Thesis, «*Nuclear Paramagnetic Relaxation*», Leiden, 1948, p. 40. Here BLOEMBERGEN considers transitions caused by dipolar interaction rather than those caused by radiation, but the adaptation to our case is immediate.

where N is the total number of atoms. Here and elsewhere we suppose that the Zeeman energy is small compared to kT_z so that higher powers of the ratio $\beta H/kT_z$ can be disregarded. If we utilize (21) and (22), then (20) is the same as

$$(23) \quad dN_M/dt = 2AMN_M$$

to terms of the lowest, i.e. zero order in $\beta H/kT$. The important thing is that the rate of change of N_M is directly proportional to the product according to (23) of N_M and the magnetic quantum number M , with a proportionality factor independent of S or M . The redistribution of states yielded by (23) is thus the same as if the temperature in the Boltzmann factor changes at a rate given by

$$(24) \quad \frac{dT_z}{dt} = \frac{2AkT_z^2}{g\beta H}.$$

Our point is that we can use this same calculation more generally interpreting S and M as the total spin and total magnetic quantum number of the whole crystal, which we may denote by S' , M' . The absorption is determined by the resultant magnetic moment (assuming, as is well warranted, that the crystal dimensions are small compared to the r.f. wave length) and so the formula (21) for the transition probability still applies (*). Since the proportionality factor A does not involve S' or any of the other crystalline quantum numbers, the growth of population of any state of the crystal, regarded as a unit, is proportional to its population and the magnetic quantum number, with the proportionality constant unaffected by the exchange eigenvalue problem. Hence, the redistribution of states produced by the r.f. field is simply one that corresponds to a change in Zeeman temperature.

These arguments break down as soon as we consider the effect of crystalline fields, or if the perturbing effect of dipolar interaction is too large. The classification in Fig. 2 is predicated on the assumption that the exchange is large compared with the dipolar coupling, and it is the dipolar coupling which makes possible energy flow between the Zeeman (magnetic) and exchange systems.

The concepts of simultaneous Zeeman, exchange, and lattice temperatures help clarify the physical meaning of an adiabatic susceptibility. This quantity is usually introduced in a purely thermodynamic fashion that gives no particular insight into how it is generated. Adiabatic conditions clearly imply that

(*) It may be objected that if S' is large, $g\beta HS'/kT$ is not small compared to unity, so that development in the ratio $\beta H/kT$ is not warranted. However, states of small S' are vastly more abundant than those where S' is of the order N , and so the resulting error is not serious in a paramagnetic material where the distribution is not strongly polarized by the applied field.

heat flow between the lattice and spin system is slow, so that different spin and lattice temperature can co-exist. If there were no coupling of dipolar structure, the magnetic field would merely alter the Zeeman temperature, and the spin system having two temperatures (Zeeman and exchange) would not be in internal thermodynamical equilibrium. The concept of an adiabatic susceptibility assumes that there is such equilibrium. It could never be brought about if there were only Zeeman and exchange energy, for these energies commute in matrix multiplications. It is necessary to have some perturbing mechanism that spoils the constancy of the magnetic moment in order to bring about equalization of the two temperatures. Such a mechanism is provided by dipolar or pseudo-dipolar coupling. The necessity of such interaction as an equilibrator is not sufficiently appreciated. Without it we would have what BROER⁽⁷⁾ calls the isolated susceptibility, in which the moment changes only in virtue of induced moments rather than changes of population among the various Zeeman components. Such induced terms arise from a second order Zeeman effect, and are absent in the simple model which we have used, but appear when the complications of the crystalline field or spin-orbit interaction are introduced. A very rapidly varying alternating field whose period is short compared with the characteristic time associated with dipolar interaction may be too fast for an adiabatic susceptibility to be achieved. As a result an additional absorption or dispersion may be expected when the impressed frequency is comparable with the reciprocal of the dipolar relaxation time. In some of the Leiden relaxation experiments⁽⁸⁾, at very high frequencies there are indications of such an effect.

3. - Negative temperatures.

As our final example of strange thermal effects in magnetism, we shall consider the negative temperatures produced by PURCELL and POUND⁽⁹⁾. Their experiments are not just of interest as an obviously spectacular *tour de force*, but primarily because of the light which they throw on relaxation processes involving nuclear spins and because their interpretation requires close scrutiny of the meaning of temperature. The paper of PURCELL and POUND gives only the barest outline of the experiments. The purely philosophical or conceptual aspects are discussed in a later paper by RAMSEY⁽¹⁰⁾.

(7) L. J. F. BROER: *Physica*, **17**, 531 (1951). In this article BROER discusses the concept of adiabatic susceptibility in considerable detail.

(8) F. W. DE VRIJER and C. J. GORTER: *Physica*, **18**, 549 (1952).

(9) E. M. PURCELL and R. V. POUND: *Phys. Rev.*, **81**, 279 (1951).

(10) N. F. RAMSEY: *Phys. Rev.*, **103**, 20 (1956).

Before discussing the experiments specifically, we should mention first of all that there is nothing philosophically or physically unreasonable in the existence of negative temperatures, provided the range permitted for the energy of the system in question is bounded. This requirement is obviously necessary, as the Boltzmann factor $\exp[-E/kT]$ does not converge for $T < 0$ if the upper limit of E is infinite. (Correspondingly, we could not have positive temperatures if the lower limit of E were $-\infty$). It thus makes sense to talk about negative temperatures for a spin system decoupled from the lattice, since the secular equation for the spin system, which can include spin-spin and Zeeman energy, is of finite order, and there is a finite number of eigenvalues for the energy. On the other hand, it is not possible to have a negative temperature, for say, the translational energy of a gas, as it has no upper bound. The existence of a negative temperature simply means that the states of high energy are more probable than those of low energy. If one examines the statistical theory by which the Boltzmann distribution is derived, one finds that there is nothing a priori objectionable in the parameter $\lambda = 1/kT$ being negative; this situation simply means that the mean energy is higher rather than lower than that corresponding to the limit $T = \pm \infty$, where all states are populated equally. Even with $T < 0$ the various thermodynamical relations can be derived from statistical mechanics in the usual way; such mechanisms as the Carnot cycle, however, require some discussion⁽¹⁰⁾. Instead of using the temperature itself, it is in some ways more satisfactory and clearer to introduce the parameter $\lambda = 1/kT$ for it is less disturbing mentally to think of λ changing sign than of T switching from $-\infty$ to $+\infty$, as is the case when a system at negative temperatures cools off. A negative temperature implies that a system is very hot rather than very cold; as it cools off by thermal contact with the rest of the world, its temperature drops to $-\infty$, switches to ∞ (corresponding to sign change in λ) and then cools to the final equilibrium positive temperature.

The key to the experiments of PURCELL and POUND is found in two properties of the nuclear spin system of LiF, the material which they use. In the first place, the spin-lattice relaxation time for the Li and F nuclear spins at a temperature around 1 °K is quite large. Previous experiments of POUND⁽¹¹⁾ show that it is about 15 seconds; in fact small samples can be moved around in a time shorter than that required for spin and lattice temperatures to be equilibrated. In the second place, and this is even more fundamental, audio frequency resonance experiments of RAMSEY and POUND⁽¹²⁾ show that the spin-spin relaxation time, even in zero fields, is about 1/50 of a millisecond.

⁽¹¹⁾ R. V. POUND: *Phys. Rev.*, **81**, 156 (1951).

⁽¹²⁾ N. F. RAMSEY and R. V. POUND: *Phys. Rev.*, **81**, 278 (1951).

The latter time is sufficiently long, since a small magnetic field can be reversed in a shorter interval.

In the Purcell and Pound experiments the LiF crystal is first placed for some time at room temperature in a large magnet giving a field of 6400 gauss. The specimen is then quickly removed and placed inside a small solenoid, the axis of which is parallel to a field of about 100 gauss provided by a small permanent magnet. The transplanting is performed in a time short compared to the spin-lattice relaxation time, but long compared to the spin-spin relaxation time in small fields. The effect is the same as though the material were demagnetized adiabatically to a field of 100 gauss; the temperature of the LiF spin system becomes approximately $293(100/6400) \sim 5^\circ\text{K}$. The transplanting of the material from the large to the small permanent magnet is simply a matter of experimental convenience, as one cannot reverse an ordinary electromagnet rapidly, but one can create a field suddenly in a solenoid joined to a condenser. By discharge of a condenser, the solenoid is made to generate a field of -200 gauss very rapidly. The time constant of the process is only $0.2\ \mu\text{s}$, and hence short in comparison to the spin-spin relaxation time. The specimen is thus exposed very suddenly to a field of -100 rather than 100 gauss. The field from the solenoid decays with a time constant of about $1\ \text{ms}$, and thereafter the field to which the specimen is exposed reaches substantially its original value of 100 gauss.

A natural explanation of what is going on in these experiments is provided by our concept of unequal spin-spin and Zeeman temperatures. By the spin-spin temperature we mean that to be used in connection with the Hamiltonian function for dipolar coupling between the spins. The reversal of the field from $+100$ to -100 can be considered as taking place with infinite rapidity for practical purposes, so that if the initial spin temperature of the specimen in the small magnet is, say, 5°K , the spin-spin temperature after reversal is 5°K and the Zeeman temperature -5°K . In other words, the density matrix is $\exp[-(H_{ss}/5k) + (H_z/5k)]$; the occurrence of the negative Zeeman temperature merely says that the contribution of the Zeeman energy to the Boltzmann factor is a function only of H/T , and so reversal of H requires reversal of T if the same distribution is maintained. There is no reversal in the sign of T_{ss} , since the spin-spin (dipole-dipole) Hamiltonian function does not involve the applied field. Ultimately, of course, the spin-spin and Zeeman temperatures must be the same, i.e. the spin system must be in equilibrium with itself. If the initial field of -100 after reversal could somehow be maintained, and there be no transfer to the lattice system, the final spin temperature would be that which corresponded to the same total internal energy as immediately after reversal. The mean energy of any part of the system is inversely proportional to its corresponding effective temperature (*), since the

(*) Both the spin-spin and Zeeman energies average to zero when all states are

energy quanta with which we are concerned are small compared to kT . The spin-spin interaction energy corresponds to an «inner» or effective magnetic field of about 30 gauss, and the energy in arbitrary units is $(H_0^2 + H^2)/T$ with $H_0 = 30$, $H = 100$. The effective final spin temperature T_H in the presence of the field is thus given approximately by the relation

$$\frac{1}{T_H} [(30)^2 + (100)^2] = \frac{(30)^2}{5} - \frac{(100)^2}{5},$$

so that T_H is about -6°K . Only qualitative or at most semi-quantitative significance should, however, be given to our estimates of negative temperatures, for the distribution of spin-spin eigenvalues is too complex to be represented by any artifice as simple as a single inner field. With our inner field approximation the entropy S is readily shown to be proportional to $(H_0^2 + H^2)/T^2$, so that in adiabatic demagnetization, the temperature is proportional to $(H^2 + H^2)^{1/2}$. If the specimen is taken out of the field, and if cooling (sic.) due to contact with the lattice system has not become appreciable, the final temperature T in the field-free state will be given by

$$T = -6 \cdot 30 / [(30)^2 + (100)^2]^{1/2} = -1.7^\circ\text{K}.$$

This is presumably the order of magnitude of the final negative spin temperature achieved in the experiment of Purcell and Pound⁽⁹⁾. Contact with the lattice ultimately makes the spin temperatures cool down to $T = \pm \infty$ and finally back to room temperature.

We may also consider what happens if the specimen is left in the solenoid rather than being taken out of it. As the field gradually returns from -100 to $+100$ as the condenser is discharged, the temperature sinks from -6° to -1.7° and then returns to -6° (neglecting elements of irreversible flow described later, which always tend to make the alignment less perfect at each stage than it would be otherwise.) Contacts with the lattice, regardless of whether the specimen is left in the solenoid or taken out of it, make the temperature ultimately go to $-\infty$, equivalent to $+\infty$ (corresponding to passage through $\lambda = 0$), and from $T = \infty$ through positive temperatures finally down to room temperature.

In connection with the interpretation of the Purcell-Pound experiment there is, however, one complication pointed out to the writer by Dr. ABRAGAM. The preceding discussion gives the impression that the spin-spin relaxation

equally populated, i.e. at $T = \pm \infty$. Hence

$$\sum_i E_i \exp [-E_i/kT] \sim -\frac{1}{kT} \sum_i E_i^2.$$

time, while long compared to the reversal time from 100 to -100 , is short if compared to the time of decay of the field from its most negative value -100 . This decay arises from the gradual attenuation of the solenoid current (a process of the order 1 ms) or removal of the specimen from the material. The spin-spin relaxation time τ_{ss} at low fields (less than about 30 gauss) is indeed less than the relaxation time 1 ms of the condenser discharge in the Purcell-Pound experiments. However, τ_{ss} increases rapidly when a magnetic field is applied. The reason for this is not hard to see. If a spin is reversed, its change in Zeeman energy must be counterbalanced by a corresponding change in the spin-spin energy. In large fields, however, the Zeeman quanta are so large that but few spin-spin eigenvalue differences are as large. For instance, in a field of 100 gauss, spin reversal leads to Zeeman quanta of 200 gauss, whereas the average spin-spin quantum is only 30 gauss. Of course there is actually a distribution of inner fields rather than a unique value; with a Gaussian distribution the probability of a value as high as 200 is very remote if the r.m.s. is only 30. The Gaussian estimate is doubtless too pessimistic, as there may be multiple spin-spin processes, etc. Nevertheless the fact remains that it is doubtful whether at fields as high as 100 gauss the spin-spin relaxation times are shorter than the current attenuation times, and possibly even the spin-lattice times.

This fact does not, however, imply that the Purcell-Pound experiment is spoiled. It simply means that the equilibration of spin-spin and Zeeman temperatures is achieved only after the applied field is somewhat reduced from its maximum absolute value of 100 gauss, for as soon as the applied field becomes comparable with the inner field, the spin-spin processes take place with high rapidity, i.e. a characteristic time of about $1/50$ ms. In consequence the Purcell-Pound experiments may not be as perfect as they would otherwise be, i.e. the final negative temperature may be greater in absolute value. Suppose, for instance, for the sake of simplicity, that when the field is reduced in absolute value from -100 , equilibration between the spin-spin and Zeeman temperatures does not take place until the field is reduced in magnitude to 30 gauss, and then sets in suddenly. The Zeeman temperature at 30 gauss just before equilibration is $(30/100)(-5^\circ) = -1.5^\circ\text{K}$ since without thermal contacts with the spin-spin reservoir the moment has the ideal behavior $M \sim H/T$, and so the Zeeman temperature is directly proportional to the applied field if the same spin alignment is maintained. On the other hand, since the spin-spin energy does not involve the applied field strength, the spin-spin temperature will remain $+5^\circ\text{K}$ until exchange of energy between the two parts of the Hamiltonian takes place. After sudden equilibration at 30 gauss, the temperature is given by

$$\frac{1}{T}[(30)^2 + (30)^2] = \frac{(30)^2}{5} - \frac{(30)^2}{1.5}, \quad \text{i.e. } T = 4.2^\circ$$

When the field is removed completely, the temperature becomes $-4.2/\sqrt{2} = -3.0$ °K, about 75% larger than our previous estimate -1.7 °K. The higher absolute value implies less perfect demagnetization, or in other words, more irreversibility. This probably is an excessively large estimate of the correction, as some of the irreversible heat flow doubtless takes place gradually before the field is reduced to 30 gauss, rather than all at once, and this reduces the correction. The fact that the Purcell and Pound experiments work as well as they do, and involve comparatively little irreversibility, is evidence that the ABRAGAM difficulty is not too serious. As ABRAGAM notes, quantitative measurements of the amount of reversibility should not be unduly difficult, and should yield interesting results.

When the field is suddenly reversed, it is essential not only that it be changed rapidly compared to the spin-spin relaxation time, but also rapidly compared to the Larmor period of any constant magnetic field that may be present. One might, for instance, naively imagine that one could obtain results as good as Purcell and Pound's by rotating the magnetic field slowly through 180° rather than reversing it, especially since in large fields the spin-spin relaxation times are abnormally large. This procedure, however, will not work, as then the spins simply rotate with the field. If one uses a system of representation in which the quantization is always along the field, the process can be considered adiabatic with respect to distribution in the stationary states as long as the rotation period is large compared to the Larmor period generated by the field. Our previous requirement that the reversal time be short compared to the spin-spin relaxation time is equivalent to requiring that the reversal be rapid compared with the Larmor precessions in the inner field. The earth's magnetic field is always present, and in their paper PURCELL and POUND make considerable reference to it; however, it is sufficiently weak that the requirement of rapid variation compared with its Larmor frequency causes no trouble. The inner field is over 100 times larger, and thus much more of a controlling factor.

So far we have considered mainly the principle of the Purcell-Pound experiment. What is the experimental evidence that the negative temperatures are really achieved? To prove their actual existence, PURCELL and POUND place the specimen back in the original field of about 6 400 gauss, in order to make resonance experiments on the ^7Li nucleus at a convenient radio-frequency (about 10 MHz). This procedure provides an excellent method of verifying negative temperatures. A negative temperature corresponds to a greater population in the upper rather than lower states, and hence to negative absorption (i.e. emission) rather than true absorption. This phenomenon is illustrated in Fig. 3, which shows one of the records obtained by sweeping the impressed frequency periodically back and forth through the resonance frequency. The peak at the extreme left is the normal resonance curve, before

the field is reversed. Just to the right of this sweep the field has been reversed, and the next resonance peak is seen to point downwards, corresponding to negative absorption. The negative peaks get weaker until finally the state $T = \pm \infty$ is reached where the positive and negative absorption cancel out because of equal population of the upper and lower states. The gradually increasing positive peaks show the cooling down of the temperature from $+\infty$ to the final room temperature. The first negative peak is not quite as large as the initial positive one, and shows that the first recorded negative temperature in the field of 6 400 gauss is about -350°K instead of -300°K . Such a phenomenon is to be expected, for there is irreversible heat flow involved in the equilibration of the Zeeman and spin-spin temperatures after the rapid reversal of the field.

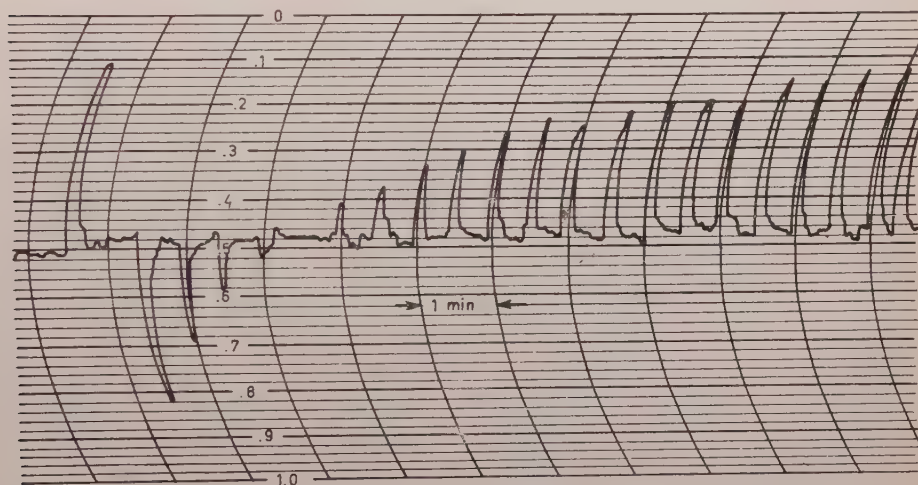


Fig. 3.

A particularly striking feature of the Purcell-Pound experiments is that regardless of how the specimen is oriented when it is placed back in the strong field, the spins always remember to point in the «wrong» direction, or in other words, the negative temperature is always achieved, showing clearly that the negative temperatures have a physical reality.

It is to be stressed that the success of the Purcell-Pound experiment is due to the fact that immediately after the reversal of the field, the spin-spin and Zeeman temperatures are not equal, but one is the negative of the other. So their experiment has furnished another example of the analysis of systems for which it is meaningful and helpful to think of different parts of the spin Hamiltonian as being at different temperatures. If the spin-spin and Zeeman

temperatures had remained equal during the reversal of the field, the experiment would have been equivalent to adiabatic demagnetization down to $H = 0$ and then remagnetization with the field applied in the opposite direction. The resulting temperatures would then always be positive, and the spins would always manage to point in the «right» direction.

At first sight it may seem that negative temperatures are a rather confusing subject, but actually their study tends to clarify one's basic understanding of thermodynamics.

* * *

The writer is much indebted to Professor E. M. PURCELL for stimulating discussions.

Magnetism at Very Low Temperatures and Nuclear Orientation.

N. KURTI

The Clarendon Laboratory - Oxford

1. - Introduction.

Professor PRYCE's lectures mainly deal with situations in which the splitting δ of the energy of the ground state of the paramagnetic ion is small compared with kT . My main object will be to deal with the macroscopic behaviour of paramagnetic salts, such as the thermal and magnetic properties of the electronic elementary magnets or with the behaviour of the nuclear spins, and to examine what happens when these systems pass into the temperature region where kT is of the order of the energy splitting and when, therefore, a rearrangement among the various energy levels takes place. There are many such regions but I shall almost entirely concentrate on temperatures below 1°K , i.e. on phenomena which occur in systems in which the separation between the energy levels is given by $\delta/k < 1^\circ\text{K}$.

This seemingly arbitrary choice can be justified on two grounds:

a) Let us look at the general problem of producing low temperatures. The essential condition is that we must have a system which at the starting temperature has a large entropy. If, by an isothermal change of an external parameter this entropy can be reduced, then, the subsequent isentropic (i.e. adiabatic and reversible) change of the external parameter in the reverse direction will result in a lowering of temperature. The classic and most important example is the process of gas liquefaction. Cooling by means of a gas becomes impossible when the vapour pressure becomes too small. The practical limit is about 1°K .

It is precisely in this temperature range that certain paramagnetic salts become very useful cooling agents. If the paramagnetic substance has a ground state which is practically degenerate at 1°K ($\delta/k < 0.5^\circ\text{K}$ is usually a good enough approximation), its entropy at this temperature will be

$S/R \sim \ln(2J+1)$ (J — angular momentum quantum number); moreover, this entropy can be reduced appreciably by modest magnetic fields of the order of 10 kOe. So it came about that following the proposal by GIAUQUE ⁽¹⁾ and by DEBYE ⁽²⁾ isentropic demagnetization of paramagnetic salts became the most powerful method for reaching temperatures below 1 °K.

Now the history of gas liquefaction is intimately connected with the study of the equation of state of fluids, that is of gases and liquids. In fact, gas liquefaction, in its various phases has been one of the most valuable means for determining deviations from the ideal behaviour and for studying intermolecular forces in fluids. The same is largely true about the magnetic cooling method. The temperature one can reach with a given paramagnetic substance will be largely determined by the deviation from «ideal» behaviour. I shall give later a thermodynamic definition of an ideal paramagnetic substance; in the statistical sense I mean by this a system of spins which have such weak interactions with each other or with their surroundings that for $H = 0$: $S/R = \ln(2J+1)$. Now deviations from this «ideal» state give information about the nature and magnitude of the interactions. Until the advent of paramagnetic resonance practically all the experimental information about these interaction came from magnetic cooling and paramagnetic relaxation.

b) The second reason for the particular interest in paramagnetic salts

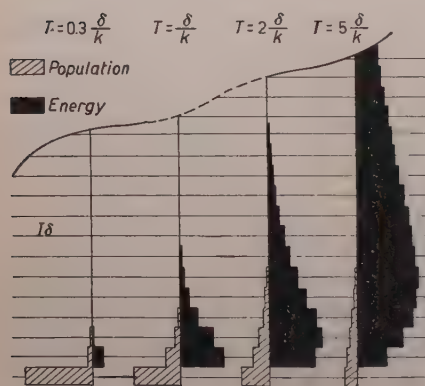


Fig. 1. — Distribution among levels and energy of a system of harmonic oscillators.

with $\delta/k < 1$ °K is that below 1 °K the thermodynamic properties, such as specific heat, entropy of these substances are almost entirely determined by the spins; the contribution from lattice vibrations being negligible.

Such an «isolated» (*) spin system has certain interesting features. Let us compare the statistical picture of a system of spins with that of, say, the lattice vibrations. In Fig. 1 the lattice vibrations are, approximately, represented by a system of harmonic oscillators. As this diagram shows in this system both the entropy (qualita-

⁽¹⁾ W. F. GIAUQUE: *Journ. Am. Chem. Soc.*, **49**, 1870 (1927).

⁽²⁾ P. DEBYE: *Ann. der Phys.*, **81**, 1154 (1926).

(*) «Isolated» is here used in the sense that the equilibrium or quasi-static properties of the substance as a whole are the same as those of a truly isolated spin-system. The spins are, of course, coupled to the lattice and the dynamic behaviour (e. g relaxation effects) depends on this coupling.

tively represented by the spread among the energy levels) and the energy increase with increasing temperature, and at sufficiently high temperatures the theorem of the equipartition of energy holds. This is possible because the energy spectrum extends to infinity.

The position is fundamentally different for a spin system, as shown in Fig. 2. (Four energy levels, $J = \frac{3}{2}$). Here the energy spectrum is bounded and as a result, both energy and entropy remain finite at infinite temperature. The theorem of equipartition of energy loses its meaning for such a system and so does the conventional and naive definition of temperature, which relates temperature to energy. Since only a finite amount of

energy is required to bring such a system to an infinite temperature it is, a priori, possible to reach higher than infinite, or negative temperatures, as was demonstrated with nuclear spins, by PURCELL, POUND and RAMSEY⁽³⁾.

It should be mentioned that, for most purposes, a spin system in contact with another system of practically zero heat content has the same thermodynamic characteristics as a completely isolated spin system. Another approximation to an isolated spin system is one in which the coupling between the spins and say, the lattice is so weak that the relaxation time is long compared with the duration of the experiment. This was the case in the negative temperature experiment of PURCELL, POUND and RAMSEY⁽³⁾.

2. - Magnetic cooling.

2.1. *Thermodynamical considerations.* - Let us now see how a paramagnetic salt may be used for producing low temperatures. The first and second law of thermodynamics may be written

$$dU = TdS + \delta W,$$

where dU is the change of the internal energy and δW is the work received by the system. What is δW in the magnetic case? By analogy with the work occurring in volume changes, $-pdV$, one intuitively tends to write HdM (M = magnetic moment), since both H and p are intensive variables and v

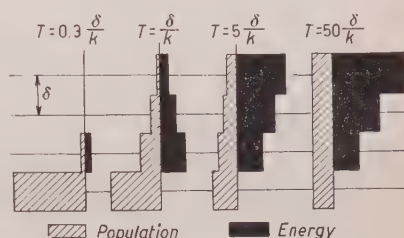


Fig. 2. - Distribution among levels and energy of a system of elementary magnets.

⁽³⁾ N. F. RAMSEY and R. V. POUND: *Phys. Rev.*, **81**, 278 (1951); E. M. PURCELL and R. V. POUND: *Phys. Rev.*, **81**, 279 (1951).

and M are extensive variables. Although in what follows I shall use this definition it should be mentioned that many authors prefer $\delta W = -M dH$ as definition. (For an extensive discussion of this question see GUGGENHEIM ⁽⁴⁾ and, more recently, HEINE ⁽⁵⁾). Either definition, if used logically, is equally justified. If we write $dU = T dS + H dM$ then U may be regarded as the internal energy of the magnetic substance, the energy which, as it were, is localized in the specimen and does not depend directly on the apparatus producing the magnetic field.

With the other definition we have

$$dE = d(U - HM) = T dS - M dH,$$

where E is the enthalpy, which includes the potential energy of the specimen in the field produced by the external magnet. For the discussion of the magnetic cooling the definition $\delta W = H dM$ has advantages (*).

It is instructive to calculate the work of magnetization in one concrete example. Consider a magnetically isotropic sphere, of radius a placed in a long solenoid with n turns per unit length, zero resistance and carrying a current i . We want to calculate the work δW done in changing the magnetic moment of the specimen from M to dM while the field in the solenoid changes from H_0 to $H_0 + dH_0$. Here $H_0 = 4\pi ni$ is the field in the absence of the specimen.

As we increase i by di there is a change in the flux Φ through the solenoid; this produces a counter e.m.f. $d\Phi/dt$ which has to be counteracted by mechanical work (additional torque applied to the dynamo supplying the current). This work is $\delta W = i dt \cdot d\Phi/dt = i d\Phi$.

Now even in the absence of the magnetic specimen an increase of i would require work to increase the magnetic energy $\frac{1}{2}Li^2 = (1/8\pi)H_0^2V$. This part of the work is obviously of no importance for our calculation. Since we are interested in the work to magnetize the specimen we need only consider that part of Φ which is due to the magnetized sphere.

(4) E. A. GUGGENHEIM: *Proc. Roy. Soc., A* **155**, 49, 70 (1936).

(5) V. HEINE: *Proc. Camb. Phil. Soc.*, **52**, 546 (1956).

(*) The following analogy is quite instructive. If one wants to *measure* the work of compression of a gas, all one needs to do is to place increasing weights m on the piston and record the corresponding displacements dl . $-\int_{l_1}^{l_2} m dl$ is the work received by the gas, provided the cylinder rests on a solid support, say a laboratory bench. If, however, the cylinder is placed on a spring mattress, then the work so calculated (l is measured in a system of co-ordinates fixed in the laboratory) also includes the work spent on increasing the potential energy of the springs. I understand that Professor PURCELL uses a similar argument when he treats this question in his classes at Harvard.

The induction B inside the sphere is:

$$\begin{aligned} B &= H_0 - (4\pi/3)I + 4\pi I \\ &= H_0 + (8\pi/3)I, \end{aligned}$$

where I is the magnetic moment per unit volume.

The flux inside the sphere due to the material (see Fig. 3) is given by

$$\Phi^{(i)} = \int_{-a}^a (8\pi/3)I \cdot \pi(a^2 - z^2) n \, dz = (8\pi/3)nM.$$

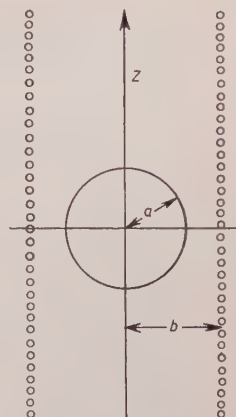


Fig. 3.

Remembering that the field produced by the sphere at external points is that of a dipole M situated at its centre, we have for the contribution to the flux from the region outside the specimen

$$\Phi^{(o)} = 2 \int_0^\infty \left\{ \int_\xi^b M [-(\varrho^2 + z^2)^{-\frac{3}{2}} + 3z^2(\varrho^2 + z^2)^{-\frac{5}{2}}] 2\pi\varrho \, d\varrho \right\} n \, dz = (4\pi/3)nM,$$

where

$$\begin{aligned} \xi &= 0 & \text{for } z > 0, \\ \xi &= (a^2 - z^2)^{\frac{1}{2}} & \text{for } z < 0. \end{aligned}$$

Then the total flux is $\Phi = \Phi^{(i)} + \Phi^{(o)} = 4\pi nM$ and

$$\delta W = i \, d\Phi = i4\pi n \, dM = H_0 \, dM.$$

From $dU = T \, dS + H \, dM$ we can derive the Maxwell relations for the magnetic case, e.g.

$$(1) \quad \left(\frac{\partial S}{\partial H} \right)_T = \left(\frac{\partial M}{\partial T} \right)_H, \quad (2) \quad \left(\frac{\partial T}{\partial H} \right)_S = - \left(\frac{\partial M}{\partial S} \right)_H.$$

As mentioned before, the first step in a magnetic cooling experiment consists in the isothermal reduction of the entropy by an external magnetic field. It is clear from (1) that the required condition is that $(\partial M / \partial T)_H$ should be finite. If $(\partial M / \partial T)_H$ is known the entropy of our elementary magnets can be calculated from

$$S(T, H) = S(T, 0) + \int_0^H \left(\frac{\partial M}{\partial T} \right)_H \, dH = S_0(T) - \Delta S_m(T, H).$$

If the case of an ideal paramagnetic $S_0 = R \ln (2J+1)$ and $(\partial M / \partial T)_H$ can be obtained from the magnetization curve given by a Brillouin function

$$M / N_0 g \beta J = \frac{2J+1}{2J} \coth (2J+1) \frac{\alpha}{2} - \frac{1}{2J} \coth \frac{\alpha}{2}, \text{ where } \alpha = \frac{g \beta H}{kT},$$

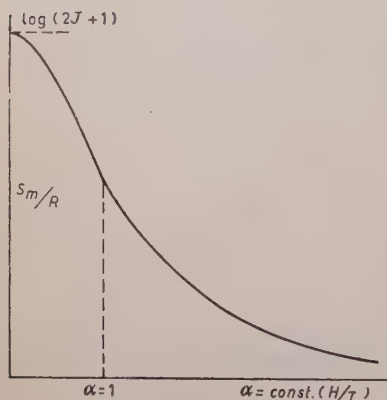


Fig. 4. — Magnetic entropy of an ideal paramagnetic salt as a function of $\alpha = g \beta H / kT$.

($\alpha = g \cdot 0.067 (H/T)$, hence, very roughly $\alpha = 1$ for $H/T \approx 10 \text{ kOe}/^\circ\text{K}$).

Fig. 4 shows qualitatively the entropy as a function of α . Tabulated values of the entropy can be found in various publications ⁽⁶⁾.

We can now write down the fundamental equation for the magnetic cooling process. For an isentropic demagnetization

$$S(T_i, H_i) = S(T_f, H_f),$$

where the subscripts i and f refer to the initial and the final state respectively.

Now,

$$S(T_i, H_i) = S_0(T_i) - \Delta S_m(T_i, H_i) = \int_0^{T_i} \frac{C_0}{T} dT - \Delta S_m(T_i, H_i),$$

and similarly,

$$S(T_f, H_f) = \int_0^{T_f} \frac{C_0}{T} dT - \Delta S_m(T_f, H_f).$$

Hence, the final temperature reached when the field is reduced isentropically to H_f is given by

$$\int_{T_f}^{T_i} \frac{C_0}{T} dT = \Delta S_m(T_i, H_i) - \Delta S_m(T_f, H_f) \quad (*).$$

⁽⁶⁾ J. R. HULL and R. A. HULL: *Journ. Chem. Phys.*, **9**, 465 (1941); W. F. GIAUQUE, J. W. STOUT, C. J. EGAN and C. W. CLARK: *Journ. Am. Chem. Soc.*, **63**, 405 (1941); L. P. SCHMID and J. S. SMART: *U.S. Naval Ordnance Rep. No.* 3640, 954.

(*) This equation can also be obtained from the Maxwell relation (2) given above, which can be written

$$(3) \quad \left(\frac{\partial T}{\partial H} \right)_S = - \frac{(\partial M / \partial T)_H}{(\partial S / \partial T)_H}.$$

In particular for $H_f = 0$ (demagnetization to zero field)

$$\int_{T_f}^{T_i} \frac{C_0}{T} dT = \Delta S_m(H_i, T_i).$$

Fig. 5 shows this process in an S - T diagram. The full line represents the entropy of an ideal paramagnetic salt in which the lattice vibrations are appreciably excited at T_i . The essence of the magnetic cooling process is this: On demagnetization to zero field the magnetic entropy returns to its full value $R \ln(2J+1)$; the system will cool until the original entropy reduction ΔS_m is used up to reduce the entropy of the thermal «ballast», the

lattice in this instance. The same argument applies when adiabatic demagnetization is used to cool other systems.

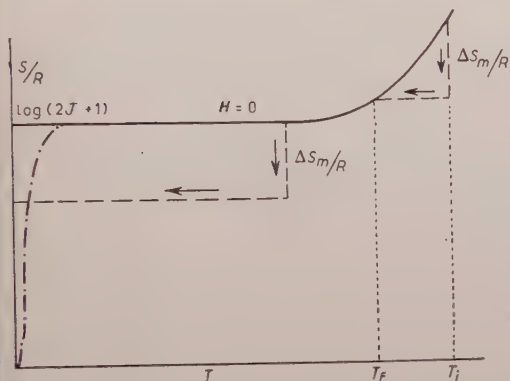


Fig. 5. — Representation of the magnetic cooling process in the entropy-temperature diagram. — Ideal paramagnetic; - - - - Real paramagnetic; Path of the magnetic cooling process.

Since

$$(4) \quad S = S_0 + \int_0^H \left(\frac{\partial M}{\partial T} \right)_H dH, \quad \text{we have} \quad \left(\frac{\partial S}{\partial T} \right)_H = \frac{C_0}{T} + \frac{\partial}{\partial T} \left[\int_0^H \left(\frac{\partial M}{\partial T} \right)_H dH \right]_H.$$

We can integrate (3) for an isentropic process between the limits T_i , H_i and T_f , H_f , after having substituted (4) into it,

$$dT = - \frac{(\partial M / \partial T)_H dH}{C_0/T + [\partial / \partial T \int_0^H (\partial M / \partial T)_H dH]_H},$$

$$\frac{C_0}{T} dT = - \left(\frac{\partial M}{\partial T} \right)_H dH - \left[\frac{\partial}{\partial T} \int_0^H \left(\frac{\partial M}{\partial T} \right)_H dH \right]_H dT = - d \left[\int_0^H \left(\frac{\partial M}{\partial T} \right)_H dH \right].$$

Hence

$$\int_{T_f}^{T_i} \frac{C_0}{T} dT = \int_0^{H_i(T_i)} \left(\frac{\partial M}{\partial T} \right)_H dH - \int_0^{H_f(T_f)} \left(\frac{\partial M}{\partial T} \right)_H dH = \Delta S_m(H_i, T_i) - \Delta S_m(H_f, T_f).$$

The figure also shows that demagnetization of our ideal paramagnetic from a temperature at which the lattice entropy is negligible would lead to absolute zero. One is saved from such a catastrophe by the reduction of the entropy through interactions.

The influence of the lattice entropy on the temperature reached by demagnetization of a «real» paramagnetic can be readily seen with the help of this diagram. This influence becomes important if the lattice entropy is of the order of either the magnetic entropy reduction or the absolute magnetic entropy. To give some rough numerical data: The lattice entropy for most paramagnetic salts is $S_l/R = 10^{-4}T^3 \div 10^{-3}T^3$. For $T_i = 1^\circ\text{K}$, and if we take the higher entropy value, this becomes important if either:

$$\Delta S_m/R < 10^{-3}, \quad \text{i.e.} \quad H/T < 0.2 \text{ kOe/degree},$$

or

$$S_m/R < 10^{-3}, \quad \text{i.e.} \quad H/T > 100 \text{ kOe/degree}.$$

2.2. *The ideal paramagnetic.* — It is interesting to examine what happens if an ideal paramagnetic with zero lattice entropy is demagnetized adiabatically. We define an ideal paramagnetic by the condition:

$$\left(\frac{\partial U}{\partial M}\right)_T = 0.$$

It follows from the 2-nd law (analogously to the well-known relation involving p and v):

$$\left(\frac{\partial U}{\partial M}\right)_T = -T \left(\frac{\partial H}{\partial T}\right)_M + H = 0.$$

By integrating at constant M one has:

$$M = f(H/T).$$

It follows from the Maxwell relation (1) that

$$S = g(H/T),$$

provided the entropy in $H=0$ is constant. ($(\partial S/\partial T)_{H=0} = 0$ for vanishing lattice specific heat). Hence if we reduce the field isentropically ($S = \text{const}$) we have $H/T = \text{const}$ and, also $M = \text{const}$. The magnetic moment of an ideal paramagnetic having zero lattice specific heat remains constant during an isentropic process, and we have the relation:

$$(5) \quad T_f = H_f \frac{T_i}{H_i}.$$

Both these relations, $M = \text{const}$ and $H/T = \text{const}$, have been proved experimentally. The first was proved in the wellknown work in Leyden by DE HAAS and WIERSMA (7) and by CASIMIR and DE HAAS (8) on caesium titanium alum and ferric ammonium alum. They have shown that during the adiabatic reduction of the field from about 20 kOe to well below 1 kOe the magnetic moment remained constant (*).

Recent unpublished experiments in Oxford by J. S. HILL and J. H. MILNER have proved the validity of the relation $H/T = \text{const}$. A crystal of cerium magnesium nitrate was used and the temperature of the crystal during demagnetization was measured by means of a carbon resistance thermometer, which shows negligible magneto-resistance. The thermometer was calibrated in a separate experiment against the susceptibility, which is known (9) to obey Curie's law. The results are shown in Fig. 6.

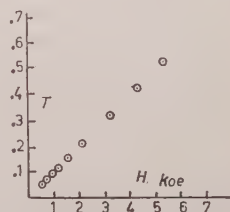


Fig. 6. — Temperature as a function of magnetic field during the isentropic demagnetization of cerium magnesium nitrate. (Experiments of J. S. HILL and J. H. MILNER in Oxford).

2.3. *The « real » paramagnetic.* — Equation (5) ceases to be valid for small fields; for $H_f = 0$ it would predict $T_f = 0$, which is impossible. The argument breaks down, because at the lowest temperatures it is no longer permissible to assume ideal behaviour, i.e. the absence of

interactions between the elementary magnet and its surroundings. If we represent these interactions by an effective, molecular field H_{eff} , then even if the external field is reduced to zero, there remains this effective field, and for $H_f = 0$ (5) becomes

$$(6) \quad T_f = H_{\text{eff}} \frac{T_i}{H_i}.$$

This is a rather rough and ready approximation but it is useful for modest values of H_i/T_i (say less than 10 kOe/°K). The values of H_{eff} for the salts most commonly used in magnetic cooling range from 40 Oe (cerium magnesium nitrate) to 400 Oe (ferric ammonium alum).

(7) W. J. DE HAAS and E. C. WIERSMA: *Physica*, **3**, 491 (1936).

(8) H. G. B. CASIMIR and W. J. DE HAAS: *Physica*, **7**, 70 (1940).

(*) It is clear that for at least part of the process the word « demagnetization » is a misnomer, and « degaussing » would seem more appropriate. I am indebted to Professor C. KITTEL for suggesting this word instead of « decamping » which I used earlier.

(9) J. M. DANIELS and F. N. H. ROBINSON: *Phil. Mag.*, **44**, 623 (1953).

It is instructive to compare the representation of the magnetic cooling process in the T - H diagram with one in the S - T diagram. Both of these are shown in Fig. 7. In the

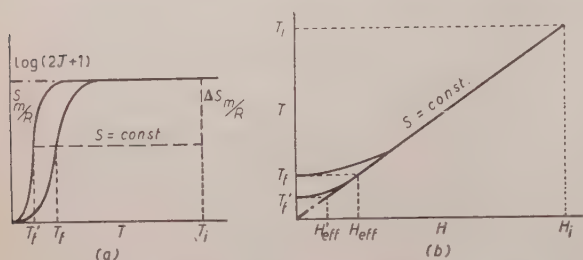


Fig. 7. - The magnetic cooling method in the S - T and H - T diagram.

energy is characterized by the temperature region in which the rapid drop of the entropy occurs. A simple relation exists between this characteristic temperature θ and H_{eff} . According to the model using the effective molecular field, the $(2J+1)$ -fold degenerate ground state is split into $2J-1$ equidistant levels separated by $g\beta H_{\text{eff}}$. If we define θ so that this separation is $k\theta$, we have $\theta = g\beta H_{\text{eff}}/k$.

The entropy representation shows the connection between the splitting or broadening of the ground state of a paramagnetic on the one hand, and, on the other hand, the cryogenic efficiency of the same salt. If we know the splitting we can, in principle, construct the S - T curve and predict the cooling effect. If, on the other hand, we carry out a series of adiabatic demagnetizations from known initial conditions we can construct the S - T curve. The analysis of such an entropy curve often enables one to establish the nature of the lifting of the degeneracy; whether it is pure splitting caused by the crystalline electric field or whether it is partly or wholly broadening caused by direct interaction between the spins.

The fundamental relation (5) for the adiabatic demagnetization can be equally well derived by a statistical mechanical argument. The partition function Z_i for an individual ion in an ideal paramagnetic is given by

$$Z_i = \sum_{-J}^{+J} \exp \left[\frac{mg\beta H}{kT} \right].$$

Now

$$S = \left(\frac{\partial}{\partial T} RT \ln Z_i \right)_H \quad \text{and} \quad M = \left(\frac{\partial}{\partial H} RT \ln Z_i \right)_T,$$

and therefore both S and M are functions of H/T only, as shown before by a thermodynamical argument.

The statistical meaning of (5) can be expressed as follows: Since entropy is a measure of disorder or of the spread of the distribution among the various energy levels, this distribution must remain unchanged during an isentropic process. But the separation of the energy levels which appears in the Boltzmann factor and hence determines the distribution is proportional to H . Hence if H is reduced, for the distribution to remain the same the temperature must drop proportionally to T .

The physical significance of (6) (demagnetization to $H = 0$ of a «real» paramagnetic salt) can similarly be expressed: During demagnetization to zero field the paramagnetic salt will cool until a temperature T_f is reached at which the degree of order produced by the internal interaction forces is the same as that produced by the external field H_i at the initial temperature T_i .

Finally, a brief remark about the inadequacy of (6).

Most of the paramagnetic ions used for magnetic cooling have Kramers degeneracy. That means that in addition to the Stark splitting of the ground level we also have a broadening due to interaction between the spins; the crystalline field cannot entirely remove the degeneracy. The levels cannot be represented as in Fig. 8a (this

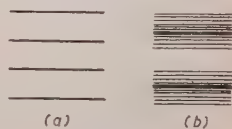


Fig. 8.

corresponds to the assumption leading to (6)); but rather as in Fig. 8b. We see that one single parameter (H_{eff} or θ) is not sufficient to describe the sys-

tem; moreover the character of the level diagram in the final state (T_f) is different from the equidistant levels of the initial state (H_i, T_i).

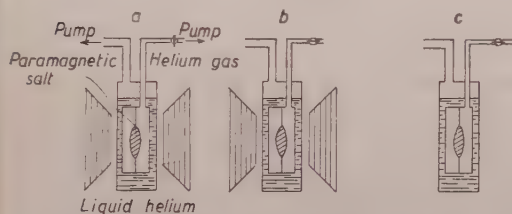


Fig. 9. — Schematic experimental arrangement for the magnetic cooling method.

tem; moreover the character of the level diagram in the final state (T_f) is different from the equidistant levels of the initial state (H_i, T_i).

2.4. *Experimental.* (*) — Fig. 9 shows schematically how the magnetic cooling process is carried out. In (a) the specimen is magnetized, the heat of magnetization

being absorbed by the liquid helium boiling at about 1°K. (In b) the helium gas surrounding the specimen is pumped out and the specimen is thermally insulated. Finally, in (c) the magnetic field is removed.

Fig. 10 shows in some detail a demagnetization cryostat as used in Oxford.

The set of coils consists of a secondary of a large number (5 000 ÷ 20 000) of turns and a primary capable of producing up to 100 ÷ 200 Oe; their mutual

(*) The first magnetic cooling was performed by F. GIAQUE and D. P. MACDOUGALL⁽¹⁰⁾ in Berkeley on 19-th March 1933.

⁽¹⁰⁾ W. F. GIAQUE and D. P. MACDOUGALL: *Phys. Rev.*, **43**, 768 (1933); see also W. J. DE HAAS, E. C. WIERSMA and H. A. KRAMERS: *Nature*, **131**, 719 (1933).

inductance depends on the susceptibility of the specimen. They form an important part of demagnetization cryostats since the susceptibility serves usually as thermometric parameter.

The mutual inductance is measured either by a ballistic method or with an A.C. bridge. The ballistic method has the advantage of simplicity coupled with adequate sensitivity, made possible by the low resistance of the coils cooled in liquid hydrogen. Its disadvantage is that individual measurements have to be at least $5 \div 10$ s apart. With the A.C. method almost continuous measurements are possible; the sensitivity is higher than that of the ballistic method. The A.C. method however suffers from the disadvantage that at very low temperature heating produced by irreversible changes (hysteresis and relaxation) may become troublesome. Also, at very low temperatures relaxation times of the order of the period of the A.C. field (usually $25 \div 100$ Hz) are common, and the susceptibility becomes frequency dependent. When a ballistic galvanometer or a flux meter is used the time-constant of the measurement can be increased to the order of a second. It is, of course, important that the reversal-time of the primary current should be controlled, e.g. with the help of the charge and discharge of condensers.

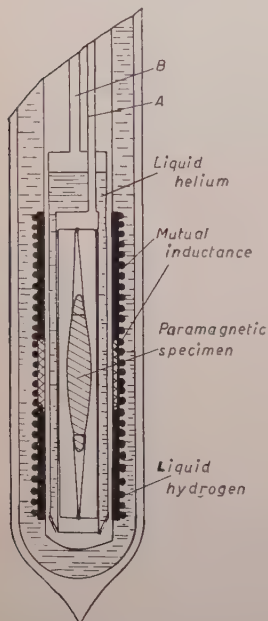


Fig. 10. — Demagnetization cryostat. (Oxford type).

It should be mentioned finally that at the low temperatures reached the paramagnetic susceptibilities are sufficiently large for demagnetizing effects to become important. Hence the need for using ellipsoidal specimens for which the demagnetizing field is homogeneous and can be calculated. The field H inside the specimen is given by

$$H = H_0 / (1 + N\kappa),$$

where H_0 is the field produced by the primary coil, N the demagnetizing factor and κ the volume susceptibility. Thus, e.g. for a spherical sample ($N = 4\pi/3$) of ferric ammonium alum at 0.1°K ($\kappa = 0.15$) we have $H = H_0/1.6$, a large correction.

3. — Determination of the absolute temperature.

The standard methods for measuring temperatures by means of gas thermometers or vapour pressure thermometers are not applicable in this temperature range because of the smallness of the vapour pressure, even of helium. In the

following we shall discuss various methods that have been used for determining absolute temperatures.

3.1. *Corrections for deviations from ideal behaviour.* — This method is somewhat similar to that used in gas thermometry. There are two ways of evaluating the corrections to Curie's law $\chi = C/T$. In the one, the essential constants (nature and magnitude of the splitting and of the broadening) are obtained from measurements at higher temperatures (paramagnetic resonance or relaxation). These constants are then substituted into the theoretical expressions ⁽¹¹⁾ and a relation between T and χ is obtained.

The other way is to carry out a series of demagnetizations, which give a relation between S and χ . Since one has the theoretical relations between S and T and χ and T , and hence between S and χ , the unknown parameters can be determined by fitting the experimental S - χ relation to the predicted one ⁽¹²⁾.

Since χ is frequently used as thermometric parameter it was found convenient to define, by means of χ , a secondary temperature scale, which, at sufficiently high temperatures, approaches the Kelvin scale. Curie's law, $\chi = C/T$ is the obvious relation, but some care has to be exercised in choosing the right definition of χ .

Curie's law is the high temperature, low field approximation of the Langevin-Brillouin magnetization curve. The field that is used in the derivation is the magnetic force acting on the individual elementary magnet. If we denote by H_i this local field and by I the magnetic moment per unit volume

$$I = CH_i/T \quad (C = \text{Curie constant/cm}^3).$$

Using the well-known Lorentz reasoning for calculating the magnetic interaction between the elementary dipoles one finds $H_i = H_0 + (4\pi/3 - N)I$. If we denote $\chi_a^{(N)} = I^{(N)}/H_0$, the apparent susceptibility measured on a specimen having N for demagnetizing factor, we have

$$\chi_a^{(N)} = \frac{C}{T - (4\pi/3 - N)C}.$$

For a spherical specimen ($N = 4\pi/3$)

$$\chi_a^{(4\pi/3)} = \frac{C}{T},$$

⁽¹¹⁾ M. H. HEBB and E. M. PURCELL: *Journ. Chem. Phys.*, **5**, 338 (1937).

⁽¹²⁾ D. DE KLERK and R. P. HUDSON: *Phys. Rev.*, **91**, 278 (1953).

that is, Curie's law should be strictly obeyed. It is therefore convenient to define a secondary temperature scale by means of the apparent susceptibility measured on a sphere ⁽¹³⁾.

$$T^{\odot} = \frac{C}{\chi_a^{\text{sphere}}}.$$

It is not necessary actually to use a spherical specimen. If we denote by $T_N^* = C/\chi_a^N$, a secondary temperature scale based on the apparent susceptibility of a specimen with a demagnetization factor N , we have

$$T^{\odot} = T_N^* + (4\pi/3 - N)C.$$

The difference between the two can be appreciable. Thus, for a slender ferric ammonium alum cylinder ($C = 0.015$, $N = 0$) $T^{\odot} - T^* = .06^\circ$; this indeed is appreciable compared with the lowest absolute temperatures ($\sim 0.02^\circ\text{K}$) one reaches with ferric alum. The relation between T^{\odot} and T_N^* is well obeyed except in the temperature region where these salts become antiferromagnetic or ferromagnetic ⁽¹⁴⁾.

3.2. Method based on the constancy of the magnetic moment along an isentropic line. — As mentioned before, the magnetic moment of an ideal paramagnetic substance remains constant during adiabatic «degaussing». Although the converse is not necessarily true (it does *not* follow from the constancy of the isentropic moment that $M = f(H/T)$), DE HAAS and WIERSMA ⁽⁷⁾ have shown that if M is constant the absolute temperature can nevertheless be calculated, although some additional measurements are needed.

Let us take the experimental fact ^(7,8) $(\partial M/\partial H)_S = 0$, or $M = f(S)$. It follows from the $dE = TdS - MdH$

$$(7) \quad \left(\frac{\partial E}{\partial H}\right)_S = -M, \quad (8) \quad \left(\frac{\partial E}{\partial S}\right)_H = T.$$

The first relation gives

$$E = -MH + g(S),$$

and hence, the second can be written

$$T = -\left(\frac{\partial M}{\partial S}\right)_H + g'(S),$$

⁽¹³⁾ N. KURTI and F. E. SIMON: *Phil. Mag.*, **26**, 849 (1938).

⁽¹⁴⁾ N. KURTI: *Journ. Phys. Radium*, **12**, 282 (1951).

and, using the Maxwell relation (2)

$$T = \left(\frac{\partial T}{\partial H} \right)_S H + g'(S).$$

Integrate this at constant S

$$\log \frac{T - g'(S)}{H} = \varphi(S).$$

or

$$\frac{T - A}{H} = B,$$

where A , B are constant along an isentropic line. Or

$$\frac{T}{T_0} = \frac{H - C}{H_0 - C},$$

where C is a function of M and is constant along an isentropic line.

If one determines $C(M)$ (usually only a small correction) by means of experiments above 1 °K this method can be useful for determining absolute temperatures down to values of H and T (of the order of 1000 Oe and 0.1 °K, and possibly less, depending on the substance) for which M is constant along an isentropic.

3.3. Calorimetric determination of *absolute* temperature changes during isentropic magnetization at low temperatures ⁽¹⁵⁾. — The de Haas-Wiersma method is not suitable for determining temperatures reached by demagnetization to zero field. Yet, one is usually interested in the χ - T correlation for $H = 0$. The method to be discussed now enables one to determine the absolute temperatures for $H = 0$, if one knows, e.g. from the de Haas-Wiersma method, the temperature in a final field on the same isentropic line. Although this method has been used very little, a description of it seems worthwhile since it offers a nice illustration of the working of the second law of thermodynamics.

It is based on the relation $\Delta Q = T \Delta S$. Figure 11 shows two entropy curves, one for $H = 0$, the other for a finite field. Starting from A let us introduce heat into the specimen until B ,

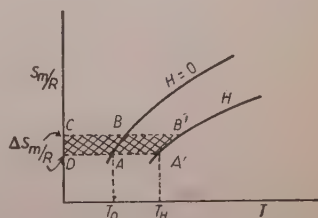


Fig. 11. — Comparison of the quantities of heat required to produce the same entropy change ΔS : in $H = 0$ ▨; in H ▩.

⁽¹⁵⁾ N. KURTI and F. E. SIMON: *Phil. Mag.*, **26**, 840 (1938).

corresponding to an entropy change ΔS , is reached. The quantity of heat Q_0 is given by the area $ABCD$, and if the temperature is small relatively to

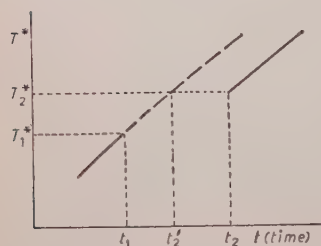


Fig. 12. — Experimental procedure for the calorimetric determination of the temperature change on isentropic demagnetization.

T_0 , $Q_0 = T_0 \Delta S$. In a second experiment let us first magnetize the substance isentropically (AA'), thereby increasing the temperature to T_H . With the field kept on we introduce heat until B' (corresponding to the same ΔS) is reached. This quantity of heat Q_H is represented by the area $A'B'CD$, or, as before $Q_H = T_H \Delta S$. Hence

$$\frac{T_0}{T_H} = \frac{Q_0}{Q_H}.$$

The actual experimental procedure is depicted in Fig. 12. The ordinates are the indications T^* of the secondary thermometer defined above. We assume that there exists a unique relation between S (in $H = 0$) and T^* . (This is always true for a restricted entropy interval, except for the limiting case $\partial S / \partial T^* = \infty$.) The specimen is heated at a constant rate ($Q \propto t$), therefore the abscissae (time) are proportional to the heat input. Having heated the sample first in $H = 0$ (solid line), let us turn on a field H at t_1 (T_1^*) and continue heating, at the same rate, until t_2 . No T^* measurements are taken during this time. At t_2 the field is reduced to zero, T^* measurements are resumed (the secondary thermometer now indicates T_2^*), and heating at the same rate is continued. If one knows what the trend of T^* would have been if the field had not been switched on (----; this can be ascertained in a separate experiment, but a graphical extrapolation is usually adequate), one can determine the time t_2' at which the specimen would have reached the same temperature T_2^* (and hence the same entropy) in zero field. This means that in the field H (and at a temperature T_H) a quantity of heat $Q_H = \text{const}(t_2 - t_1)$ produced the same entropy change as would have been produced by $Q_0 = \text{const}(t_2' - t_1)$ in $H = 0$ (and at T_0). Hence

$$\frac{T_0}{T_H} = \frac{t_2' - t_1}{t_2 - t_1}.$$

Therefore if one knows T_H , which in many cases can be determined by the de Haas-Wiersma method or, if the substance behaves ideally, from the relation $T/H = \text{const}$, such an experiment gives the absolute temperature reached by demagnetization to zero field. Alternatively, if one knows the temperature in zero field, one can determine in this way the change in temperature on isentropic magnetization.

3.4. *The « standard » method.* — Most measurements of the relation between T and T^* have been carried out by this method. The principle of this method is explained in Fig. 13. Let A represent the entropy at the temperature T_0 (known in the absolute scale, e.g. 1°K) and in a field H_1 . If the field is increased to H_2 , the temperature being maintained constant, the corresponding entropy change ΔS can be calculated, or, determined experimentally and this gives us B , which represents the entropy in H_2 and T_0 .

Let us now consider two isentropic demagnetizations to zero field, one from A , the other from B , leading to points A' and B' . We can measure the corresponding temperatures T_1^* and T_2^* in the Curie-scale. Let us now heat the specimen from T_2^* to T_1^* . If ΔQ is the quantity of heat required, we have

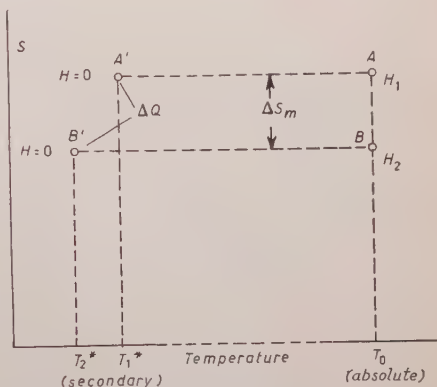


Fig. 13. — The « standard » or « Carnot-cycle » method for determining the thermodynamic temperature scale below 1°K .

$${}_1T_2^* = \frac{\Delta Q}{\Delta S},$$

where ${}_1T_2^*$ denotes the absolute temperature corresponding to the interval $T_1^* \div T_2^*$. Clearly if we use sufficiently close T^* -intervals (demagnetizations from sufficiently close values of the magnetic field) we can get a continuous T - T^* correlation.

In practice, one determines by a series of demagnetizations the S - T^* curve (Fig. 14a); by specific heat measurements ($C^* = \delta Q/dT^*$) or continuous heating the Q - T^* curve (Fig. 14b), and finally, by combining these two, one obtains a Q - S curve (Fig. 14c). The tangent to this curve gives the absolute temperature

$$T = \frac{\delta(Q/R)}{d(S/R)}.$$

The uniform introduction of heat into the specimen is difficult at low temperatures because of poor thermal conductivities and poor thermal contacts. This difficulty has been overcome by the use of γ -radiation as a heat source.

3.5. *Determination of the absolute temperature by purely magnetic measurements.* — The absolute temperature scale can be established without introducing heat into the specimen, and the desirability of using methods involving

magnetic measurements only has been particularly emphasized by GIAUQUE⁽¹⁶⁾. As we have seen before (eq. (8)) the absolute temperature may be defined as

$$T = \left(\frac{\partial E}{\partial S} \right)_H.$$

Hence if the enthalpy E is known as a function of S and H , the absolute temperature may be calculated.

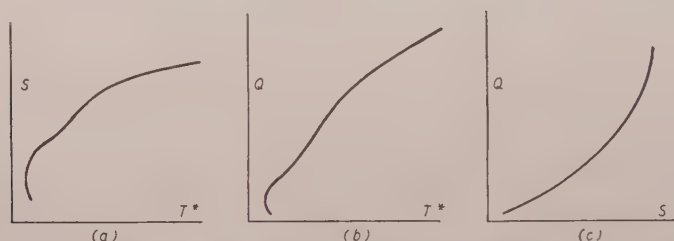


Fig. 14. - The three steps in the «standard» determination of the thermodynamic temperature scale below 1 °K. The slope of the Q - S curve gives T .

Let us try to evaluate E in terms of the differential adiabatic susceptibility $(\partial M/\partial H)_s$, a quantity that is readily determined. By integrating (7) we obtain for the enthalpy along an isentropic line (subscript S):

$$\begin{aligned} E_s(H) &= E_s(H_i) - \int_{H_i}^H M_s dH, \\ &= E_s(H_i) - \int_{H_i}^H \left[\int_0^H \left(\frac{\partial M}{\partial H} \right)_s dH \right] dH, \\ &= E_s(H_i) - H \int_0^H \left(\frac{\partial M}{\partial H} \right)_s dH \Big|_{H_i}^H + \int_{H_i}^H H \left(\frac{\partial M}{\partial H} \right)_s dH. \end{aligned}$$

Hence, if one knows $(\partial M/\partial H)_s$ along an isentropic line one can calculate the variation of the enthalpy along the same isentropic. (The second term on the right hand side can be written $H M_s(H) - H_i M_s(H_i)$, therefore in order to calculate E_s between H_i and H one needs $(\partial M/\partial H)_s$ in this field interval only, provided M at H_i and H is known).

⁽¹⁶⁾ W. F. GIAUQUE: *Phys. Rev.*, **92**, 1339 (1953).

It remains to determine $E_s(H_i)$. It is convenient to regard all isentropics as starting at the same temperature T_i . We can then integrate at constant $T = T_i$ the relation

$$dE = T dS - M dH,$$

and get

$$E(H_i, T_i) = E(0, T_i) + T_i[S(H_i, T_i) - S(0, T_i)] - \int_0^{H_i} M(T_i, H) dH.$$

$E(0, T_i)$ is an integration constant independent of H ; the other two terms can either be measured, or, if the magnetic equation of state $M = f(H, T)$ is known, calculated. If the substance behaves ideally we have:

$$E(H_i, T_i) = E(0, T_i) + M_i H_i,$$

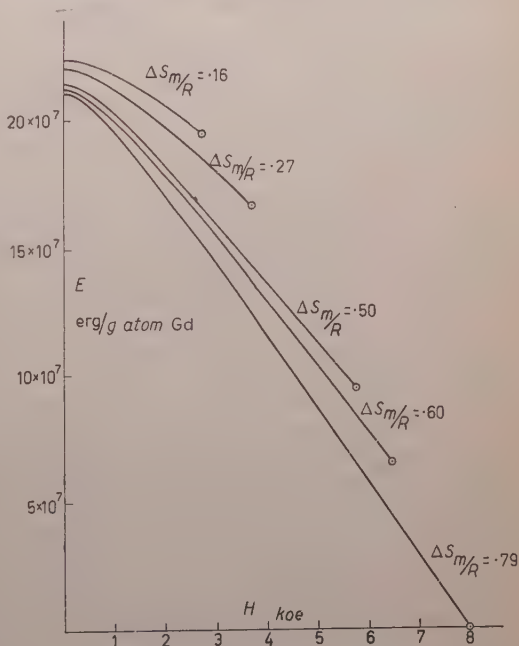
since $dE = dU - d(MH)$ and for $T = \text{const}$ $dU = 0$.

We can now plot E against H for different entropies, and if these curves are sufficiently close, calculate $T = (\partial E / \partial S)_H$ for various fields, including for $H = 0$. Since values of E for $H = 0$ are obtained by integration from H_i to 0, they are sensitive even to small errors in $(\partial M / \partial H)_S$ and this method is least accurate for $H = 0$. This difficulty is however alleviated whenever the substance behaves ideally down to a fairly low field, since then

$(\partial M / \partial H)_S = 0$ down to the same field and the errors in the integrals involving $(\partial M / \partial H)_S$ are reduced.

Fig. 15 shows, as an illustration, the enthalpies along a number of isentropics for gadolinium phosphomolybdate, a substance studied by GIAUQUE and MACDOUGALL (17).

Fig. 15. — The enthalpy of gadolinium phosphomolybdate (for one g -atom of Gd) as a function of the magnetic field for different values of the entropy (after GIAUQUE and MACDOUGALL (17)) ($T_i = 1.43^\circ \text{K}$ for all curves).



(17) W. F. GIAUQUE and D. P. MACDOUGALL: *Journ. Am. Chem. Soc.*, **60**, 376 (1938)

3'6. *Comparison of temperature scales.* – If one knows the T - T^* relation for one salt, then, in principle, this salt could be used as a thermometric standard, and the T^* scales of other salts compared with it. The difficulty is the establishment of satisfactory thermal contact between the two specimens. This is rendered even more difficult by the fact that they have to be sufficiently far from each other to avoid magnetic influence during susceptibility measurements.

These difficulties were overcome in a very elegant method developed by COOKE, MEYER and WOLF⁽¹⁸⁾. They use the magnetically anisotropic $\text{Ce}_2\text{Mg}_3(\text{NO}_3)_{12} \cdot 24\text{H}_2\text{O}$, for which $T^\odot = T$ down to 0.006°K (⁹), as thermometric standard. A solid single crystal sphere of cerium magnesium nitrate is surrounded by a spherical shell of the salt to be studied. The shell, which is made from powdered material so that it is magnetically isotropic, is firmly glued to the inner sphere. After demagnetization one measures the magnetic moment of the specimen along the two principal susceptibility axes of the single crystal. This gives the susceptibilities of both the shell and the core and hence the T - T^* correlation for the salt to be studied. This method seems to be suitable down to about 0.05°K ; below that temperature the thermal contact becomes unreliable.

Such concentric sphere specimens are also useful for determining the specific heats of paramagnetic salts. The cerium magnesium nitrate core serves as an ideal thermometer, since its specific heat is small compared with that of other paramagnetic salts and well enough known for it to be taken into account as a correction.

4. – Determination of splitting and broadening from thermodynamic data.

4'1. *General remarks.* – For the purpose of this discussion the mechanisms which are responsible for lifting the degeneracy of the ground state may be divided into two broad categories:

- (a) Individual ion picture (crystalline Stark effect, hyperfine structure splitting.)
- (b) Co-operative interactions (magnetic dipole, exchange).

The character of the S - T curves will be different in the two cases, as may be seen in Fig. 16. In case (a) (Fig. 16a), the entropy drops smoothly over a wide temperature interval. The specific heat shows a broad Schottky anomaly. In case (b) (Fig. 16b) there is a sharp drop in the entropy curve and a corresponding peak in the specific heat.

Fig. 17 shows the experimentally determined S - T curves for ferric am-

(18) A. H. COOKE, H. MEYER and W. P. WOLF: *Proc. Roy. Soc., A* **233**, 536 (1956).

monium alum (Fe^{3+} , $S = \frac{5}{2}$), chromic potassium alum (Cr^{3+} , $S = \frac{3}{2}$) and cerium magnesium nitrate (Ce^{3+} , $S = \frac{1}{2}$). The two mechanisms responsible for lifting the degeneracy are recognizable. In the case of Ce^{3+} (Kramers degeneracy!) only the co-operative interaction is present, whereas in the other two ions there is also Stark splitting, effective at higher temperatures.

Although magnetic cooling experiments were the first to give reasonably accurate information about the ground states of paramagnetic ions, one is nevertheless justified in asking whether with the advent of paramagnetic resonance they can still be of use for this type of study. After all, thermodynamic measurements give integral effects from which the individual splittings can only be inferred, while paramagnetic resonance gives the splittings directly, usually with great accuracy.

I want to indicate, however, that there are cases in which adiabatic demagnetization experiments (and paramagnetic relaxation) can provide useful and, often, essential additional information.

(a) The determination of splittings in concentrated salts is often made difficult by the broadening of the lines. Magnetic dilution (re-

placement of paramagnetic ions by diamagnetic ions) often alters the splitting, sometimes profoundly. Thermodynamic measurements are useful in these cases.

b) One is usually interested in the splitting in $H = 0$. In paramagnetic resonance the splitting is usually determined in an external field; zero field splitting is obtained by extrapolation. This extrapolation requires an exact knowledge of the symmetry of the crystalline field and here again comparison between paramagnetic resonance data and thermal data may provide useful checks.

(c) The sign of the constant D in the spin Hamiltonian (see Professor PRYCE's lectures) cannot always be obtained with certainty from paramagnetic resonance, because it involves intensity measurements. On the other hand, the sequence of the levels, that is the sign of D , affects the specific heat.

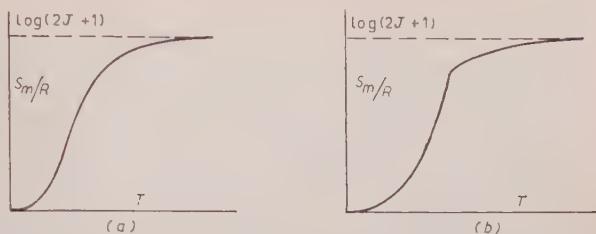


Fig. 16. — Character of the entropy-temperature curves for the two main classes of interaction: a) Stark effect, h.f.s.; b) Dipolar, exchange.

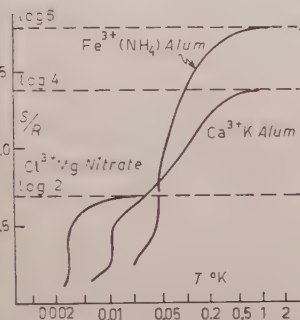


Fig. 17. — Typical entropy-temperature curves of paramagnetic salts.

(d) Finally, paramagnetic resonance can give important information about co-operative interactions, but cannot tell us what macroscopic effects these interactions will produce at the lowest temperatures.

Examples of these cases will be given later.

4.2. Theoretical basis. — The first detailed theoretical treatment of the magnetic cooling method was given in two classic papers by VAN VLECK ⁽¹⁹⁾ and by HEBB and PURCELL ⁽¹¹⁾.

The Hamiltonian of an assembly of paramagnetic ions may be written in the following form:

$$\mathcal{H} = \sum_i V_i + \sum_{i>j} w_{ij} - g\beta \sum_i \mathbf{H} \cdot \mathbf{S}_i.$$

The first term includes both the crystalline potential and the hyperfine structure coupling energy; the second represents the interaction energy between spins and finally the third term is the coupling between the external field and the spin. In the following discussion we shall be interested in the thermodynamic properties in zero field, hence $\mathbf{H} = 0$.

Let us consider the first term only, i.e. negligible interactions. If ϵ_n are the energy eigenvalues, the partition function of the individual ion is

$$Z_i = \sum_n \exp[-\epsilon_n/kT].$$

The partition function for the whole system is $Z = Z_i^{N_0}$, where N_0 is Avogadro's number. (All ions are assumed to be identical.) For $\epsilon_n/kT \ll 1$ the exponential may be expanded:

$$\begin{aligned} Z_i &= \sum_n (1 - \epsilon_n/kT + \epsilon_n^2/2k^2T^2 \dots) \\ &= \text{Tr } 1 \left(1 - \frac{1}{kT} \frac{\text{Tr } V}{\text{Tr } 1} + \frac{1}{2k^2T^2} \frac{\text{Tr } V^2}{\text{Tr } 1} \dots \right). \end{aligned}$$

From $S/R = \log Z_i + (T/Z_i) dZ_i/dT$ it follows that

$$S/R = \ln \text{Tr } 1 - \frac{1}{2k^2T^2} \left[\frac{\text{Tr } V^2}{\text{Tr } 1} - \left(\frac{\text{Tr } V}{\text{Tr } 1} \right)^2 \right] \dots,$$

where the first term $\ln \text{Tr } 1 = \ln(2S+1)$ is the entropy of the degenerate system. Using $C = T(dS/dT)$, we find for the specific heat

$$CT^2/R = \frac{(\bar{\epsilon} - \bar{\epsilon})^2}{k^2},$$

⁽¹⁹⁾ J. H. VAN VLECK: *Journ. Chem. Phys.*, **5**, 320 (1937).

in the notation used by Professor PRYCE. It is clear that a measurement of the high temperature «tail» of the specific heat or entropy gives only a mean value of the splitting but no details.

Let us next consider the case of spin-spin interactions only (Kramers doublet, no h.f.s.). The two most important types of interactions are:

(a) Magnetic dipole interaction:

$$g^2\beta^2 [S_i \cdot S_j r_{ij}^3 - 3(S_i \cdot r_{ij})(S_j \cdot r_{ij})/r_{ij}^5];$$

(b) Isotropic exchange interaction:

$$-2JS_i \cdot S_j = \frac{v_{ij}g^2\beta^2}{r_{ij}^3} S_i \cdot S_j,$$

where

$$v_{ij} = \frac{-2Jr_{ij}^3}{g^2\beta^2} \approx \frac{\text{exchange interaction}}{\text{dipolar interaction}}.$$

Then isotropic exchange can be taken into account by multiplying the first term in the magnetic interaction by $(1+v_{ij})$.

The partition function for the whole system is then

$$Z = \sum_{\lambda} \exp[-\varepsilon_{\lambda}/\kappa T],$$

where λ is a large number. Hence, as before

$$Z = \text{Tr } 1 \left[1 - \frac{1}{\kappa T} \frac{\text{Tr} \sum_{j>i} w_{ij}}{\text{Tr } 1} + \frac{1}{2\kappa^2 T^2} \frac{\text{Tr} (\sum_{j>i} w_{ij})^2}{\text{Tr } 1} \dots \right].$$

Here $\text{Tr } 1$ is the total number of states, of the order of $(2S+1)^N$; $\text{Tr} \sum_{j>i} w_{ij}$ is shown to be zero and one finds that

$$\text{Tr} (\sum_{j>i} w_{ij})^2 = \frac{1}{6} g^4 \beta^4 S^2 (S+1)^2 N \sum_j r_{ij}^{-6} (2 + v_{ji}^2).$$

(N is the number of ions per cm^3 .) Introducing the characteristic temperature for dipolar interaction $\tau = Ng^2\beta^2 S(S+1)/\kappa = 3 \times \text{Curie constant (for cm}^3\text{)}$ we find

$$Z = (2S+1)^N \left[1 + \frac{N}{12} \frac{\tau^2}{T^2} \frac{\sum_j r_{ij}^{-6} (2 + v_{ji}^2)}{N^2} \right].$$

Neglecting r_{ij} for all except nearest neighbours we can calculate the lattice sum and find, for a face centered cubic lattice (e.g. for alums)

$$\sum_j r_{ij}^{-6}(2 + v_{ij}^2)/N^2 = 12(1.20 + v^2/2).$$

Finally, we have

$$S/R = \ln(2S + 1) - (1.2 + v^2/2) \frac{\tau^2}{T^2}$$

and

$$CT^2/R = (2.4 + v^2)\tau^2.$$

It can be shown that in the $1/T^2$ approximation the « individual ion » term and the interaction term are additive and one has:

$$CT^2/R = (CT^2/R)_{\text{Stark splitting, h.f.s.}} + (CT^2/R)_{\text{interaction}}.$$

4.3. Examples of applications to experimental results.

(a) The Cr^{3+} ion has been extensively studied in chromic methylammonium alum $[\text{Cr}(\text{NH}_3\text{CH}_3)(\text{SO}_4)_2 \cdot 12 \text{H}_2\text{O}]$. The first paramagnetic resonance experiments ⁽²⁰⁾ have shown that the behaviour is described by

$$\mathcal{H} = g\beta HS + D[S_x^2 - \frac{1}{2}S(S+1)] \quad (S = \frac{3}{2}),$$

with a Stark splitting (obtained by extrapolation to $H=0$) of $\delta=2D=0.247^\circ\text{K}$. Demagnetization and relaxation experiments ⁽²¹⁾ gave for the specific heat « tail »

$$CT^2/R = 193 \cdot 10^{-4}.$$

If one assumes that exchange is negligible compared with dipolar interaction, we have

$$CT^2/R = \frac{1}{4}\delta^2 + 2.4\tau^2.$$

τ can be calculated from the known Curie-constant and one finds $\delta = 0.269^\circ\text{K}$, in disagreement with the paramagnetic resonance result.

⁽²⁰⁾ B. BLEANEY: *Proc. Roy. Soc., A* **204**, 203 (1950).

⁽²¹⁾ D. DE KLERK and R. P. HUDSON: *Phys. Rev.*, **91**, 278 (1953); W. E. GARDNER and N. KURTI: *Proc. Roy. Soc., A* **223**, 542 (1954); R. P. HUDSON and C. K. McLANE: *Phys. Rev.*, **95**, 932 (1954); J. A. BEUN, M. J. STEENLAND, D. DE KLERK and C. J. GORTER: *Physica*, **21**, 767 (1955); A. H. COOKE and W. P. WOLF (unpublished relaxation measurements).

Further resonance work ⁽²²⁾, carried out to clear up this discrepancy, showed that at low temperatures a term of rhombic symmetry has to be added to the Hamiltonian, and that the original extrapolation to $H = 0$ was at fault. The new value of the splitting (confirmed by measurements at $H = 0$) was

$$\delta = 0.255^\circ\text{K}.$$

Thus there is still a significant discrepancy. This might be explained by introducing exchange, but one finds that the value of v one would have to take would lead to a Weiss Δ of about 0.10°K , in disagreement with the susceptibility measurements. Anisotropic exchange, which affects the specific heat but does not introduce a Weiss Δ could explain the difference. The line shape in paramagnetic resonance however is not compatible with anisotropic exchange. Comparison of paramagnetic resonance and demagnetization thus shows a hitherto unexplained effect.

4.2. *Effect of dilution.* — The case of ferric rubidium alum is an interesting one. The Stark splitting of the Fe^{3+} ions has been studied by paramagnetic resonance in the potassium, ammonium, methylammonium and rubidium alums ⁽²³⁾, aluminium being used as diamagnetic diluent. The overall splitting was found to be 0.16°K , 0.20°K , 1.6°K and 0.065°K respectively. Demagnetization experiments on the concentrated ammonium and methylammonium alums showed no dependence on dilution. More recent demagnetization experiments with concentrated rubidium alum ⁽²⁴⁾ however showed a marked effect: a splitting of 0.20°K instead of 0.065°K in the diluted salt. Subsequent resonance experiments on the concentrated alum ⁽²³⁾ showed a broad, unresolved line, compatible with the splitting found from demagnetization.

For high dilutions the determination of CT^2/R by demagnetization is rendered difficult by the increased relative importance of the lattice specific heat. The paramagnetic relaxation method, which gives the spin specific heat only, is still applicable. E.g. BENZIE and COOKE ⁽²⁵⁾ studied CT^2/R as a function of magnetic dilution for isomorphous Cu^{2+}M^+ Tutton salts (where $\text{M}^+ = \text{NH}_4, \text{Na}, \text{K}, \text{Rb}, \text{Cs}$.) For infinite dilution all CT^2/R tended to the same value, corresponding to the specific heat due to hyperfine splitting. The dependence on dilution was different for the different salts, showing that the exchange interactions depended on the monovalent cation.

⁽²²⁾ J. M. BAKER: *Proc. Phys. Soc.*, B **69**, 633 (1956)l.

⁽²³⁾ B. BLEANEY and R. S. TRENAM: *Proc. Roy. Soc.*, A **223**, 1 (1954).

⁽²⁴⁾ W. E. GARDNER and N. KURTI: *Comm. Conf. Phys. Basses Temp.* (Paris, 1955), p. 206.

⁽²⁵⁾ R. J. BENZIE, A. H. COOKE and S. WHITLEY: *Proc. Roy. Soc.*, A **232**, 277 (1955).

So far we have only considered the temperature range where the $1/T^2$ approximation is valid. As far as the Stark and h.f.s. splittings are concerned, Z_i can be calculated and the temperature dependence of the entropy and of the specific heat established, whatever the value of δ/T . It is often possible to make an allowance for interactions as well, since in many cases $\tau < \delta$, and then the following approximation is possible:

$$Z = Z_i^{N_0} \left(1 + \Omega \frac{\tau^2}{T^2} + \dots \right)^{N_0},$$

where Z_i is the partition function in the absence of dipolar and exchange interactions. These are contained in the correction term Ω which also depends on δ/T .

The study of the Schottky anomaly due to Stark and h.f.s. splitting, if carried out at least down to the specific heat maximum often enables one to establish the sequence of the terms within the splitting pattern. This treatment breaks down when $\tau \approx T$.

5. - Cooperative phenomena.

When $\tau \approx T$ purely magnetic dipole interaction between spins becomes important. All paramagnetic salts, when cooled by demagnetization to such temperature show hysteresis, slight remanence⁽²⁶⁾, and the question is whether this is a sign of ferromagnetism or antiferromagnetism. There are four important theoretical treatments of this problem.

5.1. LORENTZ. - In this approximation the local field H_i is given by

$$H_i = H_0 + \frac{4\pi}{3} I \text{ (long, thin specimens assumed).}$$

Introducing H_i into Curie's law:

$$I = \frac{C(H_0 + (4\pi/3)I)}{T}, \quad \text{hence} \quad I = \frac{CH_0}{T - (4\pi/3)C}.$$

This is so-called « $4\pi/3$ catastrophe», and one would expect ferromagnetism below $T = (4\pi/3)C$, since at this temperature $I/H_0 \rightarrow \infty$.

5.2. ONSAGER⁽²⁷⁾, PIRENNE⁽²⁸⁾. - Unlike in Lorentz's treatment, where the

⁽²⁶⁾ N. KURTI, P. LAINÉ and F. E. SIMON: *Compt. Rend. Acad. Sci.*, **204**, 675 (1937); see also ref. ⁽¹³⁾.

⁽²⁷⁾ L. ONSAGER: *Journ. Am. Chem. Soc.*, **58**, 1486 (1936).

⁽²⁸⁾ J. PIRENNE: *Helv. Phys. Acta*, **22**, 479 (1949).

« sphere » has no physical reality but is solely used as a mathematical artifice (*), Onsager actually « scoops » out a sphere containing one dipole and then, by classical magnetostatics, finds that the field inside the cavity is $H_i = (3\mu/(2\mu+1))H_0$, where $\mu = 1+4\pi\kappa$ is the permeability of the medium. The dipole, when replaced into the cavity polarizes the medium and thereby produces a « reaction » field. This, however, is always parallel to the direction of the dipole and exerts no torque. Hence, as far as the Langevin-Brillouin calculation is concerned, the local field is given by

$$(9) \quad H_i = \frac{3\mu}{2\mu+1} H_0 = \frac{1+4\pi\kappa}{1+(8\pi/3)\kappa} H_0.$$

Substituting into Curie's law $I = CH_i/T$, we get

$$I = C \frac{1+4\pi\kappa}{1+(8\pi/3)\kappa} \frac{H_0}{T}.$$

It should be emphasized that κ got into this expression through the calculation of the cavity field. If we now assume that $I/H_0 = \kappa$ (see below), we have the following equation for the susceptibility:

$$\frac{8\pi}{3} \kappa^2 + \left(1 - \frac{4\pi C}{T}\right) \kappa - \frac{C}{T} = 0,$$

which for low temperatures has the asymptotic solution,

$$\kappa = \frac{3}{2} \frac{C}{T}.$$

Therefore, if we regard infinite susceptibility as the criterion for spontaneous magnetization, the Onsager model predicts no ferromagnetism.

This question has been discussed more recently by PIRENNE⁽²⁸⁾. He pointed out that I/H_0 need not be equal to κ . It is a priori possible for spontaneous magnetization to get established without the permeability of the medium becoming infinite. If one admits this possibility, then $\kappa \rightarrow \infty$ can not be regarded as the criterion for ferromagnetism. (This difficulty does not

(*) To show that the magnetic dipolar interaction field is $(4\pi/3)I$, one first of all shows, by symmetry consideration, that the field produced at the centre by a cubic array of parallel dipoles contained in a sphere is zero. The rest of the material, regarded as continuum produces a field of $(4\pi/3)I$ if the demagnetizing factor is zero. Now the symmetry argument applies equally well to an assembly of dipoles contained in a cube. And, indeed, if one calculates the effect of the material outside this cube, one finds, after a somewhat more laborious calculation, that it is $(4\pi/3)I$.

arise in the Lorentz treatment, since there the susceptibility does not appear explicitly).

PIRENNE writes for the magnetic moment quite generally:

$$I = I_{H_0=0} + \left(\frac{\partial I}{\partial H_0} \right)_{H_0=0} H_0,$$

where

$$(10) \quad \left(\frac{\partial I}{\partial H_0} \right)_{H_0=0} = \kappa,$$

the susceptibility that enters into the calculation of the cavity field. By a calculation similar to that used by ONSAGER he finds

$$(11) \quad \begin{cases} H_t = \frac{3\mu}{2\mu+1} H_0 + \frac{4\pi}{2\mu+1} I_{H_0=0} \\ \quad = H_0 + \frac{4\pi}{2\mu+1} I = H_0 + \frac{4\pi}{3+8\pi\kappa} I. \end{cases}$$

Equation (11) becomes identical with (9) if one assumes $\kappa = I/H_0$.

The magnetization is given by a Brillouin function (*)

$$(12) \quad \frac{I}{Nm} = B \left[\frac{m(H_0 + fI)}{kT} \right],$$

where $m = g\beta J$ is the elementary moment (we use m instead of the usual μ so as to avoid confusion with the permeability), and

$$(13) \quad f = 4\pi/(3 + 8\pi\kappa).$$

By differentiating (12) and with $H_0 = 0$ we get from (10)

$$(14) \quad \kappa = \frac{3}{4\pi B'(0)} \frac{T_0}{T} (1 + f\kappa) B'(x),$$

with the notation $x = m f I / \kappa T$ and

$$T_0 = \frac{4\pi}{3} \frac{Nm^2}{k} B'(0) \quad (\text{the Curie point according to Lorentz}).$$

(*) PIRENNE, who considers dielectrics, uses the Langevin function.

With these notations and for $H_0 = 0$ (12) becomes

$$(15) \quad x = \frac{3}{4\pi B'(0)} \dagger \frac{T_0}{T} B(x).$$

After eliminating κ and f between (13), (14), (15) we obtain:

$$(16) \quad \frac{T}{T_0} = \frac{1}{B'(0)} \frac{B(x)}{x} \frac{B(x)/x - 3B'(x)}{B(x)/x - B'(x)}.$$

One finds that below a temperature T_c there exists a non-zero solution, in other words the substance has a finite magnetic moment in $H_0 = 0$. If one assumes that the elementary moment is a single spin, $B(x) = \tanh x$, one finds

$$\frac{T_c}{T_0} = .340, \quad (x = 2.4),$$

i.e. the Curie point is considerably below that predicted by the Lorentz approximation. The results of the Pirenne's treatment show another, more important peculiarity. The Curie-point becomes a first order transition: at T_c the spontaneous magnetization jumps from zero to nearly saturation value. For our numerical example we find from (12)

$$\frac{I(T_c)}{Nm} = \tanh(2.4) = .98.$$

5.3. SAUER⁽²⁹⁾, LUTTINGER and TISZA⁽³⁰⁾. — These authors consider cubic arrays of classical dipoles, all oriented parallel to each other and compare the energies of the various antiferromagnetic arrangements with the ferromagnetic arrangement. They find that in several cases, e.g., for a face centered cubic lattice with dipoles aligned along face diagonals, the energy (and hence the free energy, because we are considering the system at the absolute zero) of the ferromagnetic state is lower than that of the antiferromagnetic state, provided the sample is elongated (axial ratio larger than 6:1). Such a salt, when demagnetized adiabatically from saturation should retain its full magnetic moment even when the external field is reduced to zero.

5.4. COHEN and KEFFER⁽³¹⁾. — These authors treat the same problem quantum mechanically and also find that in many cases the ferromagnetic

⁽²⁹⁾ J. A. SAUER: *Phys. Rev.*, **57**, 142 (1940).

⁽³⁰⁾ J. M. LUTTINGER and L. TISZA: *Phys. Rev.*, **70**, 954 (1946).

⁽³¹⁾ M. H. COHEN and F. KEFFER: *Phys. Rev.*, **99**, 1135 (1955).

arrangement has the lower energy. The quantum mechanical treatment shows in addition that large spins favour ferromagnetism. This is not the case in the classical dipole treatment where the magnitude of the spin only affects the Curie point but *not* the relative stability of the ferromagnetic and antiferromagnetic states.

Does the fact that no spontaneous magnetization or appreciable remanence has so far been observed in paramagnetic salts below their co-operative anomaly disprove the theories? There are two reasons why the negative results are compatible with the theoretical predictions:

(a) The essential conditions of the Sauer-Luttinger-Tisza and Cohen-Keffe theories were not satisfied in the experiments. Thus for instance in the paramagnetic alums there are four ions per unit cell, and because of the relatively strong crystalline field coupling (the Stark splitting is usually several times larger than the magnetic interaction) the dipoles, in the external field, are oriented along the four body diagonal of the cube. Such an arrangement impairs the effectiveness of the dipolar forces ⁽³²⁾. Dysprosium ethyl sulphate which has one magnetic ion per unit cell and has large moment (the lowest level is $J_z = \pm 15/2$) seems to be the ideal test substance.

(b) KITTEL ⁽³³⁾ has pointed out that a dipolar ferromagnet was likely to break up into domains. If this were so neutron diffraction might have to be used to decide whether the arrangement was ferromagnetic or antiferromagnetic.

6. - Nuclear orientation.

The limit of temperature that can be reached by isentropic demagnetization of an electron paramagnetic substance is chiefly determined by the H_{eff} ($= H_i(T_f/T_i)$) (equation (6)), which is ultimately caused by interaction between spins. It was suggested by GORTER ⁽³⁴⁾, and by KURTI and SIMON ⁽³⁵⁾ that a nuclear paramagnetic with a hundred to a thousand times smaller H_{eff} would allow much lower temperatures to be reached (*). The efforts to produce

⁽³²⁾ MARY C. M. O'BRIEN: *Phys. Rev.*, **101**, 1573 (1956).

⁽³³⁾ C. KITTEL: *Phys. Rev.*, **82**, 965 (1951).

⁽³⁴⁾ C. J. GORTER: *Phys. Z.*, **35**, 923 (1934).

⁽³⁵⁾ N. KURTI and F. B. SIMON: *Proc. Roy. Soc.*, A **149**, 152 (1935).

(*) It is true that there exist paramagnetic salts with values of H_{eff} comparable to those in nuclear paramagnetics. But, since equation (6) is based on the assumption $T_i > 0 = g\beta H_{\text{eff}}/\kappa$, the lower limit for T_i (and hence for T_f) would be about thousand times (higher ratio of electronic to nuclear Bohr magneton) for ordinary magnetic cooling than for nuclear cooling. The same thing can be expressed by saying that

an appreciable nuclear magnetization which is a prerequisite of nuclear demagnetization thus began as a purely low temperature pursuit. The emphasis shifted when it was realized (HALBAN⁽³⁶⁾, SPIERS⁽³⁷⁾ etc.) that magnetized, or more generally, oriented nuclear systems (i.e. systems in which the spatial distribution of the nuclear spin axes was not isotropic) could be useful for the study of nuclear reactions.

The following discussion will be restricted to equilibrium states, i.e. situations, in which the system comprising nuclear spins electron-spins, lattice vibrations remains in the same state as long as it does not exchange energy with the surroundings. With this restriction the various methods for producing nuclear orientation can best be discussed by the Abragam-Pryce Hamiltonian (see Professor PRYCE's lectures):

$$\mathcal{H} = -\gamma\beta_N H \cdot I + \beta\{g_{\parallel}H_zS_z + g_{\perp}(H_xS_x + H_yS_y)\} + A\{S_zI_z + B(S_xI_x + S_yI_y)\} + \\ + D\{S_z^2 - \frac{1}{3}S(S+1)\} + Q\{I_z^2 - \frac{1}{3}I(I+1)\},$$

where $Q = (q3e\partial^2V/\partial z^2)/(4I(2I-1))$, q being the electric quadrupole moment, and V the crystalline electric potential.

6.1. *External field polarization.* — Consider the first term: direct coupling between the external field and nuclear spins. The condition for appreciable nuclear polarization is $\beta_N H/kT \approx 1$, i.e. $H/T \approx 10^4$ kOe/°K e.g. 100 kOe at .01 °K. The experimental difficulties are great. The first appreciable nuclear polarization was achieved by DABBS, ROBERTS and BERNSTEIN⁽³⁸⁾ in Oak Ridge in metallic indium which was cooled by contact with a demagnetized paramagnetic salt (iron alum) to .04 °K and magnetized in a field of 13 kOe. The resulting polarization ($M/M_s = .02$) of the ¹¹⁵In nuclei was detected by the differential absorption of a polarized neutron beam. The entropy reduction in the nuclear spin system was $\Delta S/R = 5 \cdot 10^{-4}$, compared with the total nuclear entropy of $S/R = \ln 10 = 2.3$.

Considerably higher polarizations and entropy reductions were obtained in recent Oxford experiments (KURTI, ROBINSON, SIMON and SPOHR)⁽³⁹⁾ in which Cu-nuclei (in metallic copper) were cooled to .012 °K and magnetized

for a given H_{eff} the interaction energy, which roughly determines the final temperature to be reached, is about thousand times smaller for nuclear spins than for electron spins.

⁽³³⁾ H. HALBAN: *Nature*, **140**, 425 (1937).

⁽³⁷⁾ J. A. SPIERS: *Nature*, **161**, 807 (1948).

⁽³⁸⁾ J. W. T. DABBS, L. D. ROBERTS and S. BERNSTEIN: *Phys. Rev.*, **98**, 1512 (1955).

⁽³⁹⁾ N. KURTI, F. N. H. ROBINSON, F. E. SIMON and D. A. SPOHR: *Nature*, **178**, 450 (1956).

in fields up to 28 kOe. ($\Delta S/R = 1.2 \cdot 10^{-2}$ compared with $S/R = 1.4$, $M/M_s = .12$). Subsequent adiabatic demagnetizations led to temperatures, down to $2 \cdot 10^{-5}$ °K. calculated from the nuclear susceptibility by means of Curie's law. The results agreed with equation 6 and gave $H_{\text{eff}} = 25$ Oe. This value is about 10 times higher than one would expect from magnetic dipolar interactions, or from the Ruderman-Kittel⁽⁴⁰⁾ indirect exchange mechanism or from the Frohlich-Nabarro⁽⁴¹⁾ type self-polarization through the intermediary of the conduction electrons. (The satisfactory agreement with the Frohlich-Nabarro prediction mentioned in ref. (39) was found to be illusory when the best recent experimental data were used for calculating the interaction.)

The « external field polarization » or « brute force » method is the only one in which the entropy corresponding to the spatial disorder of the nuclear axes can be altered by varying an external parameter, namely the magnetic field. This is not possible for the other methods now to be discussed; the « brute force » method is thus the only one that can lead to nuclear cooling.

6'2. Magnetic hyperfine structure (h.f.s.) polarization. — Consider the second and third terms of the Hamiltonian and assume for simplicity that $g_{\parallel} = g_{\perp}$, $A = B$ ($\approx 10^{-2}$ °K). Put on \mathbf{H} in z -direction. This results in preferential population of electron spins parallel to field (2-nd term of \mathcal{H}) and, because of 3-rd term, the nuclear spins will follow if the temperature is low enough. This method (« magnetic h.f.s. polarization ») was first suggested by GORTER⁽⁴²⁾ and by ROSE⁽⁴³⁾, actually before the introduction of the Abragam-Pryce Hamiltonian, and even before the experimental discovery of h.f.s. in solids by PENROSE⁽⁴⁴⁾. The argument was that the unbalanced electron spin in a paramagnetic ion produced a strong field at the nucleus, $H_{\text{nuc.}} \approx A/\beta_N \approx \approx 10^2 \div 10^3$ kOe. Hence if all these local fields are oriented parallel, the nuclei will also be polarized. The first experiments with this method were carried out by AMBLER, GRACE, HALBAN, KURTI, DURAND, JOHNSON and LEMMER⁽⁴⁵⁾ in Oxford. The anisotropy of the γ -rays emitted by ^{60}Co incorporated in cerium magnesium nitrate (see below) was used to detect the nuclear polarization.

6'3. Electric h.f.s. alignment. — Let us consider the last term in \mathcal{H} . POUND⁽⁴⁶⁾ suggested that the coupling between the nuclear electric quadrupole moment

(40) M. A. RUDERMAN and C. KITTEL: *Phys. Rev.*, **96**, 99 (1954).

(41) H. FROHLICH and F. R. N. NABARRO: *Proc. Roy. Soc., A* **175**, 382 (1940).

(42) C. J. GORTER: *Physica*, **14**, 504 (1948).

(43) M. E. ROSE: *Phys. Rev.*, **75**, 213 (1949).

(44) R. P. PENROSE: *Nature*, **163**, 992 (1949).

(45) E. AMBLER, M. A. GRACE, H. HALBAN, N. KURTI, H. DURAND, C. E. JOHNSON and H. R. LEMMER: *Phil. Mag.*, **44**, 216 (1953).

(46) R. V. POUND: *Phys. Rev.*, **76**, 1410 (1949).

and the electric field gradient (particularly strong in certain covalent bonds) could be used for orienting nuclei. If all the field gradients have the same orientation (a uniaxial single crystal is required), the nuclear spins, too, will be oriented, if the temperature is sufficiently low ($T \sim Q/K$). Since the energy depends on I_z^2 we have here *alignment* and not *polarization*; positive and negative orientations of the nuclear spins are equally probable.

The feasibility of this method has been recently demonstrated by DABBS, ROBERTS and PARKER⁽⁴⁷⁾ who aligned ^{233}U nuclei in a diamagnetic uranyl salt. Because of the large quadrupole coupling the temperature of about 1°K was sufficiently low for this experiment. The alignment was detected by the anisotropic α -emission.

6.4. Magnetic h.f.s. alignment. — Finally consider the 3-rd and 4-th terms in \mathcal{H} . BLEANEY⁽⁴⁸⁾ pointed out that the magnetic h.f.s. coupling can also produce preferential nuclear spin orientations with respect to crystal axes. This can come about in two ways:

(i) $S \geq 1$, $D \neq 0$; and let us assume $A = B$. Because of the 4-th term the electron spins will be aligned with respect to the axis of symmetry and the 3-rd term will bring about nuclear alignment.

(ii) $S = \frac{1}{2}$, hence no D -term (Kramers doublets). If $A \neq B$ there will be nuclear alignment with respect to a crystal axis, the alignment being axial, i.e. $I_z = \pm I$ if $A > B$, or in a plane i.e. $I_z = \pm \frac{1}{2}$, if $A < B$. The first experiment using the magnetic h.f.s. alignment method (in fact the first conclusive nuclear orientation experiment) was done by DANIELS, GRACE and ROBINSON⁽⁴⁹⁾ in Oxford. The γ -ray anisotropy of ^{60}Co in a single crystal of a Tutton salt served for the detection of the alignment.

These four methods are summarized in Table I. The figures given in the table are only approximate. For instance, as mentioned before, measurable effects can in some cases be obtained at much higher temperatures, even at about 1°K .

The length of the relaxation time between the nuclear spin system and its surroundings can become a major problem at low temperatures. Thus in dielectric substances the nuclear spin-lattice relaxation time might become prohibitively large (hours or even days!) below 0.1°K . Paramagnetic impurities can be used to reduce this relaxation time. The situation is better in a metal, where the nuclear spin-conduction electron relaxation time (τ) is

⁽⁴⁷⁾ J. W. T. DABBS, L. D. ROBERTS and G. W. PARKER: *Bull. Am. Phys. Soc.* (II), **1**, 207 (1956).

⁽⁴⁸⁾ B. BLEANEY: *Proc. Phys. Soc.*, A **64**, 315 (1951).

⁽⁴⁹⁾ J. M. DANIELS, M. A. GRACE and F. N. H. ROBINSON: *Nature*, **168**, 780 (1951).

TABLE I. — *The equilibrium (or static) methods for nuclear orientation.*

Method	Parameter defining the axis of orientation		Nuclear spins	Remarks
a) External field polarization	\uparrow H 50 kOe .01 °K	(direct coupling)	$\uparrow\uparrow\uparrow\uparrow$	Relaxation time!
b) Magnetic h.f.s. polarization	\uparrow H 1 kOe .05 °K	(through electron spin)	$\uparrow\uparrow\uparrow\uparrow$	Paramagnetic salt Isotropic h. f. s. preferable
c) Magnetic h.f.s. alignment	\uparrow crystalline electric field .05 °K	(through electron spin)	$\uparrow\uparrow\downarrow\downarrow\downarrow\downarrow\uparrow\uparrow$	Paramagnetic single cryst. Anisotropic h.f.s. or <i>D</i> -term
d) Electric h.f.s. alignment	\uparrow crystalline electric field .05 °K	(through electric quadrupole moment)	$\uparrow\uparrow\downarrow\downarrow\downarrow\downarrow\uparrow\uparrow$	Single crystal covalent bond

shorter and does not increase too rapidly with falling temperature. For copper one has approximatively, $\tau = 1.0/T$ s.

Methods (b) and (c) although listed separately, are frequently used in conjunction. Thus, if one has an anisotropic hyperfine structure ($A \gg B$), but magnetic interaction between adjacent paramagnetic ions disturbs the zero field alignment, an external field, directed along the crystal axis can be used to swamp these effects ⁽⁵⁰⁾.

6'5. *Cooling procedures for the « magnetic h.f.s. » methods.* — The largest number of experiments have so far been carried out with the two magnetic h.f.s. methods. Nuclear orientation experiments are being carried out in the following places: Oxford, Leiden, Oak Ridge, the National Bureau of Standards, University of Illinois, and Ohio State University. In most cases a temperature of less than .05 °K is required, which means that adiabatic demagnetization has to be used. Since for these methods one uses nuclei in paramagnetic ions, one might think that the same ion might serve as cooling agent. This, however, is not advantageous. Take e.g. ⁵⁹Co for which $S = \frac{1}{2}$, $I = \frac{7}{2}$. The total

⁽⁵⁰⁾ M. A. GRACE, C. E. JOHNSON, N. KURTI, H. R. LEMMER and F. H. N. ROBINSON: *Phil. Mag.*, **45**, 1192 (1954).

entropy for $H = 0$ is

$$S/R = \ln(2S + 1)(2I + 1) = \ln 16.$$

But at 1°K and with the available fields only the electronic entropy, i.e. $\log 2$, can be removed. If we assume the most favourable case, namely that during demagnetization, the electron spins become completely disordered with respect to the plus and minus orientations, so that all this entropy reduction is transferred to the nuclear spins, we are still left with a nuclear entropy of $\log 4$. It is therefore better to use a separate cooling agent, preferably one with no nuclear moments. The ion whose nucleus one wants to orient is introduced in the lattice of the coolant in small concentration to form a mixed crystal. The following paramagnetic salts seem particularly useful cooling agents for these experiments:

Cerium ethylsulphate, for orienting nuclei of the rare-earths in the trivalent ions. The T - T^* correlation has been determined down to 0.02°K by JOHNSON and MEYER⁽⁵¹⁾.

Nickel fluosilicate, to orient nuclei of iron-group elements in the divalent ions. Here again, the T - T^* correlation has been determined down to 0.01°K on a mixed crystal containing 15% Ni 85% Zn⁽⁵²⁾.

Cerium magnesium nitrate, to some extent to orientate rare-earths' nuclei, but chiefly to polarize nuclei in the divalent ions of the iron group by method (b).

One of the main problems in method (b) is how to avoid the warming-up of the cooling agent when the polarizing field is switched on, especially if the cooling agent is incorporated in the same crystal. The use of magnetically anisotropic paramagnetic crystals has great advantages as was first demonstrated, in a slightly different case, by COOKE, WHITLEY and WOLF⁽⁵³⁾.

In $\text{Ce}_2\text{Mg}_3(\text{NO}_3)_{12} \cdot 24\text{H}_2\text{O}$, $g_{\parallel}/g_{\perp} \approx .10$. Therefore if one magnetizes at T_i with H_i perpendicular to the axis, and then reduces the field to H_f , turning it so that it is parallel to the axis, one has for T_f the following approximate relation:

$$\frac{g_{\perp}H_i}{T_i} = -\frac{g_{\parallel}H_f}{T_f}.$$

with $T_i = 1^\circ\text{K}$, $H_i = 20\text{ kOe}$ and $H_f = 1\text{ kOe}$ one finds $T_f \approx .005^\circ\text{K}$. If some of the Mg^{2+} is replaced by a paramagnetic ion with isotropic h.f.s. (e.g. Mn^{2+} or Co^{2+}) the conditions for magnetic h.f.s. polarization, namely low temperature and a sufficiently strong field for polarizing the electron spins, are satisfied. This method was used in the Oxford experiments⁽⁴⁵⁾.

(51) C. E. JOHNSON and H. MEYER: *Bull. Am. Phys. Soc.* (II) **2**, 184 (1957).

(52) J. S. HILL, H. MEYER and T. H. MILNER: to be published (1957).

(53) A. H. COOKE, S. WHITLEY and W. P. WOLF: *Proc. Phys. Soc.*, B **68**, 415 (1955).

6.6. *Nuclear orientation and radioactive decay.* — Let us see what information may be obtained from measurements of the anisotropy of the γ -rays emitted by oriented, radioactive nuclei. Consider a radioactive nucleus, having a nuclear spin I_γ , which decays by emission of a γ -ray of angular momentum i_γ to the ground state of spin I_0 . i_γ gives the multipole character of the radiation: $i_\gamma = 1, 2, \dots$, corresponding to dipole, quadrupole etc. Let $m = I_\gamma, I_\gamma - 1, \dots, -I_\gamma$, be the projection of I along the axis of quantization and θ the angle between this axis and the direction of observation. The intensity emitted in the direction θ by a nucleus in the magnetic substate m can be written

$$W_m(\theta) = 1 + \sum_k U(I_\gamma, I_0, i_\gamma, m) P_k(\cos \theta),$$

where P_k is the Legendre polynomial and $k = 2, \dots, 2i_\gamma$.

The population of any m -state is given by the Boltzman factor $\exp[-E_m/kT]$, where E_m depends on the constants of the Abragam-Pryce Hamiltonian and, for method (b), also on H . If we sum over all m -states, we get

$$W(\theta) = 1 - a(I_\gamma, I_0, i_\gamma, \xi) \cos^2 \theta - b(I_\gamma, I_0, i_\gamma, \xi) \cos^4 \theta - \dots,$$

where

$$\xi = \frac{\mu_N H_{\text{nuc.}}}{IkT},$$

with μ_N being the nuclear magnetic moment in nuclear Bohr magnetons. (Here it is assumed that if method (b) is used H is large enough for the electron spins to be saturated). Finally we define the anisotropy of the emission as

$$\varepsilon = \frac{W(\pi/2) - W(0)}{W(\pi/2)}.$$

It was assumed in the foregoing that one orients the nucleus in its γ -emitting state. This, in most cases, is not true since the γ -emission is usually preceded by a β or positron decay. One actually orients the nucleus (spin I_β) which through β or positron emission (or K electron capture) decays into the excited state of the daughter nucleus (spin I_γ), and one observes the γ -anisotropy from that state.

Now, even if one assumes, as one is justified in most cases, that the life of the I_γ state is so short that neither recoil effects nor the altered magnetic field due to the β -decay can disturb the orientation, there is still the change in the angular momentum $I_\beta \rightarrow I_\gamma$ (in magnitude or orientation or both) to be taken into account. Actually, by careful analysis of the temperature dependence of the anisotropy it is often possible to determine the spin change

$I_\beta \rightarrow I_\gamma$ and, also, the selection rule followed in this transition. Such an analysis has been carried out, e.g. for ^{58}Co (54). It can be said that γ -ray anisotropy measurements are useful for filling in unknown data of radioactive decay schemes, e.g. the multipole character of the radiation, the spin and parity changes, and the value of the nuclear magnetic moment of the radioactive nucleus. This latter is determined through the temperature variation of ϵ which depends on $\xi = \mu_N H_{\text{nuc}} / I k T$. If H_{nuc} is known from paramagnetic resonance experiments on the stable isotope, μ_N / I and hence (if I is known) μ_N can be determined.

The highest γ -anisotropy so far observed was 90% measured on ^{54}Mn in cerium magnesium nitrate as cooling agent (GRACE, JOHNSON, KURTI, LEMMER and ROBINSON (50)). Method (b) was used and the corresponding nuclear polarization was calculated to be about 95%. That this is indeed polarization and not alignment can be ascertained by measuring the degree of circular polarization of the γ -rays observed along the axis of orientation. Such experiments have been carried out on ^{60}Co by WHEATLEY, HUISKAMP, DIDDENS, STEENLAND and TOLHOEK (55), who detected the circular polarization by measuring forward scattering of the γ -rays on magnetization. These experiments also give the sign of the nuclear magnetic moment.

A variant, or combination of methods (b) and (c) relies on the coupling between the nuclear spins and the spontaneously magnetized electron spins in ferromagnetics. Experiments on ^{60}Co in a single crystal of cobalt (GRACE, JOHNSON, KURTI, SCURLOCK and TAYLOR (56)) showed that the h.f.s. coupling in the ferromagnetic metal is about the same as in the paramagnetic salt.

APPENDIX

The maintenance of constant temperature baths below 1 °K.

The cyclic demagnetization cryostat developed by HEER, BARNES and DAUNT (57) and made commercially available by the Arthur D. Little Co. of Cambridge, Massachusetts, offers a very satisfactory solution of this problem.

(54) J. M. DANIELS, M. A. GRACE, H. HALBAN, N. KURTI and F. N. H. ROBINSON: *Phil. Mag.*, **43**, 1297 (1952).

(55) J. C. WHEATLEY, W. J. HUISKAMP, A. N. DIDDENS, H. J. STEENLAND and R. A. TOLHOEK: *Physica*, **21**, 841 (1955).

(56) M. A. GRACE, C. E. JOHNSON, N. KURTI, R. O. SCURLOCK and R. T. TAYLOR: *Bull. Am. Phys. Soc. (II)* **2**, 136 (1957); see also G. R. KHUTSISHOILI: *Journ. Exp. Theor. Phys. USSR*, **29**, 894 (1955).

(57) C. V. HEER, C. B. BARNES and J. G. DAUNT: *Rev. Sci. Instr.*, **25**, 1088 (1954).

The method consists in principle of a magnetic Carnot-cycle, as represented in the S - T diagram of Fig. 18 (the actual numerical data in the sketch are only approximate). The four steps are as follows:

- AB*: isothermal magnetization at 1°K , $1\text{ kOe} \div 10\text{ kOe}$, heat being given up to a helium bath.
- BC*: isentropic demagnetization $10\text{ kOe} \div 2.5\text{ kOe}$, leading to about $.25^\circ\text{K}$.
- CD*: isothermal demagnetization at $.25^\circ\text{K}$ from 2.5 kOe to 0 kOe , during which heat is absorbed from the low temperature bath.
- DA*: isentropic magnetization $0 \rightarrow 1\text{ kOe}$ which brings the working substance back to 1°K .

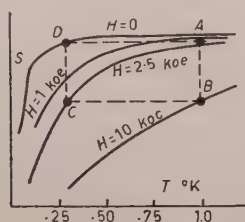


Fig. 18. — The magnetic Carnot cycle of the Heer-Barnes-Daunt cyclic refrigerator.

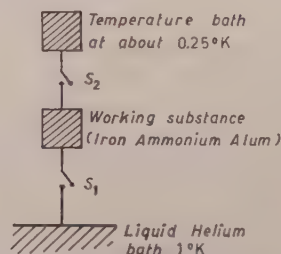


Fig. 19. — Schematic diagram of the magnetic refrigerator.

Fig. 19 shows schematically the essential parts of the apparatus. S_1 and S_2 are superconducting heat switches, which make use of the fact that the heat conductivity in the superconducting state is much smaller than in the normal state. By applying a magnetic field large enough to destroy superconductivity the thermal switch can be turned on. In the cycle illustrated in Fig. 18 both S_1 and S_2 are « off » during *BC* and *DA*; S_1 is « on » during *AB*, S_2 is « on » during *CD*. Various irreversible effects, some unavoidable, are responsible for a reduction of the efficiency of the cycle as compared with an ideal one especially at low temperatures. Thus at 0.25°K the refrigerator can absorb 4000 erg/min , which is about 10% of the ideal.

As long as one wants to absorb relatively large quantities of heat for long periods of time, or one wants to cool down large heat capacities, such a cyclic process is essential. Often, however, the entropy of the substance to be cooled is relatively small, or the heat evolved at the low temperature is small, or, finally, the experiments to be carried out do not take very long. In such cases a rather simple arrangement could be used instead of the cyclic refrigerator.

Let us assume that an electromagnet, producing 10 kOe in a pole gap of 5 cm and over an area of $5\text{ cm} \times 2\text{ cm}$ is available. (A small iron cored electromagnet weighing about 250 kg and consuming $4 \div 5\text{ kW}$ would be adequate). With such magnet dimensions it would be possible to use a paramagnetic salt specimen (say ferric ammonium alum) of 2 cm diameter and 5 cm length, i.e. $15\text{ cm}^3 \approx 1/20\text{ g-ion}$. At 1°K and 10 kOe , $\Delta S = .1\text{ cal/}^\circ\text{K}$. If one now reduces the field isentropically to 2.5 kOe the temperature will drop to about $.25^\circ\text{K}$ (provided no great thermal ballast is to be cooled down). Any heat

influx and heat generated can be compensated by suitably controlled further reduction of the field. The total quantity of heat that can be absorbed is given by

$$Q = T \Delta S \approx 0.25 \cdot 0.1 \text{ cal} = 10^6 \text{ erg}.$$

Hence a heat influx of 4000 erg/min at 0.25 °K can be absorbed during $(10^6/4 \cdot 10^3) = 250$ min, which for many experiments is quite adequate.

Finally, for the temperature range down to 0.3 °K the use of liquid ^3He offers advantages. Because of the absence of the creeping film and the relatively large vapour pressures it should be possible to maintain a ^3He bath at about 0.3 °K (vapour pressure = $2 \cdot 10^{-3}$ mm Hg) even with a rather small pump (say a diffusion pump of a speed of 50 litres/s at $5 \cdot 10^{-4}$ mm Hg). It would be necessary, or, at least, advisable, to have a ^4He bath at 0.9 °K for precooling and as a thermal shield. But, with such precautions, about 1.5 litres of ^3He (normal temperature and pressure) would be sufficient to keep a cryostat at 0.3 °K for something like 8 h.

BIBLIOGRAPHY

General references (in reverse chronological order).

- M. J. STEENLAND and H. A. TOLHOEK: *Orientation of atomic nuclei at low temperature*, in *Progress in Low Temperature Physics* (ed. GORTER), **2**, 292 (Amsterdam, 1957).
- D. DE KLERK: *Adiabatic Demagnetisation*, in *Encyclopedia of Physics*, **15**, 38 (Berlin 1956).
- E. AMBLER and R. P. HUDSON: *Magnetic cooling*, in *Rep. Progr. Phys.*, **18**, 251 (1955).
- K. D. BOWERS and J. OWEN: *Paramagnetic Resonance II*, in *Rep. Progr. Phys.*, **18**, 304 (1955).
- A. H. COOKE: *Paramagnetic Crystals in use for Low Temperature Research*, in *Progr. in Low Temp. Phys.* (ed. GORTER), **1**, 224 (Amsterdam, 1955).
- D. DE KLERK and M. J. STEENLAND: *Adiabatic demagnetization*, in *Progr. in Low Temp. Phys.* (ed. GORTER), **2**, 273 (Amsterdam, 1955).
- R. J. BLIN-STOYLE, M. A. GRACE and H. HALBAN: *Experiments with Oriented Nuclei Beta and Gamma Ray Spectroscopy* (ed. SIEGBAHN), p. 600 (Amsterdam, 1955).
- C. G. B. GARRETT: *Magnetic Cooling* (Cambridge, Mass., 1954).
- B. BLEANEY and K. W. H. STEVENS: *Paramagnetic Resonance*, in *Rep. Progr. Phys.*, **16**, 108 (1953).
- R. J. BLIN-STOYLE, M. A. GRACE and H. HALBAN: *Oriented Nuclear Systems*, in *Progr. in Nuclear Physics* (ed. FRISCH), **3**, 63 (London, 1953).
- N. KURTI: *The Temperature Range below 1° Absolute*, in *Low temperature Physics*, Four Lectures, p. 30 (London, 1952).
- A. H. COOKE: *Paramagnetic Relaxation Effects*, in *Rep. Progr. Phys.*, **13**, 276 (1950).
- J. H. VAN VLECK: *Quelques aspects de la théorie du magnétisme*. *Ann. Inst. Poincaré*, **10**, 57 (1947).
- H. B. G. CASIMIR: *Magnetism and Very Low Temperatures* (Cambridge, 1940).

Cyclotron Resonance in Crystals.

C. KITTEL

University of California - Berkeley, Cal.

In cyclotron resonance experiments electrons or holes in a crystal are caused to spiral around an applied field H_0 at the cyclotron frequency

$$(1) \quad \omega = \pm \frac{eH_0}{m^*c}.$$

A hole behaves like an electron but with a positive charge. Here m^* is the effective mass of the electron or hole in the crystal. In addition we apply an oscillating electric field perpendicular to H_0 so that one observes electric dipole transitions as an added load on the microwave apparatus. In practice the frequency of the electric field is held fixed and H is adjusted until resonance is observed as a peak in the power absorption, as in Fig. 1.

Thus one obtains m^* . It is desirable to perform the experiment on single crystals since m^* is usually anisotropic.

In principle both spin resonance and cyclotron resonance could be observed simultaneously, but cyclotron resonance absorption is about 10^{12} times as intense as spin resonance absorption which involves magnetic dipole transitions. This we can see as follows:

The ratio of the transition probabilities is

$$\frac{P_{\text{cycl.}}}{P_{\text{spin}}} = \frac{|erE_{\text{rf}}|^2}{|\mu_B H_{\text{rf}}|^2},$$

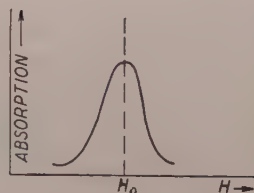


Fig. 1. — Power absorption vs. magnetic field, at constant frequency.

where r is the radius of the orbit of the particle:

$$v = v/\omega = \text{velocity of particle/angular velocity.}$$

Usually

$$E_{\text{rf}} \approx H_{\text{rf}},$$

so that

$$\frac{P_{\text{cycl.}}}{P_{\text{spin}}} \approx \left| \frac{er}{\mu_B} \right|^2.$$

For

$$m^* = 0.1 m_e, \quad v = 10^6 \text{ cm/s (at } 4^\circ\text{K)}, \quad \omega = 10^{11} \text{ s}^{-1},$$

we have

$$r = 10^6/10^{11} = 10^{-5} \text{ cm},$$

and

$$\frac{P_{\text{cycl.}}}{P_{\text{spin}}} \approx \left| \frac{5 \cdot 10^{-10} \cdot 10^{-5}}{10^{-20}} \right|^2 \approx 10^{12}.$$

To measure spin resonance absorption one likes to have $\sim 10^{16}$ spins, while $\sim 10^4$ precessing electrons may suffice for measuring cyclotron resonance absorption, for equal line widths.

It is easiest to conduct cyclotron resonance experiments in insulators or semiconductors, such as silicon and germanium. In germanium at 4°K there will be a sufficient number of carriers produced by rf ionization of the crystal impurities. These will be of one type, either electrons or holes (depending on the type of impurity) since the energy given to the carriers by the electric field is not sufficient to produce electron-hole pairs. In silicon, on the other hand, the few normally existing carriers do not gain enough energy to ionize the impurities, so electron-hole pairs are created by irradiating the sample with light. The light can be modulated at a certain frequency which will in turn modulate the microwave absorption and lead to an improved signal to noise ratio. This method is used in all recent work at microwave frequencies.

The principal requirement in observing cyclotron resonance is that the time between collisions, τ , of an electron or hole should not be too short compared to $1/\omega_0$, as $\omega_0\tau \geq 1$ gives a resolvable line. In order to make τ long enough to do the experiment, one has to use pure specimens and go to low temperatures ($\sim 4^\circ\text{K}$) in order to remove lattice phonons. For ionized impurities, the

impurity concentration should be $\lesssim 10^{14} \text{ cm}^{-3}$ while for localized non-ionized impurities, concentrations $\approx 3 \cdot 10^{20} \text{ cm}^{-3}$ can be tolerated in certain instances, as for Si in Ge.

One of the main objects of the experiment is to determine the effective mass m^* . For example, in InSb cyclotron resonance experiments have shown that $m^* = 0.014 m_e$, i.e., an electron in InSb can be accelerated approximately 70 times faster than a free electron in the same external electric field. We now consider two ways of looking at the effective mass idea.

1) One can think of a small effective mass as being analogous to the following situation: Suppose we send electrons of wave length λ through a

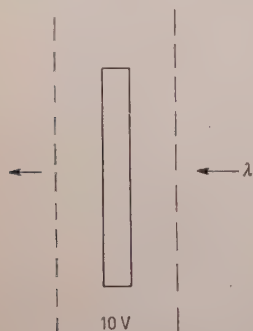


Fig. 2. - Arrangement discussed in explanation of light effective masses.

very thin crystal and suppose that λ almost, but not quite, satisfies the Bragg condition, $n\lambda = 2d \sin \vartheta$. A typical electron energy would be in the neighborhood of 1000 eV. In this case almost all the electrons will penetrate the crystal without being scattered coherently. Now suppose a small voltage is applied across the grid as in Fig. 2 so that the energy of the electrons is changed just enough to enable them to satisfy the Bragg condition. Most of the electrons will now be reflected. Thus application of a small voltage ($\sim 10 \text{ V}$) has caused a tremendous acceleration, corresponding to a light effective mass. Of course the change in momentum is absorbed by the crystal.

2) Weak binding approximation point of view:

The zero-order eigenstates of an electron moving in a regular array of atoms are the plane wave states

$$(2) \quad \psi = \exp [ikx],$$

and correspond to a uniform charge distribution, ($\psi^* \psi = 1$). For small k ,

$$E = \frac{\hbar^2}{2m} k^2,$$

and the electron behaves like a free particle. When the wave vector approaches the Bragg condition, $k = \pi/a$, the function (2) is no longer a complete description since strong reflection occurs. Thus we get a reflected wave which gives rise to standing waves

$$\psi_1 \sim \cos \frac{\pi x}{a}; \quad \psi_2 \sim \sin \frac{\pi x}{a}.$$

The charge distributions for these two possibilities are radically different, as shown in Fig. 3, and therefore correspond to very different energies.

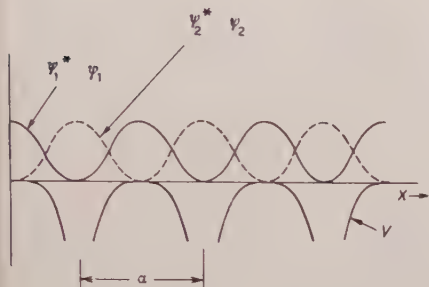


Fig. 3. - Explanation of the energy gap in band structure.

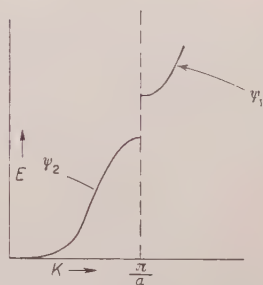


Fig. 4. - Variation of energy near a zone boundary.

This discontinuity in E at π/a is shown in Fig. 4.

Because the solutions at this point are standing waves, the group velocity is zero. A small change in k however causes a large change in velocity since $\partial E/\partial k$ varies rapidly here. A small m^* is consistent with the equation of motion of the system as a whole if the reaction of the lattice is taken into account, i.e.

$$CE = F = m^*a = MA + ma,$$

where a = acceleration of the electron;

A = acceleration of the lattice;

M = mass of lattice.

1. - Electrons in silicon and germanium.

Germanium has approximately a 20:1 anisotropy in m^* . This results in aspherical energy surfaces. For small $|\mathbf{k}|$

$$E(\mathbf{k}) = \frac{\hbar^2}{2} \left(\frac{k_z^2}{m_l} + \frac{k_x^2 + k_y^2}{m_t} \right)$$

while for a free electron

$$E(\mathbf{k}) = \frac{\hbar^2}{2m} (k_x^2 + k_y^2 + k_z^2).$$

The k_z -axis here is taken along a $[111]$ direction. The origin ($k_x = k_y = k_z = 0$) lies somewhere on the $[111]$ axis, possibly at the Brillouin zone boundary. A constant energy surface for electrons (i.e., the conduction band) consists of such an ellipsoid at corresponding equivalent points on each of the $[111]$ axes in \mathbf{k} space. Here m_l is the mass connected with acceleration in the longitudinal direction of the ellipsoid; m_t is the transverse mass. The effective mass m^* defined by Equation (1) depends on the orientation of the field relative to the z direction:

$$(3) \quad \left(\frac{1}{m^*}\right)^2 = \frac{\cos^2 \vartheta}{m_l^2} + \frac{\sin^2 \vartheta}{m_t^2},$$

where ϑ is the angle between the magnetic field and the z direction. Because electrons will be distributed over all the ellipsoids, for an arbitrary direction of the field there will be four different m^* 's and four resonance points. For \mathbf{K} parallel to a $[100]$ direction of the crystal, the effective masses connected with motion on the different ellipsoids coincide.

In order to arrive at Eq. (3) one must solve the cyclotron resonance equations for anisotropic m^* :

$$m_t \frac{dv_x}{dt} = \frac{e}{c} (\mathbf{v} \times \mathbf{H})_x;$$

$$m_t \frac{dv_y}{dt} = \frac{e}{c} (\mathbf{v} \times \mathbf{H})_y;$$

$$m_l \frac{dv_z}{dt} = \frac{e}{c} (\mathbf{v} \times \mathbf{H})_z.$$

If one puts $v_i = v_i^0 \exp[i\omega t]$ one gets a homogeneous system of three equations for the components of \mathbf{v} . Eq. (3) results from the condition that these have a non-trivial solution.

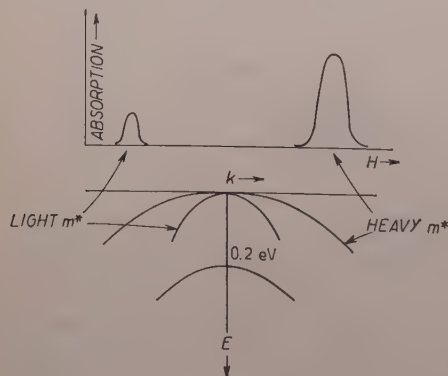


Fig. 5. - Structure of the valence band edge of Ge and Si.

2. - Holes in silicon and germanium.

The valence bands of both Si and Ge are doubly degenerate at the upper edges. The degeneracy is lifted for $k \neq 0$ as indicated in Fig. 5. Fig. 5 also shows a third band, which in the absence of spin-orbit coupling would be degenerate with the other two at $k = 0$. This third

band can be seen in germanium by infrared absorption, but the short relaxation time of holes excited in it prevents cyclotron resonance of holes in the third band from being observed.

Constant energy surfaces near the top of the valence band are distorted spheres about $k = 0$, i.e. spheres distorted in such a way as to preserve cubic symmetry. When one calculates their shape, one finds that

$$E(\mathbf{k}) = Ak^2 \pm [B^2k^4 + C^2(k_x^2k_y^2 + k_y^2k_z^2 + k_z^2k_x^2)]^{\frac{1}{2}}.$$

The cyclotron resonance experiments give A , B and C .

Holes of a given energy can therefore be associated with either of two constant energy surfaces in k space. Because of the different curvature of these surfaces, their effective masses will differ and two absorption lines will be seen.

Quantum mechanical corrections must be applied when only the low quantum numbers are excited. This occurs at low temperatures and in the presence of weak rf fields. The theory of quantum mechanical effects has been discussed by LUTTINGER, while experiments indicating their presence have been done by FLETCHER *et al.*

If a spectrum of lines is seen in the absorption curve, those due to electrons and holes can be distinguished by

- (1) Magneto-resistance measurements.
- (2) Circularly polarized microwaves will excite holes or electrons separately for surfaces which are not too highly anisotropic.
- (3) Impurity level ionization by infrared radiation.

3. Plasma resonance.

The effect of cyclotron resonance polarizes the crystal due to the coherence of the excitation. The equation of motion for a charge e with mass m^* is

$$m^* \left(\frac{d\mathbf{v}}{dt} + \frac{1}{T} \mathbf{v} \right) = e\mathbf{E}_i + \frac{e}{c} \mathbf{v} \times \mathbf{H}.$$

Here \mathbf{E}_i is the internal field given by

$$\mathbf{E}_i = \mathbf{E} - L\mathbf{p}.$$

where L is the depolarization factor. If for simplicity we neglect polarization of the host crystal itself, then the part we are interested in arises from free

carriers:

$$\mathbf{p} = Ne \int \mathbf{v} \, dt.$$

If

$$\mathbf{v} = \mathbf{v}_0 \exp[i\omega t], \quad \mathbf{E} = \mathbf{E}_0 \exp[i\omega t].$$

then

$$p = \frac{Ne v_0}{i\omega},$$

and

$$\left(i\omega + \frac{1}{\tau}\right) \mathbf{v}_0 = \frac{e\mathbf{E}_0}{m^*} - \frac{NLe^2 \mathbf{v}_0}{im^* \omega} + \frac{e}{c} \frac{\mathbf{v}_0 \times \mathbf{H}}{m^*}.$$

If we define a « plasma frequency » by

$$\omega_p^2 = \frac{NLe^2}{m^*},$$

then

$$\left[i\omega \left(1 - \frac{\omega_p^2}{\omega^2}\right) + \frac{1}{\tau}\right] \mathbf{v} = \frac{e\mathbf{E}}{m^*} + \frac{e}{c} \frac{\mathbf{v} \times \mathbf{H}}{m^*},$$

i.e., where we had ω , we have to substitute $\omega(1 - \omega_p^2/\omega^2)$ in order to take account of plasma polarization. The effect will be important when ω_p is of the order of ω or larger. A critical concentration of carriers may be defined by the relation

$$N_0 = \frac{m^* \omega^2}{Le^2}.$$

Typically N_0 might be

$$N_0 = \frac{m^* \omega^2}{Le^2} \sim \frac{10^{-24}}{25 \cdot 10^{-20}} \cdot 2.5 \cdot 10^{22} = 10^{12}/\text{cm}^3,$$

for $m^* = 0.01 m_e$.

We consider briefly the polarization of the host crystal. If χ_0 is the susceptibility exclusive of carriers, then

$$E_i = E - L \left(E_i \chi_0 + \frac{Ner}{i\omega} \right),$$

$$E_i(1 + L\chi_0) = E - \frac{NLev}{i\omega}.$$

This involves a change in two of the terms, namely we would have

$$E_i = \frac{E}{1 + L\chi_0} + \frac{iNLev}{\omega(1 + L\chi_0)}.$$

The shape of the plasma absorption line as observed by means of carriers produced by modulated light is unusual (Fig. 6).

The antisymmetry comes about because the modulation of the carrier concentration changes not only the absorption amplitude but also the position at which it takes place.

Cyclotron resonance has also been reported in the semimetals bismuth and graphite, and also in the metals tin and copper. The experimental arrangement used with the semimetals is much the same as for semiconductors. The dc magnetic field is usually normal to the surface of the specimen. The skin depth is determined essentially by majority carriers, and the minority carrier signal is superposed on that of the majority carriers. With metals a rather different arrangement

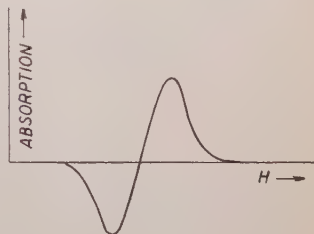


Fig. 6. — Plasma resonance absorption line shape under conditions of carrier modulation.

is used, one which in certain situations ensures freedom from depolarization effects on the resonance frequency, in spite of the high carrier concentrations present in metals. The dc magnetic field H_0 is parallel to the surface of the specimen, and the microwave electric field E_{rf} is parallel to H_0 . The carriers dip in and out of the skin depth as they circle about the magnetic field and are accelerated parallel to H_0 . That is, they are accelerated in the direction normal to the plane of the circular motion of the carriers. This arrangement minimizes plasma effects.

* * *

I am very grateful to Mr. RICHARD PETERSEN for his assistance in writing up these lectures from the course notes.

Les méthodes optiques de la résonance hertzienne.

A. KASTLER

Laboratoire de Physique de l'École Normale Supérieure - Paris

1. — Introduction.

Un phénomène de résonance hertzienne (magnétique ou électrique) est une interaction entre la matière et l'un des deux champs de l'onde électromagnétique. L'onde et la matière se trouvent modifiées dans cette interaction. Les méthodes d'investigation se divisent en deux groupes: Les méthodes radio-électriques qui étudient l'altération de l'onde (ZAVOISKY, PURCELL, F. BLOCH), les autres méthodes qui étudient l'altération de la matière. Le rôle le plus important parmi celles-ci a été joué par la méthode des jets de Rabi. A ce groupe appartiennent aussi les méthodes qui ont permis de découvrir le Lamb-shift et celles qui ont permis la mesure du moment magnétique du neutron. Les méthodes optiques se rangent également dans cette catégorie. La lumière intervient à la fois dans la genèse et dans la détection des résonances.

Une transition de résonance entre deux niveaux a pour effet d'égaliser les populations de ces niveaux. Elle n'est détectable que s'il existe au préalable une différence de population entre ces niveaux. Cette différence de population peut exister spontanément en vertu de la répartition boltzmannienne à l'équilibre thermique. Elle ne devient notable qu'à basse température. Elle peut être créée artificiellement. Dans ce but, RABI utilise la méthode de sélection magnétique de STERN et GERLACH. L'irradiation optique permet, elle aussi, de créer des différences de population notables, soit à l'état optiquement excité, soit à l'état fondamental.

Les Méthodes Optiques de la résonance hertzienne (R.H.) ont permis d'étendre les investigations de R.H. à des états atomiques optiquement excités. Elles ont été préconisées en 1949 ^(1,2), et mises en œuvre, sur des résonances

(1) F. BITTER: *Phys. Rev.*, **76**, 833 (1949); M. H. L. PRYCE: *Phys. Rev.*, **77**, 136 (1950).

(2) J. BROSSEL et A. KASTLER: *Compt. Rend. Ac. Sci.*, **229**, 1213 (1949).

Zeeman, à partir de 1950 par JEAN BROSSEL sous la direction du professeur BITTER à M.I.T. ⁽³⁾. L'extension de ces méthodes à des résonances hyperfines a permis la détermination des moments électroniques quadrupolaires des noyaux de la plupart des métaux alcalins, moments qui sont inaccessibles à l'état fondamental. Ces méthodes permettent une étude précise non seulement de l'effet Zeeman mais aussi de l'effet Stark d'un niveau optiquement excité, étude dont nous indiquerons un exemple. C'est également par une méthode optique que LAMB a pu déterminer récemment le Lamb-shift du niveau $n = 3$ de l'atome d'hydrogène. Lorsque dans la résonance optique les photons subissent des diffusions multiples avant d'être réémis, les courbes de résonance magnétique du niveau excité deviennent plus fines. Cette constatation nous oblige à admettre l'existence d'une cohérence de phase entre les atomes captant successivement le même photon.

Le procédé de pompage optique permet d'appliquer les méthodes optiques de la R.H. aux niveaux fondamentaux des atomes. L'application à des atomes de sodium a permis de mettre en évidence les effets de résonance faisant intervenir simultanément plusieurs quanta électromagnétiques (résonances multiples). Nous verrons qu'il existe deux types de « résonances multiples » à caractères différents.

Les études sur l'état fondamental des atomes en présence de gaz étrangers ont montré que l'orientation atomique de spin pur (états spectroscopiques S) est capable de survivre à des centaines de chocs et que la phase de la précession de Larmor de ces états n'est pas perturbée par le chocs, d'où la possibilité d'obtenir des raies de résonance d'une très grande finesse.

Les principes des méthodes optiques de la R.H. et les premiers résultats obtenus ont déjà fait l'objet de plusieurs exposés d'ensemble ⁽³⁾. Nous nous contentons ici de rappeler succinctement ces principes et nous renvoyons pour les détails aux articles mentionnés. Nous voudrions ici insister sur les résultats les plus récents et encore en partie inédits.

2. - Études des résonances hertziennes des états excités des atomes.

Par excitation optique d'un atome ou d'une molécule, il est possible — lorsque le vecteur excitateur est orienté dans l'espace grâce à la polarisation de la lumière incidente ou plus simplement grâce à l'emploi d'un faisceau lumineux d'une direction déterminée — d'exciter sélectivement des sous-niveaux Zeeman ou des niveaux hyperfins particuliers. Cette sélectivité se manifeste par l'ani-

⁽³⁾ A. KASTLER: *Holweek Lecture, Proc. Phys. Soc.*, A **67**, 853 (1954); J. BROSSEL: *Cahiers de Physique*, **65**, 59 (1956); A. KASTLER: *Journ. Opt. Soc. Am.*, Juin 1957 (reports of the I.C.O. Conference, M.I.T. 1956); H. KOPFERMANN: *Kernmomente*, (Frankfurt, 1956), p. 101.

sotropie d'émission et par la polarisation caractéristique de la lumière émise dans la résonance optique ou dans la fluorescence. Un champ électromagnétique de haute fréquence qui induit des transitions entre les sous-niveaux Zeeman ou hyperfins de l'état excité, modifie la population de ces niveaux et change l'intensité et l'état de polarisation de la lumière émise dans une direction donnée.

2.1. *Études des Résonances Zeeman des états optiquement excités.* — Le premier emploi de cette méthode a été l'étude par BROSSEL et BITTER ⁽⁴⁾ du niveau 6^3P_1 de l'atome de mercure atteint à partir du niveau fondamental 6^1S_0 par irradiation de la vapeur de mercure avec la raie de résonance ultraviolette 2537 Å. Pour les isotopes pairs du mercure qui forment 70% du mélange naturel le niveau supérieur se compose de trois sous-niveaux Zeeman $m = -1, 0$ et $+1$. Lorsque l'excitation est faite à l'aide d'un faisceau lumineux parallèle et polarisé rectilignement et lorsque la direction du vecteur électrique de cette lumière est celle du champ magnétique H_0 , seul le niveau central $m = 0$ est peuplé et la lumière réémise, complètement polarisée, ne contient à son tour que la composante Zeeman π de la radiation de résonance ^(5,6). L'application d'un champ magnétique de haute fréquence qui est perpendiculaire à H_0 et qui satisfait à la condition de résonance $\omega = \gamma H_0$ ou $h\nu = g\mu_B H_0$ (γ facteur gyromagnétique, g facteur de Landé, μ_B magnéton de Bohr) provoque des transitions de $m = 0$ à $m = \pm 1$ de l'état excité et fait apparaître les composantes Zeeman σ de 2537 Å dans la lumière émise. On trace une courbe

de résonance en mesurant, à fréquence ν constante, en fonction du champ H_0 , l'intensité lumineuse I_σ des composantes σ émises. La courbe I de la Fig. 1

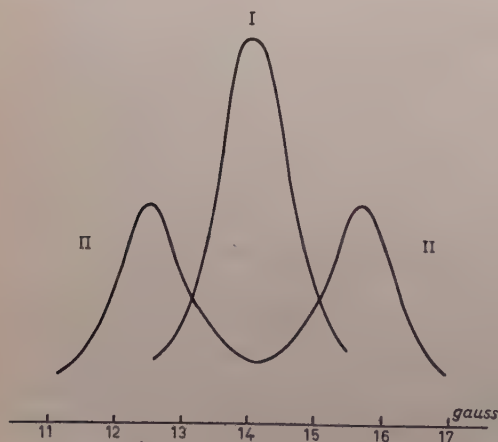


Fig. 1. — Courbes de résonances de l'état 6^3P_1 de l'atome de mercure, isotopes pairs. En ordonnée l'intensité I_σ . Fréquence: 29.625 MHz. I) Dans un champ magnétique pur. II) Dans un champ magnétique auquel est superposé un champ électrique $E = 40$ kV/cm (d'après BROSSEL et BLAMONT).

⁽⁴⁾ J. BROSSEL et F. BITTER: *Phys. Rev.*, **86**, 311 (1952); J. BROSSEL: *Thèse* (Paris, 1951); *Ann. de Phys.*, **7**, 622 (1952).

⁽⁵⁾ A. C. MITCHELL et M. W. ZEMANSKY: *Resonance Radiation and Excited Atoms*, chap. V (Cambridge, 1934), p. 258.

⁽⁶⁾ P. PRINGSHEIM: *Fluorescence a. Phosphorescence*, (New York, 1949), p. 64.

montre une telle courbe de résonance. L'abscisse de son maximum donne le facteur de Landé g , trouvé égal à 1.48. La largeur à mi-hauteur ΔH , pour les amplitudes faibles du champ oscillant H_1 est de l'ordre de 1 gauss. Elle est déterminée, en vertu du principe d'incertitude, par la durée de vie T_e du niveau excité:

$$T_e = \frac{2}{\gamma \Delta H} = \frac{h}{\pi g \mu_B \Delta H}.$$

Lorsqu'on opère à très faible densité de vapeur (-30°C), on trouve pour le niveau 6^3P_1 la valeur $T_e = 1.19 \cdot 10^{-7}$ s en bon accord avec les mesures optiques (7).

La relation entre largeur de courbe de résonance et durée de vie du niveau excité est illustrée par un autre exemple: l'étude du niveau 7^3S_1 de l'atome de mercure dont la durée de vie est beaucoup plus courte, de l'ordre de 10^{-8} s.

Mlle C. JULIENNE vient d'étudier ce niveau en irradiant la vapeur de mercure en présence d'azote avec les raies 2537 et 4046 Å d'une lampe à mercure (8). On sait que les chocs avec des molécules d'azote font passer les atomes de mercure de l'état 6^3P_1 à l'état métastable 6^3P_0 . Les atomes à cet état absorbent 4046 Å et sont portés au niveau 7^3S_1 : Cet état étant un état S , est peu sensible aux chocs: les raies émises sont fortement polarisées. L'application d'un champ magnétique de haute fréquence H_1 satisfaisant à la condition de résonance entre les sous-niveaux Zeeman de l'état 7^3S_1 modifie la polarisation des raies émises et notamment celle de 4358 Å. Les courbes de résonance obtenues (Fig. 2) ont une largeur à mi-hauteur de l'ordre d'une dizaine de gauss qui correspond à une durée de vie du niveau 7^3S_1 égale à $T_e = 1.17 \cdot 10^{-8}$ s en bon accord avec des mesures récentes faites par une méthode toute différente (9).

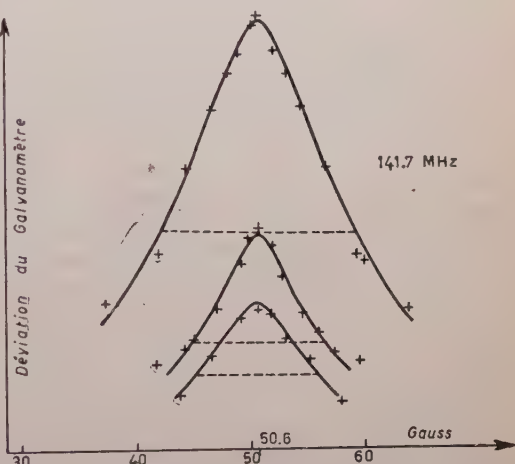


Fig. 2. — Courbe de résonance de l'état 7^3S_1 de l'atome de mercure (d'après BROSSEL et Mlle JULIENNE).

(7) J. E. BLAMONT: *Thèse* (Paris, 1956), à paraître dans *Ann. de Phys.* (1957).

(8) J. BROSSEL et Mlle C. JULIENNE: *Compt. Rend. Ac. Sci.*, **242**, 2127 (1956).

(9) E. BRANNEN, F. HUNT, R. ADLINGTON et R. NICHOLLS: *Nature*, **175**, 810 (1955);

Bull. Am. Phys. Soc., **30**, no. 4, 32-V5 (1955).

2.2. *Étude de l'effet Stark par résonance hertzienne.* — BLAMONT a repris l'étude de la résonance magnétique du niveau 6^3P_1 de l'atome de mercure en superposant au champ magnétique H_0 qui produit l'effet Zeeman un champ électrique E parallèle à H_0 qui produit des déplacements Stark (^{7,10}). Il a pu appliquer à la vapeur de mercure des champs électriques atteignant 70 kV par cm. Lorsque le champ magnétique agit seul, les deux intervalles Zeeman

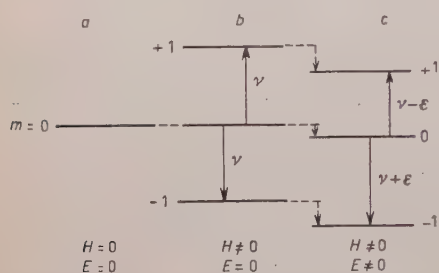


Fig. 3. — Schéma des états magnétiques m du niveau 6^3P_1 du mercure. a) sans champ; b) effet Zeeman; c) effet Zeeman + effet Stark.

à montré que le dédoublement Stark est indépendant de la valeur du champ magnétique H_0 à laquelle on opère. L'effet Stark est proportionnel au carré du champ électrique: $\Delta\nu = 2KE^2$.

La valeur numérique de la constante Stark est

$$K = (21.3 \pm 0.5) \text{ MHz pour } 100 \text{ kV/cm.}$$

Reste à déterminer le signe de la constante Stark. Nous dirons qu'elle est positive si l'application du champ électrique augmente l'intervalle $0 \rightarrow +1$ et diminue l'intervalle $0 \rightarrow -1$. On peut remarquer que les atomes portés à l'état $+1$ émettent de la lumière σ^+ circulaire droite, ceux portés à l'état -1 émettent de la lumière σ^- circulaire gauche. Les deux maxima séparés par le champ électrique doivent donc présenter des polarisations circulaires inverses lorsqu'on observe la lumière émise parallèlement aux champs, et le sens de ces polarisations détermine le signe de la constante Stark. Mais comme les électrodes employées étaient opaques à l'ultraviolet, l'observation parallèle aux champs était impossible. Fort heureusement il est possible de relier des formules théoriques simples les effets Stark de structure hyperfine des isotopes impairs à l'effet Stark des isotopes sans spin nucléaire. Or dans

(¹⁰) J. BLAMONT et J. BROSSEL: *Compt. Rend. Ac. Sci.*, **238**, 1487 (1954); *Arch. des Sci. Genève*, **9**, fasc. spécial, 152 (1956); *Compt. Rend. Ac. Sci.* **243**, 2038 (1956).

le cas des isotopes impairs le découplage progressif des vecteurs \mathbf{i} et \mathbf{J} dans un champ magnétique croissant (effet Back-Goudsmit) rend les intervalles Zeeman inégaux et permet de séparer les différentes résonances. L'addition du champ électrique produit un déplacement de chacune de ces résonances dont le sens est lié au signe de la constante Stark. A titre d'exemple, nous reproduisons (Fig. 4) les deux résonances $m_F: +\frac{3}{2} \leftrightarrow +\frac{1}{2}$ et $m_F: -\frac{3}{2} \leftrightarrow -\frac{1}{2}$ de l'état $F=\frac{3}{2}$ du mercure ^{199}Hg de spin nucléaire $\frac{1}{2}$. Ces résonances correspondent à un facteur de Landé $g_F = 1$ et se trouvent dans une région de champ magnétique éloignée de celle où l'on observe la résonance des isotopes pairs ($g = 1.48$). Pour une fréquence de 380 MHz ces deux résonances sont situées respectivement à 275 et à 270 gauss. L'application d'un champ électrique les déplace en sens inverse en les écartant l'une de l'autre. Les relations théoriques montrent que dans ces conditions le signe de la constante Stark est négatif. On trouvera une étude détaillée de ces relations et de leur vérification expérimentale dans la thèse de BLAMONT (?).

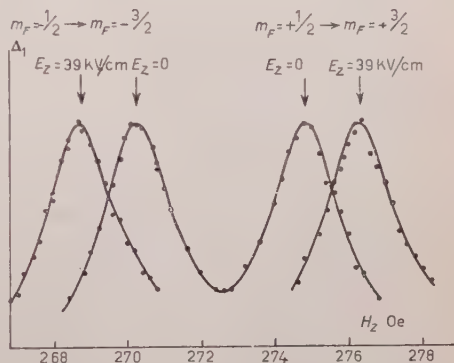


Fig. 4. — Résonance de l'état hyperfin $F = \frac{3}{2}$ de l'état 6^3P_1 de ^{199}Hg , dans un champ magnétique pur et avec addition de champ électrique (d'après BLAMONT).

2.3. L'affinement des courbes de résonance magnétique par diffusion multiple des photons. — En reprenant les expériences de Brosse sur la résonance magnétique du niveau 6^3P_1 de l'atome de mercure et en opérant à des densités de vapeur différentes, BLAMONT a constaté que, plus la densité de vapeur était élevée, plus les courbes de résonance étaient fines. Ce résultat était surprenant, car à densité de vapeur plus élevée, les chocs deviennent plus nombreux et perturbent la phase des atomes excités. On s'attend donc à trouver un élargissement des raies de résonance en vertu de la relation d'incertitude. Une étude systématique de la variation de la largeur des raies de résonance en fonction de la pression de vapeur du mercure a confirmé les observations de BLAMONT. Les résultats de cette étude faite par BARRAT et Mlle GUIOCHON sous la direction de BROUSSEL⁽¹¹⁾ sont représentés sur la Fig. 5, qui montre comment évolue la durée T_2 , inversement proportionnelle à la largeur de raie, en fonction du logarithme du nombre d'atomes par unité de volume. A faible

⁽¹¹⁾ Mlle M. A. GUIOCHON, J. E. BLAMONT, J. BROUSSEL: *Compt. Rend. Ac. Sc.*, **243**, 1859 (1956) et *Journ. de Phys.*, **18**, 99 (1957).

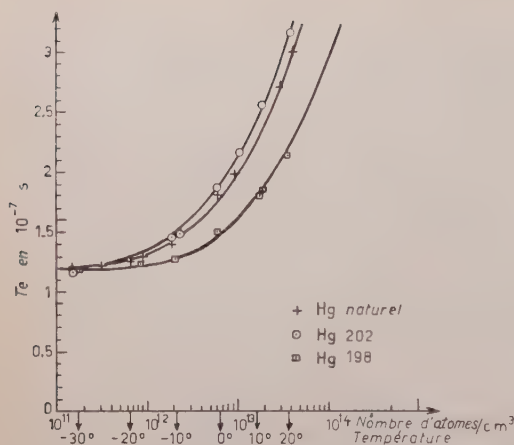


Fig. 5. — Variation de la durée de cohérence de l'état excité 6^3P_1 du mercure en fonction de la densité de vapeur de mercure (d'après BLAMONT, BROSSEL et Mlle GUIOCHON).

densité de vapeur ($N < 10^{12}$ atomes/cm³), T_c tend asymptotiquement vers une valeur limite qui correspond à la durée de vie de l'état 6^3P_1 d'un atome isolé: $1.19 \cdot 10^{-7}$ s. Cette valeur est en bon accord avec les résultats de mesure de la durée de vie par les méthodes optiques. Le désaccord constaté tout d'abord entre la valeur mesurée par BROSSEL ($1.55 \cdot 10^{-7}$ s à 0 °C) et les mesures optiques se trouve ainsi expliqué et éliminé, car à 0 °C l'affinement des courbes de résonance magnétique est déjà notable. Les conclusions générales de cette étude sont les suivantes.

La largeur de la courbe de résonance magnétique à densité de vapeur élevée n'est pas conditionnée par la durée de vie τ de l'état excité d'un atome, mais par une « durée de cohérence » T_c qui est supérieure ou égale à τ et qui augmente lorsque la densité de vapeur augmente. Cette augmentation dépend de la géométrie de la cellule de résonance. L'excitation sélective des divers isotopes montre que T_c dépend uniquement de la concentration de l'isotope étudié, et ne dépend pas de la présence des autres isotopes. Il existe un parallélisme remarquable entre l'affinement des courbes de résonance magnétique et le phénomène de dépolarisation de la radiation de résonance en fonction de la pression de vapeur du mercure. Les deux effets sont dûs à la même cause; la diffusion multiple des photons, connue sous le nom de « emprisonnement de la radiation de résonance »⁽¹²⁾. Cette diffusion est un phénomène qui se fait d'un atome à l'autre avec *conservation de la phase* de la fonction d'onde décrivant l'état excité⁽¹¹⁾.

Les chocs entre atomes de mercure qui causent des transferts entre les sous-niveaux Zeeman de l'état excité et qui, de ce fait, produisent une dépolarisation et une perturbation de phase (diminution de T_c) n'interviennent qu'à des pressions de vapeur beaucoup plus élevées ($N > 10^{14}$ atomes/cm³). Les sections efficaces de chocs anormalement élevées, auxquelles on attribuait la dépolarisation initiale de la lumière de résonance, sont à réviser (voir la remarque à ce sujet réf. (5), p. 312).

⁽¹²⁾ Mlle N. ROLLET, J. BROSSEL et A. KASTLER: *Compt. Rend. Ac. Sci.*, **242**, 240 (1956).

2.4. *Résonances hyperfines des états atomiques excités et détermination des moments électriques quadrupolaires des noyaux.* — Lorsque l'état atomique excité, atteint par irradiation en lumière polarisée, comporte une structure hyperfine, l'application d'un champ magnétique de haute fréquence dont la fréquence est convenable, produit une transition hyperfine. Les changements de population créés par cette transition se reflètent dans des modifications de la répartition spatiale et de l'état de polarisation de la lumière émise.

L'étude des intervalles hyperfins des états optiquement excités présente un intérêt particulier pour les atomes dont l'état fondamental est un état $J = 0$ ou $J = \frac{1}{2}$. Dans ce cas l'étude de cet état fondamental ne nous donne aucun renseignement sur le moment électrique quadrupolaire du noyau. Ce moment ne se manifeste que dans les états atomiques $J > \frac{1}{2}$ qui possèdent plusieurs intervalles hyperfins. La mesure de ces intervalles permet le calcul des deux constantes de couplage, la constante magnétique A et la constante quadrupolaire B qui caractérisent l'interaction entre le noyau et la configuration électronique. A l'heure actuelle la méthode optique a été appliquée à l'étude des intervalles hyperfins des états excités de type $^2P_{\frac{3}{2}}$ des atomes alcalins et de l'état 4^3P_1 de l'isotope 67 du Zinc. Le Tableau I indique les références et donne les valeurs des moments électriques quadrupolaires ainsi mesurés.

TABLEAU I.

Élément	Q en 10^{-24} cm ²	Q (RABI)	Niveau étudié	Auteurs et Références
²³ Na	+ 0.10 ± 0.06	+ 0.11 ± 0.01	$3^2P_{\frac{3}{2}}$	P. SAGALYN ⁽¹³⁾
³⁹ K	+ 0.11 ± 0.02	+ 0.07 ± 0.02	$5^2P_{\frac{3}{2}}$ (4)	G. J. RITTER et G. W. SERIES ⁽¹⁴⁾
⁸⁵ Rb	+ 0.29 ± 0.02	+ 0.27 ± 0.02	$6^2P_{\frac{3}{2}}$ (5)	U. MEYER-BERKHOUT ⁽¹⁵⁾
⁸⁷ Rb	+ 0.14 ± 0.01	+ 0.13 ± 0.01	$6^2P_{\frac{3}{2}}$ (5)	U. MEYER-BERKHOUT ⁽¹⁵⁾
¹³³ Cs	− 0.003 ± 0.002	− 0.003 3 ± 0.003 9	$7^2P_{\frac{3}{2}}$ (6)	K. H. ALTHOFF ⁽¹⁶⁾
⁶⁷ Zn	+ 0.16		4^3P_1	H. KRUGER <i>et al.</i> ⁽¹⁷⁾

Les valeurs de Q indiqués en 3^e colonne correspondent aux résultats de mesure de RABI, SENTITZKY *et al.* ⁽²³⁾. Les niveaux étudiés par eux sont indiqués en parenthèse.

⁽¹³⁾ P. L. SAGALYN: *Phys. Rev.*, **94**, 885 (1954).

⁽¹⁴⁾ G. J. RITTER et G. W. SERIES: *Proc. Phys. Soc.*, A **68**, 450 (1955); *Proc. Roy. Soc.*, A **238**, 473 (1957); G. W. SERIES: *Phys. Rev.*, **105**, 1128 (1957).

⁽¹⁵⁾ U. MEYER-BERKHOUT: *Zeits. f. Phys.*, **141**, 185 (1955).

⁽¹⁶⁾ K. H. ALTHOFF: *Zeits. f. Phys.*, **141**, 33 (1955).

⁽¹⁷⁾ K. BOCKMANN, H. KRUGER et E. RECKNAGEL: à paraître dans *Die Naturwiss.*

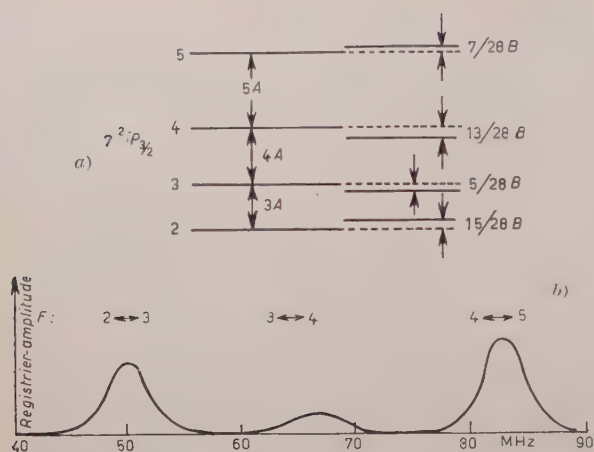


Fig. 6. — a) Schéma des niveaux hyperfins de l'état $7^2P_{3/2}$ de ^{133}Cs ; b) Résonances entre ces niveaux observées par ALTHOFF (16).

La Fig. 6 montre un exemple de courbes de résonances hyperfines, celles de l'état $7^2P_{3/2}$ du ^{133}Cs , enregistrés par ALTHOFF (16).

Notons que la mesure de la largeur de ces courbes de résonance permet aussi l'évaluation des durées de vie des états excités.

2.5. Combinaison des méthodes optiques avec d'autres méthodes. — Nous avons noté que la méthode optique joue un double rôle: elle permet par irradiation

optique d'atteindre des niveaux atomiques excités et d'y créer une sélection de population entre les sous-niveaux hyperfins et magnétiques. Elle permet de détecter les résonances hertziennes grâce aux changements d'intensité et de polarisation de la lumière émise. On peut ne faire jouer à la lumière qu'un seul de ces deux rôles et combiner la méthode optique soit avec une autre méthode de production des conditions initiales de la résonance (elle sert alors uniquement de méthode de détection), soit avec une autre méthode de détection (elle sert alors uniquement de méthode sélectrice des populations initiales).

Voici des exemples de ces deux emplois

1) *Excitation des atomes par choc électronique. Méthode optique de détection.* — L'excitation des atomes par irradiation optique ne permet d'atteindre qu'un petit nombre de niveaux. Il est possible par contre d'atteindre un grand nombre de niveaux excités par la méthode des chocs électroniques inélastiques de Franck et Hertz, et l'on sait que les radiations optiques émises dans ces conditions présentent des polarisations caractéristiques. Ceci montre qu'un choc électronique de direction donnée réalise une excitation sélective des sous-niveaux magnétiques (la théorie de cette excitation sélective mériterait d'être approfondie). Les conditions d'observation des résonances magnétiques par détection optique sont donc satisfaites (2).

Des tentatives ont été faites récemment pour combiner ainsi la méthode d'excitation électronique avec la méthode de détection optique: DEHMELT (18) a pu examiner les résonances de l'état métastable 6^3P_2 de l'atome de mercure,

(18) H. G. DEHMELT: *Phys. Rev.*, **103**, 1125 (1956).

état créé par bombardement électronique. Il se sert pour la détection, non pas des changements de polarisation de la lumière émise, mais des changements qui interviennent dans l'absorption de la raie 5461 \AA , par les atomes de ce niveau métastable. PÉBAY-PEYROULA (^{18 bis}) (mesures faites à l'École Normale Supérieure de Paris), employant également l'excitation électronique, a retrouvé la résonance hertzienne du niveau 6^3P_1 du mercure en excitant ce niveau par choc électronique et en observant l'état de polarisation de la raie 2537 \AA émise. Ces résultats sont en bon accord avec ceux de BROSEL.

W. E. LAMB qui avait déjà utilisé une méthode de détection optique pour l'étude de la structure fine du niveau $n = 2$ de l'hélium ionisé (¹⁹), vient de mesurer les intervalles de structure fine du niveau $n = 3$ de l'atome d'hydrogène (²⁰): ce niveau est atteint par choc électronique. Les atomes produits à l'état $3^2S_{\frac{1}{2}}$ de longue durée de vie, retournent à l'état fondamental en passant obligatoirement par l'état 2^2P et en émettant ainsi la raie H_{α} . Les transitions hertziennes, dipolaires électriques, font transiter des atomes de l'état $3^2S_{\frac{1}{2}}$ à l'état $3^2F_{\frac{1}{2}}$ de courte durée de vie d'où 12 % seulement d'entre eux descendent vers $2^2P_{\frac{1}{2}}$ en émettant H_{γ} alors que 88 % descendent directement à l'état fondamental en émettant Ly_{β} . La résonance hertzienne $3^2S_{\frac{1}{2}} \rightarrow 3^2P_{\frac{1}{2}}$ est donc détectée par une décroissance d'intensité de la lumière H_{α} émise. La même méthode a été appliquée par LAMB à l'étude de la structure fine dans le spectre de l'Hélium neutre (²¹).

2) *Méthode optique d'excitation. Détection par la méthode cinétique.* — En adaptant la méthode d'excitation optique à son appareil à jet, RABI (^{22,23}) a réussi à observer les résonances des états optiquement excités des atomes alcalins. La détection se fait ici en sélectionnant par un champ magnétique inhomogène de Stern et Gerlach les atomes qui ont subi des transitions Zeeman pendant qu'ils étaient à l'état optiquement excité. Ces transitions modifient en effet leur répartition parmi les niveaux Zeeman de l'état fondamental. Les résultats ainsi obtenus, dans le cas de Na, Rb et Cs, sont en bon accord avec ceux cités plus haut. Les résultats des deux procédés sont confrontés dans le Tableau I.

Nous aurons à revenir sur l'emploi des méthodes mixtes après l'étude des résonances à l'état fondamental.

(^{18 bis}) J. C. PÉBAY-PEYROULA, J. BROSEL et A. KASTLER: *Compt. Rend. Ac. Sci.*, **244**, 57 (1957).

(¹⁹) W. E. LAMB et al.: *Phys. Rev.*, **90**, 377, UAl (1953); R. NOVICK, E. ELIPWORTH et P. F. YERGIN: *Phys. Rev.*, **100**, 1153 (1955).

(²⁰) W. E. LAMB et T. M. SANDERS: *Phys. Rev.*, **103**, 313 (1956).

(²¹) T. H. MAIMAN et W. E. LAMB: *Phys. Rev.*, **98**, 1194, VA5 (1955).

(²²) I. I. RABI: *Phys. Rev.*, **87**, 379 (1952).

(²³) I. I. RABI, B. SENITZKY et al.: *Phys. Rev.*, **98**, 611 (1955); **103**, 315 (1956) et **104**, 553 (1956).

3. - Etude des résonances hertziennes de l'état fondamental.

3.1. *Orientation des atomes par le procédé de pompage optique.* - Dans une vapeur monoatomique paramagnétique à une température égale ou supérieure à la température ordinaire les différences de population entre les sous-niveau Zeeman et hyperfins de l'état fondamental restent très faibles, même dans des champs magnétiques élevés. Mais il est possible de créer des différences de population notables en irradiant la vapeur avec une raie de résonance.

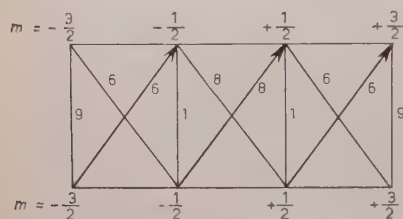


Fig. 7. - Schéma de la structure Zeeman d'une raie spectrale $J = \frac{3}{2} \rightarrow J = \frac{3}{2}$. Les nombres inscrits près des transitions représentent les valeurs relatives des probabilités de passage.

Les différences obtenues sont particulièrement importantes si la lumière incidente est polarisée circulairement ⁽²⁴⁾. Pour comprendre le mécanisme de cette action, nous allons considérer l'exemple d'une raie spectrale qui fait communiquer un état fondamental J (ou F) = $\frac{3}{2}$ avec un état excité J (ou F) = $\frac{3}{2}$. La Fig. 7 montre la structure Zeeman d'une telle raie. Dans ce diagramme les sous-niveaux magnétiques m d'un même état sont étalés horizontalement de manière à placer sur une même verticale les niveaux Zeeman de

même m des deux états atomiques qui communiquent par la raie. Avec cette convention, les trois espèces de composantes Zeeman reliant les deux états et satisfaisant aux règles de sélection sont représentées :

par des lignes verticales pour les composantes π ou $\Delta m = 0$.

par des lignes obliques à pente positive pour les composantes σ^+ ou $\Delta m = +1$.

par des lignes obliques à pente négative pour les composantes σ^- ou $\Delta m = -1$.

Si les atomes sont placés dans un champ magnétique H_0 et si la vapeur est illuminée parallèlement aux lignes de force avec de la lumière polarisée circulairement dans le sens du courant magnétisant, seules les composantes Zeeman σ^+ (marquées par des flèches) produisent l'excitation. Au cours de cette excitation les atomes se trouvant à un niveau m de l'état fondamental sont portés au niveau $m + 1$ de l'état excité d'où ils retombent, suivant le jeu des probabilités de passage, vers les niveaux m , $m + 1$, et $m + 2$ de l'état fondamental. Ce « pompage optique » concentre les atomes vers le sous-niveau Zeeman dont la valeur de m est la plus élevée (ici $m = +\frac{3}{2}$). Si le processus

⁽²⁴⁾ A. KASTLER: *Journ. de Phys.*, **11**, 255 (1950); *Physica*, **17**, 191 (1951).

de pompage se répète indéfiniment, tous les autres sous-niveaux m de l'état fondamental se vident complètement. On réalise ainsi une orientation atomique ou si l'on préfère une aimantation de la vapeur. Cette concentration vers les états m de droite modifie progressivement les caractères de la lumière de résonance émise. Dans l'exemple envisagé d'une raie $\frac{3}{2} \rightarrow \frac{3}{2}$ les atomes arrivés au niveau $m = +\frac{3}{2}$ ne sont plus susceptibles d'être excités par la lumière σ^+ . L'intensité de la lumière de résonance va donc diminuer au fur et à mesure que l'orientation atomique se produit, et la mesure de l'intensité lumineuse émise permet de suivre le processus de concentration. Un test encore plus sensible est la mesure de l'état de polarisation de la lumière de résonance émise. Les nombres inscrits à côté des composantes Zeeman de la Fig. 7 représentent les valeurs relatives des probabilités de passage. Lorsqu'on observe la lumière de résonance à angle droit du champ H_0 et du faisceau lumineux exciteur, l'état de polarisation de cette lumière, lorsque les niveaux Zeeman de l'état fondamental sont également peuplés, est caractérisé par le rapport $I_{\pi}/I_{\sigma} = 11/17$. Ce rapport augmente au cours de la concentration vers les m positifs, et lorsque les niveaux à m négatif sont dépeuplés, il est devenu égal à $\frac{3}{1}$. En fait, l'orientation atomique produite par la lumière n'est jamais complète, car des causes de désorientation et, parmi elles, notamment, les chocs des atomes contre les parois du récipient, interviennent. Mais les expériences ont montré qu'on peut obtenir par irradiation des effets d'orientation notables. Les premières expériences ont été faites sur des jets atomiques de sodium^(25,26). Elles ont été ensuite répétées avec succès sur la vapeur de sodium⁽²⁷⁾ ce qui a permis de simplifier la technique et d'étudier l'influence d'un gaz étranger sur le taux d'orientation^(29,30). On dispose ainsi d'une nouvelle méthode pour étudier le mécanisme des chocs entre atomes orientés et molécules.

Lorsqu'il y a couplage entre le moment électronique et le moment nucléaire, l'orientation atomique s'accompagne d'orientation nucléaire. C'est le cas des atomes alcalins. L'étude directe de cette orientation, par l'anisotropie des rayonnements nucléaires, n'a pas encore pu être abordée dans le cas des métaux alcalins à cause de l'adsorption de ces atomes par les parois de verre du récipient⁽³¹⁾.

(25) J. BROSSEL, A. KASTLER et J. WINTER: *Journ. de Phys.*, **13**, 668 (1952).

(26) W. B. HAWKINS et R. H. DICKE: *Phys. Rev.*, **91**, 1008 (1953); W. B. HAWKINS: *Phys. Rev.*, **98**, 478 (1956); *Thesis* (Princeton University, 1954).

(27) J. P. BARRAT, J. BROSSEL et A. KASTLER: *Compt. Rend. Ac. Sci.*, **239**, 1196 (1954).

(28) J. BROSSEL, J. MARGERIE et A. KASTLER: *Compt. Rend. Ac. Sci.*, **241**, 865 (1955).

(29) P. L. BENDER: *Thesis* (Princeton University, 1956).

(30) C. COHEN-TANNOUDJI: *Diplôme d'Études Sup.* (Paris, 1956), *Compt. Rend. Ac. Sc.*, **244**, 1027 (1957).

(31) J. BROSSEL, J. L. MOSSER et Mme M. WINTER: *Journ. de Phys.*, **16**, 814 (1955).

Dans le cas où l'état fondamental est diamagnétique, le pompage optique peut produire une orientation nucléaire pure. Les tentatives pour obtenir ainsi l'orientation nucléaire des isotopes impairs du mercure n'ont pas encore abouti ^(32,33), probablement à cause d'une intensité lumineuse insuffisante.

3.2. Résonances magnétiques à l'état fondamental sur des atomes orientés optiquement. Étude des résonances multiples. — Les différences importantes de population créées à l'état fondamental des atomes par pompage optique permettent l'étude des résonances hertziennes entre sous-niveaux de cet état. Ces résonances égalisent les populations des niveaux en jeu. Elles peuvent être détectées optiquement par les changements de polarisation de la lumière de résonance qu'elles produisent.

Ce procédé a été employé pour la première fois par BROSSEL et CAGNAC ^(34,35) pour étudier les résonances Zeeman entre niveaux m de l'état fondamental de l'atome de sodium. Le spin nucléaire de ^{23}Na étant $i = \frac{3}{2}$, cet état $3^2S_{\frac{1}{2}}$ se compose de deux états hyperfins $F = 2$ et $F = 1$. La formule de Breit-Rabi ⁽³⁶⁾ fait prévoir pour une fréquence de l'ordre d'une centaine de mégahertz quatre résonances distinctes $\Delta m = 1$. Ces résonances ont été trouvées aux valeurs prévues du champ, mais les premières mesures ont révélé l'existence de résonances intermédiaires très fines. Ces résonances sont des « résonances doubles ». Elles correspondent à une transition d'un état m à un état $m + 2$ à l'aide de deux quanta électromagnétiques de même fréquence absorbées simultanément par l'atome. La conservation de l'énergie est satisfaite et s'exprime par la relation: $E_{m+2} - E_m = 2h\nu$ entre les énergies des niveaux et la fréquence de résonance.

Chacun des quanta absorbé correspond à un champ tournant et apporte à l'atome une unité \hbar de moment cinétique. Le bilan de moment cinétique est donc également satisfait. Ces résonances doubles n'apparaissent que lorsque l'amplitude du champ de haute fréquence H_1 dépasse une certaine valeur. Lorsqu'on fait croître progressivement cette amplitude on constate que les résonances normales $\Delta m = 1$, d'abord fines pour les amplitudes faibles de H_1 , s'élargissent et finissent par se chevaucher mutuellement. C'est alors que les résonances doubles se manifestent (Fig. 8). Une explication qualitative et élémentaire de la formation de ces résonances doubles est la suivante (Fig. 9): le niveau intermédiaire qui intervient est un niveau virtuel $E' = (E_{m+2} + E_m)/2$

⁽³²⁾ F. BITTER et J. BROSSEL: *Phys. Rev.*, **85**, 1051 (1952); F. BITTER, R. F. LACEY et B. RICHTER: *Rev. Mod. Phys.*, **25**, 174 (1953).

⁽³³⁾ E. R. ANDREW: *Nuclear Magnetic Resonance* (Cambridge, 1955), p. 63.

⁽³⁴⁾ J. BROSSEL, B. CAGNAC et A. KASTLER: *Compt. Rend. Ac. Sci.*, **237**, 984 (1953).

⁽³⁵⁾ J. BROSSEL, B. CAGNAC et A. KASTLER: *Journ. d. Phys.*, **15**, 6 (1954).

⁽³⁶⁾ G. BREIT et I. I. RABI: *Phys. Rev.*, **38**, 2072 (1931).

qui ne coïncide pas avec le niveau de Bohr réel E_{m+1} . Lorsque l'amplitude du champ de radiofréquence est faible, les niveaux sont fins et seules les résonances simples ν_1 et ν_2 sont possibles. Lorsque cette amplitude augmente, les transitions de plus en plus fréquentes abrègent la durée de vie des niveaux en jeu. Ceux-ci s'élargissent en vertu du principe d'incertitude et la probabilité d'appartenance du niveau virtuel E' au niveau E_{m+1} devient grande. Ce niveau peut alors

entrer en jeu et servir de niveau intermédiaire pour permettre le saut double de E_m à E_{m+2} à l'aide de deux quanta de même fréquence (la seule fréquence présente dans le champ de rayonnement).

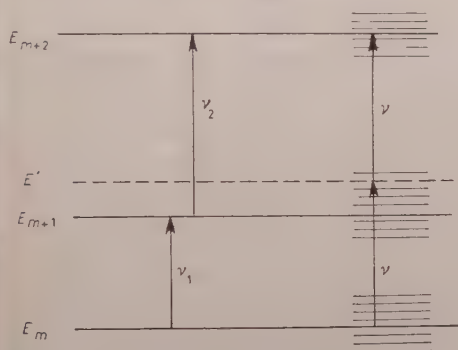


Fig. 9. — Schéma montrant les résonances simples ν_1 et ν_2 et la résonance double $\nu = (\nu_1 + \nu_2)/2$.

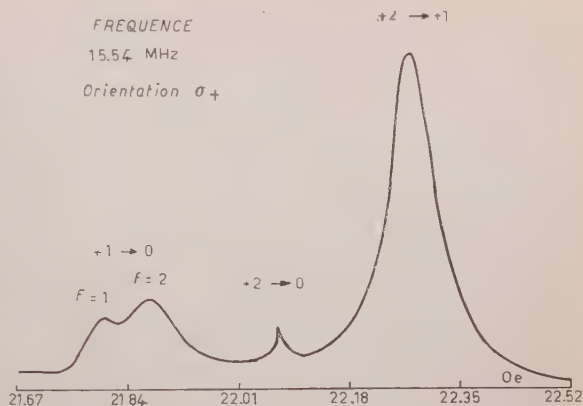


Fig. 8. — Deux résonances simples et une résonance double de l'état fondamental $3^2S_{1/2}$ de ^{23}Na . La résonance $+1 \rightarrow 0$ est dédoublée pour $F=1$ et $F=2$ (d'après WINTER).

Ces transitions $\Delta m = 2$ à deux quanta, déjà observées précédemment dans une molécule (^{85}RbF) par HUGHES et GRABNER (³⁷) ont été trouvées également par KUSCH (³⁸) par la méthode de Rabi et par HUGHES et GEIGER (³⁹) par la méthode de détection radioélectrique. Des transitions à trois, quatre et cinq quanta ont été caractérisées par la suite (^{27-40,42}).

Une transition à n quanta correspond au passage d'un état m à un état $m+n$. Elle nécessite l'apport de n unités de moment cinétique à l'atome: $\Delta m = n$. Chaque quantum électromagnétique

qui contribue à la transition est du même type: circulaire droit $\Delta m = 1$.

(³⁷) V. HUGHES et L. GRABNER: *Phys. Rev.*, **79** 314, 828 (1950).

(³⁸) P. KUSCH: *Phys. Rev.*, **93**, 1022 (1954); **101**, 627 (1956).

(³⁹) V. W. HUGHES et J. S. GEIGER: *Phys. Rev.*, **99**, 1842 (1955).

(⁴⁰) J. P. BARRAT: *Diplôme d'Études Sup.* (Paris, 1954).

(⁴¹) J. MARGERIE: *Diplôme d'Études Sup.* (Paris, 1955).

(⁴²) R. L. CHRISTENSEN, D. R. HAMILTON, A. LEMONICK, F. M. PIPKIN, J. B. REYNOLD and H. H. STROKE: *Phys. Rev.*, **101**, 1389 (1956).

La Fig. 10 due à Barrat montre comment l'augmentation progressive de

l'amplitude du champ de radiofréquence H_1 fait apparaître successivement les résonances, simples $\Delta m = 1$, doubles $\Delta m = 2$ et triples $\Delta m = 3$.

Ces courbes ont été obtenues sur l'état fondamental de l'atome de sodium par la méthode optique.

L'analyse théorique des résonances multiples (⁴³⁻⁴⁵) montre que l'intensité d'une résonance d'ordre n est proportionnelle à $(H_1/H_0)^{2n}$, H_1 étant l'amplitude du champ oscillant et H_0 la valeur du champ constant. Cette relation explique l'apparition successive des résonances d'ordre croissant quand on augmente H_1 .

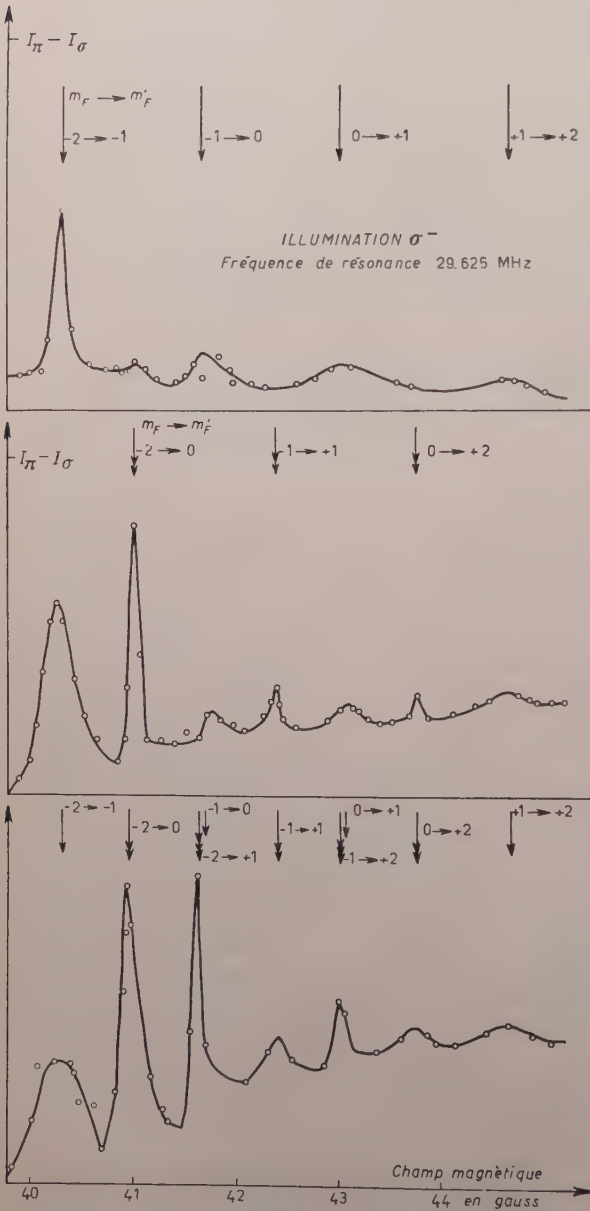


Fig. 10. - Résonance de l'état fondamental $3^2S_{1/2}$ de ^{23}Na . L'augmentation de l'amplitude du champ oscillant H_1 montre l'apparition successive des résonances simples, doubles et triples. Illumination σ^- (d'après BARRAT).

(⁴³) C. BESSET, J. HOROWITZ, A. MESSIAH et J. WINTER: *Journ. de Phys.*, **15**, 251 (1954).

(⁴⁴) H. SALWEN: *Phys. Rev.*, **99**, 1274 (1955).

(⁴⁵) M. N. HACK: *Phys. Rev.*, **104**, 84 (1956).

Un autre type de résonances multiples a été prévu par J. WINTER en 1955 et observé au laboratoire de physique de École Normale Supérieure par BROSSEL et MARGERIE ^(46,47). Ces nouvelles résonances multiples ne nécessitent pas l'existence de niveaux intermédiaires. Elles se produisent même lorsqu'il n'existe que deux niveaux énergétiques E_m et E_{m+1} . Mais elles nécessitent la présence dans le champ de rayonnement électromagnétique de quanta de trois types différents: σ^+ ($\Delta m = +1$), σ^- ($\Delta m = -1$) et π ($\Delta m = 0$). Dans l'échange entre le champ de rayonnement et l'atome, l'énergie et le moment cinétique se conservent. Lorsqu'on applique à l'atome simultanément deux radiofréquences distinctes ν_1 et ν_2 , on observe, à côté des résonances multiples correspondant à chacune de ces deux fréquences, des résonances d'intercombinaison $\Delta E/h = p\nu_1 - q\nu_2$, les entiers p et q pouvant être positifs ou négatifs. Pour les détails, nous renvoyons aux articles originaux.

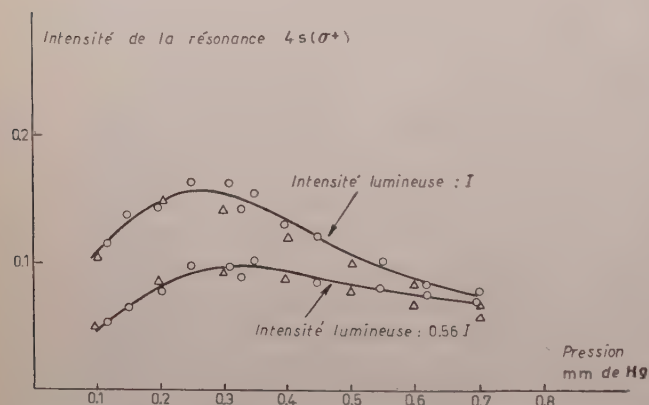
3.3. Influence des gaz étrangers. Etude des chocs. — Les premières expériences d'addition d'un gaz étranger à de la vapeur de sodium soumise au pompage optique ⁽²⁸⁻³⁰⁾ ont montré que les taux d'orientation obtenus étaient plus élevés qu'en absence de gaz. L'intensité de certaines résonances était plus que décuplée. Les gaz étudiés jusqu'à présent sont l'hydrogène, le deutérium, l'hélium, l'argon et l'azote. Leur efficacité augmente dans l'ordre de leurs masses moléculaires. COHEN-TANNOUDJI a fait une étude détaillée de l'intensité et de la finesse des courbes de résonance en fonction de la pression de l'hélium. Il a opéré dans un champ magnétique constant H_0 très uniforme et avec de faibles amplitudes de champ de radiofréquence de façon à atténuer toutes les causes d'élargissement des raies afin d'atteindre leur « largeur naturelle » déterminée par la durée de cohérence dans le champ de radiofréquence. Lorsqu'on augmente la pression de l'hélium, l'intensité des résonances croît tout d'abord régulièrement en fonction de cette pression, puis elle passe par un maximum pour une pression de l'ordre de 0,3 mm de mercure. Elle décroît ensuite lentement lorsque la pression continue à augmenter. Lorsque la pression du gaz étranger augmente, les raies deviennent plus fines. Leur largeur tend vers une valeur limite qui est de l'ordre de 2 kHz. Une partie de cette largeur est encore due à la non uniformité du champ H_0 . L'interprétation de ces résultats est la suivante. Dans la vapeur pure les atomes de sodium se meuvent en ligne droite entre les parois. Les durées de transit sont de l'ordre de 10^{-4} s. La lumière peut exercer son action orientatrice pendant ce temps et la radiofréquence agit sur les atomes orientés pendant un temps qui est nécessairement plus court. Lorsqu'on ajoute un gaz étranger, les atomes de sodium

⁽⁴⁶⁾ J. WINTER: *Compt. Rend. Ac. Sci.*, **241**, 375, 600 (1955).

⁽⁴⁷⁾ J. MARGERIE et J. BROSSEL: *Compt. Rend. Ac. Sci.*, **241**, 373, 566 (1955);

J. WINTER et J. BROSSEL: *Arch. des Sci. de Genève*, **9**, fasc. spéc., 148 (1956).

subissent des chocs contre les molécules de ce gaz et la direction de leur mouvement est changée continuellement. Le changement de direction éprouvé à chaque choc est d'autant plus grand que la masse de la molécule heurtée est plus grande. Les atomes, zigzaguant entre les molécules du gaz, touchent moins fréquemment la paroi, et la lumière peut exercer son action de pompage optique pendant une durée d'autant plus grande que la pression de gaz est plus élevée. L'accroissement considérable du taux d'orientation est dû à cette « protection » contre les parois, au contact desquelles l'orientation est détruite. Ceci montre que les chocs entre atomes orientés et molécules du gaz maintiennent l'orientation atomique car si ces chocs détruiraient l'orientation, l'addition d'un gaz étranger provoquerait une diminution de l'intensité des résonances au lieu de l'augmentation observée. L'apparition du maximum et la décroissance à pression plus élevée s'expliquent par la désorientation par chocs des atomes à l'état excité.



Gaz étranger : Hélium ○ Points expérimentaux △ Points théoriques

Fig. 11. — Variation de l'intensité d'une résonance ($m_F: -2 \rightarrow -1$) de l'atome Na en fonction de la pression de gaz étranger (He) pour 2 intensités lumineuses I et $0.56I$. Excitation σ^- (d'après COHEN-TANNOUDJI).

Lorsqu'on réduit l'intensité de la lumière excitatrice de moitié, le taux d'orientation est fortement réduit pour les faibles pressions. L'ordonnée du maximum est plus petite et son abscisse est déplacée vers des pressions plus fortes. A forte pression, le taux d'orientation devient indépendant de l'intensité lumineuse (Fig. 11). Il est possible d'en déduire qu'il n'y a pas

de désorientation des atomes à l'état fondamental, que celle-ci ne se fait qu'à l'état excité et que la lumière intervient ainsi à la fois comme cause d'orientation et comme cause de désorientation. C'est par suite de la compensation de ces deux effets que le taux d'orientation à forte pression devient indépendant de l'intensité lumineuse. La désorientation des atomes optiquement excités par les chocs est bien connue par l'étude du phénomène de dépolariation des radiations de résonance sous l'influence d'un gaz étranger (48,5,6). L'état fondamental des atomes de sodium est donc beaucoup moins vulnérable que l'état

(48) W. HANLE: *Zeit. f. Phys.*, **41**, 164 (1927).

excité. BENDER a montré ⁽²⁹⁾ que cette différence de comportement est due au fait que l'état fondamental est un état électronique *S* de symétrie sphérique alors que l'état excité est un état *P* dont la fonction d'onde est anisotrope.

L'évaluation des libres parcours moyens montre que les atomes orientés subissent des centaines de chocs à l'état fondamental sans être désorientés. Aux fortes pressions de gaz étranger, lorsque les vitesses de diffusion vers les parois deviennent faibles, la relaxation des atomes orientés se fait essentiellement par retour à l'état excité et désorientation dans cet état.

Considérons maintenant la largeur des raies de résonance. Elle est conditionnée par l'inhomogénéité résiduelle du champ magnétique et par la durée de cohérence des atomes soumis à la radiofréquence. Dans la vapeur pure la durée de cohérence est déterminée par les chocs contre les parois. Les durées de parcours sont de l'ordre de 10^{-4} s ce qui conduit à une limite inférieure de largeur de l'ordre de

$$\Delta\nu = \frac{1}{2\pi \cdot 10^{-4}} = 2 \cdot 10^3 \text{ s}^{-1} = 2 \text{ kHz}.$$

Les largeurs mesurées (3 à 4 kHz) sont plus grandes à cause de l'inhomogénéité du champ H_0 . L'addition de gaz étranger produit un léger affinement des raies. La durée de cohérence reste donc égale ou supérieure à 10^{-4} s bien que les atomes subissent pendant cette durée, à la pression où l'on fait la mesure, plusieurs centaines de chocs contre les molécules du gaz. Nous pouvons en conclure que ces chocs ne perturbent pas la phase du moment magnétique des atomes soumis à la radiofréquence, phénomène qui avait déjà été constaté sur des atomes d'hydrogène par DICKE et WITTKÉ ⁽⁴⁹⁾. Les chocs ne sont donc ni désorientants, ni déphasants. Le léger affinement des raies lorsque la pression de gaz étranger augmente, s'explique par le rétrécissement de l'espace de diffusion des atomes ce qui réduit l'influence de l'inhomogénéité du champ. Pour les pressions élevées (au-delà de l'abscisse du maximum), la durée de cohérence est essentiellement déterminée par le temps qui s'écoule entre deux excitations optiques successives de l'atome. On constate que les raies s'affinent lorsqu'on diminue l'intensité lumineuse. En appliquant la radiofréquence en une portion d'espace non éclairée, il doit être possible d'obtenir des raies encore plus fines.

BLANDIN ⁽⁵⁰⁾ vient d'appliquer la méthode optique à l'obtention de l'orientation atomique dans la vapeur de Césium et à l'étude des résonances de l'atome ^{133}Cs à l'état fondamental. Ces résonances n'ont pu être observées

⁽⁴⁹⁾ J. P. WITTKÉ et R. H. DICKE: *Phys. Rev.*, **96**, 530 (1954); J. P. WITTKÉ: *Thesis* (Princeton University, 1954).

⁽⁵⁰⁾ A. BLANDIN: *Diplôme d'Études Sup.* (Paris, 1956), extraits dans *Compt. Rend. Ac. Sci.*, **243**, 2041 (1956).

qu'en présence d'hydrogène. La Fig. 12 montre quelques courbes de résonances obtenues (*). A cause de la valeur élevée du spin nucléaire ($i = \frac{7}{2}$), le nombre de résonances est ici très grand ($F = 3$ et $F = 4$). On prévoit

8 résonances simples, 7 résonances doubles, 6 résonances triples, etc. Les identifications des transitions sont indiquées sur la figure. Les raies les plus fines correspondent à des résonances quintuples.

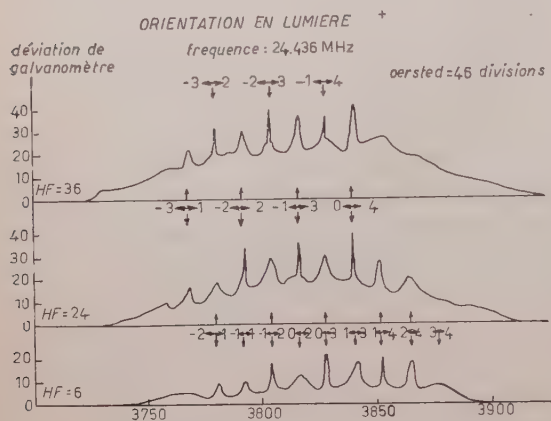


Fig. 12. — Résonance de l'état fondamental $6^2S_{\frac{1}{2}}$ de ^{133}Cs pour des intensités de radiofréquences égales, en valeur relative, à 1-4-6 (d'après BLANDIN).

4. — Perspectives d'avenir.

Je voudrais terminer par quelques remarques concernant les possibilités de développement des méthodes optiques.

1) La grande finesse des raies déjà obtenues et son insensibilité aux chocs montre que l'étude des résonances des vapeurs « protégées » par un gaz peut présenter le même intérêt pour la métrologie que la technique des jets. La persistance de l'orientation atomique au sein d'un gaz étranger permet d'entrevoir le transport des atomes orientés à distance, soit par diffusion à l'intérieur du récipient, soit par entraînement par courant gazeux, soit par déplacement mécanique du récipient. Il devient alors possible d'envisager l'emploi de la technique de Ramsey qui consiste à faire agir sur les atomes deux excitations hertziennes successives en vue d'obtenir des raies encore plus fines.

2) Nous avons vu que les chocs des molécules d'un gaz étranger désorientent les atomes à l'état optiquement excité. Lorsque la pression de gaz étranger est élevée et que cette désorientation est complète, le pompage optique peut garder son efficacité, mais il est facile de montrer que les conditions de pompage sont modifiées. Ce qui détermine dans ce cas la raréfaction des populations des divers niveaux est uniquement la vitesse avec laquelle ces niveaux se vident. Elle ne dépend que des probabilités d'absorption des composantes

(*) Ces courbes ont été obtenues après la conférence de Varenna en octobre 1956.

Zeeman employées dans la lumière incidente. Dans ces conditions, les différentes composantes de structure fine d'une raie produisent des effets de concentration en sens inverse (c'est le cas des deux raies D_1 et D_2 du sodium), et il convient de supprimer dans la lumière incidente certaines radiations ou de préférence de les polariser circulairement en sens inverse.

3) Une autre remarque que je voudrais faire est que, pour l'étude des résonances dans l'état fondamental comme dans les états excités, la méthode optique peut s'associer à d'autres méthodes d'investigation. Les faibles différences de population qui existent naturellement à la température ordinaire entre les niveaux hyperfins de l'état fondamental des atomes d'un gaz suffisent pour pouvoir observer les résonances hertziennes entre ces niveaux à l'aide de la méthode de détection radioélectrique^(51,52). En accroissant ces différences de population par le pompage optique, on doit pouvoir augmenter dans des proportions considérables les signaux radioélectriques de détection. En produisant des différences de population de sens convenable, il devient aussi possible de changer des signaux d'absorption en signaux d'émission induite, et l'on doit pouvoir s'approcher ainsi des conditions expérimentales qui amorcent l'auto-oscillation du système atomique couplé au circuit oscillant.

Dans les cristaux paramagnétiques à la température de l'hélium liquide, les composantes Zeeman d'une raie d'absorption acquièrent, comme l'a montré J. BECQUEREL⁽⁵³⁾ des intensités inégales qui reflètent les inégalités de population des niveaux Zeeman occupés. A ces inégalités est liée une polarisation rotatoire paramagnétique.

Lorsqu'on produit des résonances hertziennes entre ces niveaux, les populations s'égalisent, il en résulte un changement dans les intensités des raies d'absorption et la grandeur de la polarisation rotatoire⁽⁵⁴⁾.

Il serait intéressant d'appliquer les méthodes de détection optique à l'étude de ces résonances hertziennes dans les cristaux et aussi à la mesure des temps de relaxation spin-réseau qui, dans ces cristaux à basse température, peuvent devenir grands. On voit donc que les possibilités des méthodes optiques ne sont pas près d'être épuisées et que des domaines encore inexplorés restent à défricher.

⁽⁵¹⁾ A. ROBERTS, Y. BEERS et A. G. HILL: *Phys. Rev.*, **70**, 112, R11 (1946) et M.I.T. Technical Report no. 120 (1949).

⁽⁵²⁾ K. SHIMODA et T. NISHIKAWA: *Journ. Phys. Soc. Japan*, **6**, 512 (1951).

⁽⁵³⁾ J. BECQUEREL: *Le Radium*, **5**, 5, (1909); **6**, 327 (1909); *Phil. Mag.* **16**, 153 (1908); *Zeits. f. Phys.*, **52**, 342, 678 (1929); **57**, 11 (1929); **58**, 205 (1929).

⁽⁵⁴⁾ A. KASTLER: *Compt. Rend. Ac. Sci.*, **232**, 953 (1951).

Magnetic Properties of Superconductors.

C. J. GORTER

Kamerlingh Onnes Laboratorium der Rijksuniversiteit - Leiden

In macroscopic superconductors Meissner discovered that the induction B is always equal to zero, therefore since

$$B = H + 4\pi M,$$

where M is the magnetic moment per unit volume, we conclude that

$$M = -\frac{H}{4\pi}.$$

Because of the demagnetizing field associated with any finite magnetic specimen immersed in an external field, H_e , we have to put

$$H = H_e - NM,$$

where N is the demagnetizing coefficient and H_e is the uniform external field which exists before the specimen is brought into the field.

Solving M as a function of H_e we get

$$M = -\frac{H_e}{4\pi - N}.$$

For a very long needle-shaped specimen parallel to H_e , $N = 0$, so that in this case

$$M = -\frac{H_e}{4\pi},$$

and the specimen has an apparent volume susceptibility of $\chi = M/H_e = -1/4\pi$. The free enthalpy/unit volume is

$$G = u - TS - H_e M,$$

so that

$$\left(\frac{\partial G}{\partial H_e} \right)_T = -M,$$

and integrating this equation we get

$$G = G_{H=0} + \frac{1}{2} \frac{H_e^2}{4\pi - N}.$$

In Fig. 1 we show the three quantities B , M and G as functions of the external field for the case of an infinitely long cylinder with its axis parallel to the field ($N = 0$), and for an infinitely long circular cylinder with its axis perpendicular to the field ($N = 2\pi$).

So far we have only discussed the behaviour of a superconducting specimen for small fields. We shall discuss what happens in larger fields after discussing the caloric behaviour of superconductors.

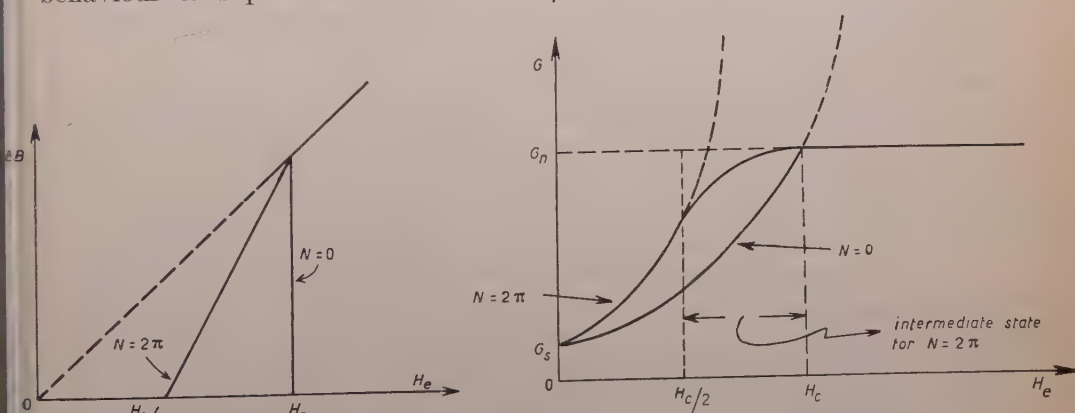


Fig. 1.

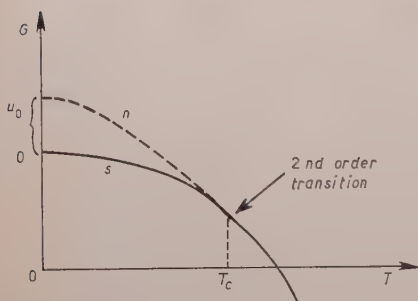
1. - Caloric behaviour.

For temperatures not too much below the critical temperature, T_c , i.e. for $T > T_c/2$, we can write approximately as a good fit to the experimental data for the specific heat in the superconducting state,

$$C_s \approx \frac{3\gamma T^3}{T_c^2}.$$

In the normal state $C_n = \gamma T$, the specific heat of the conduction electrons. In these arguments we are not concerned with the lattice contributions to the specific heats.

In zero applied field we have



$$G = - \int_0^T S dT + u_0,$$

$$S = \int_0^T \frac{C_v}{T} dT,$$

so that by integrating the specific heats twice we have

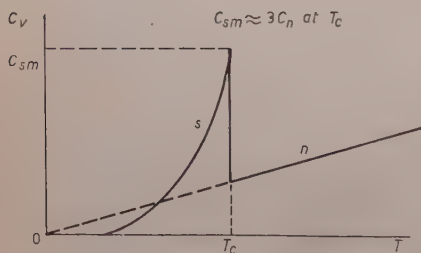


Fig. 2.

$$G_n = u_0 - \frac{1}{2} \gamma T^2,$$

$$G_s \approx - \frac{1}{4} \frac{\gamma T^4}{T_c^2},$$

where G_s has been chosen to be zero for the superconducting state at $T=0$. In Fig. 2 are shown the functions G and C_v against temperature. Note that G_s and G_n touch at $T=T_c$, indicating a second order transition, associated with which there is a discontinuity in the specific heat. This transition is observed to be an example of an ideal second order transition, i.e. it is very sharp and has no «tail» and indicates that superconductivity is a phenomenon associated with long-range order of the electrons. It is a general result that $(G_n - G_s) = H_c^2/8\pi$, and furthermore for purposes of calculation we assume for the moment that $C_s = 3\gamma(T^3/T_c^2)$.

Since at T_c , $G_n = G_s$ we have

$$u_0 = \frac{1}{2}\gamma T_c^2 = -\frac{1}{4}\gamma T_c^2$$

$$u_0 = \frac{1}{4}\gamma T_c^2$$

and

$$G_n - G_s = H_c^2/8\pi = \frac{1}{4}\gamma \left[T_c^2 - 2T^2 + \frac{T^4}{T_c^2} \right],$$

therefore

$$\frac{1}{4}\gamma \left(T_c - \frac{T}{T_c} \right)^2 = \frac{H_c^2}{8\pi},$$

so we conclude that

$$H_c = (8\pi u_0)^{\frac{1}{2}} \left(1 - \frac{T}{T_c} \right).$$

This parabolic dependence of H_c upon temperature, first found by TUXN and KAMERLINGH ONNES, has approximately been observed for all superconductors.

For a specimen which is not an infinitely long cylinder parallel to the applied field the transition from the superconducting to the normal state at constant temperature proceeds in a different manner. Referring to Fig. 1 for the case $N = 2\pi$, we note that B begins to increase from zero at $H_c = H_c/2$, whereas the negative magnetic moment begins to decrease from a maximum absolute value of $H_c/4\pi$. The reason for this is that when $H_c = H_c/2$, the field at the equator of the cylinder is actually H_c because of the demagnetizing field. Consequently the regions at the equator want to become normal. What happens is that the specimen breaks up into a composite structure consisting of both normal and superconducting laminae or filaments lying parallel to the applied field. In the s regions $B = 0$, but in the n regions $B = H_c$. This mixture of phases is called the intermediate state. The size of the intermediate state structure is determined by the balance between two opposing tendencies.

1) The finer the division into s and n regions the lower is the free enthalpy due to distortion of the field around the superconducting filaments;

2) There is a surface free enthalpy associated with the interface between superconducting and normal phases, say G_{surf} per cm^2 . In the literature one usually specifies this quantity by a length

$$A = \frac{G_{\text{surf}}}{G_n - G_s} = \delta_{\text{pen}},$$

where δ_{pen} is the penetration depth of a magnetic field into the superconductor. Δ gets larger as $T \rightarrow T_c$.

The intermediate state structure can be observed by means of magnetic powders, e.g. Ni or Nb powder.

In the case of the ferromagnetic Ni powder, the powder particles are attracted to the region of high field, i.e. the normal regions.

Since $\Delta \approx 10^{-5}$ cm the regions turn out to be of the order of 10^{-2} to 10^{-3} cm, and large specimens must be used to observe the intermediate state structure.

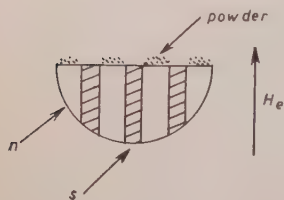


Fig. 3.

2. - Two-fluid model.

To explain the second order phase transition which occurs at $T = T_c$, in 1935 the two-fluid model was proposed, in which the «superconducting» electrons were pictured as being evaporated into normal electrons as the temperature increased.

Let x be the fraction of the total number of electrons which are normal, i.e. $x = 1$ means that the specimen is normal. Then one can write

$$G_s = xu_0 - \frac{1}{2}f(x, T)\gamma T^2,$$

since $G_n = u_0 - \frac{1}{2}\gamma T^2$, and with the assumption that the entropy of the superconducting electrons is zero. $f(x, T)$ is a weighting function which was chosen to be $x^{\frac{1}{2}}$ as a result of trial and error. So

$$G_s = xu_0 - \frac{1}{2}x^{\frac{1}{2}}\gamma T^2.$$

At equilibrium

$$\frac{\partial G_s}{\partial x} = 0 = u_0 - \frac{1}{4}x^{-\frac{1}{2}}\gamma T^2.$$

So

$$x = \frac{\gamma^2}{16} \frac{T^4}{u_0^2}.$$

Since $x = 1$ at $T = T_c$, we have

$$\gamma^2 T_c^4 = 16u_0^2$$

and

$$u_0 = \frac{1}{4}\gamma T_c^2,$$

just as was obtained before. Consequently the thermodynamic behaviour of superconductors can be described by this two-fluid model.

Experimental evidence for the validity of the two-fluid model is provided by what follows:

1) One expects $\delta_{\text{pen}} \sim (1-x)^{-\frac{1}{2}}$, so that δ_{pen} increases very rapidly as $T \rightarrow T_c$. This has been observed.

2) At high frequencies of electromagnetic radiation one gets an E_{osc} within the penetration depth which causes Joule losses in the normal electrons, giving rise to a surface impedance. The higher the frequency ν' , the less the difference between superconducting and normal surface impedances, and when $\hbar\nu \approx kT_c$, this difference seems to vanish. New American results, however, indicate the occurrence of complications.

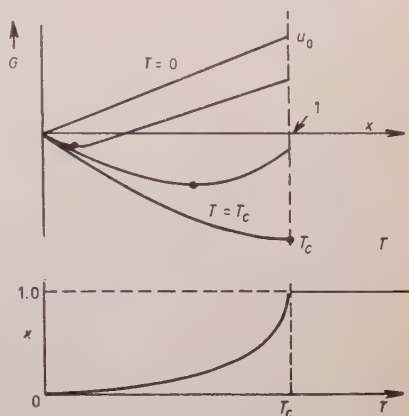


Fig. 4.

HEISENBERG and KOPPE have used statistical arguments and obtained a two-fluid model for which $x \sim T^4$ near T_c , but goes exponentially to zero near $T=0$. Experimentally this behaviour seems to be confirmed.

The two-fluid model can be correlated with an energy gap in the energy spectrum of a superconductor. At first sight one might suppose this gap to be of the order

$$u_0 \approx 10^{-7} \text{ eV},$$

the difference between G_n and G_s at $T=0$. But on the other hand it should be of the same order as

$$\frac{kT_c}{4} \approx 10^{-4} \text{ eV}.$$

The difference is explained by the fact that only the electrons on the Fermi tail are active so that

$$\frac{u_0}{kT_c/4} \approx n \approx 10^{-3},$$

where n is the relative number of active electrons and is given by

$$n \approx \frac{\gamma T_c}{k}.$$

Consequently

$$\frac{u_0}{\gamma T_c / k} = \frac{k T_c}{4},$$

or

$$u_0 = \frac{\gamma T_c^2}{4},$$

as before.

3. - The intermediate state with a current.

a) Consider the case of a long wire in a transverse magnetic field carrying a current $i \ll H_c r/2$. Experimentally one observes the ratio R/R_n , where R is the resistance of the wire, and R_n is the resistance when the wire is normal, to depend on the field as shown in Fig. 5.

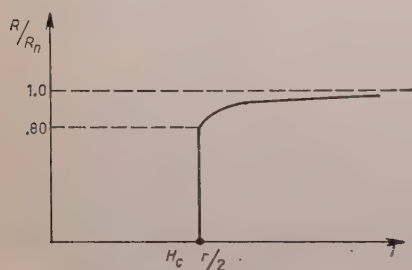


Fig. 5.

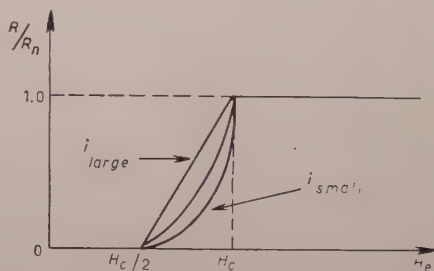


Fig. 6.

Following F. LONDON these results are usually explained by assuming that in the intermediate state normal laminae lie parallel to the external field but transverse to the cylinder axis. The ratio R/R_n then just depends on the ratio of the thickness of the normal laminae to that of the superconducting laminae.

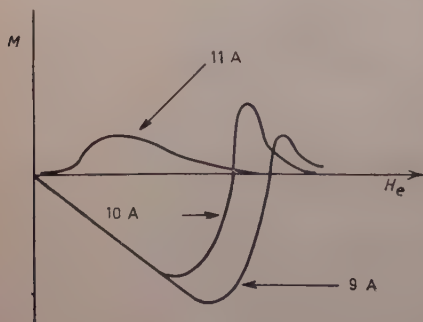


Fig. 7.

b) The case in which H_e is zero but $i > H_c r/2$. Here the behaviour of R/R_n is shown in Fig. 6.

c) The case for which the wire lies parallel to the applied field and carries a current $i < H_c r/2$. This is the so-

called quasi paramagnetic effect, because for certain values of H_c the wire develops a positive magnetic moment as shown in Fig. 7. The positive magnetic moment occurs in the neighbourhood of the point where the vector sum of

$$|\mathbf{H}_e + \mathbf{H}_i| = H_c.$$

\mathbf{H}_i is the field due to the current i .

London's model of the intermediate state configuration for large currents is shown in Fig. 8, and can be used to explain the behaviour of case b). However if one analyzes the forces acting at the boundaries between normal and superconducting regions it seem not plausible that they will place themselves perpendicular to the current.

Fig. 8. - (The height of the superconducting cones is greatly exaggerated.)

and superconducting regions it seem not plausible that they will place themselves perpendicular to the current.

In order to explain cases b) and c) as well as a) we would like to propose the following models.

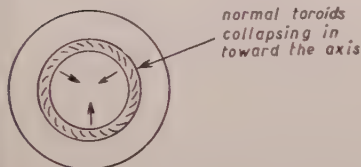


Fig. 10.

At first sight it would appear that the resistance measured across the wire should be zero because of the superconducting regions short-circuiting the normal layers. However a detailed analysis reveals that in the moving superconducting layers an induction e.m.f. is generated, while Joule heat is developed in the normal layers, and that the generated e.m.f. is of the right magnitude to explain the behaviour of the ratio R/R_n observed experimentally.

In the case b) in which H_c is zero, one pictures the normal laminae as being cylinders or toroids, concentric with the axis of the wire and collapsing inward with a velocity given by

$$\frac{dr}{dt} = -\frac{1}{4\pi\sigma r}.$$

where σ is the conductivity of the normal metal.

In Fig. 11 is shown schematically the intermediate state configuration for such a cylinder at one instant of time. Here again the motion of the collapsing

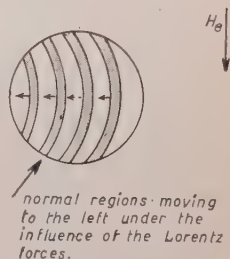


Fig. 9.

cylinders of normal material generates in the superconducting material an e.m.f. which has the character of the voltage observed.

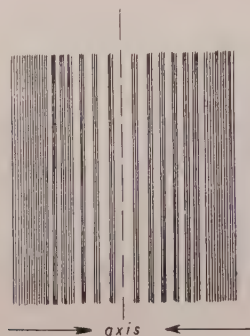


Fig. 11.

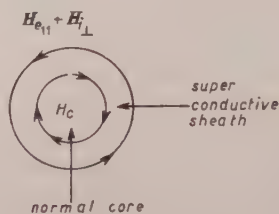


Fig. 12.

The paramagnetic effect can be understood if one notes that in the presence of a longitudinal field H_e , the contracting normal cylinders contain spiralling induction lines. The longitudinal component cannot vanish at the final collapse at the axis and that is why a normal core is built up there. The field H_c in this case may be many times larger than the external field H_e , and this would lead to the observed paramagnetism.

COMUNICAZIONI

Hall Effect in Ferromagnetics.

J. SMIT

Philips Research Laboratories N. V. Philips' Gloeilampenfabrieken - Eindhoven

It appears ⁽¹⁾ that in ferromagnetic materials the Hall voltage, measured at high fields, does not extrapolate to zero at zero field, but that a spontaneous part is left at $B = 0$. At low values of the field, where the net magnetization of the sample vanishes, F_y tends of course to zero. We can therefore write

$$F_y/i_x = R_0 B_z + R_s \cdot 4\pi M_z,$$

where $R_0 B_z$ is the normal Hall effect, with an R_0 comparable to that found in non-ferromagnetic metals, whereas $R_s \cdot 4\pi M_z$ represents the spontaneous part. This can also be expressed in terms of an effective field

$$H_{\text{eff.}} = (R_s/R_0) \cdot 4\pi M,$$

which can be as high as $(1 \div 5) \cdot 10^5$ Oe. It has been found experimentally that R_s increases strongly with increasing temperature; its value for commercial nickel at room temperature, for instance, is about ten times as large as that at low temperatures. Such a temperature dependence is similar to that of the resistivity, and we shall show that a close relationship exists between both properties. Experimentally some power law is obeyed

$$R_s \sim \varrho^n,$$

with n ranging from 1.4 to 2.

We shall show ⁽²⁾ that in a perfectly periodic lattice (pure metal at $T = 0$)

⁽¹⁾ E. M. PUGH and N. ROSTOKER: *Rev. Mod. Phys.*, **25**, 151 (1953).

⁽²⁾ J. SMIT and J. VOLGER: *Phys. Rev.*, **92**, 1577 (1953); J. SMIT: *Physica*, **21**, 877 (1955).

R_s has to be zero. The Hamiltonian, including magnetic effects, is to a first approximation

$$\mathcal{H} = \frac{p^2}{2m} + V - \frac{e}{mc} \mathbf{A} \cdot \mathbf{p} + \frac{1}{2mec} (\boldsymbol{\mu} \times \text{grad } V) \mathbf{p},$$

where V is the periodic potential, \mathbf{A} the vector potential and $\boldsymbol{\mu}$ the spin magnetic moment of the electron under consideration. If the internal magnetic field is expanded as

$$\mathbf{h}_i = \mathbf{B} + \sum_{\mathbf{g}} \mathbf{b}_{\mathbf{g}} \exp[i\mathbf{g}\mathbf{r}],$$

with \mathbf{g} a reciprocal lattice vector, then \mathbf{A} is of the form

$$\mathbf{A} = \frac{1}{2} \mathbf{B} \times \mathbf{r} + i \sum_{\mathbf{g}} (\mathbf{b}_{\mathbf{g}} \times \mathbf{g}) \exp[i\mathbf{g}\mathbf{r}]/g^2,$$

which consist of a non-periodic part $\frac{1}{2} \mathbf{B} \times \mathbf{r}$ and a periodic part. The first one gives rise to the normal Hall effect $R_0 B$, and will not be considered further.

The last term of \mathcal{H} , representing the spin-orbit interaction, is of the same form as the magnetic interaction term, and will be periodic. Therefore, apart from the term with E , the Hamiltonian will be periodic and has stationary states of the Bloch type, which can carry a stationary current, i.e. no acceleration results, so that $R_s = 0$, just for the same reason as why the resistivity vanishes. The conduction electrons therefore simply report the space-average field B , independent of their charge distribution or of the inhomogeneity of the internal magnetic fields. It may be noted that we have implicitly assumed that the conduction electrons can pass through the interior of the circular currents which produce the internal field, since otherwise the averaged field should not be equal to B .

Since the greater part of the field arises from the spins of the $3d$ electrons, one electron must be able to penetrate into the other. This can only be understood by recognizing that the spinning electron actually is a small particle (radius $\approx 10^{-13}$ cm) that is moving with the velocity of light in an orbit with radius

$$r_{\text{spin}} = \hbar/2mc \approx 2 \cdot 10^{-11} \text{ cm}.$$

This is the «Zitterbewegung» of Schrödinger. Also the contact term in the theory of the hyperfine splitting arises from this motion.

In agreement with this analysis it has been found experimentally ⁽²⁾ that in very pure nickel and probably also in iron $R_s = 0$ at very low temperatures.

In a imperfectly periodic lattice we have built up the wave function from

those for the periodic lattice

$$\psi = \sum_k a_k(t) \varphi_k(\mathbf{r}),$$

where

$$\varphi_k = u_k(\mathbf{r}) \exp[i\mathbf{k}\mathbf{r}],$$

in which u_k is a periodic function. For the sake of simplicity we used only wave functions from one band. The expectation value of a co-ordinate

$$\langle x_i \rangle = \sum_k \sum_{k'} \int a_k^* \varphi_k^* x a_{k'} \varphi_{k'} d\tau,$$

because of

$$x_i \exp[i\mathbf{k}\mathbf{r}] = -i(\partial/\partial k_i) \exp[i\mathbf{k}\mathbf{r}],$$

was found to be

$$\langle x_i \rangle = \sum_k i a_k^* \partial a_k / \partial k_i + |a_k|^2 q_i(\mathbf{k}),$$

in which

$$q_i(\mathbf{k}) = i \int u_k^* (\partial u_k / \partial k_i) d\tau,$$

is the polarization of the wave function φ_k . It has been first pointed out by KARPLUS and LUTTINGER⁽³⁾ that this q_i , which is usually zero, is now finite owing to the spin-orbit interaction. The reason for this can be easily seen. If we take μ in the z direction, the energy of an electron moving in the x - y plane will be smaller if it passes an ion on the left than on the right, because $\text{grad } V$ is opposite on both sides. Consequently the charge distribution will become asymmetrical in a direction perpendicular to both the velocity and the spin.

It has to be noted that \mathbf{q} is not a uniquely defined vector, but depends upon the choice of a phase factor in u_k , that is a gauge transformation

$$u \rightarrow u \exp[i f(\mathbf{k})]$$

changes

$$q_i \rightarrow q_i - \partial f / \partial k_i.$$

(3) R. KARPLUS and J. M. LUTTINGER: *Phys. Rev.*, **95**, 1154 (1954).

We can therefore only say that the spin-orbit interaction produced a non-zero value of $\text{curl } \mathbf{q}$, i.e. in our case

$$\partial q_x / \partial k_y - \partial q_y / \partial k_x \neq 0.$$

It is seen that now the translational motion of the electrons contributes to the angular momentum. Assuming this contribution to be of the same order of magnitude as that of the orbital motion, we arrive at

$$q \approx 10^{-9} \text{ cm}.$$

For the velocity of the wave packet we find

$$\langle v_i \rangle = \frac{d}{dt} \langle x_i \rangle = \sum_{\mathbf{k}} i \frac{d}{dt} \left(a_{\mathbf{k}}^* \frac{\partial a_{\mathbf{k}}}{\partial k_i} \right) + \frac{d|a_{\mathbf{k}}|^2}{dt} q_i.$$

The last term represents a polarization current, which is finite for an accelerated wave packet.

For the stationary state, in which we are interested,

$$d|a_{\mathbf{k}}|^2/dt = 0,$$

so such a polarization current is in the mean zero. The time derivative of the first term can be evaluated rigorously for the case that there is only a uniform electric field F_x present (in the x direction) and is then found to be for the y direction

$$i \left(\frac{d}{dt} \right)_{\text{field}} \left(a_{\mathbf{k}}^* \frac{da_{\mathbf{k}}}{dk_y} \right) = \hbar^{-1} |a_{\mathbf{k}}|^2 \left(\frac{\partial E}{\partial k_y} - e F_x \frac{\partial q_x}{\partial k_y} \right).$$

The first term on the right is the group velocity of a wave packet. The second term is of the same type and is due to the polarization energy in the applied field. Since the polarization depends upon k_y , it contributes to the group velocity. We have, therefore, the particular circumstance that the velocity operator contains the external field.

We have still to calculate the change in time due to the collisions of $ia_{\mathbf{k}}^*(\partial a_{\mathbf{k}}/\partial k_y)$. It must have a non-zero value, because it has to make the expression for the velocity gauge independent. If only the applied field is present, there are two contributions, linear in F_x , to the current, one is the polarization current, and the other stems from the electrostatic energy of the polarization in the electric field. By the application of the above mentioned gauge transformation, a current from one of the sources may be con-

verted at will into one of the other type, the total current remaining unchanged. Therefore a real distinction between the two types of current does not exist, and for the discussion of the influence of the collisions it is most convenient to write the current due to the field in terms of a polarization current only:

$$(r_y)_{\text{field}} = \sum_{\mathbf{k}} \hbar^{-1} |a_{\mathbf{k}}|^2 \frac{\partial E}{\partial k_y} + \left(\frac{d}{dt} |a_{\mathbf{k}}|^2 \right)_{\text{field}} \cdot \int_0^{\hbar} \left[\frac{\partial q_y(k'_x, k_y, k_z)}{\partial k'_x} - \frac{\partial q_x(k'_x, k_y, k_z)}{\partial k_y} \right] dk'_x.$$

According to the above arguments, this polarization current will be cancelled out exactly by the collisions. We are therefore left with the usual expression for the expectation value of the velocity of the wave packet

$$V_y \rangle = \sum_{\mathbf{k}} |a_{\mathbf{k}}|^2 \hbar^{-1} (\partial E / \partial k_y),$$

which, in the mean, can only have in a resistive material a non-zero value if a driving force in the y direction, producing transitions between states with different k_y , is present. This is a rather general statement and should apply even if some gauge independent term containing E_x in the velocity should have survived. Such a driving force in the y direction can only arise from a particular feature of the scattering process, which we have now to discuss.

In the periodic lattice the transverse spin-orbit force is exactly compensated by «electrostatic» forces for a non-zero value of the polarization. If a perturbation is present, for instance if one of the atoms is replaced by a foreign one, this equilibrium situation is destroyed and a transverse force results, which accelerates the electron in that direction. Since the polarization has the symmetry of a Lorentz force, this accelerating force represents an extra Hall effect. There are two aspects of the problem:

- 1) The spin-orbit force is changed.
- 2) The transverse electrostatic force is changed.

The first effect is due to a change of the spin-orbit interaction operator with

$$\Delta \mathcal{H}_{s.o.} = \frac{1}{2mc} (\boldsymbol{\mu} \times \text{grad } \mathcal{U}) \mathbf{p},$$

where \mathcal{U} is the perturbing potential. For the simplest case of free electrons which scatter on a spherically symmetrical rectangular potential through which depth \mathcal{U}_0 the extra Hall effect can be calculated and is of the form, expressed

in the Hall angle,

$$\varphi_H = i_y/i_x = a_1 \mathcal{U}_0 + a_2 \mathcal{U}_0^2 + \dots$$

If it is assumed that the resistivity changes by a deepening of the troughs, then

$$\varrho \sim \mathcal{U}_0^2$$

so that

$$R_s \sim b_1 \varrho^{\frac{3}{2}} + b_2 \varrho^2 + \dots$$

The order of magnitude is, however, far too small. A very much larger value of R_s is obtained by the second effect. This effect is already clear from the existence of the transverse polarization, which causes the electron not to collide centrally on the impurity atom, so that skew scattering results. In an effective mass approximation one can take this polarization into account by introducing into the Hamiltonian a term

$$\Delta \mathcal{H} = -e \mathbf{F} \cdot \mathbf{q}.$$

If \mathbf{q} is taken perpendicular and proportional to the velocity and perpendicular to the spin, this operator has the same form as the spin-orbit operator, but has a greatly increased strength. The original spin-orbit operator can also be regarded as the interaction of the electric field with an electric dipole moment with

$$q' = \frac{v}{c} \cdot \frac{\hbar}{2mc} \approx 10^{-13} \text{ cm},$$

as compared with a value of about 10^{-9} cm of q . The order of magnitude of the calculated spontaneous Hall angle is now 10^{-2} , agreeing with experiments.

For lattice vibration scattering the mean value of \mathcal{U}_0 will be zero, so that in this case the first term in R_s is that with ϱ^2 , this being in agreement with experimental finding on very pure nickel and iron at varying temperature.

Critical Scattering of Neutrons from Ferromagnets.

W. MARSHALL (*)

Theoretical Physics Division - Atomic Energy Research Establishment - Harwell

The general theory of the critical scattering of neutrons has been developed by VAN HOVE who showed how the differential cross-section was related to the pair distribution function. For ferromagnets and antiferromagnets this pair distribution function was defined as

$$(1) \quad \gamma_R(t) = \langle S_0(0) \cdot S_R(t) \rangle$$

where $S_0(0)$ is the spin of the atom zero at time zero and $S_R(t)$ is the spin of the atom R at time t . VAN HOVE showed by general arguments that

$$\gamma_R(0) = \frac{v_0 s(s+1)}{4\pi r_1^2} \frac{1}{R} \exp[-K_1 R],$$

where v_0 is the unit cell volume, r_1 some length $\approx 1 \text{ \AA}$ and $1/K_1$ a correlation length going to infinity at the Curie temperature.

K_1 and r_1 can be calculated as functions of temperature for any specific model using a modification of the Bethe-Peierls theory of order-disorder. In the usual Bethe-Peierls theory one selects a small cluster of atoms around an arbitrary atom, say R , and treats the interactions inside the cluster exactly. The influence of the other spins on the shell of spins on the outside of the cluster is represented by an internal field which is solved for self consistency. If now it is given that the spin at the origin has some particular value then an additional influence acts on the shell spins of the cluster. This additional influence is represented as a small additional field dependent on R , the spin of the origin atom, and the particular atom of the shell upon which it acts.

(*) The work to be described here was done in collaboration with Dr. R. J. ELLIOTT.

It is possible to solve self-consistently for this additional field and obtain an expression of the form (2) for $\gamma_R(0)$.

The theory shows that K_1 is zero at the Curie temperature and increases approximately linearly above and below T_c , the increase being twice as rapid below T_c : r_1 can be determined in terms of K_1 by noting that

$$(3) \quad \sum_R \gamma_R(0) = (4\mu^2 N)^{-1} \langle M^2 \rangle,$$

where M is the magnetic moment, and $\langle M^2 \rangle$ is given in terms of the susceptibility by

$$(4) \quad \langle M^2 \rangle = \langle M \rangle^2 + kT\chi,$$

from these equations it is possible to determine r_1 as a function of temperature. It is found that at T_c , $r_1 \approx 1 \text{ \AA}$.

$\gamma_R(t)$ can now be determined from $\gamma_R(0)$ as described in VAN HOVE's paper.

INTERVENTI E DISCUSSIONI

— N. KURTI:

Referring to Prof. GORTER's remark, it seems to me that at the normal Néel point ($H = 0$), the behaviour of an antiferromagnetic need not be different from that of a ferromagnetic at the Curie point.

— C. J. GORTER:

I should like to point out that statistically the situation near a Néel point is not identical with that near a Curie point of a ferromagnetic substance.

In the H - T diagram of ferromagnet one has a transition of the first order ending at the Curie temperature somewhat similar to the liquid-gas transition ending at the critical point.

In the H - T diagram of an antiferromagnet we presumably have a transition line of the second order having a vertical tangent at the Néel temperature. In contradistinction to the ferromagnetic case long-range order now disappears abruptly also if the field differs from zero.

— B. JACROT:

Dans des expériences faites à Saclay, nous avons étudié le temps de relaxation qui caractérise la dépendance temporelle de la fonction de corrélation des spins autour du point de Curie.

— H. GRÄNICH:ER:

It might be of interest to mention that an effect analogous to the critical scattering in ferromagnets occurs in ferroelectrics and was observed by W. KÄNZIG (*Helv. Phys. Acta*, **24**, 175 (1951)) in an X-ray study of BaTiO_3 single crystals. According to the quite different mechanism of ferroelectricity it is not the atomic scattering factor that changes, but the extinction properties of the crystal are greatly affected at the first order transition. BaTiO_3 crystals grown from a melt are nearly « ideal » crystals showing primary extinction. At the transition however fluctuations occur and the crystals transform to the ferroelectric state in small regions. In such regions ion shifts occur and the lattice deforms from cubic to tetragonal pseudocubic symmetry. The crystal therefore behaves at the transition as an ideal « mosaic » crystal and the integrated intensities of low order reflexions are up to 5 times more intense than above and below the transition region.

The Van Vleck Model of Ferromagnetism.

W. MARSHALL

Theoretical Physics Division - Atomic Energy Research Establishment - Harwell

Recently VAN VLECK has proposed a model of ferromagnetism (*Rev. Mod. Phys.*, **25**, 220 (1953)) which is a compromise between the extreme Heitler-London and collective models. In order to make a start on this model let us consider a few simple cases.

First consider the case of a crystal of N atoms with $N - 1$ electrons and suppose all the spins of the electrons are plus. Then with the Van Vleck model we must put one electron on each atom except one, say the n -th. The wave functions representing this will be

$$(1) \quad \varphi_n(\mathbf{r}_1, \mathbf{r}_2, \dots, \mathbf{r}_{N-1}) \alpha(1) \alpha(2) \dots \alpha(N-1),$$

which is an $(N-1) \times (N-1)$ determinant. But the « hole » on the atom n will not be stationary. Electrons will jump into it leaving a hole behind, i.e. the hole will move and the eigenfunction will be

$$(2) \quad \sum_n \exp[i\mathbf{k} \cdot \mathbf{n}] \varphi_n(\mathbf{r}_1, \mathbf{r}_2, \dots, \mathbf{r}_{N-1}) \alpha(1) \alpha(2) \dots \alpha(N-1),$$

where \mathbf{k} is the wave number of the hole.

This motion gives an energy $E(\mathbf{k})$ dependent on \mathbf{k} , i.e. an energy band. For small \mathbf{k} this will be of the form

$$(3) \quad E = E_0 + C\mathbf{k}^2.$$

Now consider the case with N atoms and $(N - 2)$ electrons. Then there are two holes, on atoms n_1 and n_2 say and the eigenfunctions will be

$$(4) \quad \sum_{n_1, n_2} \exp[i(\mathbf{k}_1 \cdot \mathbf{n}_1 + \mathbf{k}_2 \cdot \mathbf{n}_2)] \varphi_{n_1, n_2}(\mathbf{r}_1, \mathbf{r}_2, \dots, \mathbf{r}_{N-2}),$$

where $\varphi_{n_1 n_2}(\mathbf{r}_1 \dots \mathbf{r}_{N-1})$ is a $(N-2) \times (N-2)$ determinant. It is possible to show that this vanishes if $\mathbf{k}_1 = \mathbf{k}_2$: the holes obey Fermi statistics.

We can now go on to add more holes to the crystal and clearly their translational motion gives rise to a specific heat $\propto T$ which can be calculated in the usual way. But so far we have only considered the case with all the electron spins parallel. When they are not all parallel the n we also get spin waves which, if the number of holes introduced is not too large, will not be scattered too much and so will have an energy spectrum like normal spin waves in a pure Heitler-London model. So this Van Vleck model gives rise to a specific heat proportional to T coming from the translational motion of the holes, a smaller term proportional to $T^{\frac{3}{2}}$ coming from the usual spin wave motion, and a magnetization varying like $T^{\frac{3}{2}}$ and thus gives a consistent model to explain the experimental results.

There is one difficulty with this model which is connected with the use of non-orthogonal localized wave functions. This difficulty also occurs in the usual Heitler-London model and Slater has severely questioned the validity of calculations performed ignoring this difficulty. But it can be shown that this is only a formal mathematical difficulty which can be overcome by using Wannier functions in a careful way.

The coefficient C of (3) can be shown to be⁸

$$(5) \quad c = \int d\mathbf{x} \left\{ \varphi_c^*(x) \varphi(x) - \varepsilon |\varphi(x)|^2 \right\} \left\{ U(x - \mathbf{e}) + \sum_{\substack{\mathbf{m} \\ \neq 0 \text{ or } \mathbf{q}}} \left\{ U(x - \mathbf{m}) + \int d\mathbf{y} \frac{|\varphi \beta(y)|^2}{|\mathbf{x} - \mathbf{y}|} \right\} \right\}$$

where

$$\varepsilon = \int_0^{+\approx \varepsilon^2} \varphi_c^*(x) \varphi(x) d\mathbf{x}$$

Here $\varphi(x)$ is an atomic wave function centred on atom \mathbf{m} , \mathbf{q} is a nearest neighbour atom of the origin atom and $U(x - \mathbf{m})$ is the potential at x due to the core at \mathbf{m} . ε is small so terms $\approx \varepsilon^2$ can be neglected. The interesting point to note is the appearance of the term proportional to ε in the first part of (5). This term comes directly from the non-orthogonality of the atomic wave functions and has the effect of making C smaller than would be expected if the non-orthogonality were ignored i.e. the effective mass of the holes is greater than would be expected and so this Van Vleck model may give specific heats as high as those given by a pure collective electron treatment.

Influence of the Apparatus on Nuclear Magnetic Resonance.

H. PFEIFER

Physikalisches Institut der Universität - Leipzig

The first and most important problem in the theory of nuclear magnetic resonance is to find the equations of motion for the components of magnetization as functions of the applied magnetic fields and data of the spin system. For a great number of substances (mainly liquids) these equations are given by the Bloch equations. In this case the characteristic quantities of the spin system are the gyromagnetic ratio γ of the nucleus, the static susceptibility χ_0 of the nuclei and the relaxation times T_1 and T_2 .

The second problem is to transform variations of the components of the magnetization into variations of voltage; for only these variations can be amplified and recorded for measuring. This transformation is accomplished by a small coil wound round the sample. This coil generates the r-f field and at the same time voltages are induced in it by magnetization. These voltages themselves generate a new field and the sample therefore is in a somewhat altered field. Thus a variation of voltage is measured which is not only determined by the magnetization but also by the characteristics of the coil and its associated circuit. The undesirable influence of the coil and its associated circuit is always present. However we can give examples where the influence is very small.

For the theory—published in *Experiment. Techn. d. Phys.*, **2**, 127 (1954) and *Ann. d. Phys.*, **15**, 311 (1955)—the following assumptions were made.

1) The equations of motion for the magnetization are given by the Bloch-equations.

2) The direct field H_0 and the r-f field are homogeneous (the influence of inhomogeneities of the direct field is discussed by U. DOLEGA, thesis Leipzig, 1954, and the influence of inhomogeneities of the r-f field upon absorption lines, dispersion lines and spin-echoes is discussed by H. PFEIFER in *Zeits. f. angew. Phys.*, **7**, 389 (1955)).

- 3) The variation of H_0 or the frequency ω during measuring are very slow compared with the relaxation times; i.e. slow passage.
- 4) There are no saturation effects.
- 5) The filling factor of the coil is equal to unity.

In order to discuss the results we will divide the apparatuses for observing nuclear magnetic resonance in two groups A and B. To the group A belongs all devices which use a passive circuit for detecting nuclear magnetic resonance, for instance bridge type apparatus. The group B includes all devices which use an active circuit for detecting nuclear magnetic resonance. To this group for instance belong all instruments of autodyne type.

For instruments of both groups the resonance frequency is not given by $\omega = \gamma H_0$ but by $\omega_r = \sqrt{\gamma^2 H_0^2 + T_2^{-2}}$ which can be written

$$\left(\frac{\omega_r - \gamma H_0}{2/T_2} \right) \approx \frac{1}{8} \left(\frac{2/T_2}{\omega_r} \right).$$

The last term is very small, therefore the shift of resonant frequency $\omega_r - \gamma H_0$ is very small compared with the line width $2/T_2$.

For sets of group A the line width is no longer $\Delta\omega_{\frac{1}{2}} = 2/T_2$ but broadened to

$$\Delta\omega_{\frac{1}{2}} = \frac{2}{T_2} (1 + 2\pi x_0 \gamma H_0 Q T_2),$$

where Q is the quality of the circuit. We assumed $Q = 100$ and with a sample of water (i.e. $x_0 = 3.4 \cdot 10^{-1}$ cgs) we found for the relative line broadening in this case

$$\left(\frac{\Delta\omega_{\frac{1}{2}} - 2/T_2}{\gamma H_0} \right) \approx 4.26 \cdot 10^{-7}$$

that is the effect of line broadening will be important only for extremely sharp lines. About the same time as this work was published the influence of the measuring circuit upon nuclear magnetic resonance was discussed by N. BLOEMBERGEN and R. V. POUND (*Phys. Rev.*, **95**, 8 (1954)). In contrast to our calculations they found that there is no line broadening in the steady state.

Instruments of the group B show a line sharpening. The line width is

$$\Delta\omega_{\frac{1}{2}} \approx \frac{2}{T_2} \left(1 - \frac{\pi}{2} x_0 T_2^2 \gamma^2 H_0^2 \right).$$

We see from the latter equation that this sharpening becomes important for long T_2 and restricts the use of sets of group B, i.e. the autodyne type, to measuring broad lines, for instance signals from solids.

Statistical Theory of Ferro- and Antiferromagnetism.

J. VAN KRANENDONK

Instituut Lorentz - Leiden

The partition function of a spin system with an isotropic coupling between neighbouring spins can be expressed in terms of an effective Hamiltonian, H_e , for a pair of neighbouring spins. The meaning of H_e is that the pair density operator corresponding to H_e , viz. $\exp[-\beta H_e]$, describes an ensemble of isolated pairs of spins the statistical properties of which are identical with those of a pair of neighbouring spins in the actual crystal. H_e depends parametrically on the temperature and on the component S of the total spin of the spin system in the direction of the external field. The average value of S at a given temperature is obtained by minimizing the partial free energy $F(T, S)$ with respect to S . The most general expression for H_e contains ten terms, but this general form can be reduced considerably by using simple symmetry arguments. In the ferromagnetic case H_e reduces to a sum of three terms, while in the antiferromagnetic case there remain four terms for the case of a parallel, and six terms for the case of a perpendicular external field. By making specific assumptions about the remaining quantities appearing in H_e , one can construct approximations to the partition function of the spin system.

By assuming that the coupling terms appearing in H_e are zero, i.e. by assuming that the two spins of a pair of neighbouring spins are statistically uncorrelated, one obtains the Weiss molecular field theory. This shows that the Weiss theory is the best approximation that can be constructed on the basis of the assumption that the directions of neighbouring spins are uncorrelated.

As a next approximation the so-called constant coupling approximation can be obtained by assuming that the effective coupling appearing in H_e is independent of T and S and equal to the actual coupling between neighbouring spins. The approximation thus obtained is a straightforward generalization of the quasi-chemical approximation for Ising systems to the case of isotropic interaction. This constant coupling approximation is similar, though not

identical, to the Bethe-Peierls-Weiss method. However, it is easier to handle analytically, and even below T_c one can easily obtain solutions of the basic equations. By using the Opechowsky expansion method one can show that in the limit of high temperatures the exact value of the effective coupling appearing in H_c approaches the constant coupling assumed in the constant coupling approximation. One can also compare the exact power series expansion of the susceptibility above T_c in powers of $1/T$ to the power series obtained by means of the molecular field theory, the constant coupling approximation and the Bethe-Peierls-Weiss method, and one then finds that the constant coupling approximation shows the best agreement with the exact expression (*).

(*) See P. W. KASTELEYN and J. VAN KRANENDONK: *Physica*, **22**, 317, 367 (1956); and P. W. KASTELEYN: *Physica*, **22**, 387, 397 (1956).

Nuclear Relaxation in Magnetic Materials.

J. VAN KRANENDONK

Instituut Lorentz - Leiden

The resonance frequency of a nuclear spin in a magnetic crystal is determined by the sum of the external field and the time average value of the internal field at the position of the nucleus due to the surrounding magnetic ions, while the spin-lattice relaxation of the nuclear spins is due to the fluctuating part of the internal field. The fluctuations in the internal field may be due to the lattice vibrations modulating the magnetic dipolar interaction between the nuclear spins and the surrounding magnetic ions, or it may be due to the precessional motion of the magnetic ions caused by the interaction between the ions. The first relaxation process is controlled by the Debye temperature T_D of the lattice, the second one by the Curie or Néel temperature T_C of the system of interacting magnetic ions. For $T_D \ll T_C$ and for temperatures of the order of T_D only the first mechanism is of importance; for $T_C \ll T_D$ and temperatures of the order of T_C only the second mechanism is effective, while for $T_C \simeq T_D$ both mechanisms are operative.

The relaxation of the protons in antiferromagnetic $\text{CuCl}_2 \cdot 2\text{H}_2\text{O}$ has recently been measured in Leiden at temperatures below the Néel temperature of 4.3°K . In this case $T_D \ll T_N$ so that the relaxation is entirely due to the second mechanism. The fluctuations in the local field that are responsible for the proton flips are due to the precessional motions of the Cu^{++} spins caused by the antiferromagnetic interaction between the Cu^{++} ions. Quantum mechanically one can say that the proton flip is accompanied by a transition of the Cu^{++} spin system, whereby the nuclear Zeeman energy is transferred to the Cu spin system. This energy is finally transferred to the lattice in quanta that are very large compared to the nuclear Zeeman quanta, and the bottleneck for the transfer of energy from the nuclei to the lattice will be the coupling of the nuclear spins to the atomic spins and not the coupling of the atomic spins to the lattice. A general theory of this relaxation process can be deve-

loped on the basis of the assumption that the influence on the motions of the atomic spins resulting from the coupling of the atomic spins to the nuclear spins can be neglected, which condition is very well satisfied in practice.

For $T \ll T_N$ the antiferromagnetic spin system can be described by means of the spin wave approximation in which the eigenstates are analyzed with the help of two sets of $\frac{1}{2}N$ normal modes, \mathbf{k}, p , where \mathbf{k} is the wave vector and $p = 1, 2$ the polarization of the spin waves. $p = 1$ spin waves decrease the magnetization of one of the sublattices, $p = 2$ spin waves decrease that of the other sublattice. The relevant relaxation processes are Raman spin wave processes in which the nuclear flip is accompanied by the absorption of one and the emission of another spin wave, which can also be described as the inelastic scattering of a spin deviation. When one uses for the occupation numbers $n_{\mathbf{k}p}$ of the spin wave modes \mathbf{k}_p the values following from the simple spin wave treatment in which the interaction between the spin waves is neglected, one finds for the transition probability for a proton in $\text{CuCl}_2 \cdot 2\text{H}_2\text{O}$:

$$P = P_0(T/T_N)^3,$$

where P_0 is a constant characteristic of the crystal. The relaxation time $\tau = \frac{1}{2}P$ turns out to be of the correct order of magnitude, but the experimentally determined τ shows a stronger temperature dependence than T^3 . This is understandable since the simple spin wave theory gives also a too slow temperature dependence for the sublattice magnetization, viz. T^2 rather than the experimentally determined T^1 .

A similar relaxation process, though with a different temperature dependence, should occur in ferro- and ferrimagnetic materials, but no nuclear resonance has as yet been observed in such substances.

(¹) J. VAN KRANENDONK and M. BLOOM: *Physica*, **22**, 545 (1956).

The Study of Chemical Exchange Reactions by Nuclear Magnetic Resonance.

S. MEIBOOM

Department of Applied Mathematics, The Weizmann Institute of Science - Rehovot

The influence of chemical exchange on the nuclear magnetic resonance spectrum in liquids has been indicated by HAHN and MAXWELL ⁽¹⁾, who ascribed the absence of multiplet structure in the methyl-alcohol spectrum to fast chemical exchange. The effect in ethylalcohol has been described by ARNOLD ⁽²⁾.

A simple case of proton exchange reaction can be described by the equation



Here A and B symbolize the part of the molecules not involved in the reaction. The star identifies one particular proton. The proton magnetic resonance spectrum of the above system (disregarding for the moment the protons which may be present in the groups A or B) is illustrated schematically in Fig. 1. When the reaction rate is zero or very low, each of the chemical species will give its own sharp proton resonance, separated by the chemical shift Δ (top of Fig. 1). In the other extreme, when the exchange rate is very high, one sharp line will be observed, at a frequency which is the weighted average of the individual frequencies (bottom of Fig. 1). At intermediate rates of exchange the resonance lines are broadened. The greatest broadening is of the order of Δ and occurs for an average lifetime of the order of $1/\Delta$.

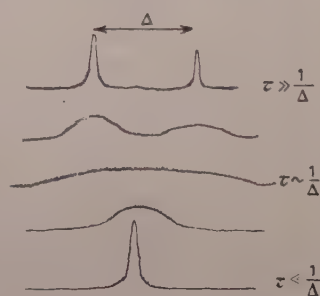


Fig. 1. - Proton magnetic resonance spectrum of the system given in equation (1) as function of mean life-time τ .

⁽¹⁾ E. L. HAHN and D. E. MAXWELL: *Phys. Rev.*, **88**, 1070 (1952).

⁽²⁾ J. T. ARNOLD: *Phys. Rev.*, **102**, 136 (1956).

In many cases proton exchange occurs between molecules of the same species. A and B in equation (1) are then identical and the chemical shift Δ is zero. In this case the exchange will be observed in the Nuclear magnetic resonance spectrum if group A contains nuclei which have spin-spin interaction with the protons, so that multiplets appear. The result of fast exchange will then be the collapsing of the multiplets into one sharp line. This is illustrated in Fig. 2, for the simplest case of two interacting non equivalent protons, one of which undergoes exchange.

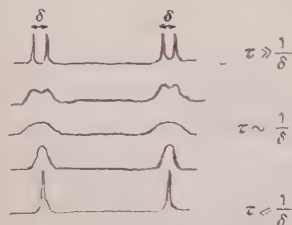


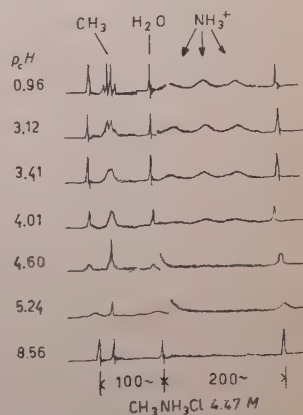
Fig. 2. - Effect of chemical exchange on multiplet structure.

A quantitative calculation of the line shapes as function of exchange rate has been given by GUTOWSKY, MCCALL and SLICHTER ⁽³⁾. This treatment

is based on the Bloch equations, and assumes perfect phase conservation during the actual exchange. The fact that one sharp line is observed at high exchange rates is the result of this assumption. This can be seen in a qualitative way from the following physical picture. The exchanging protons effectively switch their Larmor frequency back and forth between two values ω_1 and ω_2 , where $\omega_1 - \omega_2 = \Delta$. Relative to a co-ordinate system rotating with a velocity $\frac{1}{2}(\omega_1 + \omega_2)$, the magnetic moment of the protons will rotate alternately in a clockwise and counterclockwise sense, with a velocity $\Delta/2$, the reversals taking place when an exchange occurs. At higher rates of exchange this will result only in a small random motion of the magnetic vector, the amplitude of this motion being smaller the higher the exchange rate. Accordingly one sharp line will be observed. Note that it is essential to assume conservation of phase in the exchange process in order to arrive at this conclusion.

In actual systems a combination of the two cases described above frequently occurs. This is illustrated in Fig. 3, which shows actual proton resonance spectra of CH_3NH_3^+ ions in aqueous solution. The upper trace shows the spectrum at

Fig. 3. - Proton magnetic resonance spectra at 31.65 MHz of 4.47 M solutions of methylamine-hydrochloride in water. The lines at the extreme left and right are repetitions of the water line and are used for calibration. Different groups were recorded at different amplifications. So no significance should be attached to their relative intensities.



⁽³⁾ H. S. GUTOWSKY, D. W. MCCALL and C. P. SLICHTER: *Journ. Chem. Phys.*, **21**, 279 (1953). See also H. S. GUTOWSKY and A. SAIKA: *Journ. Chem. Phys.*, **21**, 1688 (1953).

very low rate of exchange. The CH_3 group appears as a sharp quadruplet, and the NH_3^+ group is a broadened triplet due to spin-spin interaction with the ^{14}N nucleus (spin 1), the broadening being due to quadrupole relaxation of the ^{14}N . The quadruplet structure due to the interaction with the CH_3 group is only barely discernible because of this broadening. In this system the rate of exchange of the NH_3^+ protons can be changed by varying the hydrogen-ion concentration. The effect of increasing the rate of exchange is shown in Fig. 3. At high rates the NH_3^+ and the water give a single sharp line, slightly shifted to the right relative to the position of the water line in the solutions having slow exchange. This indicates that the water takes part in the exchange reaction, as otherwise the water and the NH_3^+ protons would give separate lines.

It is possible to obtain quantitative data on the proton exchange rates by comparing experimental and calculated line shapes. The theory of GUTOWSKY, McCALL and SLICHTER can easily be generalized to apply to the present case. By varying the concentrations of the components involved in the exchange reaction a kinetic analysis can be made, and definite conclusions as to the detailed mechanism of the exchange reaction can be arrived at. The results of this analysis have been published elsewhere (4).

In conclusion it should be remarked that broadening due to chemical exchange might occur in systems where it is not expected at first sight. A case in point is water. It is probably an oversimplification to picture water as consisting of stable H_2O molecules. In the first place there exist OH^- and H_3O^+ ions, the protons of which exchange with H_2O molecules. In pure water the concentration of these ions is probably too low to give an appreciable broadening, even if the exchange rate happened to be such as to give maximum effect. However, it is known that water shows pronounced hydrogen bonding, so that complexes exist which continually break up and reform. This could well cause an appreciable reduction of the T_2 in water, and provide an explanation of the experimental result that $T_1 > T_2$ in pure water.

(4) E. GRUNWALD, A. LOEWENSTEIN and S. MEIBOOM: *Journ. Chem. Phys.*, in press,

Résonance paramagnétique des impuretés dans un semi-conducteur.

A. ABRAGAM et J. COMBRISSE

Centre d'Etudes Nucléaires de Saclay - France

Le phénomène de résonance paramagnétique des impuretés dans les semi-conducteurs, observé pour la première fois par FLETCHER *et al.* ⁽¹⁾, a été abondamment étudié pendant les deux dernières années ⁽¹⁻¹¹⁾, et présente un grand nombre de particularités remarquables.

Après une introduction générale, nous nous limiterons dans cet article à un exposé des résultats obtenus dans ce domaine au Laboratoire de Résonance Magnétique de Saclay en nous contentant de signaler les études faites ailleurs et en particulier les travaux remarquables de Mr. G. FEHER aux Bell Telephone Laboratories ⁽⁵⁻⁸⁾.

1. - Introduction.

On peut se faire de l'état d'un atome d'impureté « donneur » comme le phosphore ou l'arsenic introduit dans le silicium, l'image suivante, suffisante pour comprendre qualitativement les phénomènes. Les atomes de silicium sont

⁽¹⁾ R. C. FLETCHER, W. A. YAGER, G. L. PEARSON, A. N. HOLDEN, W. T. READ et F. R. MERRITT: *Phys. Rev.*, **94**, 1392 (1954).

⁽²⁾ R. C. FLETCHER, W. A. YAGER, G. L. PEARSON et F. R. MERRITT: *Phys. Rev.*, **95**, 844 (1954).

⁽³⁾ A. HONIG et A. F. KIP: *Phys. Rev.*, **95**, 1686 (1954).

⁽⁴⁾ A. HONIG: *Phys. Rev.*, **96**, 234 (1954).

⁽⁵⁾ G. FEHER: *Phys. Rev.*, **103**, 500 (1956).

⁽⁶⁾ G. FEHER et E. A. GERE: *Phys. Rev.*, **103**, 501 (1956).

⁽⁷⁾ G. FEHER: *Phys. Rev.*, **103**, 834 (1956).

⁽⁸⁾ G. FEHER, R. C. FLETCHER et E. A. GERE: *Phys. Rev.*, **100**, 1784 (1955).

⁽⁹⁾ A. HONIG et J. COMBRISSE: *Phys. Rev.*, **102**, 917 (1956).

⁽¹⁰⁾ A. ABRAGAM et J. COMBRISSE: *Compt. Rend. Acad. Sci.*, **243**, 276 (1956).

⁽¹¹⁾ A. ABRAGAM et J. COMBRISSE: *Compt. Rend. Acad. Sci.*, **243**, 650 (1956).

tétravalents et forment 4 liens tétraédraux avec leurs voisins. Lorsqu'on introduit dans le réseau un atome pentavalent il peut s'intégrer dans le réseau en perdant un électron de valence. Il devient alors un ion positif et peut retenir cet électron dans son voisinage par attraction coulombienne. La description correcte de la fonction d'onde de cet électron est extrêmement complexe mais on peut essayer de s'en faire une idée grossière en considérant l'ensemble de l'ion positif et de l'électron qui gravite autour de lui comme une espèce d'atome hydrogénoïde. Ainsi formellement le phénomène de résonance paramagnétique peut se décrire de la même façon que la résonance de l'hydrogène atomique. On observe la transition électronique $\Delta m_s = \pm 1$ à laquelle l'interaction avec le spin nucléaire superpose une structure hyperfine. On voit 2 raies dans le cas du phosphore ($I = \frac{1}{2}$), 4 pour l'arsenic ($I = \frac{3}{2}$), 6 et 8 respectivement pour les deux isotopes de l'antimoine ($I = \frac{5}{2}$ et $\frac{7}{2}$). Une approximation grossière pour calculer l'énergie d'ionisation E et le rayon a de l'orbite de Bohr de l'atome hydrogénoïde consiste, comme il est bien connu, à utiliser les formules suivantes:

$$(1) \quad a = \frac{e\hbar^2}{m^*e^2} = a_0 \varepsilon \frac{m}{m^*},$$

$$(2) \quad E = \frac{e^4 m^*}{2\varepsilon^2 \hbar^2} = E_0 \frac{m^*}{m} \frac{1}{\varepsilon^2}.$$

Dans ces formules ε est la constante diélectrique du milieu, m^* la masse efficace, a_0 et E_0 les grandeurs relatives à l'atome d'hydrogène.

Considérons à titre d'exemple le phosphore dans le silicium. Le nombre atomique du phosphore étant voisin de celui du silicium on peut espérer que ce traitement sera moins grossier que dans le cas d'une impureté comme l'arsenic ou l'antimoine. Nous prendrons $\varepsilon = 11.7$ et pour E la valeur expérimentale 0.045 eV.

On en tire par (2) la valeur 0.45 pour m^*/m (en fait la masse efficace dans Si est anisotrope et la valeur moyenne des valeurs de m^*/m mesurées dans différentes directions par la résonance cyclotron est 0.25 mais nous négligerons ce désaccord dans nos considérations approchées).

On trouve alors

$$a = 0.528 \cdot \frac{11.7}{0.45} \text{ \AA} = 14 \text{ \AA},$$

(ou 25 \AA en prenant $m^*/m = 0.25$).

A cause de cet énorme rayon atomique l'électron a une probabilité de

(12) A. ABRAGAM: *Compt. Rend. Acad. Sci.*, **242**, 1720 (1956).

présence non nulle à l'emplacement des noyaux de silicium voisins, 4,7° de ceux-ci sont des noyaux de ^{29}Si de spin $\frac{1}{2}$, ayant un moment magnétique et le couplage du spin de l'électron avec ces moments magnétiques a pour effet d'élargir les raies de résonance, qui autrement seraient extrêmement fines, jusqu'à une largeur de 2 à 3 gauss. Il s'agit là d'un élargissement « inhomogène » dont les propriétés de saturation signalées pour la première fois en résonance électronique à propos des centres F⁽¹³⁾ ont été l'objet de nombreuses études théoriques et expérimentales.

Une autre conséquence de la grande extension spatiale de la fonction d'onde est la possibilité d'un couplage d'échange entre deux spins électroniques appartenant à des impuretés voisines, et cela malgré la grande dilution (10^{16} à 10^{17} par cm^3) des impuretés.

Ces interactions d'échange se manifestent par l'apparition de lignes satellites, observées par FLETCHER *et al.* (2), étudiées systématiquement par G. FEHER *et al.* (8) et expliquées quantitativement par C. SLICHTER (14). Le calcul de l'intervalle hyperfin à partir des premiers principes a été fait pour le phosphore par KOHN et LUTTINGER (15).

Le principe de ce calcul consiste à écrire la fonction d'onde sous la forme:

$$(3) \quad \Psi(\mathbf{r}) = F^{(1)}(\mathbf{r}) \cdot \Psi_1(\mathbf{r})$$

Dans cette formule $F^{(1)}(\mathbf{r})$ est la fonction d'onde amplitude représentée (du moins à grande distance) par la fonction d'onde hydrogénoïde:

$$\frac{1}{\sqrt{\pi a^3}} \cdot \exp[-r/a].$$

$\Psi_1(\mathbf{r})$ est une fonction de Bloch de la forme

$$(4) \quad \Psi_1(\mathbf{r}) = \exp[i\mathbf{k}\mathbf{r}] u_k(\mathbf{r}),$$

normalisée à l'unité dans un volume atomique.

Si nous appelons $\varphi(r)$ la fonction d'onde 3s de l'atome silicium, on aura en ordre de grandeur

$$(5) \quad |\Psi_1(0)|^2 \simeq |\varphi(0)|^2 \Omega'$$

où Ω' est le volume atomique.

Si pour $|\varphi(0)|^2$ on prend $40 \cdot 10^{24} \text{ cm}^{-3}$ tiré des fonctions de Hartree pour

(13) A. F. KIP, C. KITTEL, R. A. LÉVY et A. M. PORTIS: *Phys. Rev.*, **91**, 1066 (1953).

(14) C. SLICHTER: *Phys. Rev.*, **99**, 479 (1955).

(15) W. KOHN et J. M. LUTTINGER: *Phys. Rev.*, **97**, 883 (1955).

Si^{+3} , et pour $\Omega' = 20 \cdot 10^{-24} \text{ cm}^3$, on trouve :

$$(6) \quad \Psi^2(0) = [\Psi^2(0)]_{\text{Hydr.}} \times \left(\frac{r_0}{r}\right)^3 \times 40 \cdot 10^{24} \times 20 \cdot 10^{-24}.$$

Il en résulte que l'intervalle ΔH entre deux raies de structure hyperfine voisines sera :

$$(7) \quad \begin{aligned} (\Delta H)_{\text{Phos.}} &= (\Delta H)_{\text{Hydr.}} \times \left(\frac{r_0}{r}\right)^3 \times 800 \times \frac{(\mu_n/I)_{\text{P}}}{(\mu_n/I)_{\text{H}}} \\ &= 506 \times \left(\frac{0.45}{11.7}\right)^3 \times 800 \times \frac{1.13}{2.79} \\ &\simeq 15 \text{ G.} \end{aligned}$$

La valeur expérimentale est 12 gauss ce qui, vu la grossièreté des calculs, est satisfaisant. On trouvera des raffinements de ce calcul dans la référence ⁽¹⁴⁾. Pour l'arsenic l'approximation précédente est encore moins justifiée. La valeur expérimentale est $\Delta H \simeq 73$ gauss.

2. — Relaxation spin-réseau.

Nous avons étudié ⁽¹⁰⁾ à 3 000 gauss et 2 °K la résonance paramagnétique des atomes d'arsenic introduits à une concentration de $10^{17}/\text{cm}^3$ environ dans un cristal de silicium (prêté obligeamment par Monsieur A. HONIG, dont le concours et l'expérience ont été d'un grand secours dans les expériences préliminaires). La relaxation spin-réseau de cette résonance présente des caractères remarquables.

1) *Longueur des temps de relaxation.* — Elle se traduit par :

a) La saturation de l'absorption χ'' même pour des valeurs très faibles du champ H.F. d'où nécessité pratique d'observer la dispersion.

b) La nécessité même dans ce cas, d'attendre plusieurs minutes après passage sur une raie pour revoir un signal comparable.

c) La possibilité de polariser les spins dans un champ élevé (9 000 gauss) puis d'observer en revenant rapidement à $H_0 = 3 000$ gauss un signal beaucoup plus important, qui correspond au facteur de Boltzmann du champ élevé.

d) La possibilité d'effectuer un passage rapide sur une raie et donc de placer, pendant un temps de l'ordre de T_1 , les spins dans un état de « température négative ».

2) Caractère complexe de la relaxation spin-réseau.

a) Nous avons observé que les deux raies extrêmes étaient systématiquement plus petites que les deux raies médianes. Cette différence a été attribuée à une croissance plus lente des raies extrêmes par suite d'un mécanisme de relaxation différent de celui des raies médianes. Nous avons effectivement observé l'égalité des quatre raies lorsque l'échantillon restait suffisamment longtemps (40 min) dans le champ H_0 .

b) Nous avons envisagé l'existence simultanée de deux mécanismes de relaxation ⁽¹⁰⁾ (considérés indépendamment par BLOEMBERGEN, SOLOMON et BARDEEN, SLICHTER et PINES ⁽¹⁶⁾).

— Le renversement du spin électronique sans changement du spin nucléaire (relaxation électronique habituelle).

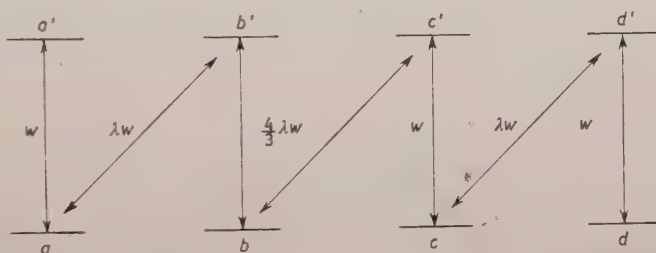


Fig. 1. — Schéma de relaxation spin-réseau dans l'arsenic.

— Le renversement simultanée en sens inverse du spin électronique et du spin nucléaire (flip-flop) par suite de la modulation de l'interaction hyperfine $\mathbf{AI} \cdot \mathbf{S}$ par les vibrations du réseau cristallin (Fig. 1). Soit W la probabilité par unité de temps des transitions $a'a$, $b'b$, $c'c$, $d'd$. Les probabilités des transitions ab' , bc' , cd' sont respectivement λW , $\frac{4}{3}\lambda W$, λW où λ est un coefficient sans dimension qui dépend de l'importance respective des deux mécanismes de relaxation.

c) Si l'échantillon après un séjour prolongé dans un champ nul est placé dans le champ H_0 pendant un temps t tel que $Wt \ll 1$ on montre facilement que le rapport raies extrêmes sur raies médianes :

$$(8) \quad \frac{E(t)}{\bar{M}(t)} \simeq \frac{6 + 3\lambda}{6 + 7\lambda}.$$

Expérimentalement :

$$\lim_{t \rightarrow 0} \frac{E(t)}{\bar{M}(t)} \simeq 0.6 \quad \text{d'où } \lambda \simeq 2.$$

⁽¹⁶⁾ J. BARDEEN, C. SLICHTER et D. PINES : à paraître.

d) Pour confirmer cette hypothèse nous avons observé la croissance d'une raie extrême dans les conditions suivantes:

— L'échantillon après être resté longtemps dans un champ nul est placé pendant un temps t ($Wt \ll 1$) dans le champ H_0 . Soit $E_\alpha(t)$ la hauteur de la première raie.

— L'échantillon étant resté très longtemps dans le champ H_0 on sature la première raie puis on observe sa valeur $E_\beta(t)$, t secondes plus tard. On montre que

$$(9) \quad \frac{E_\alpha(t)}{E_\beta(t)} = \frac{4 + 2\lambda}{4 + \lambda}.$$

Cette expérience conduit aussi à une valeur de λ de l'ordre de 2.

e) Pour déterminer W , on compare la taille de la première raie après un séjour t bref dans le champ H_0 , avec sa taille définitive atteinte après un séjour très long dans H_0 .

On montre facilement que:

$$(10) \quad \frac{E(t)}{E(\infty)} \simeq (2 + \lambda)Wt.$$

L'expérience donne $1/W \simeq 20$ min, ce qui justifie de prendre dans les expériences précédentes $t = 2$ min.

f) Une étude expérimentale sommaire montre que le temps de relaxation ne dépend pas de H_0 d'une façon critique. En particulier entre 1000 et 10 000 gauss une variation de W en H_0^2 est exclue. Par contre la variation avec la température est très rapide: les ordres de grandeur des temps de relaxation sont: 1 s vers 8 °K, 1 min à 4 °K.

La nécessité de comparer les lectures de l'appareil faites à des intervalles de temps importants est une sérieuse difficulté. Nous avons pu éliminer l'influence des variations de gain de l'appareil en utilisant un signal de résonance de référence (D.P.P.H.). Toutefois la variations très rapide des temps de relaxation spin-réseau avec la température exigerait pour une étude plus quantitative un contrôle très rigoureux de la température. Par ailleurs il est probable que des échantillons de différentes origines contenant un nombre d'impuretés différent présenteraient des temps de relaxation différents.

3) *Les lignes satellites* correspondant au cas où deux atomes d'impuretés sont particulièrement rapprochés, on peut penser que la modulation de leur interaction d'échange par les vibrations du réseau entraîne pour ces lignes un temps de relaxation plus court que pour les lignes principales. L'expérience suivante confirme cette vue. L'échantillon ayant la polarisation d'équilibre dans un champ de 3 000 gauss, on porte celui-ci à 9 000 gauss pendant 2 à

3 minutes. Après retour à 3 000 gauss on observe une valeur accrue (un facteur 1.5 environ) pour le rapport ligne satellite sur ligne principale.

Une étude théorique détaillée des mécanismes de relaxation a été faite par BARDEEN, SLICHTER et PINES ⁽¹⁶⁾. Les ordres de grandeur théoriques obtenus pour le temps de relaxation « en biais » ($1/\lambda W$) (dans la notation de BSP $W=1/T_s$, $\lambda W=1/T_x$) sont en accord raisonnable avec les valeurs expérimentales. Par contre les valeurs théoriques qu'ils trouvent pour T_s (renversement du spin électronique seul) dépassent par plusieurs ordres de grandeur les valeurs expérimentales pour tous les mécanismes qu'ils ont envisagés.

De plus leur théorie prévoit pour la variation des temps de relaxation, avec le champ appliqué et la température une loi en $H^{-2}T^{-1}$, en désaccord avec l'expérience. Il est possible que d'autres impuretés que les donneurs considérés jouent un rôle dans la relaxation spin-réseau.

3. - Polarisation nucléaire.

Plusieurs méthodes de polarisation nucléaire basées, sur la longueur des temps de relaxation ont été proposées. Parmi celles-ci certaines sont indépendante de l'existence de T_x ⁽⁵⁾ tandis que d'autres reposent sur l'hypothèse $T_x \ll T_s$ ⁽¹⁶⁾.

Une méthode de chaque type a été envisagée par nous ^(10,12).

a) Méthode indépendante de l'existence du mécanisme de relaxation « en biais ».

Considérons pour fixer les idées le cas du phosphore $I=\frac{1}{2}$ (Fig. 2).

Dans un champ élevé le spin nucléaire et le spin électronique sont complètement découplés et les fonctions d'onde des quatre états d'énergie de l'atome de phosphore sont respectivement: $a' = |+, +\rangle$, $b' = |\frac{+}{-}, -\rangle$, $b = |-, -\rangle$, $a = |-, +\rangle$, où le premier signe correspond à la valeur $\pm\frac{1}{2}$ pour S_z et le second à $\pm\frac{1}{2}$ pour I_z . Lorsque H décroît et tend vers zéro ces états tendent d'une façon continue vers les quatre états: $\bar{a}' = |+, +\rangle$, $\bar{b}' = (1/\sqrt{2})\{|+-\rangle + +|-+\rangle\}$, $\bar{b} = |-, -\rangle$, $\bar{a} = (1/\sqrt{2})\{|+-\rangle - +|-+\rangle\}$.

Soit H_M la valeur maximum du champ et T la température d'équilibre

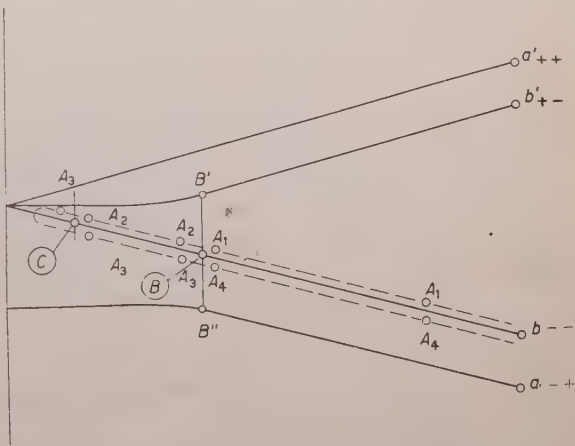


Fig. 2. - Niveaux d'énergie et évolution des populations lorsque l'on fait varier le champ magnétique.

de l'échantillon. Si $\beta H_M/kT \gg 1$, $\Delta H/kT \ll 1$, les populations des états a' et b' sont négligeables, celles de a et b sont toutes les deux $\frac{1}{2}$ et la polarisation nucléaire $P_1 = \langle I_z \rangle / I$ est négligeable. Si l'on réduit adiabatiquement le champ jusqu'à une valeur très faible H_m en un temps court par rapport au temps de relaxation spin-réseau T_1 on obtient des populations nulles pour \bar{a}' et \bar{b}' et $\frac{1}{2}$ pour \bar{a} et \bar{b} . Mais l'état \bar{a} ne fournit aucune contribution à $\langle I_z \rangle$ et l'on a donc $P_1 = -\frac{1}{2}$. Cette polarisation nucléaire décroît vers zéro avec une constante de l'ordre du temps de relaxation T_1 dans le champ H_m (qui peut être différent de T_1 dans H_M).

Ces résultats se généralisent immédiatement au cas où $kT/\beta H_M$ n'est pas très petit et où $I > \frac{1}{2}$.

On montre que la polarisation maximum P_1 est donnée dans ce cas par

$$(11) \quad P_1 = \frac{\mp 1}{2I + 1} \operatorname{tgh} \left(\frac{\beta H_M}{kT} \right),$$

(suivant le signe de A , constante de structure hyperfine).

On peut ainsi définir le coefficient d'alignement:

$$P_2 = \frac{\langle I_z^2 \rangle - \frac{1}{3}I(I+1)}{\frac{1}{3}I(I+1)},$$

et l'on montre que

$$(12) \quad P_2 = \frac{2I-1}{(I+1)(2I+1)} \operatorname{tgh} \left(\frac{\beta H_M}{kT} \right).$$

Les formules (11) et (12) reposent essentiellement sur l'hypothèse que le passage du champ fort H_M au champ faible H_m peut se faire adiabatiquement au sens d'Ehrenfest, c'est-à-dire que les populations des différents niveaux demeurent constantes. Nous verrons plus loin comment l'existence des interactions spin-spin modifie cette hypothèse. Si des isotopes radioactifs sont utilisés, ces polarisations sont décelées par l'anisotropie des rayonnements émis. Les structures hyperfines (et donc, par comparaison avec les isotopes stables, les moments magnétiques) de ces isotopes peuvent être mesurées en induisant par un champ magnétique de radiofréquence des transitions entre des niveaux d'énergie du système dans le champ H_m , le passage par la résonance étant détecté par un changement dans l'anisotropie du rayonnement émis. Cette dernière méthode avait été proposée par BLOEMBERGEN et TEMMER⁽¹⁷⁾ pour des noyaux radioactifs orientés par la méthode de BLEANEY ou

(17) N. BLOEMBERGEN et G. TEMMER: *Phys. Rev.*, **89**, 883 (1953).

GORTER et avait en fait échoué, probablement par suite de l'échauffement non résonant de l'échantillon par le champ HF. Cet échauffement ne devrait pas se produire dans le cas présent, le réseau restant en contact thermique avec l'hélium liquide.

Un premier essai infructueux de cette méthode a été fait à l'Université de Harvard (communication privée de R. V. POUND).

Nous verrons un peu plus loin une raison possible de cet échec.

b) A cause du mécanisme de relaxation en biais les noyaux d'un échantillon d'arsenic placé dans un champ magnétique présentent une polarisation spontanée $P_1 = I_z I$ qui part de zéro, passe par un maximum et retombe à zéro.

Avec $\lambda = 20$, $W = 20$ minutes on trouve que $P_{1\max} \simeq 0.15 \text{ tgh} (\beta H_M / kT)$ est atteint au bout de 10 minutes.

Pour $t = 1$ heure, P_1 est encore 0.1 tgh $(\beta H_M / kT)$. Il faut remarquer que le coefficient d'alignement

$$P_2 = \frac{3I_z^2 - I(I+1)}{I(I+1)},$$

est constamment nul, ce qui rend ce phénomène impropre à l'observation de l'anisotropie du rayonnement γ des noyaux radioactifs. (Ce point semble avoir échappé à BSP qui ont indépendamment proposé cette méthode de polarisation). Toutefois depuis la découverte de la non-conservation de la parité cette méthode paraît admirablement adaptée à l'étude de l'anisotropie du rayonnement.

On remarquera que ni l'une ni l'autre de ces méthodes ne nécessite de champ de radiofréquence et n'impose aucune condition sur l'homogénéité du champ H_0 .

4. - Interactions spin-spin.

Nous avons dans une publication antérieure ⁽¹¹⁾ supposé que le passage par un champ nul avait pour effet d'égaliser entre elles les populations des deux sous-niveaux $F=2$ et $F=1$ des atomes d'arsenic et nous avons expliqué ainsi la réduction considérable de la raie correspondant à la transition (4) Fig. 3, après le passage dans un champ nul.

Ce raisonnement est incorrect.

Si l'on considère un système de spins possédant dans un champ H_0 des niveaux Zeeman équidistants et si les populations de ces niveaux forment une distribution de Boltzmann, l'expérience montre que le passage de ce système par un champ nul, (ou du moins beaucoup plus faible que le champ local)

est une opération réversible (à condition bien entendu que la durée en soit beaucoup plus courte que le temps de relaxation spin-réseau T_1).

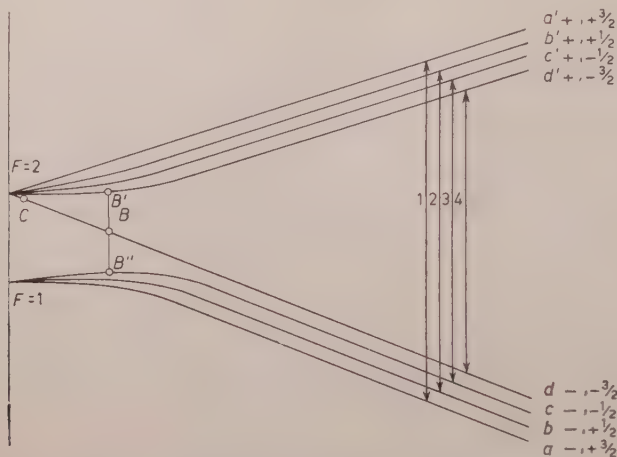


Fig. 3. — Niveaux d'énergie de l'arsenic.

Cette réversibilité qui est liée à l'existence d'une température de spins avait été démontrée par POUND dans une expérience de résonance nucléaire sur LiF⁽¹⁸⁾ et étudiée récemment en détail par ABRAGAM et PROCTOR⁽¹⁹⁾. En fait, comme nous l'avons du reste signalé dans (11), avant d'arriver dans un champ nul les spins des atomes d'arsenic pénètrent dans la région où les sous-niveaux de $F=2$ et $F=1$ deviennent équidistants (d'une façon précise où l'écart par rapport à l'équidistance est inférieur à la largeur produite par l'interaction entre les spins) et dans cette région l'interaction spin-spin établit entre les populations des 5 sous-niveaux $F=2$ une distribution de Boltzmann en progression géométrique. Cette transition qui est irréversible se produit dans un champ faible mais ensuite le passage par un champ nul est lui réversible.

D'autre part nous n'avions pas pensé à un autre effet très important qui nous a été signalé par Monsieur P. W. ANDERSON et qui est le passage par la valeur critique H_0 où le niveau B , $M_F = -(I + \frac{1}{2})$, se trouve à égale distance des deux niveaux B' et B'' où $m_F = -(I - \frac{1}{2})$. Il ressort des équations de Breit-Rabi que ceci se produit pour $H_1 = \Delta H$. Au moment de ce passage l'interaction spin-spin établit pour ces trois niveaux des populations en progression géométrique.

(18) R. V. POUND: *Phys. Rev.*, **79**, 685 (1950).

(19) A. ABRAGAM et W. PROCTOR: *Phys. Rev.*, à paraître.

Examinons d'abord le cas du phosphore ($I = \frac{1}{2}$) qui est plus simple que celui de l'arsenic (Fig. 2).

Partons d'un point A_1 dans un champ élevé où les quatre populations a, b, a', b' ont des valeurs de Boltzmann a_1, b_1, a'_1, b'_1 correspondant à la structure des niveaux en ce point, c'est-à-dire que a_1 et b_1 sont pratiquement égaux entre eux ainsi que a'_1 et b'_1 . Ces populations restent inchangées jusqu'à l'arrivée au point B . Au passage par B les trois populations b', b, a prennent de nouvelles valeurs b'_2, b_2, a_2 déterminées par la conservation du nombre de spins et de l'énergie et l'établissement d'une température de spin entre ces trois niveaux

$$(13) \quad b'_2 a_2 = b_2^2, \quad b'_2 + a_2 + b_2 = b'_1 + a_1 + b_1, \quad b'_2 - a_2 = b'_1 - a_1,$$

a' n'est pas changé par ce passage, $a'_2 = a'_1$. Ces populations sont symbolisées par le point A_2 sur la figure. Si à ce moment on revenait aux champs élevés on reviendrait avec les populations A_2 . Si, au contraire, on continue vers les champs bas, les populations demeurent inchangées jusqu'au passage par C où a reste inchangé mais a', b', b sont modifiées avec les relations

$$(14) \quad a'_3 b_3 = b_3'^2, \quad a'_3 + b'_3 + b_3 = a'_2 + b'_2 + b_2, \quad a'_3 - b_3 = a'_2 - b_2,$$

a garde sa valeur $a_3 = a_2$.

Il ne doit plus y avoir d'autres changements de populations lorsqu'on passe par la valeur zéro ni lorsqu'au retour on repasse par le point C .

Un nouveau changement se reproduit en B avec des populations A_4 données par:

$$(15) \quad b'_4 a_4 = b_4^2, \quad b'_4 + b_4 + a_4 = b'_3 + b_3 + a_3, \quad b'_4 - a_4 = b'_3 - a_3, \quad a'_4 = a'_3.$$

On garde ensuite ces populations jusqu'au retour dans le champ élevé où l'on peut de nouveau observer la résonance.

Les différentes populations se calculent facilement lorsque la température est suffisamment haute et donc toutes les populations suffisamment voisines pour que l'on puisse remplacer les progressions géométriques par des progressions arithmétiques. C'est le cas à 3 000 gauss et 2 °K.

Ecrivons pour simplifier, les populations sous la forme

$$(16) \quad P_i = \frac{1}{2(2I+1)} (1 + \alpha_i \varepsilon).$$

Les valeurs des coefficients α_i sont tabulées ci-dessous :

	A_1	A_2	A_3	A_4
a'	-1	-1	-10/9	-30/27
b'	-1	-2/3	-4/9	-14/27
b	1	1/3	2/9	10/27
a	1	4/3	12/9	34/27

La vérification expérimentale peut se faire comme suit. Au départ les deux raies ont des hauteurs proportionnelles à $(a_1 - a'_1)$ et $(b_1 - b'_1)$, c'est-à-dire à $\varepsilon/2$. Après le passage par le point B (sans descendre jusqu'en C) ces raies devraient être comme

$$a_2 - a'_2 = 7\varepsilon/12 \quad \text{et} \quad b_2 - b'_2 = 3\varepsilon/12.$$

Leur rapport devrait donc être $7/3$.

De même si l'on descend au-delà de C , après retour dans un champ élevé, les raies proportionnelles à $a_4 - a'_4$ et $b_4 - b'_4$ devraient être $16\varepsilon/27$ et $6\varepsilon/27$, c'est-à-dire dans un rapport $8/3$.

Bien entendu les considérations précédentes présupposent que toutes les opérations se font en un temps court par rapport à T_1 .

Dans l'échantillon de phosphore sur lequel nous avons travaillé cette condition n'était pas réalisée, ce qui rendait difficile l'interprétation quantitative des résultats. Nous avons toutefois constaté nettement une diminution par un facteur de l'ordre de 2 de la raie bb' par rapport à la raie aa' , lorsque l'on descendait le champ jusqu'à 30 gauss (c'est-à-dire au dessous de 42 gauss, qui est la valeur du champ H_1 correspondant au point B), alors que les deux raies demeuraient égales si l'on descendait seulement jusqu'à 60 gauss.

Les corrections dues à T_1 étaient trop importantes pour qu'une différence significative dans le rapport des raies apparaisse entre le cas où l'on descend jusqu'à 30 gauss (passage par B) et celui où on passe par zéro (passage par B et C).

Il semble que Monsieur G. FEHER (communication privée) ait pu obtenir des résultats plus quantitatifs que les nôtres en opérant à température plus basse (1,25 °K au lieu de 2 °K) d'où un temps de relaxation T_1 plus long.

Un renseignement théorique important sur la nature des couplages entre les spins électroniques est fourni par le fait qu'en B il se passe des transitions. Lorsqu'on passe par le point B , deux spins situés dans les deux état B' et B'' qui correspondent tous deux à $m_F = 0$ peuvent venir tous deux dans l'état $m_F = -1$ avec conservation de l'énergie. Une telle interaction ne conserve

done pas le M_F total des deux atomes. Ce n'est donc pas une interaction d'échange scalaire du type $J \mathbf{s}_1 \cdot \mathbf{s}_2$, ce qui nous permet d'affirmer que l'effet des interactions dipôle-dipôle n'est pas négligeable.

Les transitions au point C, elles, pourraient aussi bien résulter d'interactions dipolaires que d'interactions d'échange.

Finalement il peut être intéressant de calculer les populations dans le cas de H_0 suffisamment élevé et T suffisamment bas pour que le remplacement des progressions géométriques par des progressions arithmétiques ne soit pas justifié. Nous avons fait le calcul dans le cas où :

$$\begin{aligned} a_1 = b_1 = \frac{1}{2} & \quad \text{ce qui est une bonne approximation pour} \\ a'_1 = b'_1 = 0 & \quad T = 1.25^\circ \text{K}, H_0 = 30\,000 \text{ gauss.} \end{aligned}$$

On trouve alors :

$$\begin{array}{lll} a'_2 = 0 & a'_3 = 0.029 & a'_4 = 0.020 \\ b'_2 = 0.116 & b'_3 = 0.076 & b'_4 = 0.096 \\ b_2 = 0.267 & b_3 = 0.287 & b_4 = 0.247 \\ a_2 = 0.617 & a_3 = 0.617 & a_4 = 0.637 \end{array}$$

A l'aide de ces populations on peut calculer la polarisation obtenue en descendant dans un champ très faible, c'est-à-dire en A_3 après un passage par B et par C .

On trouve facilement :

$$P_{A_3} = -0.267.$$

Ceci est à comparer à la valeur -0.5 donnée par la formule (11) qui ne tient pas compte des transitions qui se produisent au point B . On calcule de même la polarisation que l'on obtiendrait si après être descendu jusqu'à un champ très faible, c'est-à-dire après passage par C , on remontait en champ élevé.

On trouve $P_{A_4} = +0.314$ au lieu de la valeur $1/(2I+2) = \frac{1}{3}$ donnée dans la référence ⁽¹¹⁾.

Le cas de l'arsenic, quoique beaucoup plus complexe, se traite de la même façon.

Nous nous limiterons, pour simplifier, au cas où l'on peut remplacer les progressions géométriques par les progressions arithmétiques. Les quantités α_i définies précédemment sont :

	A_1	A_2	$A_3(1/105)$	$A_4(1/105)$
a'	— 1	— 1	— 112	— 112
b'	— 1	— 6/7	— 92	— 100
c'	— 1	— 6/7	— 72	— 80
d'	— 1	— 6/7	— 52	— 60
d	1	1/7	— 32	16
c	1	8/7	100	92
b	1	8/7	120	112
a	1	8/7	140	132

On en déduit que les quatre raies de résonance dont les hauteurs initiales étaient comme $\varepsilon/4$, deviennent après passage par B comme les nombres

$$(20) \quad (15, 14, 14, 7) \frac{\varepsilon}{56},$$

et après passage par B et C comme

$$(21) \quad (61, 53, 43, 19) \frac{\varepsilon}{210}.$$

La valeur du champ critique au point B étant $H_1 = \Delta H \simeq 75$ gauss, en descendant à 100 gauss environ, le retour en champ élevé doit être réversible, en descendant à 50 gauss les rapports des raies doivent être donnés par (20) et en passant par un champ nul ils sont donnés par (21).

Ce sont bien là approximativement les résultats que nous avons obtenus expérimentalement. Mais dans la référence ⁽¹¹⁾ nous avons faussement interprété la réduction considérable de la 4^e raie, par l'égalisation dans un champ nul des populations des sous-niveaux $F=2$.

La longueur des temps de relaxation spin-réseau dans l'arsenic est telle que les corrections dues à la valeur finie de T_1 pendant que l'on fait varier le champ sont faibles. Par contre les résultats (19) sont établis en supposant qu'on part d'une distribution d'équilibre des populations, ce qui étant donné, a longueur de T_1 n'était sans doute pas réalisé dans toutes nos expériences.

Ceci rend incertaine une confrontation précise des résultats expérimentaux avec les prédictions (20) et (21).

5. — Remarque sur les méthodes de polarisation nucléaire.

Dans ce qui précède nous avons implicitement supposé que toutes les impuretés paramagnétiques en interaction étaient identiques. En fait, si l'on cherche à polariser un isotope radioactif dont la concentration dans le cristal

est extrêmement faible, l'atome paramagnétique de cet isotope aura comme voisins les atomes de l'isotope normal qui auront une structure hyperfine différente et donc des fréquences de résonance différentes.

Si sur un graphique on porte en abscisses le champ appliqué H_0 et en ordonnées les fréquences de résonance des deux espèces d'atomes, des changements de populations pourront intervenir aux intersections d'une courbe de l'isotope radioactif avec une courbe de l'isotope normal.

On ne peut tracer ce graphique pour l'isotope radioactif puisqu'on ne connaît pas son moment magnétique nucléaire mais on se convainc aisément que ces points d'intersection sont nombreux et que le passage de H_M à H_m pourrait conduire à une polarisation bien plus faible que celle donnée par les formules (11) et (12).

On pourrait tourner cette difficulté en désaimantant de H_M à H_m suffisamment vite pour que les transitions en question n'aient pas le temps de se produire. Avec une concentration de 10^{17} atomes par cm^3 , le champ moyen δH produit par un atome à l'emplacement d'un plus proche voisin est de l'ordre de 10^{-3} gauss et la fréquence angulaire $\delta\omega = \gamma\delta H$ correspondante de l'ordre de $2 \cdot 10^4$.

La condition pour qu'une transition n'ait pas le temps de se produire pendant qu'on passe par un point d'intersection, s'écrit :

$$\frac{dH_0}{dt} \gg \gamma(\delta H)^2 \simeq 20 \text{ G s}^{-1}.$$

On voit que cette condition n'est pas très critique. Toutes ces difficultés ne sont évidemment associées qu'avec la méthode de polarisation a). La méthode b), où le champ garde une valeur fixe en est exempté.

* * *

Nous voudrions pour terminer, remercier Monsieur GEORGE FEHER et Monsieur PINES qui nous ont aimablement fait parvenir les textes de leurs articles avant publication. Nous avons tiré grand profit de discussions avec MM. ANDERSON, FEHER, POUND, PIPKIN, MESSIAH.

Enfin nous voudrions remercier encore Monsieur HONIG sans qui ces recherches n'auraient sans doute ni commencé, ni abouti.

INTERVENTI E DISCUSSIONI

— C. J. GORTER:

Quoique les temps de relaxation dans les sels dilués de manganèse, et d'autres ions paramagnétiques, ne sont que de l'ordre d'une seconde au plus on pourrait essayer de les aligner également par la méthode Abragam.

Serait la longueur enorme des temps de relaxation des atomes introduits dans le Silicium due à l'absence de toute contribution orbitale au moment magnétique?

— A. ABRAGAM:

La longueur des temps de relaxation des atomes paramagnétiques introduits comme impuretés dans le Silicium, est effectivement due à l'absence de contribution orbitale au moment magnétique.

Une étude détaillée de ce problème par BARDEEN, PINES et SLICHTER vient de paraître dans la *Physical Review* du 1^{er} Mai.

Nuclear Magnetic Relaxation in Mixtures of Liquids.

L. GIULOTTO, G. LANZI and L. TOSCA

Istituto di Fisica dell'Università - Pavia

In a letter which appeared in *Journ. Chem. Phys.* we have shown that it is possible to reveal the formation of molecular clusters in liquids by means of measurements of nuclear thermal relaxation times. In fact, the theory of Purcell, Bloembergen and Pound gives a dependence of T_1 on the volume of the molecule: actually a decrease can be predicted for T_1 when molecules associate together to give clusters. The published results refer to measurements on solutions of phenol and chlorobenzene in carbon tetrachloride and they substantially support this view.

Recently we have carried out some more measurements of T_1 on mixtures of liquids whereby the formation of molecular complexes can be expected to occur. These measurements have been performed on: 1) mixtures of one proton-containing liquid with a liquid non containing protons; 2) mixtures of two liquids both proton-containing.

Referring to the first group of mixtures we can show the type of results that we obtain from solutions of ethyl alcohol with carbon tetrachloride. The behaviour of $T_1\eta$ is somewhat similar to the one already observed for phenol in carbon tetrachloride and shows rather clearly the effect of complex formation.

In the case of mixtures of water with alcohols the behaviour of the absorption coefficient for ultrasounds seems to indicate that association phenomena are present. However, in the case of ethyl alcohol with water, plotting $T_1\eta$ versus concentration does not give any clear indication on molecular clustering.

Magnetic After Effect and Internal Friction at High Temperatures in Iron and some Iron Alloys.

A. FERRO (*) and G. MONTALENTI

Centro Studi Elettrofisica, Istituto Elettrotecnico Nazionale «G. Ferraris» - Torino

A short account is given of some work on magnetic after effects that occur in iron and iron alloys at high temperatures.

To obtain a better understanding of the origin of these effects comparison is done in the same range of temperatures with elastic internal friction.

In fact apart of the well known magnetic after effects and damping phenomena due to diffusion of carbon and nitrogen in αFe , already studied by SNOEK (1), NÉEL (2) and others, some other new effects of this type can be found. As a matter of fact in his theory of magnetic relaxation NÉEL had already pointed out that, for instance, also vacant lattice points could originate this type of phenomena.

As those due to C or N in αFe also all the effects observed in the present work are controlled by some diffusion process in the lattice and thus the relaxation time depends on temperature as usually with a law of the type:

$$\tau = \tau_0 \exp \left[\frac{Q}{RT} \right],$$

where τ_0 and Q are respectively the relaxation time for infinite temperature and Q is the activation energy. These two quantities are characteristic of the diffusion mechanism involved.

Magnetic after effect is measured, as usually, as the decrease in course

(*) Fiat Laboratory, Turin.

(1) J. SNOEK: *Physica*, **5**, 633 (1938) and **6**, 161, 321, 591, 797 (1939).

(2) L. NÉEL: *Journ. Phys. et Rad.*, **12**, 339 (1951).

of time of the initial permeability after demagnetizing. Measures of permeability are carried on in alternate current at 30 Hz with a field of 0.012 Oe; the decrease of permeability is observed for 15 min. Internal friction is measured with a torsion pendulum at a frequency of about 1 Hz.

The intensity of both the magnetic and mechanical relaxation are determined as a function of temperature and compared and the characteristic relaxation times τ_0 and the energy of activation of the phenomena are evaluated.

In iron for a relaxation time of 3 min magnetic after effects begin to be observed above 350 °C with a maximum at 400° of the order of 10% and an activation energy of about 80000 cal mole. This effect corresponds to a strong mechanical after effect that occurs in the same range of temperature, but it is interesting to observe that for still higher temperatures, while the mechanical internal friction increases continuously the magnetic after effect tends to disappear. Thus at very high temperatures, but still well under the Curie point, there are some elastic relaxation processes that do not produce any magnetic after effect.

Similar results in the same temperature range are observed also in other alloys as one with 45% Ni and seem to be quite general.

Only in pure Nickel no high temperature magnetic relaxation is observed probably as the Curie point is reached at too low temperature.

As to the origin of the phenomena it may so far only be observed that these effects are produced in a temperature region where several types of diffusion processes such as diffusion of vacancies, self diffusion, diffusion of dislocations, grain boundary relaxation, may be supposed to become possible.

On the contrary a very strong magnetic after effect of the order of 80% is found in 4% Silicon iron at about 400° degrees, with an activation energy of 47000 cal/mole and a τ_0 value of about 10^{-14} , in correspondence of a small internal friction peak with the same time and energy constants.

This effect seems to be quite peculiar of this alloy and seems to have characteristics very similar to those of the effects due to an interstitial diffusion mechanism.

A more complete description of these results will be presented at the Congress of the Società Italiana di Fisica in Turin.

Röntgenographic and Paramagnetic Resonance Experiments with (Gd-La)AlO₃ Mixed Crystals.

H. GRÄNICHER and K. A. MÜLLER

Physikalisches Institut der E.T.H. - Zürich

Compounds of the general formula ABO₃ crystallize in the cubic Perovskite structure over a considerable range of ionic radii of the cations A and B. Actually in most cases the structure is slightly deformed to pseudocubic symmetry in order to minimize the effect of the misfit of ionic size and to allow partially covalent bonds. Many substances of the Perovskite type structure possess remarkable dielectric properties, i.e. they show paraelectric, ferro- and antiferroelectric behavior. In a research on structural and dielectric properties of Perovskite compounds a number of rare-earth meta-aluminates such as LaAlO₃, CeAlO₃, PrAlO₃, NdAlO₃, EuAlO₃, GdAlO₃ and scandates such as LaScO₃ and NdScO₃ have been prepared and their structures examined by X-rays.

Most of the aluminates studied show a deformation to trigonal symmetry, as if the elementary cube had been compressed along the cube diagonal. The deviation from the ideal cubic lattice can be analyzed by the line splitting of back-reflexion lines of Debye-Scherrer patterns. A measure for this deviation is the value of $\Delta\beta$, since it is defined by $\beta = 90^\circ - \Delta\beta$, where β is the rhombohedral angle. The following results were obtained for LaAlO₃:

Temperature °K	Lattice constant kX	$-\Delta\beta$
294°	3.7827 ± 0.0002	$5.25' \pm 0.1'$
198°	3.7801 ± 0.0004	$6.0' \pm 0.1'$
83°	3.7781 ± 0.0002	$7.3' \pm 0.1'$

The study of the paramagnetic properties of such substances, which can be magnetically diluted by forming mixed crystals with the diamagnetic LaAlO₃,

will give interesting information on the changes of the crystalline field and of the bond character. We therefore prepared mixed crystals of LaAlO_3 with concentrations of 10^{-1} and 10^{-2} atomic percent of GdAlO_3 and other rare-earth aluminates in ceramic, polycrystalline form.

The paramagnetic resonance absorption of $(\text{Gd-La})\text{AlO}_3$ samples was studied with a frequency of 9.4 kHz at temperatures of 295 °K, 195 °K, 83 °K and 4.2 °K. As might be expected

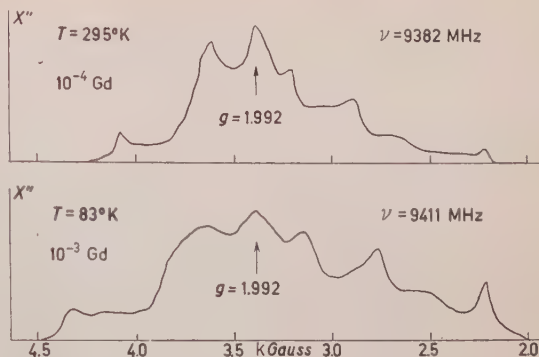


Fig. 1. — Resonance absorption lines of Gd^{3+} for 295 °K and 83 °K.

(see Fig. 1). The central peak is the highest one. It lies at $g = 1.992 \pm 0.002$ and is not shifted by temperature changes. The other six peaks are almost symmetrically grouped around the central peak. They are split over a range of about ± 1000 gauss, which corresponds to a range of g -values between 1.55 and 2.7. The lines shift markedly away from the central line with decreasing temperature, as can be seen from the upper part of Fig. 2. Some additional weak lines were observed at lower fields, but showed no shift with temperature and could not be interpreted as second order transitions ($\Delta m_s = \pm 2$).

The lines are relatively broad and two of the lines are not well resolved at all temperatures. Using published data (1) for the nuclear moments of ^{155}Gd and ^{157}Gd the hyperfine splitting was estimated to be about 12 gauss and is therefore of no importance.

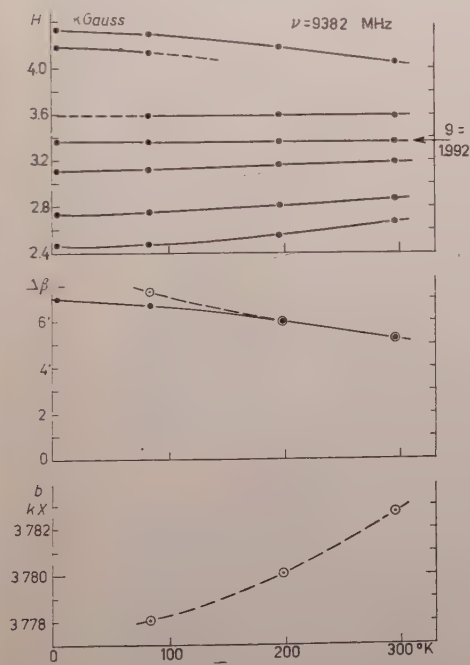


Fig. 2. — Paramagnetic resonance data (—) and röntgenographic data (—○—○—) as a function of temperature.

(1) D. R. SPECK: *Phys. Rev.*, **101**, 1725 (1956).

A change of the Gd concentration by a factor of 10 did not alter the line-width appreciably, which indicates that the dipole-dipole interaction is sufficiently reduced by dilution. The large linewidth has to be ascribed to configurational broadening due to the random orientation of crystallites in the ceramic.

The ground-state of Gd^{3+} is the eight-fold degenerate ${}^8S_{7/2}$ and one would in first order expect no interaction with the crystalline field. However a higher order interaction between the crystalline field and the spin-orbit interaction exists and is responsible for the observed splitting. The case of Gd^{3+} is similar to Mn^{2+} and Fe^{3+} , which have been discussed by Prof. M. H. L. PRYCE in his lecture. The spherical symmetric wave-function of the S -state becomes deformed due to an admixture of a higher state, presumably ${}^6P_{5/2}$.

Low ⁽²⁾ studied the paramagnetic resonance of Eu^{2+} , which has the same electronic configuration as Gd^{3+} , in a crystal of cubic symmetry and observed three energy levels. According to his results the splitting in a cubic field is small ($50 \div 100$ gauss). In comparison our observed splitting in $(\text{Gd-La})\text{AlO}_3$ is by a factor of 10 to 20 larger and is therefore due mainly to the splitting in the *trigonal* field. This interpretation also accounts for the line shift as a function of temperature. The change of the lattice constant with decreasing temperature only affects the cubic field splitting, which is too small to be detected. But since the trigonal field splitting is very large, it is clear that the increasing trigonality with lowering temperature considerably increases the line splitting. Therefore a roughly linear correlation exists between $-\Delta\beta$ and the mean relative line displacement, which was normalized to fit the room temperature value of $-\Delta\beta$ (Fig. 2, middle part).

Further experiments on mixed crystals with other rare-earth elements and other Perovskite host crystals, partly in the form of single crystals, are in progress. Very recently the orientational dependence of three paramagnetic resonance lines (presumably due to Fe^{3+} or Cr^{3+}) has been investigated with a single crystal of SrTiO_3 at room temperatures; the line width in this case being only a few gauss.

Finally we emphasize that double oxides with small concentrations of rare-earth elements might prove very useful for cooling by adiabatic demagnetization. Compared to the widely used double salts, which contain water of crystallization (e.g. alums), double oxides have the following advantages:

- a) They are mechanically rugged materials, which can be prepared in any desired shape by ceramic processes.
- b) They are insoluble in water and most other reagents except strong acids.

(2) W. Low: *Phys. Rev.*, **101**, 1827 (1956).

c) Since they contain no water of crystallization, they will give more reproducible results, smaller values of H_{crit} and thus enable to reach lower temperatures.

d) According to their higher elastic stiffness, they possess higher Debye-temperatures and have therefore a smaller lattice specific heat.

The most promising material seems to be CeO_2 crystals of cubic Fluorite structure containing small concentrations of Ce_2O_3 or PrO_2 , since neither ^{140}Ce nor ^{16}O possess nuclear moments.

The Electric Analogue to Antiferromagnetism: Antiferroelectricity.

H. GRÄNICHNER

Physikalisches Institut der E.T.H. - Zürich

Prof. GORTER has shown in his lecture that an antiferromagnetic state of a paramagnetic crystal is defined by an antiparallel arrangement of the electron spins. The magnetic superstructure observable by neutron diffraction and the splitting of nuclear magnetic resonance lines (proton resonance in $\text{CuCl}_2 \cdot 2\text{H}_2\text{O}$ observed by POULIS) provide direct evidence for the antiferromagnetic state. In contrast in the electric analogue, in antiferroelectricity difficulties arise which will be discussed in the following.

KITTEL ⁽¹⁾ introduced the notion of antiferroelectricity in 1951 and defined it as a state with spontaneous polarized lines of ions, neighbouring lines being polarized in antiparallel direction. He showed by a thermodynamical treatment, which was later refined ⁽²⁾, that with lowering temperature a drop of the dielectric constant should occur at the transition point. If the dielectric constant above the transition point has not a high value, the anomaly will be small. This might be the reason, why antiferroelectric crystals had not been observed before.

One knows that in ferroelectricity the spontaneous polarization is mainly due to ionic shifts. (The question whether ionic shifts are the cause or the consequence of ferroelectricity needs not be discussed in this connection). Therefore for the antiferroelectric state antiparallel ionic shifts must be expected. In special cases the shift will be compatible with the space-group requirements of the high-temperature phase, provided that the positions of the ions involved have free parameters. But in general some symmetry elements are lost and the space-group will change. In crystals having only a

⁽¹⁾ C. KITTEL: *Phys. Rev.*, **82**, 729 (1951).

⁽²⁾ A. F. DEVONSHIRE: *Phil. Mag. Suppl.*, **3**, 85 (1954).

small number of molecules per unit cell. (e.g. in the Perovskite structure $Z = 1$), antiferroelectric shifts are only possible in a larger unit cell having at least a doubled lattice constant along one crystallographic direction. The superstructure is then easily recognized from the superstructure lines on the X-ray patterns. By definition the antiferroelectric state is non-polar, having a centre of symmetry and thus showing no piezoelectric effect.

The difficulty in defining antiferroelectricity is not the distinction between ferro- and antiferroelectric phases, but between antiferroelectric and ordinary non-polar crystals: In normal ionic crystals the dielectric constant slightly increases with raising temperature ($d\epsilon/dT > 0$). Therefore if a phase transition occurs, which—as is generally the case—is connected with lowering temperature with a decrease of the volume, a drop of the dielectric constant is to be expected. In addition there will be involved a certain change of entropy and anomalies of the elastic properties and it cannot be excluded that superstructure might occur. Such a behaviour might thus show all the characteristic features of antiferroelectricity, but the mechanism leading to the transition is quite different.

HELEN MEGAW⁽³⁾ showed that from a crystal-chemical point of view the ionic bond arrangement of the Perovskite structure is not very stable. Oxygen and B atoms such as Ti, Zr, Nb, etc., tend to form covalent bonds and require other bond angles. She demonstrates that if the bond angle requirements of the oxygen atoms predominate, antiparallel atomic shifts occur, the structure becomes puckered and shows superstructure. She therefore considers the notion of antiferroelectricity as having no physical meaning. As a matter of fact transitions due to bond angle requirements are relatively frequent in the Perovskite structure family leading to the many deformed pseudocubic structure types. As examples one may quote the transition of SrTiO_3 crystals⁽⁴⁾, which below 100 °K show deviations from the Curie-Weiss law, and the transition in $\text{Ca}_{0.2}\text{Sr}_{0.8}\text{TiO}_3$ mixed crystals at 110 °K, where a drop of the dielectric constant was observed⁽⁵⁾.

However we do not share Megaw's point of view that ferro- and antiferroelectricity are merely due to the tendency toward stronger covalency. Many experimental facts can only be explained by assuming that in ferroelectric crystals at all temperatures an electrostatic dipole-dipole interaction exists among the induced dipoles in the crystal. But if the electric interaction leads to a transition, the ionic shifts will be such as to fulfill covalent bond requirements as well as possible.

⁽³⁾ H. MEGAW: *Acta Cryst.*, **5**, 739 (1952); **7**, 187 (1954).

⁽⁴⁾ H. GRÄNICHER: *Helv. Phys. Acta*, **29**, 211 (1956).

⁽⁵⁾ H. GRÄNICHER and O. JAKITS: *Suppl. Nuovo Cimento*, **11**, 480 (1954).

The behaviour of the dielectric constant in the paraelectric (high temperature) range is described by the empirical relation:

$$\varepsilon = \varepsilon_0(T) + \frac{C}{T - \theta} \quad (6),$$

ε_0 is called the background dielectric constant (« Untergrunds-DK »), which is of the order of 10 and shows a small positive temperature coefficient. In ferroelectrics the Curie temperature θ is practically identical with the transition temperature. In general θ may also have very low, often negative values in other substances. In ferroelectrics and many antiferroelectrics the Curie-Weiss term in the expression above is predominant. The occurrence of this strong temperature dependence with a negative temperature coefficient can be explained by dipolar interaction. It is therefore reasonable to restrict the use of the name « antiferroelectric » to cases, where the interaction is essentially of the same nature as in ferroelectrics.

If this restriction is adopted, then two additional criteria exist, which permit a phenomenological distinction between phase transformations leading to antiferroelectricity in the restricted sense and transformations which are exclusively caused by covalent bond requirements or other crystal-chemical reasons:

1) As a necessary, though not sufficient condition for antiferroelectricity we require that the temperature coefficient of the dielectric constant ($d\varepsilon/dT$) be negative in the unpolarized high temperature phase, at least in the temperature range just above the transition.

2) Since we only consider cases where dipolar interaction exists, there must also be an interaction between the polarization of the sublattices and an applied electric field, the influence of this electric field being especially important in the neighbourhood of the transition. A further necessary condition for antiferroelectricity is therefore that the transition temperature must be shifted by an external electric field (²). This shift is very marked in the case of first order transitions, but may be hard to detect in the case of higher order transitions (e.g. in the periodates $(\text{NH}_4)_2\text{H}_3\text{IO}_6$ and $\text{Ag}_2\text{H}_3\text{IO}_6$).

The difficulties in defining the antiferroelectric state in comparison to the magnetic case arise from the fact that all insulators have a dielectric constant $\varepsilon > 0$ and might possibly be antiferroelectrics, whereas antiferromagnetism obviously only occurs in crystals containing paramagnetic ions in sufficient concentration.

(⁶) H. GRÄNICHNER: *Helv. Phys. Acta*, **24**, 619 (1951).

INTERVENTI E DISCUSSIONI

— C. KITTEL:

The distinction between ferromagnetic and antiferromagnetic behaviour is usually very sharp, depending on the sign of the exchange integral. However the condition for a ferroelectric state may be very close to the condition for an antiferroelectric state. In the Perovskite structure a fractional change of 10^{-2} or 10^{-3} in the Lorentz local field interaction constant may throw the crystal from a ferroelectric to an antiferroelectric state. This sensitivity reflects the anisotropy character of the dipolar interaction.

Magnetic Susceptibility of Electrons in Periodic Fields.

C. P. ENZ

Physikalisches Institut der E.T.H. - Zürich

The problem of the magnetic susceptibility of electrons in a periodic field already treated by PEIERLS ⁽¹⁾ in 1933 and later on by WILSON ⁽²⁾ and ADAMS ⁽³⁾ in 1953, is reformulated by means of a formula due to SCHAFROTH ⁽⁴⁾. The practical purpose of the investigation to be summarized in this communication, was to try to understand the temperature dependence of the susceptibility of germanium and silicon as measured by the Zürich ⁽⁵⁾ and the Oak Ridge ⁽⁶⁾ groups.

Two different problems were envisaged both being analysed by means of the Schafroth formula. The first is a more detailed treatment of the susceptibility of the holes in Ge already studied in an earlier paper ⁽⁷⁾ but now taking fully into account the warped shape of the energy surfaces. The second application consists in a detailed investigation of the structure of the general susceptibility formula, but with neglect of spin-orbit coupling and other relativistic corrections in the field free Hamiltonian. This was done with the hope to provide an explanation for the increase of the diamagnetism with decreasing temperature experimentally found in Si and Ge ^(5,6). In fact this behaviour is not well understood and an attempt to explain it has been put forward only recently ⁽⁸⁾.

(1) R. PEIERLS: *Zeits. Phys.*, **80**, 763 (1933).

(2) A. H. WILSON: *Proc. Cambridge Phil. Soc.*, **49**, 292 (1953).

(3) E. N. ADAMS: *Phys. Rev.*, **89**, 633 (1953).

(4) M. R. SCHAFROTH: *Helv. Phys. Acta*, **24**, 645 (1951).

(5) G. BUSCH and coworkers: *Helv. Phys. Acta*, **27**, 201 (1954); G. BUSCH: in *Halbleiterprobleme IV*, edited by W. SCHOTTING, in press.

(6) D. K. STEVENS and J. H. CRAWFORD: *Phys. Rev.*, **100**, 1085 (1955) and *Bull. Am. Phys. Soc.*, **1**, 117 (1956).

(7) C. P. ENZ: *Helv. Phys. Acta*, **28**, 158 (1955).

(8) J. A. KRUMHANSL and H. BROOKS: *Bull. Am. Phys. Soc.*, **1**, 117, F5 (1956).

Let us start with a Hamiltonian of the form

$$\mathcal{H} = \mathcal{H}_0 + \omega \mathcal{H}',$$

ω being a perturbation parameter, and let $F_0(x)$ be any function which is regular in the neighbourhood of the real x -axis. We now express $F_0(\mathcal{H})$ as a formal expansion in ω . Following NAKAJIMA ⁽⁹⁾ this can be done by writing Cauchy's formula

$$F_0(\mathcal{H}) = \frac{1}{2\pi i} \oint \frac{F_0(x) dx}{x - \mathcal{H}},$$

and expanding the denominator according to

$$(x - \mathcal{H})^{-1} = (x - \mathcal{H}_0)^{-1} + \omega \cdot (x - \mathcal{H}_0)^{-1} \mathcal{H}' (x - \mathcal{H}_0)^{-1} + \\ + \omega^2 \cdot (x - \mathcal{H}_0)^{-1} \mathcal{H}' (x - \mathcal{H}_0)^{-1} \mathcal{H}' (x - \mathcal{H}_0)^{-1} + \dots$$

In the representation by eigenfunctions of \mathcal{H}_0

$$\mathcal{H}_0 |n\rangle = E_n |n\rangle,$$

we then get Schafroth's formula

$$(1) \quad (n | F_0(\mathcal{H}) | n') = (n | n') \cdot F_0(E_n) + \omega (n | \mathcal{H}' | n') F_1(E_n, E_{n'}) + \\ + \omega^2 \sum_{n''} (n | \mathcal{H}' | n'') (n'' | \mathcal{H}' | n') F_2(E_n, E_{n''}, E_{n'}) + \dots,$$

where

$$(1') \quad F_r(E_0, E_1, \dots, E_r) = \frac{1}{2\pi i} \oint \frac{F_0(x) dx}{\prod_{s=0}^r (x - E_s)}; \quad r = 0, 1, 2, \dots$$

In the case of electrons in a periodic field, \mathcal{H}_0 is periodic even with spin-orbit coupling and other relativistic corrections included and the eigenstates are of the Bloch type. Thus replacing $|n\rangle$, E_n and \sum_n by $|n\mathbf{k}\rangle$, $E_n(\mathbf{k})$ and $\sum_n d^3k$ respectively where n is now a band index and \mathbf{k} varies within the reduced zone, (1) and (1') take the form to be used here.

In the case of a homogeneous magnetic field H in the x_3 -direction we have

$$(2) \quad \mathcal{H}' = \frac{1}{2m} \left[\left(\mathbf{p} - \frac{e}{c} \mathbf{A} \right)^2 - \mathbf{p}^2 \right] - \frac{1}{2} \sigma_3 = \mathcal{H}_1 + \omega \mathcal{H}_2,$$

$$(2') \quad \omega = \frac{eH}{mc} = 2\mu H,$$

⁽⁹⁾ S. NAKAJIMA: *Adv. in Phys.*, 4, 363 (1955).

where c_3 is a Pauli spin matrix, $\frac{1}{2}$ the Bohr magneton and units are chosen such that $\hbar = 1$ throughout. For the analysis of the structure of the final formula it is useful to write the vector potential in the form

$$(3) \quad A = -H \cdot (\lambda x_2, (\lambda - 1)x_1, 0),$$

which means that a one-parameter gauge group is retained. $\lambda = \frac{1}{2}$ is the gauge in which

$$\mathcal{H}_1 = -\frac{1}{2}(l_3 + \sigma_3); \quad \mathcal{H}_2 = \frac{m}{8}(x_1^2 + x_2^2),$$

with

$$l_3 \equiv x_1 p_2 - x_2 p_1.$$

If now F_0 is taken as

$$(4) \quad F_0(E) \equiv -\frac{1}{\theta} \log (1 + \exp [-\theta(E - \zeta)]); \quad \theta \equiv \frac{1}{\hbar T},$$

the trace of $F_0(\mathcal{H})$ represents the thermodynamical potential

$$\Omega = F - N \cdot \zeta$$

for Fermi-Dirac statistics, F being the free energy. The field independent susceptibility (we are not interested here in a de Haas-Van Alphen type behaviour) is then given by

$$\chi = -\frac{4\mu^2}{V} \left(\frac{\partial^2 \Omega}{\partial \omega^2} \right)_{\zeta, m=0},$$

V being the crystal volume. Since no permanent magnetic moment exists we must have

$$\Omega = \Omega_0 + \omega^2 \Omega_2 + 0(\omega^3),$$

where from (1) and (2) it follows that

$$\Omega_2 = \frac{V}{(2\pi)^3} \sum_n (D_n + P_n),$$

with

$$(5) \quad D_n = \int_{\varepsilon} d^3k \int_{\varepsilon} d^3k' (n\mathbf{k} | \mathcal{H}_2 | n\mathbf{k}') \cdot F_1(E_n(\mathbf{k}), E_n(\mathbf{k}')),$$

$$(6) \quad P_n = \sum_{n''} \int_{\varepsilon} d^3k \int_{\varepsilon} d^3k' \int_{\varepsilon} d^3k'' (n\mathbf{k} | \mathcal{H}_1 | n''\mathbf{k}'') \cdot (n\mathbf{k}'' | \mathcal{H}_1 | n\mathbf{k}') F_2(E_n(\mathbf{k}), E_{n''}(\mathbf{k}''), E_n(\mathbf{k}')).$$

In these expressions the \mathbf{k}' integration is to be taken within a sphere $|\mathbf{k}' - \mathbf{k}| < \varepsilon$ with $\varepsilon \rightarrow 0$. This extra integration comes in because we take \mathbf{k} to vary continuously so that the normalization is

$$(n\mathbf{k} | n'\mathbf{k}') = \delta_{nn'} \delta(\mathbf{k} - \mathbf{k}')$$

and it is not allowed to put $\mathbf{k} = \mathbf{k}'$ in performing the trace. With (5) and (6) the susceptibility is simply

$$(7) \quad \chi = -\frac{\mu^2}{\pi^2} \sum_n (D_n + P_n).$$

This is a rigorous formula in so far as correlation effects between the electrons are neglected.

Since the structure of D_n and P_n is rather complicated the grouping together of terms in χ causes some trouble. This is why the reduced gauge group is retained in (3). In fact χ has to be independent of λ so that the introduction of this parameter provides a general means for the grouping together and also for a check.

Let us now examine more closely some of the features of D_n and P_n , fixing the gauge to $\lambda = \frac{1}{2}$. D_n gives purely diamagnetic contributions, the leading terms being those which contain a factor $F'_0(E_n(\mathbf{k}))$, i.e. the Fermi distribution function. This means that the summation over the band index n , for this part of D_n , extends over all filled bands and gives the familiar atomic diamagnetism

$$\chi_a = -\frac{Ne^2}{6mc^2} \sum_i \langle r_i^2 \rangle,$$

caused by the inner shell electrons.

On the other hand the sign of terms in P_n is not unique. For instance $\sum_n P_n$ contains the Landau-Peierls orbital diamagnetism

$$\chi_{LP} = +\frac{m^2\mu^2}{24\pi^3} \sum_n \int d^3k \left[\frac{\partial^2 E_n}{\partial k_1^2} \frac{\partial^2 E_n}{\partial k_2^2} - \left(\frac{\partial^2 E_n}{\partial k_1 \partial k_2} \right)^2 \right] F'_0(E_n),$$

and the Pauli spin paramagnetism

$$\chi_s = -\frac{m^2}{8\pi^3} \sum_n \int d^3k F_0''(E_n),$$

which are contributions from the free carriers alone since both terms contain the factor F_0'' , i.e. the derivative of the Fermi function.

It should be mentioned however that the splitting of the free carrier susceptibility into χ_{LP} and χ_s is rigorously true only if spin-orbit coupling is ineffective, otherwise there is a mixing of the two terms. This is just what occurs for the holes in Ge since there the energy band structure is strongly influenced by spin-orbit coupling as was shown by KITTEL in the interpretation of the cyclotron resonance experiments (¹). We shall not go into the details of the calculation here. It may be said however that though the mixing effect mentioned above shows up explicitly in the calculation it does not seem to have an appreciable influence on the total susceptibility.

Going back to the general discussion of the expressions D_n and P_n it should be noted that the terms χ_{LP} and χ_s usually considered as the essential ones cannot account for the increase of the diamagnetism with decreasing temperature found in Si and Ge (¹¹). This is so because at the temperatures in question the concentration of free carriers is negligibly small. Since moreover it is found experimentally that the susceptibility in this temperature range is not influenced by the impurity content it has to be concluded that the effect is caused entirely by the electrons in filled bands. This means that the important terms will be those containing a factor F_0' , i.e. χ_a and corresponding terms in $\sum_n P_n$.

It can be seen that these terms in $\sum_n P_n$ have a formal resemblance to a Van Vleck paramagnetism

$$\chi_v \sim \sum_n \frac{|(n|l_z|0)|^2}{E_n - E_0}.$$

This is just the type of term considered by KRUMHANSL and BROOKS (⁸) in their attempt to explain the effect. They consider the filled valence band as the important one and attribute the temperature dependence of χ to the variation of the energy gap between valence and conduction band which is known to be of the form

$$E_g = E_g^0 - \beta T.$$

(¹⁰) G. DRESSELHAUS, A. F. KIP and C. KITTEL: *Phys. Rev.*, **98**, 368 (1955).

(¹¹) It may be mentioned that ADAMS (³) faced a somewhat similar situation in the case of Bismuth.

This in fact gives qualitatively the right χ - T dependence provided that the matrix element in the numerator is essentially temperature independent. It should be pointed out however that a more detailed analysis making use of the $\hat{\lambda}$ gauge group and, more explicitly, of the relations between the matrix elements of x_j and p_j shows that the part of $\sum_n D_n$ leading to χ_a is of the same structure as the terms of $\sum_n P_n$ giving rise to a χ_v -like contribution. Thus it follows that the Krumhansl-Brooks treatment cannot be complete.

Proton Spin Relaxation in Gaseous and Liquid Hydrogen.

M. BLOOM

Dept. of Physics, University of British Columbia - Vancouver B.C., Canada

The work I am going to describe was carried out at the Kamerlingh Onnes Laboratory in Leiden. Since the last measurements were only completed a few days before this school began, the results are not yet digested and I will only discuss them in a qualitative manner. I think that this is worthwhile at this time, because the measurements show that certain quantities in the domains of molecular interactions and quantum statistical mechanics of gases are directly measurable by means of nuclear spin relaxation measurements. A detailed report of this work will shortly be submitted to *Physica*.

In the temperature region of 20 °K and lower, all H₂ molecules in thermal equilibrium are, to a good approximation, in their lowest rotational state, which for ortho-H₂ corresponds to $J=1$ and for para-H₂ to $J=0$. In a nuclear magnetic resonance experiment one observes only the protons of ortho-H₂ since para-H₂ has a total nuclear spin of zero. The quantity which we wish to discuss is the spin-lattice relaxation time t_1 of the protons. SCHWINGER has shown theoretically that the protons of H₂ come into thermal equilibrium due to interactions within the molecule which are affected by collisions between molecules. Associated with \mathbf{J} , the molecule has a rotational magnetic moment μ_J . The interaction between the protons' magnetic moments and μ_J may be pictured in terms of a magnetic field H' at the positions of the protons. Furthermore, the protons feel an effective magnetic field H'' due to their mutual dipole-dipole interaction. When the molecule undergoes a collision which changes the orientation of \mathbf{J} , the orientations of H' and H'' are also affected. Except for H₂ gas at very low pressure, such collisions occur quickly enough to cause the resonance lines to collapse into one line. The relaxation time has been calculated by SCHWINGER to be

$$\frac{1}{t_1} = (aH'^2 + bH''^2) \tau_c,$$

where a , b are quantities which depend only on the nuclear spins and gyro-magnetic ratios and on J . τ_c is the average time that a molecule spends in an m_J state. This formula is valid in the region $\omega_0^2 \tau_c^2 \ll 1$, where ω_0 is the angular frequency of the proton resonance.

Since H' and H'' are accurately known from molecular beam measurements, a measurement of t_1 uniquely determines τ_c . It is the measurement and interpretation of τ_c with which we are concerned (*). In a gas, τ_c is a function of the number of molecules per cm^3 N , the cross-section σ for collisions which produce a change in m_J (the magnetic quantum number of J) and the relative velocity of the colliding particles v . We can write

$$\tau_c \propto \frac{1}{N\sigma v},$$

where $\overline{\sigma v}$ represents an averaging over the velocity distribution of the molecules.

If σ is independent of velocity, Bloembergen writes, $\tau_c = (1.4/N\sigma\bar{v})$. One therefore expects that $t_1 \propto N$. This has been roughly verified by BLOEMBERGEN, PURCELL and POUND in measurements at room temperature. In our experiments we also verify this proportionality within the experimental accuracy of $\cong \pm 10\%$, at 20.4°K with pressures ranging⁸ from 0.2 to 1 atmosphere. To check the validity of this relaxation mechanism, we note that for 1 atmosphere of 75% ortho and 25% para- H_2 , $t_1 = 2.7 \cdot 10^{-3} \text{ s}$ corresponding to $\tau_c = 1.4 \cdot 10^{-10}$. Assuming that σ is independent of v and inserting $N = 4 \cdot 10^{20} \text{ mol/cm}^3$ and $v = 5 \cdot 10^4 \text{ cm/s}$ we obtain $\sigma = \pi r^2 = 5 \cdot 10^{-16}$ corresponding to an effective radius $r \cong 1.25 \cdot 10^{-8} \text{ cm}$, which is the right order of magnitude.

To check whether σ is really independent of velocity, we carried out experiments on the saturated vapour in equilibrium with the liquid at different temperatures. If N_T is the density of the saturated vapour at a temperature T , we expect, for σ independent of v

$$\frac{t_1(N_T)}{t_1(N_{20.4})} = \frac{N_T}{N_{20.4}} \cdot \left(\frac{T}{20.4} \right),$$

as shown by the full line in Fig. 1.

The experimental points indicated by crosses show that σ is a function of velocity. Apparently slower moving molecules have a larger σ than faster moving molecules, at least in the range over which velocities were varied in this experiment. The lowest temperature measured was 15.5°K .

(*) All the measurements on t_1 were done by the pulse method developed by E. HAHN.

From the fact that σ describes the collisions between H_2 molecules which result in a change in the orientation of \mathbf{J} , we see that it must depend on that part of the $\text{H}_2\text{--H}_2$ interaction which is anisotropic. In any sample of H_2 , there

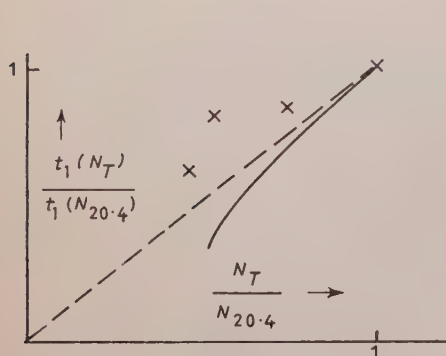


Fig. 1.

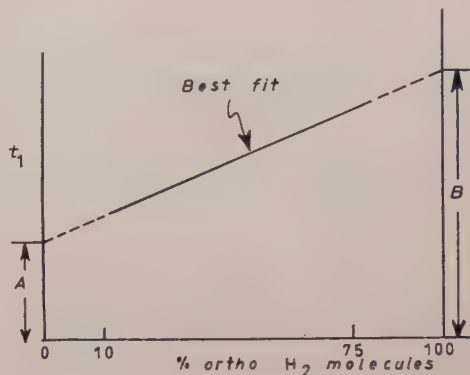


Fig. 2.

will be a mixture of ortho- and para- H_2 . Since para- H_2 is in the state $J=0$ it is spherically symmetric while ortho- H_2 is egg shaped, one would expect therefore that the σ for ortho-ortho collisions σ_o and that for ortho-para collisions σ_p may be different. For example, one of the important interactions between two ortho- H_2 molecules is the interaction between the quadrupole moments of their charge distributions. This interaction is zero for ortho-para pairs. For N_o ortho molecules per cm^3 and N_p para molecules per cm^3 , one therefore expects

$$t_1 \propto (N_o \bar{\sigma}_o \bar{v} + N_p \bar{\sigma}_p \bar{v}).$$

Experimentally, such a dependence is realized in measurements carried out in samples containing 10 to 25% ortho molecules. The interpretation of the experiments is shown in Fig. 2, where the straight line represents the best fit for data with a spread of $\cong \pm 15\%$ about it.

Extrapolation of the experimental measurements to 0 and 100% ortho- H_2 gives

$$\frac{\sigma_o \bar{v}}{\sigma_p \bar{v}} = \frac{B}{A} \cong 3 \pm 1.$$

This measurement therefore provides a means for testing the anisotropic interaction between hydrogen molecules.

Measurements in liquid H_2 give $t_1 = 180 \cdot 10^{-3} \text{ s}$ for 25% ortho- H_2 at 20.4 °K. Therefore $t_{1(\text{liquid})}/t_{1(\text{gas})} \cong 63$.

If the liquid was behaving just like a dense gas, one would expect

$$\frac{t_{1(\text{liquid})}}{t_{1(\text{gas})}} \simeq \frac{N_{\text{liquid}}}{N_{\text{gas}}}.$$

The measured ratio of the t_1 's is quite close to the ratio of the densities, which is 55. t_1 increases at lower temperatures in the liquid to a value of $230 \cdot 10^{-3}$ s at 14°K, i.e. the molecules reorient more quickly as the temperature is lowered. For lower concentrations of ortho- H_2 , t_1 becomes smaller in a similar manner to the gas.

Experiments were also carried out on HD. This is of interest because HD, having no symmetry, has as its lowest rotational state $J=0$. For 20.4°K, only one HD molecule in 100 is in the $J=1$ state. Since H' and H'' are equal to zero for $J=0$, one expects the relaxation behavior of HD to be somewhat different from H_2 . Indeed, one finds that for 0.5 atmospheres HD at 20.4°K, $t_1 = 2$ s which is approximately 1600 times as long as for H_2 . One can account for this long relaxation time by assuming that the nuclei can only relax while the molecule is in the $J=1$ state and that the time spent in the $J=1$ state is not too much longer than the time required for reorientation of the molecule. However, we do not attempt to reproduce the detailed argument here. In HD liquid, one finds $t_1 \simeq 40$ s, which is consistent with the formula given by Bloembergen, Purcell and Pound for nuclear spin relaxation in a liquid due to translational motion of the neighbouring molecules.

As a last remark, we note another quantity which should be measurable by nuclear spin relaxation in gases. It has been pointed out to the author by I. OPPENHEIM that in dense gases, the velocity distribution may depart considerably from the classical distribution. In particular v is changed in H_2 at $\simeq 30 \div 35$ °K and 40 ÷ 50 atmospheres pressure by order of magnitude 1. This would have a great effect on t_1 and should be detectable by measurements on t_1 as a function of pressure. In fact, it is possible that more accurate measurements of t_1 as a function of pressure even at 20.4°K and up to 1 atmosphere might be able to detect such effects.

The Production of Very Uniform Magnetic Fields.

E. M. PURCELL

Department of Physics, Harvard University - Cambridge, Mass.

Summary. — A magnetic field uniform to 1 part in 10^7 or better, over a volume of a few mm^3 , is needed for high resolution work in nuclear magnetic resonance. We discuss practical problems involved in producing such fields, with particular reference to permanent magnets, and suggest a new approach to some of them. A method is outlined for calculating the field variation within the gap between cylindrical poles. The results indicate that if the pole surfaces can be made magnetic equipotentials, the inhomogeneity will be slight, even for a diameter gap ratio as small as 4:1, and easily removable by simple compensating coils. To make sure the pole surfaces of a permanent magnet are equipotentials, the pole caps may be laminated transverse to the field direction. A « magnetic filter » of this sort is much more effective than a solid pole cap of the same thickness. Given suitably fine-grained material for the final pole surfaces, there appears to be no reason why a rather small permanent magnet cannot provide a field uniform enough for high resolution spectroscopy. Preliminary measurements on such a magnet will be presented.

The Antiferromagnetic State in the Chrome Alums.

J. H. VAN VLECK

Harvard University - Cambridge, Mass.

Summary. — This paper is a report on a calculation made by Miss Mary O'Brien which she has presented briefly at the Yale meeting of the American Physical Society, and which she plans to publish more fully in the *Phys. Rev.* The most striking result of Miss O'Brien's work is that purely dipolar interaction can lead to an antiferromagnetic Curie (NÉEL) point even though the paramagnetic ions are cubically spaced. It is usually assumed that cubic symmetry precludes this result, but calculations which are an extension of those previously made by DANIELS show that when different atoms in the unit cell have different directions for their crystalline fields, antiferromagnetism can ensue at sufficiently low temperatures. The predicted Néel point for methylamine chrome alum agrees with experiment ($.015 \div .020$ °K) practically within the limits of error of the latter. The calculated isentropic curves of moment versus field strength also agree quite well with experiment if a small amount of exchange is included.

The Magnetic Susceptibility of Oxygen in a Clathrate Compound.

J. H. VAN VLECK

Harvard University - Cambridge, Mass.

Summary. — COOKE, MEYER, WOLF, EVANS and RICHARDS (*Proc. Roy. Soc.*, **225**, 112 (1954)) have measured at low temperatures the susceptibility of oxygen dissolved in a β -quinol compound, wherein the oxygen molecules are 8 Å apart, and the deviation of the susceptibility from that in the gaseous state may hence be small. They find that $^{16}\text{O}^{18}\text{O}$ and $^{16}\text{O}^{16}\text{O}$ have the same susceptibility, although at low temperatures the magnetic behavior in the gaseous state should be different, inasmuch as only odd values of K are allowed for $^{16}\text{O}^{16}\text{O}$. The present paper shows that the magnetic behavior can be explained on the assumption that at helium temperatures the O_2 molecules do not rotate freely, but instead are aligned along a particular spatial direction. Calculations by Miss O'BRIEN show that the susceptibility curves can be fitted by assuming the axis of the O_2 molecule is « frozen » in space and that the spin-spin parameter is about 25 percent lower than in the gas. This apparent reduction can be explained on the basis that the molecule is not rigidly frozen, and instead has a potential barrier of about 50 cm^{-1} .

The Dependence of Nuclear Magnetic Resonance Absorption in Metals on Specimen Shape and Size.

P. RHODES

Department of Physics, University of Leeds - Leeds

Summary. — Calculations have been made of the effective distortion and shift of nuclear resonance lines in metals and alloys due to eddy currents. Expressions have been obtained appropriate to specimens in the form of flat plates, cylinders and spheres, and covering the whole range of the relevant parameters.

INDICE DEL SUPPLEMENTO

AL VOLUME VI, SERIE X, DEL

NUOVO CIMENTO

Anno 1957

Onoranze ad Amedeo Avogadro di Quaregna nel 1° Centenario della sua morte - Rendiconti del Congresso Internazionale sulle Costanti Fondamentali della Fisica e XLII Congresso Nazionale di Fisica - Torino, 6-11 Settembre 1956	pag.	1
C. FRANZINETTI and G. MORPURGO - An Introduction to the Physics of the New Particles	»	469
Rendiconti del IV Corso che nella Villa Monastero di Varenna dal 15 Luglio al 4 Agosto 1956 fu tenuto a cura della Scuola Internazionale di Fisica della Società Italiana di Fisica	»	805

Fine del *Supplemento* al Vol. VI, Serie X
del *Nuovo Cimento*, 1957

PROPRIETÀ LETTERARIA RISERVATA

Direttore responsabile: G. POLVANI

Tipografia Compositori - Bologna

Questo fascicolo del *Supplemento* è stato licenziato dai torchi il 28-XII-1957